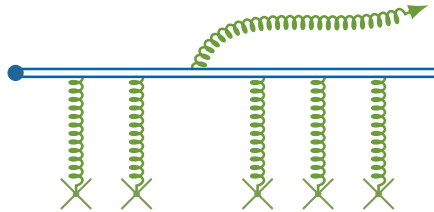


WILSON LINES

Applications in QCD

Frederik Van der Veken



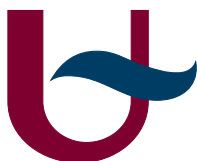
PROEFSCHRIFT

voorgelegd tot het behalen van de graad van
doctor in de Wetenschappen: Fysica

Department Fysica
Faculteit Wetenschappen
Universiteit Antwerpen

Promotor: Pierre Van Mechelen
Co-Promotor: Igor O. Cherednikov

Antwerpen, December 2014



TAQ
Theoretical
Aspects of QCD

To my little daughter Eva-Lotta, who, although repeatedly succeeding in drawing my focus away, was and remains an inspiring motivation.

°2013

SAMENVATTING

De theorie van de sterke kernkracht, kwantum chromodynamica (QCD), is niet zo grondig begrepen als we zouden willen, ook al lijkt dit op het eerste zicht misschien wel het geval. Voor een correcte interpretatie van moderne experimenten in de zoektocht naar nieuwe fysica, is een diepgaand inzicht in QCD noodzakelijk, omdat het het onderliggende mechanisme is van hadronbotsingen die de basis vormen van deze experimenten. Elke berekening in QCD kan ruwweg in twee delen opgesplitst worden: een perturbatief deel dat met behulp van standaard veldentheorie berekend kan worden, en een deel dat volledig vervat zit in zogenaamde parton dichtheidsfuncties (PDFs). Deze objecten kunnen niet berekend worden, maar wel afgeschat (door ze te discretiseren op een rooster) of gemodelleerd (en gematched met data). Maar bovenal is het mogelijk om exacte evolutievergelijkingen af te leiden die ons toe staan gemodelleerde data te extrapoleren van de ene energieschaal naar de andere.

Er bestaan verschillende methodes om het gedrag van PDFs te beschrijven. Eén van deze is de small- x methode, die vooral probeert om voorspellingen in diep inelastische verstrooiingsexperimenten te maken die ook geldig blijven bij hoge energieën en dichtheden. Daarom ligt zijn grootste toepassingsgebied in nucleaire en zware-ionen fysica. We wijden één hoofdstuk aan een introductie van deze methode. Een andere aanpak is het transversale impulsdichtheid (TMD) formalisme, dat een volledig driedimensionele kijk op de inhoud van het proton probeert te geven. Dit formalisme haalt nieuwe informatie uit semi-inclusieve experimenten door extra deeltjes in de eindtoestand waar te nemen. Deze thesis speelt zich vooral in dit formalisme af, en hoewel het niet zozeer TMDs zelf behandelt is het volledig opgebouwd rond één van de belangrijkste bestanddelen van TMDs, namelijk Wilson lijnen.

Wilson lijnen zijn opvallende wiskundige objecten. Als pad-geordende exponenten van de ijkvelden bevatten ze alle kinematische en dynamische informatie van de ijktheorie. Ze vervangen coördinaten door pad afhankelijkheid, en geven zo een meetkundige beschrijving van QCD. Ze zijn bovendien onmisbaar in een ikinvariante definitie van bilokale operatoren, en dus ook in een consequente beschrijving van elke ijktheorie. Zolang er geen externe velden zijn zal een Wilson lijn altijd een lineair pad volgen tot ze plots in een andere richting wordt gestuurd door een kortstondige externe impuls. In deze thesis stellen we een nieuwe methode voor om stuksgewijs lineaire Wilson lijnen op een eenvoudige manier te berekenen. Deze methode heeft reeds veelbelovende resultaten en een hele reeks toepassingen. Een bijzonder type Wilson lijnen zijn Wilson lussen, gedefinieerd op een gesloten pad. Ze kunnen gebruikt worden als basis elementen om ijktheorie te beschrijven zonder coördinaten of velden, waar alle dynamica door hun meetkundige evolutie gestuurd wordt. Hierop verder bouwend onderzoeken we het meetkundig gedrag van TMDs, wat tot eenvoudigere evolutievergelijkingen zal leiden, en ons dus een stap dichterbij een volledig inzicht in QCD.

ABSTRACT

Although at first sight maybe not so obvious to the unaccustomed eye, the quantum field theory of the strong force, quantum chromodynamics or QCD for short, is not as thoroughly understood as we would like it to be. A deep understanding is imperative to properly interpret modern experimental searches for new physics, as QCD is the theory that underlies the hadronic collisions that drive the experiment. Roughly speaking, every QCD calculation consists of two parts, a perturbative part, calculable by standard non-Abelian field theory methods, and a non-perturbative part, described by parton density functions (PDFs). These non-perturbative objects are not calculable, but can be estimated (on a lattice) or modelled (and fitted to data). But more importantly, it is possible to derive exact evolution equations. For a PDF that is fitted to data at a given scale, these can be used to predict it at any scale.

There exist several frameworks to investigate the behaviour of PDFs. One of these is the small- x approach, which mainly aims at maintaining correct predictions in deep inelastic scattering (DIS) even at high energies and high densities. For this reason, its main applications lie in nuclear and heavy ion physics. We devote one chapter to an introduction to small- x physics. Another popular framework is the transverse momentum density (TMD) formalism, which tries to give a complete 3-dimensional description of the contents of the proton. Instead of limiting itself to deep inelastic scattering, it will acquire information on the structure of the proton by observing particles in the final state, using semi-inclusive experiments. This thesis is mainly situated in this formalism, and although it won't deal much with TMDs themselves, it is centred around one of its key ingredients, namely Wilson lines.

Wilson lines are curious mathematical objects. Path-ordered exponentials of the gauge fields, they contain all kinematical and dynamical information of the gauge sector. They replace coordinate dependence with path dependence, and allow as such for a geometrical approach to QCD. They are indispensable for a gauge invariant description of bilocal operators, and hence for a consistent definition of any gauge theory. In the absence of external fields, all Wilson lines will be piecewise linear, that is, linear until abruptly forced in another direction by instantaneous external influences. Being the main topic of this thesis, we will demonstrate a new approach to simplify calculations with piecewise linear Wilson lines, that has promising results and a whole spectrum of applications.

A special class of Wilson lines are closed lines, or Wilson loops. They can be used as basic objects to fully describe gauge theory without coordinates nor fields. Dynamics are governed by their geometrical evolution, and inspired by this we investigate the geometrical behaviour of TMDs. This will lead to evolution equations that are easier to handle, bringing us one step closer to a full understanding of QCD.

PUBLICATIONS

BOOKS

Published

- [1] I. O. CHEREDNIKOV, T. MERTENS, and F. F. VAN DER VEKEN (2014). *Wilson Lines in Quantum Field Theory*. De Gruyter Studies in Mathematical Physics. De Gruyter, Berlin.

PEER-REVIEWED PAPERS AND PROCEEDINGS

Published

- [2] I. O. CHEREDNIKOV, T. MERTENS, and F. F. VAN DER VEKEN (2013). “Cusped light-like Wilson loops in gauge theories.” *Phys. Part. Nucl.* **44**, 250–259. [arXiv:1210.1767 \[hep-ph\]](#)
- [3] I. O. CHEREDNIKOV, T. MERTENS, and F. F. VAN DER VEKEN (2012). “Evolution of cusped light-like Wilson loops and geometry of the loop space.” *Phys. Rev. D* **86**, 085035. [arXiv:1208.1631 \[hep-th\]](#)

Accepted

- [4] F. F. VAN DER VEKEN (2014). “Piecewise linear Wilson lines.” EPJ Web Conf. In print. [arXiv:1409.3190 \[hep-ph\]](#)

In Preparation

- [5] F. F. VAN DER VEKEN (2014). “Calculation of colour traces and generators.” In preparation to submit to *Phys. Lett. B*.
- [6] F. F. VAN DER VEKEN (2014). “Working with piecewise linear Wilson lines.” In preparation to submit to *Phys. Rev. D*.

REGULAR PROCEEDINGS

Published

- [7] I. O. CHEREDNIKOV, T. MERTENS, P. TAEELS, and F. F. VAN DER VEKEN (2014). “Evolution of transverse-distance dependent parton densities at large- x_B and geometry of the loop space.” Int. J. Mod. Phys. Conf. Ser. **25**, 1460006. [arXiv:1308.3116](#) [hep-ph]
- [8] F. F. VAN DER VEKEN (2013). “Evolution and dynamics of cusped light-like Wilson loops.” PoS **Hadron2013**, 134. [arXiv:1405.4017](#) [hep-ph]
- [9] F. F. VAN DER VEKEN (2013). “Evolution and dynamics of cusped light-like Wilson loops.” Nuovo Cim. **C36**, 89–94. [arXiv:1302.6765](#) [hep-th]
- [10] F. F. VAN DER VEKEN, I. O. CHEREDNIKOV, and T. MERTENS (2012). “Evolution and dynamics of cusped light-like Wilson loops in loop space.” AIP Conf. Proc. **1523**, 272–275. [arXiv:1212.4345](#) [hep-th]
- [11] I. O. CHEREDNIKOV, T. MERTENS, and F. F. VAN DER VEKEN (2012). “Loop space and evolution of the light-like Wilson polygons.” Int. J. Mod. Phys. Conf. Ser. **20**, 109–117. [arXiv:1208.5410](#) [hep-th]

Submitted

- [12] F. F. VAN DER VEKEN (2014). “A new approach to piecewise linear Wilson lines.” Submitted to Int. J. Mod. Phys. Conf. Ser. [arXiv:1411.3372](#) [hep-ph]

WORK IN PROGRESS

- [13] L. P. GAMBERG, M. SCHLEGEL, and F. F. VAN DER VEKEN (2014). “Final state interactions and the Boer-Mulders function.” Work in Progress.
- [14] M. GARCÍA ECHEVARRÍA, A. S. IDILBI, I. SCIMEMI, and F. F. VAN DER VEKEN (2014). “Universality of the soft function in QCD.” Work in Progress.
- [15] F. F. VAN DER VEKEN (2014). “Calculational techniques for Wilson lines.” Work in Progress.

ACKNOWLEDGMENTS

First of all I would like to thank my two supervisors, Prof. Dr. Pierre Van Mechelen and Dr. Igor O. Cherednikov, for the unique opportunity of doing the first theoretical physics Ph.D. in their group. I feel honoured by their trust, and am thankful for the large amount of internships, summer schools and conferences I was allowed to attend. An extra word of thank to Igor for his continuous support—both technical and emotional—during the sometimes difficult calculations, and during moments of incertitude.

I would also like to thank Dr. Krzysztof Kutak, for his supervision during the first three months of my Ph.D. and his important contribution in helping me make the switch from Supergravity to QCD. Furthermore, I am really grateful to Prof. Dr. Edmond Iancu for accepting me for a six month internship at CEA-Saclay under his supervision. I admire his clear way of thinking, and am thankful that he was willing to share a piece of his knowledge with me by regular personal meetings, and I really appreciate his still continuing support.

Also a word of gratitude to my fellow Ph.D. students Tom Mertens and Pieter Tael for our frequent discussions and shared insights, and for their friendship. In the same line, I would like to thank my fellow students and postdocs at CEA-Saclay—Fabio, Yacine, Ekatarina, Julien, Thomas and Piotr—and at the summer schools in Varenna—Giovanni, Suzanna, Irina and Maarten—and Trento—Eduardo, Mike, Irina B., Ilnur, Jasone, Jonathan, Viacheslav, David, Tianbo, Joshua, Irina P., Felix and Jiakai. Thanks for the excellent atmosphere, the fruitful knowledge exchanges and especially for the warm friendships.

I am thankful as well to the lecturers of the summer schools for their personal involvement with the students, as it was highly beneficial. In particular, I would like to express my thanks to Prof. Dr. Mauro Anselmino, Prof. Dr. Alessandro Bacchetta, Prof. Dr. Barbara Pasquini and Prof. Dr. Abhay Deshpande for their support. Also, a special word of thanks to Prof. Dr. Marco Radici, who spent several nights preparing my application for the Marie Curie fellowship. His clear writing inspired me to rephrase some sections in this thesis.

On a more recent note, I would like to thank Prof. Dr. Leonard Gamberg, Dr. Ahmad Idilbi and Dr. Miguel García-Echevarría for the openness with which

they accepted me into their research activities, and for the fruitful discussions, which often gave me a decent base to write some sections of this thesis on.

Last—but certainly not least—I would like to thank my family, in particular my loving girlfriend Jolien, who provided me with the necessary back support to fulfil this Ph.D., and my cute little daughter Eva-Lotta, who had to miss her father on quite some occasions, not the least those last three months where he locked himself up in his desk, writing. I am thankful that, even then, she never lost her smile, and for the oh-so-needed moments of joy when she re-motivated me.

Thank you all, I couldn't have done it without your support.

φασὶ γὰρ εἶναι τὰ πρῶτα μεγέθη πλήθει μὲν ἄπειρα, μεγέθει δὲ ἀδιαίρετα, καὶ οὐτ' ἐξ ἑνὸς πολλὰ γίγνεσθαι οὔτε ἐκ πολλῶν ἔν, ἀλλὰ τῇ τούτων συμπλοκῇ καὶ περιπλέξει πάντα γεννᾶσθαι.

The ultimate units of matter are infinite in number, are indivisible and cannot be merged, but all things are formed by their plaiting.

— Δημόκριτος, as cited by *Arist. de caelo III 4.303a5; 67A15.*

FOREWORD

As far as written history knows, Democritus was the first philosopher to postulate the idea that everything that exists—all matter—is built from extremely small entities that are ἄτομος—*atomos*, ‘indivisible’. In a time where the concept of a ‘particle’ is non-existent, where matter is always conceived as either solid (earth), liquid (water), gaseous (air) or plasma (fire) without the addition of any internal structure, making such a postulate is not only a bold leap forward, but it also testifies of great intuition for physics and life, for it has taken more than two millennia to prove him right.

Far more important is the implication it had on (meta)physics, as now the quest of understanding the universe became the quest for the smallest, the search for elementary particles. Many, many years later, this quest was toughened by the additional search after the true nature of light (and forces in general), the scientific community being divided into a group of particle-believers (led by Newton) and a group of wave-believers (led by Huygens). Along came quantum mechanics, demonstrating that forces are particles as well, but just behaving as a wave. Everybody happy, end of story.

Not exactly, because something fundamentally had changed since Democritus’ postulate. Something so deeply rooted in physics that today we take it for granted. It is the quest to understand every fundamental gear that makes the universe tick, to understand the elementary forces and the elementary particles they do bind and influence. Not to be satisfied, unless we understand every tiny piece of the elementary workings of the universe (which in my humble opinion is a dream that is asymptotically free), always smaller and smaller. For this reason a

large part of the modern day physics community will remain to be devoted to elementary particles and their forces.

This thesis is no exception to that rule. It is a product made to contribute in the search to solve one of elementary particle physics' main issues that is not fully understood, namely the behaviour of the strong force. On paper, we elementary particle physicists have it all figured out.¹ We have deciphered the underlying theory for the afore mentioned force, viz. the so-called 'theory of colour' or quantum chromodynamics (QCD). But we cannot wield it. Because this theory—which we know has to be the correct one—is of such calibre that it tends to blow itself up. It works as long as we don't focus on the contents of hadrons (non-elementary particles like a proton). But that's where the core of the problem lies. Thanks to Democritos' legacy, we want to delve into it, deeper and deeper, smaller and smaller. We want to take a proton and—because we know it isn't elementary—break it open to investigate its contents. And that's where QCD starts complicating things—the more we zoom in to smaller and smaller scales, the more substructures we will find, until suddenly we find more particles than can reasonably fit inside one proton. Did our theory break? No, we just cannot wield it.

That is, we cannot *blindly* wield it. But we can manage it. For starters, we separate out the well-understood hard scattering from the interesting hadron contents. This is the core principle of modern QCD and is known as *factorisation*, and it has a strong mathematical background supporting it. A large fraction of the present day scientific QCD community is devoted to finding an accurate description of the 3-dimensional hadron content, be it in coordinate space (known as the GPD framework) or momentum space (known as the TMD framework). This thesis is part of the latter framework, be it on a more technical note. It is a dissertation on the topic of *Wilson lines*, which are paramount to define gauge-invariant TMDs, objects that will be used to describe the contents of a hadron. The usability of Wilson lines is however not limited to the investigation of the contents of the hadron. In the small- x formalism for instance—which is a formalism where one investigates QCD by zooming in and zooming in, it hence naturally adds a saturation mechanism to avoid the above scenario of an 'overfull' proton—Wilson lines emerge as a resummation of all gauge interactions on a given particle. Hence the investigation and simplification of Wilson line calculations is bound to be beneficial for a lot of people.

¹ If we may just ignore gravity, which is so weak compared to the other three forces that we can put it to zero anyway (for all practical calculations at the subatomic scale).

OUTLINE OF THE THESIS

I realise that this thesis is quite extensive, but this is mainly due to the fact that I tried to make it into a reference work as well. Having struggled myself trying to get acquainted with QCD and TMDs (coming from a Supergravity background), I hope that this thesis can serve future students as a helpful entry work.

The thesis is roughly divided into 3 parts. Part i is a basic introduction to QFT in general and QCD in particular. I start with an enumeration of possible symmetries in QFTs in Chapter 1, describing different terms in the Lagrangian and exploring Noether's theorems. In Chapter 2 I construct a general $\mathfrak{su}(n)$ gauge theory purely from geometrical arguments. This is not new research, but not so easily found in existing literature. It is also a natural first introduction to both Wilson lines and Wilson loops, as they are the geometrical objects that bring the gauge field into play. Chapter 3 is a detailed chapter that introduces quantisation using path integrals. It is an almost insurmountable task to quantise Wilson lines using canonical quantisation because the time ordering coming from the quantisation may interfere with the path ordering from the Wilson line. Quantisation with path integrals avoids this problem. Chapter 4 is a continuation on the quantisation procedure, as it shows some typical quantum effects which we will need in later chapters, like the anomalous mass dimension and the final-state cut. In the last chapter of this part, Chapter 5, I give a brief introduction on how factorisation emerges in QCD using the most common experimental setup to introduce it (namely DIS).

Part ii is what I would call the core of this thesis, and it contains the latest of my research. In Chapter 6 I reintroduce Wilson lines in a more formal way, and derive Feynman rules that are as general as possible. The description of the finite and infinite Wilson lines in Section 6.3 is as far as I know unique, in that sense that it has never been done before with the same mathematical rigourousity. The Sections 6.2, 6.4 and 6.5 form the basis for a new methodology to calculate piecewise linear Wilson lines (the most common type) in an easier way. This was the main topic of my research in the last year, and has lead to a few papers [4, 6, 12]. These first results provide a firm basic and will be extended and developed further in my current and planned work. Section 6.6 describes the eikonal approximation which is a common tool to approximate all gauge interactions on a quark. Chapter 7 is a collection of tools to simplify calculations with Wilson lines—like a direct, non-recursive calculation of colour traces in Section 7.1 [5]—and some first results of the new methodology. The full chapter is new research, and although the results in Section 7.4 are already known, the methodology used to calculate them is not and might lead to new insights. The two chapters that follow are both frameworks in QCD that rely on Wilson lines.

The TMD framework is introduced at a basic level in [Chapter 8](#). I first review DIS in a more formal way, giving an operator definition for the PDF, using Wilson lines to make it gauge invariant. Next we apply the same principle to SIDIS, leading to operator definitions for TMDs. In the last section I briefly review the evolution of TMDs, as I will come back to it when investigating the geometrical evolution of Wilson loops in [Chapter 11](#). The last chapter in this part is [Chapter 9](#), where the small- x framework is reviewed. This framework describes the behaviour of QCD in the limit of a small longitudinal momentum fraction. This chapter includes in [Section 9.3](#) a small research project which I did together with Dr. Krzysztof Kutak in the first three months of my Ph.D. It is the calculation of the transversal energy flow in a saturation framework.

[Part iii](#) is all about Wilson loops and their geometric evolution, which are results from a collaboration with Dr. Igor Cherednikov, Tom Mertens and Pieter Taelens [[2](#), [3](#), [7–11](#)]. In [Chapter 10](#) I review how Wilson loops can be used as basic building bricks to recast QCD in loop space. I start with an introduction on colour diagrams—which are useful in any QCD calculation—and investigate these diagrams in the large- N_c limit, which naturally leads to the emergence of Wilson loops. In the second part of this chapter, I review the necessary procedures in order to renormalise Wilson loops. This is a section of high relevance, as the singularity structure of Wilson lines—and hence of e.g. TMDs—is completely analogous to that of Wilson loops. I have put some special attention on light-like segments, as the latter are most relevant both for TMDs and the geometric evolution of loops. And last, in [Chapter 11](#), I present our results on the geometric behaviour of Wilson loops. I start with a motivation based on a duality between super Yang-Mills and loop space, and continue with the investigation of rectangular light-like loops. This eventually leads to our conjecture of a geometric evolution equation, which is motivated to be valid at all orders. The chapter ends with an application of the geometric evolution on TMDs. This research has since been continued by Tom Mertens and Igor Cherednikov with a larger focus on the mathematical preliminaries of loop space, further strengthening the conjecture [[16](#), [17](#)].

This thesis is concluded with two appendices that contain a lot of reference formulae, and are meant both as a support for the calculations in this thesis, and as a general reference.

—Frederik Van der Veken, December 2014.

CONTENTS

SAMENVATTING	iii	
ABSTRACT	iv	
PUBLICATIONS	v	
ACKNOWLEDGMENTS	vii	
FOREWORD	ix	
CONTENTS	xiii	
LIST OF FIGURES	xviii	
ACRONYMS	xx	
LIST OF IMPORTANT EQUATIONS	xxii	
i	INTRODUCTION TO QFT AND QCD	1
1	SYMMETRIES IN QUANTUM FIELD THEORIES	2
1.1	Classical Field Theory	2
	Equations of Motion	3
	Characteristics of the Lagrangian	6
	Scalar Fields	8
	Vector Fields	9
	Spinor Fields	11
1.2	Symmetries of the Lagrangian	13
1.3	Spacetime Symmetries	15
1.4	Global Symmetries	17
	Free Dirac Lagrangian	19
	The Yang-Mills Lagrangian	20
1.5	Local Symmetries	22
	Localised Equations of Motion	23
	Noether's Second Theorem	25
2	GEOMETRY OF QUANTUM FIELD THEORIES	28
2.1	Parallel Transport and Wilson Lines	28
	The Parallel Transporter	29
	Non-Abelian paths	32
	The Covariant Derivative	36

2.2	The Gauge Field Tensor and Wilson Loops	38
2.3	Summary	43
3	QUANTISATION OF QUANTUM FIELD THEORIES	46
3.1	Formal Definition of Path Integrals	46
	QM Propagator as a Path Integral	47
	Definition of the Path Integral	49
	Gaussian Path Integral	51
	n -Point Gaussian Integrals	53
3.2	Quantisation of The Scalar Field	59
	The Free Scalar Field	60
	The Interacting Scalar Field	66
3.3	Quantisation of the Dirac Field	71
	Grassmann Numbers	72
	The Free Dirac Field	75
3.4	Quantisation of the Gauge Field	79
	Abelian Gauge Fields	82
	Non-Abelian Gauge Field: Lorentz Gauge	84
	Non-Abelian Gauge Field: Axial Gauge	86
4	QUANTUM CORRECTIONS	89
4.1	Working With Quantised Fields	89
	Regularisation	91
	Mass Dimension Analysis	96
	One-Loop Example: Gluon Propagator with Fermion Loop	100
4.2	From Theory to Experiment	104
	Renormalisation	107
	The Callan-Symanzik equation	114
	Running Coupling in QCD: Asymptotic Freedom	116
5	BASICS OF QCD	120
5.1	Deep Inelastic Scattering	121
	Kinematics	122
	Invitation: The Free Parton Model	124
	A More Formal Approach	127
5.2	Parton Distribution Functions	134
5.3	Collinear Factorisation and Evolution of PDFs	137
ii	WILSON LINES	148
6	WILSON LINES	149
6.1	A Wilson Line Along a Path	149
	Properties of Wilson Lines	150
	Path Ordering	151

6.2	Piecewise Wilson Lines	154
6.3	Wilson Lines on a Linear Path	159
	Bounded from Below	159
	Bounded from Above	161
	Path Reversal	162
	Finite Wilson Line	166
	Infinite Wilson line	171
	External Momenta	175
6.4	Relating Different Path Topologies	176
6.5	Piecewise Linear Wilson Lines	180
	Path Functions	185
	Diagrams with Final-State Cuts	187
6.6	Eikonal Approximation	191
7	SIMPLIFYING WILSON LINE CALCULATIONS	195
7.1	Advanced Colour Algebra	196
	Calculating Products of Fundamental Generators	196
	Calculating Traces in the Adjoint Representation	201
7.2	Self-Interaction Blobs	204
	Two-Gluon Blob	204
	Three-Gluon Blob	207
7.3	Wick Rotations	210
	Regular Wick Rotation	211
	Wick Rotation with Wilson Lines	213
	Light-Cone Coordinates: Double Wick Rotation	217
7.4	Wilson Integrals	218
	2-Gluon Blob Connecting Two Adjoining Segments	220
8	INTRODUCTION TO TMDs	229
8.1	Revision of DIS	229
	Operator Definition for PDFs	230
	Gauge Invariant Operator Definition	233
8.2	Semi-Inclusive Deep Inelastic Scattering	237
	Conventions and Kinematics	238
	Structure Functions	240
	Transverse Momentum Dependent PDFs	242
	Gauge Invariant Definition for TMDs	245
8.3	Evolution of TMDs	248
	About the Rapidity Cut-Offs	251
9	QCD TOWARDS SMALL- x	254
9.1	Evolution in Longitudinal Momentum Fraction	254
9.2	The BK Equation and Saturation	261

	Comparison to Population Statistics	264
	The GBW model	265
9.3	Transversal Energy Flow	267
	Calculation of the Structure Functions	270
	Numerical Evaluation of the E_T -Flow	271
iii	WILSON LOOPS AND EVOLUTION	275
10	WILSON LOOPS AND LOOP SPACE	276
10.1	Large N_c -Limit	276
	Colour Representation	277
	Colour Representation in the Large- N_c Limit	281
10.2	Renormalisation of Wilson Loops and Γ_{cusp}	285
	Renormalisation of Wilson Loops on the Light-Cone	289
11	GEOMETRIC EVOLUTION	291
11.1	Motivation: Wilson Loops in Super Yang-Mills	291
	Super Yang-Mills Theory	292
	Planar Scattering Amplitudes	293
11.2	Wilson Loops in Loop Space	295
11.3	Evolution of Light-Like Rectangular Loops	297
	Rectangular Light-Like Loop Calculation at One-Loop	299
11.4	Geometric Evolution of TMDs	302
	CONCLUSION AND OUTLOOK	306
iv	APPENDICES	309
A	CONVENTIONS AND REFERENCE FORMULAE	310
A.1	Notational Conventions	310
A.2	Vectors and Tensors	312
A.3	Spinors and Gamma Matrices	313
A.4	Light-Cone Coordinates	316
A.5	Fourier Transforms and Distributions	318
A.6	Lie Algebra	321
	Representations	321
	Properties	322
	Useful Formulae	325
A.7	Summary of the Noether Theorems	327
A.8	Feynman rules for QCD	329
B	INTEGRATIONS	333
B.1	Reference Integrals	333
	Algebraic Integrals	333
	Logarithmic Integrals	334

	Cyclometric Integrals	335
	Gaussian Integrals	336
	Discrete Integrals	337
B.2	Special Functions and Integral Transforms	337
	Gamma Function	338
	Beta Function	340
	Polylogarithms	341
	Elliptic K -Function	342
	Integral Transforms	343
B.3	Dimensional Regularisation	345
	Euclidian Integrals	346
	Wick Rotation and Minkowskian Integrals	347
B.4	Path Integrals	349
	Properties	349
	BIBLIOGRAPHY	351

LIST OF FIGURES

Figure 2.1	Path equivalence of the parallel transporter.	31
Figure 2.2	Transitivity of the parallel transporter.	32
Figure 2.3	Transitivity with a point outside the path.	33
Figure 2.4	Discretising the path.	35
Figure 2.5	Stokes' theorem.	39
Figure 2.6	Smallest Wilson loop on the lattice.	41
Figure 3.1	Different propagator pole structures.	61
Figure 3.2	Scalar 4-point correlator.	65
Figure 3.3	Complex scalar 4-point correlator.	65
Figure 3.4	Vacuum diagram for ϕ^4 -theory.	67
Figure 3.5	Dirac 6-point correlator.	77
Figure 4.1	Fermion loop correction to the gluon propagator.	100
Figure 4.2	Running coupling constants for QED and QCD.	118
Figure 5.1	Four-jet event in electron-positron annihilation.	122
Figure 5.2	DIS kinematics.	123
Figure 5.3	DIS in the FPM.	125
Figure 5.4	DIS to all orders.	127
Figure 5.5	Hadron tensor.	132
Figure 5.6	Difference between structure functions and PDFs.	138
Figure 5.7	Factorisation in DIS at LO.	138
Figure 5.8	First order corrections to DIS.	139
Figure 5.9	Initial and final state gluon radiation.	139
Figure 5.10	Illustration of the factorisation scale.	145
Figure 5.11	Boson-gluon fusion in DIS.	145
Figure 6.1	n -th order term of a Wilson line.	151
Figure 6.2	A path with cusps.	155
Figure 6.3	Physical interpretation of piecewise integrals.	159
Figure 6.4	Linear Wilson line, bounded from below.	161
Figure 6.5	Linear Wilson line, bounded from above.	162
Figure 6.6	Linear Wilson line on a reversed path.	164
Figure 6.7	Linear Wilson line, fully infinite.	175

Figure 6.8	An incoming quark radiating two soft gluons.	191
Figure 6.9	A quark radiating n soft gluons.	192
Figure 6.10	Eikonal quark.	193
Figure 7.1	Contour for Wick rotation.	212
Figure 7.2	Pole of Wilson propagator.	214
Figure 7.3	Contour for Wick rotation with extra poles.	215
Figure 7.4	Contour for second Wick rotation in LC coordinates.	218
Figure 8.1	Gauge invariant quark correlator.	234
Figure 8.2	A first order correction to the PDF.	235
Figure 8.3	Boson-gluon fusion in DIS.	236
Figure 8.4	Kinematics of electron-proton SIDIS.	238
Figure 8.5	Kinematics of SIDIS.	239
Figure 8.6	Hadronic tensor in SIDIS.	242
Figure 8.7	TMD Wilson line structure.	245
Figure 8.8	FF Wilson line and Wilson lines in DY.	247
Figure 8.9	Wilson lines in DY.	248
Figure 8.10	Soft factor in TMDs.	249
Figure 8.11	Factorisation in SIDIS.	250
Figure 9.1	Typical ladder diagram.	255
Figure 9.2	DGLAP Evolution.	257
Figure 9.3	BFKL Evolution.	259
Figure 9.4	QCD evolution roadmap.	260
Figure 9.5	Dipole picture.	262
Figure 9.6	BFKL evolution in the dipole picture.	264
Figure 9.7	Quadratic terms in population statistics.	265
Figure 9.8	Plot of the GBW dipole cross section.	267
Figure 9.9	Definition of E_T flow.	268
Figure 9.10	Plots of E_T in the GBW model at different Q^2 .	273
Figure 10.1	Wilson loop with one cusp.	286
Figure 11.1	Duality between SYM and Wilson loops.	292
Figure 11.2	Rectangular LC Wilson loop.	298
Figure 11.3	Rectangular light-like loop at LO.	299
Figure 11.4	Hidden cusp in TMD.	304

ACRONYMS

- 1PI** one-particle irreducible
- BFKL** Balitsky-Fadin-Kuraev-Lipatov
- BK** Balitsky-Kovchegov
- CCFM** Catani-Ciafaloni-Fiorani-Marchesini
- CERN** Conseil Européen pour la Recherche Nucléaire
now *European Organisation for Nuclear Research*
- CKM** Cabibbo-Kobayashi-Maskawa
- COM** centre-of-mass
- CS** Collins-Soper
- DGLAP** Dokshitzer-Gribov-Lipatov-Altarelli-Parisi
- DIS** deep inelastic scattering
- DLLA** double leading-logarithm approximation
- D.O.F.** degree of freedom
- DVCS** deeply virtual Compton scattering
- DY** Drell-Yan
- ELEM** Euler-Lagrange equation of motion
- EPA** electron-positron annihilation
- FF** fragmentation function

- FPM free parton model
- GBW Golec-Biernat Wüsthoff
- GPD generalised parton density function
- HERA Hadron-Electron Ring Accelerator (at DESY)
- IR infra-red
- LC light-cone
- LEP Large Electron Positron Collider (at CERN)
- LHC Large Hadron Collider (at CERN)
- L.H.S. left-hand-side (of an equation)
- LIPS Lorentz-invariant phase space
- LO leading order
- LSZ Lehmann-Symanzik-Zimmermann
- MM Makeenko-Migdal
- MS minimal subtraction renormalisation scheme
- $\overline{\text{MS}}$ modified minimal subtraction renormalisation scheme
- MNS Maki-Nakagawa-Sakata
- NLO next-to-leading order
- NNLO next-to-next-to-leading order
- N^3LO next-to-next-to-next-to-leading order
- OPERA Oscillation Project with Emulsion-tRacking Apparatus (at CERN)
- PDF parton density function *or* parton distribution function
- PM parton model
- PQCD perturbative QCD
- QCD quantum chromodynamics
- QED quantum electrodynamics

QFT quantum field theory
 QM quantum mechanics
 RGE renormalisation-group equation
 R.H.S. right-hand-side (of an equation)
 SIDIS semi-inclusive deeply inelastic scattering
 SM Standard Model
 SYM super Yang-Mills
 TMD transverse momentum density *or* transverse momentum dependent PDF
 UV ultra-violet
 v.e.v. vacuum expectation value
 YM Yang-Mills

LIST OF IMPORTANT EQUATIONS

Chapter 1.	Euler-Lagrange Equations of Motion.	6
	Noether Current.	15
	Variational Derivative.	24
	Local Noether Current.	26
	Local Noether Tensor.	26
Chapter 2.	Parallel Transporter.	35
	Non-Abelian Vector Transformation.	36
	Covariant Derivative.	36
	Yang-Mills $\mathfrak{su}(n)$ Lagrangian.	44
	Yang-Mills Gauge Content.	44
	Local Gauge Transformations.	44

Chapter 3.	Path Integral.	50	
	Gaussian Path Integral.	52	
	Completing the Square in a Path Integral.	54	
	Functional Derivative.	55	
	n -point Gaussian Path Integral.	57	
	Complex Gaussian Path Integral.	58	
	Klein-Gordon Propagator Equation.	61	
	Feynman Scalar Propagator.	61	
	Feynman Propagator as Path Integrals.	64	
	Momentum Feynman Rules for Scalar Fields.	71	
	Gaussian Path Integral over Grassmanian Fields.	74	
	Completing the square with Grassmanian Fields.	74	
	Dirac Propagator Equation.	75	
	Dirac Feynman Propagator.	75	
	Momentum Feynman Rules for the Dirac Field.	79	
	Vector Propagator Equation.	83	
	Vector Feynman Propagator.	83	
	Feynman Ghost Propagator.	86	
	Vector Feynman Propagator in Axial Gauge.	87	
Chapter 4.	Cut-Off Regularisation.	92	
	Dimensional Regularisation.	95	
	General Result for Dimensional Regularisation.	96	
	Mass Dimension.	100	
	Gluon Propagator with a Fermion Loop.	103	
	LSZ Reduction Formula.	105	
	Cross Section.	105	
	$\overline{\text{MS}}$ Subtraction.	111	
	Counterterms.	113	
	Callan-Symanzik Equation.	116	
	Renormalisation Group Equations.	116	
	Running Coupling.	117	
Chapter 5.	Orthonormal Basis Vectors.	130	
	Transversal Tensors.	130	
	Physical Vectors in Orthonormal Basis.	130	
	Factorisation in the PM.	136	
	Collinear Factorisation.	147	
	DGLAP Evolution.	147	
	Splitting Functions.	147	
Chapter 6.	Properties of Wilson Lines.	151	
	Piecewise Path Ordered Integrals.	157	
	Feynman Rules for Linear Wilson Lines.	161	

	Schematic Representation of Wilson Line Segments.	165
	Mirror Relation for Hermitian Conjugate Line.	166
	Eikonal Identity.	168
	Finite Wilson Line.	170
	Extra Feynman Rule for Infinite Line.	175
	Feynman Rule in External Momentum Space.	181
	Feynman Rule in Partial External Momentum Space.	182
	Wilson Line With Blob but Without Colour.	186
	Eikonal Quark.	193
Chapter 7.	Calculation of Colour Factors.	198
	Traces of Adjoint Generators.	202
	2-Gluon Self-Interaction Blob.	205
	3-Gluon Self-Interaction Blob.	209
	Wick Rotation with Wilson Propagator.	216
	Wick Rotation in LC-Coordinates.	218
	2-Gluon Blob Connecting 2 On-LC Segments.	223
	2-Gluon Blob Connecting 2 Off-LC Segments.	226
	2-Gluon Blob Connecting an Off-LC Segment to an On-LC Segment.	228
Chapter 8.	Hadron Tensor and Quark Correlator.	231
	Gauge Invariant Quark Correlator.	233
	Unpolarised Collinear Quark PDF.	236
	Unpolarised Collinear Gluon PDF.	237
	Quark Correlator and Quark Fragmentator.	243
	Factorisation in SIDIS.	244
	Gauge Invariant TMD Quark Correlator.	246
	Factorisation in SIDIS.	249
	CS Evolution Equations for TMDs and FFs.	251
	CS Renormalisation Group Equation.	251
Chapter 9.	Gluon Distribution at Small- x .	257
	BFKL Equation.	258
	Dipole BFKL Equation.	263
	Dipole BK Equation.	263
	GBW Model.	266
Chapter 10.	Matrix-Field Propagator.	277
	3-Matrix Vertex.	280
	4-Matrix Vertex.	281
	Gauge-Invariant Wilson loop.	284
	Cusp Anomalous Dimension.	287
	Cusp Anomalous Dimension at One Loop.	289
	On-LC Cusp Anomalous Dimension.	289

	On-LC Cusp Anomalous Dimension at One Loop.	290
	On-LC Cusp Anomalous Dimension at Two Loop.	290
Chapter 11.	Makeenko-Migdal Equation.	295
	Logarithmic Area Derivative.	301
	Geometric Evolution of On-LC Planar Loop.	301
	Geometric Evolution for TMD.	305

Part I

INTRODUCTION TO QFT AND QCD

SYMMETRIES IN QUANTUM FIELD THEORIES

Before we tackle more advanced concepts and delve into the core of this thesis, we need to review some basic knowledge of quantum field theories (QFTs) and QCD, which is what the following five chapters are devoted to. Our approach will be a bit different from the common way to do this, because we like to stress the naturalness and elegance of a QFT. In this chapter, we almost purely deal with the field aspect of QFTs, treating them as classical fields and keeping quantisation for Chapter 3. The main topic of interest is Noether's theorem, which describes the deep relation between the symmetries of a theory and its conserved quantities.

Assuming that the reader already is acquainted with quantum field theories to a basic level, we will try to avoid too much details and sketch the main lines instead. There are many excellent introductory books to this subject, see e.g. [18–22] for a more profound treatment.

1.1 CLASSICAL FIELD THEORY

Let us start by constructing the essential tools to work with QFTs. While in quantum mechanics (QM) everything was built around the Hamiltonian, and basic physical quantities were represented by 3-vectors, in QFT the basic object will be the Lagrangian and physical quantities will be represented in a Lorentz-covariant way, by 4-vectors.

The fundamental variables in QFT are *fields*, defined in function of spacetime coordinates x^μ . After quantisation, excitations of these fields will be identified as particles (see Chapter 3). A field is a function in a Hilbert space that is quadratically integrable, i.e. for two fields ϕ_a and ϕ_b , the integral

$$\int_{-\infty}^{+\infty} d^4x \phi_b^*(x) \phi_a(x)$$

has to be finite. The most important practical consequence is that any field has to vanish at $\pm\infty$ in each of its coordinates.¹

We consider a system that is fully described by a set of n fields $\{\phi_i\}$. We don't specify the nature of the fields, they can be of any form including scalar, spinor or vector fields. Non-scalar fields can be expressed in function of their components—scalar quantities on their own—so that the full system only contains scalar fields or scalar field components (e.g. two vector fields form a set of 8 field components). Any obtained results will hence be applicable to spinor and vector fields as well.

The cornerstone in any field theory is the action S , the time integral of the Lagrangian L . To represent the latter in a Lorentz-covariant way, we define the *Lagrangian density* \mathcal{L} as the spatial extension of the Lagrangian, depending on the set of fields $\{\phi_i\}$, their derivatives $\{\partial_\mu\phi_i\}$, and possibly directly on the spacetime coordinates x^μ :

$$L(t) = \int d^3\mathbf{x} \mathcal{L}(x, \phi_i, \partial_\mu\phi_i). \quad (1.1)$$

The action is simply the integral of the Lagrangian density over the position four-vector:

$$S = \int d^4x \mathcal{L}(x, \phi_i, \partial_\mu\phi_i). \quad (1.2)$$

Since for the remainder of this thesis we will only work with the Lagrangian density, we will simply refer to it as the Lagrangian.

Equations of Motion

What really characterises a Lagrangian, is its behaviour—or more generally the action's behaviour—under specific transformations, be it transformations acting on the coordinates, or transformations acting on the fields. The Newtonian *principle of least action* states that, for a transition between two states, nature will always select the path that minimises the action. Transformations leaving the action invariant, commonly called *symmetries*, are hence favoured. Translated to fields, the least action principle tells us that the requirement of invariance

¹ It is possible to relax this requirement by a proper modification of the theory. In fact, e.g. in axial gauges (like the light-cone gauge) it is impossible to let the field vanish at *both* boundaries in x^0 . The technicalities of this adaptation are beyond the scope of this thesis, and whenever working in axial gauges, we will treat the fields as well-behaving.

of the action will lead to a set of equations describing the motion of the fields. Mathematically, this invariance is expressed as

$$\delta S = S' - S \equiv 0. \quad (1.3)$$

The variation of the action is of course fully determined by the variation of the Lagrangian, but we cannot simply integrate over $\delta\mathcal{L}$,

$$\delta S \neq \int d^4x \delta\mathcal{L},$$

because the integration measure d^4x and the integration region Ω transform as well:

$$\delta S = \int_{\Omega'} d^4x' \mathcal{L}(x'^{\mu}, \phi'_i(x'), \partial_{\mu}\phi'_i(x')) - \int_{\Omega} d^4x \mathcal{L}(x^{\mu}, \phi_i(x), \partial_{\mu}\phi_i(x)).$$

Because in the first integral x' is just a dummy variable, we can rename it x :

$$\delta S = \int_{\Omega'} d^4x \mathcal{L}(x^{\mu}, \phi'_i(x), \partial_{\mu}\phi'_i(x)) - \int_{\Omega} d^4x \mathcal{L}(x^{\mu}, \phi_i(x), \partial_{\mu}\phi_i(x)),$$

but the integration regions remain different. It can be shown (see e.g. [23]) that up to first order:

$$\int_{\Omega+\delta\Omega} d^4x \mathcal{L}(x) = \int_{\Omega} d^4x \partial_{\mu}(\delta x^{\mu}\mathcal{L}),$$

such that we can write

$$\delta S = \int_{\Omega} d^4x \left[\mathcal{L}(x^{\mu}, \phi'_i(x), \partial_{\mu}\phi'_i(x)) - \mathcal{L}(x^{\mu}, \phi_i(x), \partial_{\mu}\phi_i(x)) + \partial_{\mu}(\delta x^{\mu}\mathcal{L}) \right].$$

Note that the difference between the two Lagrangians acts only on the *form* of the fields, not on their arguments. Ignoring for a moment the last term, we can thus write

$$\delta\mathcal{L} = \frac{\partial\mathcal{L}}{\partial\phi_i} \Delta\phi_i + \frac{\partial\mathcal{L}}{\partial\partial_{\mu}\phi_i} \partial_{\mu}\Delta\phi_i,$$

where the transformation only acts on the field structure itself, not on x :

$$\Delta\phi_i(x) = \phi'_i(x) - \phi_i(x). \quad (1.4)$$

There is a small subtlety here. If we would literally follow the variational chain rule, the second term of $\delta\mathcal{L}$ would be linear in $\Delta\partial_\mu\phi_i$. This is not the same as what we wrote, because the variation operator acts on the derivative as well, i.e. $\Delta\partial_\mu\phi_i = \partial_\mu\Delta\phi_i + \text{corrections}$. However, we restrict ourselves to transformations of the field ϕ_i , avoiding transformations that would act on the derivative field separately. Every transformation of the form

$$\phi_i(x) \rightarrow \phi_i'(x) = \phi_i(x) + \Delta\phi_i(x),$$

will induce a variation in the derivative field literally of the form $\partial_\mu\Delta\phi_i$, hence we can drop the correction terms. See e.g. [23–25] for a mathematical proof of this statement. The variation of the action now simplifies into

$$\delta S = \int_{\Omega} d^4x \left[\frac{\partial\mathcal{L}}{\partial\phi_i} \Delta\phi_i + \frac{\partial\mathcal{L}}{\partial\partial_\mu\phi_i} \partial_\mu\Delta\phi_i + \partial_\mu(\mathcal{L}\delta x^\mu) \right]$$

Using Leibniz' rule, we can collect terms linear in $\Delta\phi_i$, and write what remains as a divergence of some quantity \mathcal{J}^μ . We will collect the transformation of the integration region in $\delta\mathcal{L}$:

$$\delta\mathcal{L} = \left(\frac{\partial\mathcal{L}}{\partial\phi_i} - \partial_\mu \frac{\partial\mathcal{L}}{\partial\partial_\mu\phi_i} \right) \Delta\phi_i + \partial_\mu \mathcal{J}^\mu. \quad (1.5)$$

\mathcal{J}^μ is the so-called *Noether current*:²

$$\mathcal{J}^\mu = \frac{\partial\mathcal{L}}{\partial\partial_\mu\phi_i} \Delta\phi_i + \mathcal{L}\delta x^\mu, \quad (1.6)$$

named after Emmy Noether. We will see in [Section 1.2](#) that it is a key concept when exploring the effect of the action's symmetries. By absorbing the transformation of the integral into $\delta\mathcal{L}$, we can now simply integrate over it:

$$\begin{aligned} \delta S &= \int d^4x \delta\mathcal{L}, \\ &= \int d^4x \left[\left(\frac{\partial\mathcal{L}}{\partial\phi_i} - \partial_\mu \frac{\partial\mathcal{L}}{\partial\partial_\mu\phi_i} \right) \Delta\phi_i + \partial_\mu \mathcal{J}^\mu \right], \\ &= \int d^4x \left(\frac{\partial\mathcal{L}}{\partial\phi_i} - \partial_\mu \frac{\partial\mathcal{L}}{\partial\partial_\mu\phi_i} \right) \Delta\phi_i. \end{aligned} \quad (1.7)$$

² See e.g. [25].

where we were allowed to drop the term $\partial_\mu \mathcal{J}^\mu$ because all fields in the Lagrangian are supposed to be well-behaving, and thus have to vanish at $\pm\infty$. Equation 1.7 holds for arbitrary $\Delta\phi_i$, implying that the integrand must be zero if we want to satisfy the condition $\delta S \equiv 0$. This gives rise to the famous classical *Euler-Lagrange equations of motion (ELEM)s*:

Euler-Lagrange Equations of Motion

$$\partial_\mu \left(\frac{\partial \mathcal{L}}{\partial \partial_\mu \phi_i} \right) \equiv \frac{\partial \mathcal{L}}{\partial \phi_i}, \quad (1.8)$$

which will be of great use when dealing with specific types of fields.

Characteristics of the Lagrangian

In any Lagrangian, we can classify the possible terms that it contains into three categories. These are kinetic terms, mass terms, and interaction terms. The first two are terms that are quadratic in the fields, while the latter can be any combination of fields.

Kinetic and mass terms describe the behaviour of the field when free of interaction with other fields. Kinetic terms are built from two fields of the same type and describe the *dynamics* of this field. After quantisation, they will give rise to the *propagator*, which is the amplitude of the field to go from one state to another. The dynamical structure of the kinetic terms requires the presence of field derivatives. On the other hand, mass terms are built from two fields of the same type as well, but describe the *statics* of this field. After quantisation, they will give rise to a constant factor in the propagator, viz. the mass. One could interpret the mass as the constant of proportionality at which the field struggles with itself when moving.³

It should be noted that the requirement of quadratic terms to be of the same type can be relaxed, i.e. it is possible for so-called *mixing* to occur. Mixing of kinetic terms would imply one type of field to dynamically create its propagation by the aid of another type of field. This would mean that the first field would dynamically transform in the second while propagating. Example theories where kinetic mixing is allowed include most supersymmetric and supergravity theor-

³ Recently, evidence from the LHC at CERN has proven the existence of a new kind of particle, the Brout-Englert-Higgs particle. This is a scalar field excitation, and as such can acquire a non-zero vacuum expectation value (v.e.v.). By interacting with other fields it passes this v.e.v. as a mass term. So in the Standard Model (SM), any mass term isn't interpreted as a struggle of a field with itself, but as a struggle of a field with the Higgs field.

ies, where the fields inside the kinetic terms are multiplied with a so-called Kähler metric tensor. To some extent, the recently discovered neutrino oscillation at OPERA could also be interpreted as a mixing of kinetic terms.⁴

A mixing of mass terms is more common, as it simply implies that mass eigenstates and flavour eigenstates don't coincide. After orthogonalisation, it is possible to recover mass terms that are expressed diagonally in the fields. However, this immediately implies that interaction terms are no longer diagonal in flavour, i.e. the process under consideration won't conserve flavour. The paramount example is that of quarks in the weak interaction, where interactions between different quarks can mix with proportionality factors given by the CKM matrix.

The last possible type of terms in the Lagrangian, interaction terms, are built from at least three fields that can, but don't have to, be of the same type. Terms built from a single field aren't allowed in the Lagrangian (unless for real scalar fields). If our theory has to be renormalisable (see Section 4.1), a maximum of four bosonic fields, or two fermionic fields and one bosonic field is imposed, by arguments of Mass Dimension analysis (see 96). Interaction terms tell us how the different fields couple to each other by giving the correct constant of proportionality. If no interaction terms between two fields are present, they simply don't interact with each other (as is the case with e.g. leptons and gluons).

It is not a necessary condition for a field to have quadratic terms in the Lagrangian. But any field that lacks these, automatically lacks a dynamic description. Such a field is thus necessarily an *external* field, for which the dynamics are defined outside of the system under consideration.⁵ As we will deal in this thesis exclusively with Lagrangians describing systems at a global scale, we won't treat external fields.

-
- ⁴ But for small distances, the mixing parameters are extremely small as compared to the non-mixing parameters, making the mixing undetectable at standard collision experiments. For this reason, one prefers to write down the neutrino Lagrangian without mixed kinetic terms, preferring to interpret the oscillation as a mixed long-distance evolution of quantum states. Also, the quantisation procedure puts the constraint that mixing can only occur for neutrinos that are not massless. This constrained can be relaxed in e.g. supersymmetric theories.
- ⁵ It is technically possible that a field has only mass terms without dynamics. Such a field is called an auxiliary field, and is unphysical, as it can be removed from the Lagrangian by filling in its ELEMs (Equation 1.8). This will lead to extra mass or interaction terms for the other fields.

Scalar Fields

Let us now investigate an example of possible field terms in the Lagrangian. We start with a real scalar field, which has no components and thus no substructure. From classical mechanics, it is known to have the Lagrangian

$$\mathcal{L}_0^{\text{scalar}} = \frac{1}{2} \partial_\mu \phi \partial^\mu \phi - \frac{1}{2} m^2 \phi^2. \quad (1.9)$$

We can interpret the first term as the energy cost of moving the field in spacetime, and the second term as the energy cost for the field simply to exist. Using the [ELEM](#)s that we derived in [Equation 1.8](#), we construct the so-called Klein-Gordon equations:

$$(\square + m^2) \phi \equiv 0 \quad (1.10)$$

The square is a common notation to denote the fully contracted second derivative, i.e. $\square = \partial_\mu \partial^\mu$. Note that scaling both the kinetic and the mass terms in the Lagrangian with the same factor won't change the Klein-Gordon equation. The factor $1/2$ is chosen to be consistent with common literature.⁶ In the case of a complex scalar field, the Lagrangian is normally expressed without this factor in front:⁷

$$\mathcal{L}_0^{\text{scalar}} = \partial_\mu \phi \partial^\mu \phi^* - m^2 |\phi|^2. \quad (1.11)$$

As a complex field, it exists of two independent fields, namely its real and imaginary parts, but most of the time we prefer to express it in function of the field and its complex conjugate. Now there are two Klein-Gordon equations, one for each field:

$$(\square + m^2) \phi \equiv 0 \quad (1.12a)$$

$$(\square + m^2) \phi^* \equiv 0 \quad (1.12b)$$

The Lagrangian $\mathcal{L}_0^{\text{scalar}}$ describes the free field,⁸ without interactions. We can add for instance a four-field interaction term as follows (going back to a real scalar field):

$$\mathcal{L}^{\text{scalar}} = \frac{1}{2} \partial_\mu \phi \partial^\mu \phi - \frac{1}{2} m^2 \phi^2 - \frac{1}{4!} \lambda \phi^4. \quad (1.13)$$

⁶ It is commonly chosen to be $1/2$ in order to have a propagator without coefficients in front.

⁷ For the same reason as above.

⁸ We will always use the label 0 to indicate a free field theory.

Then the Klein-Gordon equation is no longer homogeneous, but gains a source term:

$$(\square + m^2) \phi \equiv -\frac{1}{3!} \lambda \phi^3. \quad (1.14)$$

The important observation is that the free fields, obeying [Equation 1.10](#), can be expanded as a Fourier series and quantised accordingly (in the canonical quantisation framework), or can be evaluated as Gaussian path integrals (in the path integral framework). This is not possible for the interacting fields, obeying [Equation 1.14](#). Instead one has to separate out the interaction part from the Lagrangian, quantise the free field, and treat the interaction as *perturbations* on the free field. See [Chapter 3](#) for more details.

Vector Fields

Another example to investigate is the Lagrangian for vector fields. A vector field will commonly be associated with a force field, like the electromagnetic force, as we will discover later on. Both a scalar field and a vector field represent particles with integer spin, i.e. they are *bosonic* fields. We therefore expect the Lagrangian of a vector field to be of the same form of the one of a scalar field. For a real vector field A_μ , we naively write

$$\mathcal{L}_0^{\text{vector}} \stackrel{?}{=} \frac{1}{2} \partial_\mu A_\nu \partial^\mu A^\nu - \frac{1}{2} m^2 A_\mu A^\mu,$$

where we also contracted the ν index on the field in the kinetic term, because the Lagrangian has to be a scalar, and hence cannot have any open indices left. But there is another contraction possible, namely doing

$$\partial_\mu A_\nu \partial^\nu A^\mu.$$

We add this term to the Lagrangian with the same factor in front, but with an opposite sign

$$\mathcal{L}_0^{\text{vector}} \stackrel{?}{=} \frac{1}{2} \partial_\mu A_\nu \partial^\mu A^\nu - \frac{1}{2} \partial_\mu A_\nu \partial^\nu A^\mu - \frac{1}{2} m^2 A_\mu A^\mu.$$

The reason for the opposite sign is to be in accordance with classical electrodynamics, where the electromagnetic field tensor is defined as

$$F_{\mu\nu} = \partial_\mu A_\nu - \partial_\nu A_\mu. \quad (1.15)$$

Indeed, we can rewrite this Lagrangian as

$$\mathcal{L}_0^{\text{vector}} \stackrel{?}{=} \frac{1}{4} F_{\mu\nu} F^{\mu\nu} - \frac{1}{2} m^2 A_\mu A^\mu.$$

In [Chapter 2](#), we will demonstrate why the factor $\partial_\mu A_\nu \partial^\nu A^\mu$ has to have an opposite sign, motivated by geometric arguments. There are two more remarks however. The first one is a really important remark. As we will see in the next section, any theory that is supposed to represent a realistic quantum system, is required to be invariant under local phase rotations. It can easily be shown (see [44](#)) that a vector mass isn't invariant under such a rotation, so we drop this term. The second remark is just a matter of convention, as it is common to define the kinetic field term with a minus sign in front.⁹ So we finally have a realistic free-field vector Lagrangian:

$$\mathcal{L}_0^{\text{vector}} = -\frac{1}{4} F_{\mu\nu} F^{\mu\nu}. \quad (1.16)$$

Again using [Equation 1.8](#), we can construct the ELEM for A_μ :

$$\partial_\mu F^{\mu\nu} = (g^{\mu\nu} \square - \partial^\mu \partial^\nu) A_\nu \equiv 0. \quad (1.17)$$

But this equation cannot be solved, as it is represented by a singular (and hence non-invertible) matrix. The difficulty resides in the fact that this problem already arises at the level of the free vector field, leaving us no clue how to continue. However, there is one key property of the vector field A_μ that we overlooked: it is *over-determined*. As a spin-1 field, it has exactly three independent degrees of freedom (d.o.f.s). But the Lorentz index μ runs over all four dimensions of spacetime, giving us one d.o.f. too many. We can remove one d.o.f. by enforcing a constraint equation on A_μ . This is called “*gauging away one d.o.f.*”, or simply “*choosing a gauge*”. Two common examples are:

A. The Lorentz gauge: $\partial_\mu A^\mu \equiv 0,$ (1.18a)

B. The axial gauge: $n_\mu A^\mu \equiv 0,$ (1.18b)

where n_μ is any constant directional vector. Using the Lorentz gauge drops the second term in [Equation 1.17](#), restoring the Klein-Gordon equation:

$$\square A_\mu = 0,$$

⁹ Note the important difference: the minus sign in front of $F^{\mu\nu}$ is merely a scale factor of the Lagrangian. But the minus *inside* $F^{\mu\nu}$, as in [Equation 1.15](#), defines the dynamics of the system. Changing the latter, changes the theory, and we need it to be a minus sign to reproduce the realistic electromagnetic interaction.

which we know is quantisable. Using the axial gauge gives quantisable results as well, this is however less straightforward to reveal. Because of this, vector fields are often called *gauge fields*, and a theory containing them is called a *gauge theory* (especially when the theory is invariant under local transformations, see further).

There are several possible interaction terms to add to the Lagrangian, but the most straightforward is to contract one A_μ with an external current vector \mathcal{J}^μ :

$$\mathcal{L}^{\text{vector}} = -\frac{1}{4}F_{\mu\nu}F^{\mu\nu} - \mathcal{J}^\mu A_\mu. \quad (1.19)$$

Just as in the case of a scalar field, this renders the [ELEM](#) inhomogeneous:

$$\partial_\mu F^{\mu\nu} = \mathcal{J}^\nu, \quad (1.20)$$

such that after choosing a gauge we will continue with the quantisation of the free field, and treat the interaction as perturbations on the free field. If the current is a scalar quantity, the interaction term contains two vector fields:

$$\mathcal{L}^{\text{vector}} = -\frac{1}{4}F_{\mu\nu}F^{\mu\nu} - \mathcal{J} A_\mu A^\mu.$$

Self-interactions of the vector field are possible as well, made with terms of three or four vector fields, but for this we need to collect several vector fields into one multiplet. We will illustrate this in [Section 1.4](#).

Spinor Fields

The last example that is relevant for this thesis, is the Lagrangian for spinor fields. We know for sure that we cannot blindly use the Klein-Gordon Lagrangian for these, as they represent particles of half-integer spin, i.e. they are *fermionic* fields. These fields will be associated with *matter* (in contrast with vector fields, that are associated with forces).

Because matter particles have half-integer spin, it follows from the Pauli-exclusion principle that spinor fields anticommute:

$$\psi(x)\psi(y) = -\psi(y)\psi(x),$$

from which we automatically deduce that the square of a spinor field is zero:

$$\psi(x)\psi(x) \equiv 0. \quad (1.21)$$

From classical quantum mechanics, we know that the Dirac equation for a fermion field ψ is given by (see [Equation A.20](#)):

$$(i\cancel{\partial} - m)\psi = 0, \quad (1.22)$$

where ψ is a complex valued spinor field, and $\cancel{\partial}$ is the contraction of the derivative with a gamma matrix:

$$\cancel{\partial} = \gamma^\mu \partial_\mu. \quad (1.23)$$

A first attempt to construct a Lagrangian that reproduces [Equation 1.22](#) is

$$\mathcal{L}_0^{\text{Dirac}} \stackrel{?}{=} \bar{\psi} (i\cancel{\partial} - m) \psi.$$

However, this cannot be right, as here the mass term would be zero by definition, using [Equation 1.21](#). We thus need a second, independent field, which we will choose to be the hermitian conjugate of ψ . From symmetry considerations concerning the gamma matrices, we add a γ^0 . The conjugate field, of which the excitation will be identified with an antiparticle, is then defined as $\bar{\psi} = \psi^\dagger \gamma^0$, and obeys a slightly modified Dirac equation ([Equation A.23](#)). See [Appendix A.3](#) and [18] for more on Dirac spinors and gamma matrices. It is now not difficult to check that the Dirac equations are the [ELEM](#)s ([Equation 1.8](#)) for the following Lagrangian:

$$\mathcal{L}_0^{\text{Dirac}} = \bar{\psi} (i\cancel{\partial} - m) \psi. \quad (1.24)$$

A possible interaction term can be introduced by using the Dirac fields as a current for [Equation 1.19](#), i.e.

$$\mathcal{J}^\mu = g \bar{\psi} \gamma^\mu \psi,$$

where we added a dimensionless constant g . The resulting Lagrangian is exactly the Lagrangian for quantum electrodynamics ([QED](#)), describing the electromagnetic force:

$$\mathcal{L}^{\text{QED}} = \bar{\psi} (i\cancel{\partial} - m) \psi + g \bar{\psi} \cancel{A} \psi - \frac{1}{4} F_{\mu\nu} F^{\mu\nu}, \quad (1.25)$$

where the slashed notation is used as before, i.e. $\cancel{A} \stackrel{\text{N}}{=} A_\mu \gamma^\mu$.

1.2 SYMMETRIES OF THE LAGRANGIAN

Let us now investigate how the symmetries of a theory influence the quantities within. This will eventually lead us to Noether's famous theorem, that states that every symmetry can be associated with a conserved current and charge.

Any transformation can be parameterised in function of its effect on the spacetime coordinates and on the fields:

$$x^\mu \rightarrow x^\mu + \delta x^\mu, \quad (1.26a)$$

$$\phi_i \rightarrow \phi_i + \delta \phi_i. \quad (1.26b)$$

The two transformations are not independent, as a coordinate transformation will also manifest itself as a field transformation:

$$\phi_i(x) \rightarrow \phi_i(x + \delta x) \approx \phi_i(x) + \delta x^\mu \partial_\mu \phi_i(x).$$

Let us add some notational clarity. When writing $\Delta \phi_i$, we refer to a transformation that only affects the *form* of the field:

$$\Delta \phi_i = \phi'_i(x) - \phi_i(x),$$

while $\delta \phi_i$ is the full transformation, including the effect from the coordinate transform:

$$\delta \phi_i = \phi'_i(x') - \phi_i(x).$$

In other words, we have (up to first order):

$$\delta \phi_i = \Delta \phi_i + \delta x^\mu \partial_\mu \phi_i(x). \quad (1.27)$$

Because we absorbed the transformation of the integration parameters into the variation of \mathcal{L} , the variation of the action is easily recovered:

$$\delta S = \int d^4x \delta \mathcal{L}, \quad (1.28)$$

where the variation of the Lagrangian is, because of [Equation 1.5](#), simply the divergence of the Noether current as defined in [Equation 1.6](#):

$$\delta \mathcal{L} = \partial_\mu \mathcal{J}^\mu. \quad (1.29)$$

To satisfy the requirement $\delta S \equiv 0$, we see that $\delta \mathcal{L}$ has to vanish as well, or can be at most a divergence of any four-vector K^μ , i.e.

$$\delta \mathcal{L} \equiv \partial_\mu K^\mu \quad (1.30)$$

leaves the action invariant. By subtracting K^μ from the current and using Equation 1.27 to remove $\Delta\phi_i$,

$$\mathcal{J}^\mu = \frac{\partial \mathcal{L}}{\partial \partial_\mu \phi_i} \delta\phi_i - \left(\frac{\partial \mathcal{L}}{\partial \partial_\mu \phi_i} \partial_\nu \phi_i - \mathcal{L} \delta_\nu^\mu \right) \delta x^\nu - K^\mu, \quad (1.31)$$

we have constructed a conserved current, i.e.

$$\partial_\mu \mathcal{J}^\mu = 0. \quad (1.32)$$

The approach is as follows: we start with a certain transformation, and apply it to the Lagrangian. If this transformation leaves the Lagrangian invariant, or if it leaves the Lagrangian invariant up to a divergence, we know that the Noether current in Equation 1.31 will be conserved.

Also, for every conserved current there is an associated charge

$$Q(t) = \int d^3 \mathbf{x} \mathcal{J}^0, \quad (1.33)$$

which is conserved as well:

$$\dot{Q} = \int d^3 \mathbf{x} \partial_\mu \mathcal{J}^\mu + \int d^3 \mathbf{x} \partial \cdot \mathcal{J} = 0. \quad (1.34)$$

The first term vanishes by current conservation, and the second by use of Gauss' divergence theorem and assuming the fields vanish at $\pm\infty$.

We have now all necessary ingredients to present Noether's first theorem.

NOETHER'S FIRST THEOREM: Each continuous symmetry transformation that leaves the Lagrangian invariant up to a divergence is associated with a conserved current as defined in Equation 1.31. The spatial integral over this current's zeroth component yields a conserved charge, as given in Equation 1.33.

It is important that the symmetries have to be continuous symmetries, because this guarantees that we can start from infinitesimal variations and exponentiate the result. E.g. we can start with an small translation to describe a macroscopic shift. But for instance inversion symmetry in three dimensions (parity) is not a continuous symmetry, so we cannot apply Noether's theorem on it.

We can explore and simplify the theorem further, by parameterising the transformations in [Equations 1.26](#) in function of a set of infinitesimal parameters ϵ_r ($r = 1 \dots R$):

$$\delta x^\mu = \epsilon_r X_r^\mu, \quad (1.35a)$$

$$\delta \phi_i = \epsilon_r \Phi_{ir}, \quad (1.35b)$$

$$K^\mu = \epsilon_r K_r^\mu. \quad (1.35c)$$

The functions X_r^μ and Φ_{ir} can depend on the other coordinates resp. fields, thus allowing transformations to mix coordinates resp. fields. If we plug these parameterisations in the Noether current, we can extract the common parameter ϵ_r and define a Noether current per component of the symmetry:

Noether Current

$$\mathcal{J}_r^\mu = \frac{\partial \mathcal{L}}{\partial \partial_\mu \phi_i} \Phi_{ir} - \left(\frac{\partial \mathcal{L}}{\partial \partial_\mu \phi_i} \partial_\nu \phi_i - \mathcal{L} \delta_\nu^\mu \right) X_r^\nu - K_r^\mu. \quad (1.36)$$

These currents will be independently conserved for each symmetry component r . Note that the expression between parentheses is simply the *stress-energy tensor*:

$$T^\mu_\nu = \frac{\partial \mathcal{L}}{\partial \partial_\mu \phi_i} \partial_\nu \phi_i - \mathcal{L} \delta_\nu^\mu, \quad (1.37)$$

so that we can rewrite the current as

$$\mathcal{J}_r^\mu = \frac{\partial \mathcal{L}}{\partial \partial_\mu \phi_i} \Phi_{ir} - T^\mu_\nu X_r^\nu - K_r^\mu.$$

1.3 SPACETIME SYMMETRIES

Let us first investigate how spacetime symmetries influence a theory. We are looking at any transformation of the form

$$x^\mu \rightarrow x^\mu + \delta x^\mu. \quad (1.38)$$

But these transformations don't leave the Lagrangian invariant on their own, as they propagate into the field transformations because of [Equation 1.27](#). We thus have to transform the form of the field as well, using $\Delta \phi_i$ to compensate

the effect of the coordinate transformation. We won't delve into the details here, see e.g. [26] for a good treatment.

The first spacetime symmetry we investigate is a translation, defined as

$$x^\mu \rightarrow x^\mu + a^\mu, \quad (1.39)$$

for a constant vector a^μ . The Lagrangian will be fully invariant ($K^\mu = 0$) if we let the *total* variation of the field vanish, i.e. $\delta\phi_i \equiv 0$. There are four independent symmetry components, one for each spacetime direction. It is thus natural to replace the index r with a Lorentz index ν . Using the parameterisation in [Equations 1.35](#), we identify

$$\epsilon_r \stackrel{N}{=} a^\nu, \quad X_r^\mu \stackrel{N}{=} \delta_\nu^\mu.$$

Using [Equation 1.36](#) we can construct the Noether current, which is conserved for any Lagrangian that is invariant under spacetime translations. It is a contraction of the translation parameter with the energy-momentum tensor of the field ϕ_i :

$$\mathcal{J}^\mu = -a^\nu T^\mu{}_\nu. \quad (1.40)$$

Because the conservation law states that $-a^\nu \partial_\mu T^\mu{}_\nu \equiv 0$ must hold for any a^ν , the energy-momentum tensor is conserved in all of its components separately:

$$\partial_\mu T^\mu{}_\nu \equiv 0. \quad (1.41)$$

There will be four conserved charges as well, one for each spacetime direction. The charge of the time component is the Hamiltonian

$$H = \int d^3\mathbf{x} T^{00}, \quad (1.42)$$

and the charges of the space components of $T^\mu{}_\nu$ are associated with the momentum components of the field

$$P^i = \int d^3\mathbf{x} T^{0i}. \quad (1.43)$$

This already demonstrates the power of Noether's theorem: we derived the conservation of four-momentum from first principles without specifying a Lagrangian, only requiring it to be invariant under spacetime translations! Similarly, the requirement of invariance under Lorentz transformations (rotations and boosts)

$$x^\mu \rightarrow M^\mu{}_\nu x^\nu,$$

will result in conservation of angular momentum.

1.4 GLOBAL SYMMETRIES

Now we turn our attention towards transformations that act on the form of the field only, i.e. $X_r^\mu = 0$ always. If such a transformation is a symmetry, it is called an *internal* symmetry.

We consider a set of fields that are in a representation of a Lie algebra (see [Appendix A.6](#)), i.e. they are collected into multiplets:

$$\begin{pmatrix} \phi_1(x) \\ \vdots \\ \phi_n(x) \end{pmatrix}.$$

When a field is organised as a singlet (i.e. exactly one field in the multiplet), the only possible Lie structure is a $u(1)$ algebra. Such a field is called *Abelian* and is hence a commuting field, in contrast to fields organised in multiplets that are called *non-Abelian*. The latter are inherently more difficult to work with, because of the non-commutative nature of the underlying generators.

A theory can combine several multiplets, not necessary of the same size. For simplicity we consider now one such multiplet, but the generalisation to more is easily made. A field ϕ_a in a multiplet can transform in function of all fields in the multiplet (other fields and itself). We call this a rotation of the multiplet, and write

$$\phi_i \rightarrow \phi_i + i\alpha^a (t^a)_{ij} \phi^j, \quad (1.44)$$

where the t^a are the generators of the Lie algebra (see [Equation 1.5](#)), and the α^a are constant parameters. Note that there are two different indices in use:

- A. The indices i, j, \dots are for the fields, they can be organised in multiplets of any representation. The most common choice is the fundamental representation, where $i = 1 \dots n$ for a n -dimensional Lie algebra. It is common not to write out these indices.
- B. The indices a, b, \dots are the contraction of the parameters α^a with the generators. For any representation of a $su(n)$ algebra, there are $n^2 - 1$ generators, so $a = 1 \dots n^2 - 1$. Most of the time, these indices are written out.

If the fields are complex, then the conjugate fields simply transform with a minus sign:

$$\phi_i^* \rightarrow \phi_i^* - i\alpha^a (t^a)_{ij} \phi^{*j},$$

Note that these transformations are just the infinitesimal forms of a global phase rotation:

$$\phi_i \rightarrow e^{i\alpha^a(t^a)_{ij}}\phi^j, \quad \phi_i^* \rightarrow e^{-i\alpha^a(t^a)_{ij}}\phi^{*j}. \quad (1.45)$$

It is called a *global* transformation, because it holds globally, at every spacetime point. In contrast, if α^a wouldn't be constant but depending on x , the Noether theorem has to be adapted, as we will see in the next section.

If we compare the transformation with the parameterisation in [Equations 1.35](#), we see that

$$\epsilon^a \stackrel{\text{N}}{=} \alpha^a \quad \Phi_i^a \stackrel{\text{N}}{=} i(t^a)_{ij}\phi^j.$$

Plugging these in [Equation 1.36](#), we find the Noether current for a global phase rotation for real fields:

$$\mathcal{J}_\mu^a = \frac{\partial \mathcal{L}}{\partial \partial_\mu \phi_i} i(t^a)_{ij}\phi^j. \quad (1.46)$$

Note that that the presence of Lie generators in the current make the latter a *non-commuting operator*. This has important consequence for e.g. quantisation, as in the canonical quantisation framework this fact interferes with the canonical commutation relations. For complex fields, we have the apparent choice of putting the minus sign of the conjugate field's transform in the parameter ϵ^a or in Φ_i^a . But in the definition of [Equation 1.36](#), we have extracted the same parameter ϵ^a everywhere, so we have to move the minus sign into Φ_i^a , giving the Noether current

$$\mathcal{J}_\mu^a = \frac{\partial \mathcal{L}}{\partial \partial_\mu \phi_i} i(t^a)_{ij}\phi^j - \frac{\partial \mathcal{L}}{\partial \partial_\mu \phi_i^*} i(t^a)_{ij}\phi^{*j} \quad (1.47)$$

for complex fields.

Why would invariance to phase rotations be relevant from a physical point of view? Remember that in [QM](#) the amplitude $\Psi(\mathbf{x})$ is a complex-valued field that is only a mathematical construct, while its complex square $|\Psi(\mathbf{x})|^2$ represents the probability and is a physical observable. But there is some freedom on the choice of $\Psi(\mathbf{x})$, as multiplying it with a phase factor doesn't affect the probability. I.e. the transformation $\Psi(\mathbf{x}) \rightarrow e^{i\theta}\Psi(\mathbf{x})$ leaves the probability and hence the system invariant, and will give rise to conservation laws that can be constructed by Noether's theorem.

Free Dirac Lagrangian

To investigate an easy example, take e.g. the Lagrangian for the free Dirac field as defined in [Equation 1.24](#):

$$\mathcal{L}_0^{\text{Dirac}} = \bar{\psi} (i \not{\partial} - m) \psi,$$

where now the field forms a multiplet. The fields carry both Lie indices i, j and spinor indices α, β :

$$\mathcal{L}_0^{\text{Dirac}} = \bar{\psi}_\alpha^i \left[i (\gamma^\mu)^{\alpha\beta} \partial_\mu - \delta^{\alpha\beta} m \right] \delta_{ij} \psi_\beta^j, \quad (1.48)$$

This Lagrangian is manifestly invariant under a phase rotation

$$\psi \rightarrow e^{i\alpha^a t^a} \psi. \quad (1.49)$$

There are $n^2 - 1$ conserved Noether currents (see [Equation 1.46](#)):

$$\mathcal{J}^{\mu a} = \bar{\psi} \gamma^\mu t^a \psi, \quad (1.50)$$

where we have chosen to extract $-\alpha^a$ as the parameter ϵ^a to get a positive current (but of course, this is a matter of convention). These currents are commonly known as the Dirac or *vector* currents. We can easily check that they are indeed conserved by using [Equations 1.22](#) and [A.23](#). The associated charges are

$$Q^a = \int d^3 \mathbf{x} \bar{\psi} \gamma^0 t^a \psi = \int d^3 \mathbf{x} \psi^\dagger t^a \psi, \quad (1.51)$$

because $\bar{\psi} = \psi^\dagger \gamma^0$ and $(\gamma^0)^2 = \mathbb{1}$. In case of an $u(1)$ symmetry, we can associate the charge with the number operator:

$$Q = \int \frac{d^3 \mathbf{p}}{(2\pi)^3} \sum_s \left(a_{\mathbf{p}}^{s\dagger} a_{\mathbf{p}}^s - b_{\mathbf{p}}^{s\dagger} b_{\mathbf{p}}^s \right), \quad (1.52)$$

which holds up to an infinite constant (that vanishes after renormalisation). The number operator is the baryon number (or lepton number, depending on the fields). Noether's first theorem gives us a natural proof that the baryon and lepton numbers are conserved quantities. Also note that it clearly shows that what is conserved is the *difference* between the number of particle states ($a_{\mathbf{p}}^{s\dagger} a_{\mathbf{p}}^s$) and antiparticle states ($b_{\mathbf{p}}^{s\dagger} b_{\mathbf{p}}^s$). The two separately are not invariant.

We can construct an analogous transformation, using γ^5 as defined in [Equation A.27a](#):

$$\psi \rightarrow e^{i\alpha^a t^a \gamma^5} \psi, \quad (1.53)$$

a so-called *chiral* transformation. The transformation of $\bar{\psi}$ is a bit more intricate:

$$\bar{\psi}' = \bar{\psi}' = \overline{e^{i\alpha\gamma^5}\psi} = \left(e^{i\alpha\gamma^5}\psi\right)^\dagger \gamma^0 = \psi^\dagger e^{-i\alpha\gamma^5} \gamma^0 = -\psi^\dagger \gamma^0 e^{-i\alpha\gamma^5} = -\bar{\psi} e^{-i\alpha\gamma^5},$$

where the minus sign in front emerges because $\gamma^\mu \gamma^5 = -\gamma^5 \gamma^\mu$ (see [Equation A.29](#)). This implies

$$i\bar{\psi}\not{\partial}\psi \rightarrow i\bar{\psi}\not{\partial}\psi, \quad m\bar{\psi}\psi \rightarrow -m\bar{\psi}\psi,$$

i.e. the Dirac Lagrangian is only invariant under chiral transformations if $m = 0$. Indeed, if we calculate the associated current:

$$\mathcal{J}^{5\mu a} = \bar{\psi}\gamma^\mu\gamma^5 t^a \psi, \quad (1.54)$$

its derivative is given by

$$\partial_\mu \mathcal{J}^{5\mu a} = 2m\bar{\psi}\gamma^5 t^a \psi.$$

This current is often called the *axial vector current*, or axial current for short. It is only conserved for $m = 0$, as expected from symmetry considerations. Chiral transformations and γ^5 are essential ingredients for parity-violating theories like the electroweak theory.

The Yang-Mills Lagrangian

Next we investigate the global symmetries of a general $\mathfrak{su}(n)$ Lagrangian, also called the Yang-Mills (YM) Lagrangian, which we will construct in the next chapter, more specifically in [Equation 2.45](#):

$$\mathcal{L} = \bar{\psi}(i\not{\partial} - m)\psi + g\bar{\psi}\not{A}\psi - \frac{1}{2}\text{tr} F_{\mu\nu}F^{\mu\nu}, \quad (1.55)$$

where the factor g is the *coupling strength* of the $\mathfrak{su}(n)$ interaction. The Dirac fields are organised in a multiplet (see [Equation 1.48](#)), and the vector fields are used as operators:

$$A_\mu \stackrel{\text{N}}{=} A_\mu^a t^a, \quad (1.56a)$$

$$F_{\mu\nu} \stackrel{\text{N}}{=} F_{\mu\nu}^a t^a = \partial_\mu A_\nu - \partial_\nu A_\mu - ig[A_\mu, A_\nu]. \quad (1.56b)$$

The latter makes sure that

$$\frac{1}{2}\text{tr} F_{\mu\nu}F^{\mu\nu} = \frac{1}{2}\text{tr}(t^a t^b) F_{\mu\nu}^a F^{\mu\nu b} = \frac{1}{4}F_{\mu\nu}^a F^{\mu\nu a}.$$

The Lagrangian has a manifest $u(1)$ symmetry:

$$\psi_i \rightarrow e^{i\alpha} \psi_i, \quad A_\mu \rightarrow A_\mu,$$

which leads to a conservation of baryon or lepton number, as we saw in [Equation 1.51](#). However, the YM Lagrangian is not invariant under global $\mathfrak{su}(n)$ symmetries (with $n > 1$) that only act on the Dirac fields, as was the case in [Equation 1.49](#), instead we have to extend the transformation to the vector fields as well:

$$\psi_i \rightarrow \psi_i + i g \alpha^a (t^a)_{ij} \psi^j, \quad (1.57a)$$

$$A_\mu^a \rightarrow A_\mu^a + g f^{abc} A_\mu^b \alpha^c, \quad (1.57b)$$

where we extracted g from α . This is just a matter of convention. These are the infinitesimal forms of the rotations

$$\psi \rightarrow e^{i g \alpha^a t^a} \psi, \quad (1.58a)$$

$$\bar{\psi} \rightarrow \bar{\psi} e^{-i g \alpha^a t^a}, \quad (1.58b)$$

$$A_\mu \rightarrow e^{i g \alpha^a t^a} A_\mu e^{-i g \alpha^a t^a}, \quad (1.58c)$$

$$F_{\mu\nu} \rightarrow e^{i g \alpha^a t^a} F_{\mu\nu} e^{-i g \alpha^a t^a}. \quad (1.58d)$$

To see how the exponentiation of the infinitesimal transformation of A_μ leads to the rotation in [Equation 1.58c](#), note that [Equation 1.57b](#) can be written in operator form as

$$A_\mu \rightarrow A_\mu - i g [A_\mu, \alpha].$$

It is not difficult to show that the Lagrangian in [Equation 1.55](#) is invariant under the full transformation in [Equations 1.58](#) (the kinetic term of the vector field is invariant, because it sits inside a trace, which is cyclic). Using again $-\alpha^a$ as the transformation parameter ϵ^a , we can construct $n^2 - 1$ conserved Noether currents:

$$\begin{aligned} \mathcal{J}^{\mu a} &= i g \frac{\partial \mathcal{L}}{\partial \partial_\mu \psi} t^a \psi + g f^{abc} \frac{\partial \mathcal{L}}{\partial \partial_\mu A_\nu^b} A_\nu^c \\ &= g \bar{\psi} \gamma^\mu t^a \psi + g f^{abc} F^{\mu\nu b} A_\nu^c. \end{aligned} \quad (1.59)$$

The associated conserved charges are the charges of the symmetry under consideration. E.g. for $\mathfrak{su}(2)$ this is the *weak hypercharge* (and the vector fields represent the weak bosons), and for $\mathfrak{su}(3)$ this is the *colour charge* (and the vector fields represent the gluons).

An interesting remark is the fact that the $u(1)$ symmetry leaves the vector fields invariant. This is a strong fact: all vector fields have a vanishing $u(1)$ charge (e.g. photons and gluons carry no electromagnetic charge).

It is also interesting to explicitly calculate the **ELEM** for the vector field. For a general **YM** Lagrangian, these are given by

$$D_\mu^{ab} F^{\mu\nu b} = -J^{\nu a}, \quad (1.60a)$$

$$D_\mu^{ab} = \delta^{ab} \partial_\mu - g f^{abc} A_\mu^c, \quad (1.60b)$$

$$J^{\nu a} = g \bar{\psi} \gamma^\nu t^a \psi, \quad (1.60c)$$

and are commonly called the *Yang-Mills* equations. In operator form, these are:

$$[D_\mu, F^{\mu\nu}] = -J^{\nu a} t^a \quad (1.61a)$$

$$D_\mu = \partial_\mu - i g A_\mu, \quad (1.61b)$$

but watch out, we cannot simply absorb t^a in $J^{\nu a}$, because we need a Fierz identity (see [Equation A.77](#)) for this.

1.5 LOCAL SYMMETRIES

Now we move on to the most important concept in **QFT**, viz. that of *gauge symmetries*. In [Section 1.4](#) we motivated the need for global phase invariance from a **QM** point of view. But there is no reason why the phase parameter ϵ^a couldn't be dependent on spacetime coordinates, as the **QM** amplitude is invariant under these transformations as well. Motivated by classical **QM**, we thus require any realistic **QFT** to be invariant under a *local* phase transformation:

$$\psi \rightarrow e^{i g \alpha^a(x) t^a} \psi, \quad (1.62)$$

which varies from point to point.

Demanding local phase invariance is a much stricter requirement than global phase invariance. Indeed, e.g. the simple free Dirac Lagrangian in [Equation 1.24](#) is not locally invariant:

$$\delta \mathcal{L}^{\text{Dirac}} = -g \bar{\psi} \not{\partial} \alpha \psi.$$

The move to local phase invariance has serious implications, as both the **ELEM** and Noether's first theorem are no longer valid.

In order to adapt these theorems, we parameterise any field transformation in function of spacetime-dependent parameters $\epsilon^a(x)$ and their derivatives $\partial_\mu \epsilon^a(x)$:

$$\delta\phi_i = \epsilon^a \Phi_i^a + (\partial_\mu \epsilon^a) \Omega_i^{\mu a}. \quad (1.63)$$

The only condition on the functions $\epsilon^a(x)$ is that they are expected to be twice differentiable. As all local symmetries of interest are automatically internal symmetries (spacetime are spacetime-dependent anyway, and already treated in [Section 1.4](#)), we can safely assume $\delta x^\mu \equiv 0$.

Localised Equations of Motion

The variation of the Lagrangian is given by

$$\delta\mathcal{L} = \frac{\partial\mathcal{L}}{\partial\phi_i} \delta\phi_i + \frac{\partial\mathcal{L}}{\partial\partial_\mu\phi_i} \partial_\mu\delta\phi_i.$$

Filling in the variation in [Equation 1.63](#), we can collect the terms linear in ϵ^a and its derivatives:

$$\delta\mathcal{L} = A^a \epsilon^a + B^{\mu a} \partial_\mu \epsilon^a + C^{\mu\nu a} \partial_\mu \partial_\nu \epsilon^a, \quad (1.64)$$

with

$$A^a = \frac{\partial\mathcal{L}}{\partial\phi_i} \Phi_i^a + \frac{\partial\mathcal{L}}{\partial\partial_\mu\phi_i} \partial_\mu \Phi_i^a, \quad (1.65a)$$

$$B^{\mu a} = \frac{\partial\mathcal{L}}{\partial\phi_i} \Omega_i^{\mu a} + \frac{\partial\mathcal{L}}{\partial\partial_\mu\phi_i} \Phi_i^a + \frac{\partial\mathcal{L}}{\partial\partial_\nu\phi_i} \partial_\nu \Omega_i^{\mu a}, \quad (1.65b)$$

$$C^{\mu\nu a} = \frac{\partial\mathcal{L}}{\partial\partial_\mu\phi_i} \Omega_i^{\nu a}. \quad (1.65c)$$

The necessary condition for the action to be invariant, is that the variation of the Lagrangian vanishes up to a divergence, i.e.

$$\delta S \equiv 0 \quad \Rightarrow \quad \delta\mathcal{L} \equiv \partial_\mu(\dots).$$

With help of partial integration, we can rewrite [Equation 1.64](#) as

$$\delta\mathcal{L} = (A^a - \partial_\mu B^{\mu a} + \partial_\mu \partial_\nu C^{\mu\nu a}) \epsilon^a + \partial_\mu(\dots).$$

The first terms have to vanish independently of ϵ^a , giving us the invariance requirement

$$A^a - \partial_\mu B^{\mu a} + \partial_\mu \partial_\nu C^{\mu\nu a} \equiv 0.$$

Plugging in the definitions of A , B^μ , and $C^{\mu\nu}$ gives

$$\left(\frac{\partial \mathcal{L}}{\partial \phi_i} - \partial_\mu \frac{\partial \mathcal{L}}{\partial \partial_\mu \phi_i} \right) (\Phi_i^a - \partial_\mu \Omega_i^{\mu a}) - \left(\partial_\mu \frac{\partial \mathcal{L}}{\partial \phi_i} - \partial_\mu \partial_\nu \frac{\partial \mathcal{L}}{\partial \partial_\nu \phi_i} \right) \Omega_i^{\mu a} \equiv 0. \quad (1.66)$$

The *variational derivative* of \mathcal{L} is defined as (see e.g. [24]):

Variational Derivative

$$\frac{\delta \mathcal{L}}{\delta \phi_i} \stackrel{\text{def}}{=} \frac{\partial \mathcal{L}}{\partial \phi_i} - \partial_\mu \frac{\partial \mathcal{L}}{\partial \partial_\mu \phi_i}. \quad (1.67)$$

In the case of global symmetries, the **ELEM** are equivalent to the constraint

$$\frac{\delta \mathcal{L}}{\delta \phi_i} \equiv 0. \quad (1.68)$$

Hence the variational derivative gives a measure of the extent at which the local **ELEM**s diverge from the global ones. We can express the invariance requirement (Equation 1.66) in function of the variational derivative:

$$\frac{\delta \mathcal{L}}{\delta \phi_i} \Phi_i^a \equiv \partial_\mu \left(\frac{\delta \mathcal{L}}{\delta \phi_i} \Omega_i^{\mu a} \right). \quad (1.69)$$

Removing the spacetime dependence of ϵ^a recovers the global **ELEM** as expected, because then $\Omega_i^{\mu a} = 0$, which gives us

$$\frac{\delta \mathcal{L}}{\delta \phi_i} \Phi_i^a \equiv 0 \quad \Rightarrow \quad \frac{\delta \mathcal{L}}{\delta \phi_i} \equiv 0,$$

because it should hold independently of Φ_i^a .

Consider for instance the Yang-Mills Lagrangian as given in Equation 1.55. It is invariant under the local gauge transformation

$$\psi \rightarrow \psi + i g \alpha^a t^a \psi \quad (1.70a)$$

$$A_\mu^a \rightarrow A_\mu^a + \partial_\mu \alpha^a \quad (1.70b)$$

Comparing this with Equation 1.63, we see that the common parameter is given by $\epsilon^a = \alpha^a$. For the ψ field, we have

$$\Phi_i^a \stackrel{\text{N}}{=} i g t^a \psi \quad \Omega_i^{\mu a} = 0.$$

Identifying the transformation component for the field A_μ might be a bit confusing, as the field itself also carries Lie and Lorentz indices. The field index i on Ω thus accounts for ν and b on the field:

$$\Phi_i^a = 0 \quad \Omega_i^{\mu a} \stackrel{\text{N}}{=} \delta_\nu^\mu \delta^{ab}.$$

Local gauge invariance then implies the following local equations of motion:

$$ig \left(\frac{\delta \mathcal{L}}{\delta \psi} t^a \psi - \frac{\delta \mathcal{L}}{\delta \bar{\psi}} t^a \bar{\psi} \right) \equiv \partial_\mu \left(\frac{\delta \mathcal{L}}{\delta A_\nu^b} \delta_\nu^\mu \delta^{ab} \right)$$

$$g \partial_\mu (\bar{\psi} \gamma^\mu t^a \psi) \equiv g \partial_\mu (\bar{\psi} \gamma^\mu t^a \psi) + \partial_\mu \partial_\nu F^{\mu\nu a}.$$

Or, in other words:

$$\partial_\mu \partial_\nu F^{\mu\nu a} \equiv 0. \quad (1.71)$$

This tells us amongst other things that the field tensor should be antisymmetric.

Noether's Second Theorem

When working with local symmetries, it isn't always possible to derive conserved currents and charges, as was the case for global symmetries. However, the invariance of the Lagrangian under local symmetries will give rise to a set of differential equations constraining the fields. This is Noether's second theorem.

Instead of allowing the Lagrangian to vary up to a divergence, we require it to fully vanish, i.e. $\delta \mathcal{L} \equiv 0$. Comparing this to [Equation 1.64](#), we see that every term has to vanish separately, because the requirement has to be met independently of ϵ^a . This naturally implies $A^a \equiv 0$, $B^{\mu a} \equiv 0$, and $C^{\mu\nu a} \equiv 0$. However, because C is contracted with a fully symmetric tensor ($\partial_\mu \partial_\nu$), it is sufficient for C to be fully antisymmetric for the last term to vanish. We thus have the following requirements:

$$A^a \equiv 0 \quad \Rightarrow \quad \frac{\partial \mathcal{L}}{\partial \phi_i} \Phi_i^a \equiv - \frac{\partial \mathcal{L}}{\partial \partial_\mu \phi_i} \partial_\mu \Phi_i^a, \quad (1.72a)$$

$$B^{\mu a} \equiv 0 \quad \Rightarrow \quad \frac{\partial \mathcal{L}}{\partial \phi_i} \Omega_i^{\mu a} + \frac{\partial \mathcal{L}}{\partial \partial_\nu \phi_i} \partial_\nu \Omega_i^{\mu a} \equiv - \frac{\partial \mathcal{L}}{\partial \partial_\mu \phi_i} \Phi_i^a, \quad (1.72b)$$

$$C^{(\mu\nu)a} \equiv 0 \quad \Rightarrow \quad \frac{\partial \mathcal{L}}{\partial \partial_\mu \phi_i} \Omega_i^{\nu a} \equiv - \frac{\partial \mathcal{L}}{\partial \partial_\nu \phi_i} \Omega_i^{\mu a}. \quad (1.72c)$$

We define the local Noether current as

Local Noether Current

$$\mathcal{J}^{\mu a} = \frac{\partial \mathcal{L}}{\partial \partial_\mu \phi_i} \Phi_i^a + \frac{\delta \mathcal{L}}{\delta \phi_i} \Omega_i^{\mu a}. \quad (1.73)$$

Then the first equation $A^a \equiv 0$ reduces to

$$\partial_\mu \mathcal{J}^{\mu a} + \frac{\delta \mathcal{L}}{\delta \phi_i} \Phi_i^a - \partial_\mu \left(\frac{\partial \mathcal{L}}{\partial \phi_i} \Omega_i^{\mu a} \right) \equiv 0,$$

or, after using the local ELEM (Equation 1.69),

$$\partial_\mu \mathcal{J}^{\mu a} \equiv 0, \quad (1.74)$$

again demonstrating current conservation. We could derive a conserved charge from this current just a before, but it wouldn't make much sense as it isn't linked to any physical observable.

We can also construct a Noether tensor, defined as

Local Noether Tensor

$$F^{\mu\nu a} \stackrel{\text{def}}{=} \frac{\partial \mathcal{L}}{\partial \partial_\nu \phi_i} \Omega_i^{\mu a}. \quad (1.75)$$

Watch the order of the indices! We chose to reverse them ($F^{\mu\nu} = C^{\nu\mu}$), to make the identification with the gauge field tensor identical. The third equation $C^{(\mu\nu)a} \equiv 0$ tells us that it is antisymmetric:

$$F_{\mu\nu}^a = -F_{\nu\mu}^a,$$

and we can use it to rewrite the second equation $B^{\mu a} \equiv 0$ as

$$\partial_\nu F^{\nu\mu a} \equiv \mathcal{J}^{\mu a}. \quad (1.76)$$

Current conservation (and the fact that $F^{\mu\nu}$ is antisymmetric) implies conservation of the Noether tensor as well:

$$\partial^\mu \partial^\nu F_{\mu\nu}^a \equiv 0. \quad (1.77)$$

Note that we can combine the local ELEM with current conservation, to get a new set of equations:

$$\frac{\partial \mathcal{L}}{\partial \phi_i} \Phi_i^a + \frac{\partial \mathcal{L}}{\partial \partial_\mu \phi_i} \partial_\mu \Phi_i^a \equiv 0. \quad (1.78)$$

However, most of the time these equations are trivially satisfied and hence carry no new information. Now we can state Noether's second theorem:

NOETHER'S SECOND THEOREM: Each continuous local symmetry transformation that leaves the Lagrangian invariant is associated with a conserved current as defined in Equation 1.73 and a conserved tensor as defined in Equation 1.75. They are related to each other by Equation 1.76. For each symmetry component a , there are local ELEMs acting on all fields, as given by Equation 1.69.

Can we extend the second Noether theorem for the case where the Lagrangian is invariant up to a divergence $\partial_\mu (\epsilon^a K^{\mu a})$? Filling the definitions of the Noether current and Noether tensor in Equation 1.64, the variation of the Lagrangian is given by:

$$\delta\mathcal{L} = (\partial_\mu \mathcal{J}^{\mu a}) \epsilon^a + (\mathcal{J}^{\mu a} - \partial_\nu F^{\nu\mu a}) \partial_\mu \epsilon^a + F^{\mu\nu a} \partial_\mu \partial_\nu \epsilon^a \equiv \partial_\mu (\epsilon^a K^{\mu a}) .$$

We see that the Noether equations remain valid if we subtract K^μ from the current.

Returning to the Yang-Mills Lagrangian in Equation 1.55, the first thing we note is that the Noether tensor (Equation 1.75) identically equals the gauge field strength, validating our naming choice. Next we can construct the local Noether current using the parameterisation in Equations 1.70:

$$\begin{aligned} \mathcal{J}^{\mu a} &= i g \frac{\partial \mathcal{L}}{\partial \partial_\mu \psi} t^a \psi + \frac{\delta \mathcal{L}}{\delta A_\nu^b} \delta_\nu^\mu \delta^{ab} \\ &= -g \bar{\psi} \gamma^\mu t^a \psi + g \bar{\psi} \gamma^\mu t^a \psi + \partial_\nu F^{\nu\mu a} \\ &= \partial_\nu F^{\nu\mu a} , \end{aligned}$$

which is a trivial identity because of Equation 1.76. Also note that indeed Equation 1.78 doesn't bring any new information, as it states

$$-i \bar{\psi} t^a (i \not{\partial} - m) \psi - i \bar{\psi} t^a \psi - \bar{\psi} \not{\partial} t^a \psi \equiv 0 ,$$

i.e. $0 \equiv 0$, which is trivially satisfied.

At first sight, it would seem that Noether's second theorem isn't all that helpful, because it doesn't give us new information on the theory. But this is because the Yang-Mills Lagrangian is already a perfectly gauged Lagrangian, a 'finished' one. As the power of the second Noether theorem lies in its strong relations and constraints, it is an especially handy tool to make existing theories gauge invariant.

GEOMETRY OF QUANTUM FIELD THEORIES

We will now try to construct the Yang-Mills Lagrangian, as defined in [Equation 1.55](#), only from geometric arguments and past knowledge from quantum mechanics. From experiment it is known that matter particles, like leptons and quarks, have spin $1/2$, obeying Fermi-Dirac statistics and the Pauli exclusion principle. And from [QM](#) we know that such particles obey the Dirac equation.

We start by only considering a Dirac field, as in our simple-minded ansatz we have no idea yet about the true nature of gauge fields, only knowing they act on particles that are charged under the $\mathfrak{su}(n)$ symmetry. Our basic building brick is the free Dirac Lagrangian ([Equation 1.24](#)), on which we will impose invariance under local phase rotations.

2.1 PARALLEL TRANSPORT AND WILSON LINES

In [Sections 1.4](#) and [1.5](#) we motivated the need for global and local phase invariance with classical quantum mechanics, because the [QM](#) probability $|\Psi(\mathbf{x})|^2$ is supposed to be invariant under phase rotations, both global and local.

We know the free Dirac Lagrangian is not gauge invariant. Consider a local $\mathfrak{su}(n)$ phase rotation

$$\psi(x) \rightarrow e^{\pm i g \alpha^a(x) t^a} \psi(x), \quad (2.1)$$

where g is just a constant (which will be identified later as the coupling constant), and we leave the sign unspecified. The antiparticle field $\bar{\psi}$ transforms with an opposite sign in the exponent:

$$\bar{\psi}(x) \rightarrow \bar{\psi}(x) e^{\mp i g \alpha^a(x) t^a}.$$

The mass term is behaving nicely and remains unchanged under the transformation:

$$-m \bar{\psi} \psi \rightarrow -m \bar{\psi} e^{\mp i g \alpha^a(x) t^a} e^{\pm i g \alpha^a(x) t^a} \psi = -m \bar{\psi} \psi.$$

However, the derivative term is giving problems, as it pulls out a factor $\partial_\mu \alpha$ from the exponential:

$$i \bar{\psi} \not{\partial} \psi \rightarrow i \bar{\psi} \not{\partial} \psi - g \bar{\psi} \not{\partial} \alpha^a t^a \psi.$$

The Parallel Transporter

The standard way to proceed, is to introduce a so-called *gauge field* A_μ^a , that transforms in such a way that it cancels the problematic terms. But instead of introducing a field ad hoc, we investigate the problem at hand a bit deeper, and see if we can pinpoint the erratic behaviour (and solve it) purely by geometric arguments.

Actually, it is not surprising that the derivative spoils local transformations, as it is not a local but a bi-local operator, viz. it is defined in two spacetime points instead of one. The definition of the derivative of $\psi(x)$ in the direction of a vector n^μ is namely

$$n^\mu \partial_\mu \psi = \lim_{\epsilon \rightarrow 0} \frac{1}{\epsilon} (\psi(x + \epsilon n) - \psi(x)). \quad (2.2)$$

This definition is not well-defined, as $\psi(x + \epsilon n)$ and $\psi(x)$ obey different transformation laws. In other words, there isn't a sensible transformation for the quantity $\partial_\mu \psi$.

If we would have an object that is able to transport the transformation properties of a field at a point x to those of a field at a point y , we could use it to adapt the derivative to have a single transformation. Let us assume that we have found such a quantity $\mathcal{U}_{(x;y)}$ that is scalar, only depending on x and y , and transforms under the symmetry in [Equation 2.1](#) as

$$\mathcal{U}_{(y;x)} \rightarrow e^{\pm i g \alpha^a(y) t^a} \mathcal{U}_{(y;x)} e^{\mp i g \alpha^a(x) t^a}, \quad (2.3)$$

so we can use it to transport a field at x to a field at y :

$$\mathcal{U}_{(y;x)} \psi(x) \rightarrow e^{\pm i g \alpha^a(y) t^a} \mathcal{U}_{(y;x)} \psi(x). \quad (2.4)$$

For this reason it is often called a *parallel transporter*, or a comparator. Other common names are a gauge link, or a *Wilson line*. We will mostly stick to the latter naming convention. We will treat them extensively in [Chapter 6](#) and later. In principle, the requirement in [Equation 2.3](#) is the only constraint on \mathcal{U} so far, leaving a whole list of functions as possible candidates. In an attempt to narrow down this list, we will add some additional constraints that seem logical to enforce.

First of all, transporting a field from x to y , and then from y to z , should yield the same result as transporting it directly from x to z . Hence the parallel transporter should be transitive:

$$\mathcal{U}_{(z;y)}\mathcal{U}_{(y;x)} = \mathcal{U}_{(z;x)}. \quad (2.5)$$

This is not yet a rigorous definition, but it is accurate enough to help us understand the structure of \mathcal{U} a bit more. Next, if we place the transporter in between a bi-local product $\bar{\psi}(y)\psi(x)$ to make it invariant, we can use [Equation 2.5](#) to split it at some point z :

$$\bar{\psi}(y)\mathcal{U}_{(y;x)}\psi(x) = \bar{\psi}(y)\mathcal{U}_{(y;z)}\mathcal{U}_{(z;x)}\psi(x). \quad (2.6)$$

But we could as well redefine ψ by absorbing the transporter, i.e.

$$\Psi(z) \stackrel{\text{N}}{=} \mathcal{U}_{(z;x)}\psi(x),$$

allowing us to write the bi-local product as $\bar{\Psi}(z)\Psi(z)$. By writing out the barred field:

$$\bar{\Psi}(z) = \overline{\mathcal{U}_{(z;y)}\psi(y)} = \bar{\psi}(y) \left[\mathcal{U}_{(z;y)} \right]^\dagger,$$

and identifying with [Equation 2.6](#), we see that the dagger operation switches the endpoints:

$$\left[\mathcal{U}_{(z;y)} \right]^\dagger \equiv \mathcal{U}_{(y;z)}. \quad (2.7)$$

Furthermore, moving a field from x to y , and then back to x , should have no final effect. This immediately implies that \mathcal{U} should be *unitary*:

$$\mathcal{U}_{(x;y)}\mathcal{U}_{(y;x)} \stackrel{\text{def}}{=} 1 \quad \Rightarrow \quad \left[\mathcal{U}_{(y;x)} \right]^\dagger \mathcal{U}_{(y;x)} \equiv 1 \quad (2.8)$$

Every unitary object can be represented as a pure phase, i.e.

$$\mathcal{U}_{(y;x)} \stackrel{\text{N}}{=} e^{\pm i g f(y,x)}, \quad (2.9)$$

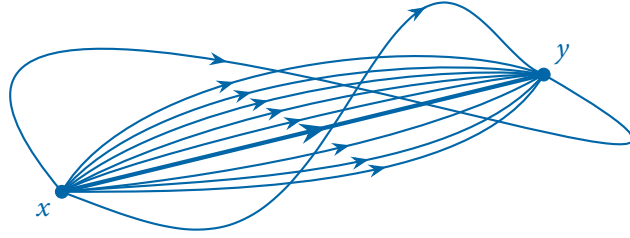


Figure 2.1: As a parallel transporter transforms in function of its path endpoints only, all paths shown will give rise to equivalent $\mathcal{U}_{(y;x)}$'s, shifting a field at x to a field at y .

where f is a real function, and the sign in front of ig is for convenience the same as the one chosen in the transformation Equation 2.1. We extracted the same factor g from $f(y, x)$ as in the transformation rules. Because of the transitivity of \mathcal{U} , this function has to be transitive with respect to addition, particularly $f(y, x) = f(y, z) + f(z, x)$. Also, because of the Hermiticity of \mathcal{U} , the function f has to be antisymmetric in its arguments, viz. $f(y, x) = -f(x, y)$. This suggests something of the form

$$f(y, x) \stackrel{?}{=} f(y) - f(x).$$

All these prerequisites are typical for a path-dependent function. This is a function that takes a coordinate as an argument, but is evaluated at the endpoints of the path. For a path \mathcal{C} , we can write this as

$$\mathcal{C} : z^\mu = x^\mu \dots y^\mu \quad \Rightarrow \quad f(y, x) \stackrel{\text{def}}{=} f^{\mathcal{C}}(z)|_x^y. \quad (2.10)$$

We thus succeeded in limiting the list of possible candidates for $\mathcal{U}_{(y;x)}$ to all pure phases that are functions of a path connecting x and y . This is illustrated in Figure 2.1, where every path leads to a different parallel transporter that is a valid candidate for $\mathcal{U}_{(y;x)}$. This is why we added the label \mathcal{C} to f ; each path can have its own function. There is no restriction on the possible paths, except that they should all be continuous and have the same endpoints.

From the physical point of view, this makes a lot of sense. Intuitively, it feels logical that, when transporting a field from one point to another, this is done in a continuous way without abrupt jumps, i.e. along a path in spacetime. As the only property we are interested in is its transformation, depending only on the endpoints, we end up with an infinite set of possible parallel transporters, each one defined along a different path, and all equally valid. Whenever it is needed

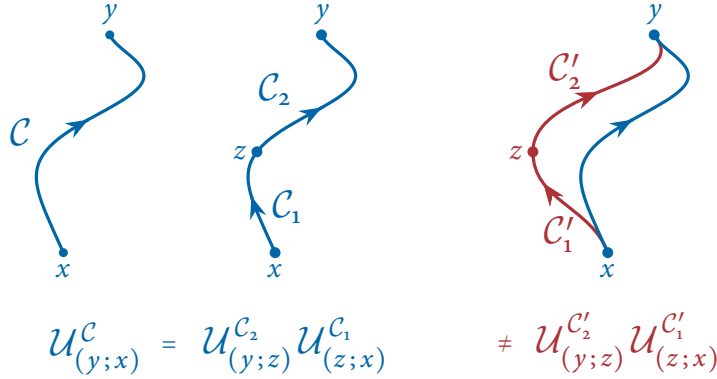


Figure 2.2: When a parallel transporter is split in a point z that lies on its path, it can be written as the product of the two new parallel transporters, i.e. it is transitive. This is not correct when z lies outside the original path.

to make a distinction between parallel transporters on different paths, we can write $U_{(y;x)}^C$ to identify the chosen path.

Non-Abelian paths

Now we have to stop for a moment, because there is a really important caveat that we overlooked. From the transitivity requirement in [Equation 2.5](#), we deduced that $f(y, x) = f(y, z) + f(z, x)$. However, because the transformation exponentials in [Equation 2.3](#) are possibly Lie algebra valued functions, it is to be expected that f is Lie algebra valued as well. But in that case, we cannot simply split the exponential, i.e.

$$e^{f(y,z)+f(z,x)} \neq e^{f(y,z)}e^{f(z,x)},$$

but we have to use the Baker-Campbell-Hausdorff formula instead, involving chained commutators of f at different spacetime points.

We decide to turn a different road, and *order* the f along the path. More specifically, in the expansion of the exponential, all f are ordered in such a way that the f that is first on the path (having the largest path parameterisation parameter) is written leftmost. We will use the symbol \mathcal{P} in front of the exponential to show that it is a path-ordered exponential. Path-ordering is treated in much more detail in [Section 6.1](#) on page 151 and onwards. Then the transitivity property is valid:

$$\mathcal{P} e^{f(y,x)} = \mathcal{P} e^{f(y,z)} \mathcal{P} e^{f(z,x)}. \quad (2.11)$$

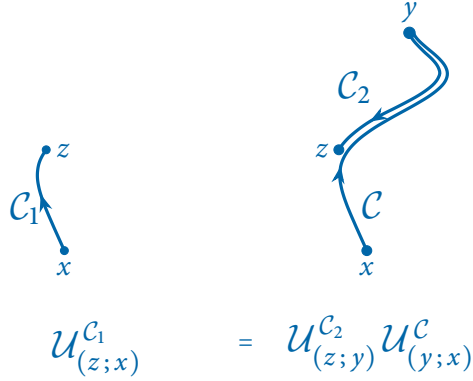


Figure 2.3: The transitivity rule can be also applied to points outside the path C on the condition that the path returns on itself, cancelling the overlapping segments.

There is, however, another caveat: this property is only valid if z already lies on the path connecting x and y , because we cannot blindly split the path in a point outside of it, see Figure 2.2. The correct definition of the transitivity property is then

$$\forall C_1 + C_2 = C: \quad U_{(y;x)}^C = U_{(y;z)}^{C_2} U_{(z;x)}^{C_1}. \quad (2.12)$$

Note that it is not impossible to use the transitivity rule with a point outside of the path. If we multiply both sides of the last equation with $U_{(z;y)}^{C_2}$, we get

$$U_{(z;y)}^{C_2} U_{(y;x)}^C = U_{(z;x)}^{C_1}, \quad (2.13)$$

because $U_{(z;y)}^{C_2} U_{(y;z)}^{C_2} = \left[U_{(y;z)}^{C_2} \right]^\dagger U_{(y;z)}^{C_2} = 1$. We can interpret this as saying that the path C_1 can be “split” at a point outside of the path if, and only if, the path returns on top of itself to cancel the superfluous part, i.e. if

$$C_1 = C - C_2. \quad (2.14)$$

This is illustrated in Figure 2.3.

Let us now try to parameterise f^C for a given path C . We approximate the path connecting x and y by dividing it into n infinitesimal linear segments:

$$f^C(y, x) \approx \sum_{i=1}^n f^C(x_{i+1}, x_i) \quad (2.15)$$

This is illustrated in [Figure 2.4](#). From symmetry considerations we expect f^C to depend in the infinitesimal limit on the centre of the segment:¹

$$f^C(x_{i+1}, x_i) \stackrel{?}{=} \tilde{f}^C\left(\frac{x_{i+1} + x_i}{2}\right).$$

Yet this cannot be correct, as now f^C is symmetric instead of antisymmetric. This was to be anticipated as we discarded information, going from a function of two variables to one of one variable. If we choose to describe a linear line segment $[x, y]$ in function of its centre $(x + y)/2$, we have to add the separation vector $y - x$ as a second variable. But instead of making \tilde{f}^C dependent on the separation vector, we interpret it as though its structural form *itself* changes, in function of the direction it is evaluated over. In other words, we promote \tilde{f}^C to a vector function which we will call A_μ , and contract it with the separation vector. Then f^C is defined as

$$f^C(y, x) \approx \sum^n (x_{i+1} - x_i)^\mu A_\mu\left(\frac{x_{i+1} + x_i}{2}\right).$$

Note that we dropped the label C from A_μ , because the path dependence is now fully moved to the coordinates x_i and x_{i+1} , while the structural form of A_μ is path independent. In other words, the same A_μ is used for every parallel transporter, for any path, in contrast with f^C , which is different for every path. The path dependence manifests itself through the factor $(x_{i+1} - x_i)^\mu$ in front, in the index μ of A_μ , and in the argument $(x_{i+1} + x_i)/2$ of A_μ .² As we discussed before, $f^C(y, x)$ is expected to be Lie algebra valued, because the transformation of \mathcal{U} is Lie algebra valued as well. It is then logical to put the Lie dependence inside A_μ , i.e. $A_\mu \stackrel{\text{def}}{=} A_\mu^a t^a$.

Taking the limit $n \rightarrow \infty$, the discrete formula becomes a line integral (see [Equation B.5c](#)), i.e. :

$$f^C(y, x) = \int_C dz^\mu A_\mu^a(z) t^a. \quad (2.16)$$

This is in perfect accordance with our physical intuition of a path with fixed endpoints. Inserting this result in [Equation 2.9](#) gives us the final definition for the parallel transporter:

-
- 1 Using Itô-calculus, one can show that taking the centre of the segment is even a necessity in order to get a correct definition.
 - 2 It is important to realise that although we intentionally named $A_\mu(x)$ as is to simplify identification with the gauge field later on, at the moment it is nothing but a generic vector function of x , without specifying its further structure.

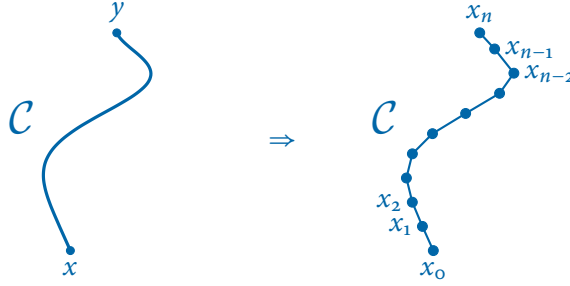


Figure 2.4: Any path C can be discretised by dividing it into n linear segments. In the limit $n \rightarrow \infty$, the original path is recovered.

Parallel Transporter

$$\mathcal{U}_{(y;x)} \stackrel{\text{def}}{=} \mathcal{P} e^{\pm i g \int_x^y dz^\mu A_\mu^a(z) t^a}. \quad (2.17)$$

This newly constructed definition for the parallel transporter allows us to interpret the transformation rules in Equation 2.3 as a transformation of A_μ , because the latter is the only dynamic component of \mathcal{U} . To see this, we take the parameters from the exponentials in Equation 2.3 and insert them in the integral using the gradient theorem (see Equation B.14):

$$\pm i g \alpha(y) \mp i g \alpha(x) = \pm i g \int_x^y dx^\mu \partial_\mu \alpha. \quad (2.18)$$

This implies that we have to define the transformation of the vector function A_μ^a as follows:

$$A_\mu^a(x) \rightarrow A_\mu^a(x) + \partial_\mu \alpha^a. \quad (2.19)$$

Note that the sign in the transformation of A_μ^a is always a plus, independent of the sign chosen in Equation 2.1, because $\partial_\mu \alpha$ has the same sign as A_μ (compare Equation 2.18 with Equation 2.17 to see this). This result is only approximately true, because we assumed that we can simply combine the exponentials. This is however not true in the non-Abelian case, as the presence of Lie generators makes the field behave like operators (see the end of Appendix A.1 for a short discussion on the usage of operators in this thesis). It is generally known that for any two operators X, Y with Y invertible, the following relation holds:

$$e^{YXY^{-1}} = Y e^X Y^{-1},$$

which, applied on the transformation of a Wilson line, gives:

$$e^{\pm i g \alpha^a(y) t^a} \mathcal{U}_{(y;x)} e^{\mp i g \alpha^a(x) t^a} = \mathcal{P} e^{\pm i g \int_x^y dz^\mu A_\mu^a(z) t^a} e^{\mp i g \alpha^a(x) t^a}. \quad (2.20)$$

We can simplify this result by partial integration and the gradient theorem:

$$\mathcal{P} e^{\pm i g \int_x^y dz^\mu e^{\pm i g \alpha^a(z) t^a} \left(A_\mu^a(z) t^a \pm \frac{i}{g} \partial_\mu \right) e^{\mp i g \alpha^a(z) t^a}}, \quad (2.21)$$

from which we deduce the correct transformation rule for a non-Abelian field:

Non-Abelian Vector Transformation

$$A_\mu^a(x) t^a \rightarrow e^{\pm i g \alpha^a(x) t^a} \left(A_\mu^a(x) t^a \pm \frac{i}{g} \partial_\mu \right) e^{\mp i g \alpha^a(x) t^a}, \quad (2.22)$$

which indeed reduces to [Equation 2.19](#) for Abelian fields.

The Covariant Derivative

Let us return to the original goal for which the comparator was constructed, viz. formulating a sensible definition for the derivative in [Equation 2.2](#). This is now straightforward; we simply transport the field at x to $x + \epsilon n$. The result is called a *covariant derivative*:

Covariant Derivative

$$n^\mu D_\mu \psi \stackrel{\text{def}}{=} \lim_{\epsilon \rightarrow 0} \frac{1}{\epsilon} \left(\psi(x + \epsilon n) - \mathcal{U}_{(x+\epsilon n;x)} \psi(x) \right). \quad (2.23)$$

Because the comparator connects two points that are separated by an infinitesimal distance ϵn , we can expand its definition in [Equation 2.17](#) up to first order in ϵ . Applying the discrete definition of the line integral ([Equation B.14](#)), this leads to

$$\mathcal{U}_{(x+\epsilon n;x)} \approx \mathcal{P} e^{\pm i \epsilon g n^\mu A_\mu(x + \frac{1}{2} \epsilon n)} \approx 1 \pm i \epsilon g n^\mu A_\mu(x). \quad (2.24)$$

The covariant derivative is then given by:

$$D_\mu \psi = \partial_\mu \psi \mp ig A_\mu^a t^a \psi, \quad (2.25)$$

and it indeed transports the transformation of the field:

$$\begin{aligned} D_\mu \psi &\rightarrow \partial_\mu (e^{\pm ig\alpha} \psi) \mp ig (A_\mu + \partial_\mu \alpha) e^{\pm ig\alpha} \psi \\ &= \pm ig (\partial_\mu \alpha) e^{\pm ig\alpha} \psi + e^{\pm ig\alpha} \partial_\mu \psi \mp ig A_\mu e^{\pm ig\alpha} \psi \mp ig (\partial_\mu \alpha) e^{\pm ig\alpha} \psi \\ &= e^{\pm ig\alpha} D_\mu \psi. \end{aligned}$$

To derive the transformation rule of the covariant derivative itself, we simply insert $1 = e^{\pm ig\alpha(x)} e^{\mp ig\alpha(x)}$ between D_μ and ψ . We see that it transforms similarly to a parallel transporter $\mathcal{U}_{(x;x)}$ on a closed path:³

$$D_\mu \rightarrow e^{\pm ig\alpha^a(x)t^a} D_\mu e^{\mp ig\alpha^a(x)t^a}. \quad (2.26)$$

From this, we can also express the transformation rule for A_μ in a different way:

$$A_\mu^a t^a \rightarrow \pm \frac{i}{g} e^{\pm ig\alpha^a t^a} D_\mu e^{\mp ig\alpha^a t^a}. \quad (2.27)$$

With help from the covariant derivative, we can now define a Dirac Lagrangian that is invariant under local transformations like those in [Equation 2.1](#):

$$\mathcal{L}_{\text{Dirac}} = \bar{\psi} (i\not{D} - m) \psi. \quad (2.28)$$

The vector field part in the covariant derivative gives rise to an interaction term between the Dirac fields and the vector field:

$$\mathcal{L}_{\text{Dirac}}^I = \pm g \bar{\psi} \not{A} \psi. \quad (2.29)$$

This is the main result of our approach: by making the derivative a well-defined mathematical object, we let a vector field emerge naturally in the form of interactions with the Dirac field. Of course, this vector field will be identified as the $\mathfrak{su}(n)$ gauge field, but let's not be too rash in our conclusion. There are still some missing parts in our approach.

³ We are *not* insinuating that the covariant derivative is a special type of $\mathcal{U}_{(x;x)}$. This cannot be true, because the latter lacks a derivative in its definition. But we do observe that they have the same transformation behaviour, which is to be expected as D_μ is constructed from \mathcal{U} .

2.2 THE GAUGE FIELD TENSOR AND WILSON LOOPS

In a QFT, the next step to proceed after defining a classical Lagrangian is to quantise the theory, so that every function of spacetime coordinates inside the Lagrangian will be interpreted as a particle field. This is exactly what we will do in [Chapter 3](#). However, our Lagrangian isn't 'complete' yet. To understand this, note that the quantisation procedure is split into two parts per field:

- A. Quadratic terms are treated as the dynamics for the field and quantised,
- B. Remaining terms are treated as interactions using perturbation theory.

We argued in [Section 1.1](#) on page 6 that any field without dynamics is automatically an external field, for which the dynamics are defined outside the system under consideration. As we are now constructing the Lagrangian at a global scale, we conclude that we are missing kinetic terms for the field A_μ .

Of course, the standard approach is to continue in a heuristic manner, as we did more or less in [Section 1.1](#) on page 9. We prefer however to let the kinetic terms emerge in the Lagrangian in a natural and elegant fashion, in the same way the interaction term emerged in the previous section. We want to base our approach on geometrical arguments only, starting from the parallel transporter. Because the kinetic terms can only contain A_μ fields, we have start with a gauge invariant version of the Wilson line (as we have no other fields to balance the transformation rules). If we evaluate a line on a closed path and trace it, i.e.

$$\mathcal{U}^\circ \stackrel{\text{def}}{=} \text{Tr} \mathcal{P} e^{\pm i g \oint_{\mathcal{C}} dz^\mu A_\mu(z)}, \quad (2.30)$$

it is automatically invariant:

$$\text{Tr} \mathcal{U}_{(x;x)} \rightarrow \text{Tr} \left(e^{\pm i g \alpha(x)} \mathcal{U}_{(x;x)} e^{\mp i g \alpha(x)} \right) = \text{Tr} \mathcal{U}_{(x;x)}. \quad (2.31)$$

Such an object is called a Wilson loop, and it contains—as we will show—all dynamics of the vector field.

We use Stokes' theorem to transform the line integral over a vector into a surface integral over the gradient:

$$\oint_{\mathcal{C}} dz \cdot A(z) = \int_{\Sigma} d\sigma^{\mu\nu} \partial_{[\mu} A_{\nu]}, \quad (2.32)$$

where Σ is the surface that is spanned by the closed path \mathcal{C} . Note that because the path is oriented, the surface is oriented as well. The orientating of the normal of the surface follows the corkscrew-rule: making a fist, if your fingers follow the

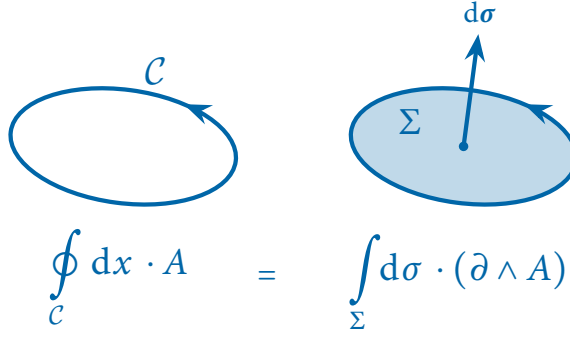


Figure 2.5: Stokes' theorem relates a line integral over a closed path C with a surface integral over the enclosed surface Σ .

path, your thumb points in the normal direction of the surface. This is illustrated in [Figure 2.5](#).

Just as we can parameterise a curve in function of a parameter λ as

$$C : z^\mu(\lambda) \Rightarrow dz^\mu = d\lambda \frac{\partial z^\mu}{\partial \lambda}, \quad (2.33)$$

we can parameterise a surface in function of two parameters λ and κ :

$$\Sigma : z^\mu(\lambda, \kappa) \Rightarrow d\sigma^{\mu\nu} = dz^\mu \wedge dz^\nu = 2d\lambda d\kappa \frac{\partial z^{[\mu}}{\partial \lambda} \frac{\partial z^{\nu]}{\partial \kappa}. \quad (2.34)$$

So we write the surface integral as

$$\int_{\Sigma} d\lambda d\kappa \frac{\partial z^\mu}{\partial \lambda} \frac{\partial z^\nu}{\partial \kappa} (\partial_\mu A_\nu - \partial_\nu A_\mu). \quad (2.35)$$

Our next move is a bit peculiar. We have to find a loop that makes sense from a physical point of view, i.e. it should be as general as possible. The most natural case is to choose a 'zero'-loop, infinitesimally small, starting from and ending in a point x . To achieve this, we discretise spacetime and define our theory *on a lattice* with grid spacing ϵ . Discretising spacetime is only allowed in an Euclidian space, so we make our space Euclidian by doing a Wick rotation (see [Section 7.3](#)):

$$z^0 \stackrel{\text{def}}{=} i z_E^0, \quad \mathbf{z} \stackrel{\text{def}}{=} \mathbf{z}_E, \quad (2.36a)$$

$$\partial^0 \stackrel{\text{def}}{=} i \partial_E^0, \quad \partial \stackrel{\text{def}}{=} \partial_E, \quad (2.36b)$$

$$A^0 \stackrel{\text{def}}{=} i A_E^0, \quad \mathbf{A} \stackrel{\text{def}}{=} \mathbf{A}_E, \quad (2.36c)$$

which changes a vector product by $v_\mu w^\mu = -v_{E\mu} w_E^\mu$, but leaves a matrix product invariant, i.e. $\omega_{\mu\nu} \rho^{\mu\nu} = \omega_{E\mu\nu} \rho_E^{\mu\nu}$. Then we can rewrite the Wilson loop as

$$\mathcal{U}^\circ = \text{Tr } \mathcal{P} \text{Exp} \left\{ \pm i g \int_{\Sigma} d\lambda d\kappa \frac{\partial z_E^\mu}{\partial \lambda} \frac{\partial z_E^\nu}{\partial \kappa} (\partial_\mu A_{E\nu}^a - \partial_\nu A_{E\mu}^a) t^a \right\}. \quad (2.37)$$

A short remark: for the Wick rotation to be valid, we assume that A_μ is well-behaving on the contour \mathcal{C} , especially that it doesn't introduce poles that would hit the Wick rotation (invalidating the result). Similarly, we assumed spacetime and the loop Σ to be continuously enough for Stokes' theorem to hold. In fact, Stokes' theorem is only well-defined for smooth paths and manifolds (which is now not the case), but we use an extension to Stokes' theorem that is well-defined for *piecewise smooth* paths. There is a strong mathematical background for this extension, but this would go much too far beyond the scope of an introductory approach to QFTs, so we don't pay much attention to it and assume all necessary conditions to be satisfied.

A 'zero'-loop is of course the smallest possible loop possible; on a lattice this is a rectangular planar loop spanning the lattice spacing, as is illustrated in [Figure 2.6](#). We will naturally choose our coordinate system along the grid, such that the sides of the square loop lie along the basis directions. We can parameterise such a loop as:

$$\Sigma : z_E^\mu(\lambda, \kappa) = x^\mu + n^\mu \lambda + \tilde{n}^\mu \kappa \quad \lambda, \kappa = 0 \dots \epsilon, \quad (2.38)$$

where n^μ and \tilde{n}^μ are perpendicular basis vectors (i.e. $n \cdot \tilde{n} \equiv 0$). It is necessary to expand [Equation 2.37](#) up to second order, because the first order vanishes due to the tracelessness of the Lie generators $\text{tr } t^a = 0$. Even in the Abelian case—where the only generator is the identity with non-vanishing trace—the first order terms vanish, by cancellation, which is easy to prove. Ignoring the constant first term, the expansion gives

$$\mathcal{U}^\circ \approx -g^2 \frac{1}{2} n^\mu \tilde{n}^\nu n^\rho \tilde{n}^\sigma \int_0^\epsilon d\lambda_1 d\kappa_1 \int_0^{\lambda_1, \kappa_1} d\lambda_2 d\kappa_2 (\partial_\mu A_{E\nu}^a - \partial_\nu A_{E\mu}^a) (\partial_\rho A_{E\sigma}^a - \partial_\sigma A_{E\rho}^a),$$

where the factor $1/2$ comes from the trace of the generators $\text{tr } t^a t^b = 1/2 \delta^{ab}$. We satisfied the path ordering requirement by chaining the integrals (see [Section](#) for more information on how this works). Note that we can simplify the factor $n^\mu \tilde{n}^\nu n^\rho \tilde{n}^\sigma$ by collecting similar vectors. The tensor product $n^\mu n^\nu$ can be repres-

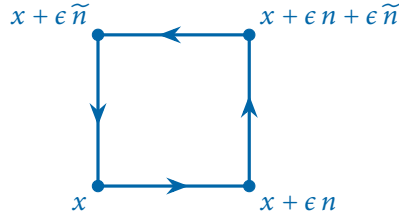


Figure 2.6: On a lattice, the smallest loop possible is a planar square with sides equal to the lattice spacing.

ented by a matrix that is zero everywhere except on the diagonal entry of the directional vector, where it is one, i.e.

$$n_1^\mu n_1^\nu \doteq \begin{pmatrix} 1 & 0 & 0 & 0 \\ 0 & 0 & 0 & 0 \\ 0 & 0 & 0 & 0 \\ 0 & 0 & 0 & 0 \end{pmatrix}, \quad n_2^\mu n_2^\nu \doteq \begin{pmatrix} 0 & 0 & 0 & 0 \\ 0 & 1 & 0 & 0 \\ 0 & 0 & 0 & 0 \\ 0 & 0 & 0 & 0 \end{pmatrix}, \quad n_3^\mu n_3^\nu \doteq \begin{pmatrix} 0 & 0 & 0 & 0 \\ 0 & 0 & 0 & 0 \\ 0 & 0 & 1 & 0 \\ 0 & 0 & 0 & 0 \end{pmatrix}, \quad n_4^\mu n_4^\nu \doteq \begin{pmatrix} 0 & 0 & 0 & 0 \\ 0 & 0 & 0 & 0 \\ 0 & 0 & 0 & 0 \\ 0 & 0 & 0 & 1 \end{pmatrix}.$$

If we take e.g. the infinitesimal square loop spanned by the n_1 and n_2 vectors, the integrand automatically becomes

$$(\partial_1 A_{E2}^a - \partial_2 A_{E1}^a)(\partial_1 A_{E2}^a - \partial_2 A_{E1}^a),$$

in other words, both factors get the same indices. As this starts to look as a sum over indices, we try to exploit this further. In a four dimensional Euclidian space, there are twelve independent planes, viz. the planes spanned by $n_1^\mu n_2^\nu$, $n_1^\mu n_3^\nu$, $n_1^\mu n_4^\nu$, $n_2^\mu n_3^\nu$, $n_2^\mu n_4^\nu$ and $n_3^\mu n_4^\nu$, and the planes oppositely oriented to them. There is no reason why one plane would be preferred over the other, so we define our Wilson loop as the sum of all twelve square loops, one for each independent infinitesimal plane. Note that summing these planes gives a straightforward result:

$$\sum_{\text{planes}} n_i^\mu n_i^\rho \tilde{n}_j^\nu \tilde{n}_j^\sigma = \delta^{\mu\rho} \delta^{\nu\sigma} - g^{\mu\rho\sigma\nu}, \quad (2.39)$$

where $g_{\mu\nu\rho\sigma} = 1$ only when $\mu = \nu = \rho = \sigma$. Because both factors of the integrand are already antisymmetric in $\mu\nu$ resp $\rho\sigma$, only the first term of the right-hand-side (r.h.s.) will contribute, and we can just make the contractions. Then the second order term in the expansion becomes:

$$\mathcal{U}^{\mathcal{O}} \approx -g^2 \int_0^\epsilon d\lambda_1 d\kappa_1 \int_0^{\lambda_1, \kappa_1} d\lambda_2 d\kappa_2 (\partial_\mu A_{E\nu}^a - \partial_\nu A_{E\mu}^a)(\partial^\mu A_E^{a\nu} - \partial^\nu A_E^{a\mu}). \quad (2.40)$$

Because ϵ is an infinitesimal parameter, going to zero in the continuum limit, we can approximate the integrals with help from [Equation B.5c](#). The innermost integral then equals

$$\int_0^{\lambda_1, \kappa_1} d\lambda_2 d\kappa_2 (\partial^\mu A_E^{v a} - \partial^v A_E^{\mu a}) \approx \lambda_1 \kappa_1 (\partial^\mu A_E^{v a} - \partial^v A_E^{\mu a}) \Big|_{x + \frac{1}{2} \lambda_1 n + \frac{1}{2} \kappa_1 \tilde{n}},$$

so that the outermost integral becomes

$$\begin{aligned} \int_0^\epsilon d\lambda_1 d\kappa_1 \lambda_1 \kappa_1 (\partial_\mu A_{E v}^a - \partial_v A_{E \mu}^a) \Big|_{x + \lambda_1 n + \kappa_1 \tilde{n}} (\partial^\mu A_E^{v a} - \partial^v A_E^{\mu a}) \Big|_{x + \frac{1}{2} \lambda_1 n + \frac{1}{2} \kappa_1 \tilde{n}} \\ \approx \frac{\epsilon^4}{4} (\partial_\mu A_{E v}^a - \partial_v A_{E \mu}^a) \Big|_{x + \frac{\epsilon}{2} n + \frac{\epsilon}{2} \tilde{n}} (\partial^\mu A_E^{v a} - \partial^v A_E^{\mu a}) \Big|_{x + \frac{\epsilon}{4} n + \frac{\epsilon}{4} \tilde{n}}. \end{aligned}$$

Because the arguments of the fields in both factors are the same in the limit $\epsilon \rightarrow 0$, we already drop the linear parts in ϵ from the arguments. We then have:

$$\mathcal{U}^\circ \approx -g^2 \frac{\epsilon^4}{4} (\partial_\mu A_{E v}^a - \partial_v A_{E \mu}^a)^2 \Big|_x + \mathcal{O}(\epsilon^4). \quad (2.41)$$

Unfortunately, these are not the only terms of order ϵ^4 . If we expand the exponential further to third and up to fourth order, additional terms of order ϵ^4 emerge. We won't show the calculation here, as it is trivial to do but really long, but just give the result instead. The extra terms are

$$\mp g^3 f^{abc} A_{E \mu}^a A_{E v}^b \partial^\mu A_E^{v a} - \frac{1}{4} g^4 f^{abx} f^{xcd} A_{E \mu}^a A_{E v}^b A_E^{\mu c} A_E^{v d}.$$

So we can conclude that, up to an irrelevant constant term in front,

$$\mathcal{U}^\circ \approx -g^2 \epsilon^4 \frac{1}{4} F_{E \mu\nu}^a F_E^{\mu\nu a} + \mathcal{O}(\epsilon^5). \quad (2.42)$$

Now comes the tricky part. We cannot simply take the continuum limit $\epsilon \rightarrow 0$, as the action, the fields, and the coupling constant are subject to rescalings and renormalisation to be able to reproduce the correct continuum theory. When summing over all lattice points (i.e. when integrating over x), we have to divide by the lattice spacing to the fourth, i.e. ϵ^4 , before taking the limit $\epsilon \rightarrow 0$. See e.g. [\[27\]](#) for a profound treatment on the continuum limit.

So finally, after rescaling the coupling constant, moving back to the continuum theory and un-Wick rotating, we find

$$\mathcal{U}^\circ \equiv -\frac{1}{4} F_{\mu\nu}^a F^{\mu\nu a}, \quad (2.43)$$

up to an irrelevant constant term (which will be subtracted from the action anyway). The gauge field tensor is given by

$$F_{\mu\nu}^a = \partial_\mu A_\nu^a - \partial_\nu A_\mu^a \pm g f^{abc} A_\mu^b A_\nu^c. \quad (2.44)$$

This is exactly what we hoped for. We have shown how the kinetic terms for the gauge field naturally emerge from the Wilson loop. Because the latter is gauge invariant by definition, the gauge field tensor is automatically gauge invariant as well.

2.3 SUMMARY

We cannot stress enough how deep the implications of our results in this chapter are. They show us that every gauge theory has a deep geometric structure, in fact, that every gauge theory is a geometric effect in se.

Starting only from the free Dirac Lagrangian and the demand of local phase invariance, we constructed a full gauge theory. More specifically, the requirement for the derivative to be well-behaving, viz. having a sensible local definition instead of bi-local, leads to:

- A. The construction of a parallel transporter, or Wilson line, and with it the introduction of the gauge field.
- B. The transformation rules for the gauge field.
- C. The definition of the covariant derivative, and hence with it the description of *interactions* between matter fields and the gauge fields.
- D. The construction of a gauge-invariant Wilson loop, and the demonstration that it is intimately related to the gauge field dynamics and kinetic terms.

Note that the last statement is a direct indication that the gauge sector of any gauge theory can be fully recast in function of Wilson loops. This methodology, firmly based on the mathematics of loop space, replaces coordinate and momentum dependence with path dependence. We will elaborate on this in [Chapter 11](#).

The full Yang-Mills Lagrangian for a $\mathfrak{su}(n)$ symmetry is thus given by

Yang-Mills $\mathfrak{su}(n)$ Lagrangian

$$\mathcal{L}_{\text{YM}} = \bar{\psi} (i \not{D} - m) \psi - \frac{1}{2} \text{Tr} F_{\mu\nu} F^{\mu\nu}. \quad (2.45)$$

For the rest of this thesis we will stick to the convention of a positive sign in the gauge transformation exponential. The opposite convention is easily recovered by making the substitution $g \rightarrow -g$. This sign convention propagates through the definition of the covariant derivative and the gauge field tensor:

Yang-Mills Gauge Content

$$D_\mu = \partial_\mu - i g A_\mu^a t^a, \quad (2.46a)$$

$$F_{\mu\nu}^a = \partial_\mu A_\nu^a - \partial_\nu A_\mu^a + g f^{abc} A_\mu^b A_\nu^c, \quad (2.46b)$$

and the local gauge transformations

Local Gauge Transformations

$$\psi \rightarrow e^{i g \alpha^a(x) t^a} \psi, \quad (2.47a)$$

$$\bar{\psi} \rightarrow \bar{\psi} e^{-i g \alpha^a(x) t^a}, \quad (2.47b)$$

$$A_\mu^a t^a \rightarrow \frac{i}{g} e^{i g \alpha^a(x) t^a} D_\mu e^{-i g \alpha^a(x) t^a}, \quad (2.47c)$$

$$D_\mu \rightarrow e^{i g \alpha^a(x) t^a} D_\mu e^{-i g \alpha^a(x) t^a}, \quad (2.47d)$$

$$F_{\mu\nu} \rightarrow e^{i g \alpha^a(x) t^a} F_{\mu\nu} e^{-i g \alpha^a(x) t^a}, \quad (2.47e)$$

which leave the Lagrangian invariant.

Four final remarks:

- A. Note that these gauge transformation rules immediately invalidate mass terms for the gauge field; indeed, terms of the form $m^2 A_\mu^a A^{\mu a}$ are not gauge invariant.
- B. This is not the most general Lagrangian possible that conserves a $\mathfrak{su}(n)$ symmetry. We could add terms of the form $\epsilon_{\mu\nu\rho\sigma} \text{Tr} F^{\mu\nu} F^{\rho\sigma}$. However, these terms are parity violating, and hence beyond the scope of this thesis.
- C. Note that the covariant derivative and the gauge field tensor can be related by $[D_\mu, D_\nu] = -i g F_{\mu\nu}$.

- d. The minus sign between the derivative terms inside the gauge field tensor (Equation 2.44) is a direct result of the wedge product in the infinitesimal surface element in Stokes' theorem (Equation 2.34), hence it is a pure geometrical effect.
-

QUANTISATION OF QUANTUM FIELD THEORIES

In the two previous chapters, we constructed the gauge-invariant Lagrangian for a classical field theory, based on symmetric and geometric arguments. The logical next step towards a decent QFT is of course the quantisation of the fields. Abelian theories are commonly quantised using the canonical formulation of quantum field theory, in which the fields are represented by non-commuting operators. This approach comes straight from classical (non-relativistic) QM, and puts the emphasis on the physical interpretation of the formalism. It is however difficult to apply to non-Abelian theories, because then the conserved charges do not commute with each other (see Equation 1.46). The solution is to do the quantisation in the path integral formalism, as it perfectly allows to quantise non-Abelian theories, and naturally shows the emergence of ghosts. We will try to give a decent outline of the methods, without delving too much into details, as it might lead us too far away from the main topic. See e.g. [18–21] for more details.

3.1 FORMAL DEFINITION OF PATH INTEGRALS

Before we can start quantising the different fields, we need to introduce the definition of a path integral and develop some calculational methods. We will start with a short motivation for the use of path integrals, coming from the propagator in classical non-relativistic QM. This is done by using the transitivity property to discretise the path along which the propagator is evaluated. The path integral then naturally emerges when taking the continuum limit.

QM Propagator as a Path Integral

In non-relativistic quantum mechanics, the Green's function G is defined as a solution of the Schrödinger equation:

$$\left(i\hbar \frac{\partial}{\partial t} - H\right) G(\mathbf{x}, t; \mathbf{x}_0, t_0) = i\hbar \delta^{(3)}(\mathbf{x} - \mathbf{x}_0) \delta(t - t_0). \quad (3.1)$$

It is often called a “propagator”, as it propagates a wavefunction from a time t_0 to a time t :

$$\psi(\mathbf{x}, t) = \int d^3\mathbf{y} \ G(\mathbf{x}, t; \mathbf{y}, t_0) \psi(\mathbf{y}, t_0) \quad \text{for } t_0 < t. \quad (3.2)$$

In the Schrödinger picture, the propagator is also often written as

$$G(\mathbf{x}, t; \mathbf{x}_0, t_0) = \langle \mathbf{x} | \mathcal{T} e^{-\frac{i}{\hbar} \int_{t_0}^t \hat{H}(t') dt'} | \mathbf{x}_0 \rangle, \quad (3.3)$$

for a general—possibly time-dependent—Hamiltonian. If the Hamiltonian doesn't commute at different times, the exponential needs to be ordered along the time direction; this is indicated by the symbol \mathcal{T} . Next we divide the time interval $[t_0, t_1]$ into two parts by inserting a t_1 (with $t_0 < t_1 < t$), using [Equation 3.2](#) to split the propagator at t_1 :

$$\begin{aligned} \psi(\mathbf{x}_1, t_1) &= \int d^3\mathbf{x}_0 \ G(\mathbf{x}_1, t_1; \mathbf{x}_0, t_0) \psi(\mathbf{x}_0, t_0), \\ \psi(\mathbf{x}, t) &= \int d^3\mathbf{x}_1 \ G(\mathbf{x}, t; \mathbf{x}_1, t_1) \psi(\mathbf{x}_1, t_1), \\ &= \int d^3\mathbf{x}_1 \ G(\mathbf{x}, t; \mathbf{x}_1, t_1) \int d^3\mathbf{x}_0 \ G(\mathbf{x}_1, t_1; \mathbf{x}_0, t_0) \psi(\mathbf{x}_0, t_0). \end{aligned} \quad (3.4)$$

But the latter should also equal

$$\psi(\mathbf{x}, t) = \int d^3\mathbf{x}_0 \ G(\mathbf{x}, t; \mathbf{x}_0, t_0) \psi(\mathbf{x}_0, t_0). \quad (3.5)$$

Comparing [Equation 3.5](#) with [Equation 3.4](#) we get

$$G(\mathbf{x}, t; \mathbf{x}_0, t_0) = \int d^3\mathbf{x}_1 \ G(\mathbf{x}, t; \mathbf{x}_1, t_1) G(\mathbf{x}_1, t_1; \mathbf{x}_0, t_0) \quad \text{for } t_0 < t_1 < t. \quad (3.6)$$

In other words, we can view the propagator from t_0 to t as the sum of all possible propagators going from t_0 to t_1 , and then from t_1 to t for any given t_1 . We can

iterate this procedure, and slice the time interval into $n + 1 \rightarrow \infty$ infinitesimal segments of length $\epsilon = t_i - t_{i-1}$:

$$G(\mathbf{x}, t; \mathbf{x}_0, t_0) = \lim_{n \rightarrow \infty} \int d^3 \mathbf{x}_1 \cdots d^3 \mathbf{x}_n G(\mathbf{x}, t; \mathbf{x}_n, t_n) \cdots G(\mathbf{x}_1, t_1; \mathbf{x}_0, t_0). \quad (3.7)$$

The i -th segment is given by (see [Equation 3.3](#))

$$\begin{aligned} G(\mathbf{x}_i, t_i; \mathbf{x}_{i-1}, t_{i-1}) &= \langle \mathbf{x}_i | \mathcal{T} e^{-\frac{i}{\hbar} \int_{t_{i-1}}^{t_i} dt' \hat{H}(t')} | \mathbf{x}_{i-1} \rangle, \\ &= \delta^{(3)}(\mathbf{x}_i - \mathbf{x}_{i-1}) - \frac{i}{\hbar} \int_{t_{i-1}}^{t_i} dt' \langle \mathbf{x}_i | \hat{H}(t') | \mathbf{x}_{i-1} \rangle, \end{aligned} \quad (3.8)$$

up to $\mathcal{O}(\frac{1}{\hbar^2})$. We now make the ansatz

$$\hat{H}(t) = \frac{\hat{p}^2}{2m} + \hat{V}(\hat{x}, t). \quad (3.9)$$

The first term then gives

$$\begin{aligned} \langle \mathbf{x}_i | \frac{\hat{p}^2}{2m} | \mathbf{x}_{i-1} \rangle &= \int d^3 \mathbf{p}_i d^3 \mathbf{p}_{i-1} \langle \mathbf{x}_i | \mathbf{p}_i \rangle \langle \mathbf{p}_i | \frac{\hat{p}^2}{2m} | \mathbf{p}_{i-1} \rangle \langle \mathbf{p}_{i-1} | \mathbf{x}_{i-1} \rangle, \\ &= \frac{1}{2\pi\hbar} \int d^3 \mathbf{p}_i e^{\frac{i}{\hbar} \mathbf{p}_i \cdot (\mathbf{x}_i - \mathbf{x}_{i-1})} \frac{\mathbf{p}_i^2}{2m}, \end{aligned}$$

while the second term gives

$$\begin{aligned} \langle \mathbf{x}_i | \hat{V}(\hat{x}, t) | \mathbf{x}_{i-1} \rangle &= V(\mathbf{x}_i, t) \delta^{(3)}(\mathbf{x}_i - \mathbf{x}_{i-1}), \\ &= \frac{1}{2\pi\hbar} \int d^3 \mathbf{p}_i e^{\frac{i}{\hbar} \mathbf{p}_i \cdot (\mathbf{x}_i - \mathbf{x}_{i-1})} V(\mathbf{x}_i, t). \end{aligned}$$

Plugging these results back in [Equation 3.8](#), we get

$$\begin{aligned} G(\mathbf{x}_i, t_i; \mathbf{x}_{i-1}, t_{i-1}) &\approx \frac{1}{2\pi\hbar} \int d^3 \mathbf{p}_i e^{\frac{i}{\hbar} \mathbf{p}_i \cdot (\mathbf{x}_i - \mathbf{x}_{i-1})} \left(1 - \frac{i}{\hbar} \int_{t_{i-1}}^{t_i} dt' H(\mathbf{x}_i, \mathbf{p}_i, t') \right), \\ &= \frac{1}{2\pi\hbar} \int d^3 \mathbf{p}_i e^{\frac{i}{\hbar} \mathbf{p}_i \cdot (\mathbf{x}_i - \mathbf{x}_{i-1})} \mathcal{T} e^{-\frac{i}{\hbar} \int_{t_{i-1}}^{t_i} dt' H(\mathbf{x}_i, \mathbf{p}_i, t')}. \end{aligned}$$

To retrieve the full propagator, we combine all segments using the transitivity:

$$G(\mathbf{x}, t; \mathbf{x}_0, t_0) = \lim_{n \rightarrow \infty} \int \prod_{i=1}^n d^3 \mathbf{x}_i \prod_{j=1}^{n+1} \frac{d^3 \mathbf{p}_j}{2\pi\hbar} \mathcal{T} e^{\frac{i}{\hbar} \sum_0^n \left[\mathbf{p}_i \cdot (\mathbf{x}_i - \mathbf{x}_{i-1}) - \frac{i}{\hbar} \int_{t_{i-1}}^{t_i} dt' H(\mathbf{x}_i, \mathbf{p}_i, t') \right]}.$$

We can write the product between the momentum and position vectors in the exponential as a time integral

$$\sum_0^\infty \mathbf{p}_i \cdot (\mathbf{x}_i - \mathbf{x}_{i-1}) = \sum_0^\infty \epsilon \mathbf{p}_i \cdot \frac{\mathbf{x}_i - \mathbf{x}_{i-1}}{\epsilon} = \int_{t_0}^t dt' \mathbf{p}(t') \dot{\mathbf{x}}(t'), \quad (3.10)$$

such that we can combine the two terms in the exponential. So we finally get

$$G(\mathbf{x}, t; \mathbf{x}_0, t_0) = \int \mathcal{D}\mathbf{x} \mathcal{D}\mathbf{p} e^{\frac{i}{\hbar} \int_{t_0}^t dt' [\mathbf{p} \cdot \dot{\mathbf{x}} - H]} = \int \mathcal{D}\mathbf{x} \mathcal{D}\mathbf{p} e^{\frac{i}{\hbar} S}. \quad (3.11)$$

In other words, the Green's function that propagates a space point \mathbf{x}_0 at time t_0 to a space point \mathbf{x} at time t can be written as an integral over all possible paths; a path integral of the action. This is a result on which we will build when going to quantum field theory.

Definition of the Path Integral

Let us now try to develop the formalism a bit more formal, starting with path integrals of scalar fields. The result in [Equation 3.11](#) is a path integral over coordinates and momenta, but in [QFT](#) we of course would like to express it as an integral over the fields. First we expand the scalar field in an arbitrary basis $\{u_i\}$:

$$\phi(x) \stackrel{\text{def}}{=} \sum \alpha_i u_i(x), \quad (3.12)$$

where the coefficients are just real numbers, and the basis is chosen to be orthonormal:

$$\int d^4x u_i(x) u_j(x) \stackrel{\text{def}}{=} \delta_{ij}. \quad (3.13)$$

Because of the orthonormality of the basis, we can retrieve the α_i coefficient by projecting ϕ on u_i :

$$\alpha_i = \int d^4x \phi(x) u_i(x). \quad (3.14)$$

If we cut off the series in Equation 3.12 at a value n , we can write any functional of the field in function of the n coefficients α_i :

$$F[\phi] \xrightarrow{\text{cut at } n} F^n(\alpha_1, \dots, \alpha_n).$$

Now it is straightforward to give a sensible definition of the path integral. First note that integrating over all possible fields is the same as integrating over all possible field coefficients α_i . So for the series expansion cut at n , the path integral over a functional F is simply

$$\int \mathcal{D}^{\text{cut}} \phi F[\phi] = \int_{-\infty}^{+\infty} d\alpha_1 \cdots d\alpha_n F^n(\alpha_1, \dots, \alpha_n).$$

It is thus logical to define the path integral for an uncut series expression as

Path Integral

$$\int \mathcal{D}\phi F[\phi] \stackrel{\text{def}}{=} \lim_{n \rightarrow \infty} \int_{-\infty}^{+\infty} d\alpha_1 \cdots d\alpha_n F^n(\alpha_1, \dots, \alpha_n), \quad (3.15)$$

under the condition that this limit exists. The path integral is linear and translation invariant:

$$\int \mathcal{D}\phi (aF[\phi] + bG[\phi]) = a \int \mathcal{D}\phi F[\phi] + b \int \mathcal{D}\phi G[\phi], \quad (3.16a)$$

$$\int \mathcal{D}\phi F[\phi + \chi] = \int \mathcal{D}\phi F[\phi], \quad (3.16b)$$

where the latter is of course only valid if χ doesn't depend on ϕ . Instead of translating the field, we could also rotate it:

$$\bar{\phi}(y) \stackrel{\text{def}}{=} \int d^4x L(y, x) \phi(x). \quad (3.17)$$

In this case the coefficients of $\bar{\phi}$ are related to those of ϕ by the coefficients of L :

$$\bar{\alpha}_i = \sum_j L_{ij} \alpha_j.$$

This variable change will modify the integration measure with a determinant:

$$\prod \alpha_i \rightarrow \prod \bar{\alpha}_i = \det L^n \prod \alpha_i,$$

and hence

$$\mathcal{D}\phi \rightarrow \mathcal{D}\bar{\phi} = \det L \mathcal{D}\phi . \quad (3.18)$$

We can combine translation and rotation in one formula:

$$\int \mathcal{D}\phi F[L\phi + \chi] = \det L \int \mathcal{D}\phi F[\phi] , \quad (3.19)$$

where we adopted the shorthand notation

$$L\phi \stackrel{\text{N}}{=} \int d^4x L(y, x)\phi(x) , \quad (3.20)$$

which is a notation that we will often use, as a matter of saving space.

Gaussian Path Integral

By far the most important path integral is a Gaussian integral, because—as we will see—field correlators are related to the path integral of an exponential of the action. Because the kinetic field terms in the action are quadratic by nature, they lead to a Gaussian path integral. A general Gaussian path integral can be written as:

$$\int \mathcal{D}\phi e^{-\int d^4x d^4y \phi(x)K(x, y)\phi(y)} , \quad (3.21)$$

where $K(x, y)$ is a real symmetric operator by definition,¹ and is commonly called a Kähler metric. Expanding the fields in their coefficients, we can write

$$\int d^4x d^4y \phi(x)K(x, y)\phi(y) = \sum_{i, j} \int d^4x d^4y \alpha_i u_i(x)K(x, y)\alpha_j u_j(y) . \quad (3.22)$$

If we expand K in the same basis as ϕ :

$$K(x, y) \stackrel{\text{def}}{=} \sum_{i, j} K_{ij} u_i(x)u_j(y) , \quad (3.23)$$

we can retrieve its coefficients by projecting—now twice—on the basis functions:

$$K_{ij} = \int d^4x d^4y u_i(x)K(x, y)u_j(y) . \quad (3.24)$$

¹ If it is not symmetric, only its symmetric part contributes to the result.

This is exactly the integral in Equation 3.22, i.e. we can write

$$\int d^4x d^4y \phi(x)K(x,y)\phi(y) = \sum_{i,j} \alpha_i K_{ij} \alpha_j, \quad (3.25)$$

So the Gaussian path integral is now given by:

$$\lim_{n \rightarrow \infty} \int \prod d\alpha_i e^{-\sum_{i,j} \alpha_i K_{ij}^n \alpha_j}.$$

The components of K^n represent a $n \times n$ matrix which can be orthogonalised as

$$K_{ij}^n = \sum_{k,l} O_{ik} B_{kl} O_{lj},$$

where B is diagonal, i.e.

$$B_{kl} = \lambda_k \delta_{kl} \quad (\text{no sum over } k),$$

and where the orthogonal matrices O have unit determinant. We absorb them by redefining α_i :

$$\beta_i \stackrel{\text{def}}{=} \sum_j O_{ij} \alpha_j,$$

so that we can rewrite

$$\sum_{i,j} \alpha_i K_{ij}^n \alpha_j = \sum_i \lambda_i \beta_i^2. \quad (3.26)$$

The integration measures remain invariant:

$$\prod d\beta_i = \det O \prod d\alpha_i = \prod d\alpha_i. \quad (3.27)$$

The exponential can now be rewritten as a product of n exponentials:

$$e^{\sum_i \lambda_i \beta_i^2} = \prod_i e^{\lambda_i \beta_i^2},$$

so the Gaussian path integral becomes a product of n Gaussian integrals:

Gaussian Path Integral

$$\int \mathcal{D}\phi e^{-\int d^4x d^4y \phi(x)K(x,y)\phi(y)} = N_G \frac{1}{\sqrt{\det K}}, \quad (3.28)$$

where

$$N_G = \lim_{n \rightarrow \infty} \sqrt{\pi^n} \quad (3.29)$$

is an infinite constant that we will divide out in a later stage, and

$$\det K = \lim_{n \rightarrow \infty} \det K^n,$$

provided that this limit exists. Let us investigate a trivial example, where

$$K(x, y) = \delta^{(4)}(x - y).$$

The components of K are then:

$$K_{ij} = \int d^4x \ u_i(x)u_j(x) = \delta_{ij},$$

which is simply the identity matrix with determinant $\det K^n = 1$. Because the determinant is independent of n , taking the limit doesn't change it, i.e. $\det K = 1$ as well. We hence have

$$\int \mathcal{D}\phi \ e^{-\int d^4x \ \phi^2(x)} = N_G. \quad (3.30)$$

n-Point Gaussian Integrals

Now that we know how to path-integrate Gaussian functions, we investigate what to do when the exponential contains, next to quadratic terms, linear terms as well:

$$A[\phi, J] = - \int d^4x \ d^4y \ \phi(x)K(x, y)\phi(y) + \int d^4x \ J(x)\phi(x).$$

If this would be a regular (non-path) integration, the way to proceed would be to 'complete the square', i.e.

$$\int dx \ e^{-ax^2+bx} = e^{\frac{b^2}{4a}} \int dx \ e^{-a(x-\frac{b}{2a})^2} = e^{\frac{b^2}{4a}} \int dx \ e^{-ax^2}. \quad (3.31)$$

We will now try a similar approach on the functionals. First we define

$$\bar{\phi}(x) = \phi(x) - \frac{1}{2} \int d^4x' \ K^{-1}(x, x')J(x'), \quad (3.32)$$

where K^{-1} is the inverse Kähler metric, satisfying

$$\int d^4z \ K(x, z)K^{-1}(z, y) = \delta^{(4)}(x - y). \quad (3.33)$$

Next we can write $A[\phi, J]$ in function of the new fields $\bar{\phi}$:

$$\begin{aligned} A[\phi, J] = & - \int d^4x d^4y \left(\bar{\phi}(x) + \frac{1}{2} \int d^4x' K^{-1}(x, x') J(x') \right) \\ & \times K(x, y) \left(\bar{\phi}(y) + \frac{1}{2} \int d^4y' K^{-1}(y, y') J(y') \right) \\ & + \int d^4x J(x) \left(\bar{\phi}(x) + \frac{1}{2} \int d^4x' K^{-1}(x, x') J(x') \right), \end{aligned}$$

which gives after using [Equation 3.33](#):

$$A[\phi, J] = - \int d^4x d^4y \left[\bar{\phi}(x) K(x, y) \bar{\phi}(y) - \frac{1}{4} J(x) K^{-1}(x, y) J(y) \right].$$

Because in the path integral formalism fields are *functions*, not operators, they commute and we can always factor out the exponential, writing the sum as a product of two exponentials.² Furthermore, from [Equation 3.32](#) we see that the shift in $\bar{\phi}$ is independent on ϕ , it hence leaves the integration invariant (because of translation invariance). So the path integral is given by:

Completing the Square in a Path Integral

$$\int \mathcal{D}\phi e^{-\phi K \phi + J \phi} = e^{\frac{1}{4} J K^{-1} J} \int \mathcal{D}\phi e^{-\phi K \phi}, \quad (3.34)$$

with the abbreviations

$$\phi K \phi \stackrel{\text{N}}{=} \int d^4x d^4y \phi(x) K(x, y) \phi(y), \quad (3.35a)$$

$$J \phi \stackrel{\text{N}}{=} \int d^4x J(x) \phi(x), \quad (3.35b)$$

$$J K^{-1} J \stackrel{\text{N}}{=} \int d^4x d^4y \frac{1}{4} J(x) K^{-1}(x, y) J(y). \quad (3.35c)$$

Look how closely it resembles the regular integration technique in [Equation 3.31](#).

² Even when the fields are Lie algebra-valued they commute, because we assume that in general the Kähler is diagonal in Lie indices, i.e. $K \sim \delta^{ab}$, which implies both fields have the same generator so that they commute.

A last thing we want to investigate is how to make path integrations of Gaussians with fields in front of the exponential, evaluated at different points, i.e.

$$\int \mathcal{D}\phi \phi(x_1) \cdots \phi(x_n) e^{-\phi K \phi}. \quad (3.36)$$

We will call this an n -point *Gaussian path integral*. For odd n , the path integral cancels because the integrand is an odd function, so let us start with a 2-point integral. If this would be a regular integration, the way to proceed would be to make a derivation w.r.t. the coefficient in front of x^2 in the exponent:

$$\int dx x^2 e^{-ax^2} = -\frac{d}{da} \int dx e^{-ax^2} = -\frac{d}{da} \sqrt{\frac{\pi}{a}}.$$

If we want to do something similar in the path integral formalism, we first need to find a sensible derivative. Without going too much into the formal details, we define the *functional derivative* of a functional by its action on a test function:

Functional Derivative

$$\frac{\delta J(y)}{\delta J(x)} \stackrel{\text{def}}{=} \delta^{(4)}(x-y). \quad (3.37)$$

It commutes with integration, so that

$$\frac{\delta}{\delta J(x)} \int d^4 y J(y) \phi(y) = \phi(x). \quad (3.38)$$

For all other calculations it can be treated as a normal derivative on the functions. It obeys e.g. the same Leibniz' rule as the standard derivative:

$$\frac{\delta}{\delta J(x)} \left(F[J] G[J] \right) = \frac{\delta F[J]}{\delta J(x)} G[J] + F[J] \frac{\delta G[J]}{\delta J(x)}. \quad (3.39)$$

just as it obeys the chain rule as well:

$$\begin{aligned} \frac{\delta}{\delta J(x)} e^{\int d^4 y J(y) \phi(y)} &= \left(\frac{\delta}{\delta J(x)} \int d^4 y J(y) \phi(y) \right) e^{\int d^4 y J(y) \phi(y)}, \\ &= \phi(x) e^{\int d^4 y J(y) \phi(y)}, \end{aligned} \quad (3.40)$$

The latter allows us to write the 2-point integral as a double derivative:

$$\int \mathcal{D}\phi \phi(x_1)\phi(x_2) e^{-\phi K\phi} = \frac{\delta}{\delta J(x_1)} \frac{\delta}{\delta J(x_2)} \int \mathcal{D}\phi e^{-\phi K\phi + J\phi} \Big|_{J=0}. \quad (3.41)$$

And we know how to calculate the integral in the r.h.s., as we calculated it in Equation 3.34. The J -dependence then sits in the exponential in front of the path integral:

$$\int \mathcal{D}\phi \phi(x_1)\phi(x_2) e^{-\phi K\phi} = \left(\frac{\delta}{\delta J(x_1)} \frac{\delta}{\delta J(x_2)} e^{\frac{1}{4}JK^{-1}J} \right)_{J=0} \int \mathcal{D}\phi e^{-\phi K\phi}. \quad (3.42)$$

The chain rule brings the term $JK^{-1}J$ in front of the exponential, which we can easily calculate:

$$\begin{aligned} & \frac{\delta}{\delta J(x_2)} \int d^4x d^4y J(x)K^{-1}(x,y)J(y) \\ &= \int d^4x d^4y \left[\delta^{(4)}(x-x_2) K^{-1}(x,y)J(y) + J(x)K^{-1}(x,y) \delta^{(4)}(y-x_2) \right], \\ &= \int d^4y K^{-1}(x_2,y)J(y) + \int d^4x J(x)K^{-1}(x,x_2), \\ &= 2 \int d^4x J(x)K^{-1}(x,x_2). \end{aligned}$$

The last step is valid because K^{-1} is symmetric. Using the shorthand $J_i \stackrel{\text{N}}{=} J(x_i)$ we then have:

$$\begin{aligned} \frac{\delta}{\delta J_1} \frac{\delta}{\delta J_2} e^{\frac{1}{4}JK^{-1}J} &= \frac{1}{2} \frac{\delta}{\delta J_1} J_x K_{x2}^{-1} e^{\frac{1}{4}JK^{-1}J}, \\ &= \frac{1}{2} \left(\frac{\delta}{\delta J_1} J_x K_{x2}^{-1} \right) e^{\frac{1}{4}JK^{-1}J} + \frac{1}{2} J_x K_{x2}^{-1} \frac{\delta}{\delta J_1} e^{\frac{1}{4}JK^{-1}J}, \\ &= \frac{1}{2} K_{12}^{-1} e^{\frac{1}{4}JK^{-1}J} + J_x K_{x2}^{-1} J_y K_{y1}^{-1} e^{\frac{1}{4}JK^{-1}J}, \\ &\stackrel{J=0}{=} \frac{1}{2} K^{-1}(x_1, x_2). \end{aligned}$$

This gives us the final result for a 2-point Gaussian path integral:

$$\int \mathcal{D}\phi \phi(x_1)\phi(x_2) e^{-\phi K\phi} = \frac{1}{2} K^{-1}(x_1, x_2) \int \mathcal{D}\phi e^{-\phi K\phi}. \quad (3.43)$$

Generalising this to an n -point integral is trivial, as we just can write

n -point Gaussian Path Integral

$$\int \mathcal{D}\phi \phi_1 \cdots \phi_n e^{-\phi K \phi} = \frac{\delta}{\delta J_1} \cdots \frac{\delta}{\delta J_n} e^{\frac{1}{4} J K^{-1} J} \Big|_{J=0} \int \mathcal{D}\phi e^{-\phi K \phi}, \quad (3.44)$$

where we introduced the shorthand notation $\phi_n \stackrel{N}{=} \phi(x_n)$. However, we have to be careful as Leibniz' rule chains non-trivially at higher orders. E.g. for the case with four fields, we get

$$\begin{aligned} \frac{\delta}{\delta J_1} \frac{\delta}{\delta J_2} \frac{\delta}{\delta J_3} \frac{\delta}{\delta J_4} e^{\frac{1}{4} J K^{-1} J} &= \frac{1}{2} \frac{\delta}{\delta J_1} \frac{\delta}{\delta J_2} \frac{\delta}{\delta J_3} J_x K_{x4}^{-1} e^{\frac{1}{4} J K^{-1} J}, \\ &= \frac{\delta}{\delta J_1} \frac{\delta}{\delta J_2} \left(\frac{1}{2} K_{34}^{-1} + \frac{1}{4} J_x K_{x4}^{-1} J_y K_{y3}^{-1} \right) e^{\frac{1}{4} J K^{-1} J}, \\ &= \frac{\delta}{\delta J_1} \left(\frac{1}{4} K_{34}^{-1} J_x K_{x2}^{-1} + \frac{1}{4} K_{23}^{-1} J_x K_{x4}^{-1} + \frac{1}{4} J_y K_{y3}^{-1} K_{24}^{-1} \right. \\ &\quad \left. + \frac{1}{4} J_y K_{y3}^{-1} J_x K_{x4}^{-1} J_z K_{z2}^{-1} \right) e^{\frac{1}{4} J K^{-1} J}, \\ &= \frac{1}{4} \left(K_{34}^{-1} K_{12}^{-1} + K_{23}^{-1} K_{14}^{-1} + K_{13}^{-1} K_{24}^{-1} + \mathcal{O}(J) \right) e^{\frac{1}{4} J K^{-1} J}, \\ &\stackrel{J=0}{=} \frac{1}{4} \left(K_{12}^{-1} K_{34}^{-1} + K_{13}^{-1} K_{24}^{-1} + K_{14}^{-1} K_{23}^{-1} \right). \end{aligned}$$

So any n -point Gaussian path integral is just a set of all possible combinations of $n/2$ inverse Kähler metrics in front of a standard Gaussian, when n is even. Indeed, for any n even, we have found that

$$\int \mathcal{D}\phi \phi_{i_1} \cdots \phi_{i_n} e^{-\phi K \phi} = \frac{(n-1)!!}{2^{\frac{n}{2}}} K_{(i_1 i_2}^{-1} \cdots K_{i_{n-1} i_n}^{-1})} \int \mathcal{D}\phi e^{-\phi K \phi}. \quad (3.45)$$

The factor in front deserves a short explanation. First of all, the factor $2^{-n/2}$ comes from the fact that every K^{-1} gets a $1/2$ in front (see Equation 3.43).³ On the other hand, the double factorial

$$(n-1)!! = (n-1) \cdot (n-3) \cdot \cdots \cdot 3 \cdot 1 \quad (3.46)$$

represents the number of possible combinations to pick unordered pairs from an even set of n elements. It is needed to cancel the normalisation factor from the symmetrisation procedure, but we can ignore this factor if we instead of normalising the symmetry just make all possible unique permutations of the

3 This is the reason why one commonly chooses to put a factor $1/2$ in front of the kinetic terms in the scalar Lagrangian, as it will manifest in the Kähler as a factor 2, cancelling the overall factor $2^{-n/2}$.

indices. Note that relating the n -point integral to a combination of 2-point integrals is exactly the same as making a Wick contraction, so we have found a nice mathematical explanation for a relation that is otherwise—arguably—a bit less elegant to prove.

Until now we have only considered a real scalar field. Generalising this to a complex scalar field is trivial. First of all, the Gaussian can be calculated in the same way as before, by expanding the field in function of a set of basis vectors $u_i(x)$, and cutting the series at a value n . Then using the result for a standard integral in Equation B.4j, we find:

Complex Gaussian Path Integral

$$\int \mathcal{D}\phi^* \mathcal{D}\phi e^{-\phi^* K \phi} = \frac{N_G^*}{\det A}, \quad (3.47)$$

where $N_G^* = \lim_{n \rightarrow \infty} (2\pi i)^n$. Note that now the dependence on the determinant is without the square root; a consequence of the fact that we have two path integrations. Completing the square goes the same as before, but because we now have two source terms (J and J^*), the result is without the factor $1/4$:

$$\int \mathcal{D}\phi^* \mathcal{D}\phi e^{-\phi^* K \phi + J^* \phi + J \phi^*} = e^{J^* K^{-1} J} \int \mathcal{D}\phi^* \mathcal{D}\phi e^{-\phi^* K \phi}. \quad (3.48)$$

Finally, n -point Gaussians can be calculated in the same way as well, where this time we use two functional derivatives, one to J and one to J^* (note that to bring down a ϕ we need to derive w.r.t. J^* and vice versa):

$$\begin{aligned} \int \mathcal{D}\phi^* \mathcal{D}\phi \phi_{i_1} \cdots \phi_{i_m} \phi_{j_1}^* \cdots \phi_{j_n}^* e^{-\phi^* K \phi} &= \frac{\delta}{\delta J_{i_1}^*} \cdots \frac{\delta}{\delta J_{i_m}^*} \frac{\delta}{\delta J_{j_{m+1}}} \cdots \frac{\delta}{\delta J_{j_n}} e^{J^* K^{-1} J} \Big|_{J, J^* = 0} \\ &\times \int \mathcal{D}\phi^* \mathcal{D}\phi e^{-\phi^* K \phi}. \end{aligned} \quad (3.49)$$

Note that this is an $n + m$ -point integral. There are however two important differences, as compared to the real field, when identifying the derivatives with the inverted Kähler metric. First of all, if in the above equation $m \neq n$, i.e. when the number of δ_J doesn't equal the number of δ_{J^*} , the result will automatically be zero after setting $J, J^* = 0$. So we have the natural requirement $m \equiv n$. But more importantly, as compared to the real n -point Gaussian, the number of possible combinations will be smaller. Where in the real case the number of possible combinations equals $(n - 1)!!$, in the complex case this is only $(n/2)!$,

for a total number of n derivatives.⁴ Consider e.g. the calculation of the 4-point integral:

$$\begin{aligned}
 \frac{\delta}{\delta J_1} \frac{\delta}{\delta J_2} \frac{\delta}{\delta J_3^*} \frac{\delta}{\delta J_4^*} e^{J^* K^{-1} J} &= \frac{\delta}{\delta J_1} \frac{\delta}{\delta J_2} \frac{\delta}{\delta J_3^*} \left(K_{x4}^{-1} J_x e^{J^* K^{-1} J} \right), \\
 &= \frac{\delta}{\delta J_1} \frac{\delta}{\delta J_2} \left(K_{x4}^{-1} J_x K_{y3}^{-1} J_y e^{J^* K^{-1} J} \right), \\
 &= \frac{\delta}{\delta J_1} \left(K_{24}^{-1} K_{y3}^{-1} J_y + K_{x4}^{-1} J_x K_{23}^{-1} \right) e^{J^* K^{-1} J}, \\
 &\stackrel{J, J^* = 0}{=} K_{13}^{-1} K_{24}^{-1} + K_{14}^{-1} K_{23}^{-1}. \tag{3.50}
 \end{aligned}$$

When comparing this to the real result, we see that the missing term is $K_{12}^{-1} K_{34}^{-1}$, which would connect two coordinates that are both belonging to non-conjugated fields, and two coordinates that are both belonging to conjugated fields. It is easy to show that

$$\int \mathcal{D}\phi^* \mathcal{D}\phi \phi_1 \phi_2 e^{-\phi^* K \phi} = \int \mathcal{D}\phi^* \mathcal{D}\phi \phi_1^* \phi_2^* e^{-\phi^* K \phi} = 0. \tag{3.51}$$

Hence when making all possible combinations, we only make those that cross conjugated and non-conjugated fields. Using index notation, we can write this as:

$$\begin{aligned}
 \int \mathcal{D}\phi^* \mathcal{D}\phi \phi_{i_1} \phi_{j_1}^* \cdots \phi_{i_n} \phi_{j_n}^* e^{-\phi^* K \phi} &= n! \binom{-1}{i_1} \cdots \binom{-1}{i_n} \\
 &\times \int \mathcal{D}\phi \mathcal{D}\phi^* e^{-\phi^* K \phi}, \tag{3.52}
 \end{aligned}$$

where again the factor $n!$ in front is only needed to cancel the normalisation of the symmetrisation.

3.2 QUANTISATION OF THE SCALAR FIELD

Let us see how we can use the path integral formalism in order to quantise any field theory, starting with a scalar field theory—as this is the most trivial to work

⁴ To appreciate the difference: the real 8-point correlator has 105 terms, while for the complex there are only 24.

with, and as the results can be easily ported to higher-spin fields. Motivated by [Equation 3.11](#), we expect the propagator to be related to

$$\int \mathcal{D}\phi \, e^{iS}.$$

Note that from now on we will work in natural units, hence $\hbar \equiv 1$ and $c \equiv 1$.

The Free Scalar Field

The action for a free scalar field is given by [Equation 1.9](#) (we still consider the field to be real-valued):

$$S_0^{\text{scalar}} = \int d^4x \left(\frac{1}{2} \partial_\mu \phi \partial^\mu \phi - \frac{1}{2} m^2 \phi^2 \right).$$

Using partial integration, we can rewrite this as

$$S_0^{\text{scalar}} = -\frac{1}{2} \int d^4x \, d^4y \, \phi(x) \delta^{(4)}(x-y) (\square + m^2) \phi(y), \quad (3.53)$$

hence the Kähler metric is given by

$$K(x, y) = \frac{i}{2} \delta^{(4)}(x-y) (\square + m^2). \quad (3.54)$$

Note that the Kähler includes the Klein-Gordon operator $\square + m^2$ (see [Equation 1.10](#)). Its inverse is defined so to satisfy

$$\int d^4z \, K(x, z) K^{-1}(z, y) \equiv \delta^{(4)}(x-y).$$

Here we hence have

$$\frac{i}{2} (\square + m^2) K^{-1}(x, y) \equiv \delta^{(4)}(x-y). \quad (3.55)$$

Now comes the important part. In the canonical quantisation framework, quantisation is implemented by imposing canonical commutation relations on the fields. Next these are used in order to construct the free scalar propagator D_F as a 2-point correlation. Applying the Klein-Gordon [Equation 1.10](#) on this propagator then yields the equation:

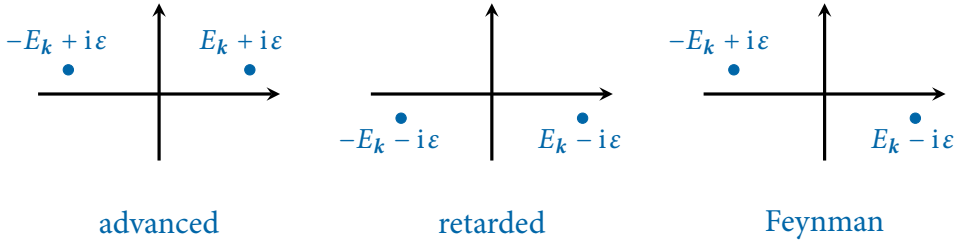


Figure 3.1: Pole structures for the three most common propagators, from left to right: the advanced, retarded and Feynman propagator. Their definitions are given in [Equation 3.58](#) and [Equations 3.59](#), while the energy is simply $E_k = \sqrt{\mathbf{k}^2 + m^2}$.

Klein-Gordon Propagator Equation

$$(\square + m^2) D_F(x, y) \equiv -i \delta^{(4)}(x - y). \quad (3.56)$$

But we didn't impose commutation relations, and so we don't yet have derived a sensible definition for the propagator. We can avoid the need for canonical commutation relations by comparing [Equation 3.56](#) with [Equation 3.55](#). Instead of trying to derive the propagator, we simply *define* it as

$$D_F(x, y) \stackrel{\text{def}}{=} \frac{1}{2} K^{-1}(x, y). \quad (3.57)$$

So this is the main difference between the two formalisms: while in the canonical quantisation framework, quantisation itself lies in the canonical commutation relations (which will eventually lead to the above identification between the inverse Kähler and the propagator), in the path integral quantisation framework we skip the commutation relations, and directly impose this identification. Hence [Equation 3.57](#) summarises the fundamental basis of quantisation in the path integral formalism.

[Equation 3.56](#) can be easily solved in momentum space, giving the definition of the Feynman scalar propagator:

Feynman Scalar Propagator

$$D_F(x, y) = \int \frac{d^4k}{(2\pi)^n} \frac{i}{k^2 - m^2 + i\epsilon} e^{-ik \cdot (x-y)}, \quad (3.58)$$

where ϵ is a pole-prescription that follows from the technicalities in the calculation. The solution is not unique, and different prescriptions lead to propagators

that have different causal behaviours. Two examples are the advanced and retarded propagators:

$$D_{\text{adv}} = \int \frac{d^4 k}{(2\pi)^n} \frac{i}{(k^0 - i\varepsilon)^2 - \mathbf{k}^2 - m^2} e^{-ik \cdot (x-y)}, \quad (3.59a)$$

$$D_{\text{ret}} = \int \frac{d^4 k}{(2\pi)^n} \frac{i}{(k^0 + i\varepsilon)^2 - \mathbf{k}^2 - m^2} e^{-ik \cdot (x-y)}. \quad (3.59b)$$

The pole structures for these three propagators are shown in [Figure 3.1](#). In what remains of this thesis, we will exclusively deal with the Feynman propagator in [Equation 3.58](#). See e.g. [18–20] for more detail.

Now that we have identified the propagator with the inverse Kähler, we investigate how it emerges from (possibly a combination of) path integrals of the exponentiated action. The path integral over the action is just a standard zero-point Gaussian, which we already solved in [Equation 3.28](#):

$$\int \mathcal{D}\phi e^{iS} = \frac{N_{\mathcal{G}}}{\sqrt{\det \frac{i}{2} \delta^{(4)}(x-y) (\square + m^2)}} \quad (3.60)$$

To calculate its determinant, we again expand K in function of the basis functions $u_i(x)$, and cut the series again at n . It is clear that this determinant is merely a constant—as there is no field dependence inside—but as an illustration of the techniques involved it is interesting to calculate it. First we express the basis functions as discrete Fourier series, so that we can let the derivatives work on them:

$$u_i(x) = \frac{1}{V} \sum_m^n e^{-ik_m \cdot x} u_i(k_m), \quad (3.61)$$

where

$$k_m^\mu = \frac{2\pi m^\mu}{L}, \quad V = L^4,$$

and where m^μ is an integer. So the elements of K are given by:

$$\begin{aligned} K_{ij} &= \frac{i}{2} \int d^4 x d^4 y u_i(x) \delta^{(4)}(x-y) (\square + m^2) u_j(y), \\ &= \frac{i}{2} m^2 \delta_{ij} + \frac{i}{2} \frac{1}{V^2} \sum_{m,l} \int d^4 x e^{-ik_n \cdot x} u_i(k_m) \partial^2 e^{-ik_l \cdot x} u_j(k_l), \\ &= \frac{i}{2} m^2 \delta_{ij} - \frac{i}{2} \frac{1}{V^2} (2\pi)^4 \sum_{m,l} k_l^2 \delta^{(4)}(k_m + k_l) u_i(k_m) u_j(k_l), \\ &= \frac{i}{2} m^2 \delta_{ij} - i \frac{8\pi^4}{V^2} \sum_m k_m^2 u_i(k_m) u_j(-k_m). \end{aligned}$$

This determinant can be calculated, because for any $n \times n$ matrix that has this form, the determinant is simply given by

$$\begin{vmatrix} a + x_1 y_1 & x_1 y_2 & \cdots & x_1 y_n \\ x_2 y_1 & a + x_2 y_2 & \cdots & x_2 y_n \\ \vdots & \vdots & \ddots & \vdots \\ x_n y_1 & x_n y_2 & \cdots & a + x_n y_n \end{vmatrix} = a^{n-1} \left(a + \sum_1^n x_i y_i \right). \quad (3.62)$$

Applied to the Kähler this is

$$\det K^n = \left(\frac{i}{2} \right)^n m^{2n-2} \left[m^2 - \frac{(2\pi)^4}{V^2} \sum_i^n \sum_m^n k_m^2 u_i(k_m) u_i(-k_m) \right].$$

In other words, the path integral is again a constant:

$$\int \mathcal{D}\phi \, e^{iS_0^{\text{scalar}}} = N_\phi, \quad (3.63)$$

where the infinite constant now equals

$$N_\phi = \lim_{n \rightarrow \infty} \sqrt{\frac{(-2i\pi)^n}{m^{2n} - \sum_i^n k_i^2 f(k_i)}}, \quad (3.64)$$

$$f(k_m) = m^{2n-2} \frac{(2\pi)^4}{V^2} \sum_i^n \int d^4x \, d^4y \, e^{ik_m \cdot (x-y)} u_i(x) u_i(y). \quad (3.65)$$

I.e. the constant resums all possible mass and momentum modes up to infinity.

Now we are a bit stuck, as we wanted to relate the propagator to the path integral of the action, but the latter equals a constant without any dynamics, which is even infinite to make things worse. However, as we motivated in [Equation 3.57](#), the propagator is directly related to the inverse Kähler metric, which in turn emerges from the 2-point Gaussian path integral in [Equation 3.43](#):

$$\int \mathcal{D}\phi \, \phi_1 \phi_2 e^{-\phi K \phi} = \frac{1}{2} K_{12}^{-1} \int \mathcal{D}\phi \, e^{-\phi K \phi} = D_F(x_1, x_2) N_\phi. \quad (3.66)$$

If we divide this result by the zero-point integral (which equals N_ϕ), the bothersome infinite constant cancels out. In other words, we define the propagator to be equal to

Feynman Propagator as Path Integrals

$$D_F(x_1, x_2) \stackrel{\text{def}}{=} \frac{\int \mathcal{D}\phi \phi_1 \phi_2 e^{iS_0}}{\int \mathcal{D}\phi e^{iS_0}} . \quad (3.67)$$

The physical interpretation of the propagator follows from the fact that it is a solution to the Klein-Gordon Equation 3.56. Hence it remains the same as in QM but now expressed in spacetime, i.e. it is the amplitude for a particle travelling from a spacetime point x_1 to a spacetime point x_2 , and vice versa (because the propagator is symmetric).

The Feynman propagator equals the time-ordered 2-point correlation function of a field as defined in the canonical quantisation framework, i.e.

$$D_F(x, y) \equiv \langle 0 | \mathcal{T} \phi(x) \phi(y) | 0 \rangle .$$

Because in the path integral framework time-ordering is irrelevant (remember that the fields are mere functions, no operators), we can drop the \mathcal{T} from this notation. If one wants to relate results between the two formalisms, adding a \mathcal{T} in the correlator will do (at least from a notational point of view).

It is then trivial to generalise this definition to higher order correlation functions:

$$\langle 0 | \phi_1 \phi_2 \cdots \phi_n | 0 \rangle \stackrel{\text{def}}{=} \frac{\int \mathcal{D}\phi \phi_1 \phi_2 \cdots \phi_n e^{iS_0}}{\int \mathcal{D}\phi e^{iS_0}} , \quad (3.68)$$

These integrals are solved in Equation 3.45. E.g. for the 4-point correlator we find

$$\langle 0 | \phi_1 \phi_2 \phi_3 \phi_4 | 0 \rangle = D_F^{12} D_F^{34} + D_F^{13} D_F^{24} + D_F^{14} D_F^{23} . \quad (3.69)$$

So it represents 2 particles that are travelling from any of the four points to any of the other points. This is illustrated in Figure 3.2. Such pictures are called *Feynman diagrams*, after the famous physicist that invented them. The relation we found is true at any order: the n -point correlator represents $n/2$ identical particles that connect any two out of the n spacetime points.

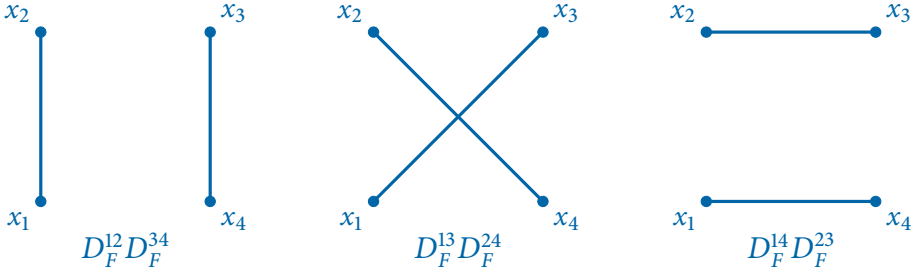


Figure 3.2: The scalar 4-point correlator can be interpreted in a physical way by using Feynman diagrams. Here two particles are created at different spacetime points. Each propagates to one of the remaining points and is annihilated. This can be done in three ways only, because the particles are indistinguishable.

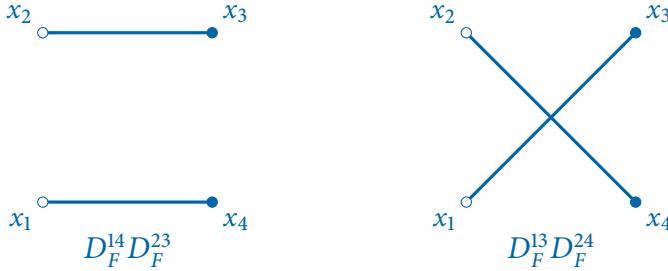


Figure 3.3: The complex scalar 4-point correlator represents all different possibilities for two complex scalar fields. A complex scalar propagator connects a conjugated field (represented as open dots) with a non-conjugated field (represented as filled dots).

Note in the case of complex scalar fields, the propagator can only connect a non-conjugated with a conjugated field, as was explained in Equation 3.50. This means e.g. :

$$\langle 0 | \phi_1^* \phi_2^* \phi_3 \phi_4 | 0 \rangle = D_F^{13} D_F^{24} + D_F^{14} D_F^{23}, \tag{3.70a}$$

$$\langle 0 | \phi_1 \phi_2^* \phi_3 \phi_4^* | 0 \rangle = D_F^{12} D_F^{34} + D_F^{14} D_F^{23}. \tag{3.70b}$$

The first relation is illustrated in Figure 3.3.

The Interacting Scalar Field

Let us now advance to an interacting scalar field theory. The most common is ϕ^4 -theory, so we will choose it as an example to quantise interacting scalar field theory. Its Lagrangian given by (see also [Equation 1.13](#)):

$$S^{\text{scalar}} = \int d^4x \left(\frac{1}{2} \partial_\mu \phi \partial^\mu \phi - \frac{1}{2} m^2 \phi^2 - \frac{\lambda}{4!} \phi^4 \right). \quad (3.71)$$

While it is in principle possible to calculate the Gaussian path integral that contains this action, it becomes quickly unmanageable to calculate n -point correlators, as we cannot use the derivation trick anymore. Instead, for any coupling constant λ smaller than one, we can expand interacting part of the action exponential:

$$e^{-\phi K \phi - \phi^4} = \left(1 - i \frac{\lambda}{4!} \int d^4x \phi(x) \phi(x) \phi(x) \phi(x) + \dots \right) e^{-\phi K \phi}. \quad (3.72)$$

The first $\mathcal{O}(\lambda)$ term is just a 4-point correlator, but with every field in the same point:

$$\int d^4x \int \mathcal{D}\phi \phi_x \phi_x \phi_x \phi_x e^{-\phi K \phi} = 3N_\phi \int d^4x D_F(x, x) D_F(x, x). \quad (3.73)$$

This can be interpreted (up to an irrelevant constant N_ϕ) as the creation of two particles at some point x , that propagate over an undefined distance only to be annihilated again in exactly the same point. Furthermore, this result is integrated over all possible spacetime points. Higher orders give the same result, be it with more particles as intermediate steps (but every diagram is ‘closed’, i.e. there are no external points, instead every point is integrated over). It hence symbolises the natural excitation of an interacting scalar field over all spacetime, better known as the *vacuum energy*. However, this vacuum diagrams are a bit troublesome, as they are infinite by definition—and not only due to the factor N_ϕ (we don’t mind the latter, as we will divide it out anyway). We can see this by using the Fourier transform of the propagator:

$$\begin{aligned} \int d^4x D_F(x, x) D_F(x, x) &= \int d^4x \frac{d^4k_1}{(2\pi)^4} \frac{d^4k_2}{(2\pi)^4} \frac{i e^{-ik_1 \cdot (x-x)}}{k_1^2 - m^2 + i\epsilon} \frac{i e^{-ik_2 \cdot (x-x)}}{k_2^2 - m^2 + i\epsilon}, \\ &= \left(\int d^4x \right) \int \frac{d^4k_1}{(2\pi)^4} \frac{d^4k_2}{(2\pi)^4} \frac{i}{k_1^2 - m^2 + i\epsilon} \frac{i}{k_2^2 - m^2 + i\epsilon}, \end{aligned}$$

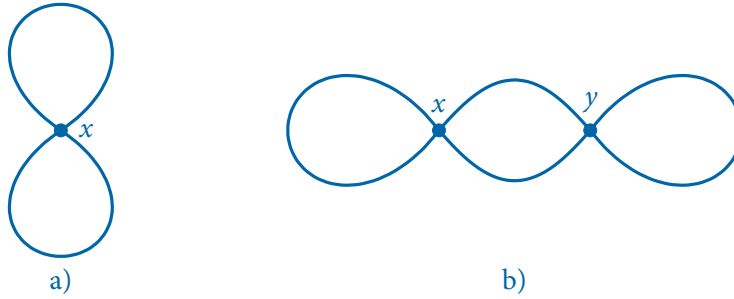


Figure 3.4: a) The **NLO** vacuum Feynman diagram for ϕ^4 -theory, where two particles are created and annihilated in the same point. b) An **NNLO** example.

where the factor in front explodes to infinity. The only solution we have to get a finite result, is to divide these modes out, just as we did in the free case. we will soon see how to accomplish this.

Now for a more interesting example, we investigate the situation where we have two extra fields at different spacetime point in front of the expansion (we already divided by N_ϕ —the path integral over the free action—in order to cancel it):

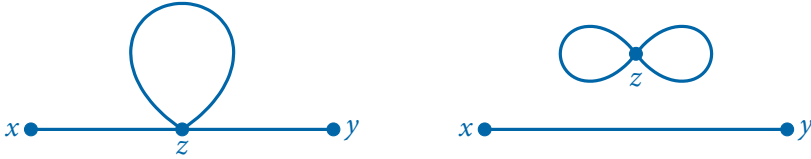
$$\begin{aligned} \frac{1}{N_\phi} \int \mathcal{D}\phi \phi_x \phi_y \left(1 - i \frac{\lambda}{4!} \int d^4z \phi_z \phi_z \phi_z \phi_z + \dots \right) e^{-\phi K \phi}, \\ = D_F(x, y) - i \frac{\lambda}{4!} \frac{1}{N_\phi} \int d^4z \int \mathcal{D}\phi \phi_x \phi_y \phi_z \phi_z \phi_z \phi_z e^{-\phi K \phi} + \dots \end{aligned} \quad (3.74)$$

The first term is again the propagator, and the next terms are $\mathcal{O}(\lambda)$ corrections. We will interpret this result as the *full propagator*, i.e. the propagator for the interacting field. The propagator for the free field is the ‘leading order’ (**LO**) approximation to the full propagator, and the one that includes the first-order correction in λ the ‘next-to-leading order’ (**NLO**) approximation, and so on. The **NLO** correction term is a 6-point correlator, which we can express in terms of free-field propagators:

$$\frac{1}{N_\phi} \int \mathcal{D}\phi \phi_x \phi_y \phi_z \phi_z \phi_z \phi_z e^{-\phi K \phi} = 12 D_F^{xz} D_F^{zz} D_F^{zy} + 3 D_F^{xy} D_F^{zz} D_F^{zz}. \quad (3.75)$$

We only have two terms; one where both x and y are connected to one of the z ’s (there are 12 equal terms of these form), and one where x and y are connected and

all z are interconnected (of which there are 3 equal terms). Their corresponding Feynman diagrams are given by:



The first diagram is what we will call a *one-loop correction* to the propagator. The second diagram is the free propagator multiplied with an **NLO** vacuum diagram. Remember that there is an integral over all possible z ; this is exactly the superposition principle of **QM**: when a process can happen in different ways, we sum over all possible paths.

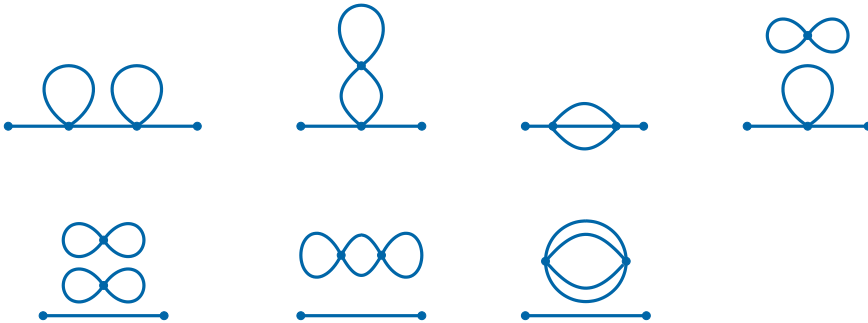
Let us out of curiosity investigate the **NNLO** contribution, the second order in λ . It is given by

$$-\frac{1}{2} \frac{\lambda^2}{(4!)^2} \frac{1}{N_\phi} \int d^4z \int d^4w \int \mathcal{D}\phi \phi_x \phi_y \phi_z \phi_z \phi_z \phi_z \phi_w \phi_w \phi_w \phi_w e^{-\phi K \phi}. \quad (3.76)$$

The solution is a bit more involving than before, as it is now a sum of terms consisting of 5 free propagators:

$$144 D_F^{xz} D_F^{zz} D_F^{zw} D_F^{ww} D_F^{wy} + 144 D_F^{xz} D_F^{zw} D_F^{zw} D_F^{zw} D_F^{wy} + 96 D_F^{xz} D_F^{zw} D_F^{ww} D_F^{wz} D_F^{zy} \\ + 36 D_F^{xz} D_F^{zz} D_F^{zy} D_F^{ww} D_F^{ww} + 9 D_F^{xy} D_F^{zz} D_F^{zz} D_F^{ww} D_F^{ww} + 36 D_F^{xy} D_F^{zz} D_F^{zw} D_F^{zw} D_F^{ww} \\ + 24 D_F^{xy} D_F^{zw} D_F^{zw} D_F^{zw} D_F^{zw} + z \leftrightarrow w.$$

The coefficients just follow from summing equal terms, as before. The diagrams corresponding to these terms are:



So we have three 2-loop corrections, one 1-loop correction plus an **NLO** vacuum diagram, and three free propagators plus an **NNLO** vacuum diagram. Now what to do with the troublesome vacuum diagrams, that are infinite? It is not difficult to understand that when calculating the propagator to all orders, in the end we will have all possible combinations between ‘pure’ propagator corrections and vacuum diagrams. In other words, symbolically we can write:

$$\text{all orders} = \left(\text{---} + \text{---} \circlearrowleft + \text{---} \circlearrowleft \circlearrowleft + \dots \right) \left(1 + \text{---} \circlearrowleft + \text{---} \circlearrowleft \circlearrowleft + \dots \right).$$

So we can factor out all vacuum contributions. This in turn means that we can define the full interacting propagator in function of the full action:

$$D_F^{\text{full}}(x_1, x_2) \stackrel{\text{def}}{=} \frac{\int \mathcal{D}\phi \phi_1 \phi_2 e^{-iS}}{\int \mathcal{D}\phi e^{-iS}}, \quad (3.77)$$

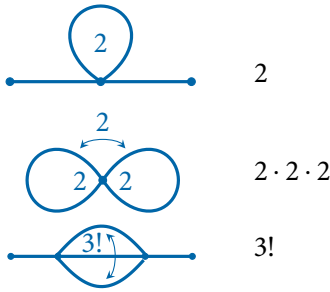
where we have the full interacting action in the numerator to include all loop corrections, and in the denominator to divide out the infinite constant N_ϕ plus all vacuum diagrams. Totally similar, we can define the full interaction higher order correlation functions:

$$\langle \Omega | \phi_1 \phi_2 \dots \phi_n | \Omega \rangle \stackrel{\text{def}}{=} \frac{\int \mathcal{D}\phi \phi_1 \phi_2 \dots \phi_n e^{-iS}}{\int \mathcal{D}\phi e^{-iS}}, \quad (3.78)$$

where $\langle \Omega | \Omega \rangle$ denotes the normalised interacting vacuum state.


It is much easier to draw all possible diagrams than to calculate all possible combinations resulting from the path integral. The only thing we need to know, is how to calculate the combinatorics coefficient in front, only based on the diagram. Let us build it step by step. First there is a factor $n!$ from the interchange of the coordinates that are integrated over (the *vertices*)—this factor cancels with the factor $1/n!$ from the expansion of the exponential. Furthermore, every vertex has four legs that can be interchanged at will, giving a factor $4!$ that cancels with the $1/4!$ from the interaction term in the Lagrangian. However, in doing this we might have a factor that is too large, as the combinations in the path integral are only those that are distinguishable. More specific, if a vertex has its four legs connected to four different points, then it is distinguishable and we add a factor $4!$, cancelling the vertex factor. However, if two legs are connected to each other, interchanging them doesn't make a difference and it will show up in the path integral as only one term. Hence this gives a factor $4 \cdot 3$ instead. So a symmetry in the diagram *lowers* the coefficient in front. To incorporate this in our calculations,

we just keep the cancellation of the vertex coefficient $4!$, but divide out the by *symmetry factor* of the diagram. Any self-connection gives a factor of 2, and any interchange of n lines or vertices that leaves the diagram invariant also gives a factor of $(n!)$. Diagrams are considered equivalent if they can be related by a continuous deformation, or, literally, if one can be transformed into the other by moving—not tearing—the legs whilst keeping the external points fixed. A few examples:



Feynman was the first to acknowledge the possibility to relate amplitudes with diagrams so he created the tool of Feynman diagrams, which are accompanied by a set of *Feynman rules* that dictate how to retrieve the correct mathematical amplitude for a given diagram. For ϕ^4 -theory, we have derived everything we need to present these rules:

A. *Scalar propagator:* $x \text{---} y = D_F(x, y), \quad (3.79a)$

B. *Scalar vertex:*  $= -i\lambda \int d^4z, \quad (3.79b)$

C. *Scalar external point:* $x \bullet = 1, \quad (3.79c)$

D. Divide by the symmetry factor. (3.79d)

Since the formula for the propagator is expressed in momentum space:

$$D_F(x, y) = \int \frac{d^4k}{(2\pi)^n} \frac{i}{k^2 - m^2 + i\epsilon} e^{-ik \cdot (x-y)}, \quad (3.80)$$

it is often easier to calculate the diagrams in momentum space. We then label each scalar line with an extra arrow indicating the direction of momentum flow.

What happens is that the integration in each vertex eats the exponentials to give a delta function:

$$\begin{array}{ccc}
 k_2 & & k_3 \\
 \swarrow & & \nearrow \\
 & \times & \\
 \nwarrow & & \searrow \\
 k_1 & & k_4
 \end{array}
 \sim \int d^4z \, e^{ik_1 \cdot z} e^{-ik_2 \cdot z} e^{ik_3 \cdot z} e^{-ik_4 \cdot z} = \delta^{(4)}(k_2 + k_4 - k_1 - k_3),$$

where we defined the short-hand notation

$$\delta^{(n)}(x) \stackrel{N}{=} (2\pi)^n \delta^{(n)}(x), \tag{3.81}$$

because a δ -function will often be accompanied with powers of 2π .

Note that the vertex rule in momentum space is essentially the same as *conservation of momentum* at each vertex. The only exponentials that remain, are those from the propagators that end in an external point. The generalisation to Feynman rules in momentum space is now trivial:

Momentum Feynman Rules for Scalar Fields

A. <i>Scalar propagator:</i>	\xrightarrow{k}	=	$\frac{i}{k^2 - m^2 + i\epsilon}$,	(3.82a)
B. <i>Scalar vertex:</i>	\times	=	$-i\lambda$,	(3.82b)
C. <i>Scalar external point:</i>	$\xrightarrow{k} \bullet x$	=	$e^{-ik \cdot x}$,	(3.82c)
D. <i>Impose momentum conservation at each vertex,</i>				(3.82d)
E. <i>Integrate over all undetermined momenta:</i>			$\int \frac{d^4k}{(2\pi)^4}$	(3.82e)
F. <i>Divide by the symmetry factor.</i>				(3.82f)

3.3 QUANTISATION OF THE DIRAC FIELD

We have chosen to start with the quantisation of scalar fields, as they form the easiest subject to develop the framework because both Dirac and gauge fields have some intricate details that need to be dealt with. We now move to the

investigation of the quantisation of the former, however, the difficulty arises in the fact that Dirac fields are Grassmannian functions, i.e. they anticommute.

Grassmann Numbers

Before we can define path integrals over Dirac fields, we have to define Dirac fields themselves in a rigorous manner. In the path integral formalism, we try to avoid the use of operators. When expanding a Dirac field in the same basis as in Equation 3.12:

$$\psi(x) \stackrel{\text{def}}{=} \sum \theta_i u_i(x), \quad (3.83)$$

where now the coefficients anticommute

$$\theta_i \theta_j = -\theta_j \theta_i.$$

These are called *Grassmann numbers*, and form an extension to standard number theory. Anti-commutation has some strong consequences, e.g. the square of a Grassmann number is always zero:

$$\theta^2 = 0,$$

and more specifically, any product of n Grassmann numbers

$$\theta_{i_1} \cdots \theta_{i_m}$$

will be zero from the moment two indices are equal, as we can anticommute until the two numbers with the same indices are next to each other and hence vanish. Also because of this property, a Taylor series is cut after the first order, i.e.

$$f(\theta) = f(0) + \theta f'(0) \quad (3.84)$$

is an exact relation for any function that satisfies the requirements to be eligible for a Taylor expansion. Differentiation of Grassmann numbers can be introduced by the logical requirement

$$\frac{\partial \theta_i}{\partial \theta_j} \stackrel{\text{def}}{=} \delta_{ij}, \quad (3.85)$$

but care has to be taken, as the differentiation operator is Grassmann-valued itself:

$$\frac{\partial}{\partial \theta_1} (\theta_1 \theta_2) = \frac{\partial \theta_1}{\partial \theta_1} \theta_2 = \theta_2, \quad \frac{\partial}{\partial \theta_1} (\theta_2 \theta_1) = -\theta_2 \frac{\partial \theta_1}{\partial \theta_1} = -\theta_2. \quad (3.86)$$

Considering integration, the only type we have to investigate is a linear integral, due to the cut in the Taylor series:

$$\int d\theta (A + B\theta),$$

which is defined to equal

$$\int d\theta (A + B\theta) = B. \quad (3.87)$$

there is a strong mathematical background for this statement, which would lead us to far away, so we just accept it as is. Note that it essentially makes derivation and integration the same thing. When having a multiple integration, we postulate the sign convention that if inner integrals can be calculated first, the result is positive:

$$\int d\theta_1 d\theta_2 \theta_2 \theta_1 \stackrel{\text{def}}{=} +1. \quad (3.88)$$

Complex Grassmann number are a logical extension, with the fact that complex conjugation reverses the order of the numbers:

$$(\theta_1 \theta_2)^* = \theta_2^* \theta_1^*. \quad (3.89)$$

It is now straightforward to calculate e.g. a Gaussian integral over a complex variable:

$$\int d\theta^* d\theta e^{-\theta^* b \theta} = \int d\theta^* d\theta (1 - \theta^* b \theta) = \int d\theta^* d\theta (1 + \theta \theta^* b) = b. \quad (3.90)$$

If this would have been a normal, non-Grassmann number, the result would have been $2\pi/b$. So with Grassmann integration, the Kähler factor comes out in the numerator rather than in the denominator. With an additional factor $\theta\theta^*$ we get:

$$\int d\theta^* d\theta \theta \theta^* e^{-\theta^* b \theta} = \int d\theta^* d\theta (\theta \theta^* - \theta \theta^* \theta^* b \theta) = \int d\theta^* d\theta \theta \theta^* = 1,$$

which we can interpret as $1/b$, i.e. the factor $\theta\theta^*$ brings down an additional factor $1/b$. We can easily generalise this to higher dimensions:

$$\int d\theta_1^* d\theta_1 \cdots d\theta_n^* d\theta_n e^{-\theta_i^* K^{ij} \theta_j} = \det K. \quad (3.91)$$

Inserting extra fields brings down the inverse of K :

$$\int d\theta_1^* d\theta_1 \cdots d\theta_n^* d\theta_n \theta_k \theta_l^* e^{-\theta_i^* B^{ij} \theta_j} = (K^{-1})_{kl} \det K. \quad (3.92)$$

So the Grassmannian Gaussian behaves exactly like the regular one, except for the position of the determinant.

To derive the calculation of path integrals now goes complete analogous to the complex scalar case. E.g. the Gaussian path integral is given by:

Gaussian Path Integral over Grassmanian Fields

$$\int \mathcal{D}\bar{\psi} \mathcal{D}\psi e^{-\bar{\psi} K \psi} = \det K, \quad (3.93)$$

where the bar operation is defined in Equation A.22. It is easy to verify that it doesn't change the integral. Completing the square goes totally analogous as well, now with η and $\bar{\eta}$ as Grassmanian source terms:

Completing the square with Grassmanian Fields

$$\int \mathcal{D}\bar{\psi} \mathcal{D}\psi e^{-\bar{\psi} K \psi + \bar{\eta} \psi + \bar{\psi} \eta} = \det K e^{\bar{\eta} K^{-1} \eta}. \quad (3.94)$$

Again we define n -point integrals by derivation to the sources (and as was the case for the complex scalar, we need to derive to $\bar{\eta}$ to bring down a ψ and vice versa):

$$\int \mathcal{D}\bar{\psi} \mathcal{D}\psi \psi_1 \bar{\psi}_2 \cdots \psi_{n-1} \bar{\psi}_n = \det K \frac{\delta}{\delta \bar{\eta}_1} \frac{\delta}{\delta \eta_2} \cdots \frac{\delta}{\delta \bar{\eta}_{n-1}} \frac{\delta}{\delta \eta_n} e^{\bar{\eta} K^{-1} \eta}, \quad (3.95)$$

but remember that Dirac fields anticommute, and derivatives w.r.t. a Dirac source as well. Two common examples

$$\int \mathcal{D}\bar{\psi} \mathcal{D}\psi \psi_1 \bar{\psi}_2 e^{-\bar{\psi} K \psi} = K_{12}^{-1} \det K, \quad (3.96a)$$

$$\int \mathcal{D}\bar{\psi} \mathcal{D}\psi \psi_1 \bar{\psi}_2 \psi_3 \bar{\psi}_4 e^{-\bar{\psi} K \psi} = [K_{12}^{-1} K_{34}^{-1} + K_{14}^{-1} K_{32}^{-1}] \det K. \quad (3.96b)$$

Note that the inverse Kähler is now naturally antisymmetric in its arguments, which means that the order of its arguments becomes significant, e.g. in the last term $K_{32}^{-1} = -K_{23}^{-1}$.

The Free Dirac Field

The action for a free Dirac field is given by [Equation 1.24](#):

$$S_0^{\text{Dirac}} = \int d^4x \left(i\bar{\psi}\not{\partial}\psi - m\bar{\psi}\psi \right),$$

where the slashed notation is explained in [Appendix A.3](#). The Kähler metric is hence given by

$$K(x, y) = -i \delta^{(4)}(x - y) (i\not{\partial}_y - m). \quad (3.97)$$

The inverse Kähler satisfies

$$-i (i\not{\partial}_x - m) K^{-1}(x, y) \equiv \delta^{(4)}(x - y). \quad (3.98)$$

From [QM](#) it is known that the Dirac propagator Δ_F has to satisfy

Dirac Propagator Equation

$$(i\not{\partial}_x - m) \Delta_F(x, y) \equiv i \delta^{(4)}(x - y), \quad (3.99)$$

so we make the logical definition

$$\Delta_F(x, y) \stackrel{\text{def}}{=} K^{-1}(x, y). \quad (3.100)$$

Note that the Dirac propagator can be related to the scalar propagator in a straightforward way, by relating [Equation 3.56](#) to [Equation 3.99](#):

$$\Delta_F(x, y) = (i\not{\partial} + m) D_F(x, y). \quad (3.101)$$

We can solve the Dirac [Equation 3.99](#) exactly, with result:⁵

Dirac Feynman Propagator

$$\Delta_F(x, y) = \int \frac{d^4k}{(2\pi)^4} \frac{i}{\not{k} - m + i\varepsilon} e^{-ik \cdot (x-y)}. \quad (3.102)$$

Because this function is odd, the propagator is automatically antisymmetric:

$$\Delta_F(x, y) = -\Delta_F(y, x). \quad (3.103)$$

⁵ In this case the $+i\varepsilon$ isn't merely a pole prescription, but it ensures the proper ordering of the fields. See [\[20, 21\]](#) for a more detailed explanation.

This antisymmetry tells us that we have to choose a *direction* for the propagator. It is common to define $\Delta_F(x, y)$ as the propagator from y to x ,⁶ which we will denote with an arrow:

$$\Delta_F(x, y) = y \bullet \longrightarrow \bullet x . \quad (3.104)$$

Note that this implies that in a Feynman diagram, a Dirac propagator is read from *right to left*. This will generalise to any Dirac structure, hence from now on we adopt the convention that any Feynman diagram has to be read from right to left (which we can do without changing the results for scalar and gauge fields, as these are symmetric anyway). If we now make the convention that in a Feynman diagram time runs in the horizontal direction, from left to right, we can make the distinction between a particle and an antiparticle based on the direction of the arrow (as the latter ‘moves back in time’):

$$\text{A. Particle:} \quad y \bullet \longrightarrow \bullet x \quad y^0 < x^0, \quad (3.105a)$$

$$\text{B. Antiparticle:} \quad x \bullet \longleftarrow \bullet y \quad y^0 > x^0. \quad (3.105b)$$

Exactly as in the scalar case, we define the propagator and n -point function as a fraction of path integrals:

$$\Delta_F(x_1, x_2) \stackrel{\text{def}}{=} \frac{\int \mathcal{D}\bar{\psi} \mathcal{D}\psi \psi_1 \bar{\psi}_2 e^{iS_0}}{\int \mathcal{D}\bar{\psi} \mathcal{D}\psi e^{iS_0}}, \quad (3.106a)$$

$$\langle 0 | \psi_{i_1} \cdots \psi_{i_n} \bar{\psi}_{j_1} \cdots \bar{\psi}_{j_n} | 0 \rangle \stackrel{\text{def}}{=} \frac{\int \mathcal{D}\bar{\psi} \mathcal{D}\psi \psi_{i_1} \cdots \psi_{i_n} \bar{\psi}_{j_1} \cdots \bar{\psi}_{j_n} e^{iS_0}}{\int \mathcal{D}\bar{\psi} \mathcal{D}\psi e^{iS_0}}. \quad (3.106b)$$

The ordering of the fields inside the path integral matters because of the antisymmetry, so we adopted the common convention to order the barred integration measure first, i.e. $\mathcal{D}\bar{\psi} \mathcal{D}\psi$, but for the fields we put the unbarred fields first, i.e. $\psi \bar{\psi} \cdots$. Note that the convention in [Equation 3.104](#) now implies that a Dirac propagator goes *from a $\bar{\psi}$ field to a ψ field*.

The $2n$ -point Gaussian equals as before all possible combinations for n particles to propagate to one of the remaining spacetime points. However because the Dirac field is complex, less combinations are possible, as was the case

⁶ This is a result from the positive $i\epsilon$.

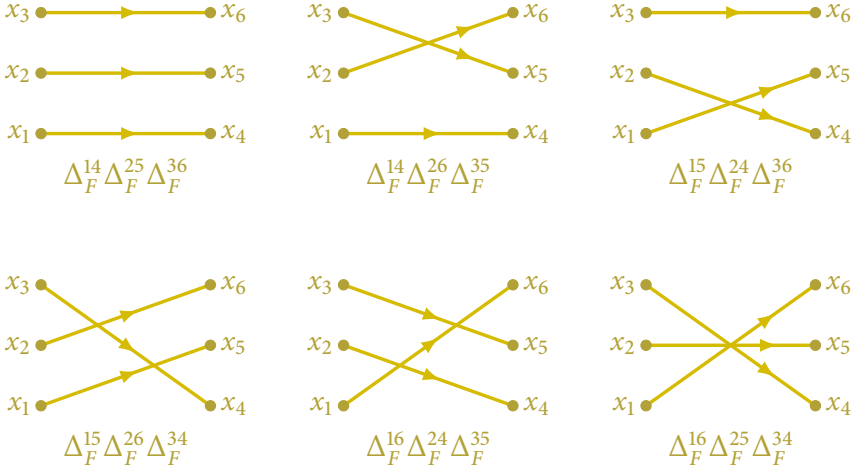


Figure 3.5: The Dirac 6-point correlator represents six possible (equivalent) diagrams. Note that every propagator starts in one of the first three points and ends in one of the last three. This comes from the fact that the Dirac field is complex, as we have already seen in the case of a complex scalar field.

for the complex scalar field in [Equations 3.70](#). The ordering of the fields as in $\psi\psi\cdots\bar{\psi}\bar{\psi}\cdots$ makes sure that no minus signs enter in the sum of possibilities, as long as we express all propagators from a $\bar{\psi}$ field to a ψ field. As an example we calculate the 6-point correlator:

$$\begin{aligned} \langle 0 | \psi_1 \psi_2 \psi_3 \bar{\psi}_4 \bar{\psi}_5 \bar{\psi}_6 | 0 \rangle &= \Delta_F^{14} \Delta_F^{25} \Delta_F^{36} + \Delta_F^{14} \Delta_F^{26} \Delta_F^{35} + \Delta_F^{15} \Delta_F^{24} \Delta_F^{36} + \Delta_F^{15} \Delta_F^{26} \Delta_F^{34} \\ &\quad + \Delta_F^{16} \Delta_F^{24} \Delta_F^{35} + \Delta_F^{16} \Delta_F^{25} \Delta_F^{34}, \end{aligned}$$

which is illustrated in [Figure 3.5](#).

The only thing left to do before we can define Feynman rules for the free Dirac field (the interacting Dirac field includes gauge bosons, which we will treat in the next section), is derive appropriate rules for external Dirac field lines. From standard [QM](#) and spinor theory, we know that a Dirac field acts on a particle momentum state as:

$$\psi(x) |p, s\rangle = e^{-i p \cdot x} u^s(p) |0\rangle, \quad (3.107a)$$

$$\langle p, s | \psi(x) = 0, \quad (3.107b)$$

$$\bar{\psi}(x) |p, s\rangle = 0, \quad (3.107c)$$

$$\langle p, s | \bar{\psi}(x) = \langle 0 | \bar{u}^s(p) e^{+i p \cdot x}, \quad (3.107d)$$

and on an antiparticle momentum state as:

$$\psi(x) |p, s\rangle = 0, \quad (3.108a)$$

$$\langle p, s | \psi(x) = \langle 0 | v^s(p) e^{+i p \cdot x}, \quad (3.108b)$$

$$\bar{\psi}(x) |p, s\rangle = e^{-i p \cdot x} \bar{v}^s(p) |0\rangle, \quad (3.108c)$$

$$\langle p, s | \bar{\psi}(x) = 0, \quad (3.108d)$$

where u and v are spinors (see e.g. [Equations A.24](#)), that satisfy the *completeness relations*:

$$\sum_s u^s(p) \bar{u}^s(p) = \not{p} + m, \quad (3.109a)$$

$$\sum_s \bar{v}^s(p) v^s(p) = \not{p} - m, \quad (3.109b)$$

which will prove to be very useful to simplify calculations with external spinors.

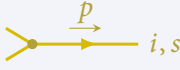
In Feynman diagram notation, we make the difference between a particle and an antiparticle state with the direction of the arrow. The exponentials will be absorbed into δ -functions to account for the conservation of momentum, but the sign in front of $p \cdot x$ will define the direction of the momentum flow: a negative sign implies towards the δ -function, i.e. *towards the vertex*. As the state $|p, s\rangle$ is an initial state (remember that we read Dirac fields from right to left), the momentum flow for a regular particle will be parallel to the arrow indicating the Dirac field:

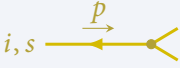
$$\psi(x) |p, s\rangle = i, s \begin{array}{c} \xrightarrow{p} \\ \text{---} \text{---} \end{array}$$

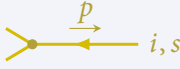
It is easy to verify that in general the momentum of a particle is parallel to its field arrow, and that of an antiparticle antiparallel. So finally we have the following momentum space Feynman rules for the free Dirac field:


Momentum Feynman Rules for the Dirac Field

A. *Initial fermion:*  = $u_i^s(p)$, (3.110a)

B. *Final fermion:*  = $\bar{u}_i^s(p)$, (3.110b)

C. *Initial antifermion:*  = $\bar{v}_i^s(p)$, (3.110c)

D. *Final antifermion:*  = $v_i^s(p)$, (3.110d)

E. *Fermion propagator:*  = $\frac{i}{\not{p} - m + i\epsilon}$. (3.110e)

3.4 QUANTISATION OF THE GAUGE FIELD

Last we need to quantise gauge fields. As vector fields commute, a path integral over a vector field is just one scalar path integral per component, i.e.

$$\int \mathcal{D}A \stackrel{\text{N}}{=} \int \mathcal{D}A^0 \mathcal{D}A^1 \mathcal{D}A^2 \mathcal{D}A^3 . \quad (3.111)$$

However the fact that there is gauge freedom on the field makes this much less straightforward. To see this, we take the regular action for a free vector field from [Equation 1.16](#):

$$S_0^{\text{vector}} = -\frac{1}{4} \int d^4x F_{0\mu\nu} F_0^{\mu\nu} , \quad (3.112)$$

where the free gauge tensor is given by

$$F_0^{\mu\nu} = (\partial^\mu A^{a\nu} - \partial^\nu A^{a\mu}) t^a , \quad (3.113)$$

with t^a a generator of the underlying Lie algebra (see [Appendix A.6](#)). After partial integration, we can rewrite the action as

$$S_0^{\text{vector}} = \frac{1}{2} \int d^4x d^4y A_\mu^a(x) \delta^{(4)}(x-y) \delta^{ab} (g^{\mu\nu} \square - \partial^\mu \partial^\nu) A_\nu^b(y) ,$$

so the Kähler metric is given by

$$K(x, y) = -\frac{i}{2} \delta^{(4)}(x - y) \delta^{ab} (g^{\mu\nu} \square - \partial^\mu \partial^\nu) . \quad (3.114)$$

But this is exactly the core of the problem: this metric is a singular 4×4 matrix, and hence has no inverse. This is due to gauge freedom, i.e.

$$A_\mu(x) + \partial_\mu \alpha(x)$$

leaves the action invariant (see [Equation 2.19](#)). The modes $A_\mu = \partial_\mu \alpha$ are gauge-equivalent to $A = 0$, hence these are the troublesome modes. The path integral is badly divergent, as we are redundantly integrating over an infinite set of equivalent fields.

We can fix the problem with a trick due to Faddeev and Popov [28]. First we define the functional $G[A]$ as a gauge-fixing condition, i.e. it is zero for a given gauge. The two most common types of gauges are the Lorentz gauge and the axial gauge:

$$\text{A. Lorentz gauge:} \quad G[A] = \partial_\mu A^\mu , \quad (3.115a)$$

$$\text{B. Axial gauge:} \quad G[A] = n_\mu A^\mu . \quad (3.115b)$$

We would like to constrain the path integral to only contain the gauge-fixed modes, so that all redundancy disappears. This is achieved with a functional δ -function. The formula

$$\int \mathcal{D}A \delta(G[A]) \quad (3.116)$$

will only select these fields that satisfy $G[A] = 0$, i.e. that are gauge-fixed. However, we cannot blindly input something inside the path integral, as that would change its value. But note that in the one-dimensional case, a δ of another function can be simplified by using the Jacobian of this function:

$$\int dx \delta(g(x)) f(x) = \sum_{\text{roots}} f(x_i) \left| \frac{\partial g}{\partial x} \right|_{x_i}^{-1} ,$$

and more specifically, when $f(g(x)) = 1$, we have

$$\int dx \delta(g(x)) = \sum_{\text{roots}} \left| \frac{\partial g(x)}{\partial x} \right|_{x_i}^{-1} .$$

This is easily generalised to higher dimensions:

$$\int dx_1 \cdots dx_n \delta^n(\mathbf{g}(\mathbf{x})) = \det \left(\frac{\partial g_i}{\partial x_j} \right)^{-1} ,$$

and we can hence define a similar relation for path integrations, putting the determinant on the *l.h.s.* to get an expression equal to 1:

$$\det\left(\frac{\delta G[A^\alpha]}{\delta\alpha}\right) \int \mathcal{D}\alpha \delta(G[A^\alpha]) = 1, \quad (3.117)$$

where A^α is the gauge transformed field. So now we can input this into the path integral over $\mathcal{D}A$, as it is just 1:

$$\int \mathcal{D}A \det\left(\frac{\delta G[A^\alpha]}{\delta\alpha}\right) \int \mathcal{D}\alpha \delta(G[A^\alpha]) e^{iS[A]}. \quad (3.118)$$

The action is gauge-invariant, so we can replace $S[A] \rightarrow S[A^\alpha]$:

$$\int \mathcal{D}A \det\left(\frac{\delta G[A^\alpha]}{\delta\alpha}\right) \int \mathcal{D}\alpha \delta(G[A^\alpha]) e^{iS[A^\alpha]}.$$

Also, making a gauge transformation is equivalent to a constant shift, and hence it leaves the integration measure invariant, i.e. $\mathcal{D}A^\alpha = \mathcal{D}A$. So we can write:

$$\int \mathcal{D}A^\alpha \det\left(\frac{\delta G[A^\alpha]}{\delta\alpha}\right) \int \mathcal{D}\alpha \delta(G[A^\alpha]) e^{iS[A^\alpha]}.$$

Now we note that A^α is just a dummy variable, so we can rename it back to A :

$$\int \mathcal{D}A \det\left(\frac{\delta G[A]}{\delta\alpha}\right) \int \mathcal{D}\alpha \delta(G[A]) e^{iS[A]}.$$

There is no α -dependence left, and we can factor out the integral

$$\left(\int \mathcal{D}\alpha\right) \int \mathcal{D}A \det\left(\frac{\delta G[A]}{\delta\alpha}\right) \delta(G[A]) e^{iS[A]}. \quad (3.119)$$

This is just another infinite constant that will be divided out later, so we already drop it. Note that it represents the infinite number of redundant field configurations, which we wanted to remove. In other words, the integral

$$\int \mathcal{D}A \det\left(\frac{\delta G[A^\alpha]}{\delta\alpha}\right) \delta(G[A]) e^{iS[A]}$$

is finite, as the functional δ ensures that only non-equivalent field configurations are integrated over. Note that we re-added the α -dependence inside the Jacobian,

which is valid as the Jacobian is gauge-invariant itself.⁷ It will allow us to do a specific calculation of the determinant, and we can turn the α -dependence in the Jacobian on and off, depending on what suits us most. What follows will be different for Abelian and non-Abelian fields, so we will treat each case separately.

Abelian Gauge Fields

If the fields are Abelian, the gauge transformation is given by (see [Equation 2.19](#)):

$$A_\mu^\alpha(x) \stackrel{N}{=} A_\mu(x) + \partial_\mu \alpha(x).$$

This implies that the functional determinant is invariant of the field itself, i.e. it is $\det(\square)$ (in Lorentz gauge), and we can factor it out the integral:

$$\det\left(\frac{\delta G[A^\alpha]}{\delta \alpha}\right) \int \mathcal{D}A \delta(G[A]) e^{iS[A]},$$

which again implies that we can drop the determinant, as it will cancel out anyway. Now we will loosen our gauge-fixing condition a bit, and consider the class of Lorentz gauges given by

$$G[A] = \partial_\mu A^\mu - \omega(x), \quad (3.120)$$

where ω is any scalar function. This doesn't change the Jacobian, so the former derivation remains valid. So far we have found the equality

$$\int \mathcal{D}A e^{iS[A]} = \det(\square) \left(\int \mathcal{D}\alpha \right) \int \mathcal{D}A \delta(\partial_\mu A^\mu - \omega) e^{iS[A]}, \quad (3.121)$$

but because ω is unspecified, this equation remains valid if we replace the [r.h.s.](#) with any linear combination of different ω . We can even multiply the integrand with a Gaussian weighting function that is normalised to one:

$$N_\xi e^{-i \int d^4x \frac{\omega^2}{2\xi}}, \quad (3.122a)$$

$$N_\xi = \left(\int \mathcal{D}\omega e^{-i \int d^4x \frac{\omega^2}{2\xi}} \right)^{-1} = \lim_{n \rightarrow \infty} \sqrt{(2i \xi \pi)^n}. \quad (3.122b)$$

Finally we integrate over all possible ω (which is the same as the continuous limit of making all possible linear combinations):

⁷ This is not so straightforward to demonstrate, however quite logical. See [\[20\]](#) for a nice explanation.

$$\begin{aligned} \int \mathcal{D}A e^{iS[A]} &= N_\xi \det(\square) \left(\int \mathcal{D}\alpha \right) \int \mathcal{D}\omega \mathcal{D}A \delta(\partial_\mu A^\mu - \omega) e^{-i \int d^4x \frac{\omega^2}{2\xi}} e^{iS[A]}, \\ &= N_\xi \det(\square) \left(\int \mathcal{D}\alpha \right) \int \mathcal{D}A e^{-i \int d^4x \frac{(\partial_\mu A^\mu)^2}{2\xi}} e^{iS[A]}, \end{aligned}$$

where we used the δ -function and the integration over ω to make the replacement $\omega = \partial_\mu A^\mu$. Effectively, we have added a new term to the Lagrangian:

$$\mathcal{L}^{\text{gauge-fixed}} = \frac{1}{2} A_\mu^a (g^{\mu\nu} \square - \partial^\mu \partial^\nu) A_\nu^b - \frac{1}{2\xi} \partial_\mu A^\mu \partial_\nu A^\nu. \quad (3.123)$$

So now the Kähler metric is given by

$$K(x, y) = -\frac{i}{2} \delta^{(4)}(x - y) \left(g^{\mu\nu} \square - \left(1 - \frac{1}{\xi}\right) \partial^\mu \partial^\nu \right), \quad (3.124)$$

which is no longer singular! In analogy with the scalar field in [Equation 3.57](#), we define the vector propagator as:

$$D_F^{\mu\nu}(x, y) \stackrel{\text{def}}{=} \frac{1}{2} (K^{-1}(x, y))^{\mu\nu}, \quad (3.125)$$

which now satisfies the equation

Vector Propagator Equation

$$\left(g_{\mu\nu} \square - \left(1 - \frac{1}{\xi}\right) \partial_\mu \partial_\nu \right) D_F^{\nu\rho} \equiv i \delta_\mu^\rho \delta^{(4)}(x - y). \quad (3.126)$$

We can solve this equation exactly, giving

Vector Feynman Propagator

$$D_F^{\mu\nu}(x, y) = \int \frac{d^4k}{(2\pi)^4} \frac{-i}{k^2 + i\epsilon} \left(g^{\mu\nu} - (1 - \xi) \frac{k^\mu k^\nu}{k^2} \right) e^{-ik \cdot (x - y)}. \quad (3.127)$$

So now we have another gauge choice, namely the choice of ξ . A few common examples are:

A. $\xi = 0$ Landau gauge, (3.128a)

B. $\xi = 1$ Feynman gauge, (3.128b)

C. $\xi = 3$ Yennie gauge. (3.128c)

By far the most commonly used choice is the Feynman gauge. It is often possible to cancel divergences for a given (piece of a) diagram by choosing an appropriate gauge (see e.g. [Equation 7.31](#)). However, it is rare that different diagrams combine in a finite way with the same gauge choice. Finally, note that in the Feynman gauge $\xi = 1$ [Equation 3.126](#) transforms into the simpler form we found in [Equation 1.17](#).

Now that we have successfully quantised the Abelian gauge field, all other properties are analogous to the scalar case. I.e. we define the free propagator as

$$D_F^{\mu\nu}(x_1, x_2) \stackrel{\text{def}}{=} \frac{\int \mathcal{D}A A^\mu(x_1) A^\nu(x_2) e^{iS_0}}{\int \mathcal{D}A e^{iS_0}}, \quad (3.129a)$$

$$\langle 0 | A_1 \cdots A_n | 0 \rangle \stackrel{\text{def}}{=} \frac{\int \mathcal{D}A A_1 \cdots A_n e^{iS_0}}{\int \mathcal{D}A e^{iS_0}}. \quad (3.129b)$$

Non-Abelian Gauge Field: Lorentz Gauge

What changes when we try to quantise non-Abelian gauge fields? The important fact is that the gauge transformation is now more intricate (see [Equation 2.27](#)):

$$\begin{aligned} A_\mu^a t^a &\rightarrow e^{ig\alpha^a t^a} \left(A_\mu^a t^a + \frac{i}{g} \partial_\mu \right) e^{-ig\alpha^a t^a}, \\ &\approx (A_\mu^a + D_\mu \alpha^a) t^a, \end{aligned}$$

where D_μ is the derivative acting in the adjoint representation:

$$D_\mu^{ab} = \delta^{ab} \partial_\mu - g f^{abc} A_\mu^c.$$

In particular the functional determinant in [Equation 3.119](#) is no longer independent of A , so we cannot factor it out from the $\mathcal{D}A$ path integral:

$$\det \left(\frac{\delta G[A]}{\delta \alpha} \right) = \det (\partial_\mu D^\mu), \quad (3.130)$$

where we again adopted the Lorentz gauge condition $G[A] = \partial_\mu A^\mu$. We have no hope in calculating the remaining integral

$$\left(\int \mathcal{D}\alpha \right) \int \mathcal{D}A \det(\partial_\mu D^\mu) \delta(G[A]) e^{iS[A]}, \quad (3.131)$$

as the dependence of the determinant on A spoils any path integration techniques we know. However, again we can use a trick, and again due to Faddeev and Popov. This time we make the observation that a determinant in a numerator can be the result of a path integration over Grassmanian fields. So instead of trying to calculate it, we exponentiate it:

$$\det(\partial_\mu D^\mu) = \int \mathcal{D}\bar{c} \mathcal{D}c e^{-i \int d^4x \bar{c} \partial_\mu D^\mu c}. \quad (3.132)$$

These fields are a bit peculiar, as they obey the path integral formalism for spinor fields—having the determinant in the numerator—but have the kinetic terms of scalar fields, with a double derivative. Hence they cannot have any correspondence to real particles, but that shouldn't be a big problem, as long as we use them as a mathematical tool. These new fields and their particle excitations are called *Faddeev-Popov ghosts*, and have to be included in every Feynman diagram calculation in a non-Abelian theory that is quantised in the Lorentz gauge.

The main point is that their dependence on the A -field is only linear, and not quadratic. This means we can treat this term as an interaction term to the gauge field, and ignore it while quantising the free gauge field. In other words, the quantisation of the gauge field now goes exactly the same as in the Abelian case, resulting in the propagator in Equation 3.127 (with an added factor δ^{ab} for the colour, which is merely a δ because the Kähler is diagonal in its colour indices). However, for a non-Abelian field this steps are only possible if we have exponentiated the determinant, i.e. if we include ghosts in our theory.

The ghost Lagrangian is given by:

$$\mathcal{L}^{\text{ghost}} = -\bar{c}^a \square c^a - g f^{abc} \bar{c}^a \partial^\mu A_\mu^b c^c. \quad (3.133)$$

Using the same methods as before, we can calculate the ghost propagator:

Feynman Ghost Propagator

$$\Sigma_F^{ab}(x, y) = \int \frac{d^4 k}{(2\pi)^4} \frac{i}{k^2 + i\varepsilon} \delta^{ab} e^{-ik \cdot (x-y)}. \quad (3.134)$$

The interaction term gives a factor $gf^{abc}k^\mu$, with k the outgoing ghost momentum after the vertex. As ghost fields anticommute, they naturally have a field arrow similarly to Dirac fields. But as ghosts will never be external, they will only appear in loops, and we don't really have to worry about the arrow as long as we use it consistently. Every loop will then give an extra minus sign, just as in the Dirac case. The Feynman rules for ghosts are given in [Equations A.99](#).

Non-Abelian Gauge Field: Axial Gauge

Now we will make an important investigation. When using a different class of gauges, namely axial gauges, ghosts fully decouple from our theory. Let us investigate this a bit more. Any axial gauge is defined as

$$G[A] \stackrel{\text{def}}{=} n_\mu A^\mu - \omega, \quad (3.135)$$

for some arbitrary directional vector n_μ . The functional determinant is then given by

$$\det \left(\frac{\delta G[A]}{\delta \alpha} \right) = \det (\partial_\mu D^\mu) = \det (n \cdot \partial - gn \cdot A) = \det (n \cdot \partial - g\omega), \quad (3.136)$$

which is independent of A ! So we don't have to introduce ghosts at all in an axial gauge, we can just factor out the determinant from the integral. The trick we used, is to apply the constraint given by the functional δ -function—as it is fully integrated over, this constraint will be in effect anyway. Couldn't we have done the same in the Lorentz gauge? Yes, but then we shouldn't forget to apply Leibniz' rule on the derivative:

$$\det \left(\frac{\delta G[A]}{\delta \alpha} \right) = \det (\partial_\mu D^\mu) = \det (\square - g\partial \cdot A - gA \cdot \partial) = \det (\square - g\omega - gA \cdot \partial),$$

so we still have a term in the determinant that depends on A . In general, any gauge that is defined using derivatives, will give rise to ghosts. So it seems the axial gauge is much easier to work with. However, because we have a different gauge

condition, we need to redo the calculation leading to the propagator, starting from Equation 3.120 but now with the class of axial gauges as in Equation 3.135:

$$\int \mathcal{D}A e^{iS[A]} = \det(n \cdot \partial) \left(\int \mathcal{D}\alpha \right) \int \mathcal{D}A \delta(n \cdot A - \omega) e^{iS[A]}, \quad (3.137)$$

Again, we make an integration over ω , weighted with the Gaussian in Equations 3.122:

$$\begin{aligned} \int \mathcal{D}A e^{iS[A]} &= N_\xi \det(n \cdot \partial) \left(\int \mathcal{D}\alpha \right) \int \mathcal{D}\omega \mathcal{D}A \delta(b \cdot A - \omega) e^{-i \int d^4x \frac{\omega^2}{2\xi}} e^{iS[A]}, \\ &= N_\xi \det(n \cdot \partial) \left(\int \mathcal{D}\alpha \right) \int \mathcal{D}A e^{-i \int d^4x \frac{(n \cdot A)^2}{2\xi}} e^{iS[A]}, \end{aligned}$$

The new term in the Lagrangian is now:

$$\mathcal{L}^{\text{gauge-fixed}} = \frac{1}{2} A_\mu^a (g^{\mu\nu} \square - \partial^\mu \partial^\nu) A_\nu^b - \frac{1}{2\xi} n_\mu A^\mu n_\nu A^\nu, \quad (3.138)$$

and the Kähler metric is given by

$$K(x, y) = -\frac{i}{2} \delta^{(4)}(x - y) \left(g^{\mu\nu} \square - \partial^\mu \partial^\nu - \frac{1}{\xi} n^\mu n^\nu \right). \quad (3.139)$$

Of course we use the same definition for the propagator:

$$D_F^{\mu\nu}(x, y) \stackrel{\text{def}}{=} \frac{1}{2} (K^{-1}(x, y))^{\mu\nu}, \quad (3.140)$$

which now satisfies the slightly different equation

$$\left(g_{\mu\nu} \square - \partial_\mu \partial_\nu - \frac{1}{\xi} n_\mu n_\nu \right) D_F^{\nu\rho} \equiv i \delta_\mu^\rho \delta^{(4)}(x - y). \quad (3.141)$$

We can again solve this equation exactly, giving finally the propagator in a general axial gauge:

Vector Feynman Propagator in Axial Gauge

$$D_F^{\mu\nu}(x, y) = \int \frac{d^4k}{(2\pi)^4} \frac{-i \delta^{ab}}{k^2 + i\varepsilon} \left(g^{\mu\nu} - \frac{k_\mu n_\nu + k_\nu n_\mu}{k \cdot n} + (n^2 + \xi k^2) \frac{k_\mu k_\nu}{(k \cdot n)^2} \right) e^{-ik \cdot (x-y)}.$$

Like was the case with Lorentz gauges, ξ induces an additional gauge choice. We are however only interested in the so-called *light-cone* (LC) gauge, where

$n^2 = 0$. Furthermore, we take $\xi = 0$ (the homogeneous LC gauge), such that the term proportional to k^2 vanishes.

Most of the time, calculations are easier in Lorentz gauges, because ghost loop diagrams resemble a lot to gauge boson loop diagrams, hence the calculation can be ‘copied’. On the other hand, calculations in axial gauges are far more challenging, due to the extra terms $1/k \cdot n$ in the propagator, which makes integrations more tricky. A few common pole prescriptions to regulate this factor are:

$$\text{A. Advanced:} \quad \frac{1}{[n \cdot k]} = \frac{1}{n \cdot k - i\eta}, \quad (3.142a)$$

$$\text{B. Retarded:} \quad \frac{1}{[n \cdot k]} = \frac{1}{n \cdot k + i\eta}, \quad (3.142b)$$

$$\text{C. Principal Value:} \quad \frac{1}{[n \cdot k]} = \frac{1}{2} \left(\frac{1}{n \cdot k + i\eta} + \frac{1}{n \cdot k - i\eta} \right). \quad (3.142c)$$

The principal value prescription is less suited for the LC gauge and should be avoided in this case [29]. A particular prescription that is more adequate is the Mandelstam-Leibbrandt prescription (see [30]):

$$\text{D. Mandelstam-Leibbrandt:} \quad \frac{1}{[n \cdot k]} = \frac{\tilde{n} \cdot k}{n \cdot k \tilde{n} \cdot k + i\eta}, \quad (3.142d)$$

$$\tilde{n}^2 \equiv 0, n \cdot \tilde{n} \neq 0, \text{ e.g. :} \quad \frac{1}{[k^+]} = \frac{k^-}{k^+ k^- + i\eta}. \quad (3.142e)$$

There are also special considerations depending on the axial structure of the gauge. See e.g. [29] for a good treatment.

QUANTUM CORRECTIONS

Although at first sight maybe not so clear, quantised fields have a behaviour that is totally different from classical fields. Loop integrations require appropriate regularisation schemes, which in turn spawn the theory with unphysical divergences. The theory needs to be properly renormalised to treat these divergences, and this renormalisation procedure will in turn influence the physical parameters of the theory, and more, it will deeply change our understanding of physical quantities. Besides the divergences, the regularisation procedure leaves behind unphysical energy scales as well. From the requirement of invariance under rescalings, we will derive a set of renormalisation group equations, and show how these equations lead to an asymptotically free behaviour of QCD, violating perturbative methods at low energies.

4.1 WORKING WITH QUANTISED FIELDS

In the previous chapter we succeeded in quantising the free field theory for the [YM Lagrangian](#) (see [Equation 2.45](#)). Fully expanded, the interacting Lagrangian reads in Lorentz gauge:

$$\mathcal{L}_{\text{Lorentz}}^{\text{YM}} = \mathcal{L}_0^{\text{gauge}} + \mathcal{L}_0^{\text{ghost}} + \mathcal{L}_0^{\text{Dirac}} + \mathcal{L}_I, \quad (4.1a)$$

$$\mathcal{L}_0^{\text{gauge}} = -\frac{1}{4} (\partial_\mu A_\nu^a - \partial_\nu A_\mu^a)^2 - \frac{1}{2\xi} \partial_\mu A^\mu \partial_\nu A^\nu, \quad (4.1b)$$

$$\mathcal{L}_0^{\text{ghost}} = -\bar{c}^a \square c^a, \quad (4.1c)$$

$$\mathcal{L}_0^{\text{Dirac}} = \bar{\psi} (i \not{\partial} - m) \psi, \quad (4.1d)$$

$$\begin{aligned} \mathcal{L}_I = & g \bar{\psi} \not{A} \psi - g f^{abc} \bar{c}^a \partial^\mu A_\mu^b c^c - g f^{abc} (\partial_\mu A_\nu^a) A^{\mu b} A^{\nu c} \\ & - \frac{1}{2} g^2 f^{abx} f^{xcd} A_\mu^a A_\nu^b A^{\mu c} A^{\nu d}. \end{aligned} \quad (4.1e)$$

The only difference with the axial gauge is the omission of ghosts and a different gauge-fixing term:

$$\mathcal{L}_{\text{axial}}^{\text{YM}} = \mathcal{L}_0^{\text{gauge}} + \mathcal{L}_0^{\text{Dirac}} + \mathcal{L}_I, \quad (4.2a)$$

$$\mathcal{L}_0^{\text{gauge}} = -\frac{1}{4} (\partial_\mu A_\nu^a - \partial_\nu A_\mu^a)^2 - \frac{1}{2\xi} n_\mu A^\mu n_\nu A^\nu, \quad (4.2b)$$

$$\mathcal{L}_0^{\text{Dirac}} = \bar{\psi} (i\not{\partial} - m) \psi, \quad (4.2c)$$

$$\begin{aligned} \mathcal{L}_I = & g \bar{\psi} \not{A} \psi - g f^{abc} (\partial_\mu A_\nu^a) A^{\mu b} A^{\nu c} \\ & - \frac{1}{2} g^2 f^{abx} f^{xcd} A_\mu^a A_\nu^b A^{\mu c} A^{\nu d}. \end{aligned} \quad (4.2d)$$

We didn't calculate the Feynman rules for the interaction terms yet, and we won't do so either, as they are really straightforward to derive, totally analogous to the scalar case in [Section](#) . All Feynman rules for **YM** are listed in [Appendix A.8](#) as a quick reference.

As we have seen in Subsection [The Interacting Scalar Field](#) on page 66 and onwards, all interaction terms in the Lagrangian are expanded in orders of the coupling constant, to form a perturbative series. In a **YM** theory this coupling constant will often be denoted by g . It entered for the first time in the gauge transformation of the Dirac field, [Equation 2.1](#), where we extracted it arbitrarily from the gauge parameter α . Starting from there, it propagated through the theory to become the interaction strength between the gauge field and the Dirac fields, between the gauge fields themselves and between the gauge and ghost fields (if in Lorentz gauge). The fact that all this couplings are the same, follows from the simple requirement of gauge invariance. Hence, there is only one constant that governs the dynamics of a typical **YM** theory, viz. g , that has to be matched against experiment. Considering the kinematics, there are much more constants that govern it, these are the masses of the fields.

As long as $g \ll 1$, we can validate a perturbative regime, and can tune our theory to higher accuracy by including higher order diagrams, for instance when higher resolution data becomes available from experiment. However, it is not always possible to keep g small, as we will see later in this chapter. A suitable way to solve this, is to separate the process in two regimes depending on the value of g , and combine the regimes accordingly. Such an approach is known as *factorisation*, and is the main topic of the next chapter.

When calculating diagrams of **NLO** and higher orders, we encounter many apparent divergences. Of course, observable quantities always have to be finite, and therefore we expect divergences to cancel out when calculating a full result. However, the emergence of such divergences in intermediate steps might prove challenging to deal with. We hence need some methods to *regulate* the divergences.

Regularisation

Any integration over loop momenta will automatically introduce divergences, which correspondingly have to be regulated. There are two types of divergences, ultra-violet (**UV**) divergences, that appear for momenta $\rightarrow \infty$, and infra-red (**IR**) divergences, that appear in the soft region, i.e. for momenta $\rightarrow 0$. The former are the most common and most well-known how to treat. A typical loop integral has the form

$$\int \frac{d^4 k}{(2\pi)^4} \frac{1}{(k^2 - m^2)^n}. \quad (4.3)$$

This is badly divergent in the **UV**-region. The standard procedure to calculate this integral, would be to first make a Wick rotation, such that the momentum is now an Euclidian vector:

$$k_E^0 \stackrel{\text{def}}{=} -i k^0, \quad (4.4a)$$

$$(k_E)^2 = -k^2. \quad (4.4b)$$

This transforms the integral into

$$i(-)^n \int \frac{d^4 k_E}{(2\pi)^4} \frac{1}{(k_E^2 + m^2)^n}.$$

Because it is Euclidian, we can move to 4-dimensional spherical coordinates:

$$d^4 k_E \rightarrow d^3 \Omega dk_E k_E^3, \quad k_E^2 \rightarrow k_E^2.$$

The angular part of the integration is given by

$$\int d^3 \Omega = \int_0^{2\pi} d\phi \int_0^\pi d\chi \sin^2 \theta \sin \chi = 2\pi^2, \quad (4.5)$$

hence the integral is now

$$i \frac{(-)^n}{8\pi^2} \int_0^\infty dk_E \frac{k_E^3}{(k_E^2 + m^2)^n},$$

which is divergent for $n = 1$ and $n = 2$. One way to proceed, is to avoid the singular part by introducing a cut-off:

Cut-Off Regularisation

$$-\frac{i}{8\pi^2} \int_0^\Lambda dk_E \frac{k_E^3}{k_E^2 + m^2} = -\frac{i}{16\pi^2} m^2 \left(\frac{\Lambda^2}{m^2} - \ln \frac{\Lambda^2}{m^2} \right), \quad (4.6a)$$

$$\frac{i}{8\pi^2} \int_0^\Lambda dk_E \frac{k_E^3}{(k_E^2 + m^2)^2} = \frac{i}{16\pi^2} \left(\ln \frac{\Lambda^2}{m^2} - 1 \right), \quad (4.6b)$$

where we already dropped the terms where we could take the limit $L \rightarrow \infty$ safely. So the cut-off acts as a regulator, as it regulates the divergence. The original integral can be retrieved by letting $\Lambda \rightarrow \infty$. The first integral is called *quadratically divergent*, as it is quadratic in Λ . Similarly, the second divergence is called *logarithmically divergent* as it behaves like $\ln \Lambda$. What we now expect is that other diagrams will give similar contributions, but with opposite signs, such that the dependence on the regulator vanishes.

However, the cut-off regularisation—being the easiest regulator available—has some shortcomings, the most important of which being the violation of translational invariance. There exist several other regularisation procedures, like Pauli-Villars regularisation, analytic regularisation, ζ -regularisation, etc... We won't treat these. Instead, we investigate the—arguably—most useful regularisation procedure, that of *dimensional regularisation*.

Consider again the same integral as above. For $n = 1$, it behaves at large momenta as $|\mathbf{p}|^{-2}$, and for $n = 2$ it behaves at large momenta as $|\mathbf{p}|^{-4}$. The momentum integrals are therefore divergent for dimensions $d \geq 2$ resp. $d \geq 4$. The idea is to subtract a small infinitesimal number 2ϵ from the number of spacetime dimensions,¹ in order to make the integral convergent. E.g. the following integrals are convergent:

$$\int \frac{d^{2-2\epsilon} k}{(2\pi)^{2-2\epsilon}} \frac{1}{k^2 - m^2}, \quad (4.7a)$$

$$\int \frac{d^{4-2\epsilon} k}{(2\pi)^{4-2\epsilon}} \frac{1}{(k^2 - m^2)^2}. \quad (4.7b)$$

There is no physical meaning to a theory with $4-2\epsilon$ dimensions, so we are allowed to use it as a mathematical tool, as long as we make the limit $\epsilon \rightarrow 0$ in the final

¹ The factor 2 in front of ϵ follows from normalisation considerations, because every pole in $4-\epsilon$ will be of the form $2/\epsilon$, so choosing $4-2\epsilon$ gives 'clean' poles of the form $1/\epsilon$. In older literature it was common to use the convention $\omega = 4 - \epsilon$, so care should be taken when comparing references. Most of the time one can deduce the convention used by inspecting the factor in front of the pole.

result. But how do we integrate in non-integer dimensions? There are several ways to do this (see e.g. [31, 32]), but the most straightforward is when used in combination with spherical coordinates, especially for integrands that do not depend on the angular part. The extrapolation to non-integer dimensions will be based on the extrapolation from the integer factorial to the real numbers by use of the Gamma function. Consider a function f that only depends on the momentum squared, and is divergent when integrated in d dimensions, e.g.

$$\int \frac{d^d k}{(2\pi)^d} f(k^2). \quad (4.8)$$

We will regulate this integral by making the shift $\omega = d - 2\epsilon$. The first steps are straightforward: again we make a Wick rotation, and move to spherical coordinates:

$$i \int \frac{d^{\omega-1} \Omega}{(2\pi)^\omega} \int_0^\infty dk_E k_E^{\omega-1} f(-k_E^2).$$

We moved the non-integer part of the spacetime dimensions into the angular part, because then we can calculate it separately, and the result will be applicable to all integrals for which the integrand only depends on k^2 . To calculate the angular part, we use a trick. An ω -dimensional Gaussian function can be written as a product of ω Gaussians, or, more generally:

$$\int d^\omega x e^{-x^i x^i} = \left(\int dx e^{-x^2} \right)^\omega = \sqrt{\pi^\omega}.$$

We can make this step because all x_i are independent from each other. We can calculate a ω -dimensional Gaussian as well by moving to spherical coordinates:

$$\int d^\omega x e^{-x^i x^i} = \int d^{\omega-1} \Omega \int_0^\infty dx x^{\omega-1} e^{-x^2} = \left(\int d^{\omega-1} \Omega \right) \frac{1}{2} \Gamma\left(\frac{\omega}{2}\right).$$

So we have

$$\left(\int d^{\omega-1} \Omega \right) = \frac{2\pi^{\frac{\omega}{2}}}{\Gamma\left(\frac{\omega}{2}\right)}, \quad (4.9)$$

which we use to give the result for a general dimensionally regularised integrand that depends on k^2 only:

$$\int \frac{d^d k}{(2\pi)^d} f(k^2) = \lim_{\epsilon \rightarrow 0} \frac{2i}{(4\pi)^{\frac{\omega}{2}} \Gamma\left(\frac{\omega}{2}\right)} \int_0^\infty dk_E k_E^{\omega-1} f(-k_E^2). \quad (4.10)$$

As an example, we calculate the 4-dimensional integral in Equation 4.3 (with $n = 2$, so that it is at most logarithmically divergent):

$$\int \frac{d^4 k}{(2\pi)^4} \frac{1}{(k^2 - m^2)^2} = \lim_{\epsilon \rightarrow 0} \frac{2i}{(4\pi)^{\frac{\omega}{2}} \Gamma\left(\frac{\omega}{2}\right)} \int_0^\infty dk_E \frac{k_E^{\omega-1}}{(k_E^2 + m^2)^2}$$

The last integral can be related to a Beta function by making the substitution $\alpha = m^2/(k^2 + m^2)$:

$$\begin{aligned} \int_0^\infty dk_E \frac{k_E^{\omega-1}}{(k_E^2 + m^2)^2} &= \frac{1}{2} \int_0^\infty d(k_E^2) \frac{(k_E^2)^{\frac{\omega}{2}-1}}{(k_E^2 + m^2)^2}, \\ &= \frac{1}{2} m^{\omega-4} \int_0^1 d\alpha \alpha^{1-\frac{\omega}{2}} (1-\alpha)^{\frac{\omega}{2}-1}, \\ &= \frac{1}{2} m^{\omega-4} \int_0^1 d\alpha B\left(2 - \frac{\omega}{2}, \frac{\omega}{2}\right), \end{aligned}$$

and because we can write the Beta function as a combination of Gamma functions, i.e.

$$B(\alpha, \beta) = \frac{\Gamma(\alpha)\Gamma(\beta)}{\Gamma(\alpha + \beta)}, \quad (4.11)$$

the final result is given by (using $\omega = 4 - 2\epsilon$):

$$\int \frac{d^4 k}{(2\pi)^4} \frac{1}{(k^2 - m^2)^2} = \lim_{\epsilon \rightarrow 0} \frac{i}{(4\pi)^2} \left(\frac{4\pi}{m^2}\right)^\epsilon \Gamma(\epsilon). \quad (4.12)$$

We can investigate the behaviour in the limit $\omega \rightarrow 4$ using the expansion of the Gamma function near zero:

$$\Gamma(\epsilon) \approx \frac{1}{\epsilon} - \gamma_E + \mathcal{O}(\epsilon), \quad (4.13)$$

where $\gamma_E \approx 0.5772$ is the Euler-Mascheroni constant. The ϵ -power can be approximated as well:

$$x^\epsilon \approx 1 + \epsilon \ln x + \mathcal{O}(\epsilon^2). \quad (4.14)$$

This then gives:

Dimensional Regularisation

$$\int \frac{d^4 k}{(2\pi)^4} \frac{1}{(k^2 - m^2)^2} \rightarrow \frac{i}{(4\pi)^2} \left(\frac{1}{\epsilon} - \gamma_E + \ln 4\pi - \ln m^2 \right). \quad (4.15)$$

When comparing this to the result in [Equation 4.6b](#), i.e.

$$\int \frac{d^4 k}{(2\pi)^4} \frac{1}{(k^2 - m^2)^2} \rightarrow \frac{i}{(4\pi)^2} (\ln \Lambda^2 - \ln m^2 - 1), \quad (4.16)$$

we see that the Λ -regulator naturally emerged with a logarithm, while in the case of dimensional regularisation this is an inverse pole. Note that the ‘core’ result of the integration is in both cases the same, namely $-\ln m^2$, while each procedure adds a different regulator, but also different finite terms:

$$\text{A. Cut-off regularisation:} \quad \ln \Lambda^2 - 1, \quad (4.17a)$$

$$\text{B. Dimensional regularisation:} \quad \frac{1}{\epsilon} - \gamma_E + \ln 4\pi. \quad (4.17b)$$

We will mainly work in the dimensional regularisation scheme in this thesis.

We can now repeat the same calculation, but for general dimension and general n :

$$I = \int \frac{d^d k}{(2\pi)^d} \frac{1}{(k^2 - m^2)^n} = \lim_{\epsilon \rightarrow 0} i(-)^n \frac{m^{d-2n}}{(4\pi)^{\frac{d}{2}}} \left(\frac{4\pi}{m^2} \right)^\epsilon \frac{\Gamma\left(n - \frac{d}{2} + \epsilon\right)}{\Gamma(n)}. \quad (4.18)$$

The Gamma function has poles in 0 and all negative numbers, hence the result is divergent when d is even and $d \geq 2n$. If this is not the case, the integral is convergent and we can just take the limit $\epsilon \rightarrow 0$. We can find a general expression for the divergent integral, by using the more general expansion of the Gamma function (see [Equation B.6l](#)):

$$\Gamma(\epsilon - n) = \frac{(-)^n}{n!} \left(\frac{1}{\epsilon} + \psi^{(0)}(n+1) + \mathcal{O}(\epsilon) \right) \quad n \geq 0, \quad (4.19)$$

where $\psi^{(0)}$ is the digamma function, defined as the logarithmic derivative of the Gamma function:

$$\psi^{(0)}(z) = \frac{\Gamma'(z)}{\Gamma(z)}.$$

For integer values $n > 0$ it equals

$$\psi^{(0)}(n) = -\gamma_E + \sum_{j=1}^{n-1} \frac{1}{j}. \quad (4.20)$$

We can now give the general result for the integral in [Equation 4.18](#):

General Result for Dimensional Regularisation

$$I = i (-)^n \frac{m^{d-2n}}{(4\pi)^{\frac{d}{2}}} \frac{\Gamma\left(n - \frac{d}{2}\right)}{(n-1)!} \quad (d < 2n \text{ or } d \text{ odd}),$$

$$I = i \frac{m^{d-2n}}{(4\pi)^{\frac{d}{2}}} \frac{(-)^{\frac{d}{2}}}{(n-1)! \left(\frac{d}{2} - n\right)!} \left(\frac{1}{\epsilon} - \gamma_E + \sum_{j=1}^{\frac{d}{2}-n} \frac{1}{j} + \ln 4\pi - \ln m^2 \right) \quad (d \geq 2n).$$

We give a list of common integrals in dimensional regularisation in [Appendix B.3](#). Note that the change of dimensions to a non-integer value also reflects itself in tensor contractions. In particular

$$g_{\mu\nu} g^{\mu\nu} = \omega. \quad (4.21)$$

Dirac γ -matrices are however dimensionally normalised such that $\text{Tr}(\mathbb{1}) \equiv d$, i.e. while Lorentz indices live in an ω -dimensional spacetime, Dirac indices always live in an (integer) d -dimensional spacetime. This implies that the contraction identities for γ -matrices are in function of ω (see [Equations A.30](#)), while the trace identities are in function of d (see [Equations A.31](#), in 4 dimensions). This works fine for every γ -matrix but γ^5 , hence dimensional regularisation is not suited to regularise parity-violating theories. As this thesis solely deals with (parity-conserving) QCD, we can adopt the dimensional regularisation framework without problem.

Mass Dimension Analysis

Dimensional analysis is a useful tool in physics, as it helps us to keep track of the right physical quantities. The *Dimension* of an expression is a collection of powers of the basic physical quantities, and is intimately related to the unit of a quantity. There are 7 basic physical quantities in physics, the *base quantities* (with their corresponding SI units in brackets):

[M] Mass (kg, kilogram),

[L] Length (m, metre),

- [T] Time (s, second),
- [Θ] Temperature (K, Kelvin),
- [N] Amount of substance (mole),
- [I] Electric current (A, Ampère),
- [J] Luminous intensity (cd, candela).

Any physical quantity can be expressed in powers of these base units.² E.g. acceleration is $[L][T^{-2}]$, force is $[M][L][T^{-2}]$, electric resistance is $[M][L^2][T^{-3}][I^{-2}]$, and energy is $[M][L^2][T^{-2}]$. The important fact is that any physically meaningful equation must have the same Dimensions on the *l.h.s.* and *r.h.s.*, hence checking this is a useful tool to check the validity of an equation.

But we are working in natural units (more specifically, Lorentz-Heaviside natural units), where $c \stackrel{\text{def}}{=} \hbar \stackrel{\text{def}}{=} k_B \stackrel{\text{def}}{=} \epsilon_0 \stackrel{\text{def}}{=} 1$. This implies that $[M]$, $[L]$, $[T]$ and $[\Theta]$ are now related to each other, because:

$$c = \lambda\nu \stackrel{\text{def}}{=} 1 \Rightarrow [L] \equiv [T], \quad (4.22a)$$

$$E = \hbar\omega \stackrel{\text{def}}{=} \omega \Rightarrow [M][L^2][T^{-2}] \equiv [T^{-1}] \Rightarrow [M] \equiv [L^{-1}], \quad (4.22b)$$

$$S = k_B \ln W \stackrel{\text{def}}{=} \ln W \Rightarrow [M][L^2][T^{-2}] \equiv [\Theta]. \quad (4.22c)$$

We will choose Mass as the basic Dimension, with $[M]=[L^{-1}]=[T^{-1}]=[\Theta]$. Using natural units leads to a simplified relation between the elementary charge and the fine-structure constant:

$$\alpha \equiv \frac{e^2}{4\pi} \Rightarrow [Q] \equiv 0. \quad (4.23)$$

We can exploit this to relate the dimension of the electric current to the dimension of mass:

$$I = \frac{dQ}{dt} \Rightarrow [I] \equiv [M]. \quad (4.24)$$

The two remaining base quantities (amount of substance and luminous intensity) are of lesser importance in pure QFT, so we state that every expression we will encounter will—when in natural units—have its Dimension exactly defined by its Mass Dimension. Some common Mass Dimensions are (from now on, we use the notation $[...]$ to denote the Mass Dimension of an expression):

$$[m] = +1, \quad [x^\mu] = -1, \quad [d^4x] = -4, \quad [\partial_\mu] = +1, \quad [E] = +1, \quad [p^\mu] = +1.$$

² An exception to this are dimensionless quantities, for which it is not guaranteed that they can be expressed in function of the base quantities. The best examples are the radian and steradian, that are considered the standard units of (solid) angular measure.

The derivative has positive Mass Dimension because it equals one over length. The action is required to be a dimensionless quantity:

$$[S] \equiv 0 \quad \Rightarrow \quad [\mathcal{L}] \equiv 4, \quad (4.25)$$

because the integral over x has Mass Dimension $[f d^4 x] = f [d^4 x] = -4$. We can use this requirement to derive the Mass Dimension of the different fields, because every term in the Lagrangian has to have Mass Dimension equal to 4. For scalar fields we have:

$$[\partial_\mu \phi \partial^\mu \phi] \equiv 4 \quad \Rightarrow \quad [\phi] \equiv 1, \quad (4.26)$$

for spinor fields:

$$[\bar{\psi} \not{\partial} \psi] \equiv 4 \quad \Rightarrow \quad [\psi] \equiv \frac{3}{2}, \quad (4.27)$$

and for gauge fields:

$$[\partial_\mu A_\nu \partial^\mu A^\nu - \partial_\mu A_\nu \partial^\nu A^\mu] \equiv 4 \quad \Rightarrow \quad [A_\mu] \equiv 1. \quad (4.28)$$

The n -point correlators have Mass Dimension equal to n times the mass of the field, as

$$[\langle \phi_1 \cdots \phi_n \rangle] = \frac{[f \mathcal{D} \phi \phi_1 \cdots \phi_n e^{iS}]}{[f \mathcal{D} \phi e^{iS}]} = \frac{[f \mathcal{D} \phi] [\phi_1 \cdots \phi_n] [e^{iS}]}{[f \mathcal{D} \phi] [e^{iS}]} = [\phi_1] \cdots [\phi_n],$$

and similar for the Dirac and gauge fields. Note that $[\mathcal{D} \phi] = \infty$, but is divided out as usual. Using the fact that the δ -function has Mass Dimension opposite to that of its argument:

$$[\delta^n(x)] = \left[\int \frac{d^n p}{(2\pi)^n} e^{ip \cdot x} \right] = n, \quad [\delta^n(p)] = \left[\int \frac{d^n x}{(2\pi)^n} e^{ip \cdot x} \right] = -n, \quad (4.29)$$

we can as well calculate the Mass Dimension of the propagator based on its equation of motion. E.g., the gauge field propagator has to satisfy [Equation 3.126](#):

$$\left[\left(g_{\mu\nu} \square - \left(1 - \frac{1}{\xi} \right) \partial_\mu \partial_\nu \right) D_F^{\nu\rho} \right] \equiv [i \delta_\mu^\rho \delta^{(4)}(x-y)] \quad \Rightarrow \quad [D_F^{\nu\rho}] \equiv 2. \quad (4.30)$$

We can verify from the mass terms $[m \bar{\psi} \psi]$ and $[m^2 \phi^2]$ that these parameters m indeed have the Dimension of a mass. The coupling constant is dimensionless, as we can see from $[g \bar{\psi} \not{A} \psi]$.

Now comes the important part. In dimensional regularisation, we modified the number of spacetime dimensions by subtracting a small parameter 2ϵ . But this changes the Mass Dimension of the Lagrangian if we want to satisfy the requirement that the action remains dimensionless, because now

$$\left[\int d^\omega x \mathcal{L} \right] \equiv 0 \quad \Rightarrow \quad [\mathcal{L}] \equiv \omega. \quad (4.31)$$

Hence the Mass Dimensions of the fields change as well:

$$[\partial_\mu \phi \partial^\mu \phi] \equiv \omega \quad \Rightarrow \quad [\phi] \equiv 1 - \epsilon, \quad (4.32a)$$

$$[\bar{\psi} \not{\partial} \psi] \equiv \omega \quad \Rightarrow \quad [\psi] \equiv \frac{3}{2} - \epsilon, \quad (4.32b)$$

$$[\partial_\mu A_\nu \partial^\mu A^\nu - \partial_\mu A_\nu \partial^\nu A^\mu] \equiv \omega \quad \Rightarrow \quad [A_\mu] \equiv 1 - \epsilon. \quad (4.32c)$$

But now the coupling constant is no longer dimensionless:

$$[g \bar{\psi} \not{A} \psi] \equiv \omega \quad \Rightarrow \quad [g] \equiv \epsilon. \quad (4.33)$$

A dimensionful coupling constant hinders perturbative theories quite a lot, if not makes them totally unmanageable. So we define a dimensionless coupling constant \bar{g} as:

$$\bar{g} \mu^\epsilon \stackrel{\text{def}}{=} g, \quad (4.34)$$

with μ an arbitrary energy scale, which we will refer to as the *renormalisation scale* (see the next section). For convenience, we will only use \bar{g} in calculations, so that we can drop the bar in the notation and always write g . In practice this means we need to add a factor μ^ϵ in front of every g .

Until now we have derived the Mass Dimension based on first principles: either we could just read it from the powers of the underlying quantities, or we could derive from a relation to other quantities (like we derived the Mass Dimension of the fields from the requirement that the action is dimensionless). But how do we compute the Mass Dimension for a general quantity F , if nothing is known about its underlying structure? We will try to give a simple intuitive statement here. Suppose that F has Mass Dimension n , then we can write:

$$F = c m^n.$$

By differentiating w.r.t. m , the exponent comes in front:

$$\frac{\partial F}{\partial m} = n c m^{n-1},$$

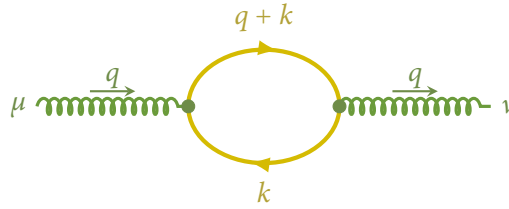


Figure 4.1: Fermion loop correction to the gluon propagator. Because the γ -matrices are traced, they give rise to a negative sign in front. Quark momenta are in the direction of the field arrow.

and by multiplying with m , we retrieve the original function:

$$m \frac{\partial F}{\partial m} = n c m^n = n F.$$

So we define the Mass Dimension as

Mass Dimension

$$[F] \stackrel{\text{def}}{=} \frac{\partial \ln F}{\partial \ln m} = \frac{m}{F} \frac{\partial F}{\partial m}. \quad (4.35)$$

This is of course a bit simplistic, so we will give a more formal approach when deriving the Callan-Symanzik Equation 4.81.

One-Loop Example: Gluon Propagator with Fermion Loop

We have now all necessary tools to make an example calculation. We will calculate one of the NLO corrections diagrams to the gluon propagator, namely the one with an internal fermion loop as depicted in figure Figure 4.1.

Using the Feynman rules in Appendix A.8, we can write down the amplitude for this diagram:

$$i \Pi_2^{\mu\nu}(q) = - (ig)^2 \text{tr}(t^a t^b) \mu^{2\epsilon} \int \frac{d^\omega k}{(2\pi)^\omega} \text{Tr} \left(\gamma^\mu \frac{i}{\not{k} - m} \gamma^\nu \frac{i}{\not{k} + \not{q} - m} \right). \quad (4.36)$$

Note that we added a factor $\mu^{2\epsilon}$ coming from the Mass Dimension of the coupling constant. Because we are calculating the *correction* to the gluon propagator, the two gluon lines are not included in the calculation. The trace

over the colour generators can be calculated using [Equation A.70](#). We bring the γ -matrices up from the denominator:

$$\frac{1}{\not{k} - m} \frac{\not{k} + m}{\not{k} + m} = \frac{\not{k} + m}{k^2 - m^2},$$

and next we use Feynman parameters (see [Appendix B.2](#)) to combine the two denominators into one:

$$\frac{1}{k^2 - m^2} \frac{1}{(k + q)^2 - m^2} = \int_0^1 dx \frac{1}{(\ell^2 - \Delta)^2},$$

where

$$\ell^\mu = k^\mu + xq^\mu, \quad \Delta = m^2 - x(1-x)q^2.$$

The amplitude then becomes

$$\begin{aligned} i\Pi_2^{\mu\nu}(q) &= -g^2 \text{Tr}(\gamma^\mu \gamma^\rho \gamma^\nu \gamma^\sigma) \frac{1}{2} \delta^{ab} \mu^{2\epsilon} \int \frac{d^\omega k}{(2\pi)^\omega} dx \frac{\ell_\rho \ell_\sigma - x(1-x)q_\rho q_\sigma}{(\ell^2 - \Delta)^2} \\ &\quad - g^2 \text{Tr}(\gamma^\mu \gamma^\nu) \frac{1}{2} \delta^{ab} \mu^{2\epsilon} \int \frac{d^\omega k}{(2\pi)^\omega} dx \frac{m^2}{(\ell^2 - \Delta)^2}, \end{aligned}$$

where we used the fact that the integration over odd powers of ℓ vanishes, just as the trace of an odd number of γ -matrices. Now we use the trace identities for the Dirac matrices (see [Equations A.31](#)), which gives:

$$\begin{aligned} i\Pi_2^{\mu\nu}(q) &= -2g^2 \delta^{ab} \mu^{2\epsilon} \int \frac{d^\omega k}{(2\pi)^\omega} dx \left(g^{\mu\nu} \frac{2-\omega}{\omega} \frac{\ell^2}{(\ell^2 - \Delta)^2} \right. \\ &\quad \left. + (g^{\mu\nu} m^2 - x(1-x)(2q^\mu q^\nu - g^{\mu\nu} q^2)) \frac{1}{(\ell^2 - \Delta)^2} \right). \end{aligned}$$

These two integrals are given in [Equations B.25](#). Note that we can rewrite

$$g^{\mu\nu} m^2 - x(1-x)(2q^\mu q^\nu - g^{\mu\nu} q^2) = g^{\mu\nu} \Delta - 2x(1-x)(q^\mu q^\nu - g^{\mu\nu} q^2).$$

This Δ will cancel the extra Δ coming from the integration with ℓ^2 (after taking the limit $\epsilon \rightarrow 0$ where possible):

$$\begin{aligned} \int \frac{d^\omega k}{(2\pi)^\omega} dx \frac{\ell^2}{(\ell^2 - \Delta)^2} &= i \frac{\Delta}{(4\pi)^2} \frac{\omega}{2} \left(\frac{1}{\epsilon} - \gamma_E + \ln 4\pi - \ln \Delta + 1 \right), \\ \int \frac{d^\omega k}{(2\pi)^\omega} dx \frac{1}{(\ell^2 - \Delta)^2} &= i \frac{1}{(4\pi)^2} \left(\frac{1}{\epsilon} - \gamma_E + \ln 4\pi - \ln \Delta \right). \end{aligned}$$

The result is then

$$i\Pi_2^{\mu\nu}(q) = (q^2 g^{\mu\nu} - q^\mu q^\nu) i\delta^{ab}\Pi_2(q^2), \quad (4.37a)$$

$$\Pi_2(q^2) = -\frac{\alpha_s}{\pi} \int dx \, x(1-x) \left(\frac{1}{\epsilon} - \gamma_E + \ln 4\pi - \ln \frac{\Delta}{\mu^2} \right), \quad (4.37b)$$

where we used the definition of the fine-structure constant as in [Equation A.2](#). This last integral can be calculated as well. The first part is trivial:

$$\left(\frac{1}{\epsilon} - \gamma_E + \ln 4\pi + \ln \mu^2 \right) \int dx \, x(1-x) = \frac{1}{6} \left(\frac{1}{\epsilon} - \gamma_E + \ln 4\pi + \ln \mu^2 \right). \quad (4.38)$$

For the last term we have to make a distinction whether the polynomial can be factored or not. In case $q^2 \geq 4m^2$, we can:

$$m^2 - x(1-x)q^2 = q^2(x-x_1)(x-x_2), \quad x_{1,2} = \frac{1}{2} \pm \frac{1}{2} \sqrt{1 - 4\frac{m^2}{q^2}}.$$

The integral then breaks up into 5 pieces:

$$\begin{aligned} - \int dx \, x(1-x) \ln(m^2 - x(1-x)q^2) = \\ - \frac{1}{6} \ln q^2 - \int dx \, x \ln(x-x_1) - \int dx \, x \ln(x-x_1) \\ + \int dx \, x^2 \ln(x-x_1) + \int dx \, x^2 \ln(x-x_1). \end{aligned}$$

These integrals are listed in [Equations B.2](#):

$$\begin{aligned} \int dx \, x \ln(x-x_i) &= \frac{1}{2}(1-x_i^2) \ln(1-x_i) - \frac{x_i}{2} - \frac{1}{4} + \frac{1}{2}x_i^2 \ln(-x_i), \\ \int dx \, x^2 \ln(x-x_i) &= \frac{1}{3}(1-x_i^3) \ln(1-x_i) - \frac{x_i^2}{3} - \frac{x_i}{6} - \frac{1}{9} + \frac{1}{3}x_i^3 \ln(-x_i). \end{aligned}$$

We can simplify this sum further by noting that $x_1 = 1 - x_2$ and vice versa. This gives:

$$\begin{aligned} - \int dx \, x(1-x) \ln(m^2 - x(1-x)q^2) = \\ - \frac{1}{6} \left[\ln m^2 - 4\frac{m^2}{q^2} - \frac{5}{3} + i\pi + \sqrt{1 - 4\frac{m^2}{q^2}} \left(1 + 2\frac{m^2}{q^2} \right) \ln \frac{1 + \sqrt{1 - 4\frac{m^2}{q^2}}}{1 - \sqrt{1 - 4\frac{m^2}{q^2}}} \right]. \end{aligned}$$

On the other hand, in case $q^2 < 4m^2$, we can only break the integral in 3 pieces because we cannot factor the polynomial. The result is then:

$$- \int dx \, x(1-x) \ln(m^2 - x(1-x)q^2) = -\frac{1}{6} \left[\ln m^2 - 4 \frac{m^2}{q^2} - \frac{5}{3} + i \sqrt{4 \frac{m^2}{q^2} - 1} \left(1 + 2 \frac{m^2}{q^2} \right) \ln \frac{1 + i \sqrt{4 \frac{m^2}{q^2} - 1}}{1 - i \sqrt{4 \frac{m^2}{q^2} - 1}} \right].$$

The only difference with the case $q^2 > 4m^2$ is the term $i\pi$. This is not so surprising, as the logarithm has a branch cut at $q^2 = 4m^2$. So the final result is then

Gluon Propagator with a Fermion Loop

$$i\Pi_2^{\mu\nu}(q) = (q^2 g^{\mu\nu} - q^\mu q^\nu) i\delta^{ab} \Pi_2(q^2), \quad (4.39a)$$

$$\Pi_2(q^2) = -\frac{\alpha_s}{6\pi} \left(\frac{1}{\epsilon} - \gamma_E + \ln 4\pi - \ln \frac{m^2}{\mu^2} + C(q^2) \right), \quad (4.39b)$$

$$C(q^2) = -4 \frac{m^2}{q^2} - \frac{5}{3} + \sqrt{1 - 4 \frac{m^2}{q^2}} \left(1 + 2 \frac{m^2}{q^2} \right) \ln \frac{1 + \sqrt{1 - 4 \frac{m^2}{q^2}}}{1 - \sqrt{1 - 4 \frac{m^2}{q^2}}} + i\pi \theta(q^2 - 4m^2).$$

Most of the time we are only interested in the coefficient of the pole; the finite coefficients only matter when going to NNLO and higher. But note that $C(q^2)$ is finite at $q^2 = 0$, although maybe not obvious at first sight. We can make this clear by expanding the square root and the logarithm around $q^2 = 0$:

$$\sqrt{1 - 4 \frac{m^2}{q^2}} = 2i \left(\frac{q}{m} \right)^{-1} - \frac{i}{4} \frac{q}{m} + \mathcal{O}(q^3), \quad (4.40a)$$

$$\ln \frac{1 + \sqrt{1 - 4 \frac{m^2}{q^2}}}{1 - \sqrt{1 - 4 \frac{m^2}{q^2}}} = -i \frac{q}{m} - \frac{i}{24} \left(\frac{q}{m} \right)^3 + \mathcal{O}(q^5), \quad (4.40b)$$

such that their combination becomes

$$\sqrt{1 - 4 \frac{m^2}{q^2}} \left(1 + 2 \frac{m^2}{q^2} \right) \ln \frac{1 + \sqrt{1 - 4 \frac{m^2}{q^2}}}{1 - \sqrt{1 - 4 \frac{m^2}{q^2}}} = 4 \frac{m^2}{q^2} + \frac{5}{3} + \mathcal{O}(q), \quad (4.41a)$$

$$\Rightarrow C(0) = 0. \quad (4.41b)$$

In other words, the NLO correction doesn't add any poles in $q^2 = 0$.

4.2 FROM THEORY TO EXPERIMENT

What we have derived so far, is how to calculate n -point field correlators. These are, depending on normalisation and convention, exactly the same as the bare Green's functions of the theory. As the difference is at most a constant factor, we will use the two naming conventions interchangeable.

By themselves, Green's functions are not physical observables, as their external legs are not necessarily on mass-shell, and as e.g. correlators of gauge fields aren't even gauge invariant. So we need to relate them to physical quantities that are directly linked to observables. We will apply the most common approach, the S -matrix expansion, that is due to Dyson. The Dyson expansion of the S -matrix contains the complete information about all collision processes. We define it as the probability amplitude for a process to go from an initial state $|\text{in}\rangle$ to a final state $\langle\text{out}|$:

$$S_{\beta\alpha} = \langle\beta|\alpha\rangle. \quad (4.42)$$

Note that this S is not the same as the action S .³ We can also introduce an operator \hat{S} that transforms an in-state into an out-state:

$$\langle\beta, \text{out}| \stackrel{\text{def}}{=} \langle\beta, \text{in}| \hat{S},$$

which gives

$$S_{\beta\alpha} = \langle\beta, \text{in}| \hat{S} |\alpha, \text{in}\rangle. \quad (4.43)$$

It is a unitary operator, because

$$\langle\beta, \text{in}| \hat{S} \hat{S}^\dagger |\alpha, \text{in}\rangle = \langle\beta, \text{in}| \alpha, \text{in}\rangle = \delta_{\beta\alpha}.$$

It is possible to construct this operator from the Green's functions with the so-called *Lehmann-Symanzik-Zimmermann (LSZ) reduction formula*. We won't treat its technicalities here as that would lead us too far, but we will just state the formula itself. The S -matrix for a process with m initial particles (labelled with momenta p_i) and n final particles (labelled with momenta p'_i) can be derived from the $n + m$ -point correlation function as follows:

³ There simply aren't enough letters available in the alphabet.

LSZ Reduction Formula

$$\langle p'_1 \cdots p'_n | \hat{S} | p_1 \cdots p_m \rangle \sim \int \left(\prod_i^n \prod_j^m d^4 x_i d^4 y_j e^{i p'_i \cdot x_i} e^{-i p_j \cdot y_j} (\square'_{x_i} + m^2) (\square_{y_j} + m^2) \right) \langle \Omega | \phi'_{x_1} \cdots \phi'_{x_n} \phi_{y_1} \cdots \phi_{y_m} | \Omega \rangle. \quad (4.44)$$

On the other hand, we can also retrieve observable quantities from the *transition matrix* T , which is defined as the shift that S makes from the identity:

$$\hat{S} \stackrel{\text{def}}{=} \hat{1} + i \hat{T}. \quad (4.45)$$

It can be shown that the transition matrix for processes with two initial particles directly relates to the amplitude:

$$i \langle p'_1 \cdots p'_n | \hat{T} | p_1 p_2 \rangle = \mathfrak{G}^{(4)} \left(p_1 + p_2 - \sum_i^n p'_i \right) \mathcal{M}(p_1 + p_2 \rightarrow p'_1 + \cdots + p'_n),$$

where we used the short-hand notation defined in [Equation 3.81](#). \mathcal{M} is the sum of all possible Feynman diagrams consisting of two incoming particles with momenta p_1 and p_2 , and n outgoing particles with momenta p'_1, \dots, p'_n . Furthermore, we only consider diagrams that are *fully connected* and *amputated*. A diagram is fully connected when it is not separable into subdiagrams, and is amputated if every external leg can be cutted as close to the nearest vertex as possible without making a difference. The following diagrams will hence not be included in amplitude calculations:



The first because it consists of two subdiagrams and is hence not fully connected, the second because the lower right leg isn't fully amputated; we still have to amputate the loop, as indicated by the dashed red line (of course, loop corrections are allowed inside the diagram, i.e. for virtual particles—amputation only concerns external particles).

From this definition for the amplitude, we can construct—using the Lehmann-Symanzik-Zimmermann (LSZ) reduction formula—an observable known as the cross section:

Cross Section

$$d\sigma(12 \rightarrow 1'2' \cdots n') \stackrel{\text{def}}{=} \frac{1}{4\sqrt{(p_1 \cdot p_2)^2 - m_1^2 m_2^2}} d\Phi |\mathcal{M}|^2. \quad (4.46)$$

The first factor is the *flux factor* and depends on the 4-momentum of the

incoming particles. The measure $d\Phi$ is the *Lorentz-invariant phase space* (LIPS), and represents the on-shell conditions for the final particles:

$$d\Phi = \left(\prod_i^n \frac{d^4 p'_i}{(2\pi)^4} \delta^+(p_i'^2 - m^2) \right) \delta^{(4)}\left(p_1 + p_2 - \sum_i^n p'_i\right), \quad (4.47)$$

where δ is defined in Equation 3.81, and δ^+ is a combination of Equation 3.81 and Equation A.54:

$$\delta^+(p^2 - m^2) \stackrel{\text{N}}{=} 2\pi \delta^+(p^2 - m^2) \stackrel{\text{N}}{=} 2\pi \delta(p^2 - m^2) \theta(p^0). \quad (4.48)$$

For each subset of k indistinguishable particles in the final state, we have to divide by a symmetry factor

$$\frac{1}{k!}, \quad (4.49)$$

that compensates for double counting the same state $k!$ times. This is additional to the symmetry factor of the diagram, which only manages the double counting of the internal lines. The cross section is directly observable, as it represents the ‘effective interaction surface’ of a certain process, and can be hence retrieved from experiment by counting events, normalised against a background.

A common approach is to calculate diagrams directly for the amplitude squared $|\mathcal{M}|^2$. The amplitude is then associated with the left side of the diagram, the conjugate amplitude with the right side, and they are separated by a so-called *final-state cut*. The Feynman rules on the left side remain the same, while the rules on the right are hermitian conjugated (in particular, also the propagator pole prescription changes sign to $-\mathrm{i}\epsilon$). Particles that cross the cut are external particles, so they have to be on-shell, which means we add a factor $\delta^+(p^2 - m^2)$. Because we would like to treat it as one diagram, momenta in the right side are flipped. This changes the sign of the 3-gluon vertex and the ghost vertex. We can easily motivate this schematically:

$$F_{\mu\nu\rho}^{abc}(k, p, q) \quad (F_{\mu\nu\rho}^{abc}(k, p, q))^{\dagger} = F_{\mu\nu\rho}^{abc}(k, p, q)$$

where F is the 3-gluon coefficient:

$$F_{\mu\nu\rho}^{abc}(k, p, q) = g f^{abc} [g^{\mu\nu} (k-p)^{\rho} + g^{\nu\rho} (p-q)^{\mu} + g^{\rho\mu} (q-k)^{\nu}].$$

If we now calculate the same probability with the cut diagram method, we get:

$$F_{\mu\nu\rho}^{abc}(k, p, q) F_{\mu\nu\rho}^{abc}(-k, -p, -q) = -F_{\mu\nu\rho}^{abc}(k, p, q)$$

So indeed, by flipping the momenta we get a minus sign difference. The same is true for the ghost vertex. This then gives rise to the following extra Feynman rules for cut diagrams:

A. *Cut Fermion*: $i \xrightarrow{p} j$ = $\delta^{ij} \delta^+(p^2 - m^2)$

B. *Cut Gluon*: $a, \mu \xrightarrow{k} b, \nu$ $\stackrel{\text{Lorentz}}{=} -\delta^{ab} \delta^+(k^2) g^{\mu\nu}$
 $\stackrel{\text{LC}}{=} -\delta^{ab} \delta^+(k^2) \left(g^{\mu\nu} - 2 \frac{k_{(\mu} n_{\nu)}}{k \cdot n} \right)$

- D. All Feynman diagrams at the right side of the cut are complex conjugated.
 C. The 3-gluon vertex and the ghost vertex get an extra minus sign when on the right side of the cut.

The advantage of this approach is that it is easier to directly calculate interference diagrams. It is especially common when calculating PDFs and structure functions, as we will see e.g. in [Equation 5.35](#).

Renormalisation

There is an important matter that we yet have to match with experiment. When doing loop calculations, as we saw before, we regularise the integral using dimensional regularisation. However, in doing so we introduced two new parameters to the theory, namely the UV regulator ϵ and the renormalisation scale μ . These are unphysical leftovers from a mathematical tool, so we somehow have to adapt our theory to manage these.

We start with the UV regulators. The poles are an indication that some of our physical quantities tend towards infinity at higher orders. This behaviour is of course pathological, because we expect the corrections to become smaller and smaller at higher order, converging to a finite value. Let us illustrate this in an intuitive way. Consider e.g. a free electron propagating through spacetime.

It has a charge equal to the elementary charge e . As we go to higher orders in perturbation theory, the electron gets more and more ‘dressed’ with virtual photons and virtual electron-positron pairs, and these corrections add to the apparent charge as we observe it macroscopically. However, these corrections pull the value of the charge to infinity instead of some reasonable value. Now, we have to understand that when we make a real-life experiment, there are no order calculations involved—it is an all-order result—the only limiting factor is the resolution of the detector. But even when the resolution is extremely bad, it will always be good enough to make the difference between a stable value, and a value that explodes towards infinity. In other words, experiment contradicts the theoretical prediction. There is something fundamentally wrong.

In fact, as it happens, there is something *conceptually* wrong with our intuitive explanation. We *assumed* that the elementary charge equals the bare electron charge e_0 (which is the charge as it appears in \mathcal{L} , i.e. before corrections), but of course this is totally wrong. The elementary charge as we know it, is a result drawn from experiment, hence it is the charge *after making all order corrections*. If the reason that the charge explodes is that we took the wrong starting assumption, then maybe we have to reverse the idea. Instead of a finite (unmeasurable) bare charge, that explodes when calculating all order corrections towards an infinite (measurable) macroscopic charge, we take the bare charge to be infinite, such that it becomes finite after including all order corrections. This is the key concept behind *renormalisation*.

Is it counter-intuitive—or even unphysical—to make the bare charge divergent? Actually, no, it isn’t, as the bare charge itself is unphysical. It is not an observable, because no real-world electron will ever be free of virtual corrections dressing it. Hence the renormalised charge is the correct physical observable.

Let us try to forge this into in a mathematical statement. We start with an investigation of the gluon propagator. We define the one-particle irreducible (1PI) diagram as the sum of all diagrams that cannot be separated by cutting maximally one gluon line:

$$i\Pi^{\mu\nu}(q) \equiv \mu \overset{q}{\curvearrowright} \text{1PI} \curvearrowleft \nu . \quad (4.50)$$

In the calculation we have done before, we have used the notation $\Pi_2^{\mu\nu}$ to denote the contribution that is second order in g . Note that we were able to factorise out the tensor structure in [Equation 4.39a](#). In fact, it is possible to prove that this is a general statement to all orders:

$$\Pi^{\mu\nu}(q) = (q^2 g^{\mu\nu} - q^\mu q^\nu) \Pi(q^2), \quad (4.51)$$

where Π doesn’t introduce extra poles in $q^2 = 0$. The full gluon two-point function is then given by:

$$\begin{aligned}
 \text{gluon loop} &= \text{gluon} + \text{gluon} \text{ (1PI)} + \text{gluon} \text{ (1PI)} \text{ (1PI)} + \dots \\
 &= \frac{-i g^{\mu\nu}}{q^2} + \frac{-i g^{\mu\rho}}{q^2} i (q^2 g_{\rho\sigma} - q_\rho q_\sigma) \Pi(q^2) \frac{-i g^{\sigma\nu}}{q^2} + \dots,
 \end{aligned}$$

which we can abbreviate as

$$\text{gluon loop} = \frac{-i g^{\mu\nu}}{q^2 (1 - \Pi(q^2))}.$$

Note that this relation is only valid inside an S -matrix calculation, and that its derivation relies heavily on the validity of so-called *Ward identities* $k_\mu \mathcal{M}^\mu = 0$, for which the treatment goes beyond the scope of this thesis. Because $\Pi(q^2)$ doesn't add extra poles in q^2 , the manifest singularity in the exact propagator for $q^2 = 0$ remains, and the gluon remains massless after higher order corrections. The residue of this pole is

$$\frac{1}{1 - \Pi(0)} \stackrel{N}{=} \mathcal{Z}_A, \tag{4.52}$$

so that we can write

$$\text{gluon loop} = \mathcal{Z}_A \frac{-i g^{\mu\nu}}{q^2} + \text{finite terms}. \tag{4.53}$$

The constant \mathcal{Z}_A , which we will call a *renormalisation constant*, is infinite after taking the limit $\epsilon \rightarrow 0$. E.g. using the result in [Equations 4.39](#), we can calculate the $\mathcal{O}(\alpha_s)$ -shift in the propagator due to the fermion loop correction:

$$\delta \mathcal{Z}_A^\psi = \mathcal{Z}_A^\psi - 1 \stackrel{\mathcal{O}(\alpha_s)}{=} -\frac{\alpha_s}{6\pi} \left(\frac{1}{\epsilon} - \gamma_E + \ln 4\pi - \ln \frac{m_q^2}{\mu^2} \right). \tag{4.54}$$

We can repeat the same calculation for the quark propagator. The **1PI** diagram is defined as:

$$-i\Sigma(p) \equiv \text{quark line with 1PI loop}. \tag{4.55}$$

The full quark propagator is then given by:

$$\begin{aligned}
 \text{full quark propagator} &= \text{free quark} + \text{quark} \text{ (1PI)} + \text{quark} \text{ (1PI)} \text{ (1PI)} + \dots \\
 &= \frac{i}{\not{p} - m_0} + \frac{i}{\not{p} - m_0} [-i\Sigma(\not{p})] \frac{i}{\not{p} - m_0} + \dots.
 \end{aligned}$$

Note that these are the bare masses, as the observable mass will be the mass after corrections. The sum of all iPI diagrams resums into

$$\text{---} \circ \text{---} = \frac{i}{\not{p} - m_0 - \Sigma(\not{p})}. \quad (4.56)$$

The pole $\not{p} = m_0 + \Sigma(\not{p})$ represents the condition for the propagator to go on-shell, it hence defines the new mass, after corrections, which is thus defined as the solution of

$$m \equiv m_0 + \Sigma(m). \quad (4.57)$$

The mass shift is given by:

$$\delta m = m - m_0 = \Sigma(m). \quad (4.58)$$

For first-order corrections, it can be approximated by:

$$\delta m \approx \Sigma(m_0). \quad (4.59)$$

Close to the pole $\not{p} = m$, we can expand the denominator as

$$(\not{p} - m) \left(1 - \left. \frac{d\Sigma}{d\not{p}} \right|_{\not{p}=m} \right) + \mathcal{O}((\not{p} - m)^2).$$

The residue of the propagator pole is given by

$$\frac{1}{1 - \left. \frac{d\Sigma}{d\not{p}} \right|_{\not{p}=m}} \stackrel{\text{N}}{=} \mathcal{Z}_\psi, \quad (4.60)$$

so that we can write

$$\text{---} \circ \text{---} = \mathcal{Z}_\psi \frac{i}{\not{p} - m} + \text{finite terms}. \quad (4.61)$$

Again, the factor \mathcal{Z}_ψ is infinite in the limit $\epsilon \rightarrow 0$. Similarly, the ghost field propagators will gain a factor \mathcal{Z}_c . What makes things somewhat cumbersome, is that because the Green's functions gain a renormalisation factor, i.e.

$$\langle \Omega | \phi_1 \cdots \phi_n | \Omega \rangle \rightarrow (\sqrt{\mathcal{Z}_\phi})^n \langle \Omega | \phi_1 \cdots \phi_n | \Omega \rangle,$$

the [LSZ formula in Equation 4.44](#) also gains this factor:

$$\begin{aligned}
& (\sqrt{\mathcal{Z}_\phi})^{n+m} \langle p'_1 \cdots p'_n | \hat{S} | p_1 \cdots p_m \rangle \sim \\
& \int \left(\prod_i^n \prod_j^m d^4 x_i d^4 y_j e^{i p'_i \cdot x_i} e^{-i p_j \cdot x_j} (\square'_{x_i} + m^2) (\square_{y_j} + m^2) \right) \langle \Omega | \phi'_{x_1} \cdots \phi'_{x_n} \phi_{y_1} \cdots \phi_{y_m} | \Omega \rangle .
\end{aligned} \tag{4.62}$$

We will see in a moment how we can deal with this.

In [Equations 4.53](#) and [4.61](#) we separated the pole part from the finite parts. However, it is often convenient to absorb some of the finite terms into the constants \mathcal{Z}_A and \mathcal{Z}_ψ (or equivalently, in the renormalisation scale). This choice is totally free, as long as it is kept consistently. This is called a *renormalisation scheme*. Two common choices are

- A. **MS** (*minimal subtraction renormalisation scheme*): No finite terms, only the pole $1/\epsilon$ is absorbed.
- B. **$\overline{\text{MS}}$** (*modified minimal subtraction renormalisation scheme*): The pole $1/\epsilon$ and the regularisation ‘remnants’ $\ln 4\pi$ and $-\gamma_E$ are absorbed.

It is convenient to define the $\overline{\text{MS}}$ scheme in a more rigorous way. We will subtract the remnants by absorbing them in the renormalisation scale. For this we define a factor S_ϵ such that $\bar{\mu}$, defined as

$$\bar{\mu}^{2\epsilon} \stackrel{\text{def}}{=} \mu^{2\epsilon} S_\epsilon = \mu^\epsilon [1 + \epsilon (\ln 4\pi - \gamma_E) + \mathcal{O}(\epsilon^2)] , \tag{4.63}$$

contains the remnants. The most common choice for S_ϵ is

$$S_\epsilon = (4\pi e^{-\gamma_E})^\epsilon , \tag{4.64}$$

but we prefer to follow the convention by Collins [\[33\]](#):

$\overline{\text{MS}}$ Subtraction

$$S_\epsilon = \frac{(4\pi)^\epsilon}{\Gamma(1-\epsilon)} . \tag{4.65}$$

Up to first order in ϵ , the two conventions are equal. We prefer the last one, because it maximally simplifies loop calculations with a double pole at first order, which are common when using Wilson lines (see e.g. [Equation 7.72](#) for a calculation where we demonstrate the difference). In practice, every coupling constant is automatically accompanied by the renormalisation scale (see [Equation 4.34](#)), so to express the results in function of the subtracted scale, we have to divide it by S_ϵ :

$$g \stackrel{\text{def}}{=} \bar{g} \mu^\epsilon \stackrel{\text{def}}{=} \bar{g} \bar{\mu}^\epsilon \sqrt{S_\epsilon^{-1}} , \tag{4.66}$$

where g is the dimensionful and \bar{g} the dimensionless coupling constant, i.e. $[g] = \epsilon$ and $[\bar{g}] = 0$. We will only use the dimensionless coupling constant \bar{g} and the subtracted scale $\bar{\mu}$, so for convenience, we drop the bar notation. Also, in order not to overload our calculations, we won't explicitly write the factors $\sqrt{S_\epsilon^{-1}}$. We will just remind ourselves to divide by a factor S_ϵ per loop (and mention when we do this). To see how S_ϵ subtracts the remnants, we first note that the $(4\pi)^\epsilon$ factor is directly cancelled, and that the Euler-Mascheroni constant is cancelled because

$$\Gamma(\epsilon)\Gamma(1-\epsilon) = \frac{1}{\epsilon} + \mathcal{O}(\epsilon). \quad (4.67)$$

This can be illustrated with e.g. [Equation 4.15](#):

$$\begin{aligned} S_\epsilon^{-1} \int \frac{d^\omega k}{(2\pi)^\omega} \frac{1}{(k^2 - m^2)^2} &= \frac{\Gamma(1-\epsilon)}{(4\pi)^\epsilon} \frac{i}{(4\pi)^2} \left(\frac{4\pi}{m^2}\right)^\epsilon \Gamma(\epsilon), \\ &\rightarrow \frac{i}{(4\pi)^2} \left(\frac{1}{\epsilon} - \ln m^2\right). \end{aligned}$$

To renormalise our theory we can now proceed in two different ways.

RENORMALISED PERTURBATION THEORY: In this approach we remove the infinite renormalisation constants from the n -point correlators. To achieve this, we rescale the bare fields:

$$A_0^\mu \rightarrow \sqrt{\mathcal{Z}_A} A_r^\mu, \quad (4.68a)$$

$$\psi_0 \rightarrow \sqrt{\mathcal{Z}_\psi} \psi_r, \quad (4.68b)$$

$$c_0 \rightarrow \sqrt{\mathcal{Z}_c} c_r. \quad (4.68c)$$

This is indeed the renormalisation procedure as we described it in an intuitive way in the beginning of this section. We define the bare fields as infinite, such that they become finite after corrections. Here the A_r^μ , ψ_r and c_r are the *renormalised fields*, i.e. the fields as we measure them in experiment. In a way, they are the bare fields after extraction of an infinite factor. Thanks to these rescalings, the [LSZ](#) formula is cast in its original form, as in [Equation 4.44](#) without the infinite factors in front of the S-matrix, and in function of the renormalised fields. The rescalings also propagate into the Lagrangian, which is now given by:

$$\begin{aligned} \mathcal{L} = & -\frac{1}{4} \mathcal{Z}_A (\partial^\mu A_r^\nu - \partial^\nu A_r^\mu)^2 - \frac{1}{2\xi} \mathcal{Z}_A \partial_\mu A_r^\mu \partial_\nu A_r^\nu - \mathcal{Z}_c \bar{c}_r \square c_r \\ & + \mathcal{Z}_\psi \bar{\psi}_r (i \not{\partial} - m_0) \psi_r + g_0 \sqrt{\mathcal{Z}_A} \mathcal{Z}_\psi \bar{\psi}_r A_r \psi_r - g_0 \sqrt{\mathcal{Z}_A} \mathcal{Z}_c f^{abc} \bar{c}_r \partial^\mu A_{\mu r}^b c_r \\ & - g_0 \mathcal{Z}_A^{\frac{3}{2}} f^{abc} (\partial_\mu A_{\nu r}^a) A_r^{\mu b} A_r^{\nu c} - \frac{1}{2} g_0^2 \mathcal{Z}_A^2 f^{abx} f^{xcd} A_{\mu r}^a A_{\nu r}^b A_r^{\mu c} A_r^{\nu d}. \end{aligned}$$

If we now define

Counterterms

$$\delta_\psi \stackrel{\text{def}}{=} Z_\psi - 1, \quad \delta_A \stackrel{\text{def}}{=} Z_A - 1, \quad \delta_c \stackrel{\text{def}}{=} Z_c - 1, \quad (4.69a)$$

$$\delta_m \stackrel{\text{def}}{=} Z_\psi m_0 - m, \quad \delta_1 \stackrel{\text{def}}{=} \frac{g_0}{g} Z_c \sqrt{Z_A} - 1, \quad \delta_2 \stackrel{\text{def}}{=} \frac{g_0}{g} Z_\psi \sqrt{Z_A} - 1, \quad (4.69b)$$

$$\delta_3 \stackrel{\text{def}}{=} \frac{g_0}{g} \left(\sqrt{Z_A} \right)^3 - 1, \quad \delta_4 \stackrel{\text{def}}{=} \frac{g_0^2}{g} Z_A^2 - 1, \quad (4.69c)$$

we can write the Lagrangian as

$$\mathcal{L} = \mathcal{L}_{\text{renorm}} + \mathcal{L}_{\text{counter}}, \quad (4.70)$$

where the first is the renormalised Lagrangian, i.e. the standard Lagrangian expressed in function of renormalised fields, physical masses, and physical coupling constants:

$$\begin{aligned} \mathcal{L}_{\text{renorm}} = & -\frac{1}{4} (\partial^\mu A_r^\nu - \partial^\nu A_r^\mu)^2 - \frac{1}{2\xi} \partial_\mu A_r^\mu \partial_\nu A_r^\nu - \bar{c}_r \square c_r \\ & + \bar{\psi}_r (i\cancel{\partial} - m) \psi_r + g \bar{\psi}_r \cancel{A}_r \psi_r - g f^{abc} \bar{c}_r \partial^\mu A_{\mu r}^b c_r \\ & - g f^{abc} (\partial_\mu A_{\nu r}^a) A_r^{\mu b} A_r^{\nu c} - \frac{1}{2} g^2 f^{abx} f^{xcd} A_{\mu r}^a A_{\nu r}^b A_r^{\mu c} A_r^{\nu d}, \end{aligned}$$

and the second contains the so-called *counterterms*:

$$\begin{aligned} \mathcal{L}_{\text{counter}} = & -\frac{1}{4} \delta_A (\partial^\mu A_r^\nu - \partial^\nu A_r^\mu)^2 - \frac{1}{2\xi} \delta_A \partial_\mu A_r^\mu \partial_\nu A_r^\nu - \delta_c \bar{c}_r \square c_r \\ & + \delta_\psi \bar{\psi}_r (i\cancel{\partial} - \delta_m) \psi_r + g \delta_2 \bar{\psi}_r \cancel{A}_r \psi_r - g \delta_1 f^{abc} \bar{c}_r \partial^\mu A_{\mu r}^b c_r \\ & - g \delta_3 f^{abc} (\partial_\mu A_{\nu r}^a) A_r^{\mu b} A_r^{\nu c} - \frac{1}{2} g^2 \delta_4 f^{abx} f^{xcd} A_{\mu r}^a A_{\nu r}^b A_r^{\mu c} A_r^{\nu d}. \end{aligned}$$

The eight parameters in [Equations 4.69](#) depend on five quantities (3 fields, a mass and a coupling constant), so there are three relations between them. These are known as the *Slavnov-Taylor* identities, and can be derived from Noether's current conservation theorem and gauge invariance (see e.g. [31]):

$$\delta_1 - \delta_c \equiv \delta_2 - \delta_\psi \equiv \delta_3 - \delta_A \equiv \frac{1}{2} (\delta_4 - \delta_A). \quad (4.71)$$

The definitions in [Equations 4.69](#) only make sense if we give a precise definition for the physical mass and coupling constant. For this we need to define a set of *renormalisation conditions*, from which we can derive constraints on the counterterms. One such condition is e.g. that the physical mass is defined as

the pole of the quark propagator at all orders. Then we proceed as follows: the terms in $\mathcal{L}_{\text{counter}}$ will give rise to extra Feynman rules, viz. the counterterm diagrams. We then can compute any amplitude by considering all possible diagrams, including the counterterm diagrams (which are power-counted as one order in α_s higher than the corresponding regular diagrams). The amplitude will be expressed in the unknown parameters $\delta_A, \delta_\psi, \delta_c, \delta_1, \delta_2, \delta_3, \delta_4$, and δ_m . These parameters are then retrieved by matching the amplitude against the renormalisation conditions. The result will be naturally free of divergences, and independent of the regulator. See e.g. [18, 31] for an expanded treatment.

BARE PERTURBATION THEORY: Another approach is to keep all quantities in their bare form during the computation of amplitudes. It will give us an expression in function of the regulator ϵ and the bare parameters m_0 and g_0 . Next we calculate the physical mass and coupling constant up to the order that is relevant for the first calculation. We then express the bare mass and coupling constant in function of the physical parameters. We retrieve the cross section by using the LSZ-formula, but *with* the renormalisation factors. In the end the result is free of divergences, and independent of the regulator. This approach is more straightforward to implement, as we can keep the same calculations as before but expressed in bare quantities. It requires however double the number of calculations, as we have to calculate the physical quantities separately, and becomes quite complicated at higher orders. But the advantage is that if the physical masses and coupling constants have already been calculated, they can be reused in other calculations. We prefer to use this approach, as it allows us to do regular calculations as before, forgetting about renormalisation or counterterms, and still renormalise the result later on. Of course the two approaches are totally equivalent, but not interchangeable; one has to use one approach consistently.

The Callan-Symanzik equation

In the previous subsection we investigated how we use renormalisation to handle one of the unphysical leftovers of the regularisation process, namely the UV regulator. However, there is another unphysical remnant that we need to deal with, viz. the renormalisation scale μ , which follows from a shift in spacetime dimensions to non-integer values (see Equation 4.34). After renormalising the fields, all the parameters will depend on this renormalisation scale, i.e.

$$\mathcal{Z}(\mu), \quad g(\mu), \quad m(\mu). \quad (4.72)$$

But logically, the bare parameters are renormalisation-scale independent:

$$\frac{\partial \phi_0}{\partial \mu} \equiv 0, \quad \frac{\partial g_0}{\partial \mu} \equiv 0, \quad \frac{\partial m_0}{\partial \mu} \equiv 0. \quad (4.73)$$

Now consider a Green's function of n fields, for simplicity all of the same type. The bare Green's function depends on the bare parameters, the fields, and the momenta in the external legs, but not on the renormalisation scale:

$$\mathcal{G}_0^n \equiv \mathcal{G}_0^n(g_0, m_0, \{\phi_i\}, \{p_i\}), \quad (4.74a)$$

$$\frac{d\mathcal{G}_0^n}{d\mu} = 0. \quad (4.74b)$$

The renormalised Green function follows from the rescaling of the fields:

$$\mathcal{G}^n \stackrel{\text{def}}{=} (\sqrt{\mathcal{Z}_\phi})^{-n} \mathcal{G}_0^n, \quad (4.75)$$

and gains now scale dependence through its parameters, but possibly also directly (note that the momenta don't scale with μ):

$$\mathcal{G}^n \equiv \mathcal{G}^n(\mu, g(\mu), m(\mu), \{\phi_i(\mu)\}, \{p_i\}). \quad (4.76)$$

Using [Equation 4.74b](#) we can investigate its behaviour under a scale shift:

$$\frac{d}{d\ln \mu} \left((\sqrt{\mathcal{Z}_\phi})^n \mathcal{G}^n \right) \equiv 0 \quad \Rightarrow \quad \left(n \gamma_\phi + \frac{d}{d\ln \mu} \right) \mathcal{G}^n \equiv 0, \quad (4.77)$$

where

$$\gamma_\phi \stackrel{\text{N}}{=} -\frac{1}{2} \frac{\partial \ln \mathcal{Z}}{\partial \ln \mu} \quad (4.78)$$

is the *anomalous dimension* of the field. We have chosen to differentiate w.r.t. $\ln \mu$ instead of μ , such that γ_ϕ is dimensionless. We can use the chain rule for the differentiation of the Green's function:

$$\frac{d}{d\ln \mu} \mathcal{G} = \left(\frac{\partial}{\partial \ln \mu} + \beta(g) \frac{\partial}{\partial g} + \gamma_m \frac{\partial}{\partial \ln m} \right) \mathcal{G},$$

where

$$\gamma_m \stackrel{\text{N}}{=} \frac{\partial \ln m(\mu)}{\partial \ln \mu}, \quad \beta(g) \stackrel{\text{N}}{=} \frac{\partial g(\mu)}{\partial \ln \mu}. \quad (4.79)$$

Combining this with Equation 4.77, we get

$$\left(\frac{\partial}{\partial \ln \mu} + \beta(g) \frac{\partial}{\partial g} + \gamma_m \frac{\partial}{\partial \ln m} + n \gamma_\phi \right) \mathcal{G}^n \equiv 0. \quad (4.80)$$

If we consider a general renormalised n -point Green's function in Yang-Mills theory:

$$\begin{aligned} \mathcal{G}^{n,k,l} &\stackrel{N}{=} \langle \Omega | \psi_1 \cdots \psi_{\frac{n}{2}} \bar{\psi}_{\frac{n}{2}+1} \cdots \bar{\psi}_n A_1^{\mu_1} \cdots A_k^{\mu_k} c_1 \cdots c_{\frac{l}{2}} \bar{c}_{\frac{l}{2}+1} \cdots \bar{c}_l | \Omega \rangle, \\ &= \mathcal{Z}_\psi^{-n} \left(\sqrt{\mathcal{Z}_A} \right)^{-k} \mathcal{Z}_c^{-l} \mathcal{G}_0^{n,k,l}, \end{aligned}$$

we now know that it has to satisfy the equation

Callan-Symanzik Equation

$$\left(\frac{\partial}{\partial \ln \mu} + \beta(g) \frac{\partial}{\partial g} + \gamma_m \frac{\partial}{\partial \ln m} + n \gamma_\psi + k \gamma_A + l \gamma_c \right) \mathcal{G}^{n,k,l} \equiv 0, \quad (4.81)$$

with

Renormalisation Group Equations

$$\beta(g) \stackrel{N}{=} \frac{\partial g(\mu)}{\partial \ln \mu}, \quad \gamma_\psi \stackrel{N}{=} -\frac{1}{2} \frac{\partial \ln \mathcal{Z}_\psi}{\partial \ln \mu}, \quad \gamma_A \stackrel{N}{=} -\frac{1}{2} \frac{\partial \ln \mathcal{Z}_A}{\partial \ln \mu}, \quad (4.82a)$$

$$\gamma_c \stackrel{N}{=} -\frac{1}{2} \frac{\partial \ln \mathcal{Z}_c}{\partial \ln \mu}, \quad \gamma_m \stackrel{N}{=} \frac{\partial \ln m}{\partial \ln \mu}. \quad (4.82b)$$

This is called the *Callan-Symanzik* equation, and the set of equations defining the β -function and the anomalous dimensions are commonly called the *renormalisation-group equation (RGE)*. We can calculate the β and γ functions by calculating a few diagrams at a given order (e.g. the gluon propagator and the 3-gluon vertex) and compare the respective Callan-Symanzik equations. The renormalised perturbation theory is the best suited framework for this type of calculations.

Running Coupling in QCD: Asymptotic Freedom

At **NLO**, the β -function can be written as:

$$\beta(g) = b_0 \frac{g^3}{(4\pi)^2}, \quad (4.83)$$

which we can solve exactly:

Running Coupling

$$g^2(\mu) = \frac{g_0^2}{1 - \frac{g_0^2}{(4\pi)^2} b_0 \ln \frac{\mu^2}{\mu_0^2}}. \quad (4.84)$$

There is a huge difference between Abelian and non-Abelian theories. In an Abelian theory, like QED, we have

$$b_0^{\text{QED}} = \frac{4}{3}, \quad (4.85)$$

which gives a plot as shown in Figure 4.2a, where the coupling goes towards zero in the limit $\mu \rightarrow 0$, and rises towards infinity for $\mu \rightarrow \infty$. This is quite intuitive, as high energies imply short-distance physics. If we imagine e.g. two magnets approaching, they will attract each other (assuming opposite poles) stronger and stronger the closer they get.

On the other hand, in a non-Abelian theory like $\text{su}(n)$, the b_0 coefficient is given by:

$$b_0^{\text{su}(n)} = -\frac{11}{3}N_c + \frac{2}{3}N_f, \quad (4.86)$$

where N_c is the number of gauge elements (colour charges, 3 for QCD) and N_f the number of quark flavours (6 for QCD). If $\frac{11}{3}N_c > \frac{2}{3}N_f$, the coefficient will be negative (as is the case for QCD). This gives a plot as shown in Figure 4.2b, where the coupling goes towards zero at infinity, and rises sharply in the limit $\mu \rightarrow 0$. This is quite counter-intuitive, as it implies that particles at an infinitesimally small separation don't attract each other (colourwise). Such a theory is called *asymptotically free*. There is a useful metaphor, namely that of two particles connected by a rubber band. If you leave the band relaxed, nothing happens. But from the moment you try to pull the particles apart, tension will accumulate, and the more you pull, the more you try to increase the separation between the two particles, the stronger the tension. It is hence also a metaphor for *confinement*, describing how quarks can never exist as free particles, because the harder you try to separate them from a bound state, the harder they resist. But the metaphor goes even further, because if you pull too hard on the rubber band, it will snap in half. Similarly, if you keep on trying to separate quarks, after a while the gluon binding energy will 'snap', i.e. it will create two new quarks to bind with the existing ones, such that there are now two independent bound states that can be separated at will.

But the most important consequence is that at a given energy scale, namely roughly $\Lambda_{\text{QCD}} \approx 250 \text{ MeV}$, the coupling constant α_s will become bigger than one,

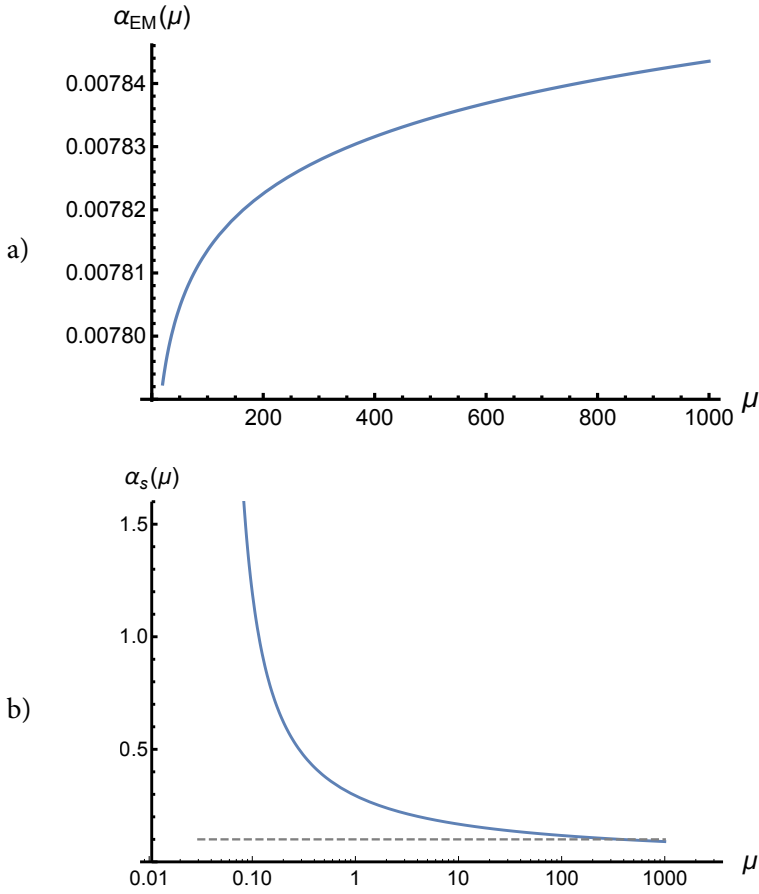


Figure 4.2: a) Running coupling for QED. As for any Abelian theory, it is slowly increasing. b) Running coupling for QCD (with log scale on the horizontal axis). Because $\frac{11}{3}N_c > \frac{2}{3}N_f$, the β -function is negative, and the coupling rises towards small energies. The dashed line shows $\alpha_s \approx 0.1$, the common value for high-energy calculations.

and the perturbative framework is invalidated. This is pathological. Of course, also in QED there could be energies high enough to render the coupling $\alpha_{EM} > 1$, but at least these energies are high enough not to influence with the physics at hand, i.e. we can still treat the perturbative theory as an effective theory up to some upper cut-off scale. This is not the case in QCD, as the energies at which a perturbative treatment fails are energies that are present in every experiment, namely inside the hadrons.

Luckily there is a way to deal with it. The asymptotic freedom essentially divides QCD into two parts: a part where $\mu > \Lambda_{QCD}$ and a perturbative approach

is valid—we can hence use perturbative QCD (pQCD) as an effective theory in this region—and a part that is not calculable, but has to be extracted from experiment. This is the basis for the *factorisation* framework, which we will study in the next chapter.

BASICS OF QCD

QCD, as a non-Abelian theory, has a peculiar behaviour due to the anti-screening of gluons which makes it asymptotically free, as was discussed in the previous chapter. Essentially it means that it is cut into two regimes: a perturbative regime called perturbative QCD (**pQCD**) where $\alpha_s < 1$, such that hard processes can be calculated by standard field theory methods (using **pQCD** as an effective theory to **QCD**), and a non-perturbative regime that is not calculable. Real-life scattering experiments are never limited to hard processes, so it is necessary to somehow combine both regimes into meaningful observables. The use of *factorisation* is a key method to achieve this, as it allows us to separate the two regimes as a separation of energy scales. As the separation is arbitrary, we add the natural requirement that the resulting process cannot depend on the separation point. This then leads to the emergence of evolution equations, describing how the non-perturbative part evolves in function of energy. A few common processes in **QCD** are:

EPA Electron positron annihilation was one of the first processes used to investigate **QCD**. The lepton pair annihilates into a virtual photon, which consequently decays into a quark-antiquark pair (events where the photon decays into a lepton pair are ignored). It was intensively studied in the **LEP** experiments between 1981 and 2000, and lead to deep insights in the theory of the strong force. Angular distributions of two jet events demonstrated the $\text{spin-}1/2$ nature of quarks, angular distributions of three jet events demonstrated the $\text{spin-}1$ nature of gluons and the rate of three-jet events to two-jet events provided a good estimate of the strength of the strong coupling constant (10% rate, hence $\alpha_s \approx 0.1$ at standard energies). Finally, four-jet events (see [Figure 5.1](#)) are sensitive to the three-gluon vertex, and hence allow for an investigation of the non-Abelian nature of **QCD**, and literary for a check of $SU(3)$ to be the underlying group theory. It remains to date an interesting experimental setup to investigate the workings behind jet fragmentation and hadronisation, as there are no initial-state interactions that could blur data and calculations.

- DIS** Deep inelastic scattering, in which an highly relativistic electron is collided onto a heavy proton (or any other hadron), is a process mainly useful to probe the hadronic contents. Its investigation at the **HERA** experiment has lead to the development of the so-far most successful factorisation approach, namely *collinear factorisation*. It is the process that we will use in this chapter as a starting ground to develop the framework of parton density functions (**PDFs**) and collinear factorisation.
- SIDIS** Semi-inclusive deep inelastic scattering allows for a much richer phenomenology, because it includes the identification of one final hadron. However, The underlying theory becomes much more involving, as in this case collinear factorisation is broken, and dependence of the **PDFs** on transverse momentum has to be included. As this is the ideal process to develop the transverse momentum density (**TMD**) framework, we will study it extensively in **Chapter 8**.
- DY** The Drell-Yan process, where two hadrons are collided and form a lepton pair, is a very interesting process as it is free of final-state interactions, and can as such be considered the reverse of the **EPA** process. It is however quite rare and hard to measure, leading to low statistics and making it difficult to interpret. One of the key results in **DY** experiments is the discovery of the light quark flavour asymmetry in the proton. We will briefly investigate the topological differences between **DY** and **SIDIS** in the **TMD** framework in the end of **Section 8.2**.
- DVCS** Deeply virtual Compton scattering, in which a photon is scattered elastically on a hadronic target, is a process that allows a direct view on the hadron contents as expressed in coordinate space, hence it is the most appropriate experimental setup to investigate generalised parton density functions (**GPDs**). We will not address it in this thesis.

More reading on the basics of **pQCD** can be found in [18, 22, 33–38]

5.1 DEEP INELASTIC SCATTERING

To investigate the framework of factorisation, we will introduce it in the **QCD** process where it is easiest (because collinear) and best understood, namely **DIS**. Here an electron is collided with a proton, but in the final state only the electron is measured while all other final states are integrated out. What simplifies this process as compared to other factorised processes, is that there is only one

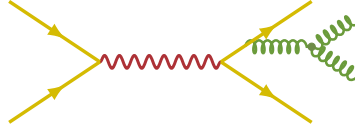


Figure 5.1: Four-jet events demonstrate the non-Abelian behaviour of QCD, because they consist of two distinct sub-processes. In the Abelian sub-process, a gluon is radiated twice from a quark, proportional to C_F , but in the non-Abelian sub-process, a gluon is radiated and then split into two gluons, as shown here. The latter is proportional to C_A , and angular correlations between the two sub-processes allow for the extraction of the rate of the constants.

hadronic state, i.e. only one non-perturbative region. A process where two protons are collided would be much more difficult to investigate, due to the mixture of two non-perturbative regions (unless severely restricted, like the way that **DY** is limited to events that produce a lepton pair).

This also implies that in **DIS** we can integrate out the transversal component of the momentum of the struck quark, leaving only longitudinal dependence in the **PDF**. In **Section 8.2** we go one step further by identifying a final state hadron, implying the need of two **PDFs** concurrently, and the preservation of transversal momentum dependence.

Kinematics

Deep inelastic scattering is the most straightforward process to probe the insides of a hadron. An electron is collided head-on with a proton (or whatever hadron), destroying it maximally. The kinematic diagram is shown in **Figure 5.2**. We will always neglect electron masses. The centre-of-mass energy squared s is then given by:

$$s = (P + l)^2 = m_p^2 + 2P \cdot l, \quad (5.1)$$

and q is the momentum transferred by the photon:

$$q^\mu \stackrel{\text{N}}{=} l^\mu - l'^\mu. \quad (5.2)$$

Because $q^2 = 2E_e E'_e (\cos \theta_{ee'} - 1) \leq 0$, we define $Q^2 \stackrel{\text{N}}{=} -q^2 \geq 0$. The invariant mass of the final state X is then given by

$$m_X^2 = (P + q)^2 = m_p^2 + 2P \cdot q - Q^2. \quad (5.3)$$

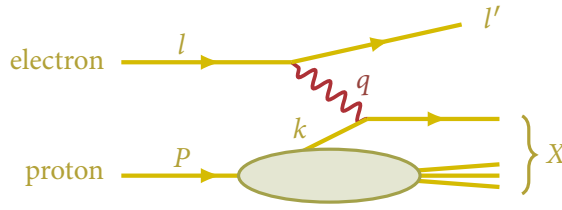


Figure 5.2: Kinematics of deep inelastic electron-proton scattering.

In order for the photon to probe the contents of the proton, it should have a wavelength $\lambda \ll r_p$ with $\lambda \sim \frac{1}{Q}$ and r_p the radius of the proton. The latter is fully destroyed if we have *deep* ($Q^2 \gg m_p^2$) and *inelastic* ($m_x^2 \gg m_p^2$) scattering. The two Lorentz invariants of interest in the process are Q^2 and $P \cdot q$, but it is convenient to use the variables Q and x_B instead, where

$$x_B \stackrel{N}{=} \frac{Q^2}{2P \cdot q} \quad (5.4)$$

is called the *Bjorken-x*. Unless necessary to avoid confusion, we will always drop the index 'B', just remember that x always denotes the Bjorken- x (and thus not a general fraction, see further). Its kinematics restrain x to lie between $\frac{Q^2}{s+Q^2}$ (neglecting terms of $\mathcal{O}\left(\frac{M^2}{Q^2}\right)$) and 1 (the elastic limit). Another useful variable is

$$y \stackrel{N}{=} \frac{P \cdot q}{P \cdot l}, \quad (5.5a)$$

$$= \frac{Q^2}{x(s - m_p^2)}. \quad (5.5b)$$

In the rest frame this equals $y = \frac{E-E'}{E}$, the fractional energy loss of the lepton. It is not an independent variable because

$$Q^2 = x y (s - m_p^2). \quad (5.6)$$

Let us finish this subsection on kinematics with two trivial relations:

$$2x P \cdot l = \frac{Q^2}{y}, \quad (5.7a)$$

$$l \cdot q = -l' \cdot q = -\frac{Q^2}{2}. \quad (5.7b)$$

The latter can be demonstrated by calculating $(l - q)^2 = l'^2 = 0$.

Invitation: The Free Parton Model

A *parton* is a terminology used to denote any pointlike constituent of the proton, being quarks, antiquarks or gluons. The parton model (PM) describes the proton as a black box containing an undetermined amount of such partons. The mutual interactions of these partons have large timescales compared to the interaction with the photon, allowing us to separate the latter from the former. For instance, inside the proton a gluon could fluctuate into a quark-antiquark pair. The photon would enter the proton and kick out one of the quarks, much faster than the pair can recombine. The pair looks ‘frozen’ to the photon: because of the much larger timescale of the parton interactions, all dynamics are hidden for the photon. From the latter’s viewpoint, all partons are hence ‘free’.

As we will see in Equation 5.10, in DIS the momentum of a parton is defined as a fraction ξ of the original parent hadron. The size of this fraction will define the dominant type of parton that arises in this regime. We have three types:

- A. *Valence quarks:* $10^{-2} \leq \xi \leq 1$. These are the quarks that normally form the parent hadron. E.g. for a proton there are 3 valence quarks, viz. 2 up quarks and a down quark.
- B. *Sea quarks:* $10^{-4} \leq \xi \leq 10^{-2}$. These quarks always come in a quark-antiquark pair, and are created from a virtual gluon.
- C. *Gluons:* $10^{-8} \leq \xi \leq 10^{-2}$. At large- x , gluons can be neglected as the valence quarks are by far the dominant partons. However, at small- x gluons quickly dominate all partons and one can neglect all quarks (see Chapter 9).

Note that the regions in ξ are just vague approximations, as there is no way to sharply separate the different parton types. Furthermore, at higher energy scales, the gluons become dominant much faster. Also note that the existence of both valence and sea quarks makes that the quark number operator is not well-defined, as it is not conserved. We anticipated this in the construction of conserved Noether charges (see Equation 1.52), where it naturally follows that it is the difference between particle and antiparticle states that is conserved. Hence if we write the number of valence u quarks as N_{u_v} , the number of u quarks as N_u , the number of \bar{u} antiquarks as $N_{\bar{u}}$, and similarly for the d quarks, the following equations are valid (conserved and Lorentz invariant) in the case of the proton:

$$N_{u_v} = N_u - N_{\bar{u}} \equiv 2, \quad (5.8a)$$

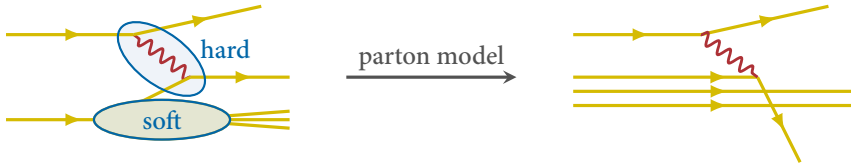


Figure 5.3: DIS in the FPM. The virtual photon strikes one of the quarks, while the other two quarks are left unharmed and don't influence the process anyhow.

$$N_{d_v} = N_d - N_{\bar{d}} \equiv 1. \quad (5.8b)$$

When applied on parton density functions (see later), these sum rules are known as the *Gottfried sum rules*.

It is convenient to let the short-distance process—the interaction between the photon and one of the partons—be named the *hard* part, which we will often denote with a hat, e.g. \hat{s} is the hard CoM energy squared. In contrast to this stands the *soft* part, which—as we will see in later sections—contains all interactions at large distances. For now, we can make an intuitive distinction: everything inside the proton is soft, everything outside the proton plus the interaction point—the photon and the struck parton—is hard. This is illustrated in the left picture of Figure 5.3. Later on we will give a more rigorous formulation for this distinction. The PM thus describes DIS without the strong interaction participating, as all effects of the strong force are absorbed in the proton, without giving any clue for the structure of the latter except one, viz. that we can extract a parton from it.

Before we really delve into the PM, we try to get a general idea by investigating an extreme case: the free parton model (FPM). In this toy model the proton has no dynamic structure, but merely consists of exactly three quarks, totally unaware of each other's existence. From the point of view of the photon it doesn't matter how the proton structure looks, be it in the FPM or the standard PM, it just hits a parton like it would hit any electromagnetically charged particle, ignoring all other structure in the proton. The leading order hard part of DIS is therefore genuine electron-quark scattering, which we can describe similarly to electron-muon scattering.¹ This is illustrated schematically in Figure 5.3. Of course, at timescales much larger than the process, the remains of the proton and the struck parton will *hadronise* into jets, as free quarks can only exist for a short amount of time due to the asymptotic freedom of QCD.

¹ Note that we deliberately choose $e^- \mu^+$ scattering over $e^- e^+$ scattering, because the latter also contains a diagram where the two electrons annihilate into a virtual photon, which has no correspondence with $e^- q$ scattering.

The differential cross section for (unpolarised) $e^- \mu^+$ scattering can be calculated by basic QED techniques and equals

$$\frac{d\sigma}{dy}(e^- \mu^+ \rightarrow e^- \mu^+) = \frac{4\pi\alpha^2 s}{Q^4} \left(1 - y + \frac{y^2}{2}\right), \quad (5.9)$$

where $\alpha \approx \frac{1}{137}$ is the electromagnetic fine-structure constant (see Equation A.2). The only difference between the cross section for $e^- \mu^+$ scattering and that for $e^- q^+$ scattering is the charge of the quark:

$$\frac{d\hat{\sigma}}{dy}(e^- q^\pm \rightarrow e^- q^\pm) = e_q^2 \frac{4\pi\alpha^2 \hat{s}}{Q^4} \left(1 - y + \frac{y^2}{2}\right),$$

but now $\hat{s} = (l + k)^2$, the centre-of-mass energy squared of the electron and the quark. In order to relate the hard cross section to the full cross section, we define the quark momentum as a fraction of the proton momentum:

$$k = \xi P \quad 0 < \xi < 1, \quad (5.10)$$

such that

$$\hat{s} = \xi s \quad \hat{y} = y.$$

For the outgoing quark to be on-shell, we have the requirement

$$(k + q)^2 \approx 2\xi P \cdot q - Q^2 \equiv 0, \\ \Rightarrow \xi \equiv x.$$

In this case, the on-shellness constraint fixes the momentum fraction to equal the Bjorken variable, but this is certainly not a general result. The Bjorken- x is a kinematical constraint defining the process, while ξ is nothing more than a momentum fraction (totally independent of the process). Keeping both x and ξ as independent variables (which will simplify comparisons with later results), the electron-quark cross section is given by

$$\frac{d^3 \hat{\sigma}_q}{dx dy d\xi} = \frac{4\pi\alpha^2 s}{Q^4} \left(1 - y + \frac{y^2}{2}\right) e_q^2 \xi \delta(x - \xi), \quad (5.11)$$

Going to the electron-proton cross section is obvious in the FPM. We simply integrate over all possible quark fractions ξ and make a weighted sum over the three quarks:

$$\frac{d^2 \sigma^{\text{FPM}}}{dx dy} = \frac{1}{3} \sum_q \int d\xi \frac{d^3 \hat{\sigma}_q}{dx dy d\xi}, \\ = \frac{4\pi\alpha^2 s}{Q^4} \left(1 - y + \frac{y^2}{2}\right) x \frac{1}{3} \sum_q e_q^2. \quad (5.12)$$

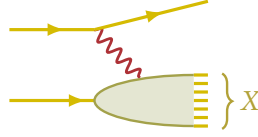


Figure 5.4: DIS to all orders: a photon hitting a proton and breaking it.

A More Formal Approach

Let us redo our intuitive derivation from the previous section in a more formal way. We will treat the proton as a ‘black box’ (contrary to the FPM representation where it is an exact packet of three partons), which we deeply probe with a highly virtual photon. This is depicted in Figure 5.4. We know that in the PM, it is assumed that the photon interacts with one constituent of the proton only (a quark, an antiquark, or at higher orders possibly a gluon), on a timescale sufficiently small to allow the struck parton to be considered temporarily ‘free’. To motivate this quantitatively, we write the components of the proton momentum P and the parton momentum k in light-cone coordinates (see Appendix A.4):

$$P^\mu = (P^+, \frac{m_p^2}{2P^+}, \mathbf{0}_\perp), \quad k^\mu = (k^+, k^-, \mathbf{k}_\perp).$$

In the rest frame of the proton, the distribution of its constituents is isotropic, i.e. all components of p^μ are of the order $\lesssim m_p$. In the limit $P^+ \rightarrow \infty$, the so-called *infinite-momentum frame*, the only remaining component of the proton momentum is its plus-component. The parton naturally follows the proton in the boost. Then the 4-momenta become:

$$P_{\text{IMF}}^\mu = (P^+, 0^-, \mathbf{0}_\perp), \quad k_{\text{IMF}}^\mu \approx (k^+, 0^-, \mathbf{0}_\perp).$$

The parton’s transverse component $\mathbf{p}_\perp \sim m_p$ can be trivially neglected when compared to $p^+ \rightarrow \infty$. The ratio of the plus momenta is boost invariant, so that we can write:

$$\xi = \frac{k^+}{P^+}, \quad \Rightarrow \quad k_{\text{IMF}}^\mu = \xi P_{\text{IMF}}^\mu.$$

As long as we can boost to a frame where P^+ is the only remaining large component of the proton momentum, the parton is fully collinear to the parent proton and can thus be considered to be ‘free’. From now on we will always parameterise the proton momentum and the struck quark momentum based on the dominantly large P^+ :

$$P^\mu = \left(P^+, \frac{m_p^2}{2P^+}, \mathbf{0}_\perp \right), \quad k^\mu = \left(\xi P^+, \frac{k^2 + \mathbf{k}_\perp^2}{2\xi P^+}, \mathbf{k}_\perp \right), \quad (5.13)$$

where we can safely assume $k^2, \mathbf{k}_\perp^2 \ll 2\xi P^+$ and $m_p^2 \ll 2P^+$, reproducing the IMF limit. Furthermore, we choose a frame such that

$$q^\mu = \left(0^+, \frac{Q^2}{2xP^+}, \mathbf{q}_\perp \right), \quad (5.14)$$

where $\mathbf{q}_\perp^2 = Q^2$.

Returning our attention to the mechanics behind the process, we write the matrix element for a given final state X in function of the leptonic and hadronic states:

$$\mathcal{M}_X = \langle l' | J_{\text{leptonic}}^\mu | l \rangle D_{\mu\nu}(q) \langle X | J_{\text{hadronic}}^\nu | P \rangle, \quad (5.15)$$

such that the differential cross section is given by (see [Equation 4.46](#)):

$$\begin{aligned} d\sigma &= \frac{1}{4P \cdot l} \frac{d^3 l'}{(2\pi)^3 2E'_l} \sum_X \int \frac{d^3 p_X}{(2\pi)^3 2E_X} \delta^{(4)}(P+l-p_X-l') |\mathcal{M}|^2, \\ E'_l \frac{d^3 \sigma}{d l'^3} &= \frac{2}{s - m_p^2} \frac{\alpha^2}{Q^4} L_{\mu\nu} W^{\mu\nu}. \end{aligned} \quad (5.16)$$

Before we continue, we will define a set of Cartesian basis vectors, which will show to be especially convenient when investigating [SIDIS](#) in the [TMD](#) framework in [Section 8.2](#). We start by choosing a spacelike normal vector in the direction of q^μ . We thus define the normal vector \hat{q}^μ as

$$\hat{q}^\mu \stackrel{\text{def}}{=} \frac{q^\mu}{Q}, \quad (5.17)$$

which is indeed spacelike normal because $\hat{q}^2 = -1$. Next we construct the timelike basis vector from the proton momentum P^μ by subtracting from it its projection on \hat{q} , and dividing by its total length:

$$\begin{aligned} \hat{t}^\mu &\stackrel{\text{def}}{=} \frac{1}{\sqrt{m_p^2 + (P \cdot \hat{q})^2}} (P^\mu + P \cdot \hat{q} \hat{q}^\mu), \\ &= \frac{1}{\kappa} \frac{1}{Q} (2xP^\mu + q^\mu), \end{aligned} \quad (5.18)$$

where x is the Bjorken- x and

$$\kappa = \sqrt{4x^2 \frac{m_p^2}{Q^2} + 1} \rightarrow 1 \quad (5.19)$$

in the limit $Q^2 \gg m_p^2$. Also note that the projection on \hat{q}^μ equals $\frac{P \cdot \hat{q}}{\hat{q} \cdot \hat{q}} \hat{q}^\mu = -P \cdot \hat{q} \hat{q}^\mu$. The next basis vector is then constructed by subtracting from it its projection on \hat{q}^μ and \hat{t}^μ . This is the same as contracting it with the tensor

$$g_{\perp}^{\mu\nu} \stackrel{\text{def}}{=} g^{\mu\nu} + \hat{q}^\mu \hat{q}^\nu - \hat{t}^\mu \hat{t}^\nu, \quad (5.20)$$

which has the following useful properties:

$$\hat{q}_\mu g_{\perp}^{\mu\nu} = g_{\perp}^{\mu\nu} \hat{q}_\nu = 0, \quad (5.21a)$$

$$\hat{t}_\mu g_{\perp}^{\mu\nu} = g_{\perp}^{\mu\nu} \hat{t}_\nu = 0, \quad (5.21b)$$

$$g_{\perp}^{\mu\nu} g_{\perp\nu\rho} = \delta_\rho^\mu + \hat{q}^\mu \hat{q}_\rho - \hat{t}^\mu \hat{t}_\rho, \quad (5.21c)$$

$$g_{\perp}^{\mu\nu} g_{\perp\mu\nu} = 2. \quad (5.21d)$$

Note that this definition of $g_{\perp}^{\mu\nu}$ is compatible with the definition in [Equations A.45](#). We can hence construct a third orthonormal (spacelike) vector from, say, l^μ :

$$\begin{aligned} \hat{l}^\mu &\stackrel{\text{def}}{=} \frac{1}{\sqrt{-l_\mu g_{\perp}^{\mu\nu} g_{\perp\nu\rho} l^\rho}} g_{\perp}^{\mu\nu} l_\nu, \\ &= \frac{1}{\sqrt{1 - y - \frac{\kappa^2 - 1}{4} y^2}} \left(\kappa \frac{y}{Q} l^\mu - \kappa \frac{y}{2} \hat{q}^\mu - \frac{2 - y}{2} \hat{t}^\mu \right), \end{aligned}$$

where we used the relations in [Equations 5.7](#). It is again a spacelike orthonormal vector:

$$\hat{l}_\perp^\mu \hat{l}_\mu = \hat{l}_\perp^\mu g_{\mu\nu} \hat{l}_\perp^\nu = \hat{l}_\perp^\mu g_{\perp\mu\nu} \hat{l}_\perp^\nu = -1. \quad (5.22)$$

Now normally we would proceed with the construction of the last orthonormal basis vector, but we don't have any independent physical vectors left in our process. But we still can define an antisymmetric projection tensor as follows:

$$\varepsilon_{\perp}^{\mu\nu} \stackrel{\text{def}}{=} \varepsilon^{\mu\nu\rho\sigma} \hat{t}_\rho \hat{q}_\sigma. \quad (5.23)$$

As with $g_{\perp}^{\mu\nu}$, this definition of $\varepsilon_{\perp}^{\mu\nu}$ is compatible with the definition in [Equations A.47](#). It is easy to show that

$$\varepsilon_{\perp}^{\mu\nu} \hat{t}_\nu = 0, \quad (5.24a)$$

$$\varepsilon_{\perp}^{\mu\nu} \hat{q}_\nu = 0, \quad (5.24b)$$

$$\varepsilon_{\perp}^{\mu\nu} g_{\perp\nu\rho} = \varepsilon_{\perp\rho}^\mu, \quad (5.24c)$$

$$\varepsilon_{\perp}^{\mu\nu} g_{\perp\mu\nu} = \varepsilon_{\perp\mu}^\mu = 0, \quad (5.24d)$$

by use of the antisymmetry of $\varepsilon^{\mu\nu\rho\sigma}$. Note that $\varepsilon_{\perp\nu}^{\mu}$ has the same components as $\varepsilon_{\perp}^{\mu\rho}$ but with opposite signs. Furthermore, because in general

$$\varepsilon^{\mu\nu\rho\sigma}\varepsilon_{\mu\nu\tau\nu} = -2(\delta_{\tau}^{\rho}\delta_{\nu}^{\sigma} - \delta_{\nu}^{\rho}\delta_{\tau}^{\sigma}), \quad (5.25)$$

we have

$$\varepsilon_{\perp}^{\mu\nu}\varepsilon_{\perp\mu\nu} = 2. \quad (5.26)$$

Let's summarise our new basis:

Orthonormal Basis Vectors

$$\hat{q}^{\mu} = \frac{q^{\mu}}{Q}, \quad (5.27a)$$

$$\hat{t}^{\mu} = \frac{1}{\kappa} \frac{1}{Q} (2xP^{\mu} + q^{\mu}), \quad (5.27b)$$

$$\hat{l}^{\mu} = \frac{1}{\sqrt{1-y-\frac{\kappa^2-1}{4}y^2}} \left(\kappa \frac{y}{Q} l^{\mu} - \kappa \frac{y}{2} \hat{q} - \frac{2-y}{2} \hat{t} \right). \quad (5.27c)$$

Transversal Tensors

$$g_{\perp}^{\mu\nu} = g^{\mu\nu} + \hat{q}^{\mu}\hat{q}^{\nu} - \hat{t}^{\mu}\hat{t}^{\nu}, \quad (5.28a)$$

$$\varepsilon_{\perp}^{\mu\nu} = \varepsilon^{\mu\nu\rho\sigma} \hat{t}_{\rho} \hat{q}_{\sigma}. \quad (5.28b)$$

Now we can express all the relevant momenta in the process in our new basis using Equation 5.13 (remember that the projections on \hat{q}^{μ} and \hat{l}^{μ} give an extra minus sign, because $\hat{q}^2 = \hat{l}^2 = -1$):

Physical Vectors in Orthonormal Basis

$$q^{\mu} = Q \hat{q}^{\mu}, \quad (5.29a)$$

$$P^{\mu} = \kappa \frac{Q}{2x} \hat{t}^{\mu} - \frac{Q}{2x} \hat{q}^{\mu}, \quad (5.29b)$$

$$k^{\mu} \approx \frac{\xi}{x} \frac{Q}{2} \hat{t}^{\mu} - \frac{\xi}{x} \frac{Q}{2} \hat{q}^{\mu}, \quad (5.29c)$$

$$l^{\mu} = \frac{1}{\kappa} Q \frac{2-y}{2y} \hat{t}^{\mu} + \frac{Q}{2} \hat{q}^{\mu} + \frac{1}{\kappa} \frac{Q}{y} \sqrt{1-y-\frac{\kappa^2-1}{4}y^2} \hat{l}^{\mu}, \quad (5.29d)$$

$$l'^{\mu} = \frac{1}{\kappa} Q \frac{2-y}{2y} \hat{t}^{\mu} - \frac{Q}{2} \hat{q}^{\mu} + \frac{1}{\kappa} \frac{Q}{y} \sqrt{1-y-\frac{\kappa^2-1}{4}y^2} \hat{l}^{\mu}. \quad (5.29e)$$

It is easy to verify that these formulae indeed reproduce the correct definitions.

E.g. one can quickly check the on-shell conditions $q^2 = -Q^2$, $k^2 = \xi^2 m_p^2$, $l^2 = l'^2 = 0$.

Let us return to [Equation 5.16](#), and specify the lepton and hadron tensor in our new basis. We consider the electron beam to be polarised, say longitudinally, but we don't measure the polarisation of the outgoing electron, implying we have to sum over outgoing polarisation states using [Equations A.26](#). Then the lepton tensor $L^{\mu\nu}$ is given by

$$\begin{aligned} L^{\mu\nu} &\stackrel{\text{N}}{=} \sum_{\lambda'} \left(\bar{u}^\lambda(l) \gamma^\mu u^{\lambda'}(l') \right) \left(\bar{u}^{\lambda'}(l') \gamma^\nu u^\lambda(l) \right), \\ &= -Q^2 g^{\mu\nu} + 4l^{(\mu} l'^{\nu)} + 2i\lambda \varepsilon^{\mu\nu\rho\sigma} l_\rho l'_\sigma. \end{aligned} \quad (5.30)$$

Writing it in our new basis gives:

$$\begin{aligned} L^{\mu\nu} &= \frac{Q^2}{y^2} \left[-y^2 g_\perp^{\mu\nu} + 4(1-y) (\hat{t}^\mu \hat{t}^\nu + \hat{l}^\mu \hat{l}^\nu) + 4\sqrt{1-y} (2-y) \hat{t}^{(\mu} \hat{l}^{\nu)} \right. \\ &\quad \left. -i\lambda y (2-y) \varepsilon_\perp^{\mu\nu} + i2\lambda y \sqrt{1-y} \varepsilon^{\mu\nu\rho\sigma} \hat{q}_\rho \hat{l}_\sigma \right]. \end{aligned} \quad (5.31)$$

This might look more difficult than the original expression, but the advantage lies in the fact that it is now expressed in an orthonormal basis, simplifying contractions with other tensors.

On the other hand, from [Equation 5.16](#) we see that the hadronic tensor is defined as

$$W^{\mu\nu} \stackrel{\text{N}}{=} 4\pi^3 \sum_X \int \frac{d^3 \mathbf{p}_X}{(2\pi)^3 2E_X} \delta^{(4)}(P+q-p_X) \langle P | J^{\dagger\mu}(0) | X \rangle \langle X | J^\nu(0) | P \rangle, \quad (5.32)$$

$$= \frac{1}{4\pi} \int d^4 z e^{iq \cdot z} \langle P | J^{\dagger\mu}(z) J^\nu(0) | P \rangle, \quad (5.33)$$

where we used the translation operator

$$\langle P | J^{\dagger\mu}(0) | X \rangle e^{i(P-p_X) \cdot z} = \langle P | J^{\dagger\mu}(z) | X \rangle, \quad (5.34)$$

and integrated out a complete set of states by use of the completeness relation:

$$\int |X\rangle \langle X| = \mathbb{1}, \quad \int \stackrel{\text{N}}{=} \sum_X \int \frac{d^3 \mathbf{p}_X}{(2\pi)^3 2E_X} = \sum_X \int \frac{d^4 p_X}{(2\pi)^4} \delta^+(p_X^2 - m_X^2), \quad (5.35)$$

where

$$\delta^+(p_X^2 - m_X^2) \stackrel{\text{N}}{=} 2\pi \delta(p_X^2 - m_X^2) \theta(p^0). \quad (5.36)$$

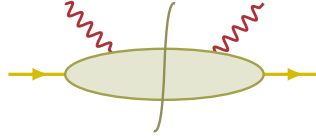


Figure 5.5: The hadronic tensor is a squared amplitude defined with a sum over all possible external states. This sum, and the separation between the amplitude and its conjugate, is represented by the vertical final-state cut line.

Figure 5.5 shows the common convention to draw the hadronic tensor. It is a squared amplitude for a proton absorbing a photon going to any final state X , while summing over all possible final states. The vertical curve, a so-called ‘final-state cut’, acts both as a separator (everything to the left is the amplitude \mathcal{M} , everything to the right is the complex conjugate \mathcal{M}^*) and as a symbol representing the completeness relation (reminding us that we have to sum over all final states and integrate out their momenta). It is straightforward to use the final-state cut in perturbative calculations: every particle crossing it, is a real particle and thus has to be on-shell. This can be incorporated by adding a $\delta^+(p^2 - m^2)$, matching the particle’s momentum squared to its mass squared (see also the discussion on page 106). We have no information about the contents of the hadronic tensor, as it sits in the highly non-perturbative region of QCD; the proton constituents are strongly *confined*. But we can parameterise the hadronic tensor based on its mathematical structure. In this thesis, we will restrict ourselves only to work with unpolarised hadron tensors, as polarisation brings some technicalities with it, which would distract us too much from our main topic of interest at the moment.

For an unpolarised proton, $W^{\mu\nu}$ will only exist in the vector space spanned by the orthonormal vectors we derived before. But as the electron momentum l^μ doesn’t have any physical significance inside the hadron tensor, we will use \hat{q}^μ , \hat{t}^μ , and their crossings. Thus we can expand the former as:

$$W^{\mu\nu} = A g^{\mu\nu} + B \hat{q}^\mu \hat{q}^\nu + C \hat{q}^\mu \hat{t}^\nu + D \hat{t}^\mu \hat{q}^\nu + E \hat{t}^\mu \hat{t}^\nu + i F \epsilon^{\mu\nu\rho\sigma} \hat{t}_\rho \hat{q}_\sigma,$$

where the scalar functions A, \dots, F only depend on m_p^2, Q^2 and x (because there are no other invariants in the proton system). In the case of polarised hadrons, the spin vector S^μ and its combinations should be added to the basis. Next we impose current conservation, which requires $\partial_\mu J^\mu = 0$. Applying this to Equation 5.33 we find $\hat{q}_\mu W^{\mu\nu} = W^{\mu\nu} \hat{q}_\nu = 0$. This condition gives:

$$A \equiv B,$$

$$C \equiv D \equiv 0.$$

$W^{\mu\nu}$ should also be Hermitian and time-reversal invariant, and for the electromagnetic and the strong force it should be parity invariant as well. By using the transformation matrix

$$\Lambda_{\mu}^{\nu} = \begin{pmatrix} 1 & 0 & 0 & 0 \\ 0 & -1 & 0 & 0 \\ 0 & 0 & -1 & 0 \\ 0 & 0 & 0 & -1 \end{pmatrix}. \quad (5.37)$$

we can write out these conditions (adding spin-dependence for future reference):

$$\text{Hermiticity:} \quad W_{\mu\nu}^*(q, P, S) \equiv W_{\nu\mu}(q, P, S), \quad (5.38a)$$

$$\text{parity-reversal:} \quad \Lambda_{\mu}^{\rho} \Lambda_{\nu}^{\sigma} W_{\mu\nu}(q, P, S) \equiv W_{\rho\sigma}(\tilde{q}, \tilde{P}, -\tilde{S}), \quad (5.38b)$$

$$\text{time-reversal:} \quad \Lambda_{\mu}^{\rho} \Lambda_{\nu}^{\sigma} W_{\mu\nu}^*(q, P, S) \equiv W_{\rho\sigma}(\tilde{q}, \tilde{P}, \tilde{S}). \quad (5.38c)$$

where $\tilde{q}^{\mu} = \delta^{\mu 0} q^0 - \delta^{\mu i} q^i$. The effect of these conditions is that A, \dots, F should be real functions, and the parity-reversal requirement sets $F = 0$. But parity is not conserved in weak interactions; in that case F is allowed to have a non-zero value. We can rewrite $W^{\mu\nu}$ as (taking $S = 0$ again):

$$W^{\mu\nu} = -\frac{1}{2x} \left[g_{\perp}^{\mu\nu} F_T(x, Q^2) - \hat{t}^{\mu} \hat{t}^{\nu} F_L(x, Q^2) - i \varepsilon_{\perp}^{\mu\nu} F_A(x, Q^2) \right]. \quad (5.39)$$

where

$$F_T = -2x A, \quad F_L = 2x (A + E), \quad F_A = 2x F.$$

These are called the transversal resp. longitudinal resp. axial *structure functions* of the proton. They are non-perturbative (and thus non-calculable) objects, which have to be extracted from experiment. In parallel to these, a different notation is also used in literature:

$$F_1 = \frac{1}{2x} F_T, \quad F_T = 2x F_1, \quad (5.40a)$$

$$F_2 = \frac{1}{\kappa^2} (F_L + F_T), \quad F_L = \kappa^2 F_2 - 2x F_1, \quad (5.40b)$$

$$F_3 = \frac{1}{x \kappa^2} F_A, \quad F_A = x \kappa^2 F_3. \quad (5.40c)$$

We can express the hadron tensor in function of the last three structure functions as well:

$$W^{\mu\nu} = -g_{\perp}^{\mu\nu} F_1 + \hat{t}^{\mu} \hat{t}^{\nu} \left(\frac{\kappa^2}{2x} F_2 - F_1 \right) + i \frac{\kappa^2}{2} \varepsilon_{\perp}^{\mu\nu} F_3. \quad (5.41)$$

The difference between F_T, F_L, F_A and F_1, F_2, F_3 is just a matter of historic convention. However, there exist different conventions for the normalisation of the structure functions, if so often differing by a factor of 2 or $2x$. We follow the same convention as e.g. in [39], as we believe it to be the most commonly accepted one. The structure functions can be extracted from the hadronic tensor by projecting with appropriate tensors:

$$F_1 = -\frac{1}{2} g_{\perp}^{\mu\nu} W_{\mu\nu}, \quad F_T = -x g_{\perp}^{\mu\nu} W_{\mu\nu}, \quad (5.42a)$$

$$F_2 = \frac{x}{\kappa^2} (2\hat{t}^{\mu} \hat{t}^{\nu} - g_{\perp}^{\mu\nu}) W_{\mu\nu}, \quad F_L = 2x \hat{t}^{\mu} \hat{t}^{\nu} W_{\mu\nu}, \quad (5.42b)$$

$$F_3 = -\frac{2i}{\kappa^2} \varepsilon_{\perp}^{\mu\nu} W_{\mu\nu}, \quad F_A = -2x i \varepsilon_{\perp}^{\mu\nu} W_{\mu\nu}. \quad (5.42c)$$

For the rest of this thesis we will ignore weak interactions, dropping F_A from the hadronic tensor.

Combining the result from the leptonic and the hadronic tensor, we get

$$L_{\mu\nu} W^{\mu\nu} = \frac{2Q^2}{x y^2} \left[\left(1 - y + \frac{y^2}{2} \right) F_T(x, Q^2) + (1 - y) F_L(x, Q^2) \right].$$

Plugging this result in [Equation 5.16](#) gives us the final expression for the unpolarised cross section for electron-proton deep inelastic scattering (neglecting terms of order $\frac{m_p^2}{Q^2}$):

$$\frac{d^2\sigma}{dx dy} = \frac{4\pi\alpha^2 s}{Q^4} \left[\left(1 - y + \frac{y^2}{2} \right) F_T(x, Q^2) + (1 - y) F_L(x, Q^2) \right] \quad (5.43)$$

If we compare this with the result in [Equation 5.12](#), we find the following structure functions for the free parton model:

$$F_T^{\text{FPM}}(x, Q^2) = \frac{1}{3} x \sum_q e_q^2, \quad (5.44a)$$

$$F_L^{\text{FPM}}(x, Q^2) = 0. \quad (5.44b)$$

5.2 PARTON DISTRIBUTION FUNCTIONS

In Subsection [Invitation: The Free Parton Model](#) on page 124 and onwards, we succeeded in deriving a lowest order result for the cross section, starting from

a static proton. On the other hand, in Subsection [A More Formal Approach](#) on page 127 and onwards, we followed a more formal approach, without any assumptions about the proton structure but one: that we can separate the hard interaction from the proton contents. This is the concept of *factorisation*: in any process containing hadrons we try to separate the perturbative hard part (the scattering Feynman diagram) from the non-perturbative part (the hadron contents). The latter is not-calculable, and consequently it has to be described by a *parton density function* (or parton distribution function, **PDF** for short) that gives the probability to find a parton with momentum fraction ξ in the parent hadron. However, one has to proceed with caution because factorisation has not been proven but for a small number of processes, including [EPA](#), [DIS](#), [SIDIS](#) and [DY](#).

The **PDF** is literally the object that describes the proton as a black box. You give it a fraction ξ and it returns the probability to hit a parton carrying this longitudinal momentum fraction when you bombard the proton with a photon. It is commonly written as

$$f_q(\xi),$$

where q is the type of parton for which the **PDF** is defined. There are thus 7 **PDFs**, one for each quark and antiquark, and one for the gluon. A parton distribution function is not calculable; they have to be extracted from experiment. However, as we will see in [Section 5.3](#), we can calculate its *evolution equations*, such that we can evolve an extracted **PDF** from a given kinematic region to a new kinematic region. It is a probability density, but it is also a distribution in momentum space; by plotting the **PDF** in function of x one gets a clear view of the distribution of the partons in the proton. Furthermore we assume that the **PDF** only depends on ξ , and not e.g. on the parton's transverse momentum. This doesn't mean that we automatically neglect the struck parton's transverse momentum component! But because we don't identify any hadron in the final state, and because we have to sum over all final states and integrate out their momenta (the final-state cut), any transverse momentum dependence in the **PDF** or the hard part is integrated out. Factorisation in [DIS](#)—also called *collinear* factorisation because of the collinearity of the struck quark to the proton—is a factorisation over x (plus an energy scale). We can write this formally as

$$\frac{d\sigma}{dx} \sim f_q(x, \mu_F^2) \otimes \hat{H}(x, \mu_F^2),$$

which is just a schematic. We will treat the technical details soon, in [Section 5.3](#).

Whenever information on the transverse momentum is needed, e.g. when identifying a final hadron like in [SIDIS](#), collinear factorisation won't do, and

\mathbf{k}_\perp -factorisation is needed instead, where a *transverse momentum dependent PDF*, or **TMD** for short, is convoluted with the hard part:

$$\frac{d\sigma}{dx} \sim f_q(x, \mathbf{k}_\perp, \mu_F^2) \otimes \hat{H}(x, \mathbf{k}_\perp, \mu_F^2).$$

Formally, a **PDF** and a **TMD** should be related by integrating out the transverse momentum dependence:

$$f_q(\xi) = \int d^2\mathbf{k}_\perp f_q(\xi, \mathbf{k}_\perp),$$

however, **QCD** corrections make this equality invalid.

In the parton model, the concept of (collinear) factorisation can be painlessly implemented:

Factorisation in the **PM**

$$d\sigma \stackrel{\text{PM}}{\equiv} \sum_q \int d\xi f_q(\xi) d\hat{\sigma}_q\left(\frac{x}{\xi}\right), \quad (5.45a)$$

$$\stackrel{\text{N}}{\equiv} f_q \otimes d\hat{\sigma}_q. \quad (5.45b)$$

Note that this is not the common convolution definition, i.e. $\int d\tau f(\tau)g(t-\tau)$. This is because the latter is a convolution *as defined in Fourier space*. In **QCD**, a lot of theoretical progress has been made by the use of *Mellin moments*. These form an advanced mathematical tool, which would take use too long to delve into. The thing to keep in mind is that the type of convolution as in [Equations 5.45](#) is a convolution in Mellin space (see [Equations A.66](#) for the definition of the Mellin transform).

We can express the structure functions of the proton in terms of the structure functions of the quark, where the latter are defined at leading order as

$$\hat{F}_T^q(x) \stackrel{\text{def}}{=} x e_q^2 \delta(1-x). \quad (5.46)$$

To do this, we use [Equations 5.45](#) to relate the electron-quark cross-section in [Equation 5.11](#) with the electron-proton cross-section in [Equation 5.43](#). Then it is easy to show that:

$$F_T^{\text{PM}}(x, Q^2) = \sum_q \int_x^1 d\xi f_q(\xi) \hat{F}_T^q\left(\frac{x}{\xi}\right), \quad (5.47a)$$

$$= \sum_q e_q^2 x f_q(x), \quad (5.47b)$$

$$F_L^{\text{PM}}(x, Q^2) = 0. \quad (5.47c)$$

Note that F_T^{PM} does not depend on Q^2 ! This is called the “Bjorken scaling” prediction: the structure functions scale with x , independently of Q^2 . Because this prediction is a direct result from the parton model, it should be clearly visible in leading order (up to first-order QCD corrections, where the Bjorken scaling is broken). This is indeed confirmed by experiment.

Also note that by comparing [Equations 5.47](#) to [Equations 5.44](#), we can easily find the quark PDFs in the free parton model:

$$f_q^{\text{FPM}}(x) = \frac{1}{3}, \quad (5.48)$$

which is exactly what the initial assumption for the FPM is: the proton equals exactly three quarks, thus the probability of finding one of those is always one third per quark, regardless the value of x .

A small remark on the difference between structure functions and PDFs. A structure function emerges in the parametrisation of the hadronic tensor, the latter being *process dependent*. If we have a look at its definition for DIS in [Equation 5.33](#), we see that the hadronic tensor contains information both on the proton content and the photon hitting it. This is illustrated in [Figure 5.5](#), where the blob represents the hadronic tensor, describing the process of a photon hitting a (black box) proton. As a structure function is just a parametrisation of the hadronic tensor, the same applies to it. If we change the process to, say, deep inelastic neutrino scattering, our structure functions change as well, because now they describe the process of a W^\pm or Z^0 boson hitting a proton.

But the main idea behind factorisation is that, inside the structure functions, we can somehow factorise out the proton content (which is process independent) from the process dependent part. This is shown in [Figure 5.6](#), where the smaller blob now represents a quark PDF. The factorisation of structure functions in the parton model is demonstrated in [Equations 5.47](#). The initial factorisation ansatz, [Equations 5.45](#), is required to be valid for any cross section, given an unique set of PDFs, i.e. the PDFs are *universal*. We can extract these PDFs in one type of experiment, like electron DIS, and reuse them in another experiment like neutrino DIS. In contrast with the structure functions, PDFs emerge in the parametrisation of the quark correlator—as we will see in [Section](#) —which is universal by definition.

5.3 COLLINEAR FACTORISATION AND EVOLUTION OF PDFS

We started the idea of a separation between soft and hard parts in the crude PM (see [Equations 5.45](#)); [Figure 5.7](#) shows our current view on factorisation in DIS.

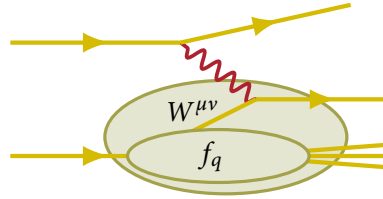


Figure 5.6: Difference between structure functions and PDFs.

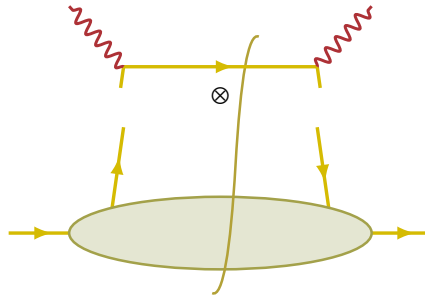


Figure 5.7: Factorisation in DIS at LO.

However, until now we haven't given a rigorous definition for the separation between the hard and the soft part. At leading order (LO) this is trivial (we just cut the struck quark before the interaction with the photon, as in Figure 5.7), but we need a fail-proof approach at higher orders. E.g. at NLO an additional gluon can be radiated from the struck quark before the interaction with the photon (as in the four leftmost diagrams in Figure 5.8). How do we define whether the radiated gluon belongs to the PDF or in the hard part? As we will see, the correct way to approach this—at least in the collinear case—is to define a separation in energy scales. The requirement of independence of the process on this separation will then lead to evolution equations for the PDFs.

Let us now continue with an investigation of DIS at first order in α_s , and see how that changes our factorisation rules:

$$F_T(x, Q^2) = \sum_q e_q^2 x f_q(x) + \mathcal{O}(\alpha_s),$$

$$F_L(x, Q^2) = 0 + \mathcal{O}(\alpha_s).$$

In what follows we will continue by using $F_2 = F_T + F_L$, to be in accordance with common literature. The correct approach to continue is as such: we calculate $\hat{W}^{\mu\nu}$ for a single quark from the amplitude

$$\hat{W}^{\mu\nu} = \int d\Phi |\mathcal{M}|^2 \tag{5.49}$$

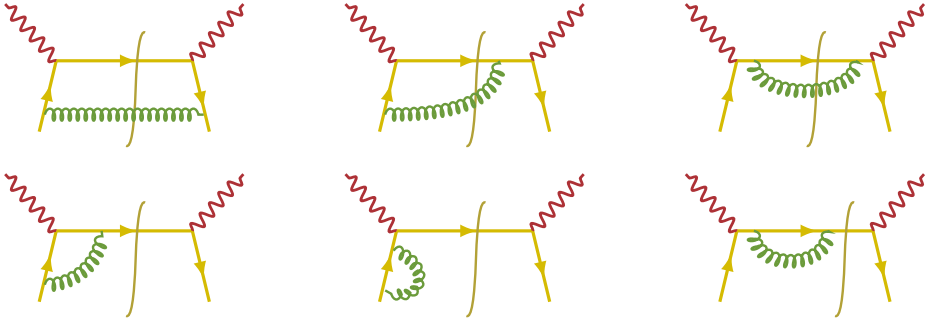


Figure 5.8: All types of first order corrections to the DIS process. Real corrections are on the upper line; virtual on the lower line.

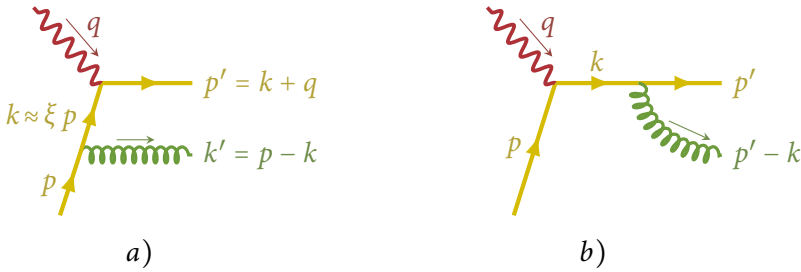


Figure 5.9: a) Initial state gluon radiation. b) Final state gluon radiation.

up to first order in α_s , then we extract \hat{F}_2 for a single quark using [Equations 5.42](#). We compare the result with [Equation 5.46](#), plug it in [Equation 5.47a](#) and see how it changes the PDF.

There are 3 types of real gluon exchanges at first order, where the exchanged gluon is on-shell, and 3 types of virtual gluon exchanges, shown in [Figure 5.8](#). We will calculate the real contributions in LC-gauge—as the latter gives the natural interpretation of the PDF as a number density—and label the momenta as shown in [Figure 5.9](#). The corresponding amplitude for the initial state gluon radiation ([Figure 5.9a](#)) is (see also [Equations A.99](#) for the QCD Feynman rules):

$$\mathcal{M}_i^{a,\lambda,\lambda'} = \bar{u}^\lambda(p') (ie_q \gamma^\mu) \frac{i \not{k}}{k^2 + i\epsilon} (ig \not{\epsilon}(k) t^a) u^{\lambda'}(p).$$

We average over colour and incoming spin states, and sum over final spin (see [Equations A.26](#)) and gluon polarisation states, i.e.

$$|\mathcal{M}|^2 \stackrel{\text{N}}{=} \frac{1}{N_c} \sum_{a,b} \frac{1}{2} \sum_{\lambda} \sum_{\lambda'} \sum_{\text{pol}} \mathcal{M}^{a,\lambda,\lambda'} \mathcal{M}^{*b,\lambda,\lambda'}. \quad (5.50)$$

We hence get for the complex squared amplitude

$$|\mathcal{M}|^2 = \frac{1}{2} C_F e_q^2 g^2 \frac{1}{k^4} \sum_{\text{pol}} \text{tr}(\not{\epsilon} \not{p} \not{k} \gamma^\mu \not{p}' \gamma^\nu \not{k}), \quad (5.51)$$

where we used [Equation A.72b](#) to simplify the colour generators. We can sum over the gluon polarisation states by using [Equation A.98b](#), this simplifies the trace into

$$\begin{aligned} \text{tr}(\dots) &= -\text{tr}(\gamma_\rho \not{p} \gamma^\rho \not{k} \gamma^\mu \not{p}' \gamma^\nu \not{k}) \\ &\quad + \frac{1}{p^+ - k^+} \text{tr}(\gamma^+ \not{p} (\not{p} - \not{k}) \not{k} \gamma^\mu \not{p}' \gamma^\nu \not{k}) \\ &\quad + \frac{1}{p^+ - k^+} \text{tr}((\not{p} - \not{k}) \not{p} \gamma^+ \not{k} \gamma^\mu \not{p}' \gamma^\nu \not{k}). \end{aligned}$$

The first term can be simplified using [Equation A.30b](#):

$$-\text{tr}(\gamma_\rho \not{p} \gamma^\rho \not{k} \gamma^\mu \not{p}' \gamma^\nu \not{k}) = (\omega - 2) \text{tr}(\not{p} \not{k} \gamma^\mu \not{p}' \gamma^\nu \not{k}),$$

which can further simplified using

$$\not{k} \not{p} \not{k} = 2p \cdot k \not{k} - k^2 \not{p}.$$

The other two traces can be simplified by using the fact that $\not{p} \not{p} = p^2 \approx 0$, the mass of the quark and $\not{k} \not{k} = k^2$, the virtuality of the quark (also using the cyclicity of the trace):

$$\begin{aligned} \text{tr}(\gamma^+ \not{p} (\not{p} - \not{k}) \not{k} \gamma^\mu \not{p}' \gamma^\nu \not{k}) &= -k^2 \text{tr}(\not{k} \gamma^+ \not{p} \gamma^\mu \not{p}' \gamma^\nu), \\ \text{tr}((\not{p} - \not{k}) \not{p} \gamma^+ \not{k} \gamma^\mu \not{p}' \gamma^\nu \not{k}) &= -k^2 \text{tr}(\not{p} \gamma^+ \not{k} \gamma^\mu \not{p}' \gamma^\nu). \end{aligned}$$

Their sum can be further simplified with the same trick as before:

$$(\not{k} + \not{p}) \gamma^+ (\not{k} + \not{p}) = 2(k + p)^+ (\not{k} + \not{p}) - (k^2 + 2k \cdot p) \gamma^+. \quad (5.52)$$

Now we assume that the longitudinal component of the virtual quark is a fraction of the longitudinal momentum of the parent quark, i.e.

$$k^+ = \xi p^+. \quad (5.53)$$

The full trace is then given by:

$$\begin{aligned} \text{tr}(\dots) &= \left[(\omega - 2) 2p \cdot k - 2k^2 \frac{1 + \xi}{1 - \xi} \right] \text{tr}(\not{k} \gamma^\mu \not{p}' \gamma^\nu) \\ &\quad - k^2 \left[(\omega - 2) + 2 \frac{1 + \xi}{1 - \xi} \right] \text{tr}(\not{p} \gamma^\mu \not{p}' \gamma^\nu) \\ &\quad + \frac{1}{1 - \xi} \frac{k^2}{p^+} (k^2 + 2k \cdot p) \text{tr}(\gamma^+ \gamma^\mu \not{p}' \gamma^\nu). \end{aligned} \quad (5.54)$$

We parameterise the quark and photon momenta as in [Equations 5.13](#) and [5.14](#), neglecting the transverse momentum components of the original quark. However, after radiating the gluon it will acquire transverse momentum which cannot be neglected, but will be integrated out as we are integrating over final states. The momenta are thus given by:

$$p^\mu = (p^+, 0^-, \mathbf{0}_\perp), \quad k^\mu = \left(\xi p^+, \frac{k^2 + \mathbf{k}_\perp^2}{2\xi p^+}, \mathbf{k}_\perp \right), \quad q^\mu = \left(0^+, \frac{Q^2}{2\hat{x} p^+}, \mathbf{q}_\perp \right),$$

where $q_\perp^2 = Q^2$ and \hat{x} is the Bjorken- x for the quark-photon system. The phase space integral is given by

$$\begin{aligned} \int d\Phi &= \int \frac{d^4 k'}{(2\pi)^4} \frac{d^4 p'}{(2\pi)^4} \delta^+(k'^2) \delta^+(p'^2) \delta^{(4)}(p + q - p' - k'), \\ &= \int \frac{d^4 k}{(2\pi)^2} \delta^+((p - k)^2) \delta^+((k + q)^2), \end{aligned}$$

and using

$$\begin{aligned} (p - k)^2 &= \frac{1}{\xi} [k^2 (\xi - 1) - k_\perp^2], \quad (k + q)^2 = k^2 + \frac{Q^2}{\hat{x}} (\xi - \hat{x}) - 2\mathbf{k}_\perp \cdot \mathbf{q}_\perp, \\ d^4 k &= \frac{d\xi}{2\xi} dk^2 d^2 \mathbf{k}_\perp. \end{aligned}$$

it can be rewritten as

$$\int d\Phi = \frac{1}{2} \int d\xi dk^2 \frac{d^2 \mathbf{k}_\perp}{(2\pi)^2} \delta((\xi - 1)k^2 - k_\perp^2) \delta\left(k^2 + \frac{Q^2}{\hat{x}} (\xi - \hat{x}) - 2\mathbf{k}_\perp \cdot \mathbf{q}_\perp\right).$$

Note that the θ -part of the δ^+ -functions dropped out, as it is automatically satisfied due to the fact that $0 \leq \xi \leq 1$:

$$p^+ - k^+ = p^+(1 - \xi) > 0, \quad k^+ + q^+ = \xi p^+ > 0,$$

because the quark moves with the proton in the positive n^+ -direction. To rewrite the trace, we first define a notational shorthand:

$$\begin{aligned} l^+ &= -4 \frac{1 + \xi^2}{1 - \xi} k^2 p^+, \\ l^- &= \frac{2}{p^+} k^4, \\ l_\perp &= 4 \frac{\xi}{1 - \xi} k^2 \mathbf{k}_\perp. \end{aligned}$$

We already used the fact that $k_{\perp}^2 \equiv (\xi - 1)k^2$ due to the δ 's in the phase space integral. This shorthand allows us to simply write

$$\text{tr}(\dots) = \text{tr}(l\gamma^{\mu}\not{p}'\gamma^{\nu}) = 8l^{(\mu}p'^{\nu)} - 4g^{\mu\nu}l\cdot p'.$$

To retrieve the structure functions of the quark from the hadronic tensor, we project on the orthonormal basis using [Equations 5.42](#) (and using [Equation 5.51](#) to get the correct terms in front):

$$\begin{aligned}\hat{F}_2 &= \int d\Phi \ x (2\hat{t}^{\mu}\hat{t}^{\nu} - g_{\perp}^{\mu\nu}) \frac{1}{2} C_F e_q^2 g^2 \frac{1}{k^4} (8l_{(\mu}p'_{\nu)} - 4g_{\mu\nu}l\cdot p'), \\ &= 4x C_F e_q^2 g^2 \int d\Phi \ \frac{1}{k^4} (2l\cdot t p'\cdot t + l_{\perp}\cdot p'_{\perp}).\end{aligned}\quad (5.55)$$

Note that $(2\hat{t}^{\mu}\hat{t}^{\nu} - g_{\perp}^{\mu\nu})g_{\mu\nu} = 0$ and $l_{\mu}g_{\perp}^{\mu\nu}p'_{\nu} = -l_{\perp}\cdot p'_{\perp}$. The basis vector \hat{t} is in this frame given by

$$\hat{t}^{\mu} = \left(\frac{2xp^+}{Q}, \frac{Q}{2xp^+}, \frac{\mathbf{q}_{\perp}}{Q} \right),$$

and p' is simply the sum of the virtual quark and photon momentum $p' = k + p$:

$$p' = \left(\xi p^+, \frac{1}{2p^+} \left(k^2 + \frac{Q^2}{x} \right), \mathbf{k}_{\perp} + \mathbf{q}_{\perp} \right).$$

The next steps are straightforward but tedious; we will just give the result:

$$\hat{F}_{2\text{div}} = e_q^2 \frac{\alpha_s}{2\pi} x P_{qq}(x) \int_{\mu_0}^{Q^2} \frac{dk^2}{k^2}, \quad (5.56)$$

where the integral is regulated in the [IR](#) region with a lower cut-off μ_0^2 . The [UV](#) cut-off Q^2 follows from kinematics. The integration just gives a logarithm:

$$\hat{F}_{2\text{div}} = e_q^2 \frac{\alpha_s}{2\pi} x P_{qq}(x) \ln \frac{Q^2}{\mu_0^2}. \quad (5.57)$$

These are the only divergent terms. We didn't list the finite terms, as they are easily calculable and are of secondary importance. We could have used dimensional regularisation as well (with $\omega = 4 + 2\epsilon$, as appropriate for [IR](#) divergences), giving

$$\hat{F}_{2\text{div}} = e_q^2 \frac{\alpha_s}{2\pi} x P_{qq}(x) \frac{1}{\epsilon}. \quad (5.58)$$

However, the physical interpretation that now follows is much more natural with a cut-off, so we prefer to use that. The function $P_{qq}(x)$ is the so called *splitting function*:

$$P_{qq}(\xi) = C_F \frac{1 + \xi^2}{1 - \xi}. \quad (5.59)$$

This function is specific for the diagram in [Figure 5.9a](#). We use the notation $P_{ij}(\xi)$ to denote “the probability to get a parton of type i with a momentum fraction ξ from a parent parton of type j ”. In this case, $P_{qq}(\xi)$ represents the probability for a quark to split into a quark carrying a fraction ξ of its momentum and a gluon carrying a fraction $1 - \xi$ of its momentum. In light-cone gauge, the other real diagrams don't add any divergences, only finite, calculable parts. So do the virtual diagrams, which can be easily calculated using standard loop-integral methods, as all ultraviolet divergences which appear in individual loop diagrams, cancel out. So we can write the full result for \hat{F}_2 at leading order in α_s :

$$\hat{F}_2 = e_q^2 x \left[\delta(1-x) + \frac{\alpha_s}{2\pi} \left(P_{qq}(x) \ln \frac{Q^2}{\mu_0^2} + C(x) \right) \right], \quad (5.60)$$

where $C(x)$ contains all finite parts. Bjorken scaling is, as expected, violated; \hat{F}_2 now depends on Q^2 . The singularity which is regulated by μ_0^2 appears when the gluon is emitted collinear to the quark ($\mathbf{k}_\perp = 0$), hence it is called a *collinear divergence*. Physically the limit \mathbf{k}_\perp corresponds to a long-range (soft) interaction, where QCD can no longer be calculated in a perturbative way.

To extend our result to the proton structure, we convolute \hat{F}_2 with a [PDF](#), as in [Equation 5.47a](#):

$$F_2 = \sum_q e_q^2 x \int_x^1 \frac{d\xi}{\xi} f^q(\xi) \left[\delta\left(1 - \frac{x}{\xi}\right) + \frac{\alpha_s}{2\pi} \left(P_{qq}\left(\frac{x}{\xi}\right) \ln \frac{Q^2}{\mu_0^2} + C\left(\frac{x}{\xi}\right) \right) \right].$$

However, care has to be taken as f^q is the bare, unrenormalised [PDF](#), exactly the same situation as for the renormalisation of the coupling constant. From now on we will write it as $f_0^q(\xi)$ to make the distinction clear. We want to absorb the collinear divergence into the [PDF](#) and renormalise it up to an arbitrary scale. We choose such a scale μ_F , with $\mu_0^2 < \mu_F^2 < Q^2$, and we use it to split the logarithm:

$$\ln \frac{Q^2}{\mu_0^2} = \ln \frac{Q^2}{\mu_F^2} + \ln \frac{\mu_F^2}{\mu_0^2}, \quad (5.61)$$

and define a renormalised [PDF](#) as:

$$f^q(x, \mu_F^2) = \int_x^1 \frac{d\xi}{\xi} f_0^q(\xi) \left[\delta\left(1 - \frac{x}{\xi}\right) + \frac{\alpha_s}{2\pi} \left(P\left(\frac{x}{\xi}\right) \ln \frac{\mu_F^2}{\mu_0^2} + C\left(\frac{x}{\xi}\right) \right) \right]. \quad (5.62)$$

Then we can rewrite the factorisation formula in terms of the renormalised PDF and the factorisation scale:

$$F_2 = \sum_q e_q^2 x \int_x^1 \frac{d\xi}{\xi} f^q(\xi, \mu_F^2) \hat{H}\left(\frac{x}{\xi}, Q^2, \mu_F^2\right), \quad (5.63a)$$

$$\hat{H}\left(\frac{x}{\xi}\right) = \left[\delta\left(1 - \frac{x}{\xi}\right) + \frac{\alpha_s}{2\pi} \left(P_{qq}\left(\frac{x}{\xi}\right) \ln \frac{Q^2}{\mu_F^2} + \tilde{C}\left(\frac{x}{\xi}\right) \right) \right]. \quad (5.63b)$$

In other words, we can retrieve the structure by convoluting the PDF f^q with the partonic hard part \hat{H} . Note that we have divided the finite part into two parts:

$$C(x) = \tilde{C}(x) + C'(x). \quad (5.64)$$

C' is subtracted from the hard part and gets absorbed by the PDF, while \tilde{C} is what remains in the factorisation formula. The exact choice of how to do this is up to convention, and is called a *factorisation scheme*. This is exactly the same as the renormalisation scheme as we introduced it in the section on renormalisation on page 111. In this framework, two common schemes are the DIS scheme, where $\tilde{C} = 0$, i.e. everything is subtracted into the PDF, and the more common $\overline{\text{MS}}$ scheme, where $C' = \ln 4\pi - \gamma_E$ only.

It is very important to have a clear understanding of what is happening here. In the calculation of the correction to the hard part, we integrated out all k_\perp^2 -dependence between μ_0^2 and Q^2 . The kinematics of the system make sure that $k_\perp \leq Q$ always, i.e. the upper border of the integration is justified. In the infrared region however, there is no such kinematic restriction. By cutting the lower border of the integration at μ_0^2 we discarded gluon radiation with $k_\perp < \mu_0$ from the hard part. In order to avoid dropping these gluons entirely, we have to absorb them in the PDF, which we subsequently renormalise up to an arbitrary scale μ_F . By doing this, we hide the divergence from the process, inside an object that wasn't perturbative to begin with.

The physical interpretation goes as follows: we choose an arbitrary energy scale μ_F that separates the process in two parts, namely a hard part with k_\perp larger than this scale, and a non-perturbative part (the PDF) with k_\perp smaller than this scale. This interpretation is illustrated in Figure 5.10. Note that this supports our previous intuitive definition of factorisation at LO, namely to separate the two regions by just cutting the quark in two, before it gets struck by the photon. For this reason we will call μ_F the *factorisation scale*.

Since F_2 is a physical observable, it cannot depend on the factorisation scale (which is merely an unphysical leftover of a mathematical tool). Translated to a formal statement, this implies:

$$\frac{\partial F_2}{\partial \ln \mu_F^2} \equiv 0. \quad (5.65)$$



Figure 5.10: a) The transverse momentum of the gluon is smaller than the factorisation scale, so we absorb it in the PDF. b) The transverse momentum of the gluon is larger than the factorisation scale, so we add it to the hard part.

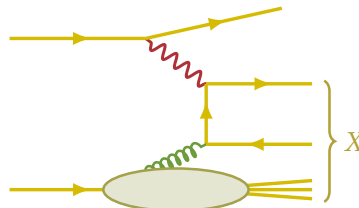


Figure 5.11: Boson-gluon fusion in DIS.

This is really a strong requirement—so strong that we can use it to derive an evolution equation for f , the so-called Dokshitzer-Gribov-Lipatov-Altarelli-Parisi (DGLAP) evolution equation:

$$\frac{\partial}{\partial \ln \mu_F^2} f^q(x, \mu_F^2) = \frac{\alpha_s(\mu_F^2)}{2\pi} \int_x^1 \frac{d\xi}{\xi} P_{qq}\left(\frac{x}{\xi}, \alpha_s(\mu_F^2)\right) f^q(\xi, \mu_F^2), \quad (5.66)$$

where we also incorporated the effect of the running coupling $\alpha_s(\mu_F^2)$. Note that P_{qq} depends on the coupling because this is an all-order equation; corrections from higher order calculations will manifest themselves inside the splitting function. The fact that the independence on the factorisation scale yields the evolution of the PDF is not so strange, after all, if we want to be able to arbitrarily choose an unphysical cut between soft and hard for a given process, we will also need to know how this energy cut affects the PDF.

Everything we have derived so far was for quarks only. Adding gluons, we can now calculate the leading-order contribution (in α_s) to \hat{F}_2 from the boson-gluon

fusion diagram in [Figure 5.11](#), and convolute this with the gluon PDF. We find for the partonic structure function:

$$\hat{F}_2^g = \sum_q e_q^2 x \frac{\alpha_s}{2\pi} \left(P_{qg}(x) \ln \frac{Q^2}{\mu_0^2} + C^q(x) \right). \quad (5.67)$$

This is quite similar to [Equation 5.60](#), especially, there is again a singularity from the integration over k_1^2 . As we already knew, there is no gluon contribution to \hat{F}_2 when $\alpha_s = 0$. The splitting function is given by

$$P_{qg}(\xi) = \frac{1}{2} (\xi^2 + (1 - \xi)^2), \quad (5.68)$$

where P_{qg} is the probability to find a quark in a gluon. Note that in \hat{F}_2^g we sum over quark flavour. We have to renormalise the gluon PDF as we did with the quark PDF, but we absorb the singularities in the quark PDF (exactly because we are looking at a quark in a gluon):

$$\begin{aligned} f^q(x, \mu_F^2) &= f_0^q(x) + \frac{\alpha_s}{2\pi} \int_x^1 \frac{d\xi}{\xi} f_0^q(\xi) \left(P_{qq}\left(\frac{x}{\xi}\right) \ln \frac{\mu_F^2}{\mu_0^2} + C'^q\left(\frac{x}{\xi}\right) \right) \\ &+ \frac{\alpha_s}{2\pi} \int_x^1 \frac{d\xi}{\xi} f_0^g(\xi) \left(P_{qg}\left(\frac{x}{\xi}\right) \ln \frac{\mu_F^2}{\mu_0^2} + C'^g\left(\frac{x}{\xi}\right) \right). \end{aligned}$$

On the other hand, higher-order calculations show that the renormalisation of the gluon PDF is given by:

$$\begin{aligned} f^g(x, \mu_F^2) &= f_0^g(x) + \frac{\alpha_s}{2\pi} \int_x^1 \frac{d\xi}{\xi} f_0^g(\xi) \left(P_{gg}\left(\frac{x}{\xi}\right) \ln \frac{\mu_F^2}{\mu_0^2} + C'^g\left(\frac{x}{\xi}\right) \right) \\ &+ \frac{\alpha_s}{2\pi} \int_x^1 \frac{d\xi}{\xi} f_0^q(\xi) \left(P_{gq}\left(\frac{x}{\xi}\right) \ln \frac{\mu_F^2}{\mu_0^2} + C'^g\left(\frac{x}{\xi}\right) \right). \end{aligned}$$

With these renormalisation definitions, we can write the factorisation formulae as:

Collinear Factorisation

$$F_2 = \sum_q e_q^2 x (f^q \otimes \hat{H}^q + f^g \otimes \hat{H}^g), \quad (5.69a)$$

$$\hat{H}^q(z) = \delta(1-z) + \frac{\alpha_s}{2\pi} \left(P_{qq}(z) \ln \frac{Q^2}{\mu_F^2} + \tilde{C}^q(z) \right), \quad (5.69b)$$

$$\hat{H}^g\left(\frac{x}{\xi}\right) = \frac{\alpha_s}{2\pi} \left(P_{qg}(z) \ln \frac{Q^2}{\mu_F^2} + \tilde{C}^g(z) \right), \quad (5.69c)$$

$$(f \otimes H)(x) \stackrel{\text{N}}{=} \int_x^1 \frac{d\xi}{\xi} f(\xi) H\left(\frac{x}{\xi}\right). \quad (5.69d)$$


Of course, in order to fully validate collinear factorisation, one needs to derive factorisation formulae for F_1 as well and verify if they agree with those for F_2 . This has been done quite thoroughly, such that we can accept collinear factorisation as a valid framework. Then finally, the full DGLAP evolution equations can be expressed in a matrix equation:

DGLAP Evolution


$$\frac{\partial}{\partial \ln \mu^2} \begin{pmatrix} q_i(x, \mu^2) \\ g(x, \mu^2) \end{pmatrix} = \frac{\alpha_s}{2\pi} \int_x^1 \frac{d\xi}{\xi} \begin{pmatrix} P_{q_i q_j} & P_{q_i g} \\ P_{g q_j} & P_{g g} \end{pmatrix} \Big|_{\frac{x}{\xi}} \cdot \begin{pmatrix} q_j\left(\frac{x}{\xi}, \mu^2\right) \\ g\left(\frac{x}{\xi}, \mu^2\right) \end{pmatrix} \quad (5.70)$$

For completeness' sake, we list all splitting functions at leading order:


Splitting Functions




$$P_{qq}(\xi) = C_F \frac{1 + \xi^2}{1 - \xi}, \quad (5.71a)$$



$$P_{qg}(\xi) = \frac{1}{2} (\xi^2 + (1 - \xi)^2), \quad (5.71b)$$



$$P_{gq}(\xi) = C_F \frac{1 + (1 - \xi)^2}{\xi}, \quad (5.71c)$$



$$P_{gg}(\xi) = 2 C_A \left(\frac{\xi}{1 - \xi} + \frac{1 - \xi}{\xi} + \xi(1 - \xi) \right). \quad (5.71d)$$

This leads us to the end of this chapter on deep inelastic scattering and collinear factorisation. In [Chapter 8](#), we will investigate what changes when we can no longer integrate over transverse momentum, e.g. when we identify a hadron in the final state.

Part II

WILSON LINES

WILSON LINES

We saw in [Chapter 2](#) that a Wilson line is a path-ordered exponential constructed from the gauge fields (see [Equation 2.17](#)), that transforms bi-locally (see [Equation 2.3](#)). It is an object that emerges naturally in gauge theories from geometrical arguments to cure the definition of the derivative, but this is not its only application. Because of its bi-local transformation properties, it is often used as a parallel transporter to render non-local terms gauge invariant, especially in QCD calculations concerning validation of factorisation schemes, and in calculations for constructing or modelling PDFs (see [Chapter 8](#)). For these reasons, Wilson lines deserve some special attention—which is why we investigate them in great detail in this chapter and the next. We focus on piecewise linear Wilson lines—which are vastly the most commonly used and the only ones used in this thesis—and will derive their properties and Feynman rules, and construct a framework meant to simplify perturbative calculations. Finally, in the last section we briefly motivate the importance of Wilson lines by explaining the eikonal approximation—one of the main applications of Wilson lines.

6.1 A WILSON LINE ALONG A PATH

A Wilson line is a path-ordered exponential of a line integral of the gauge field along a given path \mathcal{C} :

$$\mathcal{U}^{\mathcal{C}} = \mathcal{P} e^{i g \int_{\mathcal{C}} dz^{\mu} A_{\mu}(z)} . \quad (6.1)$$

The sign convention which was discussed in [Chapter 2](#) also manifests itself in the definition of the Wilson line. Choosing a positive sign in the gauge transformation of the particle field—as we do in this thesis—results in a positive sign in the path-ordered exponential. This follows from its behaviour under gauge transformations, as it has to have the correct sign to cancel the transformation

of the particle field, in order to parallel transport it to a different spacetime point (see [Equations 2.3, 2.4 and 2.18](#)).

The Wilson line we constructed in [Chapter 2](#) is valid for any group theory. We focus on [QCD](#), and as such every Wilson line we will use from now on will be an $SU(3)$ group element, expressed in the fundamental or the adjoint representation. If no statement about the representation is made, we assume it to be in the fundamental. The physical interpretation of a Wilson line becomes clear by expanding the exponential:

$$\mathcal{U}^C = \sum_{n=0}^{\infty} \frac{1}{n!} (ig)^n \mathcal{P} \int_C dz_n^{\mu_n} \cdots dz_1^{\mu_1} A_{\mu_n}(z_n) \cdots A_{\mu_1}(z_1), \quad (6.2)$$

i.e. the n -th order in the expansion represents a radiation of n gluon fields as in [Figure 6.1](#). To save writing space, we often use the shorthand notation

$$A_i \stackrel{N}{=} A_{\mu_i}^{a_i}(z_i). \quad (6.3)$$

The point z_i at which the field A_i is radiated is integrated over the full path to get all possible configurations. However, path-ordering adds the additional constraint that all fields should remain in the same order, i.e. the field A_i has to be radiated between A_{i-1} and A_{i+1} . The full exponential is thus a resummation of all possible radiations from the path. We can interpret this as a full gauge effect along the path; this can be e.g. the nett effect of a particle moving in an external medium. Resumming all gluons, a Wilson line can also represent e.g. a fast-moving quark (when in the fundamental representation) or a fast-moving gluon (when in the adjoint representation). In this case, we assume the quark resp. gluon not to deviate after radiating a gluon. This is called the *eikonal approximation* and is treated in more detail in [Section 6.6](#).

Properties of Wilson Lines

In [Chapter 2](#) we constructed a Wilson line by the requirement to satisfy a set of properties. As we discovered during the derivation, these properties led to the natural interpretation of a Wilson line being a functional of a path. We just list them here again for easy reference:

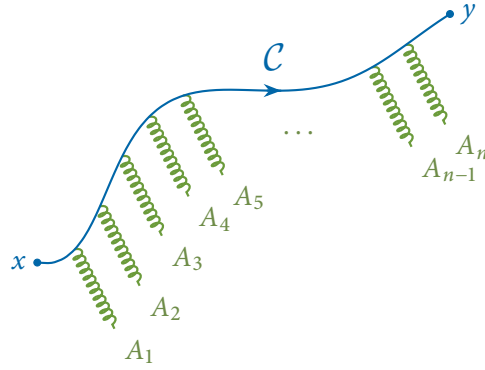


Figure 6.1: Illustration of the n -th order term in the expansion of the Wilson line $\mathcal{U}_{(y;x)}^C$. The n radiated fields A_i (using the short-hand notation defined in Equation 6.3) can be radiated at any point (due to the fact that they are integrated over along the path), but are ordered such that $\lambda_n \geq \lambda_{n-1} \geq \dots \geq \lambda_2 \geq \lambda_1$.

Properties of Wilson Lines

A. A Wilson line is unitary: $\mathcal{U}^C [\mathcal{U}^C]^\dagger = \mathbb{1}$. (6.4a)

B. Path reversion equals Hermitian conjugation: $\mathcal{U}^C = [\mathcal{U}^{-C}]^\dagger$. (6.4b)

C. It is path-transitive, i.e. if $C = C_1 + C_2$, then $\mathcal{U}^C = \mathcal{U}^{C_1} \mathcal{U}^{C_2}$. (6.4c)

D. It transforms in function of its endpoints only:

$$\mathcal{U}_{(y;x)} \rightarrow e^{ig\alpha^a(y)t^a} \mathcal{U}_{(y;x)} e^{-ig\alpha^a(x)t^a}. \quad (6.4d)$$

E. A Wilson loop is gauge-invariant: $\mathcal{U}^\circ \rightarrow \mathcal{U}^\circ$. (6.4e)

Path Ordering

The symbol \mathcal{P} in Equation 6.1 denotes path ordering, ensuring that the gauge fields are ordered in such a way that the first fields on the path are written leftmost. When associating a diagram with this formula, we will use the same convention as with Dirac lines: we read them from right to left. Getting a bit ahead, we have already written the gauge fields in a reversed order, from n to 1, such that when drawing a Wilson line on a path from left to right, we can notate

the gauge fields as 1 to n (from left to right, see [Figure 6.1](#)). This ensures that A_n is the first field on the path (having the highest value for its parameter λ , see below).

The Wilson line still has two open indices, in the fundamental or the adjoint depending on the representation chosen for the Lie generators (remember that we defined the gauge fields with the generators absorbed, $A_\mu = A_\mu^a t^a$). In case of a Wilson loop, these indices are traced.

It is convenient to parameterise the path \mathcal{C} in function of a one-dimensional parameter λ :

$$\mathcal{C} : z^\mu(\lambda) \quad \lambda = a \dots b, \quad (6.5)$$

where $z(a)$ and $z(b)$ are the start- resp. endpoints of the path. Then we can formally write out the path ordering requirement, e.g. for two fields we have

$$\mathcal{P} A_{\mu_1}(z_1) A_{\mu_2}(z_2) = \theta(\lambda_1 - \lambda_2) A_{\mu_1}(\lambda_1) A_{\mu_2}(\lambda_2) + \theta(\lambda_2 - \lambda_1) A_{\mu_2}(\lambda_2) A_{\mu_1}(\lambda_1)$$

for $z^{\mu_1}(\lambda_1)$ and $z^{\mu_2}(\lambda_2)$. This can easily be generalised to more than two fields, by chaining an appropriate number of θ -functions:

$$\mathcal{P} A_{\mu_1}(z_1) \cdots A_{\mu_n}(z_n) = \sum_{\sigma(\lambda_1, \dots, \lambda_n)} \left(\prod_{i=1}^{n-1} \theta(\lambda_{i+1} - \lambda_i) \right) A_{\mu_1}(\lambda_1) \cdots A_{\mu_n}(\lambda_n), \quad (6.6)$$

where $\sum_{\sigma(\lambda_1, \dots, \lambda_n)}$ represents a sum over all possible permutations of λ_i . Note that in case of Abelian fields all fields commute, and we can sum all θ -functions. Then the path-ordering symbol can just be ignored:

$$\mathcal{P} A_{\mu_1}(z_1) \cdots A_{\mu_n}(z_n) = A_{\mu_1}(z_1) \cdots A_{\mu_n}(z_n).$$

In this case, every term in the expansion of the exponential is just a power of the same integral:

$$\mathcal{U}_{\text{abelian}} = \mathcal{P} e^{\int_{\mathcal{C}} \text{i}g \text{d}z^\mu A_\mu(z)} = \sum_{n=0}^{\infty} \frac{1}{n!} (\text{i}g)^n \left(\int_{\mathcal{C}} \text{d}z^\mu A_\mu(z) \right)^n.$$

But of course, we are mainly interested in non-Abelian fields, as in this thesis we will be using Wilson lines in QCD. Calculating a line integral is easiest by parameterising the path as in [Equation 6.5](#). Then we make a change of variables:

$$\text{d}z^\mu \rightarrow \text{d}\lambda \frac{\text{d}z^\mu}{\text{d}\lambda},$$

in order to rewrite the path ordered exponential as

$$\mathcal{U}_{(b;a)}^C = \mathcal{P} \text{Exp} \left\{ i g \int_a^b d\lambda \ (z^\mu)' A_\mu(z) \right\}. \quad (6.7)$$

We can effectuate the path ordering in the expansion using [Equation 6.6](#). This will manifest itself as a chaining of the parameters λ_i in the upper integration borders:

$$\begin{aligned} & \mathcal{P} \int d\lambda_n \cdots d\lambda_1 \frac{dz^{\mu_n}(\lambda_n)}{d\lambda_n} \cdots \frac{dz^{\mu_1}(\lambda_1)}{d\lambda_1} \\ &= n! \int_a^b d\lambda_n \int_a^{\lambda_n} d\lambda_{n-1} \int_a^{\lambda_{n-1}} d\lambda_{n-2} \cdots \int_a^{\lambda_2} d\lambda_1 \frac{dz^{\mu_n}(\lambda_n)}{d\lambda_n} \cdots \frac{dz^{\mu_1}(\lambda_1)}{d\lambda_1}. \end{aligned} \quad (6.8)$$

This literally tells us what we anticipated: that the i -th gauge field (with parameter λ_i) has to be radiated between the $i-1$ -th and the $i+1$ -th gauge field (because with these integration borders the parameters satisfy $\lambda_{i+1} \geq \lambda_i \geq \lambda_{i-1}$).

Note that [Equation 6.8](#) is only valid for integrands of the form

$$A_{\mu_n}(z(\lambda_n)) \cdots A_{\mu_1}(z(\lambda_1)), \quad (6.9)$$

i.e. products of the same vector field function, depending on different variables. We cannot use it for e.g.

$$A_{\mu_n}(z(\lambda_n)) \cdots \partial_\nu A_{\mu_i}(z(\lambda_i)) \cdots A_{\mu_1}(z(\lambda_1)),$$

because the interchange symmetry is broken by the derivative.

It is possible to move the chaining to the lower integration borders, but in this case we need to flip the order of the parameters (to ensure that we can keep the order of the radiated gluons as is, i.e. from n to 1):

$$\begin{aligned} & \mathcal{P} \int d\lambda_n \cdots d\lambda_1 \frac{dz^{\mu_n}(\lambda_n)}{d\lambda_n} \cdots \frac{dz^{\mu_1}(\lambda_1)}{d\lambda_1} \\ &= n! \int_a^b d\lambda_1 \int_{\lambda_1}^b d\lambda_2 \int_{\lambda_2}^b d\lambda_3 \cdots \int_{\lambda_{n-1}}^b d\lambda_n \frac{dz^{\mu_n}(\lambda_n)}{d\lambda_n} \cdots \frac{dz^{\mu_1}(\lambda_1)}{d\lambda_1}. \end{aligned} \quad (6.10)$$

It is straightforward to check these formulae in an intuitive way, by verifying that in both cases $\lambda_n \geq \lambda_{n-1} \geq \cdots \geq \lambda_2 \geq \lambda_1$. Using the integrand in [Equation 6.9](#), the full expression is then automatically path ordered. Depending on the specific path calculation, [Equation 6.8](#) or [Equation 6.10](#) might be easier to use.

In order to investigate how different path structures influence a Wilson line, it is preferable to separate out the path content from the gauge field content. Luckily, this can be easily done by making a Fourier transform. The path content is then fully described by the following integrals:

$$I_n = \frac{1}{n!} (ig)^n \mathcal{P} \int d\lambda_1 \cdots d\lambda_n (z_1^{\mu_1})' \cdots (z_n^{\mu_n})' e^{i \sum_{k=1}^n k_i \cdot z_i}. \quad (6.11)$$

Note that although we use the common convention for Fourier transforms (with a negative sign in the exponent for the inverse transform, see [Equations A.58](#)),¹ we preferred to make the integration substitution $k \rightarrow -k$, to make the link with common literature concerning Wilson lines (cf. e.g. in [33], where momenta are pointing *outwards*). The n -th order term of the Wilson line expansion is then given by

$$\mathcal{U}_n = \int \frac{d^\omega k_n}{(2\pi)^\omega}, \cdots \frac{d^\omega k_1}{(2\pi)^\omega} A_{\mu_n}(-k_n) \cdots A_{\mu_1}(-k_1) I_n, \quad (6.12)$$

The negative signs in the arguments are a result from the integration substitution explained above. They remind us that the results we will derive are defined for momenta pointing outwards in a Feynman diagram.

Also, remember that the fields are ordered from n to 1 to allow them to be read from left to right.

6.2 PIECEWISE WILSON LINES

In general, most interesting and dynamically rich paths will not be smooth, but contain *cusps*. These are points in the path where the path is continuous but its derivative is not, i.e. the path looks cracked. This is illustrated in [Figure 6.2](#). The reason that cusps are more compelling is that they don't occur naturally, but are the result of external driving forces. E.g. if the Wilson line represents a resummed quark, a cusp can be the effect of an interaction with a hard photon. Cusps hence contain all information on the dynamics of a system.

At first sight, paths with cusps might seem a bit problematic from a mathematical point of view, as a general path is supposed to be smooth, i.e. continuously differentiable. What saves the day, is the transitivity property of a Wilson line, because it allows us to split the path at the cusp, and continue with a product of two Wilson lines. E.g. in [Figure 6.2](#) we have three cusps that divide the path into four segments.

¹ This implies that positive momenta are pointing *inwards* in a Feynman diagram.

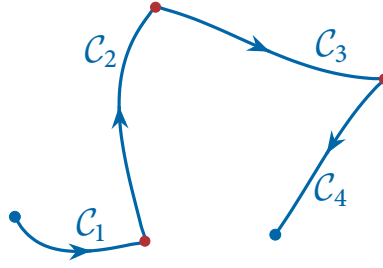


Figure 6.2: A path with cusps. Although the full path is not smooth, the three cusps divide the path into four smooth segments. The full path \mathcal{C} can be approached as a piecewise path with regions \mathcal{C}_{1-4} .

In other words, the path on which a Wilson line is evaluated can be piecewise, as long as each segment is smooth (in particular, each segment should be defined over an interval that is not a single point). Note that we don't even need the restriction that the segments should be joined, because we can always define a piecewise function (with possibly disconnected segments) in function of adjoining intervals in the parameterisation parameter:

$$f(\lambda) = \begin{cases} f^1(\lambda) & \lambda = a_1 \dots a_2, \\ f^2(\lambda) & \lambda = a_2 \dots a_3, \\ \vdots & \\ f^M(\lambda) & \lambda = a_M \dots a_{M+1}. \end{cases} \quad (6.13)$$

We will use capitalised Latin letters for the index referring to segments. Let us consider a piecewise smooth path, consisting of M continuously differentiable segments. We would like to be able to express the integrals I_n that contain all path information (see Equation 6.11) in function of the same integrals but expressed over each segment separately.

The first order integral over the J -th segment only involves the J -th part of f :

$$S_1^J = \int_{a_J}^{a_{J+1}} d\lambda f(\lambda) = \int_{a_J}^{a_{J+1}} d\lambda f^J(\lambda). \quad (6.14)$$

Then of course the first order integral I_1 can be trivially expressed in function of the first order segment integrals, as it is just their sum:

$$\int_{a_1}^{a_{M+1}} d\lambda = \left(\int_{a_1}^{a_2} + \int_{a_2}^{a_3} + \dots + \int_{a_M}^{a_{M+1}} \right) d\lambda,$$

$$I_1 = \sum_{J=1}^M S_1^J. \quad (6.15)$$

The calculation of the second order integral is a bit more tricky, as there are two points of particular interest. First, because in Equation 6.11 every incarnation of $e^{-ik_i \cdot z}$ gets another index i , we need to introduce this dependence in f , which we will do with a lower index:

$$I_2 = \int_{a_1}^{a_{M+1}} d\lambda_1 f_i(\lambda_1) \int_{a_1}^{\lambda_1} d\lambda_2 f_{i+1}(\lambda_2),$$

where of course in this case $i = 1$, but we left it open for the sake of generality. The second point is that in the definition of I_2 the inner integral has a variable upper border, and thus is a piecewise function itself:

$$\int_{a_1}^{\lambda_1} d\lambda_2 f_{i+1}(\lambda_2) = \begin{cases} \int_{a_1}^{\lambda_1} d\lambda_2 f_{i+1}(\lambda_2) & \lambda_1 = a_1 \dots a_2, \\ S^1(i+1) + \int_{a_2}^{\lambda_1} d\lambda_2 f_{i+1}(\lambda_2) & \lambda_1 = a_2 \dots a_3, \\ \vdots \\ \sum_{J=1}^{M-1} S^J(i+1) + \int_{a_M}^{\lambda_1} d\lambda_2 f_{i+1}(\lambda_2) & \lambda_1 = a_M \dots a_{M+1}. \end{cases} \quad (6.16)$$

The outermost integral will be split as well, combining the appropriate regions:

$$\begin{aligned} & \int_{a_1}^{a_{M+1}} d\lambda_1 f_i(\lambda_1) \int_{a_1}^{\lambda_1} d\lambda_2 f_{i+1}(\lambda_2) \\ &= \int_{a_1}^{a_2} d\lambda_1 f_i(\lambda_1) \int_{a_1}^{\lambda_1} d\lambda_2 f_{i+1}(\lambda_2) + \int_{a_2}^{a_3} d\lambda_1 f_i(\lambda_1) \left(S^1(i+1) + \int_{a_2}^{\lambda_1} d\lambda_2 f_{i+1}(\lambda_2) \right) \\ &+ \dots + \int_{a_M}^{a_{M+1}} d\lambda_1 f_i(\lambda_1) \left(\sum_{J=1}^{M-1} S^J(i+1) + \int_{a_M}^{\lambda_1} d\lambda_2 f_{i+1}(\lambda_2) \right). \end{aligned}$$

This can be simplified by using the notation for the first-order segment integral and by introducing the notation for the second-order segment integral:

$$S_2^J(i) = \int_{a_J}^{a_{J+1}} d\lambda_1 \int_{a_J}^{\lambda_1} d\lambda_2 f_i^J(\lambda_1) f_{i+1}^J(\lambda_2), \quad (6.17)$$

$$I_2 = \sum_{J=1}^M S_2^J(1) + \sum_{J=2}^M \sum_{K=1}^{J-1} S_1^J(1) S_1^K(2). \quad (6.18)$$

Note that S_2 only depends on the J -th segment; no mixing occurs. This will be true to all orders, and is exactly what we hoped for: we can express the full path ordered integral as path ordered integrals over the separate segments. Also note that the argument of successive segment integrals (which is the incarnation index of f) is simply incrementing; this will also be true to all orders (i.e. only terms of the form $S_{m_1}^{J_1}(i) S_{m_2}^{J_2}(i+1) \dots S_{m_k}^{J_k}(i+k)$ will appear). In what follows, we will drop this argument of S , as it is trivial to deduce as long as we keep the *ordering* of the S 's fixed.

Although we used the expression for the path-ordering given by Equation 6.8, the whole derivation is equally valid when using the chaining of the integration borders as given in Equation 6.10.

The extension to higher orders is trivial but paper-consuming, so we just give the results:

Piecewise Path Ordered Integrals

$$I_3 = \sum_{J=1}^M S_3^J + \sum_{J=2}^M \sum_{K=1}^{J-1} \left[S_1^J S_2^K + S_2^J S_1^K \right] + \sum_{J=3}^M \sum_{K=2}^{J-1} \sum_{L=1}^{K-1} S_1^J S_1^K S_1^L, \quad (6.19a)$$

$$I_4 = \sum_{J=1}^M S_4^J + \sum_{J=2}^M \sum_{K=1}^{J-1} \left[S_1^J S_3^K + S_2^J S_2^K + S_3^J S_1^K \right] + \sum_{J=4}^M \sum_{K=3}^{J-1} \sum_{L=2}^{K-1} \sum_{O=1}^{L-1} S_1^J S_1^K S_1^L S_1^O \\ + \sum_{J=3}^M \sum_{K=2}^{J-1} \sum_{L=1}^{K-1} \left[S_1^J S_1^K S_2^L + S_1^J S_2^K S_1^L + S_2^J S_1^K S_1^L \right], \quad (6.19b)$$

$$I_n = \sum_{i=1}^n \left[\left(\prod_{j=1}^i \sum_{J_j=i-j+1}^{J_{j-1}-1} \right)_{J_0-1=M} \left(\begin{array}{l} \text{All terms of the form } \prod_{j=1}^i S_{l_j}^{J_j} \\ \text{such that } \sum_{j=1}^i l_j = n \end{array} \right) \right]. \quad (6.19c)$$

It is straightforward to write out the n -th order integral for any n . All we have to do is make all possible combinations of S_i 's that give n internal f 's and adding the correct number of sum symbols while keeping the ordering. It is also possible to give a recursive definition:

$$I_n(M) = \sum_{J=1}^M S_n^J + \sum_{J=2}^M \sum_{i=1}^{n-1} S_i^J I_{n-i}(J-1). \quad (6.20)$$

The last two equations literally translate to a Wilson line; just replace every S with a \mathcal{U} , for instance:²

$$\mathcal{U}_3 = \sum_{J=1}^M \mathcal{U}_3^J + 2 \sum_{J=2}^M \sum_{K=1}^{J-1} \mathcal{U}_1^J \mathcal{U}_2^K + \sum_{J=3}^M \sum_{K=2}^{J-1} \sum_{L=1}^{K-1} \mathcal{U}_1^J \mathcal{U}_1^K \mathcal{U}_1^L, \quad (6.21)$$

where

$$\mathcal{U}_n^J = \left(\frac{ig}{16\pi^4} \right)^n \int d^4 k_1 \dots d^4 k_n A_{\mu_1}(k_1) \dots A_{\mu_n}(k_n) S_n^J. \quad (6.22)$$

Note that the ordering of the \mathcal{U}^J remains important, as the momentum integration runs over the S_i 's and the fields, which are non-commutative due to the colour generators.

The physical interpretation of the n -th order formula is a collection of all possible diagrams for n -gluon radiation from a M -segment Wilson line, as is illustrated in figure (Figure 6.3) for 3 gluons radiated from a line with 4 linear segments. Note the manifest path ordering: the \mathcal{U}^J are path ordered by definition, and the sums are such that the gluon from segment J is radiated before K which is radiated before L (here we literally see that a Wilson line is read from right to left, as the order of J , K , and L is flipped).

Consider now the product of e.g. three Wilson lines, labelled \mathcal{U}^A , \mathcal{U}^B and \mathcal{U}^C . Expanding the exponentials and collecting terms of the same order in g we get:

$$\begin{aligned} \mathcal{U}^A \mathcal{U}^B \mathcal{U}^C &= 1 + (\mathcal{U}_1^A + \mathcal{U}_1^B + \mathcal{U}_1^C) \\ &+ (\mathcal{U}_1^A \mathcal{U}_1^B + \mathcal{U}_1^A \mathcal{U}_1^C + \mathcal{U}_1^B \mathcal{U}_1^C + \mathcal{U}_2^A + \mathcal{U}_2^B + \mathcal{U}_2^C) \\ &+ (\mathcal{U}_1^A \mathcal{U}_1^B \mathcal{U}_1^C + \mathcal{U}_1^A \mathcal{U}_2^B + \mathcal{U}_1^A \mathcal{U}_2^C + \mathcal{U}_1^B \mathcal{U}_2^C + \mathcal{U}_2^A \mathcal{U}_1^B \\ &+ \mathcal{U}_2^A \mathcal{U}_1^C + \mathcal{U}_2^B \mathcal{U}_1^C + \mathcal{U}_3^A + \mathcal{U}_3^B + \mathcal{U}_3^C) + \dots, \end{aligned}$$

which equals, up to third order, the sum of Equations 6.14, 6.18 and 6.19a. In other words, we can equate a product of Wilson lines to one line with several segments. The proof easily generalises to all orders. Note that the order of the segments is reversed w.r.t. the order of the product (because we read the lines from right to left), e.g. the product $\mathcal{U}^A \mathcal{U}^B \mathcal{U}^C$ is a line with first segment C , second segment B and last segment A , i.e.

$$\mathcal{U}^A \mathcal{U}^B \mathcal{U}^C = \mathcal{U}^{ABC},$$

where we read the order of the segments in the r.h.s. from right to left.

² We use the brace notation for tensor symmetrisation, i.e. $\mathcal{U}_{(1}^J \mathcal{U}_{2)}^K = \frac{1}{2} (\mathcal{U}_1^J \mathcal{U}_2^K + \mathcal{U}_2^J \mathcal{U}_1^K)$. See Equations A.13

$$\begin{aligned}
\sum_{J=1}^M \mathcal{U}_3^J &= \text{Diagram 1} + \text{Diagram 2} + \text{Diagram 3} + \text{Diagram 4} \\
\sum_{J=2}^M \sum_{K=1}^{J-1} \mathcal{U}_1^J \mathcal{U}_2^K &= \text{Diagram 5} + \text{Diagram 6} + \text{Diagram 7} + \text{Diagram 8} \\
&\quad + \text{Diagram 9} + \text{Diagram 10} \\
\sum_{J=2}^M \sum_{K=1}^{J-1} \mathcal{U}_2^J \mathcal{U}_1^K &= \text{Diagram 11} + \text{Diagram 12} + \text{Diagram 13} + \text{Diagram 14} \\
&\quad + \text{Diagram 15} + \text{Diagram 16} \\
\sum_{J=3}^M \sum_{K=2}^{J-1} \sum_{L=1}^{K-1} \mathcal{U}_1^J \mathcal{U}_1^K \mathcal{U}_1^L &= \text{Diagram 17} + \text{Diagram 18} + \text{Diagram 19} + \text{Diagram 20}
\end{aligned}$$

The figure shows four rows of Feynman diagrams representing different gluon radiation topologies on a 4-segment Wilson line. Each diagram consists of a blue zigzag line with four segments and green wavy lines representing gluon radiation. The segments are labeled with letters J, K, L, and M. The first row shows four diagrams with a single gluon radiation on each segment. The second row shows eight diagrams with two gluon radiations on different segments. The third row shows eight diagrams with two gluon radiations on different segments. The fourth row shows four diagrams with three gluon radiations on different segments. The diagrams are arranged in a grid-like pattern, with each diagram in a row having a similar structure but different radiation positions.

Figure 6.3: Correspondence between Equation 6.21 and all possible diagrams for 3-gluon radiation on a 4-segment Wilson line. Path ordering is manifestly conserved.

6.3 WILSON LINES ON A LINEAR PATH

The results from the former section are general results, i.e. valid for any path. Let us now turn our focus towards paths built from linear segments—as these are the most commonly used in literature—and derive Feynman rules for the different linear topologies. For every segment there exist four possible path structures: it can be a finite segment connecting two points, it can be a segment connecting $\pm\infty$ and a point r^μ , or it can be a fully infinite line connecting $-\infty$ with $+\infty$. We will investigate them case by case.

Bounded from Below

We start with a path going from a point a_μ to $+\infty$ along a direction n_μ . Such a path can be parameterised as

$$z^\mu = a^\mu + n^\mu \lambda \quad \lambda = 0 \dots \infty. \quad (6.23)$$

Using the path-ordering as defined in [Equation 6.10](#), we can write [Equation 6.11](#) as:³

$$I_n^{\text{l.b.}} = (ig)^n n^{\mu_1} \dots n^{\mu_n} e^{ia \cdot \sum_j k_j} \int_0^\infty \int_{\lambda_1}^\infty \dots \int_{\lambda_{n-1}}^\infty d\lambda_1 \dots d\lambda_n e^{i \sum_j (n \cdot k_j + i\eta) \lambda_j}, \quad (6.24)$$

where the terms $+i\eta$ in the exponential (with $\eta > 0$ infinitesimal) are needed to make the integral convergent. Solving this integral is straightforward. First we calculate the innermost integral, which is just the Fourier transform of a Heaviside θ -function:

$$\int_{\lambda_{n-1}}^\infty d\lambda_n e^{i(n \cdot k_n + i\eta) \lambda_n} = \frac{i}{n \cdot k_n + i\eta} e^{i(n \cdot k_n + i\eta) \lambda_{n-1}}, \quad (6.25)$$

Note that if we would have used [Equation 6.8](#) instead of [Equation 6.10](#), this result would have contained two terms—of course valid as well but much more difficult.

We can summarise the effect of the innermost integral as a factor $\frac{1}{n \cdot k_n}$ and an extra term $n \cdot k_n$ in front of λ_{n-1} . The next integral will then give a factor $\frac{1}{n \cdot k_n + n \cdot k_{n-1}}$ and so on. In other words, we simply get:

$$I_n^{\text{l.b.}} = (ig)^n n^{\mu_1} \dots n^{\mu_n} e^{ia \cdot \sum_j k_j} \prod_{j=1}^n \frac{i}{n \cdot \sum_{l=j}^n k_l + i\eta}, \quad (6.26)$$

There is a small subtlety in this result, as we absorbed some factors in front of the $i\eta$ into η (which is something we are allowed to do as the limit $\eta \rightarrow 0$ is implicitly assumed).

We can reconstruct the result in [Equation 6.26](#) with the following Feynman rules:

³ The symbol n is used both as an index (in the n -th order expansion) and as a directional vector. The difference should be clear from context.

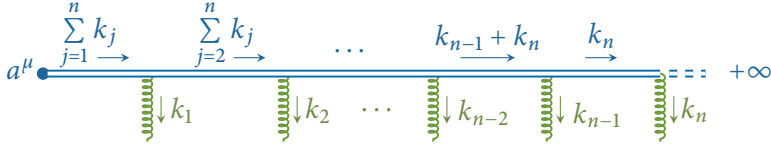


Figure 6.4: n -gluon radiation for a Wilson line going from a^μ to $+\infty$.

Feynman Rules for Linear Wilson Lines			
A. Propagator:	$\xrightarrow{\quad k \quad}$	$= \frac{i}{n \cdot k + i\eta}$,	(6.27a)
B. External point:	$a^\mu \bullet \xrightarrow{\quad k \quad}$	$= e^{i a \cdot k}$,	(6.27b)
C. Line to infinity:	$==== +\infty$	$= 1$,	(6.27c)
D. Wilson vertex:	$\begin{matrix} j \\ \xrightarrow{\quad} \\ \downarrow k \\ \mu, a \end{matrix} i$	$= i g n^\mu (t^a)_{ij}$.	(6.27d)

These Feynman rules are for momenta that start in the external point and point outwards from the Wilson line (see the discussion above Equation 6.12). If one or more momenta are inwards, the correct Feynman rule can be trivially retrieved by making the substitution $k_i \rightarrow -k_i$. As an illustration, the resulting n -th order diagram is drawn in Figure 6.4.

Bounded from Above

The logical next step is to investigate a path that starts at $-\infty$ and now goes up to a point b_μ , which we parameterise as

$$z^\mu = b^\mu + n^\mu \lambda \quad \lambda = -\infty \dots 0. \tag{6.28}$$

In this case, it is easier to reverse the integration variables as in Equation 6.8, which then gives the integral for a Wilson line with upper bound:

$$I_n^{\text{u.b.}} = (i g)^n n^{\mu_1} \dots n^{\mu_n} e^{i b \cdot \sum_j k_j} \int_{-\infty}^0 \int_{-\infty}^{\lambda_n} \dots \int_{-\infty}^{\lambda_2} d\lambda_n \dots d\lambda_1 e^{i n \cdot \sum_j k_j \lambda_j}. \tag{6.29}$$

The calculation goes as before, giving:

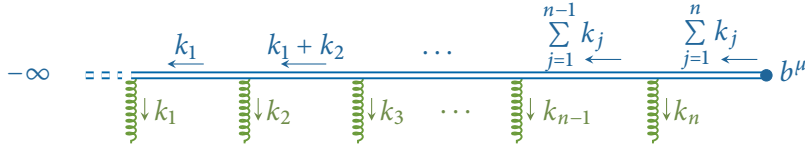


Figure 6.5: n -gluon radiation for a Wilson line going from $-\infty$ to b^μ . Path flow is opposite to momentum flow

$$I_n^{\text{u.b.}} = (ig)^n n^{\mu_1} \dots n^{\mu_n} e^{ib \cdot \sum_j k_j} \prod_{j=1}^n \frac{-i}{n \cdot \sum_{l=1}^j k_l - i\eta}, \quad (6.30)$$

which differs from Equation 6.26 only in the accumulation of momenta in the denominators (bottom-top instead of top-bottom) and the sign of the convergence terms. The Feynman rules derived before remain valid if we make the substitution $k \rightarrow -k$ in the Wilson line propagators, but not in the external point. Then it is straightforward to draw the n -th order diagram for a Wilson line going from $-\infty$ to b^μ , as demonstrated in Figure 6.5. The path still flows from left to right, but now the momenta are opposite to the path flow. However the main idea remains the same: momenta start from the external point and are spread over the outgoing gluons.

Path Reversal

Let us now investigate what changes when we reverse the path of a Wilson line. First of all, the integration borders are of course interchanged, because the path flows from the final point to the initial point. This is the same as keeping the integration borders as they are, and flipping the sign in the exponent. But the most important is that the order of the fields is reversed, because the field that normally lies first on the path will be encountered last when following the reversed path flow. This is the idea of *anti path-ordering* $\overline{\mathcal{P}}$, defined such that the field with the highest value for λ is written *rightmost* instead of leftmost. The reversed Wilson line is thus given by:

$$\mathcal{U}_{(a;b)} = \overline{\mathcal{P}} e^{-ig \int_a^b dz^\mu A_\mu}. \quad (6.31)$$

It comes as no surprise that this is exactly the same as the Hermitian conjugate, as this was one of the properties imposed during the derivation of the Wilson line in Chapter 2. Note that the reversal of the field ordering is not only a logical step when reversing the path, but also a direct result of the Hermitian

conjugate, because $(A_n \cdots A_1)^\dagger = A_1^\dagger \cdots A_n^\dagger$. By using the fact that $A(k)^\dagger = A(-k)$ is a Hermitian function⁴, and making the substitution $k \rightarrow -k$, the relation to the reversed path becomes apparent. We thus have indeed:

$$\mathcal{U}_{(a;b)} = \mathcal{U}_{(b;a)}^\dagger. \quad (6.32)$$

But of course it would be desirable to express the Hermitian conjugate line in function of normal path-ordered fields, such that we can use the same Feynman rules as before.

Let's see how e.g. a Wilson line from $-\infty$ to b^μ behaves when Hermitian conjugated (remember that in Equation 6.12 we defined the regular Wilson line with opposite momenta, i.e. with factors $A_i(-k_i)$):

$$\begin{aligned} \mathcal{U}_{(b;-\infty)}^\dagger &= \left[\sum_{n=0}^{\infty} (ig)^n \int \frac{d^\omega k_n}{(2\pi)^\omega} n \cdot A(-k_n) \cdots n \cdot A(-k_1) e^{ib \cdot \sum_{j=1}^n k_j} \prod_{j=1}^n \frac{-i}{n \cdot \sum_{l=1}^j k_l - i\eta} \right]^\dagger \\ &= \sum_{n=0}^{\infty} (-ig)^n \int \frac{d^\omega k_n}{(2\pi)^\omega} n \cdot A(k_1) \cdots n \cdot A(k_n) e^{-ib \cdot \sum_{j=1}^n k_j} \prod_{j=1}^n \frac{i}{n \cdot \sum_{l=1}^j k_l + i\eta} \\ &= \sum_{n=0}^{\infty} (-ig)^n \int \frac{d^\omega k_n}{(2\pi)^\omega} n \cdot A(-k_1) \cdots n \cdot A(-k_n) e^{ib \cdot \sum_{j=1}^n k_j} \prod_{j=1}^n \frac{-i}{n \cdot \sum_{l=1}^j k_l - i\eta}, \end{aligned}$$

where in the last step we made the integration substitution $k_i \rightarrow -k_i$. In order to make the identification with Equation 6.12, we have to relabel the fields by doing

$$1 \rightarrow n, 2 \rightarrow n-1, \dots, n \rightarrow 1,$$

which gives

$$\begin{aligned} \mathcal{U}_{(b;-\infty)}^\dagger &= \sum_{n=0}^{\infty} \int \frac{d^\omega k_n}{(2\pi)^\omega} \cdots \frac{d^\omega k_1}{(2\pi)^\omega} A_{\mu_n}(-k_n) \cdots A_{\mu_1}(-k_1) I_n^{\text{l.b.}\dagger}, \\ I_n^{\text{l.b.}\dagger} &= (ig)^n (-n^{\mu_1}) \cdots (-n^{\mu_n}) e^{ib \cdot \sum_{j=1}^n k_j} \prod_{j=1}^n \frac{i}{-n \cdot \sum_{l=j}^n k_l + i\eta}. \end{aligned}$$

⁴ Because $A(x)$ is real.

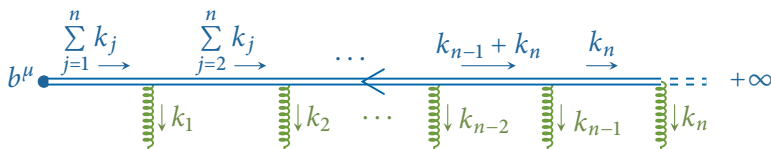


Figure 6.6: Reversing the path of a Wilson line is the same as taking the Hermitian conjugate $\mathcal{U}_{(b; -\infty)}^\dagger$. If we want to express this in standard path ordering, we have to make the substitution $n \rightarrow -n$ (shown by the blue arrow) and change the path into a line going from b^μ to $+\infty$.

We see now that this is the expansion of a Wilson line from b^μ to $+\infty$, but with opposite n^μ .⁵ The same will be true for a Wilson line from a point to $+\infty$, so we can write:

$$\mathcal{U}_{(+\infty; a)}^\dagger = \mathcal{U}_{(a; -\infty)} \Big|_{n \rightarrow -n}, \tag{6.33a}$$

$$\mathcal{U}_{(b; -\infty)}^\dagger = \mathcal{U}_{(+\infty; b)} \Big|_{n \rightarrow -n}. \tag{6.33b}$$

We will indicate the direction of n in a Feynman diagram with a blue arrow on the Wilson line, where going from left to right implies a positive n . This also indicates the direction of the path flow: an arrow from right to left implies a negative n , implying a Hermitian conjugate, implying a reversed path (from right to left).⁶ With this convention, we can draw the reversed version of $\mathcal{U}_{(b; -\infty)}$ as in Figure 6.6.

Let us have a look at how the Feynman rules change when making the substitution $n \rightarrow -n$. First for the Wilson line propagator, we see that it gets complex conjugated when the momentum flow is opposed to the path direction:

$$\begin{array}{c} \xrightarrow{k} \\ \hline \hline \end{array} = \frac{i}{n \cdot k + i\eta}, \quad \begin{array}{c} \xleftarrow{k} \\ \hline \hline \end{array} = \frac{-i}{n \cdot k - i\eta}, \tag{6.34a}$$

$$\begin{array}{c} \xleftarrow{k} \\ \hline \hline \end{array} = \frac{-i}{n \cdot k - i\eta}, \quad \begin{array}{c} \xrightarrow{k} \\ \hline \hline \end{array} = \frac{i}{n \cdot k + i\eta}. \tag{6.34b}$$

5 The important fact to realise here is that what defines whether a Wilson line is going from $-\infty$ to a^μ or from a^μ to $+\infty$ is how the momenta are summed in the denominator. For the former it is $\sum_{l=1}^j$, and for the latter $\sum_{l=j}^n$.

6 Note that the substitution $n \rightarrow -n$ is not the same as a path reversal. To appreciate the difference, remember that for a linear path $z^\mu = r^\mu + n^\mu \lambda$, so the substitution $n \rightarrow -n$ changes a path from $-\infty$ to 0 into one from $+\infty$ to 0 (ignoring the difference between path-ordering and anti path-ordering). But the reversed path goes in the *direction* $-n$; this is why we can use the blue arrow to denote both. The difference is maybe subtle, but cannot be neglected.

The vertex coefficient only depends on the path direction, (not on the momentum direction):

$$j \begin{array}{c} \text{---} \text{---} \text{---} \\ \uparrow k \\ \text{---} \end{array} i = i g n^\mu (t^a)_{ij}, \quad j \begin{array}{c} \text{---} \text{---} \text{---} \\ \uparrow k \\ \text{---} \end{array} i = -i g n^\mu (t^a)_{ij}. \quad (6.35)$$

On the other hand, the sign in the exponent for an external point doesn't depend on the direction of the path flow, but only on the momentum direction as compared to the point itself:

$$\begin{array}{c} \leftarrow k \\ \text{---} \text{---} \end{array} \bullet r^\mu = r^\mu \begin{array}{c} \text{---} \text{---} \text{---} \\ \rightarrow k \end{array} = \begin{array}{c} \leftarrow k \\ \text{---} \text{---} \end{array} \bullet r^\mu = r^\mu \begin{array}{c} \text{---} \text{---} \text{---} \\ \leftarrow k \end{array} = e^{i r \cdot k}, \quad (6.36a)$$

$$\begin{array}{c} \text{---} \text{---} \\ \rightarrow k \end{array} \bullet r^\mu = r^\mu \begin{array}{c} \text{---} \text{---} \text{---} \\ \leftarrow k \end{array} = \begin{array}{c} \text{---} \text{---} \text{---} \\ \rightarrow k \end{array} \bullet r^\mu = r^\mu \begin{array}{c} \text{---} \text{---} \text{---} \\ \rightarrow k \end{array} = e^{-i r \cdot k}. \quad (6.36b)$$

Most of the time, we will drop the arrow indicating the path flow on the Wilson line, as it obscures readability, and assume—unless specified otherwise—the path flowing from left to right.

We now introduce a shorthand notation to denote the path structure for a Wilson line segment. We represent the two structures we calculated first by:

Schematic Representation of Wilson Line Segments	
$\mathcal{U}_{(+\infty; a)} \stackrel{N}{=} \begin{array}{c} \text{---} \text{---} \text{---} \\ \rightarrow \end{array},$	(6.37a)
$\mathcal{U}_{(b; -\infty)} \stackrel{N}{=} \begin{array}{c} \text{---} \text{---} \text{---} \\ \leftarrow \end{array}.$	(6.37b)

Note that there is a subtlety in our drawing conventions. Until now we've only drawn small pieces of a segment in order to illustrate the Feynman rules. But here we give a schematic representation of a full segment (including gluons). Confusion might especially appear between the depiction of the Feynman rule for an external point and this representation, however, the correct interpretation should be clear from the context. Furthermore, from now on we will mostly use the latter notation.

For the reversed path, there is some ambiguity in the interpretation. Combining Equation 6.32 and Equations 6.33, we can write

$$\mathcal{U}_{(a; +\infty)} = \mathcal{U}_{(a; -\infty)} \Big|_{n \rightarrow -n}. \quad (6.38)$$

In both sides of the equation, the blue arrow is pointing from right to left. However, in the l.h.s. the line touches $+\infty$ and in the r.h.s. it touches $-\infty$. The l.h.s.

gives the correct physical picture, while the r.h.s. gives the correct calculational picture (assuming we keep all fields in standard path-ordering). We choose the latter, so keep in mind that this is not a correct physical representation:

$$\mathcal{U}_{(a; +\infty)} = \mathcal{U}_{(a; -\infty)} \Big|_{n \rightarrow -n} \stackrel{N}{=} \leftarrow \bullet, \quad (6.39a)$$

$$\mathcal{U}_{(-\infty; b)} = \mathcal{U}_{(+\infty; b)} \Big|_{n \rightarrow -n} \stackrel{N}{=} \bullet \leftarrow. \quad (6.39b)$$

This helps avoiding calculational mistakes, as the former representation would seem to suggest that $\mathcal{U}_{(+\infty; a)}$ and $\mathcal{U}_{(a; +\infty)}$ are related by a simple sign change in n . This is not enough, one also has to change the accumulation of momenta in the denominator of the propagator, from $\sum_j^n k_l$ (Equation 6.26) to $\sum_1^j k_l$ (Equation 6.30). A trick to remind this correctly is to remember that path reversing equals Hermitian conjugation, and the latter is easily demonstrated in our schematic notation using a “mirror relation”:

Mirror Relation for Hermitian Conjugate Line

$$\left(\bullet \rightleftharpoons \bullet \right)^\dagger = \leftarrow \bullet, \quad \left(\bullet \leftarrow \bullet \right)^\dagger = \bullet \leftarrow, \quad (6.40)$$

which is literally the same as Equations 6.33.

Finite Wilson Line

Next we investigate a Wilson line on a finite path, going from a point a^μ to a point b^μ (where now the direction is defined by $n^\mu = \frac{b^\mu - a^\mu}{\|b - a\|}$). We parameterise this as:

$$z^\mu = a^\mu + n^\mu \lambda \quad \lambda = 0 \dots \|b - a\|. \quad (6.41)$$

Of course we can simply use Equation 6.4c to split the line at $\pm\infty$, i.e.

$$\mathcal{U}_{(b; a)} = \mathcal{U}_{(b; +\infty)} \mathcal{U}_{(+\infty; a)} = \mathcal{U}_{(b; -\infty)} \mathcal{U}_{(-\infty; a)},$$

but in what follows we will do a brute-force calculation giving the same result, and this for three reasons:

- A. It is an extra, practical check of the transitivity formula.
- B. Following our calculations, we will see that this is the natural and only way to calculate a finite line in momentum space, i.e. so far no easier solutions exist.

- c. Halfway the calculation we will need to solve a recursive relation, which we can re-use when calculating the fully infinite line.

Because there are no infinities at the borders, it doesn't matter whether we choose Equation 6.10 or Equation 6.8, as both are equally difficult but will give the same results. Choosing Equation 6.10, we write the segment integral as

$$I_n^{\text{fin}} = (ig)^n n^{\mu_1} \dots n^{\mu_n} e^{ia \cdot \sum_j k_j} \int_0^{\|b-a\|} \int_0^{\lambda_n} \dots \int_0^{\lambda_2} d\lambda_n \dots d\lambda_1 e^{in \cdot \sum_j k_j \lambda_j}. \quad (6.42)$$

Dropping the factors in front of the integral, we find a recursion relation:

$$I_1^{\text{fin}}(k_1) = \int_0^{\|b-a\|} d\lambda e^{in \cdot k_1 \lambda} = \frac{-i}{n \cdot k_1} \left(e^{i(b-a) \cdot k_1} - 1 \right), \quad (6.43a)$$

$$I_n^{\text{fin}}(k_1, \dots, k_n) = \frac{-i}{n \cdot k_1} \left(I_{n-1}^{\text{fin}}(k_1+k_2, \dots, k_n) - I_{n-1}^{\text{fin}}(k_2, \dots, k_n) \right). \quad (6.43b)$$

To ameliorate notational clarity, we will drop the factors n^μ (from the fractions) and $i(b-a)^\mu$ (from the exponent) in the next calculation. The first few orders are easily calculated:

$$\begin{aligned} I_2^{\text{fin}} &= \frac{(-i)^2}{k_1(k_1+k_2)} (e^{k_1+k_2} - 1) + \frac{i(-i)}{k_1 k_2} (e^{k_2} - 1), \\ I_3^{\text{fin}} &= \frac{(-i)^3}{k_1(k_1+k_2)(k_1+k_2+k_3)} (e^{k_1+k_2+k_3} - 1) + \frac{i(-i)^2}{k_1 k_2 (k_2+k_3)} (e^{k_2+k_3} - 1) \\ &\quad + \frac{i^2(-i)}{(k_1+k_2)k_2 k_3} (e^{k_3} - 1), \\ I_4^{\text{fin}} &= \frac{(-i)^4}{k_1(k_1+k_2)(k_1+k_2+k_3)(k_1+k_2+k_3+k_4)} (e^{k_1+k_2+k_3+k_4} - 1) \\ &\quad + \frac{i(-i)^3}{k_1 k_2 (k_2+k_3)(k_2+k_3+k_4)} (e^{k_2+k_3+k_4} - 1) \\ &\quad + \frac{i^2(-i)^2}{(k_1+k_2)k_2 k_3 (k_3+k_4)} (e^{k_3+k_4} - 1) + \frac{i^3(-i)}{(k_1+k_2+k_3)(k_2+k_3)k_3 k_4} (e^{k_4} - 1), \end{aligned}$$

and so on. We see that every term has a fraction where a part of the momenta is accumulated from below, and the other part is accumulated from above. We can

thus express the n -th order term exactly as (reintroducing the factors n^μ and $(b-a)^\mu$):

$$I_n^{\text{fin.}} = \sum_{m=0}^{n-1} \left(e^{i(b-a) \cdot \sum_{m+1}^n k_j} - 1 \right) \left(\prod_{j=1}^m \frac{i}{n \cdot \sum_{l=j}^m k_l} \right) \left(\prod_{j=m+1}^n \frac{-i}{n \cdot \sum_{l=m+1}^j k_l} \right). \quad (6.44)$$

This can be simplified further. First of all, we have exactly $2n$ terms, of which n have no exponential and can thus be summed to simplify into one term (these are all terms corresponding to the -1 term in parentheses). Note that if we sum these n terms and add the $m = n$ term, we get zero:

Eikonal Identity

$$\sum_{m=0}^n \left(\prod_{j=1}^m \frac{i}{n \cdot \sum_{l=j}^m k_l} \right) \left(\prod_{j=m+1}^n \frac{-i}{n \cdot \sum_{l=m+1}^j k_l} \right) = 0, \quad (6.45)$$

which is easy to prove by induction. This is known as the *eikonal identity*, and is especially useful in the case of Abelian fields, because then it tells us that—for a given diagram where two Wilson lines are connected to each other with $n/2$ photons (or gluons when ignoring colour)—if we sum the possible emission partitions between the two lines, the result is automatically zero.⁷

Using the eikonal identity, we can replace the sum of the n terms by the opposite of the $m = n$ term:

$$- \sum_{m=0}^{n-1} \left(\prod_{j=1}^m \frac{i}{n \cdot \sum_{l=j}^m k_l} \right) \left(\prod_{j=m+1}^n \frac{-i}{n \cdot \sum_{l=m+1}^j k_l} \right) = \prod_{j=1}^n \frac{i}{n \cdot \sum_{l=j}^m k_l},$$

The important observation is now that the last term is also the $m = n$ term for the full sum including the exponential (Equation 6.44), as in this case the exponential vanishes:⁸

$$e^{i(b-a) \cdot \sum_{n+1}^n k_j} = e^0 = 1.$$

7 We don't even have to sum over all possible crossings. Any given diagram connecting the photons is represented as a product of δ -functions and propagators, and is factorised out of this calculation.

8 Remember that by definition $\sum_{j=a}^b f(j) = 0$ if $a > b$, this is an 'empty sum'. The same is true for

multiplication: $\prod_{j=a}^b f(j) = 1$ if $a > b$.

This then gives:

$$\begin{aligned} I_n^{\text{fin.}} &= \sum_{m=0}^{n-1} e^{i(b-a)\cdot\sum_{m+1}^n k_j} \left(\prod_{j=1}^m \frac{i}{n\cdot\sum_{l=j}^m k_l} \right) \left(\prod_{j=m+1}^n \frac{-i}{n\cdot\sum_{l=m+1}^j k_l} \right) + \prod_{j=1}^n \frac{i}{n\cdot\sum_{l=j}^n k_l}, \\ &= \sum_{m=0}^n e^{i(b-a)\cdot\sum_{m+1}^n k_j} \left(\prod_{j=1}^m \frac{i}{n\cdot\sum_{l=j}^m k_l} \right) \left(\prod_{j=m+1}^n \frac{-i}{n\cdot\sum_{l=m+1}^j k_l} \right). \end{aligned}$$

Reintroducing the factors in front, we see that the exponential simplifies into

$$e^{i a \cdot \sum_1^n k_j} \sum_{m=0}^n e^{i(b-a)\cdot\sum_{m+1}^n k_j} = \sum_{m=0}^n e^{i a \cdot \sum_1^m k_j} e^{i b \cdot \sum_{m+1}^n k_j}.$$

We can thus finally write the path content integral for a finite line as

$$I_n^{\text{fin.}} = \sum_{m=0}^n \left(\prod_{j=1}^m i g n^{\mu_j} \frac{i}{n\cdot\sum_{l=j}^m k_l} e^{i a \cdot k_j} \right) \left(\prod_{j=m+1}^n i g n^{\mu_j} \frac{-i}{n\cdot\sum_{l=m+1}^j k_l} e^{i b \cdot k_j} \right). \quad (6.46)$$

Using the fact that this kind of chained sum can in general be written as a product of two infinite sums:

$$\sum_{n=0}^{\infty} \sum_{m=0}^n A_m B_{n-m} = \left(\sum_{n=0}^{\infty} A_n \right) \left(\sum_{n=0}^{\infty} B_n \right),$$

we can transform [Equation 6.46](#) into a product of two half-infinite Wilson lines:⁹

$$\sum_{n=0}^{\infty} I_n^{\text{fin.}} = \left(\sum_{n=0}^{\infty} \prod_{j=1}^n i g n^{\mu_j} \frac{-i}{n\cdot\sum_{l=1}^j k_l} e^{i b \cdot k_j} \right) \left(\sum_{n=0}^{\infty} \prod_{j=1}^n i g n^{\mu_j} \frac{i}{n\cdot\sum_{l=j}^n k_l} e^{i a \cdot k_j} \right).$$

To make the identification with two half-infinite Wilson lines, we will manually add the convergence terms in the fraction (we can do this without problem

⁹ There is a small subtlety here: in [Equation 6.46](#), the propagators are ordered from 1 to n . But of course the fields are ordered from n to 1 as explained in [Equation 6.12](#). So basically, when including the momentum integrals over the fields, the two products switch places.

because in the infinitesimal limit they are zero anyway), but to be consistent, they have to have the same sign in both products:¹⁰

$$\sum_n I_n^{\text{fin.}} = \left(\sum_{n=0}^{\infty} \prod_{j=1}^n i g n^{\mu_j} \frac{-i}{n \cdot \sum_{l=1}^j k_l + i \eta} e^{i b \cdot k_j} \right) \left(\sum_{n=0}^{\infty} \prod_{j=1}^n i g n^{\mu_j} \frac{i}{n \cdot \sum_{l=j}^n k_l + i \eta} e^{i a \cdot k_j} \right),$$

which is literally the same as two lower bound Wilson lines:

$$\mathcal{U}_{(b;a)} = \mathcal{U}_{(b;-\infty)} \Big|_{n \rightarrow -n} \mathcal{U}_{(+\infty;a)} = \mathcal{U}_{(+\infty;b)}^\dagger \mathcal{U}_{(+\infty;a)} = \mathcal{U}_{(b;+\infty)} \mathcal{U}_{(+\infty;a)}. \tag{6.47}$$

Of course, we can just as well insert convergence terms with a negative sign, i.e.

$$\sum_n I_n^{\text{fin.}} = \left(\sum_{n=0}^{\infty} \prod_{j=1}^n i g n^{\mu_j} \frac{-i}{n \cdot \sum_{l=1}^j k_l - i \eta} e^{i b \cdot k_j} \right) \left(\sum_{n=0}^{\infty} \prod_{j=1}^n i g n^{\mu_j} \frac{i}{n \cdot \sum_{l=j}^n k_l - i \eta} e^{i a \cdot k_j} \right),$$

which gives us two upper bound Wilson lines:

$$\mathcal{U}_{(b;a)} = \mathcal{U}_{(b;-\infty)} \mathcal{U}_{(+\infty;a)} \Big|_{n \rightarrow -n} = \mathcal{U}_{(b;-\infty)} \mathcal{U}_{(a;-\infty)}^\dagger = \mathcal{U}_{(b;-\infty)} \mathcal{U}_{(-\infty;a)}, \tag{6.48}$$

proving the arbitrariness of the transitivity property. When putting this relations in a schematic form, it is easiest to represent the one where the finite line is cut at $+\infty$, because then the line is literally torn in two:

Finite Wilson Line

$$a^\mu \bullet \rightleftarrows b^\mu = a^\mu \bullet \rightleftarrows \otimes \leftleftarrows b^\mu .$$

The reversed path is simply the Hermitian conjugate (note that the Hermitian conjugation also flips the order of the two lines in the r.h.s.):

$$a^\mu \bullet \leftleftarrows b^\mu = b^\mu \bullet \rightleftarrows \otimes \leftleftarrows a^\mu .$$

¹⁰ The reasoning behind it is that the correct place to introduce these convergence terms is not here— at the end of the calculation—but at the start of the calculation in the exponent of Equation 6.42, i.e. $e^{i \left(n \cdot \sum_{k_j \pm i \eta} \right) \lambda_j}$. Then after doing the full calculation, both products in Equation 6.46 will have convergence terms with the same sign.

So the only things that change after reversing the path are the external points. This is of course logical, as we could interpret it as a normal finite line from b^μ to a^μ , for which the former schematic relation holds.

Infinite Wilson line

Finally, the last possible path structure for a linear segment is a fully infinite line, going from $-\infty$ to $+\infty$ along a direction n^μ and passing through a point r^μ . Such a path can be parameterised as:

$$z^\mu = r^\mu + n^\mu \lambda \quad \lambda = -\infty \dots +\infty. \quad (6.49)$$

Using [Equation 6.8](#), we can write the segment integral as

$$I_n^{\text{inf.}} = (ig)^n n^{\mu_1} \dots n^{\mu_n} e^{ir \cdot \sum_j k_j} \int_{-\infty}^{+\infty} \dots \int_{-\infty}^{\lambda_2} d\lambda_n \dots d\lambda_1 e^{in \cdot \sum_j k_j \lambda_j}.$$

Naively, one could think that $I_n^{\text{inf.}}$ consists of $n-1$ integrals that evaluate to the Fourier transform of a Heaviside θ -function (see [Equations A.63](#)), $\frac{-i}{n \cdot k - i\eta}$, and one integral, the outermost, that evaluates to a Dirac δ -function. This would give the following result (again dropping the factors in front of the integral for convenience):

$$I_n^{\text{inf.}} = (ig)^n n^{\mu_1} \dots n^{\mu_n} \left(\prod_{j=1}^{n-1} \frac{-i}{n \cdot \sum_{l=1}^j k_l - i\eta} \right) 2\pi \delta\left(n \cdot \sum_{j=1}^n k_j\right). \quad (6.50)$$

However, there is one caveat. When we explicitly write the convergence terms used in the $n-1$ innermost integrals, we see that the outermost integral doesn't equal a δ -function at all, but is badly divergent:

$$\int_{-\infty}^{+\infty} d\lambda_n e^{i(n \cdot \sum_{j=1}^n k_j - i\eta)\lambda_n}. \quad (6.51)$$

This is the Fourier transform of $e^{\eta\lambda_n}$, which is divergent.¹¹ In other words, either we drop the convergence terms ($\eta = 0$), making the δ integral representation convergent but making all $n-1$ innermost integrals divergent, or we add the

¹¹ The only square-integrable linear exponential functions are $e^{-\eta|\lambda|}$ and $e^{-\eta\lambda} \theta(\lambda)$.

convergence terms in order to make the innermost integrals convergent, but then we lose the δ function representation and are stuck with a divergent Fourier transform. Simply using the convergence terms for the $n-1$ innermost integrals, and then setting them to zero for the last integral won't do, as there is no reason to believe that we are allowed to take the limit $\eta \rightarrow 0$ halfway. Furthermore we will need the convergence terms in the Wilson line propagators when doing momentum integrations.

A consistent approach is to regularise the path, as is calculated up to second order in [40]. However, their proof is based on a not so rigorous use of the Riemann-Lebesgue lemma. We will show that it is not difficult to make a mathematically correct all-order proof, based on solving the same recursion relation as we encountered in the calculation of the finite line. The regularised path runs from $r^\mu - \frac{2}{\xi}n^\mu$ to $r^\mu + \frac{2}{\xi}n^\mu$ (with $\xi > 0$), and is parameterised as:

$$z_\xi^\mu = r^\mu + \frac{2}{\xi} \tanh\left(\frac{\xi}{2}\lambda\right) n^\mu \quad \lambda = -\infty \dots +\infty \quad (6.52)$$

If we take the limit $\xi \rightarrow 0$, we recover the same parametrisation as in Equation 6.49. The innermost integral equals:

$$\begin{aligned} I_1^{\text{inf.}} &= \int_{-\infty}^{\lambda_2} d\lambda_1 \operatorname{sech}^2\left(\frac{\xi}{2}\lambda_1\right) e^{i\frac{2}{\xi}(n \cdot k_1 - i\eta) \tanh\left(\frac{\xi}{2}\lambda_1\right)} \\ &= \frac{-i}{n \cdot k_1 - i\eta} \left(e^{i\frac{2}{\xi}(n \cdot k_1 - i\eta) \tanh\left(\frac{\xi}{2}\lambda_2\right)} - e^{-i\frac{2}{\xi}(n \cdot k_1 - i\eta)} \right) \\ &\xrightarrow{\lambda_2 \rightarrow +\infty} 2i \sin\left(\frac{2}{\xi}(n \cdot k_1 - i\eta)\right) \frac{-i}{n \cdot k_1 - i\eta} \end{aligned}$$

The factor sech^2 is the integration measure that comes from the reparameterisation of the path $dz^\mu \rightarrow (z^\mu)' d\lambda$. Note that we added the convergence terms $i\eta$, despite the fact that at first sight they don't seem necessary. However, intuitively one can expect that they are in fact indispensable, as the regularisation of the path acts on the outermost ' δ '-integral and not on the innermost ' θ '-integrals, leaving the latter unregularised. We will indeed confirm their necessity in the next step. To proceed, we observe that for higher orders the integrals obey a recursion relation (again dropping the factors in front):

$$I_n^{\text{inf.}}(k_1, \dots, k_n) = \frac{-i}{n \cdot k_1 - i\eta} \left(I_{n-1}^{\text{inf.}}(k_1 + k_2, k_3, \dots, k_n) - e^{-i\frac{2}{\xi}(n \cdot k_1 - i\eta)} I_{n-1}^{\text{inf.}}(k_2, k_3, \dots, k_n) \right). \quad (6.53)$$

This relation looks a lot like [Equations 6.43](#). In fact the result is very similar and can be simplified into

$$I_n^{\text{inf.}} = 2i \sum_{m=0}^{n-1} e^{-i \frac{2}{\xi} \left(n \cdot \sum_1^m k_j - i\eta \right)} \sin \left[\frac{2}{\xi} \left(n \cdot \sum_{m+1}^n k_j - i\eta \right) \right] \prod_1^m \frac{i}{n \cdot \sum_j^m k_l - i\eta} \prod_{m+1}^n \frac{-i}{n \cdot \sum_{m+1}^j k_l - i\eta}.$$

Note how the convergence terms $-i\eta$ ensure that the exponent converges nicely in the limit $\xi \xrightarrow{>} 0$; they are indeed indispensable. All terms thus vanish in this limit, except the $m = 0$ term where the exponent equals 1. We now move from the regularised path back to the original path by taking this limit:

$$I_n^{\text{inf.}} = (ig)^n n^{\mu_1} \dots n^{\mu_n} \left(\prod_1^{n-1} \frac{-i}{n \cdot \sum_1^j k_l - i\eta} \right) 2\pi \delta \left(n \cdot \sum_1^n k_j - i\eta \right). \quad (6.54)$$

As this is the same result as in [Equation 6.50](#), we have shown that there is no need to regularise the path and that the naive calculation leads to correct results, although seemingly divergent at first sight.

A few words on the emergence of the δ -function however. We use here the concept of a *nascent δ -function*, which is any function δ_ξ with infinitesimal parameter $\xi > 0$, that has the weak limit

$$\lim_{\xi \xrightarrow{>} 0} \delta_\xi(x) \cong \delta(x). \quad (6.55)$$

This weak limit relates δ_ξ and δ not by equality, but by the sifting property:

$$\lim_{\xi \xrightarrow{>} 0} \int_{-\infty}^{+\infty} dx \delta_\xi(x) f(x) = f(0). \quad (6.56)$$

In other words, for all practical purposes we can treat the weak limit of a nascent delta function as a normal delta function. One can construct such a nascent δ -function from any function g that is absolutely integrable and has total integral equal to 1 by defining

$$\delta_\xi(x) = \frac{1}{\xi} g \left(\frac{x}{\xi} \right) \quad (6.57)$$

As the sinc function has total integral equal to $\int dx \frac{\sin x}{x} = \pi$, we can easily construct a nascent δ -function from it:

$$\delta_\xi(x) = \frac{1}{\pi} \frac{\sin \frac{x}{\xi}}{x} \quad (6.58)$$

We still have one encumbrance to overcome, namely that in our result the argument of the sine has an infinitesimal (but non-zero) complex shift $-i\eta$, while the δ -function and nascent δ -functions are only defined for real arguments. Luckily the former steps can be proven to be valid for complex shifts as well. First note that

$$\int dx \frac{\sin(x - i\eta)}{x - i\eta} = \pi \quad (6.59)$$

from which it is straightforward to show that

$$\lim_{\xi \xrightarrow{\pm} 0} \int_{-\infty}^{+\infty} dx \frac{1}{\pi} \frac{\sin\left(\frac{x-i\eta}{\xi}\right)}{x - i\eta} f(x - i\eta) = f(0) \quad (6.60)$$

In other words, the sifting property still holds after making a small complex shift (at least for this type of nascent delta functions). We thus can make the identification:

$$\lim_{\xi \xrightarrow{\pm} 0} \frac{\sin\left(\frac{2}{\xi} \left(n \cdot \sum_1^n k_j - i\eta\right)\right)}{n \cdot \sum_1^n k_j - i\eta} \cong \pi \delta\left(n \cdot \sum_1^n k_j - i\eta\right) \quad (6.61)$$

leading to the final result in [Equation 6.54](#). Still one word of caution: as mentioned before, this weak limit doesn't ensure that it *equals* a δ -function, but merely shows that the sifting property holds. This implies that when using [Equation 6.54](#), we are *not allowed to use the integral representation of the δ -function* (the latter wouldn't make any sense, as it is a divergent integral). The correct way to make use of a δ -function with a complex argument, is to only use it in conjunction with the sifting property.

Returning to the infinite Wilson line, we can get an equivalent definition by starting from [Equation 6.10](#):

$$I_n^{\text{inf.}} = (ig)^n n^{\mu_1} \dots n^{\mu_n} \prod_1^{n-1} \frac{i}{n \cdot \sum_j k_j + i\eta} 2\pi \delta\left(n \cdot \sum_1^n k_j + i\eta\right). \quad (6.62)$$

We conclude that the correct way to draw an infinite Wilson line, is to put all radiated gluons on one side from the point r^μ , where the line piece connecting the point to a gluon is a cut propagator having the following Feynman rule:

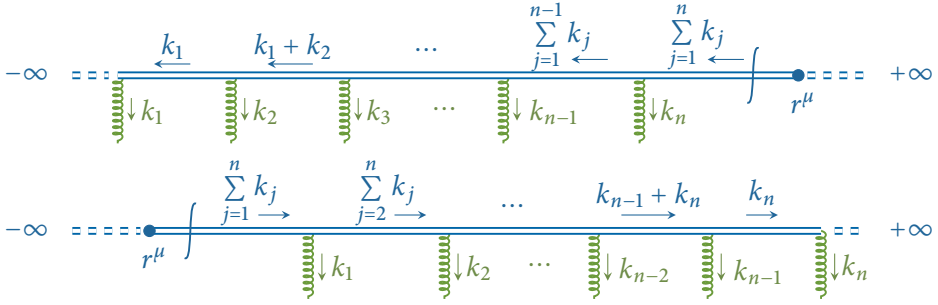


Figure 6.7: Two possible diagrams for n -gluon radiation from a Wilson line going from $-\infty$ to $+\infty$. The upper diagram corresponds to Equation 6.54 and the lower one to Equation 6.62.

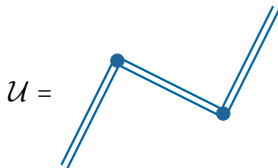
Extra Feynman Rule for Infinite Line

E. *Cut propagator:* $\frac{\vec{k}}{\not{\!|}} = \delta(n \cdot k + i\eta), \quad (6.63)$

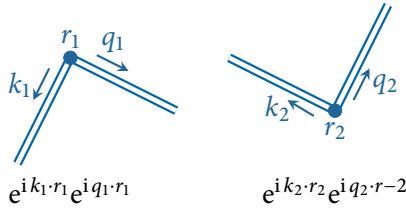
where $\delta(i)$ s defined in Equation A.56. There are hence two ways two draw a Feynman diagram for an infinite Wilson line, i.e. having all gluons radiated before or after the point r^μ . This is illustrated in Figure 6.7.

External Momenta

Sometimes it is useful to write the Feynman rule for external points in momentum representation. To achieve this, we Fourier transform the full Wilson line in all of its external points. Consider e.g. the simple line



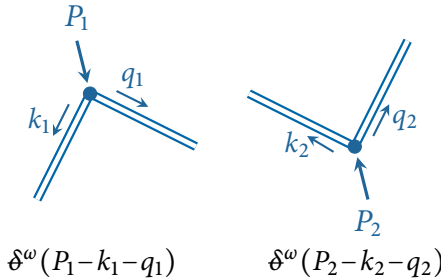
which consists of 4 segments (remember that the finite segment is split in two). It has two external points, or vertices, that each contribute a factor $e^{i kr}$ on each side of the vertex:



The Wilson line in momentum space is defined as the Fourier transform in every vertex:

$$U^{\text{momentum}} \stackrel{\text{def}}{=} \int d^\omega r_1 d^\omega r_2 e^{-i P_1 \cdot r_1} e^{-i P_2 \cdot r_2} U^{\text{coordinate}}, \tag{6.64}$$

These integrations will give rise to δ -functions:



So we can simply replace the Feynman rule for the external point with the demand of momentum conservation at every vertex, with an additional external momentum per vertex.

6.4 RELATING DIFFERENT PATH TOPOLOGIES

In the former section we have seen that there are eight possible linear path structures; two connecting a point to $\pm\infty$, next a finite line and finally a fully infinite line, all with normal or reversed path flow. We won't treat the fully infinite line anymore in the remainder of this thesis, because it has a particular way of dealing with it, and because infinite lines won't often appear as segments

of a piecewise Wilson line and are thus less relevant for what follows in the next section.¹²

The remaining six path structures are not independent. We have seen in the previous subsections that if we choose the two path topologies from Equations 6.37:¹³

$$\bullet \Longrightarrow = (ig)^n n^{\mu_1} \dots n^{\mu_n} e^{ir \cdot \sum_j k_j} \prod_{j=1}^n \frac{i}{n \cdot \sum_{l=j}^n k_l + i\eta}, \quad (6.65a)$$

$$\Longleftarrow \bullet = (ig)^n n^{\mu_1} \dots n^{\mu_n} e^{ir \cdot \sum_j k_j} \prod_{j=1}^n \frac{-i}{n \cdot \sum_{l=1}^j k_l + i\eta}, \quad (6.65b)$$

we can express the remaining four in function of them:

$$\Longleftarrow \bullet = \Longleftarrow \bullet \Big|_{n \rightarrow -n}, \quad (6.66a)$$

$$\bullet \Longrightarrow = \bullet \Longrightarrow \Big|_{n \rightarrow -n}, \quad (6.66b)$$

$$\bullet \Longrightarrow \bullet = \bullet \Longrightarrow \otimes \Longleftarrow \bullet, \quad (6.66c)$$

$$\bullet \Longleftarrow \bullet = (\bullet \Longrightarrow \otimes \Longleftarrow \bullet) \Big|_{a \leftrightarrow b}. \quad (6.66d)$$

Note that in Equations 6.65 we deliberately chose two structures that have positive convergence terms $+i\eta$, so that all calculations have the same type of poles. But these two structures aren't fully independent either, as they are related by a sign difference and an interchange of momentum indices:

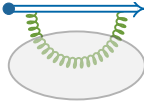
$$\Longleftarrow \bullet = (-)^n \bullet \Longrightarrow \Big|_{(k_1, \dots, k_n) \rightarrow (k_n, \dots, k_1)}. \quad (6.67)$$

We can exploit this relation when making a full calculation, i.e. connecting the Wilson line to a blob. This blob can be constructed from any combination of Feynman diagrams, but cannot contain other Wilson lines. If one is interested in interactions between different Wilson lines, it is sufficient to treat the different lines as different segments of one line (as is explained in the end of Section 6.2). We will name the blob depending on the number of gluon lines that connect it to the Wilson segment. Valid blobs are e.g. a gluon propagator connected to the Wilson segment (a 2-gluon blob), a gluon connecting a quark to the Wilson segment (a 1-gluon blob). Note that the naming of the blob isn't always faithful

¹² technically, they are relevant when considering several infinite Wilson lines and treating these as one line with multiple segments, but we avoid these scenarios as they complicate the formalism.

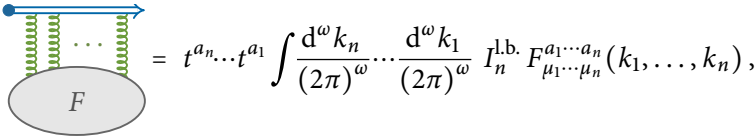
¹³ Remember that n is defined along the path flow (from starting point to ending point). A reversed path arrow thus always denotes $-n$.

to the number of gluons participating in the process. E.g. in the case of a gluon being connected to a segment (a self-energy diagram), this is clearly one gluon, but we will refer to it as a 2-gluon blob, as two gluon lines enter the blob:



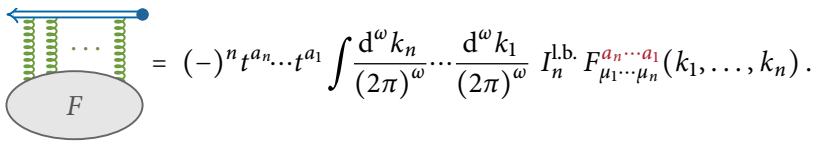
It is a matter of convention, and we chose this one as it helps categorising the blobs.

In the next section we will research how to calculate diagrams with piecewise Wilson lines, but first we investigate how to connect a blob to one segment. For the structure given in Equation 6.65a this is (again abusing the path integration measure notation):



$$= t^{a_n} \dots t^{a_1} \int \frac{d^\omega k_n}{(2\pi)^\omega} \dots \frac{d^\omega k_1}{(2\pi)^\omega} I_n^{l.b.} F_{\mu_1 \dots \mu_n}^{a_1 \dots a_n}(k_1, \dots, k_n),$$

where we absorbed the gluon propagators into the blob $F_{\mu_1 \dots \mu_n}^{a_1 \dots a_n}$. Furthermore, we always define the blob as the sum of all possible crossings; it is thus symmetric under the simultaneous interchange of Lorentz, colour, and momentum indices. Because every Lorentz index of F is contracted with the same vector n^μ , it is automatically symmetric in these. The combination of these symmetries implies that an interchange of momentum variables is equivalent to an interchange of the corresponding colour indices. In particular, it is now straightforward to relate Equation 6.65b to Equation 6.65a when connected to a symmetrised blob:



$$= (-)^n t^{a_n} \dots t^{a_1} \int \frac{d^\omega k_n}{(2\pi)^\omega} \dots \frac{d^\omega k_1}{(2\pi)^\omega} I_n^{l.b.} F_{\mu_1 \dots \mu_n}^{a_n \dots a_1}(k_1, \dots, k_n).$$

Note that the only difference is an interchange of the colour indices. Often the blob has a factorable colour structure, i.e.

$$F_{\mu_1 \dots \mu_n}^{a_1 \dots a_n}(k_1, \dots, k_n) = c^{a_1 \dots a_n} F_{\mu_1 \dots \mu_n}(k_1, \dots, k_n). \tag{6.68}$$

If we then define the following notations:

$$c = t^{a_n} \dots t^{a_1} c^{a_1 \dots a_n}, \tag{6.69a}$$

$$\bar{c} = t^{a_n} \dots t^{a_1} c^{a_n \dots a_1}, \tag{6.69b}$$

we can simply write

$$\text{Wilson line} \rightarrow \text{blob } F = c \text{ blob } F \rightarrow \text{Wilson line} \quad (6.70a)$$

$$\text{Wilson line} \leftarrow \text{blob } F = (-)^n \bar{c} \text{ blob } F \leftarrow \text{Wilson line} \quad (6.70b)$$

The yellow, ‘photon-like’ wavy lines are just a reminder that there is no colour structure left in the blob. In other words, when changing the structure of a Wilson line, we don’t have to redo the calculation of the integral! The difference is merely some colour algebra, changing c into \bar{c} and a sign difference.

Remember that due to the fact that we read a Wilson line as a Dirac line, i.e. from right to left, we have to order the generators in Equation 6.69a from n to 1. On the other hand, the blob is written from left to right—which is a matter of choice, as it is fully symmetrised¹⁴—leading to the difference in ordering between $t^{a_n} \dots t^{a_1}$ and $c^{a_1 \dots a_n}$.

For a factorable blob example, take e.g. the 3-gluon vertex:

$$F = g f^{a_1 a_2 a_3} \left[(k_1 - k_2)^\rho D_{\mu_1 \nu}^\rho(k_1) D_{\mu_2}^\nu(k_2) D_{\rho \mu_3}(k_3) + \text{cross.} \right],$$

with colour structure

$$c^{a_1 a_2 a_3} = f^{a_1 a_2 a_3} \quad \Rightarrow \quad \bar{c} = t^{a_3} t^{a_2} t^{a_1} f^{a_3 a_2 a_1} = -t^{a_3} t^{a_2} t^{a_1} f^{a_1 a_2 a_3} = -c.$$

This clearly implies that

$$\text{Wilson line} \leftarrow \text{blob } F = (-)^3 \bar{c} \text{ blob } F \rightarrow \text{Wilson line} = c \text{ blob } F \rightarrow \text{Wilson line} = \text{Wilson line} \leftarrow \text{blob } F \quad (6.71)$$

So the 3-gluon vertex is path topology-invariant. Of course, a lot of blob structures won’t be colour factorable, but we can always write these as a sum of factorable terms:

$$F_{\mu_1 \dots \mu_n}^{a_1 \dots a_n}(k_1, \dots, k_n) = \sum_i c_i^{a_1 \dots a_n} F_{i \mu_1 \dots \mu_n}(k_1, \dots, k_n),$$

¹⁴ The important fact to realise is that indeed the order doesn’t matter for a fully symmetrised blob, but it should of course have the same ordering in its momenta, i.e. we identify a_1 with k_1 . Because most references in literature write simple blobs from left to right, we keep this convention for the blob for the sake of simplicity.

such that we can repeat the same procedure as before

$$\text{Diagram (6.72a)} = \sum_i c_i \text{Diagram (6.72a)}, \quad (6.72a)$$

$$\text{Diagram (6.72b)} = (-1)^n \sum_i \bar{c}_i \text{Diagram (6.72b)}. \quad (6.72b)$$

In conclusion: whatever the structure of the Wilson line, to calculate a given diagram we can retrieve it from the calculation of the same diagram with a Wilson line bounded from below, using straightforward colour algebra. For a trivial structure containing only one segment, the gain is not that big, but for a line consisting of several segments—as we will see in the next section and the next chapter—this trick can save us quite some calculation time.

6.5 PIECEWISE LINEAR WILSON LINES

Now we turn our attention to piecewise Wilson lines, using the results from section Section 6.2. When connecting a n -gluon blob to a piecewise Wilson line, the n gluons aren't necessarily all connected to the same segment; other diagrams are possible as well, where the n -gluons are divided among several segments. This is the physical interpretation of formula Equation 6.19c. As mentioned before, the \mathcal{U}_i^J aren't commutative in se due to the non-Abelian nature of the fields. However, when connected to the same symmetrised blob that is summed over all crossings, they can be treated as if they where. This implies that multiple-segment terms can be related by straightforward substitution, e.g.

$$\mathcal{U}_1^K \mathcal{U}_2^J = \mathcal{U}_2^K \mathcal{U}_1^J \Big|_{(r_K \leftrightarrow r_J, n_K \leftrightarrow n_J)}, \quad (6.73)$$

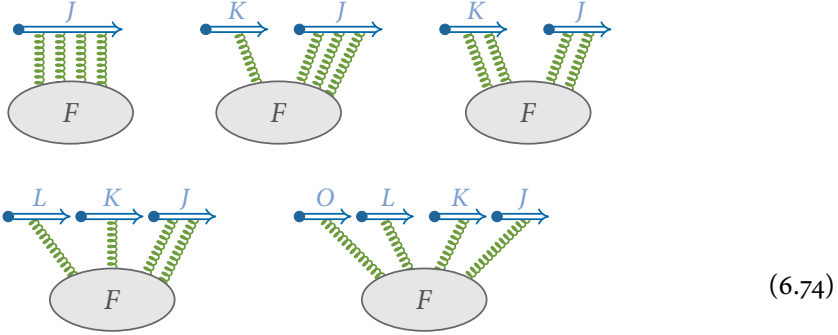
etc. To get all diagrams connecting a given n -gluon blob to a piecewise line, we have to calculate exactly $p(n)$ diagrams, the partition function from combinatorics,¹⁵ independent of the number of segments M . When connecting

¹⁵ The partition function $p(n)$ is the number of integer partitions of n ; e.g. $4 = 4, 3+1, 2+2, 2+1+1$, or $1+1+1+1$. Thus $p(4) = 5$. Other examples are $p(3) = 3$, $p(5) = 7$ and $p(6) = 11$.

e.g. a 4-gluon blob, we need to calculate exactly 5 diagrams. These are constructed from the following segments (cf. Equation 6.19b):

$$u_4^J, u_3^J u_1^K, u_2^J u_2^K, u_2^J u_1^K u_1^L, \text{ and } u_1^J u_1^K u_1^L u_1^O.$$

They are the easiest represented schematically:



In addition, there are 3 more diagrams that can be related using Equation 6.73, built from the segments

$$u_1^J u_3^K, u_1^J u_2^K u_1^L, \text{ and } u_1^J u_1^K u_2^L.$$

Now what about external momenta? We saw in Subsection *External Momenta* on page 175 and onwards that if we want to express the Wilson line in momentum space, we have to add an additional external momentum to every vertex and apply momentum conservation. However, most of the time a vertex connects two or more segments, and to be able to use our framework, we need Feynman rules that are defined per segment (not per vertex). Luckily, this can be easily achieved by using the fact that a Fourier transformation transforms a product in a convolution:

$$\mathcal{F}_k [f(r)g(r)] = \mathcal{F}_k [f(r)] \otimes \mathcal{F}_k [g(r)]. \tag{6.75}$$

This means that we can associate per segment the Fourier transform of an external point, i.e. we replace the Feynman rule for an external point with:

Feynman Rule in External Momentum Space

B. External point:

=

$\delta^{(\omega)}(P-k)$

(6.76)

An ‘empty’ segment—with no gluon radiated from it—then naturally gains a $\delta(P)$. After connecting the blob we make a convolution over the segments that are connected to the same external point.

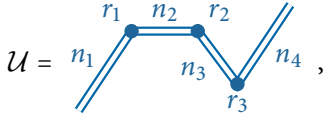
In the TMD framework (see Chapter 8), it is common to express Wilson lines only partially in momentum space. More specific, the plus and minus components are expressed in coordinate space, while the transversal components are expressed in momentum space. The Feynman rule is in this case replaced with:

Feynman Rule in Partial External Momentum Space

$$\text{B. External point: } \begin{array}{c} P \\ \swarrow \\ \bullet \\ \xrightarrow{k} \\ r \end{array} = \mathcal{D}^{(\omega-2)}(\mathbf{P}^\perp - \mathbf{k}^\perp) e^{i r^+ k^- + i r^- k^+}, \quad (6.77)$$

where the convolution is now only over \mathbf{P}^\perp .

Let us briefly sketch the steps needed to do a full calculation in this framework. We illustrate each step with an easy example, viz. the calculation of all self-interactions of the Wilson line with the following path structure:



where the path flow is assumed from left to right. The steps to undertake are:

- A. List the segments that form the Wilson line and their corresponding path constants: the segment direction n_K^μ , the external point r_K^\pm and the external momentum \mathbf{P}_K^\perp . For the given example, these are (from left to right):

$$\begin{array}{ll} \leftarrow \bullet & -n_1, P_1, r_1, \\ \bullet \rightarrow & n_2, P_1, r_1, \\ \leftarrow \bullet & n_2, P_2, r_2, \\ \bullet \rightarrow & n_3, P_2, r_2, \\ \leftarrow \bullet & n_3, P_3, r_3, \\ \bullet \rightarrow & n_4, P_3, r_3. \end{array}$$

The first segment has a minus sign in its direction because we used relation Equation 6.66a.

- B. Define the process under consideration, and identify all possible blob structures for the process, ordered by the number of gluons interchanged between the blob and the Wilson line. For the NNLO¹⁶ self-interaction

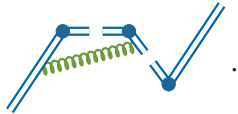
¹⁶ Note that there is a difference between referring to the order of the process and the order of the blob. As every gluon radiated from the blob already contributes a factor g , the total order of a diagram connecting an n -gluon blob to a Wilson line will be $\alpha_s^{n/2}$ plus the order of the blob. E.g. connecting a NLO 4-gluon blob gives a diagram at next-to-next-to-next-to-leading order (N³LO).

example, there are three blobs: the 2-gluon blob, which is the gluon propagator at **NLO**, the 3-gluon blob, which is the three gluon vertex, and the 4-gluon blob, which consists of two gluon propagators at **LO**.

- c. For every blob, list all possible diagrams. For the 4-gluon blob, these are listed in [Equation 6.74](#). The 2-gluon blob has two diagrams, and the 3-gluon blob three. Note that this step is *independent on the content of the blob* (only dependent on the number of interchanged gluons), and thus independent on the process.
- d. For every diagram, separate out the dependence on the path, like we did in the previous section by factorising out the colour structure. We will develop a more formal approach in the next subsection (see e.g. [Equation 6.79](#)). Next apply the Feynman rules and calculate the momentum integrals in the diagram.
- e. Apply the specific path structure to the relevant diagrams, and sum all diagrams according to [Equation 6.19c](#). If external momenta are used, assign a $\delta^{(\omega-2)}(\mathbf{P}_K^\perp)$ to all external points that do not participate in the diagram, and make a convolution over duplicate external momenta. Let's illustrate the latter with an example. The diagram connecting the 2-gluon blob to two different segments will be a function of $\mathbf{P}_J^\perp, \mathbf{P}_K^\perp, r_J^\pm, r_K^\pm, n_J^\mu$ and n_K^μ (it will also depend on the type of path structure, but let us ignore this for now):

$$\begin{array}{c} \text{---} \\ \text{---} \\ \text{---} \end{array} \begin{array}{c} \text{---} \\ \text{---} \\ \text{---} \end{array} \stackrel{N}{=} \mathcal{W}_2(\mathbf{P}_J^\perp, \mathbf{P}_K^\perp, r_J^\pm, r_K^\pm, n_J^\mu, n_K^\mu),$$

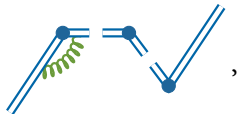
Consider now the following contribution:



The third external point isn't participating, so it gets a δ -function. The gluon isn't connecting the same external point, so no convolution is needed. The result for this term is hence simply

$$\delta^{(\omega-2)}(\mathbf{P}_3^\perp) \mathcal{W}_2(\mathbf{P}_1^\perp, \mathbf{P}_2^\perp).$$

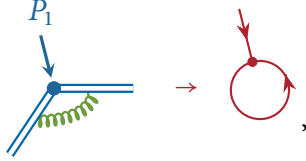
But if we consider the contribution



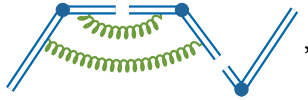
we need to do a convolution because now $\mathbf{P}_J^\perp = \mathbf{P}_K^\perp$. This can be easily done, by making the substitutions $\mathbf{P}_J^\perp \rightarrow \mathbf{P}_J^\perp - \mathbf{q}^\perp$ and $\mathbf{P}_K^\perp \rightarrow \mathbf{q}^\perp$, and integrating over \mathbf{q}_\perp . The result for this term is then

$$\delta^{(\omega-2)}(\mathbf{P}_2^\perp) \delta^{(\omega-2)}(\mathbf{P}_3^\perp) \int \frac{d^{\omega-2} \mathbf{q}^\perp}{(2\pi)^{\omega-2}} \mathcal{W}_2(\mathbf{P}_1^\perp - \mathbf{q}^\perp, \mathbf{q}^\perp).$$

Note that because this diagram essentially forms a tadpole, i.e.



momentum conservation demands the incoming momentum to vanish as well, i.e. it will give $\delta^{(\omega-2)}(\mathbf{P}_1^\perp)$. So we could have ignored the convolution from the beginning. But this is only true for 2-gluon blobs. Consider e.g. the 4-gluon blob diagram



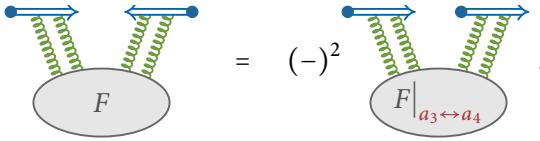
This is no tadpole, so we need to make a double convolution. The result is then

$$\delta^{(\omega-2)}(\mathbf{P}_3^\perp) \int \frac{d^{\omega-2} \mathbf{q}_1^\perp}{(2\pi)^{\omega-2}} \frac{d^{\omega-2} \mathbf{q}_2^\perp}{(2\pi)^{\omega-2}} \mathcal{W}_4(\mathbf{P}_1^\perp - \mathbf{q}_1^\perp, \mathbf{q}_1^\perp, \mathbf{P}_2^\perp - \mathbf{q}_2^\perp, \mathbf{q}_2^\perp).$$

The good thing about this framework is that the results from B, C, and D are independent of the structure of the Wilson line. Furthermore, we can already calculate the convolution integrals when calculating the momentum integrals, such that we have the result ready. In other words, once we calculated e.g. the three possible diagrams connecting a 3-gluon vertex to a piecewise Wilson line, we can retrieve this result for any Wilson line structure and never need to recalculate it again; we only need to change the colour factors and the way the different diagrams combine.

Path Functions

Now what about the different path structures, as defined in [Equations 6.65](#)? We can use the same trick as in the end of the former section, viz. a sign change and an interchange of the corresponding colour indices. For instance:



The easiest way to implement this on a general basis, is to define a function Φ per diagram for a given blob, that gives the colour structure in function of the path type, hence it depends on the segment index J . For the leading order 2-gluon blob, this is straightforward. When the gluon is connected to the same segment, flipping the segment makes no difference because we have a factor $(-)^2$, and the colour interchange has no effect ($\delta^{ba} = \delta^{ab}$). When the gluon connects two different segments, flipping one of the segments gives a sign difference because of the factor $(-)^1$. So the leading order 2-gluon blob has the following path function:

$$\text{Diagram 1} : \Phi(J) = C_F, \tag{6.78a}$$

$$\text{Diagram 2} : \Phi(J, K) = (-)^{\phi_J + \phi_K} C_F, \tag{6.78b}$$

where ϕ_J is a number representing the type of the path:

$$\phi_J = \begin{cases} 0 & J = \text{blue arrow pointing right} \\ 1 & J = \text{blue arrow pointing left} \end{cases}. \tag{6.79}$$

Keep in mind that in our original definition of the Wilson line in [Equation 6.1](#), colour indices are not yet traced, meaning that [Equations 6.78](#) should still be multiplied with a unit matrix $\mathbb{1}_{N_c \times N_c}$. Similarly, we find for the leading order 3-gluon blob:

$$\text{Diagram 3a} : \Phi(J) = -i \frac{N_c}{2} C_F, \tag{6.80a}$$

$$\text{Diagram 3b} : \Phi(J, K) = -i (-)^{\phi_J + \phi_K} \frac{N_c}{2} C_F, \tag{6.80b}$$

$$\text{Diagram 3c} : \Phi(J, K, L) = -i (-)^{\phi_J + \phi_K + \phi_L} \frac{N_c}{2} C_F. \tag{6.80c}$$

For non-factorable blobs we use the same trick as in [Equations 6.72](#), by giving Φ an extra index to identify the sub diagram it belongs to.

Let us introduce a new notation, to indicate a full diagram but without the colour content, in which a blob is connected to m Wilson line segments, with n_i gluons connected to the i -th segment:

Wilson Line With Blob but Without Colour

$$\mathcal{W}_{n_m \dots n_1}^{J_m \dots J_1} \stackrel{\text{N}}{=} \int \frac{d^\omega k_n}{(2\pi)^\omega} \dots \frac{d^\omega k_1}{(2\pi)^\omega} I_{n_m}^{\text{l.b.}, J_m} \dots I_{n_1}^{\text{l.b.}, J_1} F_{\mu_1 \dots \mu_{n_1 + \dots + n_m}}, \quad (6.81)$$

where we will write the indices from right to left to be consistent with the Wilson line being read from right to left. It is important to be consistent in the choice of the ‘base’ structure, from which all other linear topologies can be derived. We have chosen the lower bound Wilson line as the base, which can be seen in the integrals $I^{\text{l.b.}}$. If we would have chosen e.g. the upper bound line, also the definition in [Equation 6.79](#) would change.

Returning to the 4-gluon blob, we can now write the full result for a factorable blob using [Equation 6.19b](#):

$$\begin{aligned} \mathcal{U}^4 = & \sum_J^M \Phi_4 \mathcal{W}_4^J + \sum_{J=2}^M \sum_{K=1}^{J-1} [\Phi_{31} \mathcal{W}_{31}^{KJ} + \Phi_{22} \mathcal{W}_{22}^{KJ}] + \sum_{J=3}^M \sum_{K=2}^{J-1} \sum_{L=1}^{K-1} \Phi_{211} \mathcal{W}_{211}^{LKJ} \\ & + \sum_{J=4}^M \sum_{K=3}^{J-1} \sum_{L=2}^{K-1} \sum_{O=1}^{L-1} \Phi_{1111} \mathcal{W}_{1111}^{OLKJ} + \text{symm}, \quad (6.82) \end{aligned}$$

where the symmetrised diagrams $\Phi_{13} \mathcal{W}_{13}^{KJ}$, $\Phi_{121} \mathcal{W}_{121}^{LKJ}$, and $\Phi_{112} \mathcal{W}_{112}^{LKJ}$ are calculated using [Equation 6.73](#), interchanging also the ϕ_J . In other words:

$$\Phi_{13}(K, J) \mathcal{W}_{13}^{KJ} = \Phi_{31}(J, K) \mathcal{W}_{31}^{JK}, \quad (6.83a)$$

$$\Phi_{121}(L, K, J) \mathcal{W}_{121}^{LKJ} = \Phi_{211}(K, L, J) \mathcal{W}_{211}^{KLJ}, \quad (6.83b)$$

$$\Phi_{112}(L, K, J) \mathcal{W}_{112}^{LKJ} = \Phi_{211}(J, K, L) \mathcal{W}_{211}^{JKL}. \quad (6.83c)$$

For a non-factorable blob, every term is just replaced by a sum over sub diagrams, e.g.

$$\Phi_4 \mathcal{W}_4^J \rightarrow \sum_i \Phi_4^i \mathcal{W}_4^i. \quad (6.84)$$

It is important to realise that both the Φ and \mathcal{W} can be calculated independent of the path structure, giving a result depending on n_j , r_j and ϕ_j . We will call the latter the *path constants*, which fully determine a piecewise linear path. If

we have made a full calculation for a given path, we can easily port the result to another path, simply by inputting the new path constants.

Diagrams with Final-State Cuts

So far we have only calculated amplitudes. To get probabilities from these, we can do this in the standard way, viz. squaring diagrams and combining them order by order (squared terms and interference terms), or we could treat the squared diagram as one Wilson line—with double the number of segments—where the segments to the right of the cut are the hermitian conjugate of those to the left. The choice is a matter of personal taste. We choose to continue with the latter case, where we now have three distinct sectors of diagrams: a sector $\mathcal{U}_{\text{left}}$ where the blob is only connecting segments left of the cut, a sector $\mathcal{U}_{\text{right}}$ where the blob is only connecting segments right of the cut (this is just the hermitian conjugate of the former, but possibly with different path parameters r_J , n_J , and ϕ_J), and a sector \mathcal{U}_{cut} where the blob is connecting segments both left and right of the cut. In other words:

$$\mathcal{U} = \mathcal{U}_{\text{left}} + \mathcal{U}_{\text{cut}} + \mathcal{U}_{\text{right}}. \tag{6.85}$$

For the first two nothing changes, the calculations go as before. For the example of the 4-gluon blob, the first sector $\mathcal{U}_{\text{left}}^4$ is almost exactly equal to Equation 6.82, but the sums run up only to M_c , the number of segments before the cut, instead of M . The last sector $\mathcal{U}_{\text{right}}^4$ is simply the hermitian conjugate of this, starting at $M_c + 1$:¹⁷


$$\begin{aligned} \mathcal{U}_{\text{right}}^4 &= \sum_{M_c+1}^M \Phi_4^\dagger \mathcal{W}_4^\dagger + \sum_{M_c+2}^M \sum_{M_c+1}^{J-1} [\Phi_{31}^\dagger \mathcal{W}_{31}^\dagger + \Phi_{22}^\dagger \mathcal{W}_{22}^\dagger] \\ &+ \sum_{M_c+3}^M \sum_{M_c+2}^{J-1} \sum_{M_c+1}^{K-1} \Phi_{211}^\dagger \mathcal{W}_{211}^\dagger + \sum_{M_c+4}^M \sum_{M_c+3}^{J-1} \sum_{M_c+2}^{K-1} \sum_{M_c+1}^{L-1} \Phi_{1111}^\dagger \mathcal{W}_{1111}^\dagger + \text{symm}. \end{aligned}$$

For the remaining sector \mathcal{U}_{cut} we need to define a cut blob. Given a blob, several possible cut blobs might exist, depending on the number of gluons to the left and right of the cut. E.g. the leading order 4-gluon cut blobs are given by



$$\text{cut blob} = \text{left-right} + \text{right-left} + \text{cross}, \tag{6.86a}$$

¹⁷ At first sight one might expect that Hermitian conjugation also flips the order of the segments, but as explained in the paragraph above Equation 6.73 they can be treated as commutative.

$$
\quad = \quad + \text{cross}, \quad (6.86b)$$

where the crossings are to be made on the sides of the cut separately. Also note that when the cut blob is more complex, it should be summed over all possible cut locations. Consider e.g. the fermionic part of the [NLO 2-gluon cut blob](#):

$$
\quad = \quad + \quad + \quad . \quad (6.87)$$

Note that even if a blob has no lines crossing the cut, it will be considered a cut blob as long as it has gluons on both the left and the right side, as e.g. the first term in the [r.h.s.](#) of [Equation 6.86b](#). As the blob itself connects the left and the right sector (even if internally it doesn't literally), this blob is associated to the sector \mathcal{U}_{cut} .

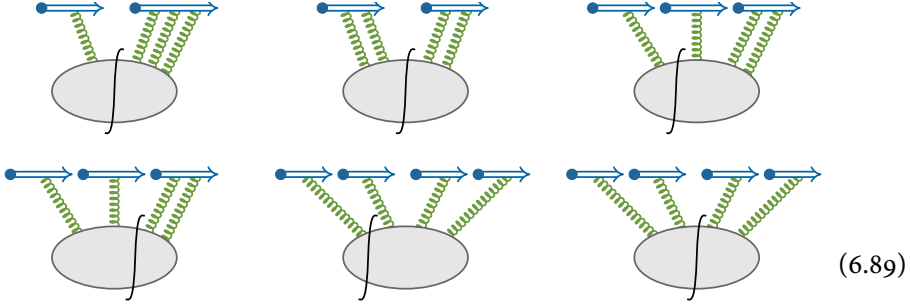
Now concerning the latter sector, we investigate how many diagrams are added in comparison to [Equation 6.74](#) due to the cut. First note that a Wilson line segment itself is never cut.¹⁸ A semi-infinite line (lower bound or upper bound) cannot be cut due to the symmetric nature of a squared amplitude, and although a finite line can be cut, we can always write it as a convolution of two semi-infinite lines, placing the cut in between.¹⁹ Another remark is that we cannot simply use relation [Equation 6.73](#) as before, because it could change the cut topology. Cut diagrams are sorted depending on how its gluons are distributed on the left resp. right side of the cut, and connected to the appropriate cut blob. For instance the second diagram of [Equation 6.74](#), namely \mathcal{W}_{31}^4 , can be cut in one way only, connecting the Wilson line to the cut blob in [Equation 6.86a](#). But the fourth diagram, \mathcal{W}_{211}^4 , can be cut in two ways: cutting with one gluon on the left (written as $\mathcal{W}_{21|1}^4$ and connected to the blob in [Equation 6.86a](#)), or cutting with two gluons on the left (written as $\mathcal{W}_{2|11}^4$ and connected to [Equation 6.86b](#)). Other cut topologies can be related by Hermitian conjugation when switching left and right sides, e.g.

¹⁸ A cut line does appear in the context of infinite Wilson lines as we saw in [Equation 6.63](#), but this is a different type of cut (not a final-state cut), and anyway we are not (yet) including infinite Wilson lines in this framework.

¹⁹ In the [TMD](#) framework it is common to associate a cut finite line with a true cut propagator, but this is merely a matter of naming conventions. E.g. in Subsection [Gauge Invariant Operator Definition](#) on page [233](#) and onwards we make the definition of a collinear [PDF](#) (a cut diagram itself) gauge-invariant by adding a finite Wilson line that is cut. In literature (see e.g. [\[33\]](#)) it is then common to also integrate over the exponential coming from [Equation 6.27b](#) leading to a delta function, which in turn can be interpreted as the Feynman rule for a cut propagator (see [Equation 6.63](#)). We prefer to avoid this approach, as it is more general to leave a^μ unintegrated. We will however adapt the same pictorial representation of a cut finite Wilson line, see e.g. [Figure 8.1](#), but we remind ourselves that it is just a cut between two lower-bound segments.

$$\mathcal{W}_{11|2}^{LKJ} = \mathcal{W}_{2|11}^{\dagger JKL}. \quad (6.88)$$

In the case of the 4-gluon blob, the following diagrams have to be added to Equation 6.74:



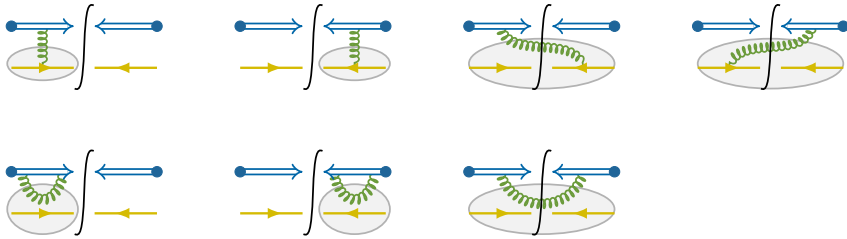
Now we have the necessary ingredients to write the cut sector for the 4-gluon blob:

$$\begin{aligned} \mathcal{U}_{\text{cut}}^4 = & \sum_{M_c+1}^M \sum_1^{M_c} \left[\left(\mathcal{W}_{3|1}^{KJ} + \text{h.c.} \right) + \mathcal{W}_{2|2}^{KJ} \right] \\ & + \sum_{M_c+2}^M \sum_{M_c+1}^{J-1} \sum_1^{M_c} \left[\left(\mathcal{W}_{2|1}^{LKJ} + \text{symm.} \right) + \mathcal{W}_{11|2}^{LKJ} \right] + \sum_{M_c+1}^M \sum_2^{M_c} \sum_1^{K-1} \text{h.c.} \\ & + \sum_{M_c+3}^M \sum_{M_c+2}^{J-1} \sum_{M_c+1}^{K-1} \sum_1^{M_c} \mathcal{W}_{11|1}^{OLKJ} + \sum_{M_c+1}^M \sum_3^{M_c} \sum_2^{K-1} \sum_1^{L-1} \text{h.c.} \\ & + \sum_{M_c+2}^M \sum_{M_c+1}^{J-1} \sum_2^{M_c} \sum_1^{L-1} \mathcal{W}_{11|11}^{OLKJ} \end{aligned} \quad (6.90)$$

Although this might look quite complex, note that it only is the way how to combine the diagrams that is a bit involving. And even then, it is a matter of good bookkeeping, making it look a lot worse than it is.

One final remark: in Equation 6.85 we assumed that the sectors $\mathcal{U}_{\text{left}}$ and $\mathcal{U}_{\text{right}}$ only use regular blobs, while the sector \mathcal{U}_{cut} only uses cut blobs. While the latter is always true—as we cannot connect a segment before the cut with a segment after the cut without including the cut line—the former is only partially correct. It is possible that the left (or right) sector connects to a blob that is cut *before* or *after all gluons*. Let us illustrate this. Consider e.g. a trivial example, namely the

interaction between a Wilson line and a quark line. Ignoring the self-interactions of the quark, we have the following possible probability diagrams at NLO:



This means we have four different blobs, namely two 1-gluon blobs:

$$\begin{array}{c} \text{blob} \\ \text{with 1-gluon} \end{array} = \text{blob} \text{ with 1-gluon}, \tag{6.91a}$$

$$\begin{array}{c} \text{blob} \\ \text{with cut} \end{array} = \text{blob} \text{ with cut}, \tag{6.91b}$$

and two 2-gluon blobs:

$$\begin{array}{c} \text{blob} \\ \text{with 2-gluons} \end{array} = \text{blob} \text{ with 2-gluons}, \tag{6.92a}$$

$$\begin{array}{c} \text{blob} \\ \text{with cut} \end{array} = \text{blob} \text{ with cut}. \tag{6.92b}$$

The two 1-gluon blobs and the first 2-gluon blob will be used in the $\mathcal{U}_{\text{left}}$ and $\mathcal{U}_{\text{right}}$ sectors, while the second 2-gluon blob is the only blob used in the \mathcal{U}_{cut} sector.

Note that it is not for every blob possible to draw a cut fully to the right or left. E.g. the LO 2-gluon self-interaction blob doesn't have this possibility, because if we would try to draw such a blob with the cut fully to the left, i.e.

$$\begin{array}{c} \text{blob} \\ \text{with 2-gluons} \end{array} = \begin{array}{c} \text{blob} \\ \text{with cut} \end{array}, \tag{6.93}$$

we immediately see that this is not a valid Feynman diagram, as the amplitude on the left side would represent two real gluons popping out from nothing. We thus conclude that self-interaction blobs cannot have cuts fully to the left or right.

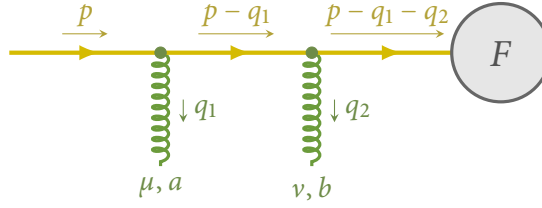


Figure 6.8: An incoming quark radiating two soft gluons.

6.6 EIKONAL APPROXIMATION

Before we delve into the calculational techniques to work with Wilson lines—as we will do in the next chapter—we will motivate the usefulness of Wilson lines by one of their most important applications, namely as a resummation of soft and collinear gluons.

In the *eikonal approximation* we assume a quark with momentum large enough to neglect the change in momentum due to the emission or absorption of a soft gluon. Even after multiple soft interactions it won't deviate much from its path, which we then take to be unaltered. Such a quark is called *eikonal*.

Let us investigate this a bit further. We take an incoming (hence real) quark with momentum p that radiates two soft gluons with momentum q_1 and q_2 . This is illustrated in [Figure 6.8](#) (where the blob represents all possible diagrams connected to the quark propagator). This diagram is equal to

$$F \frac{i(\not{p} - q_1 - q_2)}{(p - q_1 - q_2)^2 + i\epsilon} i g t^b \gamma^v \frac{i(\not{p} - q_1)}{(p - q_1)^2 + i\epsilon} i g t^a \gamma^\mu u(p). \quad (6.94)$$

Making the soft approximation is the same as neglecting q_i with respect to \not{p} , and q_i^2 with respect to $p \cdot q_j$, giving

$$F \frac{i p_\rho \gamma^\rho \gamma^v}{-2 p \cdot q_1 - 2 p \cdot q_2 + i\epsilon} i g t^b \frac{i p_\sigma \gamma^\sigma \gamma^\mu}{-2 p \cdot q_1 + i\epsilon} i g t^a u(p),$$

where we used $p^2 = 0$ because this is the momentum of a real quark. Because of the Dirac [Equation A.20](#) in momentum representation, i.e. $\not{p} u(p) = 0$, we can add a term $i p_\sigma \gamma^\mu \gamma^\sigma$ to the numerator of the rightmost fraction:

$$F \frac{i p_\rho \gamma^\rho \gamma^v}{-2 p \cdot q_1 - 2 p \cdot q_2 + i\epsilon} i g t^b \frac{i p_\sigma \{\gamma^\sigma, \gamma^\mu\}}{-2 p \cdot q_1 + i\epsilon} i g t^a u(p). \quad (6.95)$$

Next we use the anticommutation rule [Equation A.18](#) and write the momentum as $p^\sigma = |p| n^\sigma$, with n^σ a normalised directional vector, in order to get

$$F \frac{i p_\rho \gamma^\rho \gamma^v}{-2 p \cdot q_1 - 2 p \cdot q_2 + i\epsilon} i g t^b \frac{-i n^\mu}{n \cdot q_1 - i\epsilon} i g t^a u(p). \quad (6.96)$$

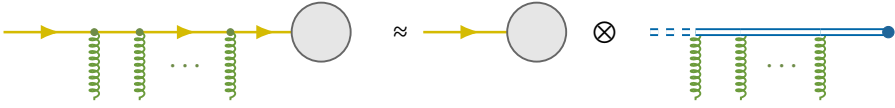


Figure 6.9: A quark radiating n soft gluons can be represented as a bare quark multiplied with a Wilson line going from $-\infty$ to 0.

Because the rightmost fraction doesn't contain any Dirac structure anymore, we can repeat the same steps on the leftmost fraction. This gives:

$$F \frac{-i}{n \cdot (q_1 + q_2) - i\epsilon} i g n^\nu t^b \frac{-i}{n \cdot q_1 - i\epsilon} i g n^\mu t^a u(p). \tag{6.97}$$

What we see is that the Dirac propagators have been replaced by Wilson line propagators, and the Dirac-gluon couplings by Wilson vertices. By using the eikonal approximation, we literally factorised out the gluon contribution from the Dirac part.

Of course this remains valid when radiating more gluons. In the latter case, the resulting formula is straightforward:

$$(i g)^n F t^{a_n} \dots t^{a_1} u(p) \frac{-i n^{\mu_n}}{n \cdot \sum q_i - i\epsilon} \dots \frac{n^{\mu_2}}{n \cdot (q_1 + q_2) - i\epsilon} \frac{n^{\mu_1}}{n \cdot q_1 - i\epsilon}.$$

This is exactly the result for an incoming bare quark connected to the blob, multiplied with a Wilson line going from $-\infty$ to 0 (we know that the external point has to be zero because there is no exponential):

$$F \mathcal{U}_{(0; -\infty)} u(p). \tag{6.98}$$

However, when using the momentum representation for the external point, the latter gives a factor $\delta^{(\omega)}(q)$, so that we can write this relation as an exact convolution:

$$F(p) \int \frac{d^\omega q}{(2\pi)^\omega} \mathcal{U}(q) u(p - q) = F(p) (\mathcal{U} \otimes u)(p), \tag{6.99}$$

where q can be interpreted as the sum of the gluon momenta. This is illustrated in the diagram in Figure 6.9. Note that Equations 6.98 and 6.99 don't give a bare multiplication either, because the t^{a_i} are placed between the $u(p)$ of the external quark and the blob. Writing out the Dirac and Lie indices makes this clear:

$$(F)_\beta^j \delta^{\beta\alpha} (t^{a_n} \dots t^{a_1})_{ji} (u(p))_\alpha^i \frac{i g n_{\mu_n}}{n \cdot \sum q_i + i\epsilon} \dots \frac{i g n_{\mu_1}}{n \cdot q_1 + i\epsilon}.$$

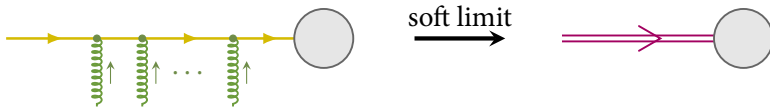


Figure 6.10: In the soft limit, a bare quark can be represented as an eikonal quark.

From this result, we introduce the concept of an *eikonal quark*. This is a quark that is only interacting softly with the gauge field, and thus doesn't deviate from its straight path. It can be understood as a bare quark convoluted with a Wilson line to all orders:

Eikonal Quark

$$|\psi_{\text{eik.}}^i\rangle = \mathcal{U}_{(0; -\infty)}^{ij} \otimes |\psi^j\rangle. \quad (6.100)$$

In other words, the net effect of multiple soft gluon interactions on an eikonal quark is just a colour rotation (nothing but a phase). It is common to denote an eikonal quark with a double line, but this gives rise to ambiguities: the double line was already used to denote a Wilson line propagator. These are, although related, not the same. The eikonal line represents a quark (carrying spinor indices) resummed with soft gluon radiation *to all orders*, while the Wilson line propagator represents gluon radiation at a *specified order* (not necessarily soft), still to be multiplied with the quark (carrying no spinor indices itself). In short, Wilson line propagators are used in the calculation of an eikonal line. To appreciate the difference, have a look at Equation 6.100: the eikonal quark is the combination $\mathcal{U}_{(0; -\infty)}^{ij} \otimes |\psi^j\rangle$, while the Wilson line propagators are components of $\mathcal{U}_{(0; -\infty)}$.

To avoid confusion, we will draw an eikonal line in red, and always explicitly draw an arrowhead (representing the quark's momentum flow):

$$\begin{array}{c} \overrightarrow{p} \\ \text{---} \\ \text{---} \end{array} \quad \text{An eikonal line, i.e. } |\psi_{\text{eik.}}^i(p)\rangle_{\alpha}, \quad (6.101a)$$

$$\begin{array}{c} \overrightarrow{q} \\ \text{---} \\ \text{---} \end{array} \quad \text{A Wilson line propagator, i.e. } \frac{i}{n \cdot q + i\epsilon}. \quad (6.101b)$$

But keep in mind that these notations are commonly interchanged in literature. Using our notation for the eikonal line, we can write down the eikonal approximation diagrammatically as in Figure 6.10.

A last remark: in the derivation of the eikonal approximation, more specifically Equation 6.95, we used the fact that the quark in question is external, by adding a term $\gamma^{\mu} \not{p} u(p) = 0$. This is a crucial step, without which we wouldn't have been

able to resum all gluons into a Wilson line, i.e. Wilson lines as a resummation of gluon radiation can only appear next to quarks that are on-shell.

It is possible to resum gluon radiation into a Wilson line even if it is not soft. E.g. in the collinear approximation, we allow for large radiated momenta q which are collinear to p , i.e. if $p^\mu = |p| n^\mu$ then $q^\mu = |q| n^\mu$ in the same direction. The Dirac equation tells us that $\not{p} u(p) = 0$ and thus $\not{q} u(p) = 0$, which implies we can add a term $\gamma^\mu \not{q} u(p)$ to Equation 6.94. If we keep the quasi on-shell constraint, $q^2 \approx 0$ as compared to $p \cdot q$, this again leads to a Wilson line, but this time with possibly big q momentum components (as long as they are collinear to p).

SIMPLIFYING WILSON LINE CALCULATIONS

In the former chapter we deeply investigated piecewise linear Wilson lines. We derived Feynman rules for the eight different possible linear topologies (four types plus their path reversals), and discovered how to relate them to each other. Finally, by collecting a set of diagrams per blob we wish to connect to a given Wilson line, we were able to develop a framework to significantly simplify calculations if the Wilson line has a lot of segments. Moreover, and this was the most important result, from the moment we have made a calculation with a given blob, we can easily port the result to any piecewise linear Wilson line. However, there is a fly in the ointment. Calculating these general integrals is quite complicated, because we have to keep the path constants (n_μ^J , r_μ^J and ϕ^J) as general as possible, while normally in a calculation these are fixed in such a way that the integral simplifies a lot (e.g. $n^2=0$, $\mathbf{n}_\perp=0$). This chapter is devoted to a few tricks that can help in simplifying the calculations encountered with piecewise linear Wilson lines.

In [Section 7.1](#), we develop an advanced technique to simplify any product or trace of fundamental Lie generators. As we separated out the colour structure in the previous chapter, this section can be a big help in calculating these factors. In [Section 7.2](#), we show how to properly define the contents of the blobs introduced in the previous chapter. We do this by using the example of self-interaction blobs—which contain no external lines and hence represent interactions between the Wilson line and itself—for a 2-gluon blob and a 3-gluon blob. In [Section 7.3](#) we explore the validity of a Wick rotation in the context of Wilson lines, and adapt the formulation where necessary. And finally in [Section 7.4](#), we make the first steps to calculate a common general Wilson line integral, and narrow it down to an easy example, a 1-gluon cusp correction, which we fully calculate for general segment directions, be it purely light-like, transversal, or mixed.

7.1 ADVANCED COLOUR ALGEBRA

The first step of any calculation in the piecewise framework is the calculation of path functions (see e.g. [Equations 6.78](#)). These functions contain a colour part and a part related to the line structure. The colour part is given by (see [Equation 6.69a](#)):

$$c = t^{a_n} \dots t^{a_1} c^{a_1 \dots a_n} .$$

The n -generator product is simply the colour structure of the n -th order expansion term of the Wilson line, while the factor $c^{a_1 \dots a_n}$ is the colour structure of the blob. Let's see if we can somehow simplify this term.

Calculating Products of Fundamental Generators

Similarly to what we did with the Fierz identity in [Equation A.78](#), any product of colour generators can be written as a linear combination of the identity operator and the generators, because the latter span the full product space. In other words:

$$t^{a_1} t^{a_2} \dots t^{a_n} = A^{a_1 a_2 \dots a_n} \mathbb{1} + B^{a_1 a_2 \dots a_n b} t^b .$$

As $A^{a_1 a_2 \dots a_n}$ and $B^{a_1 a_2 \dots a_n b}$ are just coefficients, tracing the [r.h.s.](#) simply gives $A^{a_1 a_2 \dots a_n} \text{tr}(\mathbb{1})$, because the single generator after $B^{a_1 a_2 \dots a_n b}$ is traceless. In a similar way we can recover $B^{a_1 a_2 \dots a_n b}$ by multiplying the product with a generator before making the trace. I.e. :

$$\begin{aligned} \text{tr}(t^{a_1} t^{a_2} \dots t^{a_n}) &= N_c A^{a_1 a_2 \dots a_n} , \\ \text{tr}(t^{a_1} t^{a_2} \dots t^{a_n} t^b) &= \frac{1}{2} B^{a_1 a_2 \dots a_n b} . \end{aligned}$$

But the [l.h.s.](#) of the latter can also be calculated as one order higher, i.e.

$$t^{a_1} t^{a_2} \dots t^{a_n} t^b = A^{a_1 a_2 \dots a_n b} \mathbb{1} + B^{a_1 a_2 \dots a_n b c} t^c ,$$

giving

$$\begin{aligned} \text{tr}(t^{a_1} t^{a_2} \dots t^{a_n} t^b) &= N_c A^{a_1 a_2 \dots a_n b} , \\ \Rightarrow A^{a_1 a_2 \dots a_n} &\equiv \frac{1}{2N_c} B^{a_1 a_2 \dots a_n} . \end{aligned}$$

Only one of these is linearly independent. We will adopt the notation

$$C^{a_1 a_2 \dots a_n} \stackrel{\text{N}}{=} N_c A^{a_1 a_2 \dots a_n} , \tag{7.1}$$

with C standing for ‘colour factor’. Note the difference with [Equation 6.68](#), i.e. a capital C is the colour factor that represents an n -generator product, while a lower case c represents the colour structure of a given blob. We can now rewrite the first equation as:

$$t^{a_1 \dots a_n} = C^{a_1 \dots a_n} \frac{\mathbb{1}}{N_c} + 2 C^{a_1 \dots a_n b} t^b, \quad (7.2a)$$

$$C^{a_1 \dots a_n} = \text{tr}(t^{a_1 \dots a_n}). \quad (7.2b)$$

As the colour factor identically equals the trace, it naturally has the same properties, namely cyclicity and Hermiticity:

$$C^{a_1 a_2 \dots a_n} = C^{a_2 a_3 \dots a_n a_1} = \dots, \quad (7.3a)$$

$$C^{a_1 a_2 \dots a_n} = \overline{C}^{a_n \dots a_2 a_1}. \quad (7.3b)$$

The first colour factors are straightforward to calculate:

$$C_0 = N_c, \quad (7.4a)$$

$$C^a = 0, \quad (7.4b)$$

$$C^{ab} = \frac{1}{2} \delta^{ab}, \quad (7.4c)$$

$$C^{abc} = \frac{1}{4} h^{abc}. \quad (7.4d)$$

To calculate higher orders, we use [Equation A.75](#) to deduce a recursion formula for traces in the fundamental representation—and hence for colour factors—by applying it on the last two generators (the last two indices of a colour factor):

$$C^{a_1 \dots a_n} = \frac{\delta^{a_{n-1} a_n}}{2N_c} C^{a_1 \dots a_{n-2}} + \frac{h^{a_{n-1} a_n b}}{2} C^{a_1 \dots a_{n-2} b}. \quad (7.5)$$

This gives for instance

$$C^{abcd} = \frac{1}{4N_c} \delta^{ab} \delta^{cd} + \frac{1}{8} h^{abx} h^{xcd},$$

$$C^{abcde} = \frac{1}{8N_c} (h^{abc} \delta^{de} + \delta^{ab} h^{cde}) + \frac{1}{16} h^{abx} h^{xcy} h^{yde},$$

$$C^{abcdef} = \frac{1}{8N_c^2} \delta^{ab} \delta^{cd} \delta^{ef} + \frac{1}{32} h^{abx} h^{xcy} h^{ydz} h^{zef} \\ + \frac{1}{16N_c} (h^{abx} h^{xcd} \delta^{ef} + h^{abc} h^{def} + \delta^{ab} h^{cdx} h^{xef}).$$

One extremely useful observation is that inner summations only appear between consecutive h 's, and never with a δ . This allows us to define the following short-hand notations:

$$\begin{aligned}\delta &\stackrel{N}{=} \delta^{a_i a_{i+1}}, \\ h &\stackrel{N}{=} h^{a_i a_{i+1} a_{i+2}}, \\ \underset{\square}{hh} &\stackrel{N}{=} h^{a_i a_{i+1} x} h^{x a_{i+2} a_{i+3}}, \\ \underset{\square\square}{hhh} &\stackrel{N}{=} h^{a_i a_{i+1} x} h^{x a_{i+2} y} h^{y a_{i+3} a_{i+4}}, \\ &\dots\end{aligned}$$

so that we can rewrite the former result as (note that the order of the δ 's and h 's is significant because of the indices):

$$C_2 = \frac{1}{2} \delta, \quad (7.6a)$$

$$C_3 = \frac{1}{4} h, \quad (7.6b)$$

$$C_4 = \frac{1}{4N_c} \delta\delta + \frac{1}{8} \underset{\square}{hh}, \quad (7.6c)$$

$$C_5 = \frac{1}{8N_c} (h\delta + \delta h) + \frac{1}{16} \underset{\square\square}{hhh}, \quad (7.6d)$$

$$C_6 = \frac{1}{8N_c^2} \delta\delta\delta + \frac{1}{16N_c} \left(\underset{\square}{hh}\delta + h h + \delta \underset{\square}{hh} \right) + \frac{1}{32} \underset{\square\square\square}{hhhh}. \quad (7.6e)$$

If we generalise this to an n -th order trace, we get from Equation 7.5:

Calculation of Colour Factors

$$n \text{ even: } C^{a_1 \dots a_n} = \sum_{i=0}^{\frac{n}{2}-1} \frac{1}{2^{\frac{n}{2}+i} N_c^{\frac{n}{2}-i-1}} \left(\begin{array}{l} \text{all allowed } \delta, h \text{ combinations} \\ \text{built from } 2i \text{ } h\text{'s} \end{array} \right), \quad (7.7a)$$

$$n \text{ odd: } C^{a_1 \dots a_n} = \sum_{i=0}^{\frac{n-3}{2}} \frac{1}{2^{\frac{n+1}{2}+i} N_c^{\frac{n-1}{2}-i-1}} \left(\begin{array}{l} \text{all allowed } \delta, h \text{ combinations} \\ \text{built from } 2i+1 \text{ } h\text{'s} \end{array} \right). \quad (7.7b)$$

where the δ, h combinations need to have n open indices, using

$$\begin{aligned}\delta & \text{ 2 open indices,} \\ h & \text{ 3 open indices,} \\ \underset{\square}{hh} & \text{ 4 open indices,} \\ \underset{\square\square}{hhh} & \text{ 5 open indices,}\end{aligned}$$

etc.

and where it is forbidden to put any δ or h in between two contracted h 's. So for instance $\underline{h\delta h}$ and \underline{hhh} are not allowed. With this in mind, we can tackle any trace without the need for recursive calculations. For example:

$$\begin{aligned}
C^{a_1 \cdots a_{10}} = & \frac{1}{32N_c^4} \delta\delta\delta\delta\delta + \frac{1}{64N_c^3} \left(\underline{hh\delta\delta\delta} + \underline{\delta hh\delta\delta} + \underline{\delta\delta hh\delta} + \underline{\delta\delta\delta hh} \right. \\
& + \underline{hh\delta\delta} + \underline{h\delta h\delta} + \underline{h\delta\delta h} + \underline{\delta h h\delta} + \underline{\delta h\delta h} + \underline{\delta\delta h h} \left. \right) + \frac{1}{128N_c^2} \left(\underline{hhhh\delta\delta} \right. \\
& + \underline{\delta hhhh\delta} + \underline{\delta\delta hhhh} + \underline{hhhh\delta} + \underline{hhh\delta h} + \underline{\delta hhhh} + \underline{h hhh\delta} + \\
& + \underline{h\delta hhh} + \underline{\delta h hhh} + \underline{hh hh\delta} + \underline{hh\delta hh} + \underline{\delta hh hh} + \underline{hh h h} + \underline{h hh h} \\
& \left. + \underline{h h hh} \right) + \frac{1}{256N_c} \left(\underline{hhhhhh\delta} + \underline{\delta hhhhhh} + \underline{hhhhhh} + \underline{h h h h h h} \right. \\
& \left. + \underline{h h h h h h} + \underline{h h h h h h} + \underline{h h h h h h} \right) + \frac{1}{512} \underline{h h h h h h h h} .
\end{aligned}$$

This looks quite complex, but is in its essence not that difficult, as we only have 6 ‘types’ of terms, depending on the number of h 's in a certain term. The result will simplify drastically if there exist symmetries between the indices of $C^{a_1 \cdots a_{10}}$.

As a result from [Equation 7.5](#) we can use a trick to double check our result, namely that the total number of terms should equal the $(n-1)$ -th Fibonacci number (counting 0 as the zeroth Fibonacci number). Indeed, for the 10-th order trace we have 34 terms.

Making contractions over the indices of one colour factor is straightforward using the formulae in the end of [Appendix A.6](#). E.g.

$$C^{abab} = \frac{1}{4N_c} \delta^{ab} \delta^{ab} + \frac{1}{8} h^{abx} h^{xab} .$$

The last term can be calculated by using [Equation A.87c](#):

$$h^{abx} h^{xab} = h^{abx} \bar{h}^{xba} = -\frac{4}{N_c} \delta^{bb} = -8C_F ,$$

giving

$$C^{abab} = \frac{1}{4N_c} (N_c^2 - 1) - C_F = -\frac{1}{2} C_F . \quad (7.8)$$

Similarly, if we flip the last two indices of the colour factor we have

$$C^{abba} = \frac{1}{4N_c} \delta^{ab} \delta^{ba} + \frac{1}{8} h^{abx} h^{xba} .$$

This time the last term can be calculated by using Equation A.87d:

$$h^{abx} h^{xba} = 4(N_c^2 - 2) C_F,$$

giving

$$C^{abba} = N_c C_F^2. \quad (7.9)$$

Because of the cyclicity these two are the only independent fully contracted fourth order colour factors. We will conclude this subsection with a list of properties for the colour factors. First, a listing of some common contractions of the first to fifth order colour factors:

$$C^{aa} = N_c C_F, \quad C^{aba} = 0, \quad C^{axxb} = \frac{1}{2} C_F \delta^{ab}, \quad (7.10a)$$

$$C^{axbx} = -\frac{1}{4N_c} \delta^{ab}, \quad C^{abab} = -\frac{1}{2} C_F, \quad C^{abba} = N_c C_F^2, \quad (7.10b)$$

$$C^{abcxx} = C_F C^{abc}, \quad C^{abxcx} = -\frac{1}{2N_c} C^{abc}, \quad C^{axxyy} = 0, \quad (7.10c)$$

$$C^{axyxy} = 0, \quad C^{axyyx} = 0, \quad C^{abcdxx} = C_F C^{abcd}, \quad (7.10d)$$

$$C^{abcxdx} = -\frac{1}{2N_c} C^{abcd}, \quad C^{abxcdx} = \frac{1}{8} \delta^{ab} \delta^{cd} - \frac{1}{2N_c} C^{abcd}, \quad (7.10e)$$

and the sixth order colour factors:

$$C^{abxxyy} = \frac{1}{2} C_F^2 \delta^{ab}, \quad C^{abxyxy} = -\frac{C_F}{4N_c} \delta^{ab}, \quad C^{abxyyx} = \frac{1}{2} C_F^2 \delta^{ab}, \quad (7.11a)$$

$$C^{axbxyy} = -\frac{C_F}{4N_c} \delta^{ab}, \quad C^{axbyxy} = \frac{1}{8N_c^2} \delta^{ab}, \quad C^{axbyyx} = -\frac{C_F}{4N_c} \delta^{ab}, \quad (7.11b)$$

$$C^{axxbyy} = \frac{1}{2} C_F^2 \delta^{ab}, \quad C^{axybxy} = \frac{1}{8} \frac{N_c^2 + 1}{N_c^2} \delta^{ab}, \quad C^{axybyx} = \frac{1}{8N_c^2} \delta^{ab}, \quad (7.11c)$$

$$C^{aabbcc} = N_c C_F^3, \quad C^{abacbc} = \frac{C_F}{4N_c}, \quad C^{aabcbc} = -\frac{1}{2} C_F^2, \quad (7.11d)$$

$$C^{abccba} = N_c C_F^3, \quad C^{abcabc} = \frac{N_c^2 + 1}{4N_c} C_F. \quad (7.11e)$$

We also list some contractions between two colour factors:

$$C^{ax} C^{xb} = \frac{1}{4} \delta^{ab}, \quad C^{ab} C^{ab} = \frac{N_c}{2} C_F, \quad C^{axy} C^{xyb} = -\frac{1}{4N_c} \delta^{ab}, \quad (7.12a)$$

$$C^{axy} C^{yxb} = \frac{N_c^2 - 2}{8N_c} \delta^{ab}, \quad C^{abc} C^{abc} = -\frac{C_F}{2}, \quad C^{abc} C^{cba} = \frac{N_c^2 - 2}{4} C_F, \quad (7.12b)$$

and between a colour factor and a standard colour constant:

$$C^{ab} t^a t^b = \frac{N_c}{2} C_F \frac{\mathbb{1}}{N_c}, \quad C^{axy} f^{xyb} = i \frac{N_c}{4} \delta^{ab}, \quad (7.13a)$$

$$C^{abc} f^{abc} = i \frac{N_c^2}{2} C_F, \quad C^{abxy} f^{xyc} = i \frac{N_c}{8} h^{abc}, \quad (7.13b)$$

$$C^{abcd} f^{abc} = 0, \quad C^{abcd} f^{abx} f^{xcd} = -\frac{N_c^3}{4} C_F. \quad (7.13c)$$

For contractions with longer colour factors, we can simply use the Fierz identities (see Equation A.77). Expressed in function of colour factors, these are:

$$C^{a_1 \dots a_m x a_{m+1} \dots a_p x a_{p+1} \dots a_n} = \frac{1}{2} C^{a_1 \dots a_m a_{p+1} \dots a_n} C^{a_{m+1} \dots a_p} - \frac{1}{2N_c} C^{a_1 \dots a_n}, \quad (7.14a)$$

$$C^{a_1 \dots a_m x x a_{m+1} \dots a_n} = C_F C^{a_1 \dots a_n}, \quad (7.14b)$$

$$C^{a_1 \dots a_m x C^{x a_{m+1} \dots a_n}} = \frac{1}{2} C^{a_1 \dots a_n} - \frac{1}{2N_c} C^{a_1 \dots a_m} C^{a_{m+1} \dots a_n}. \quad (7.14c)$$

Calculating Traces in the Adjoint Representation

In the adjoint representation Equation 7.2a is not true, because the set $\{\mathbb{1}, T^a\}$ isn't sufficient to reproduce all possible products of adjoint generators. Still, it would be useful to find a method to calculate adjoint traces. Unfortunately, this is not so trivial, as we have no useful expression for the anticommutation relations—which we need to get a recursion relation as in Equation 7.5. Instead of a brute-force calculation, we will relate traces in the adjoint representation to traces in the fundamental using a nifty trick. First, note that in general the product space of the fundamental and the anti-fundamental is isomorphic to the sum space of the adjoint and the identity:

$$F \otimes \bar{F} \simeq A \oplus \mathbb{1}, \quad (7.15)$$

from which we can derive (U_A denotes 'the group element U expressed in the adjoint representation'):

$$\text{tr}(U_A) = \text{tr}(U_F) \text{tr}(U_{\bar{F}}) - 1. \quad (7.16)$$

For the trivial group element $U = \mathbb{1}$, we get indeed $d_A = d_F^2 - 1$. To calculate the n -th order trace, it is sufficient to take $U = \prod_i^n e^{t_R^a \alpha_i^a}$, expand it and compare terms of the same order in α_i . Furthermore we can use

$$U_{\bar{F}} = U_F^\dagger = U_F^{-1},$$

which implies

$$e^{\bar{t}^{a_1} \alpha_1^{a_1}} \dots e^{\bar{t}^{a_n} \alpha_n^{a_n}} = e^{-t^{a_n} \alpha_n^{a_n}} \dots e^{-t^{a_1} \alpha_1^{a_1}} .$$

For example, the fourth-order trace in the adjoint can be calculated as follows:

$$\begin{aligned} \text{tr}\left(e^{T^a \alpha_1^a} e^{T^b \alpha_2^b} e^{T^c \alpha_3^c} e^{T^d \alpha_4^d}\right) &= \text{tr}\left(e^{t^a \alpha_1^a} e^{t^b \alpha_2^b} e^{t^c \alpha_3^c} e^{t^d \alpha_4^d}\right) \text{tr}\left(e^{-t^d \alpha_4^d} e^{-t^c \alpha_3^c} e^{-t^b \alpha_2^b} e^{-t^a \alpha_1^a}\right) - 1, \\ \alpha_1^a \alpha_2^b \alpha_3^c \alpha_4^d \text{tr}\left(T^a T^b T^c T^d\right) &= \alpha_1^a \alpha_2^b \alpha_3^c \alpha_4^d \left[\text{tr}\left(t^a t^b t^c t^d\right) N_c + N_c \text{tr}\left(t^d t^c t^b t^a\right) \right. \\ &\quad + 2 \text{tr}\left(t^a t^b\right) \text{tr}\left(t^c t^d\right) + 2 \text{tr}\left(t^a t^c\right) \text{tr}\left(t^b t^d\right) \\ &\quad \left. + 2 \text{tr}\left(t^a t^d\right) \text{tr}\left(t^b t^c\right) \right] . \end{aligned}$$

Using this trick we can calculate any trace in the adjoint representation in function of traces in the fundamental representation. Also note that we can derive equations similar to [Equation 7.16](#) using different representation combinations. For example in $SU(3)$ we have

$$\mathbf{3} \otimes \mathbf{3} \simeq \mathbf{6} \oplus \bar{\mathbf{3}},$$

implying

$$\text{tr}(U_{2F}) = \text{tr}(U_F) \text{tr}(U_F) - \text{tr}(U_{\bar{F}}) .$$

Now back to the adjoint generators. We can generalise their trace as

Traces of Adjoint Generators

$$\begin{aligned} \text{tr}(T^{a_1} \dots T^{a_n}) &= N_c \left(\text{tr}(t^{a_1} \dots t^{a_n}) + (-)^n \bar{\text{tr}}(t^{a_1} \dots t^{a_n}) \right) \\ &\quad + \sum_{m=2}^{n-2} (-)^{n-m} \frac{n!}{m! (n-m)!} \text{tr}\left(t^{(a_1 \dots t^{a_m})}\right) \bar{\text{tr}}\left(t^{a_{m+1} \dots t^{a_n}}\right) . \quad (7.17) \end{aligned}$$

We introduced two new notations: first we have the ‘conjugated’ trace, which is simply the trace in reversed order:

$$\bar{\text{tr}}(t^{a_1} \dots t^{a_n}) = \text{tr}(t^{a_n} \dots t^{a_1}) .$$

The only thing that changes when reversing a trace of fundamental generators, is that every h gets replaced by its complex conjugate \bar{h} (hence the notation $\bar{\text{tr}}$). The result can then be simplified further using relations as $h - \bar{h} = 2i f$,

$h_{\square}h + \overline{h}_{\square}h = 2\left(d_{\square}d - f_{\square}f\right)$, etc. The second notation we introduced, $(\cdot)^{\circ}$, is an ‘ordered’ symmetrisation which for a general tensor M is defined as:

$$M^{(a_1 \cdots a_m | a_{m+1} \cdots a_n)^{\circ}} = \frac{m!(n-m)!}{n!} \times \left(M^{a_1 \cdots a_n} + \begin{array}{l} \text{all permutations for which the first } m \\ \text{indices and the last } n-m \text{ indices are} \\ \text{ordered with respect to } (a_1 \cdots a_n) \end{array} \right). \quad (7.18)$$

For instance:

$$M^{(ab | N^{cd})^{\circ}} = \frac{1}{6} \left(M^{ab} N^{cd} + M^{ac} N^{bd} + M^{ad} N^{bc} + M^{bc} N^{ad} + M^{bd} N^{ac} + M^{cd} N^{ab} \right).$$

One handy property is that when A and B are commutative, we have:

$$A^{(a_1 \cdots a_m | B^{a_{m+1} \cdots a_n})^{\circ}} = B^{(a_1 \cdots a_{n-m} | A^{a_{n-m+1} \cdots a_n})^{\circ}},$$

e.g. $(\delta|h)^{\circ} = (h|\delta)^{\circ}$. To conclude, let us list some traces:¹

$$C_A^{a_1 a_2} = N_c \delta, \quad (7.19a)$$

$$C_A^{a_1 a_2 a_3} = \frac{N_c}{4} (h - \overline{h}), \quad (7.19b)$$

$$C_A^{a_1 a_2 a_3 a_4} = \frac{1}{2} (\delta\delta + 3(\delta\delta^{\circ})) + \frac{N_c}{8} (h_{\square}h + \overline{h}_{\square}h), \quad (7.19c)$$

$$C_A^{a_1 a_2 a_3 a_4 a_5} = \frac{1}{8} \left[(h - \overline{h}) \delta + \delta (h - \overline{h}) + 10 (\delta^{\circ} | (h - \overline{h}))^{\circ} \right] + \frac{N_c}{16} (h_{\square}h_{\square}h - \overline{h}_{\square}h_{\square}h), \quad (7.19d)$$

$$C_A^{a_1 a_2 a_3 a_4 a_5 a_6} = \frac{1}{4N_c} (\delta\delta\delta + 15(\delta\delta\delta^{\circ})) + \frac{1}{16} \left[(h_{\square}h + \overline{h}_{\square}h) \delta + (h_{\square}h + \overline{h}_{\square}h) + \delta (h_{\square}h + \overline{h}_{\square}h) + 15 (\delta^{\circ} | (h_{\square}h + \overline{h}_{\square}h))^{\circ} - 20 (h^{\circ} | \overline{h})^{\circ} \right] + \frac{N_c}{32} (h_{\square}h_{\square}h_{\square}h + \overline{h}_{\square}h_{\square}h_{\square}h), \quad (7.19e)$$

where we introduced the notation

$$C_A^{a_1 \cdots a_n} \stackrel{N}{=} \text{tr}(T^{a_1} \cdots T^{a_n}), \quad (7.20)$$

in analogy with the fundamental representation.

¹ Note that $(\delta^{\circ} | \delta)^{\circ} = (\delta\delta^{\circ})$, for any number of δ 's.

7.2 SELF-INTERACTION BLOBS

Now that we have developed some useful tools for working with the colour algebra, we make a list of path functions for some common blobs. We will list the Wilson self-interaction blobs—i.e. all blobs that connect the Wilson line to itself, not to e.g. a fermion—up to NNLO. These are the blobs that are used in the calculation of soft factors and Wilson loops. Note that we always take the convention that gluon momenta are pointing *outwards* from the Wilson line, *into* the blob.

Two-Gluon Blob

The 2-gluon blob up to NNLO is simply the gluon propagator plus one-loop and two-loop corrections:



So the formula for the blob is simply given by

$$F_{\mu_1\mu_2}^{ab}(k_1, k_2) = \delta^{ab} D_{\mu_1\nu}(k_1) \mathfrak{F}^{(\omega)}(k_1 + k_2) \mathcal{B}_{\mu_2}^{\nu}(k_1), \quad (7.21)$$

where \mathcal{B} resums all corrections:

$$\mathcal{B}_{\nu\mu}(k) = g_{\nu\mu} + \left[i\Pi_{\nu\rho}^{\text{NLO}}(k) - \Pi_{\nu\sigma_1}^{\text{NLO}}(k) D^{\sigma_1\sigma_2}(k) \Pi_{\sigma_2\rho}^{\text{NLO}}(k) + i\Pi_{\nu\rho}^{\text{NNLO}}(k) + \dots \right] D_{\mu}^{\rho}(k), \quad (7.22)$$

and where Π is the $\mathfrak{1PI}$ diagram. We anticipated the fact that we can factor out the colour structure to be δ^{ab} . This is only logical, as there are no other elements in the algebra that have exactly two adjoint indices open (and that cannot be reduced to something proportional to δ^{ab}). This also means that the path function defined in Equations 6.78 is indeed valid, because the colour structure is (see Equation 6.69a):

$$c = t^a t^b \delta^{ab} = C_F \mathbb{1},$$

and what is more, it is valid to all orders for the 2-gluon self-interaction blob, following our reasoning above. Connecting this blob to a Wilson line is trivial using the methods developed in Section 6.5. This gives:

$$\mathcal{U}^2 = \sum_J^M \Phi_2(J) \mathcal{W}_2^J + \sum_{J=2}^M \sum_{K=1}^{J-1} \Phi_{11}(J, K) \mathcal{W}_{11}^{JK}, \quad (7.23)$$

where Φ and \mathcal{W} are given by Equations 6.78 and Equation 6.81:

2-Gluon Self-Interaction Blob

$$\overline{\overline{\overline{J}}} : \quad (7.24a)$$


$$\Phi_2(J) = C_F,$$

$$\begin{aligned} \mathcal{W}_2^J &= \int \frac{d^\omega k_1}{(2\pi)^\omega} \frac{d^\omega k_2}{(2\pi)^\omega} I_2^{1.b.J}(k_1, k_2) F_{\mu_1 \mu_2}(k_1, k_2), \\ &= -i g^2 n_J^{\mu_1} n_J^{\mu_2} \frac{1}{\eta} \mu^{2\epsilon} \int \frac{d^\omega k}{(2\pi)^\omega} \frac{1}{n^J \cdot k + i\eta} D_{\mu_1 \nu}(k) \mathcal{B}_{\mu_2}^\nu(k), \end{aligned}$$

$$\overline{\overline{\overline{K}}} \overline{\overline{\overline{J}}} : \quad (7.24b)$$


$$\Phi_{11}(J, K) = (-)^{\phi_J + \phi_K} C_F,$$

$$\begin{aligned} \mathcal{W}_{11}^{JK} &= \int \frac{d^\omega k_1}{(2\pi)^\omega} \frac{d^\omega k_2}{(2\pi)^\omega} I_1^{1.b.K}(k_1) I_1^{1.b.J}(k_2) F_{\mu_1 \mu_2}(k_1, k_2), \\ &= -g^2 n_K^{\mu_1} n_J^{\mu_2} \mu^{2\epsilon} \int \frac{d^\omega k}{(2\pi)^\omega} \frac{e^{i(r^K - r^J) \cdot k}}{n^K \cdot k + i\eta} \frac{1}{n^J \cdot k - i\eta} D_{\mu_1 \nu}(k) \mathcal{B}_{\mu_2}^\nu(k), \end{aligned}$$

where ϕ_J is defined in Equation 6.79, and $I_n^{1.b.J}$ is given in Equation 6.26. In Sections 7.3 and 7.4 we will investigate some calculational tools to do these momentum integrations. Equations 7.24 are of course still gauge-invariant statements, as all gauge-dependent content is contained in $D_{\mu\nu}$ and $\mathcal{B}_{\mu\nu}$.

Now let us investigate the contents of the 2-gluon blob a bit more precise. The one-loop diagrams are the fermion loop, ghost loop (in non-axial gauges), and the two possible gluon loops:



which are (see Equation 4.36 for the fermion loop):

$$i\Pi_{v_1 v_2}^{\text{NLO}} \Big|_{\text{ferm.}} = \frac{g^2}{2} \mu^{2\epsilon} \int \frac{d^\omega q}{(2\pi)^\omega} \text{tr}(\gamma^{v_2} \Delta_F(q) \gamma^{v_1} \Delta_F(q+k)), \quad (7.25a)$$

$$i\Pi_{v_1 v_2}^{\text{NLO}} \Big|_{\text{ghost}} = g^2 N_c \mu^{2\epsilon} \int \frac{d^\omega q}{(2\pi)^\omega} (q+k)^{v_1} q^{v_2} \Sigma_F(q+k) \Sigma_F(q), \quad (7.25b)$$

$$i\Pi_{v_1 v_2}^{\text{NLO}} \Big|_{3\text{gluon}} = -\frac{g^2}{2} N_c \int \frac{d^\omega q}{(2\pi)^\omega} \mathcal{A}^{v_1 \rho_1 \sigma_1} D_{\rho_1 \rho_2}(q) D_{\sigma_1 \sigma_2}(q+k) \mathcal{A}^{v_2 \rho_2 \sigma_2}, \quad (7.25c)$$

$$\mathcal{A}^{v\rho\sigma} = g^{v\rho}(q-k)^\sigma - g^{\rho\sigma}(2q+k)^v + g^{\sigma v}(q+2k)^\rho,$$

$$i\Pi_{v_1 v_2}^{\text{NLO}} \Big|_{4\text{gluon}} = -i g^2 N_c (g^{v_1 \rho} g^{v_2 \sigma} - g^{v_1 v_2} g^{\rho\sigma}) \mu^{2\epsilon} \int \frac{d^\omega q}{(2\pi)^\omega} D_{\rho\sigma}(q). \quad (7.25d)$$

In Feynman gauge (and using dimensional regularisation, see Subsection *Regularisation* on page 91 and onwards), it is not so difficult to calculate these NLO contributions. The sum of all contributions equals (see e.g. [Equations 4.37](#) for the fermion loop):²

$$i\Pi_{\mu\nu}^{\text{NLO}} = i (g_{\mu\nu} k^2 - k_\mu k_\nu) \frac{\alpha_s}{\pi} \left[\frac{5N_c - 2N_f}{12} \left(\frac{1}{\epsilon} - \gamma_E + \ln 4\pi + \ln \mu^2 \right) + \frac{N_c}{12} - I \right],$$

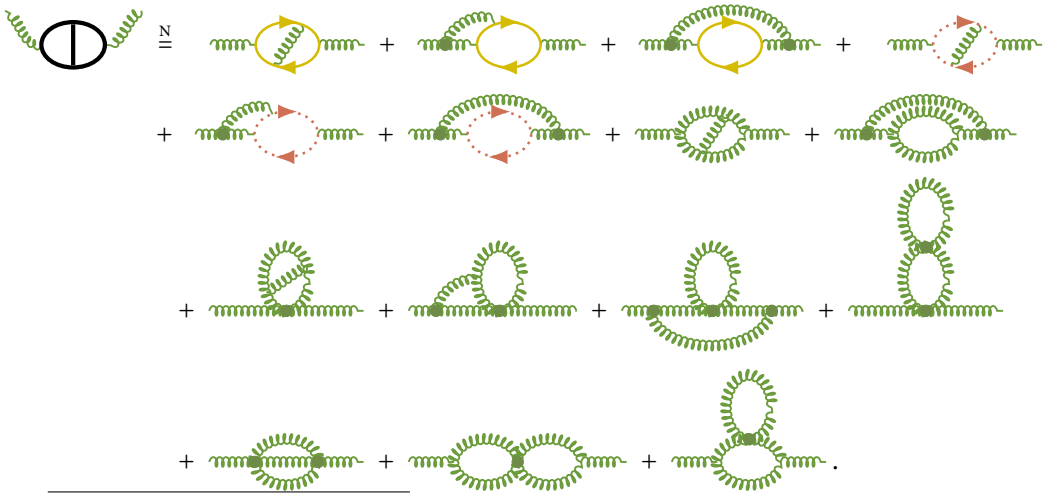
$$I = \int_0^1 dx \left[N_c \left(\frac{1}{4} + x(1-x) \right) \ln \Delta(0) - x(1-x) \sum_q^{N_f} \ln \Delta(m_q^2) \right],$$

where

$$\Delta(m^2) \stackrel{\text{N}}{=} m^2 - x(1-x)k^2.$$









We can solve I in the same way as we did in [Equations 4.39](#). However, the k^2 -integration that emerges when connecting the blob will be quite complicated due to the logarithm of square roots. For this reason, we leave the x -integration undefined until after the momentum integration.

The NNLO 1PI diagram is a lot more involving. We will not calculate it—as we don't need it—but just list its 15 sub diagrams:



² There is a very important caveat: when calculating blob diagrams that will be inserted in other diagrams, it is always preferable *not* to expand the UV poles, because a priori the parent diagram and its poles are not known, i.e. we don't now yet to which order we have to keep the finite terms. Leaving ϵ unexpanded avoids this problem.

We already deduced from first principles that at any order the colour structure has to be proportional to δ^{ab} . Using [Equations A.84 to A.89](#), we can easily double-check this:

	$\text{tr}(t^a t^x t^b t^x) = -\frac{1}{4N_c} \delta^{ab},$
	$\text{tr}(t^b t^x t^y) f^{ayx} = -i \frac{N_c}{4} \delta^{ab},$
	$\text{tr}(t^y t^z) f^{axy} f^{bzx} = -\frac{N_c}{2} \delta^{ab},$
	$f^{xay} f^{ycz} f^{zbw} f^{wcx} = \frac{N_c^2}{2} \delta^{ab},$
	$f^{avw} f^{xby} f^{y wz} f^{zvx} = \frac{N_c^2}{2} \delta^{ab},$
	$f^{awv} f^{bzw} f^{xzy} f^{yvx} = N_c^2 \delta^{ab},$
	$f^{xay} f^{ycz} f^{zbw} f^{wcx} = \frac{N_c^2}{2} \delta^{ab},$
	$f^{vaw} f^{wbz} f^{xzy} f^{yvx} = N_c^2 \delta^{ab},$

and similarly for the seven remaining diagrams.

Three-Gluon Blob

The 3-gluon blob up to [NNLO](#) is simply the 3-gluon vertex plus one-loop corrections:



So the formula for the blob is given by

$$F_{\mu_1 \mu_2 \mu_3}^{abc}(k_1, k_2, k_3) = f^{abc} D_{\mu_1 \nu_1}(k_1) D_{\mu_2 \nu_2}(k_2) D_{\mu_3 \nu_3}(k_3) \delta^\omega(k_1 + k_2 + k_3) \Gamma^{\nu_1 \nu_2 \nu_3}(k_1, k_2, k_3),$$

where Γ resums all corrections:

$$\Gamma_{\mu\nu\rho}(k, p, q) = \Gamma_{\mu\nu\rho}^{\text{LO}}(k, p, q) + \Gamma_{\mu\nu\rho}^{\text{LO+B}}(k, p, q) + \Gamma_{\mu\nu\rho}^{\text{NLO}}(k, p, q) + \dots \quad (7.26a)$$

$$\Gamma_{\mu\nu\rho}^{\text{LO}}(k, p, q) = g [g_{\mu\nu}(k-p)^\rho + g_{\nu\rho}(p-q)^\mu + g_{\rho\mu}(q-k)^\nu]. \quad (7.26b)$$

Again we anticipated the fact that we can factor out the colour structure to be f^{abc} . The same arguments as for the 2-gluon blob are however no longer valid, as now there exists a second structure—independent of f^{abc} —with three adjoint indices, namely d^{abc} . It just happens that up to first loop the colour structure only depends on f^{abc} , of which we took advantage to factor it out. Just remember that this might no longer be possible at second loop (if this is indeed the case, we will have to split the blob as a sum of two colour-factorable sub-blobs, as explained in [Section 6.4](#)). Again the path function defined in [Equations 6.80](#) is indeed valid, because the colour structure is (see [Equation 6.69a](#)):

$$c = t^c t^b t^a f^{abc} = C^{cba} f^{abc} \frac{\mathbb{1}}{N_c} + 2C^{cbax} f^{abc} t^x = -i \frac{N_c}{2} C_F \mathbb{1},$$

where we used [Equation 7.2a](#) to write the generator product as a sum of colour factors, and used the relations in [Equations 7.13](#) to simplify the result. Remember that we need to read a Wilson line as a Dirac line, i.e. from right to left, to get the correct result. Here this can be seen in the order of the generators; reversing the order would give a minus sign difference.

Investigating the colour structure, we have three different possibilities: all gluons connected to one segment, two gluons to one segment and one to another, or all to a different segment. Reversing the direction of a segment line is the same as flipping the order of the colour indices that are connected to it and multiplying with -1 for each gluon. For the situation where all gluons are connected to one segment, flipping this segment leaves the result invariant (see [Equation 6.71](#)). For the situation 1+2, flipping the segment with one gluon only gives a sign difference (because reversing one index doesn't change anything):

$$(-)^1 c = i \frac{N_c}{2} C_F \mathbb{1},$$

and flipping the segment with two gluons reverses these indices, also giving a sign difference:

$$(-)^2 t^c t^b t^a f^{acb} = C^{cba} f^{acb} \frac{\mathbb{1}}{N_c} + 2C^{cbax} f^{acb} t^x = i \frac{N_c}{2} C_F \mathbb{1}.$$

And for the situation 1 + 1 + 1, flipping any segment trivially gives a sign difference. So these effects can be combined into the path function as given in [Equations 6.80](#).

The full Wilson line result can be calculated using the methods developed in [Section 6.5](#):

$$\mathcal{U}^3 = \sum_J^M \Phi_3 \mathcal{W}_3^J + \sum_{J=2}^M \sum_{K=1}^{J-1} (\Phi_{21} \mathcal{W}_{21}^{JK} + J \leftrightarrow K) \sum_{J=3}^M \sum_{K=2}^{J-1} \sum_{L=1}^{K-1} \Phi_{111} \mathcal{W}_{111}^{JKL}, \quad (7.27)$$

where Φ and \mathcal{W} are now given by Equations 6.80 and Equation 6.81:

3-Gluon Self-Interaction Blob

$$\overline{\overline{\overline{k_1 \downarrow \text{---} \uparrow k_3}}} : \quad (7.28a)$$

$$\Phi_3(J) = -i \frac{N_c}{2} C_F,$$

$$\mathcal{W}_3^J = \int \frac{d^\omega k_1}{(2\pi)^\omega} \frac{d^\omega k_2}{(2\pi)^\omega} \frac{d^\omega k_3}{(2\pi)^\omega} I_3^{\text{l.b.},J}(k_1, k_2, k_3) F_{\mu_1 \mu_2 \mu_3}(k_1, k_2, k_3),$$

$$= i g^3 n_J^{\mu_1} n_J^{\mu_2} n_J^{\mu_3} \frac{1}{\eta} \mu^{3\epsilon} \int \frac{d^\omega k_1}{(2\pi)^\omega} \frac{d^\omega k_2}{(2\pi)^\omega} \frac{1}{n^J \cdot k_1 - i\eta} \frac{1}{n^J \cdot (k_1 + k_2) - i\eta} \\ D_{\mu_1 \nu_1}(k_1) D_{\mu_2 \nu_2}(k_2) D_{\mu_3 \nu_3}(k_1 + k_2) \Gamma^{\nu_1 \nu_2 \nu_3}(k_1, k_2, -k_1 - k_2),$$

$$\overline{\overline{\overline{k_1 \downarrow \text{---} \uparrow k_3}}} : \quad (7.28b)$$

$$\Phi_{21}(J, K) = -i (-)^{\phi_J + \phi_K} \frac{N_c}{2} C_F,$$

$$\mathcal{W}_{21}^{JK} = \int \frac{d^\omega k_1}{(2\pi)^\omega} \frac{d^\omega k_2}{(2\pi)^\omega} \frac{d^\omega k_3}{(2\pi)^\omega} I_1^{\text{l.b.},K}(k_1) I_2^{\text{l.b.},J}(k_2, k_3) F_{\mu_1 \mu_2 \mu_3}(k_1, k_2, k_3),$$

$$= -g^3 n_K^{\mu_1} n_J^{\mu_2} n_J^{\mu_3} \mu^{3\epsilon} \int \frac{d^\omega k_1}{(2\pi)^\omega} \frac{d^\omega k_2}{(2\pi)^\omega} \frac{e^{i(r^K - r^J) \cdot k_1}}{n^K \cdot k_1 + i\eta} \frac{1}{n^J \cdot k_1 - i\eta} \frac{1}{n^J \cdot (k_1 + k_2) - i\eta} \\ D_{\mu_1 \nu_1}(k_1) D_{\mu_2 \nu_2}(k_2) D_{\mu_3 \nu_3}(k_1 + k_2) \Gamma^{\nu_1 \nu_2 \nu_3}(k_1, k_2, -k_1 - k_2),$$

$$\overline{\overline{\overline{k_1 \downarrow \text{---} \uparrow k_3}}} : \quad (7.28c)$$

$$\Phi_{111}(J, K, L) = -i (-)^{\phi_J + \phi_K + \phi_L} \frac{N_c}{2} C_F,$$

$$\mathcal{W}_{111}^{JKL} = \int \frac{d^\omega k_1}{(2\pi)^\omega} \frac{d^\omega k_2}{(2\pi)^\omega} \frac{d^\omega k_3}{(2\pi)^\omega} I_1^{\text{l.b.},L}(k_1) I_1^{\text{l.b.},K}(k_2) I_1^{\text{l.b.},J}(k_3) F_{\mu_1 \mu_2 \mu_3}(k_1, k_2, k_3),$$

$$= -g^3 n_L^{\mu_1} n_K^{\mu_2} n_J^{\mu_3} \mu^{3\epsilon} \int \frac{d^\omega k_1}{(2\pi)^\omega} \frac{d^\omega k_2}{(2\pi)^\omega} \frac{e^{i(r^L - r^J) \cdot k_1}}{n^L \cdot k_1 + i\eta} \frac{e^{i(r^K - r^J) \cdot k_2}}{n^K \cdot k_2 + i\eta} \frac{1}{n^J \cdot (k_1 + k_2) - i\eta} \\ D_{\mu_1 \nu_1}(k_1) D_{\mu_2 \nu_2}(k_2) D_{\mu_3 \nu_3}(k_1 + k_2) \Gamma^{\nu_1 \nu_2 \nu_3}(k_1, k_2, -k_1 - k_2).$$

where ϕ_J is defined in Equation 6.79, and $I_n^{l.b.J}$ is given in Equation 6.26. Again these results are still gauge-invariant.

Now let us investigate the contents of the 3-gluon blob a bit more precise. There are two one-loop contributions, viz. a ‘pure’ contribution where the vertex point is substituted by a loop, and a contribution where the propagator in one of the legs is evaluated at NLO. The latter is really straightforward to calculate, because the result was already calculated in Equation 7.22:

$$\begin{aligned} \Gamma_{\mu\nu\rho}^{\text{LO}+\mathcal{B}}(k, p, q) &= \mathcal{B}_{\mu\sigma}^{\text{NLO}}(k) \Gamma_{\sigma\nu\rho}^{\text{LO}}(k, p, q) + \mathcal{B}_{\nu\sigma}^{\text{NLO}}(p) \Gamma_{\mu\sigma\rho}^{\text{LO}}(k, p, q) \\ &+ \mathcal{B}_{\rho\sigma}^{\text{NLO}}(k) \Gamma_{\mu\nu\sigma}^{\text{LO}}(k, p, q). \end{aligned} \quad (7.29)$$

The pure contribution is however a bit more complicated. The loops are—just as was the case for the propagator—a fermion loop, ghost loop, and the two possible gluon loops:

The diagram shows a 3-gluon blob (a circle with three wavy lines) on the left, followed by an equals sign and five terms separated by plus signs. The first term is a fermion loop (yellow circle with two wavy lines). The second term is a ghost loop (red circle with two wavy lines). The third and fourth terms are gluon loops (green circles with two wavy lines) with different internal gluon line connections. The fifth term is another gluon loop (green circle with two wavy lines).

This result is quite challenging to calculate and spans several pages (see e.g. [41, 42]). It is instructive to take out the pole part, as this is the most interesting part. In covariant gauges, it is given by:

$$\Gamma_{\mu\nu\rho}^{\text{NLO UV}}(k, p, q) = \frac{1}{\epsilon} \frac{\alpha_s}{4\pi} \left[\frac{2}{3} N_f - N_c \left(\frac{2}{3} + \frac{3}{4} \xi \right) \right] \Gamma_{\mu\nu\rho}^{\text{LO}}(k, p, q), \quad (7.30)$$

where $\xi = 0$ in Feynman gauge. Note that when choosing the gauge defined by

$$\xi = \frac{8}{9} \left(\frac{N_f}{N_c} - 1 \right), \quad (7.31)$$

which is $\xi = \frac{8}{9}$ for $N_f = 6$, there are no ultraviolet divergences.

7.3 WICK ROTATIONS

In this section we will investigate the possibility to use a Wick rotation when doing integrations with Wilson lines. We cannot blindly make the substitution $k^0 = i k_E^0$ as in Appendix B.3, because the rotation might hit the poles. To see what we mean with this statement, let us first investigate how a regular Wick rotation works.

Regular Wick Rotation

Naively, one could think that in a Minkowskian integral

$$\int d^\omega k f(k^2) \quad (7.32)$$

the substitution $k^0 = ik_E^0$ would suffice to change it into an Euclidian integral

$$i \int d^\omega k_E f(-k_E^2), \quad (7.33)$$

but this is of course not true, as a complex substitution changes the contour of the integration (in the same way a real substitution can change the integration borders). The transformation is hence only valid if we can prove that the integration over the real axis equals the one over the complex axis. For most calculations in quantum field theory, this is trivial, as they will primarily contain integrals where the integrand is a combination of Feynman propagators. These can always be brought into the form

$$\int \frac{d^\omega k}{(2\pi)^\omega} \frac{1}{(k^2 - \Delta + i\varepsilon)^n}, \quad (7.34)$$

by completing the square and using Feynman parameterisation. This expression has two manifest poles of order n :³

$$k^0 = \pm \sqrt{\mathbf{k}^2 + \Delta - i\varepsilon} \approx \pm \sqrt{\mathbf{k}^2 + \Delta} \mp i\varepsilon. \quad (7.35)$$

These poles lie in the second and fourth quadrant (the numbering of the quadrants follows the angular magnitude, i.e. anticlockwise, starting in the upper right quadrant). Note that even when $\Delta < -\mathbf{k}^2$, the poles will lie in the second and fourth quadrant, because then

$$k^0 = \pm \sqrt{\mathbf{k}^2 + \Delta - i\varepsilon} \approx \pm i \sqrt{-\mathbf{k}^2 - \Delta} \mp \varepsilon.$$

If we now choose the contour as in [Figure 7.1](#), the contour integral vanishes because it doesn't enclose any poles. We then have:

$$\oint_{\mathcal{C}} = \int_{\mathcal{C}_R} + \int_{\mathcal{C}_1} + \int_{\mathcal{C}_I} + \int_{\mathcal{C}_2} \equiv 0 \quad \Rightarrow \quad \int_{\mathcal{C}_R} = - \int_{\mathcal{C}_I}. \quad (7.36)$$

³ Where the second step is made using the expansion $\sqrt{x - i\varepsilon} \approx \sqrt{x} - \frac{i\varepsilon}{2\sqrt{x}}$ and absorbing \sqrt{x} in ε .

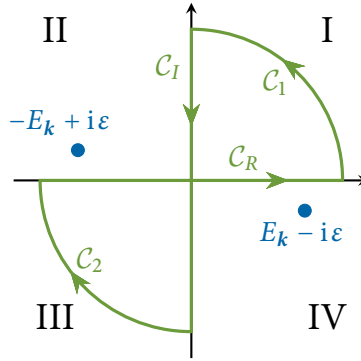


Figure 7.1: The contour chosen for a Wick rotation. Because it doesn't enclose any poles, the contour integral vanishes. If the integrand behaves as $\mathcal{O}(1/k^2)$, the real integral \mathcal{C}_R equals the imaginary integral \mathcal{C}_I . Note that although this is a contour with a self-intersection, we can split it at $(0, 0)$ into two valid contours, giving the same result (see Figure 7.3).

The integrations over the arc segments vanish because the integrand is of $\mathcal{O}(1/(k^0)^2)$. The minus sign in front of the integral over \mathcal{C}_I flips its borders, so that we indeed have

$$\int \frac{d^\omega k}{(2\pi)^\omega} \frac{1}{(k^2 - \Delta + i\varepsilon)^n} = (-)^n i \int \frac{d^\omega k_E}{(2\pi)^\omega} \frac{1}{(k_E^2 + \Delta)^n}. \quad (7.37)$$

We dropped the pole prescription in the *r.h.s.* as it is no longer needed.

Note that with this contour, it is indeed required that the integrand is of $\mathcal{O}(1/(k^0)^2)$, because e.g. exponential damping won't be sufficient. Suppose that we have an integration of the form

$$\int \frac{d^\omega k}{(2\pi)^\omega} \frac{k^0}{(k^2 - \Delta + i\varepsilon)^2} e^{i k \cdot x},$$

which is of $\mathcal{O}(1/k^0)$. To calculate the integrations over \mathcal{C}_1 and \mathcal{C}_2 , we use analytic continuation to parameterise k^0 in polar representation as

$$k^0 = R e^{i\theta}.$$

The k^0 integration over \mathcal{C}_1 then becomes:

$$\lim_{R \rightarrow \infty} iR \int_0^{\frac{\pi}{2}} d\theta e^{i\theta} \frac{R e^{i\theta}}{R^2 e^{2i\theta} - \mathbf{k}^2 - \Delta + i\varepsilon} e^{iR(\cos\theta + i \sin\theta)x^0} e^{-i\mathbf{k} \cdot \mathbf{x}} \sim \lim_{R \rightarrow \infty} e^{-R x^0 \sin\theta}.$$

The sign of $\sin \theta$ is fixed, because

$$\theta = 0 \dots \frac{\pi}{2} \Rightarrow \sin \theta > 0.$$

Hence this integral only vanishes for $x^0 > 0$. On the other hand, the integration over \mathcal{C}_2 has $\theta = -\pi/2 \dots -\pi$ and thus $\sin \theta < 0$, so this integral only vanishes for $x^0 < 0$. We cannot have both $x^0 > 0$ and $x^0 < 0$, at the same time, so exponential damping cannot make the integrations over the arcs vanish.⁴

There are hence two requirements to be allowed to make a Wick rotation:

- A. The integrand should scale as $\mathcal{O}\left(\frac{1}{(k^0)^2}\right)$,
- B. The integrand should only have poles in the 2nd and 4th quadrant.

It is however possible to relax the second requirement by adapting the Wick rotation formula a bit, as we will see in what follows.

Wick Rotation with Wilson Lines

Propagators from Wilson lines will introduce a linear dependence on k^0 in the denominator. Consider e.g. the **NLO** self-energy of a Wilson line segment (see [Equation 7.24a](#)):

$$\frac{J}{k_1 \text{---} k_2} = -ig^2 (n_J)^2 \frac{1}{\eta} \int \frac{d^\omega k}{(2\pi)^\omega} \frac{1}{n^J \cdot k + i\eta} \frac{1}{k^2 + i\epsilon}, \quad (7.38)$$

where the gluon propagator is expressed in Feynman gauge. If $(n^J)^0 = 0$, the Wilson line segment doesn't introduce additional poles, and we can safely make a Wick rotation. So from now on we suppose that $(n^J)^0 \neq 0$. Then the integrand has three poles:

$$k^0 = \pm \sqrt{\mathbf{k}^2 - \Delta} \mp i\epsilon, \quad k^0 = \frac{1}{n^0} (\mathbf{n} \cdot \mathbf{k} - i\eta). \quad (7.39)$$

The problematic pole is the last one, as it can lie in all quadrants, depending on the sign of n^0 and $\mathbf{n} \cdot \mathbf{k}$, as illustrated in [Figure 7.2](#). The troublesome quadrants are the first and the third; the integral has its poles in these quadrants when $\mathbf{n} \cdot \mathbf{k} \leq 0$. We can separate this values by splitting the integral in three parts using

⁴ Unless we forge some unphysical exponential of the form $e^{i|k^0|x^0 - i\mathbf{x} \cdot \mathbf{k}}$.

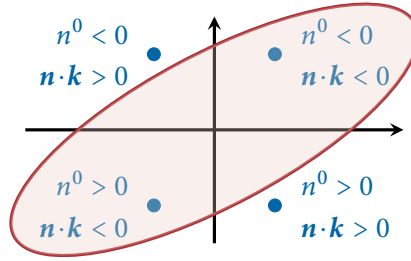


Figure 7.2: The pole of the Wilson propagator can lie in any quadrant, depending on the signs of n^0 and $\mathbf{n} \cdot \mathbf{k}$. The problematic poles are those in the first and third quadrants. These are the poles with $\mathbf{n} \cdot \mathbf{k} < 0$. The troublesome poles are marked in red.

$$1 = \theta(\mathbf{n} \cdot \mathbf{k}) + \theta(-\mathbf{n} \cdot \mathbf{k}) + \delta(\mathbf{n} \cdot \mathbf{k})^5$$

$$\int \frac{d^\omega k}{(2\pi)^\omega} \frac{\theta(\mathbf{n} \cdot \mathbf{k})}{n^J \cdot k + i\eta} \frac{1}{k^2 + i\varepsilon} + \int \frac{d^\omega k}{(2\pi)^\omega} \frac{\theta(-\mathbf{n} \cdot \mathbf{k})}{n^J \cdot k + i\eta} \frac{1}{k^2 + i\varepsilon} + \int \frac{d^\omega k}{(2\pi)^\omega} \frac{\delta(\mathbf{n} \cdot \mathbf{k})}{n^J \cdot k + i\eta} \frac{1}{k^2 + i\varepsilon}. \quad (7.40)$$

The first integral has no poles in the first and third quadrants and can hence be Wick rotated without problem. The second integral can be calculated by using the Residue theorem:

$$\oint_{\mathcal{C}} = \int_{\mathcal{C}_R} + \int_{\mathcal{C}_I} \equiv 2\pi i \text{Res} \quad \Rightarrow \quad \int_{\mathcal{C}_R} \equiv 2\pi i \text{Res} - \int_{\mathcal{C}_I}. \quad (7.41)$$

However, here we are skipping an important step: the contour in [Figure 7.1](#) is only valid because we can split it into two contours without self-intersections. The lower left contour is defined clockwise, so its Residue gains a minus sign (this doesn't matter in case of a regular Wick rotation, as then the residues are zero anyway). So we split the contour into a positive contour \mathcal{C}^+ and a negative contour \mathcal{C}^- , as in [Figure 7.3](#):

$$\oint_{\mathcal{C}^+} = \int_{\mathcal{C}_R^+} + \int_{\mathcal{C}_I^+} \equiv 2\pi i \text{Res}^+ \quad \Rightarrow \quad \int_{\mathcal{C}_R^+} \equiv 2\pi i \text{Res}^+ - \int_{\mathcal{C}_I^+}, \quad (7.42a)$$

$$\oint_{\mathcal{C}^-} = \int_{\mathcal{C}_R^-} + \int_{\mathcal{C}_I^-} \equiv -2\pi i \text{Res}^- \quad \Rightarrow \quad \int_{\mathcal{C}_R^-} \equiv -2\pi i \text{Res}^- - \int_{\mathcal{C}_I^-}, \quad (7.42b)$$

⁵ If $\mathbf{n} \cdot \mathbf{k} = 0$, the pole lies on the contour, which is treated differently. For this reason we chose to define $\theta(0) = 0$.

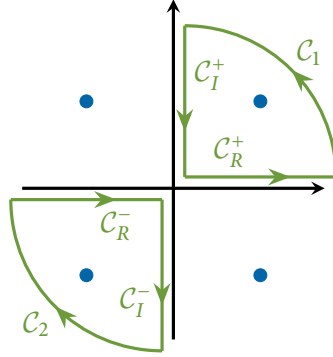


Figure 7.3: When there are extra poles in the first or third quadrant, we need to split the contour in its subcontours. The lower left contour, \mathcal{C}^- , is evaluated clockwise, hence its Residue gains a minus sign.

$$\int_{\mathcal{C}_R} = \int_{\mathcal{C}_R^+} + \int_{\mathcal{C}_R^-} = 2\pi i \text{Res}^+ - 2\pi i \text{Res}^- - \int_{\mathcal{C}_I} . \quad (7.42c)$$

We will never have Res^+ and Res^- at the same time, as these are two versions of the same Residue, depending on the sign of n^0 (see [Figure 7.2](#)), which we assumed to be non-zero (because if it is zero, we don't need to do this calculation anyway as we can just Wick-rotate the integral without problem). So we can write the Residue as:

$$2\pi i \text{Res}^+ - 2\pi i \text{Res}^- = (\theta(-n^0) - \theta(n^0)) 2\pi i \text{Res} , \quad (7.43)$$

where the full Residue is given by

$$2\pi i \text{Res} = i \int \frac{d^{\omega-1}\mathbf{k}}{(2\pi)^{\omega-1}} \frac{n^0 \theta(-\mathbf{n}\cdot\mathbf{k})}{(\mathbf{n}\cdot\mathbf{k} - i\eta)^2 - (n^0 \mathbf{k})^2} , \quad (7.44)$$

hence we can write

$$2\pi i \text{Res}^+ - 2\pi i \text{Res}^- = -i \int \frac{d^{\omega-1}\mathbf{k}}{(2\pi)^{\omega-1}} \frac{|n^0| \theta(-\mathbf{n}\cdot\mathbf{k})}{(\mathbf{n}\cdot\mathbf{k} - i\eta)^2 - (n^0 \mathbf{k})^2} . \quad (7.45)$$

We dropped the $i\epsilon$ pole-prescription, as it is no longer needed (the integration over k^0 has been done). We cannot drop the $i\eta$, as it will act as a soft regulator.

We can repeat the same calculation for the third integral in [Equation 7.40](#), but because the pole then lies on the contour, the residue only contributes a factor π instead of 2π :

$$\pi i \text{Res}^+ - \pi i \text{Res}^- = -i \int \frac{d^{\omega-1}\mathbf{k}}{(2\pi)^{\omega-1}} \frac{|n^0| \delta(\mathbf{n}\cdot\mathbf{k})}{(\mathbf{n}\cdot\mathbf{k} - i\eta)^2 - (n^0 \mathbf{k})^2} . \quad (7.46)$$

Combining the three terms in Equation 7.40, we can write a Wick rotation with a Wilson line propagator as a regular Wick rotation plus a correction term \mathcal{W}_P :

Wick Rotation with Wilson Propagator

$$\int \frac{d^\omega k}{(2\pi)^\omega} \frac{1}{n^J \cdot k + i\eta} \frac{1}{k^2 + i\varepsilon} = i \int \frac{d^\omega k_E}{(2\pi)^\omega} \frac{1}{n_E^J \cdot k_E - i\eta} \frac{1}{k_E^2} - i\mathcal{W}_P, \quad (7.47a)$$

$$\mathcal{W}_P = \int \frac{d^{\omega-1} \mathbf{k}}{(2\pi)^{\omega-1}} \frac{|n^0|}{(\mathbf{n} \cdot \mathbf{k} - i\eta)^2 - (n^0 \mathbf{k})^2} \left(\theta(-\mathbf{n} \cdot \mathbf{k}) + \frac{1}{2} \delta(\mathbf{n} \cdot \mathbf{k}) \right). \quad (7.47b)$$

It is interesting to see that the factor $(\theta(-\mathbf{n} \cdot \mathbf{k}) + 1/2 \delta(\mathbf{n} \cdot \mathbf{k}))$ in the definition of \mathcal{W}_P can be replaced by a single θ -function, if we adopt the convention $\theta(0) = 1/2$.

Equations 7.47 easy generalise to the integral of a Wilson line propagator and any function f that doesn't has poles in the first or third quadrants:

$$\int \frac{d^\omega k}{(2\pi)^\omega} \frac{1}{n^J \cdot k + i\eta} f(k) = -i \int \frac{d^\omega k_E}{(2\pi)^\omega} \frac{1}{n_E^J \cdot k_E - i\eta} f(i k_E^0, \mathbf{k}_E) - i\mathcal{W}_P, \quad (7.48)$$

where now \mathcal{W}_P is given by (assuming f is symmetric in k^0):

$$\mathcal{W}_P = \int \frac{d^{\omega-1} \mathbf{k}}{(2\pi)^{\omega-1}} \frac{1}{|n^0|} \left(\theta(-\mathbf{n} \cdot \mathbf{k}) + \frac{1}{2} \delta(\mathbf{n} \cdot \mathbf{k}) \right) f(k) \Big|_{k^0 \rightarrow \frac{1}{n^0} (\mathbf{n} \cdot \mathbf{k} - i\eta)}. \quad (7.49)$$

However, in general \mathcal{W}_P is quite difficult to calculate—especially in dimensional regularisation—because of the angular part in $\mathbf{n} \cdot \mathbf{k}$. In the Section 7.4 we will investigate a more brute-force approach. We can rewrite Equation 7.49 as (adopting the convention $\theta(0) = 1/2$):

$$\mathcal{W}_P = \int \frac{d^\omega \mathbf{k}}{(2\pi)^\omega} f(k) \mathfrak{D}^+(\mathbf{n} \cdot \mathbf{k} + i\eta), \quad (7.50)$$

which we can interpret as the ‘real emission’ of a Wilson line segment. We have argued before (on page 188) that there is no such thing as a cut Wilson segment, so this interpretation cannot be rigorous. Indeed, the \mathfrak{D}^+ implies a θ -function with a complex shift, i.e. $\theta(n^0 k^0 + i\eta)$, which is not well-defined (and we have no trick to deal with it as we did have in the case of a complex δ -function). So we leave Equation 7.50 as a vague physical interpretation without mathematical rigour, at most a curious coincidence.

Light-Cone Coordinates: Double Wick Rotation

When using LC coordinates, we have to make two consecutive Wick rotations, as now the first two components of the momentum have a positive sign. Let us investigate again a general Feynman propagator integral as in [Equation 7.34](#):

$$\int \frac{d^\omega k}{(2\pi)^\omega} \frac{1}{(k^2 - \Delta + i\varepsilon)^n}.$$

Let us first rotate the k^+ component. It has a pole in

$$k^+ = \frac{1}{2k^-} (\mathbf{k}_\perp^2 + \Delta - i\varepsilon),$$

which lies in the second or fourth quadrant, as long as $\Delta \geq -\mathbf{k}_\perp^2$. In the latter case we can safely Wick rotate it by identifying $k^+ = ik_E^+$:

$$\int \frac{d^\omega k}{(2\pi)^\omega} \frac{1}{(k^2 - \Delta + i\varepsilon)^n} = i \int \frac{d^{\omega-1} \mathbf{k} dk_E^+}{(2\pi)^\omega} \frac{1}{(2ik_E^+ k^- - \mathbf{k}_\perp^2 - \Delta + i\varepsilon)^n}.$$

But now the pole of k^- is given by

$$k^- = \frac{1}{2ik_E^+} (\mathbf{k}_\perp^2 + \Delta - i\varepsilon) = \frac{1}{2k_E^+} (-i(\mathbf{k}_\perp^2 + \Delta) - \varepsilon), \quad (7.51)$$

which now lies in the first or third quadrant for $\Delta \geq -\mathbf{k}_\perp^2$. Luckily, this doesn't pose a problem, as this is a second, independent integration, and we can just choose a different contour, like in [Figure 7.4](#). Then we have

$$\oint_C = \int_{C_R} + \int_{C_1} + \int_{C_I} + \int_{C_2} \equiv 0 \quad \Rightarrow \quad \int_{C_R} = - \int_{C_I}, \quad (7.52)$$

as before. But now we don't have to switch the borders of the integral over C_I , so we retain the minus sign. So after making the second Wick rotation by identifying $k^- = ik_E^-$, we have:

$$\int \frac{d^\omega k}{(2\pi)^\omega} \frac{1}{(k^2 - \Delta + i\varepsilon)^n} = (-)^n \int \frac{d^\omega k_E}{(2\pi)^\omega} \frac{1}{(k_E^2 + \Delta)^n}.$$

The only difference with a Wick rotation in Cartesian coordinates is the lack of the i in front. This result was only valid for $\Delta \geq -\mathbf{k}_\perp^2$. But in case $\Delta < -\mathbf{k}_\perp^2$, we just start with the second contour and end with the original contour, to get the same result. So for any function f that scales as $\mathcal{O}(1/k^2)$, we have:

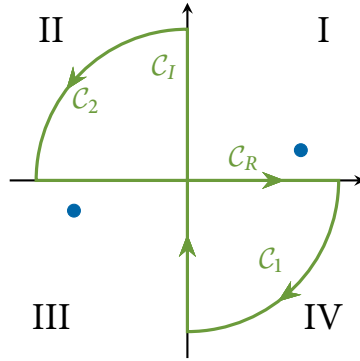


Figure 7.4: The contour chosen for the second Wick rotation when working in LC coordinates. Because of the shift $k^+ = ik_E^+$, the poles have switched quadrants, so the contour needs to be flipped.

Wick Rotation in LC-Coordinates

$$\int \frac{d^\omega k}{(2\pi)^\omega} f(k^2) = \int \frac{d^\omega k_E}{(2\pi)^\omega} f(-k_E^2). \quad (7.53)$$

Adding a Wilson line propagator will however complicate the calculation, as we will get two independent correction terms, one per rotation.

7.4 WILSON INTEGRALS

One common integral when dealing with Wilson lines is the following one:

$$I = \int \frac{d^\omega k}{(2\pi)^\omega} \prod_{i=1}^n \frac{1}{n_i \cdot (k + K_i) + A_i + i\sigma_i \eta} \prod_{j=1}^m \frac{1}{(k + P_j)^2 + B_j + i\epsilon} e^{i r \cdot k}, \quad (7.54)$$

constructed from n ‘linear propagators’ (Wilson line propagators) and m ‘squared propagators’ (regular Feynman propagators). The $+i\epsilon$ are merely pole prescriptions, but the $\pm i\eta$ act as soft regulators and can have positive or negative signs. We encapsulated their sign into the $\sigma_i = \pm 1$ in front, such that we can assert that $\eta > 0$. We also naturally assume $n \geq 1$, $m \geq 1$, and $K_i, P_i, A_i, B_i \in \mathbb{R}$, and will use light-cone coordinates. Furthermore A_i and B_j cannot depend on k .

As this framework to work with Wilson lines has been developed only recent, general results have not yet been reached. In this section, we briefly sketch the

first steps to solve this general integral, and continue with a simpler case, namely that of the LO 2-gluon blob at $r = 0$ (i.e. the two segments are connected). We will use this result in Section 10.2 to calculate the cusp anomalous dimension.

The first step in calculating the integral in Equation 7.54 is to use Schwinger parameterisations (see Equations B.10), and write it as:

$$I = \left(\prod_i^n \sigma_i \right) (-i)^{n+m} \int \frac{d^\omega k}{(2\pi)^\omega} \int_0^\infty d\alpha_1 \cdots d\alpha_n d\beta_1 \cdots d\beta_m e^{i \sum_i^n \sigma_i \alpha_i [n_i \cdot (k + K_i) + A_i] + i \sum_j^m \beta_j [(k + P_j)^2 + B_j] + i r \cdot k - \sum_i^n \alpha_i \eta}.$$

Note that we already took the limit $\varepsilon \rightarrow 0$. We can do this without problem, as it is merely a prescription, telling us which contour to use when doing the integration. Although we didn't use contour integration, the prescription served its purpose: the sign of the Schwinger parameterisation follows the sign of the pole prescription. By completing the square, we rewrite the exponential as

$$\begin{aligned} i \left(\sum \beta_j \right) \left(k + \frac{\sum \beta_j P_j}{\sum \beta_j} + \frac{\sum \sigma_i \alpha_i n_i}{2 \sum \beta_j} + \frac{r}{2 \sum \beta_j} \right)^2 - i \frac{(\sum \beta_j P_j)^2}{\sum \beta_j} - i \frac{(\sum \sigma_i \alpha_i n_i)^2}{4 \sum \beta_j} \\ - i \frac{r^2}{4 \sum \beta_j} - i \frac{\sum \sigma_i \alpha_i \beta_j n_i \cdot P_j}{\sum \beta_j} - i \frac{\sum \sigma_i \alpha_i n_i \cdot r}{2 \sum \beta_j} - i \frac{\sum \beta_j P_j \cdot r}{\sum \beta_j} \\ + i \sum \sigma_i \alpha_i (n_i \cdot K_i + A_i) + i \sum \beta_j (P_j^2 + B_j) - \sum \alpha_i \eta. \end{aligned}$$

After making the shift

$$k \rightarrow k + \frac{\sum \beta_j P_j}{\sum \beta_j} + \frac{\sum \sigma_i \alpha_i n_i}{2 \sum \beta_j} + \frac{r}{2 \sum \beta_j},$$

the k -integration is just a Gaussian, which we can solve by making a Wick rotation:

$$\begin{aligned} \int \frac{d^\omega k}{(2\pi)^\omega} e^{i(\sum \beta_j)k^2} &= i \int \frac{d^\omega k_E}{(2\pi)^\omega} e^{-i(\sum \beta_j)k_E^2}, \\ &= -\frac{i}{(4\pi)^2} (4\pi i)^\varepsilon (\sum \beta_j)^{\varepsilon-2}. \end{aligned}$$

To be mathematically rigorous, we have to mention that a purely imaginary Gaussian integral is divergent. Luckily, this is easily solved by regulating the integral with an infinitesimal negative shift:

$$\lim_{\varepsilon \rightarrow 0} \int \frac{d^\omega k_E}{(2\pi)^\omega} e^{-i[(\sum \beta_j) - i\delta]k_E^2} \quad (7.55)$$

The validity of regulating an integral (and taking the limit $\delta \rightarrow 0$) in the middle of a calculation can be questioned. But in dimensional regularisation it can be proven that all complex Gaussian integrals are well-defined, even when purely imaginary [31]. The result so far is

$$I = \left(\prod_i^n \sigma_i \right) (-i)^{n+m+1} \frac{(4\pi i)^\epsilon}{(4\pi)^2} \int_0^\infty d\alpha_1 \cdots d\alpha_n d\beta_1 \cdots d\beta_m \left(\sum \beta_j \right)^{\epsilon-2} e^{iE}, \quad (7.56)$$

where the exponent is given by:

$$E = \sum_i^n \alpha_i [\sigma_i (n_i \cdot K_i + A_i) + i\eta] + \sum_j^m \beta_j [P_j^2 + B_j] - \frac{(\sum \beta_j P_j)^2}{\sum \beta_j} - \frac{(\sum \sigma_i \alpha_i n_i)^2}{4 \sum \beta_j} - \frac{r^2}{4 \sum \beta_j} - \frac{\sum \sigma_i \alpha_i \beta_j n_i \cdot P_j}{\sum \beta_j} - \frac{\sum \sigma_i \alpha_i n_i \cdot r}{2 \sum \beta_j} - \frac{\sum \beta_j P_j \cdot r}{\sum \beta_j}. \quad (7.57)$$

The appearance of a lot of factors of the form $(\sum \beta_j)$ is a hint for the next step: we will make the substitution $\beta_j = y_j L$, such that $\sum \beta_j = L$ (see [Equations B.11](#)). The integral then becomes:

$$I = \mathcal{N} \int_0^\infty d\alpha_1 \cdots d\alpha_n d y_1 \cdots d y_m dL \delta(1 - \sum y_j) L^{m+\epsilon-3} e^{iE}, \quad (7.58)$$

where \mathcal{N} and the exponent are:

$$\mathcal{N} = \left(\prod_i^n \sigma_i \right) (-i)^{n+m+1} \frac{(4\pi i)^\epsilon}{(4\pi)^2}, \quad (7.59)$$

$$E = \sum_i^n \alpha_i [\sigma_i (n_i \cdot K_i + A_i) + i\eta] + L \sum_j^m y_j (P_j^2 + B_j) - L (\sum y_j P_j)^2 - \frac{1}{4L} (r + \sum \sigma_i \alpha_i n_i)^2 - \sum \sigma_i \alpha_i y_j n_i \cdot P_j - \sum y_j P_j \cdot r. \quad (7.60)$$

From this point on, things are getting a bit more difficult, as the exponent contains terms linear in L , but terms linear in $1/L$ as well. We continue with a much easier situation, viz. that of an **LO** 2-gluon blob connecting 2 adjoining segments.

2-Gluon Blob Connecting Two Adjoining Segments

The integral we need to calculate is given by (see [Equation 7.24b](#)):

$$\mathcal{W}_{11}^{JK} = -g^2 n_K^{\mu_1} n_J^{\mu_2} \mu^{2\epsilon} \int \frac{d^\omega k}{(2\pi)^\omega} \frac{e^{i(r^K - r^J) \cdot k}}{n^K \cdot k + i\eta} \frac{1}{n^J \cdot k - i\eta} D_{\mu_1 \nu}(k). \quad (7.61)$$

This is a specific form of our ‘master’ integral, with

$$n = 2, \quad m = 1, \quad K_i = 0, \quad A_i = 0, \quad P_j = 0, \quad (7.62a)$$

$$B_j = 0, \quad r = r^K - r^J, \quad \sigma_K = +1, \quad \sigma_J = -1. \quad (7.62b)$$

Our result so far in this specific example is then

$$\mathcal{W}_{11}^{JK} = -i g^2 n_K \cdot n_J \mu^{2\epsilon} \frac{(4\pi i)^\epsilon}{(4\pi)^2} \int_0^\infty d\alpha_1 d\alpha_2 d\beta \beta^{\epsilon-2} e^{iE}, \quad (7.63)$$

where the exponent is given by:

$$E = -\frac{1}{4\beta} (\alpha_1 n_K - \alpha_2 n_J + r)^2 + i\alpha_1 \eta + i\alpha_2 \eta. \quad (7.64)$$

We now make the substitution

$$\tilde{\beta} = \frac{1}{\beta}, \quad d\tilde{\beta} = -\frac{1}{\beta^2} d\beta.$$

This gives (dropping the factors in front):

$$I = \int_0^\infty d\alpha_1 d\alpha_2 d\tilde{\beta} \tilde{\beta}^{-\epsilon} e^{-\frac{1}{4}\tilde{\beta}(\alpha_1 n_K - \alpha_2 n_J + r)^2 - \alpha_1 \eta - \alpha_2 \eta}.$$

This is a complex Γ representation (see [Equations B.6](#)), which is convergent for $0 < \epsilon < 1$. The result is now:

$$I = \Gamma(1 - \epsilon) (-4i)^{1-\epsilon} \int_0^\infty d\alpha_1 d\alpha_2 (\alpha_1^2 n_K^2 + \alpha_2^2 n_J^2 + r^2 - 2\alpha_1 \alpha_2 n_K \cdot n_J + 2\alpha_1 n_K \cdot r - 2\alpha_2 n_J \cdot r)^{\epsilon-1} e^{-\alpha_1 \eta - \alpha_2 \eta}.$$

Next we again use x - L parameterisation :

$$\alpha_1 = xL, \quad \alpha_2 = (1-x)L, \quad L = 0 \dots \infty, \quad x = 0 \dots 1, \quad d\alpha_1 d\alpha_2 = dx dL L,$$

which gives:

$$I = \Gamma(1 - \epsilon) (-4i)^{1-\epsilon} \int_0^1 dx \int_0^\infty dL L [L(xn_K - \bar{x}n_J) + r]^{2(\epsilon-1)} e^{-L\eta}, \quad (7.65)$$

where \bar{x} is just a short-hand notation:

$$\bar{x} \stackrel{N}{=} 1 - x. \quad (7.66)$$

Now we apply the additional demand that the Wilson segments are adjoining, viz. $r_K = r_J$ and hence $r = 0$. The L integration is then again a Gamma function integral representation, and gives a factor $\eta^{-2\epsilon} \Gamma(2\epsilon)$:

$$I = \Gamma(1 - \epsilon) \Gamma(2\epsilon) \left(\frac{1}{\eta^2} \right)^\epsilon (-4i)^{1-\epsilon} \int_0^1 dx (xn_K - \bar{x}n_J)^{2(\epsilon-1)}. \quad (7.67)$$

In the case of on-LC segments, i.e. $n_K^2 = n_J^2 = 0$, the x -integral is just a Beta function (see Equation B.7a):

$$\begin{aligned} \int_0^1 dx (xn_K - \bar{x}n_J)^{2(\epsilon-1)} &= (-2n_K \cdot n_J)^{\epsilon-1} \int_0^1 dx x^{\epsilon-1} \bar{x}^{\epsilon-1}, \\ &= (-2n_K \cdot n_J)^{\epsilon-1} B(\epsilon, \epsilon), \\ &= (-2n_K \cdot n_J)^{\epsilon-1} \frac{\Gamma(\epsilon) \Gamma(\epsilon)}{\Gamma(2\epsilon)}. \end{aligned} \quad (7.68)$$

We just have to collect all missing factors from the intermediate steps to get the on-LC result. From Equation 7.63 we have a factor

$$-i g^2 n_K \cdot n_J \mu^{2\epsilon} \frac{(4\pi i)^\epsilon}{(4\pi)^2}.$$

Next we have from Equation 7.67 a factor

$$-4i \Gamma(1 - \epsilon) \Gamma(2\epsilon) \left(-\frac{1}{4i \eta^2} \right)^\epsilon,$$

and last we have the $\overline{\text{MS}}$ subtraction (which is a division by S_ϵ , see Equation 4.65) that gives an extra $\Gamma(1 - \epsilon)/(4\pi)^\epsilon$. These three factors together give:

$$-\frac{\alpha_s}{\pi} n_K \cdot n_J \Gamma(1 - \epsilon) \Gamma(1 - \epsilon) \Gamma(2\epsilon) \left(-\frac{1}{4} \frac{\mu^2}{\eta^2} \right)^\epsilon. \quad (7.69)$$

The full on-LC result is then

$$\mathcal{W}_{11}^{JK}|_{\text{LC}} = \frac{\alpha_s}{2\pi} \Gamma(1 - \epsilon) \Gamma(1 - \epsilon) \Gamma(\epsilon) \Gamma(\epsilon) \left(\frac{n_K \cdot n_J}{2} \frac{\mu^2}{\eta^2} \right)^\epsilon. \quad (7.70)$$

Expanding in function of the regulator gives our final result for the 2-gluon blob at LO connecting two adjoining on-LC segments:

2-Gluon Blob Connecting 2 On-LC Segments

$$\mathcal{W}_{11}^{JK}|_{\text{LC}} = \frac{\alpha_s}{2\pi} \left[\frac{1}{\epsilon^2} + \frac{1}{\epsilon} \left(\ln \frac{n_K \cdot n_J}{2} + \ln \frac{\mu^2}{\eta^2} \right) + \frac{1}{2} \left(\ln \frac{n_K \cdot n_J}{2} + \ln \frac{\mu^2}{\eta^2} \right)^2 + \frac{\pi^2}{3} \right]. \quad (7.71)$$

Note that the convention in Equation 4.65 subtracts the most finite terms possible when having a double pole. This is due to the fact that

$$\Gamma(1-\epsilon)\Gamma(1-\epsilon)\Gamma(\epsilon)\Gamma(\epsilon) = \frac{1}{\epsilon^2} + \frac{\pi^2}{3} + \mathcal{O}(\epsilon^2). \quad (7.72)$$

If we would use the regular convention as in Equation 4.64, the subtraction would be less strong because

$$(e^{-\gamma_E})^\epsilon \Gamma(1-\epsilon)\Gamma(\epsilon)\Gamma(\epsilon) = \frac{1}{\epsilon^2} - \frac{1}{\epsilon} 2\gamma_E + 2\gamma_E^2 + \frac{\pi^2}{4} + \mathcal{O}(\epsilon),$$

which leaves an extra pole term and an extra term with γ_E . Also note that although the result seems to be divergent in the limit $n_K \cdot n_J \rightarrow 0$, this is perfectly finite. The seemingly divergent behaviour is an artefact from the regulation. If $n_K \cdot n_J = 0$, the original contribution in Equation 7.24b is zero before we need to start a regulation procedure.

Now we will repeat this calculation, starting from Equation 7.67, but with off-LC segments. If $n_K^2, n_J^2 \neq 0$, we can parameterise the scalar product in function of a Minkowskian angle χ between the two segments:

$$\cosh \chi \stackrel{\text{def}}{=} \frac{n_K \cdot n_J}{|n_K| |n_J|}, \quad (7.73)$$

so that we can rewrite

$$(xn_K - \bar{x}n_J)^2 \equiv x^2 n_K^2 - 2x\bar{x}n_K n_J \cosh \chi + \bar{x}^2 n_J^2, \quad (7.74)$$

where now $n_K \stackrel{N}{=} |n_K|$. We will rewrite the x -integral in function of a new angle ψ , that we introduce by the relation:

$$xn_K \sinh \psi = \bar{x}n_J \sinh(\chi + \psi). \quad (7.75)$$

Or in other words:

$$x = \frac{n_J \sinh(\chi + \psi)}{n_K \sinh \psi + n_J \sinh(\chi + \psi)}, \quad (7.76a)$$

$$\bar{x} = \frac{n_K \sinh \psi}{n_K \sinh \psi + n_J \sinh(\chi + \psi)}, \quad (7.76b)$$

$$\psi = \operatorname{arcoth} \left[\operatorname{csch} \chi \frac{x n_K}{\bar{x} n_J} - \coth \chi \right], \quad (7.76c)$$

$$= \frac{1}{2} \ln \frac{x n_K - \bar{x} n_J e^{-\chi}}{x n_K - \bar{x} n_J e^{\chi}}, \quad (7.76d)$$

where we used the hyperbolic sum rule

$$\sinh(\chi + \psi) = \sinh \chi \cosh \psi + \sinh \psi \cosh \chi. \quad (7.77)$$

We can now simplify

$$\begin{aligned} (x n_K - \bar{x} n_J)^2 &= x^2 n_K^2 - 2x \bar{x} n_K n_J \cosh \chi + \bar{x}^2 n_J^2, \\ &= \frac{n_K^2 n_J^2 \sinh^2 \chi}{(n_K \sinh \psi + n_J \sinh(\chi + \psi))^2}. \end{aligned}$$

To make the integral substitution, we first note that

$$\begin{aligned} d\psi &= -n_K n_J \frac{\sinh \chi}{(x n_K - \bar{x} n_J)^2} dx, \\ \psi(x=0) &= -\chi \quad \psi(x=1) = 0, \end{aligned}$$

giving eventually:

$$\int_0^1 dx (x n_K - \bar{x} n_J)^{2(\epsilon-1)} = -(n_K n_J \sinh \chi)^{2\epsilon-1} \int_{-\chi}^0 d\psi (n_K \sinh \psi + n_J \sinh(\chi + \psi))^{-2\epsilon}.$$

To calculate this integral, we expand it in ϵ :

$$\int_{-\chi}^0 d\psi (n_K \sinh \psi + n_J \sinh(\chi + \psi))^{-2\epsilon} = \chi + 2\epsilon \int_0^{-\chi} d\psi \ln [n_K \sinh \psi + n_J \sinh(\chi + \psi)].$$

Using the exponential representation of the hyperbolic sine, i.e.

$$\sinh \psi = \frac{1}{2} (e^{\psi} - e^{-\psi}), \quad (7.78)$$

we rewrite the argument of the logarithm as

$$\begin{aligned} \ln [n_K \sinh \psi + n_J \sinh(\chi + \psi)] &= \ln \frac{1}{2} e^\psi [n_K + n_J e^\chi - (n_K + n_J e^{-\chi}) e^{-2\psi}], \\ &= -\ln 2 + \psi + \ln [n_K + n_J e^\chi - (n_K + n_J e^{-\chi}) e^{-2\psi}]. \end{aligned}$$

The integral over the first terms is trivial. Using the short-hand notations $a = n_K + n_J e^\chi$ and $b = n_K + n_J e^{-\chi}$, the integral over the logarithm can be done by making the substitution $t = -b e^{-2\psi}$. We have (see [Equation B.2e](#)):

$$\begin{aligned} -\frac{1}{2} \int_{-b e^{2\chi}}^{-b} dt \frac{\ln(a+t)}{t} &= \frac{1}{2} \left[\ln b e^{2\chi} \ln a - \text{Li}_2 \left(\frac{b e^{2\chi}}{a} \right) - \ln b \ln a + \text{Li}_2 \left(\frac{b}{a} \right) \right], \\ &= \chi \ln (n_K + n_J e^\chi) + \frac{1}{2} \left[\text{Li}_2 \left(\frac{n_K + n_J e^{-\chi}}{n_K + n_J e^\chi} \right) - \text{Li}_2 \left(\frac{n_J + n_K e^\chi}{n_J + n_K e^{-\chi}} \right) \right]. \end{aligned}$$

We can require n_K and n_J to have the same length, i.e. $|n_K| \equiv |n_J|$, because it is just a path parameterisation where only their direction matters (and their length is not zero). Then the result simplifies into

$$\chi \ln n_K + \chi \ln (1 + e^\chi) - \frac{1}{2} (\text{Li}_2 e^\chi - \text{Li}_2 e^{-\chi}).$$

So the final result for the x -integration is then

$$\int_0^1 dx (x n_K - \bar{x} n_J)^{2(\epsilon-1)} = -\frac{(n_K^2 n_J^2 \sinh^2 \chi)^\epsilon}{n_K n_J \sinh \chi} \chi (1 + \epsilon \Upsilon), \quad (7.79a)$$

$$\Upsilon = 2 \ln 2 + \ln n_K^2 + 2 \ln (1 + e^\chi) + \chi - \frac{1}{\chi} (\text{Li}_2 e^\chi - \text{Li}_2 e^{-\chi}). \quad (7.79b)$$

Now we add the missing factors from the intermediate steps (see [Equation 7.69](#)). We will write $n_K \cdot n_J$ in function of the Minkowskian angle, i.e. $n_K \cdot n_J = n_K n_J \cosh \chi$, which will combine with the $1/\sinh \chi$ into a $\coth \chi$. This gives:

$$\frac{\alpha_s}{\pi} \chi \coth \chi \Gamma(1-\epsilon) \Gamma(1-\epsilon) \Gamma(2\epsilon) \left(-\frac{n_K^2 n_J^2}{4} \sinh^2 \chi \frac{\mu^2}{\eta^2} \right)^\epsilon (1 + \epsilon \Upsilon). \quad (7.80)$$

To allow for an easy comparison with the on-LC case, we rewrite the sinh inside the ϵ exponential as

$$-n_K^2 n_J^2 \sinh^2 \chi = n_K^2 n_J^2 (1 - \cosh^2 \chi) = n_K^2 n_J^2 - (n_K \cdot n_J)^2.$$

Expanding in function of ϵ , the result becomes:

2-Gluon Blob Connecting 2 Off-LC Segments

$$\mathcal{W}_{11}^{JK}|_{\pm\epsilon} = \frac{\alpha_s}{2\pi} \chi \coth \chi \left[\frac{1}{\epsilon} + \ln \frac{n_K^2 n_J^2 - (n_K \cdot n_J)^2}{4} + \ln \frac{\mu^2}{\eta^2} + \Upsilon \right]. \quad (7.81)$$

When comparing to the on-LC result in Equation 7.71, we see that the most important difference is that in the on-LC case there is a double pole in ϵ that is not present in the off-LC case. This is true in general: light-like Wilson line segments will introduce additional divergences. Indeed, if one of the segments—or both—goes on-LC, the angle becomes infinite:

$$\chi = \operatorname{arcosh} \frac{n_K \cdot n_J}{|n_K| |n_J|} \sim -\log(|n_K| |n_J|) \xrightarrow{\text{on-LC}} \infty. \quad (7.82)$$

This is the key manifestation of LC-divergences. There is no way of retrieving the on-LC-result from the off-LC result, as we are missing a double pole and mixed terms.

Another possibility is a situation where one of the segments is on-LC and the other is not. This is a bit complicated, as the Minkowskian angle is still not well-defined, but neither can we use the Beta function integral representation as we were able to in the on-LC case (see Equation 7.68). Luckily, using a bit of trickery we can do something similar using the incomplete Beta function (see Equation B.7c). We start again from Equation 7.67, but assume now that $n_J^2 = 0$. It doesn't matter which segment we take on-LC, the results are the same, but when choosing $n_J^2 = 0$, the term with \bar{x} drops from the calculation, which is easier. The x -integration is now:

$$\begin{aligned} \int_0^1 dx (x n_K - \bar{x} n_J)^{2(\epsilon-1)} &= \int_0^1 dx (x^2 n_K^2 - 2x\bar{x} n_K \cdot n_J)^{\epsilon-1}, \\ &= (2n_K \cdot n_J)^{\epsilon-1} \int_0^1 dx x^{\epsilon-1} \left(\frac{2n_K \cdot n_J + n_K^2}{2n_K \cdot n_J} x - 1 \right)^{\epsilon-1}. \end{aligned}$$

Next we make the substitution

$$t = \frac{2n_K \cdot n_J + n_K^2}{2n_K \cdot n_J} x \stackrel{N}{=} \tilde{n} x, \quad \Rightarrow \quad dx = \frac{1}{\tilde{n}} dt,$$

which gives

$$\begin{aligned} \int_0^1 dx (xn_K - \bar{x}n_J)^{2(\epsilon-1)} &= (2n_K \cdot n_J)^{\epsilon-1} \frac{1}{\tilde{n}^\epsilon} \int_0^{\tilde{n}} dt t^{\epsilon-1} (t-1)^{\epsilon-1}, \\ &= (2n_K \cdot n_J)^{\epsilon-1} \frac{1}{\tilde{n}^\epsilon} B(\tilde{n}; \epsilon, \epsilon). \end{aligned} \quad (7.83)$$

$B(\tilde{n}; \epsilon, \epsilon)$ is the incomplete Beta function. It has a series expansion given by [Equation B.7f](#):

$$B(\tilde{n}; \epsilon, \epsilon) = \frac{1}{\epsilon} \tilde{n}^\epsilon (1 - \tilde{n})^\epsilon \left(1 + \sum_{m=0}^{\infty} \frac{B(\epsilon+1, m+1)}{B(2\epsilon, m+1)} \tilde{n}^{m+1} \right). \quad (7.84)$$

We can expand the fraction of the two Beta functions, which we have to do up to second order in ϵ (because we have a double pole, one in front of the Beta function expansion and one from $\Gamma(2\epsilon)$ in [Equation 7.67](#)):

$$\begin{aligned} \frac{B(\epsilon+1, m+1)}{B(2\epsilon, m+1)} &= \frac{\Gamma(\epsilon+1) \Gamma(2\epsilon+m+1)}{\Gamma(2\epsilon) \Gamma(\epsilon+m+2)}, \\ &\approx 2\epsilon \frac{1}{m+1} + 2\epsilon^2 \left[\frac{1}{m+1} \left(\sum_k^m \frac{1}{k} \right) - \frac{1}{(m+1)^2} \right]. \end{aligned} \quad (7.85)$$

The infinite sums running over m are just straightforward convergent series. The first and the last are just the first and the second polylogarithms (see [Equation B.8a](#) and [Equations B.8](#)), while the second sum is a bit less trivial as it is a chained sum:

$$\sum_{m=0}^{\infty} \frac{\tilde{n}^{m+1}}{m+1} = \sum_{m=1}^{\infty} \frac{\tilde{n}^m}{m} = \text{Li}_1(\tilde{n}) = -\ln(1 - \tilde{n}), \quad (7.86a)$$

$$\sum_{m=0}^{\infty} \frac{\tilde{n}^{m+1}}{(m+1)^2} = \sum_{m=1}^{\infty} \frac{\tilde{n}^m}{m^2} = \text{Li}_2(\tilde{n}), \quad (7.86b)$$

$$\sum_{m=0}^{\infty} \frac{\tilde{n}^{m+1}}{m+1} \sum_k^m \frac{1}{k} = \frac{1}{2} \ln^2(1 - \tilde{n}). \quad (7.86c)$$

So the expansion of the incomplete Beta function is now:

$$B(\tilde{n}; \epsilon, \epsilon) \approx \frac{1}{\epsilon} \tilde{n}^\epsilon (1 - \tilde{n})^\epsilon \left[1 - 2\epsilon \ln(1 - \tilde{n}) + \epsilon^2 \ln^2(1 - \tilde{n}) - 2\epsilon^2 \text{Li}_2(\tilde{n}) \right].$$

Putting everything together, we have (adding the factor in front from [Equation 7.69](#)):

$$-\frac{\alpha_s}{2\pi} \Gamma(1-\epsilon) \Gamma(1-\epsilon) \Gamma(2\epsilon) \frac{1}{\epsilon} \left(\frac{n_K^2 \mu^2}{4 \eta^2} \right)^\epsilon \left[1 + 2\epsilon \ln \left(-\frac{2n_K \cdot n_J}{n_K^2} \right) + \epsilon^2 \tilde{B} \right], \quad (7.87)$$

with

$$\tilde{B} = \ln^2 \left(-\frac{2n_K \cdot n_J}{n_K^2} \right) - 2 \operatorname{Li}_2 \left(\frac{2n_K \cdot n_J + n_K^2}{2n_K \cdot n_J} \right).$$

Giving the final result:

2-Gluon Blob Connecting an Off-LC Segment to an On-LC Segment

$$\mathcal{W}_{11}^{JK} \Big|_{\frac{1}{2}\text{LG}} = -\frac{\alpha_s}{4\pi} \left[\frac{1}{\epsilon^2} + \frac{1}{\epsilon} \left(\ln \frac{(n_K \cdot n_J)^2}{n_K^2} + \ln \frac{\mu^2}{\eta^2} \right) + \text{fin.} \right], \quad (7.88)$$

where the finite terms are given by:

$$\begin{aligned} \ln^2 \left(-\frac{n_K \cdot n_J}{2} \right) - \ln^2 \frac{n_K^2}{4} + \frac{1}{2} \left(\ln \frac{n_K^2}{4} - \ln \frac{\mu^2}{\eta^2} \right)^2 \\ + \ln \frac{(n_K \cdot n_J)^2}{4} \ln \frac{\mu^2}{\eta^2} - 2 \operatorname{Li}_2 \left(\frac{2n_K \cdot n_J + n_K^2}{2n_K \cdot n_J} \right) + \frac{\pi^2}{2} \quad (7.89) \end{aligned}$$

To conclude: general results are not that straightforward to calculate as they might seem at first sight, because the integrals at hand are quickly getting involving. On the other hand, once calculated in a given gauge, they never have to be calculated again as the results can be easily applied to any Wilson line structure using the framework developed in the previous chapter.

INTRODUCTION TO TMDS

In this chapter, we will give a brief review of the basics of the **TMD** formalism. We investigate situations where the common collinear factorisation as introduced in [Sections 5.2](#) and [5.3](#) is no longer adequate, and has to be replaced by a new factorisation approach that introduces transverse momentum dependence in the **PDF**. The main goal is to have a good description for processes that are not fully inclusive, but where e.g. a final hadron is identified. In such a process we cannot integrate over \mathbf{k}_\perp because the final hadron will have a manifest \mathbf{k}_\perp -dependence.

We start this chapter with a revision of **DIS**, where we now can construct a gauge-invariant operator definition for the **PDFs**. Then we move to a less inclusive experimental setup, viz. **SIDIS**, and introduce **PDFs** that are \mathbf{k}_\perp -dependent, the so-called **TMDs**, and construct operator definitions for these as well. In the last section of this chapter, we investigate the evolution of **TMDs**, and construct equations that will be used similarly to the **DGLAP** equations in the collinear case.

As always, we don't go too much into detail but try to give a broad picture. The formalism of **TMDs** has gone through a lot of evolution in twenty years. They were originally introduced in e.g. [[43–47](#)], later adapted into a gauge-invariant approach [[48–56](#)], and the most recent definitions are found in e.g. [[33, 57–64](#)]. For a good treatment of the renormalisation of **TMDs**, see e.g. [[65–70](#)].

8.1 REVISION OF DIS

Before we start with the investigation of the **TMD** framework, we will review **DIS** in a more formal way. This will allow us to construct gauge-invariant operator definitions for the **PDFs**, which will show to be indicative for the construction of **TMDs** later on.

Operator Definition for PDFs

As we have shown in [Section 5.1](#), we can assume that the photon scatters off a quark with mass m inside the proton, if Q^2 is sufficiently large. The final state can therefore be split in a quark with momentum p and the full remaining state with momentum p_X . Constructing the (unpolarised) hadronic tensor ([Equation 5.32](#)) for this setup is straightforward. First we remark that pulling a quark out of the proton at a spacetime point $(0^+, 0^-, \mathbf{0}_\perp)$ is simply $\psi_\alpha(0) |P\rangle$. Then we construct the diagram for the hadronic tensor, the so-called ‘handbag diagram’, step-by-step:

$$\begin{aligned}
 & \text{Diagram 1: } \langle X | \psi_\alpha(0) | P \rangle, \\
 & \text{Diagram 2: } \bar{u}_\beta^\lambda(p) (\gamma^\nu)^{\beta\alpha} \langle X | \psi_\alpha(0) | P \rangle, \\
 & \text{Diagram 3: } \sim [\gamma^\mu (\not{p} + m) \gamma^\nu]^{\beta\alpha} \langle P | \bar{\psi}_\beta(0) | X \rangle \langle X | \psi_\alpha(0) | P \rangle,
 \end{aligned}$$

where we omitted the prefactor, sums and integrations over X and p and the δ -function. Including these, the full hadronic tensor is given by

$$\begin{aligned}
 W^{\mu\nu} = & \frac{1}{4\pi} \sum_q e_q^2 \int_X \int \frac{d^3\mathbf{p}}{(2\pi)^3 2p^0} \int d^4z e^{i(P+q-p_X-p)\cdot z} \\
 & \times [\gamma^\mu (\not{p} + m) \gamma^\nu]^{\beta\alpha} \langle P | \bar{\psi}_\beta(0) | X \rangle \langle X | \psi_\alpha(0) | P \rangle, \quad (8.1)
 \end{aligned}$$

where \int_X is defined in [Equation 5.35](#). Next we replace the integral over p with an on-shell condition

$$\int \frac{d^3\mathbf{p}}{(2\pi)^3 2p^0} \rightarrow \int \frac{d^4p}{(2\pi)^4} \delta^+(p^2 - m^2),$$

where δ^+ is defined in Equation A.57. We introduce the momentum $k = p - q$, giving

$$W^{\mu\nu} = \frac{1}{4\pi} \sum_q e_q^2 \int_X \int \frac{d^4k}{(2\pi)^3} \delta^+((k+q)^2 - m^2) \int d^4z e^{i(P-k-p_X)\cdot z} \\ \times [\gamma^\mu (\not{k} + \not{q} + m) \gamma^\nu]^{\beta\alpha} \langle P | \bar{\psi}_\beta(0) | X \rangle \langle X | \psi_\alpha(0) | P \rangle .$$

Now the next steps are the same as in Equation 5.33, using the translation operator and the completeness relation:

Hadron Tensor and Quark Correlator

$$W^{\mu\nu} = \frac{1}{2} \sum_q e_q^2 \int d^4k \delta^+((k+q)^2) \text{Tr}(\Phi_q \gamma^\mu (\not{k} + \not{q}) \gamma^\nu) , \quad (8.2a)$$

$$\Phi_{\alpha\beta}^q \stackrel{\text{N}}{=} \int \frac{d^4z}{(2\pi)^4} e^{-ik\cdot z} \langle P | \bar{\psi}_\beta(z) \psi_\alpha(0) | P \rangle . \quad (8.2b)$$

Φ is the *quark correlator*, which will be used as a basic building brick to construct PDFs. Note that its Dirac indices are defined in a reversed way, this is deliberately to set the trace right. This result is quite a general result, valid for a range of processes.

Using Equation 5.13 and neglecting terms of $\mathcal{O}(1/Q)$, we can approximate the δ -function in Equation 8.2a as

$$\delta((k+q)^2) \approx P^+ \delta(\xi - x) ,$$

which again sets $\xi \equiv x$ as in the FPM. This then gives

$$W^{\mu\nu} \approx \frac{1}{4} \sum_q e_q^2 \text{Tr} \left(\Phi^q(x) \gamma^\mu \frac{P^+}{P\cdot q} (\not{k} + \not{q}) \gamma^\nu \right) , \quad (8.3)$$

where the integrated quark correlator is defined as

$$\Phi(x) = \int dk^- d^2\mathbf{k}_\perp \Phi(x, k^-, \mathbf{k}_\perp) , \\ = \frac{1}{2\pi} \int dz^- e^{-ixP^+z^-} \langle P | \bar{\psi}_\beta(0^+, z^-, \mathbf{0}_\perp) \psi_\alpha(0) | P \rangle . \quad (8.4)$$

A last simplification that we can make is to assume that the outgoing quark is moving largely in the minus direction; $k^\mu + q^\mu \approx k^- + q^-$. This is easily understood in the infinite momentum frame, where the quark ricochets back after being

struck head-on by the photon. However, it is a valid simplification in any frame, which can be shown by making a $\frac{1}{Q}$ expansion of $W^{\mu\nu}$.

With this assumption we get

$$\begin{aligned} \frac{P^+}{P \cdot q} (\not{k} + \not{q}) &\approx \gamma^+ \frac{P^+}{P \cdot q} \left(\frac{k^2 + \mathbf{k}_\perp^2}{2\xi P^+} + q^- \right), \\ &\approx 1, \end{aligned}$$

giving the final result for the unpolarised hadron tensor in DIS at leading twist (this means up to $\mathcal{O}\left(\frac{1}{Q}\right)$):

$$W^{\mu\nu} \approx \frac{1}{4} \sum_q e_q^2 \text{Tr}(\Phi^q(x) \gamma^\mu \gamma^+ \gamma^\nu). \quad (8.5)$$

Now let us investigate the unintegrated quark correlator Equation 8.2b a bit deeper. Since it is a Dirac matrix, we can expand it in function of Lorentz vectors, pseudovectors and Dirac matrices. The variables on which it depends are p^μ , P^μ and S^μ (the latter is a pseudovector in the case of fermionic hadrons). Our basis is then (see Equation A.28) spanned by

$$\{p^\mu, P^\mu, S^\mu\} \otimes \{\mathbb{1}, \gamma^5, \gamma^\mu, \gamma^\mu \gamma^5, \gamma^{\mu\nu}\},$$

where $\gamma^{\mu\nu} = \gamma^{[\mu} \gamma^{\nu]}$. The next steps go completely analogously to our derivation of the structure functions from the hadron tensor in Subsection A More Formal Approach on page 127 and onwards. The conditions to satisfy are

$$\text{Hermiticity:} \quad \Phi(p, P, S) \equiv \gamma^0 \Phi^\dagger(p, P, S) \gamma^0, \quad (8.6a)$$

$$\text{Parity:} \quad \Phi(p, P, S) \equiv \gamma^0 \Phi(\tilde{p}, \tilde{P}, -\tilde{S}) \gamma^0. \quad (8.6b)$$

For instance the integrated quark correlator can be expanded up to leading twist as

$$\Phi(x, P, S) = \frac{1}{2} \left(f_1(x) \gamma^- + g_{1L}(x) S_L \gamma^5 \gamma^- + \frac{1}{2} h_1(x) [\not{S}_T, \gamma^-] \gamma^5 \right), \quad (8.7)$$

where the three integrated PDFs f_1 , g_{1L} and h_1 are the unpolarised resp. helicity resp. transversity distributions. They can be recovered from the quark correlator by projecting on the correct gamma matrix:

$$f_1 = \frac{1}{2} \text{Tr}(\Phi \gamma^+), \quad (8.8a)$$

$$g_{1L} = \frac{1}{2} \text{Tr}(\Phi \gamma^+ \gamma^5), \quad (8.8b)$$

$$h_1 = \frac{1}{2} \text{Tr}(\Phi \gamma^+ \gamma^5 \not{S}). \quad (8.8c)$$

Gauge Invariant Operator Definition

A general Dirac field transforms under a non-Abelian gauge transformation as (see Equation 2.47a):

$$\psi(x) \rightarrow e^{ig\alpha^a(x)t^a} \psi(x) \quad (8.9a)$$

$$\bar{\psi}(x) \rightarrow \bar{\psi}(x) e^{-ig\alpha^a(x)t^a}. \quad (8.9b)$$

As a result, the quark correlator is not gauge-invariant:

$$\Phi \rightarrow \int \frac{d^4z}{(2\pi)^4} e^{-ik \cdot z} \langle P | \bar{\psi}_\beta(z) e^{-ig\alpha^a(z)t^a} e^{ig\alpha^a(0)t^a} \psi_\alpha(0) | P \rangle.$$

But we know from Equation 6.4d that a Wilson line $\mathcal{U}_{(x;y)}$ transforms as

$$\mathcal{U}_{(x;y)} \rightarrow e^{ig\alpha^a(x)t^a} \mathcal{U}_{(x;y)} e^{-ig\alpha^a(y)t^a}.$$

Hence the following definition for the quark correlator is gauge-invariant:

Gauge Invariant Quark Correlator

$$\Phi \stackrel{\text{def}}{=} \int \frac{d^4z}{(2\pi)^4} e^{-ik \cdot z} \langle P | \bar{\psi}_\beta(z) \mathcal{U}_{(z;0)} \psi_\alpha(0) | P \rangle. \quad (8.10)$$

Note that the gauge transformation of \mathcal{U} only depends on its endpoints. Although the latter are fully fixed by the quark correlator, there is still freedom in the choice of the path, influencing the result. The gauge-invariant correlator is thus path dependent, because of the path dependence of the underlying Wilson line. This will play a big role when working with the \mathbf{k}_\perp -dependent correlator, which we will investigate further in Section 8.2.

Although the requirement of gauge invariance for the correlator leaves the path unspecified, it is the precise development of factorisation proofs that uniquely dictates which path should be used in the definition of PDFs. For the integrated quark correlator the path is separated along the z^- direction, as in Equation 8.4, which leads to a straightforward Wilson line structure:¹

$$\Phi(x) = \frac{1}{2\pi} \int dz^- e^{-ixP^+z^-} \langle P | \bar{\psi}_\beta(0^+, z^-, \mathbf{0}_\perp) \mathcal{U}_{(z;0)}^- \psi_\alpha(0) | P \rangle,$$

$$\mathcal{U}_{(z;0)}^- = \mathcal{P} e^{-ig \int_0^{z^-} d\lambda A^+(0^+, \lambda, \mathbf{0}_\perp)} \quad (\text{because } n^- \cdot A = A^+).$$

¹ In the context of PDFs, Wilson lines are commonly called *gauge links*. We won't use this terminology in this thesis.

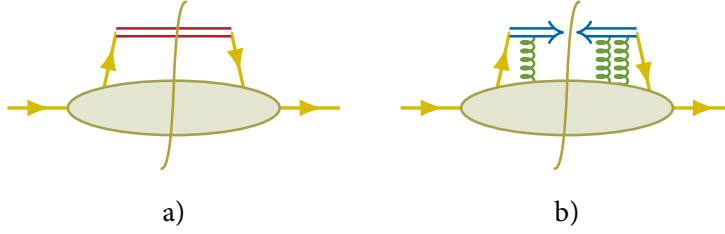


Figure 8.1: a) The gauge invariant quark correlator function, with a cut Wilson line. b) The Wilson lines inside the definition of the correlator account for the resummation of soft gluons.

In the Light-Cone gauge, we have $A^+ = 0$ and thus $\mathcal{U}^- = 1$, reducing the quark correlator to the definition in Equation 8.4. As long as one stays in the $A^+ = 0$ gauge, it is perfectly valid to neglect the Wilson line inside the PDFs. The line is a finite line, so using the transitivity property we can split it at $+\infty$ (see e.g. Equation 6.47) and write it as:

$$\mathcal{U}_{(z;0)}^- = \left[\mathcal{U}_{(+\infty;z)}^- \right]^\dagger \mathcal{U}_{(+\infty;0)}^- . \quad (8.11)$$

It is common to draw the Wilson line as a finite line being cut. Following the discussion on page 188, we know that the cut passes in between two semi-infinite lines, but we keep the representation of a cut finite line for convenience. This is illustrated in Figure 8.1. Remember from Equation 6.100 that a quark dressed with a Wilson line can be considered an eikonal quark, essentially being a quark with soft and collinear gluon resummation. The physical interpretation for the quark correlator is nothing different: it represents all soft and collinear interactions between the struck quark and the proton.

We inserted the Wilson line somewhat ad-hoc: we were looking for an object having the correct transformation properties to make the quark correlator gauge invariant, and the Wilson line happens to be such an object. It is however not so difficult to prove this in a more formal way, using the the eikonal approximation. Consider the diagram in Figure 8.2, where one soft gluon before the cut connects the struck quark with the blob. The hadronic tensor is then (see also Equation 8.5):

$$W^{\mu\nu} \sim \sum_q e_q^2 \frac{1}{2} \text{Tr} \left(\Phi_\rho^A(k, k-l) \gamma^\mu \gamma^+ \gamma^\rho \frac{\not{p} - \not{l} + m}{(p-l)^2 - m^2 + i\epsilon} \gamma^\nu \right) ,$$

where the quark-quark-gluon correlator is given by

$$\Phi^A(k, k-l) = \frac{1}{2} \int \frac{d^4z}{(2\pi)^4} \frac{d^4u}{(2\pi)^4} e^{-ik \cdot z} e^{-il \cdot (u-z)} \langle P | \bar{\psi}_\beta(z) g A_\rho(u) \psi_\alpha(0) | P \rangle .$$

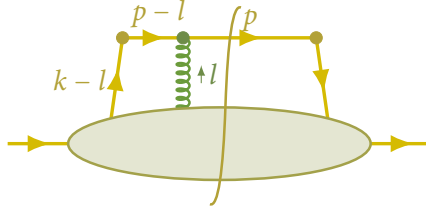


Figure 8.2: A first order correction to the PDF.

Remember that we have an on-shell quark so that we can use the eikonal approximation. The γ^+ is what's left of the real quark, after making the sum over polarisation states:

$$\sum u^s(p)\bar{u}^s(p) = \not{p} + m \rightarrow p^- \gamma^+, \tag{8.12}$$

so we can use γ^+ as though it were an $\bar{u}(p)$ on which to perform the eikonal approximation (as in Equation 6.95). Then we can make the approximation

$$\gamma^+ \gamma^\rho \frac{\not{p} - \not{l} + m}{(p-l)^2 - m^2 + i\epsilon} \approx \gamma^+ \frac{-n^\rho}{n \cdot l - i\epsilon}. \tag{8.13}$$

This is indeed a Wilson line propagator. An important remark: the definition of $\mathcal{U}_{(+\infty; z)}^\dagger$ also incorporates an exponential coming from the Feynman rule for the external point. This exponential has been extracted from \mathcal{U} (it is $e^{-ixP^+z^-}$), but this remains valid by momentum conservation. The choice to extract the exponential from the Wilson line is by historic convention.

It is straightforward to generalise this to any number of gluons, where gluons on the left of the cut will be associated with a line from 0 to $+\infty$, and gluons on the right of the cut with a line from $+\infty$ to z . In other words:

$$W^{\mu\nu} \sim \sum_q e_q^2 \frac{1}{2} \text{Tr}(\Phi_\rho(x) \gamma^\mu \gamma^+ \gamma^\nu),$$

where now the quark-quark-gluon correlator is resummed to all orders:

$$\Phi = \frac{1}{2\pi} \int dz^- e^{-ixP^+z^-} \langle P | \bar{\psi}_\beta(0^+, z^-, \mathbf{0}_\perp) \mathcal{U}_{(+\infty; z)}^{-\dagger} \mathcal{U}_{(+\infty; 0)}^- \psi_\alpha(0) | P \rangle. \tag{8.14}$$

This is indeed the anticipated result. Using Equation 8.8a, we can give a gauge-invariant formulation of the unpolarised integrated quark parton density function:

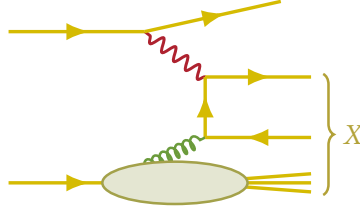


Figure 8.3: Boson-gluon fusion in DIS.

Unpolarised Collinear Quark PDF

$$f_{q/p}(x) = \frac{1}{4\pi} \int dz^- e^{-ixP^+z^-} \langle P | \bar{\psi}(z^-) \mathcal{U}_{(+\infty; z)}^{-\dagger} \gamma^+ \mathcal{U}_{(+\infty; 0)}^- \psi(0) | P \rangle, \quad (8.15)$$

where the subscript in $f_{q/p}$ is a common convention to denote “the integrated quark PDF for a quark with flavour q inside a proton”.

But what about the gluon PDF? Until now we totally ignored the possibility of the photon hitting a gluon inside the proton, because it is a higher order interaction. But while we are moving towards a more realistic approach of QCD, we cannot ignore gluon densities any further. A photon can hit a gluon by interchanging a quark. This is the boson-gluon fusion process mentioned before, and is illustrated in Figure 8.3. To construct the integrated gluon PDF, we start in the light-cone gauge $A^+ = 0$ such that we can ignore Wilson lines for now. There is a constraint equation on A^- relating it to the transverse gauge field, implying that the latter are the only independent fields. Then following the same derivation as in Subsection *Operator Definition for PDFs* on page 230 and onwards, we find (see [71] for the original derivation):

$$f_{g/p}(\xi) = \frac{1}{2\pi} \int dz^- \xi P^+ e^{-i\xi P^+ z^-} \langle P | A^{ia}(z^-) A^{ia}(0) | P \rangle.$$

The factor ξP^+ is typical for fields with even-valued spin. To make this gauge invariant, we cannot simply insert a Wilson line as before, because the gauge fields transform with an extra derivative term. However, the gauge field density $F^{\mu\nu}$ transforms without such a derivative. We can easily relate the two:

$$\begin{aligned} F_{\mu\nu}^a &= \partial_\mu A_\nu^a - \partial_\nu A_\mu^a + g f^{abc} A_\mu^b A_\nu^c \\ F_{+i}^a &= \partial_+ A_i^a \quad (A^+ = 0) \\ \Rightarrow A_i^a &= \frac{1}{\partial_+} F_{+i}, \end{aligned} \quad (8.16)$$

which we can use to redefine the gluon PDF. Inserting a Wilson line (in the adjoint representation, as it has to couple to gluons) then gives our final result for the integrated gluon PDF:

Unpolarised Collinear Gluon PDF

$$f_{g/P}(\xi) = \frac{1}{2\pi} \int \frac{dz^-}{\xi P^+} e^{-i\xi P^+ z^-} \langle P | F^{+ib}(z^-) \mathcal{U}_{(z^-,0)}^{A\ ba} F^{+ia}(0) | P \rangle. \quad (8.17)$$

There are a few subtleties when dealing with gluon PDFs (like the difference between the Weizsäcker-Williams and dipole gluon distributions, see [72]), but discussing these issues would lead us too far away from our main topics of interest.

8.2 SEMI-INCLUSIVE DEEP INELASTIC SCATTERING

Collinear factorisation is a well-explored and experimentally verified framework, but it only works when integrating out all final states. Keeping these final states, i.e. fully exclusive DIS, would maximally break collinear factorisation. In this section we investigate an intermediate solution, where we identify exactly one hadron in the final state, and integrate out all other states. This is called semi-inclusive deeply inelastic scattering (SIDIS). Because there is no restriction on the momentum of the final hadron, it can acquire a transversal part.

To put it more formally: in DIS we were able to describe our process on a plane, because it only has two independent directions, viz. the direction of the incoming proton (which is parallel to the incoming electron) and the direction of the outgoing electron. We have chosen a frame where the plus and minus components of the momenta span this plane, such that the transversal components are zero. In SIDIS a third direction emerges from the momentum of the identified hadron, which doesn't necessarily lie in the plane spanned by the incoming and outgoing electron. In this frame, the final hadron will have a non-zero transverse momentum component.

As we will discover in this section, the breaking of collinear factorisation is not an insurmountable task to overcome; we can adapt our factorisation framework to allow for \mathbf{k}_\perp -dependence, such that the convolution between the hard part and the PDF—now also dependent on \mathbf{k}_\perp , and thus from now on called a transverse momentum density (TMD)—is a convolution over \mathbf{k}_\perp . In this thesis we will not delve into the technicalities for \mathbf{k}_\perp -factorisation, as they are quite intricate and would lead us too far.

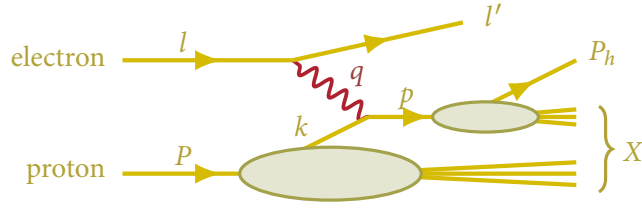


Figure 8.4: Kinematics of semi-inclusive deep inelastic electron-proton scattering.

Conventions and Kinematics

Different conventions exist in literature concerning the naming of the different **TMDs** and azimuthal angles. We will follow the *Trento conventions*, as defined in [56]. Furthermore, concerning the labelling of momenta, we will follow the same convention as used in [59]. In a **SIDIS** process, we have an electron with momentum l that scatters off a proton with momentum P . The mediated photon has momentum q , and hits a parton with momentum k , that has momentum p after scattering (i.e. $p = k + q$). The struck parton then fragments into a hadron with momentum P_h . This is shown in Figure 8.4. Note that we now have two density functions; one that represents the probability to find a parton in the proton (the **TMD**), and one that represents the probability for a parton to fragment in a specific hadron (the fragmentation function (**FF**)). For simplicity we assume the final hadron to be a spin 0 hadron, like a pion. We use x and y as defined in Equation 5.4 and Equations 5.5, and we define a new Lorentz invariant z :

$$z = \frac{P \cdot P_h}{P \cdot q}. \quad (8.18)$$

The value for z can be measured in experiment; it will approximate the fractional momentum of the detected hadron relative to its parent parton, in the same way x approximates the fractional momentum of the struck quark relative to the parent proton. Intuitively, we can add an **FF** $D^q(z)$ to Equation 5.47, giving a **PM** collinear estimate for F_2 in **SIDIS**:

$$F_2^{\text{PM}} = \sum_q e_q^2 x f^q(x) D^q(z), \quad (8.19)$$

which gives us using Equation 5.43 a first estimate for the **SIDIS** cross section:

$$\frac{d^3\sigma}{dx dy dz} \approx \frac{4\pi\alpha^2 s}{Q^4} \left(1 - y + \frac{y^2}{2}\right) \sum_q e_q^2 x f^q(x) D^q(z). \quad (8.20)$$

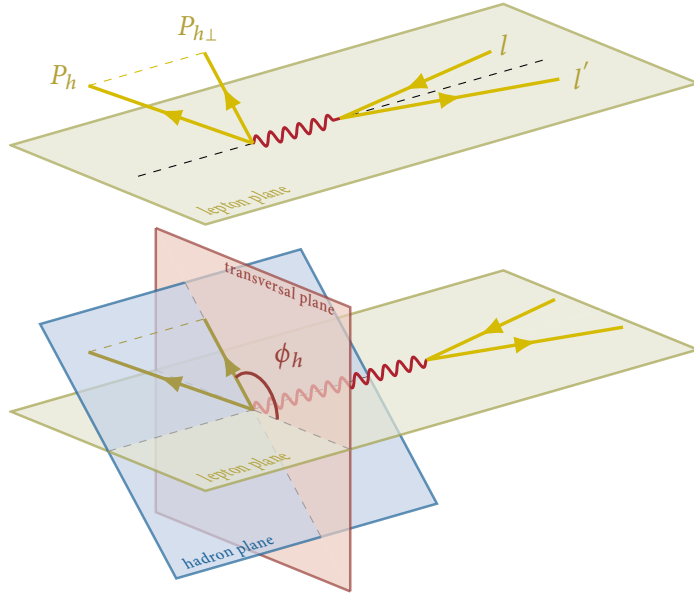


Figure 8.5: In the rest frame of the proton, $P_{h\perp}$ is the projection of P_h onto the plane perpendicular to the photon momentum. The azimuthal angle ϕ_h is the angle between $P_{h\perp}$ and the lepton plane.

Another important variable is the azimuthal angle ϕ_h , which is defined as

$$\cos \phi_h = -\frac{\hat{l} \cdot P_h}{|P_{h\perp}|},$$

where $|P_{h\perp}|$ is the length of the transversal component of the momentum of the outgoing hadron:

$$|P_{h\perp}| = \sqrt{-g_{\perp\mu\nu} P_h^\mu P_h^\nu}.$$

The geometrical construction of the azimuthal angle is shown in Figure 8.5. We can now construct the cross section:

$$\frac{d^6\sigma}{dx dy dz d\phi_h d\mathbf{P}_{h\perp}^2} = \frac{\alpha^2}{2zxsQ^2} L_{\mu\nu} W^{\mu\nu}, \quad (8.21)$$

where we approximated

$$d^3\mathbf{P}_h \approx dz d^2\mathbf{P}_{h\perp} \frac{E_h}{z}.$$

Structure Functions

The hadronic tensor is defined as (compare it to Equation 5.33):

$$\begin{aligned} W^{\mu\nu} &\stackrel{\text{N}}{=} 4\pi^3 \int_X \delta^{(4)}(P+q-p_X-p_h) \langle P | J^{\dagger\mu}(0) | X, P_h \rangle \langle X, P_h | J^\nu(0) | P \rangle, \\ &= \frac{1}{4\pi} \int d^4r e^{iq\cdot r} \langle P | J^{\dagger\mu}(r) | P_h \rangle \langle P_h | J^\nu(0) | P \rangle. \end{aligned} \quad (8.22)$$

As we will see in Subsection *Transverse Momentum Dependent PDFs* on page 242 and onwards, this is a bit simplistic as we cannot integrate out the X states without affecting P_h , but the general idea is correct. Note that because we do not integrate over P_h (we measure it in the final state), we cannot drop the state $|P_h\rangle \langle P_h|$. This leads to an important difference as compared to the hadronic tensor in DIS, viz. that we cannot naively impose the same constraints as in Equation 5.38a, because time-reversal invariance isn't automatically satisfied. We can restore this invariance by changing it slightly, namely we require invariance under the simultaneous reversal of time and of initial and final states.

For the parametrisation of the hadronic tensor, we use the same orthonormal basis as before, viz. Equations 5.27, but now we have an additional physical vector at our disposal, which we can use to construct the fourth basis-vector:

$$\hat{h}^\mu \stackrel{\text{N}}{=} \frac{g_\perp^{\mu\nu} P_{h\nu}}{|P_{h\perp}|}. \quad (8.23)$$

\hat{h}^μ is a spacelike unit vector:

$$\hat{h}^\mu \hat{h}_\mu = -1. \quad (8.24)$$

Watch out, as although we normalised this vector, it is not fully orthogonal! We have as expected

$$\hat{h} \cdot \hat{t} = 0, \quad \hat{h} \cdot \hat{q} = 0,$$

but it is not orthogonal to \hat{l}^μ :

$$\hat{h} \cdot \hat{l} = \cos \phi_h. \quad (8.25)$$

This is a deliberate choice, because now we have the azimuthal dependence hard-coded inside our new basis. Note that

$$-\hat{l}_\perp^\mu \varepsilon_{\perp\mu\nu} \hat{h}^\nu = \sin \phi_h, \quad (8.26)$$

which implies that ϕ_h is fully defined in the region $0 \dots 2\pi$. We can parametrise $W^{\mu\nu}$ in the same way as we did in Equation 5.39, now with \hat{h} added. This gives (for the unpolarised case):

$$W^{\mu\nu} = \frac{z}{x} \left[-g_{\perp}^{\mu\nu} F_{UU,T} + \hat{t}^{\mu} \hat{t}^{\nu} F_{UU,L} + 2\hat{t}^{(\mu} \hat{h}^{\nu)} F_{UU}^{\cos \phi_h} \right. \\ \left. + (2\hat{h}^{\mu} \hat{h}^{\nu} + g_{\perp}^{\mu\nu}) F_{UU}^{\cos 2\phi_h} - 2i \hat{t}^{[\mu} \hat{h}^{\nu]} F_{LU}^{\sin \phi_h} \right] \quad (8.27)$$

The subscript UU denotes a structure function for an unpolarised beam on an unpolarised target, while the labelling in function of ϕ_h will be motivated by contracting with the lepton tensor Equation 5.31:

$$L_{\mu\nu} W^{\mu\nu} = \frac{4zs}{y} \left[\left(1 - y + \frac{y^2}{2} \right) F_{UU,T} + \sqrt{1-y} (2-y) \cos \phi_h F_{UU}^{\cos \phi_h} \right. \\ \left. + (1-y) F_{UU,L} + (1-y) \cos 2\phi_h F_{UU}^{\cos 2\phi_h} + \lambda y \sqrt{1-y} \sin \phi_h F_{LU}^{\sin \phi_h} \right].$$

As anticipated, $F_{UU}^{\cos \phi_h}$ has a factor $\cos \phi_h$ in front, and so on. Note that $F_{LU}^{\sin \phi_h}$ is the structure function for a longitudinally polarised lepton beam (on an unpolarised proton target), which is confirmed by the factor λ in front (originating from the last term in the lepton tensor Equation 5.31). The cross section is then given by Equation 8.21:

$$\frac{d^6 \sigma}{dx dy dz d\phi_h d\mathbf{P}_{h\perp}^2} = \frac{2\alpha^2}{x y Q^2} \left[\left(1 - y + \frac{y^2}{2} \right) F_{UU,T} + (1-y) F_{UU,L} \right. \\ \left. + \lambda y \sqrt{1-y} \sin \phi_h F_{LU}^{\sin \phi_h} + (1-y) \cos 2\phi_h F_{UU}^{\cos 2\phi_h} \right. \\ \left. + \sqrt{1-y} (2-y) \cos \phi_h F_{UU}^{\cos \phi_h} \right], \quad (8.28a)$$

$$\frac{d^3 \sigma}{dx dy dz} = \frac{4\pi\alpha^2}{x y Q^2} \left[\left(1 - y + \frac{y^2}{2} \right) \tilde{F}_{UU,T} + (1-y) \tilde{F}_{UU,L} \right], \quad (8.28b)$$

where we integrated over $\mathbf{P}_{h\perp}$ in the last step, which got rid of the ϕ_h -dependence. The tilde structure functions are the integrated versions:

$$\tilde{F}_{UU,T}(x, z, Q^2) = \int d^2 \mathbf{P}_{h\perp} F_{UU,T}(x, z, Q^2, \mathbf{P}_{h\perp}), \quad (8.29)$$

and similarly for $\tilde{F}_{UU,L}$. From the logical demand

$$\sum_h \int dz z \frac{d^3 \sigma_{\text{SIDIS}}}{dx dy dz} \equiv \frac{d^2 \sigma_{\text{DIS}}}{dx dy},$$

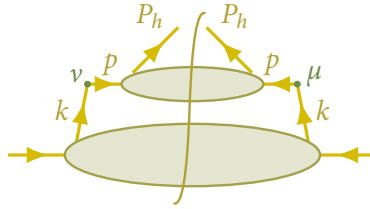


Figure 8.6: Leading order diagram for the hadronic tensor in SIDIS.

we can relate the SIDIS structure functions to the DIS structure functions:

$$\sum_h \int dz z \tilde{F}_{UU,T}(x, z, Q^2) \equiv F_T(x, Q^2), \tag{8.30a}$$

$$\sum_h \int dz z \tilde{F}_{UU,L}(x, z, Q^2) \equiv F_L(x, Q^2). \tag{8.30b}$$

Transverse Momentum Dependent PDFs

We can construct the diagram for the hadronic tensor following the same step-by-step procedure we used in DIS (see Subsection *Operator Definition for PDFs* on page 230 and onwards), this time adding a fragmentation function, as is illustrated in Figure 8.6. Remember that the amplitude for extracting a quark from a proton with momentum P is

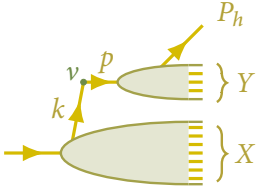
$$\psi_\alpha(0) |P\rangle .$$

Then the amplitude for a quark fragmenting in a hadron with momentum P_h is of course

$$\langle P_h | \bar{\psi}_\alpha(0) .$$

So we simply have:

$$\left. \begin{array}{c} \nu \\ k \\ \text{---} \end{array} \right\} X \quad = \quad (\gamma^\nu)^{\beta\alpha} \langle X | \psi_\alpha(0) |P\rangle ,$$



$$= \langle Y, P_h | \bar{\psi}_\beta(0) | 0 \rangle (\gamma^\nu)^{\beta\alpha} \langle X | \psi_\alpha(0) | P \rangle .$$

The QED-vertex adds a δ -function, and making the final-state cut adds two final-state sums (using the notation defined in Equation 5.35) and two δ -functions:

$$W^{\mu\nu} = \frac{1}{2} \sum_q e_q^2 \int d^4 k d^4 p \int_X \int_Y \delta^{(4)}(P-k-p_X) \delta^{(4)}(P_h+p_Y-p) \delta^{(4)}(k+q-p) \\ \times \langle P | \bar{\psi} | X \rangle \gamma^\mu \langle 0 | \psi | Y, P_h \rangle \langle Y, P_h | \bar{\psi} | 0 \rangle \gamma^\nu \langle X | \psi | P \rangle .$$

Next we will separate the proton content from the fragmentating hadron content, applying on each the same steps as before (expressing the δ -function as an exponential, using the translation operator and the completeness relation). Then we get the general leading order result:

Quark Correlator and Quark Fragmentator

$$W^{\mu\nu} = \frac{1}{2} \sum_q e_q^2 \int d^4 k d^4 p \delta^{(4)}(k+q-p) \text{tr}(\Phi(k, P) \gamma^\mu \Delta(p, P_h) \gamma^\nu) , \quad (8.31a)$$

$$\Phi_{\alpha\beta}(k, P) = \int \frac{d^4 r}{16\pi^4} e^{-ik \cdot r} \langle P | \bar{\psi}_\beta(r) \psi_\alpha(0) | P \rangle , \quad (8.31b)$$

$$\Delta_{\alpha\beta}(p, P_h) = \int \frac{d^4 r}{16\pi^4} e^{-ip \cdot r} \langle 0 | \psi_\alpha(0) | P_h \rangle \langle P_h | \bar{\psi}_\beta(r) | 0 \rangle . \quad (8.31c)$$

Next we choose a frame where the parton in the TMD carries a fraction ξ of the proton's plus momentum, and where the final hadron carries a fraction ζ of the fragmentating parton's minus momentum, i.e.

$$k^\mu = \left(\xi P^+, \frac{k^2 + \mathbf{k}_\perp^2}{2 \xi P^+}, \mathbf{k}_\perp \right) , \quad p^\mu = \left(\zeta \frac{p^2 + \mathbf{p}_\perp^2}{2 P_h^-}, \frac{P_h^-}{\zeta}, \mathbf{p}_\perp \right) , \quad (8.32)$$

such that we can write (neglecting terms that are $\frac{1}{Q}$ suppressed):

$$\delta^{(4)}(k+q-p) \approx \delta(k^+ + q^+) \delta(q^- - p^-) \delta^{(2)}(\mathbf{k}_\perp + \mathbf{q}_\perp - \mathbf{p}_\perp) , \\ \approx \frac{1}{P^+ P_h^-} \delta(\xi - x) \delta\left(\frac{1}{\zeta} - \frac{1}{z}\right) \delta^{(2)}(\mathbf{k}_\perp + \mathbf{q}_\perp - \mathbf{p}_\perp) .$$

We transform the integral measures as

$$d^4k = P^+ d\xi dk^- d^2\mathbf{k}_\perp, \quad d^4p = dp^+ d\zeta \frac{P_h^-}{\zeta^2} d^2\mathbf{p}_\perp.$$

Then we can rewrite the hadronic tensor as:

$$W^{\mu\nu} = \sum_q e_q^2 \int d^2\mathbf{k}_\perp z \text{tr}(\Phi(x, \mathbf{k}_\perp, P) \gamma^\mu \Delta(z, \mathbf{k}_\perp + \mathbf{q}_\perp, P_h) \gamma^\nu), \quad (8.33)$$

where we defined the \mathbf{k}_\perp -dependent correlators as:

$$\Phi(\xi, \mathbf{k}_\perp, P) \stackrel{\text{N}}{=} \int \frac{d^3\mathbf{r}}{8\pi^3} e^{-ixP^+ r^- + i\mathbf{k}_\perp \cdot \mathbf{r}_\perp} \langle P | \bar{\psi}(0^+, r^-, \mathbf{r}_\perp) \psi(0) | P \rangle, \quad (8.34a)$$

$$\Delta(z, \mathbf{p}_\perp, P_h) \stackrel{\text{N}}{=} \frac{1}{2z} \int \frac{d^3\mathbf{r}}{8\pi^3} e^{-i\frac{P_h^-}{z} r^+ + i\mathbf{k}_\perp \cdot \mathbf{r}_\perp} \langle 0 | \psi(0) | P_h \rangle \langle P_h | \bar{\psi}(r^+, 0^-, \mathbf{r}_\perp) | 0 \rangle. \quad (8.34b)$$

We can parametrise the quark correlator and fragmentator functions in terms of **TMDs** and **FFs**, precisely as we did with the quark correlator in the case of **DIS**. Keeping only the contributions at leading-twist, we obtain the following unpolarised **TMDs** and **FFs** [58]:

$$\Phi(\xi, \mathbf{k}_\perp) = \frac{1}{2} f_1(\xi, \mathbf{k}_\perp) \gamma^- + \frac{i}{2} h_1^\perp(\xi, \mathbf{k}_\perp) \frac{\mathbf{k}_\perp}{m_p} \gamma^-, \quad (8.35a)$$

$$\Delta(\zeta, \mathbf{k}_\perp) = \frac{1}{2} D_1(\zeta, \mathbf{k}_\perp) \gamma^+ + \frac{i}{2} H_1^\perp(\zeta, \mathbf{k}_\perp) \frac{\mathbf{k}_\perp}{m_h} \gamma^+. \quad (8.35b)$$

The correlator is built from the unpolarised **TMD** $f_1(\xi, \mathbf{k}_\perp)$ and the so-called Boer-Mulders **TMD** $h_1^\perp(\xi, \mathbf{k}_\perp)$. The fragmentator is built from the unpolarised **TMD FF** $D_1(\zeta, \mathbf{k}_\perp)$ and the so-called Collins function $H_1^\perp(\zeta, \mathbf{k}_\perp)$. If we plug this result in Equation 8.21 and Equation 8.28b, and use the approximation

$$\mathbf{q}_\perp \approx -\frac{\mathbf{P}_{h\perp}}{z}, \quad (8.36)$$

we get the factorisation formula for the unpolarised transversal structure function in **SIDIS**:

Factorisation in SIDIS

$$F_{UU,T} = \sum_q e_q^2 x f_1^q \otimes D_1^q. \quad (8.37)$$

where we defined the convolution over transverse momentum as

$$f_1^q \otimes D_1^q = \int d^2\mathbf{k}_\perp d^2\mathbf{p}_\perp \delta^{(2)}\left(\mathbf{k}_\perp - \mathbf{p}_\perp - \frac{1}{z}\mathbf{P}_{h\perp}\right) f_1^q(x, \mathbf{k}_\perp) D_1^q(z, \mathbf{p}_\perp), \quad (8.38)$$

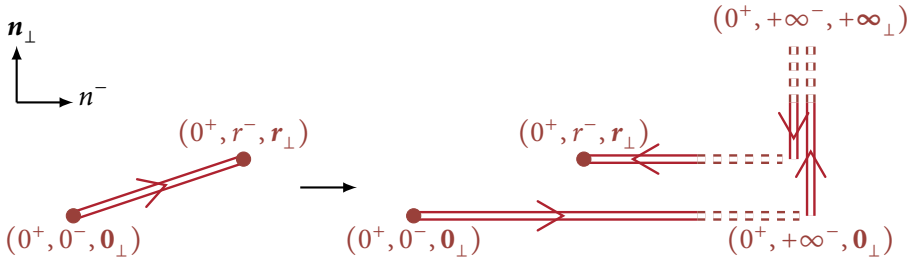


Figure 8.7: Structure of the Wilson lines in the **TMD** definition.

which is a regular convolution with ‘open’ variable $\frac{1}{z}P_{h\perp}$. Other structure functions arise when convoluting polarised **TMDs** (which arise when the target hadron is polarised), which we don’t treat in this thesis.

This factorisation formula is however not yet fully rigorous, and we will improve it in [Section 8.3](#).

Gauge Invariant Definition for TMDs

Just as was the case in the previous section for **DIS**, our **TMDs** and **FFs** defined so far ([Equations 8.34](#)) are not gauge invariant, and are only valid in the light-cone gauge $A^+ = 0$. Gauge invariance can be restored by inserting a Wilson line:

$$\Phi(\xi, \mathbf{k}_{\perp}, P) = \int \frac{d^3\mathbf{r}}{8\pi^3} e^{-i\xi P^+ r^- + i\mathbf{k}_{\perp} \cdot \mathbf{r}_{\perp}} \langle P | \bar{\psi}(r) \mathcal{U}_{(r;0)} \psi(0) | P \rangle, \quad (8.39)$$

where now the space-time point separation no longer lies on the light-cone, i.e. the Wilson line has to connect the point $(0^+, 0^-, \mathbf{0}_{\perp})$ with the point $(0^-, r^+, \mathbf{r}_{\perp})$. But a Wilson line is path-dependent, implying that different path choices give different results. How do we choose a path, or at least motivate our choice? Just as was the case for the collinear **PDF**, the gauge invariance requirement doesn’t put any constraints on the path. The correct path can however be retrieved by explicit calculations of a full process. Different processes might require different paths, that can be quite complex (see e.g. [73–75]). This is an active topic of interesting research these days, as it is intimately bound to the validity of **TMD** factorisation.

In the collinear case we were able to interpret the Wilson line as a colour rotation on the quark, making it an eikonal quark. We then split the Wilson line into two parts at infinity. This splitting had two advantages, first that we could associate a line with the quarks on each side of the cut diagram separately,

and second that we could use easy Feynman rules. In the **TMD** definition for unpolarised **SIDIS**, we can do something analogous. We add a light-like line to each quark:

$$\mathcal{U}_{(+\infty^-, \mathbf{0}_\perp; 0^-, \mathbf{0}_\perp)}^- \psi(0^+, 0^-, \mathbf{0}_\perp), \quad (8.40a)$$

$$\bar{\psi}(0^+, r^-, \mathbf{r}_\perp) \mathcal{U}_{(+\infty^-, r_\perp; r^-, r_\perp)}^{-\dagger}. \quad (8.40b)$$

But now we have because of the transverse separation

$$\mathcal{U}_{(r; 0)} \neq \mathcal{U}_{(+\infty^-, r_\perp; r^-, r_\perp)}^{-\dagger} \mathcal{U}_{(+\infty^-, \mathbf{0}_\perp; 0^-, \mathbf{0}_\perp)}^-.$$

So we need a Wilson line to connect the transverse ‘gap’, i.e.

$$\mathcal{U}_{(r; 0)} = \mathcal{U}_{(+\infty^-, r^-)}^{-\dagger} \mathcal{U}_{(r_\perp; \mathbf{0}_\perp)}^\perp \mathcal{U}_{(+\infty^-, 0^-)}^-.$$

We will split this line at $+\infty_\perp$ for the same reasons as before. Adding this to [Equations 8.40](#) gives:

$$\mathcal{U}_{(+\infty^-, +\infty_\perp; +\infty^-, \mathbf{0}_\perp)}^\perp \mathcal{U}_{(+\infty^-, \mathbf{0}_\perp; 0^-, \mathbf{0}_\perp)}^- \psi(0^+, 0^-, \mathbf{0}_\perp), \quad (8.41a)$$

$$\bar{\psi}(0^+, r^-, \mathbf{r}_\perp) \mathcal{U}_{(+\infty^-, r_\perp; r^-, r_\perp)}^{-\dagger} \mathcal{U}_{(+\infty^-, +\infty_\perp; +\infty^-, r_\perp)}^\perp, \quad (8.41b)$$

leading to the final definition for the gauge invariant **TMD** quark correlator:

Gauge Invariant TMD Quark Correlator

$$\Phi = \int \frac{d^3 \mathbf{r}}{8\pi^3} e^{-ixP^+ r^- + ik_\perp \cdot \mathbf{r}_\perp} \langle P | \bar{\psi}(r) \mathcal{U}_{(+\infty; r)}^\dagger \tilde{\mathcal{U}}_{(+\infty; 0)} \psi(0) | P \rangle, \quad (8.42a)$$

$$\tilde{\mathcal{U}}_{(+\infty; 0)} = \mathcal{U}_{(+\infty^-, +\infty_\perp; +\infty^-, \mathbf{0}_\perp)}^\perp \mathcal{U}_{(+\infty^-, \mathbf{0}_\perp; 0^-, \mathbf{0}_\perp)}^-, \quad (8.42b)$$

$$\mathcal{U}_{(+\infty; r)}^\dagger = \mathcal{U}_{(+\infty^-, r_\perp; r^-, r_\perp)}^{-\dagger} \mathcal{U}_{(+\infty^-, +\infty_\perp; +\infty^-, r_\perp)}^\perp. \quad (8.42c)$$

What about the physical interpretation? Consider again the one-gluon exchange as depicted in [Figure 8.2](#). We saw in [Equation 8.13](#) that the net contribution for a soft or collinear gluon is a factor

$$g \int \frac{d^4 l}{16\pi^4} A \frac{\not{p} - \not{l}}{(p-l)^2 + i\epsilon} \approx -g \int \frac{d^4 l}{16\pi^4} \frac{n \cdot A}{n \cdot l - i\epsilon}, \quad (8.43)$$

where l^μ is the momentum of the exchanged photon and $n^\mu = \frac{p^\mu}{|p|}$ the direction of the outgoing quark. We were able to make this simplification because in the correlator this correction stands to the right of a factor $\bar{u}(p)$, such that we can make use of the fact $\bar{u}(p)\not{p} = 0$:

$$\bar{u}(p)\not{A}\not{p} = \bar{u}(p) (\not{A}\not{p} + \not{p}\not{A}) = 2\bar{u}(p)\not{p} \cdot A.$$

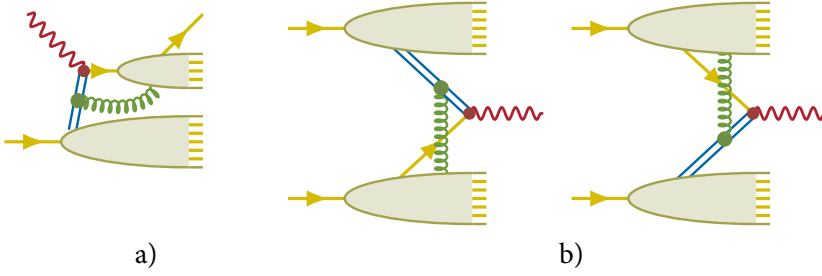


Figure 8.8: a) In *SIDIS*, the longitudinal Wilson line inside the fragmentation function represents a resummation of soft and collinear gluons connected to the incoming quark. b) In *Drell-Yan*, the longitudinal Wilson line inside one *TMD* represents a resummation of soft and collinear gluons connected to the parton extracted from the other *TMD*.

As we saw before, this contribution calculated to all orders leads to the light-like Wilson line. In the collinear case this was the end of the story. But now that we are in the *TMD* case, we cannot simply take the exchanged gluon to be collinear, instead, we need to add to [Equation 8.43](#) a term

$$g \int \frac{d^4 l}{16\pi^4} \frac{\not{A}l}{2p \cdot l + l_{\perp}^2 - i\epsilon} \approx g \int \frac{d^2 l_{\perp}}{4\pi^2} \frac{\gamma^{\mu} l_{\perp}}{l_{\perp}^2 - i\epsilon} A_{\perp}^{\mu}(0^+, \infty^-, l_{\perp})$$

It is not so straightforward to prove (see e.g. [55]), but this parts will sum up to a transversal Wilson line. So in the end, inside the *TMD* we have both a resummation of collinear gluons—coming from the line parts \mathcal{U}^- and $\mathcal{U}^{-\dagger}$ —and a resummation of soft transversal gluons, coming from the $\tilde{\mathcal{U}}$ and $\tilde{\mathcal{U}}^{\dagger}$ parts. Note however that by choosing an appropriate gauge, it is possible to cancel the contribution of one type of these lines, e.g. in the *LC* gauge only the transversal parts remain (with advanced or retarded prescriptions the *LC* gauge can cancel the transverse segment as well). Of course, the same reasoning can be repeated for the fragmentation function, but then the light-like Wilson lines will lie in the plus direction. This is illustrated in [Figure 8.8a](#).

To end this section, we give an example for the use of Wilson lines in the *Drell-Yan* process. In this setup, two protons (or a proton and an antiproton) are collided and create a photon or weak boson by quark-antiquark annihilation. We thus need two *TMDs*, which are both in the initial state. The longitudinal part of the Wilson line used to make the *TMD* gauge invariant represents a resummation of gluons connected to the parton struck from the other *TMD*. This is illustrated in [Figure 8.8b](#). Because of the fact that the Wilson line now represents initial state radiation, the line structure will be different. More specifically, the path will flow towards $-\infty$ before returning, as shown in [Figure 8.9](#). This has an important

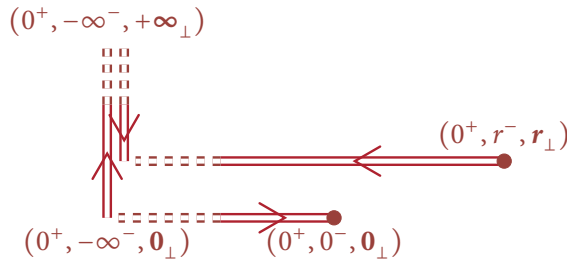


Figure 8.9: Structure of Wilson lines in the **DY TMD** definition. Because of the initial-state interactions in **DY**, the direction of the Wilson line is reversed, going now towards $-\infty$.

consequence: two out of the eight (unpolarised and polarised) **TMDs** are T-odd and will have a sign change with this line structure as compared to **SIDIS** (the Boer-Mulders **TMD** from [Equations 8.35](#) is an example). This would imply that **TMDs** are process-dependent, and not universal as they ought to be. So far it is not experimentally verified whether these T-odd **TMDs** have a non-zero value, although there is a growing amount of evidence that they exist (in particular the so-called Sivvers function). They are not universal, but they are manageable because the non-universality can usually be calculated (like the sign change in **DY** w.r.t. **SIDIS**). The latter is however not yet confirmed by experiment.

8.3 EVOLUTION OF TMDs

One thing that remains to be defined before we can really use **TMDs** in experiment, is their evolution. In the collinear case, the evolution of **PDFs** is fully governed by the **DGLAP** equations. To do something similar for **TMDs**, we first have to take a new look at our crude factorisation formula in [Equation 8.37](#), because we will have to adapt it due to the singularity structure of the **TMDs** involved.

As the Wilson line structure is now such that the light-like lines do not overlap (see [Figure 8.7](#)), we are left with overlapping **LC** divergences (originating from the double pole in [Equation 7.71](#)) and additional **IR** divergences. The latter can be managed by extracting all soft contributions into a so-called soft factor S . It is typically calculated as a **v.e.v.** of the complex square of two Wilson lines with one cusp. This is illustrated in [Figure 8.10](#).

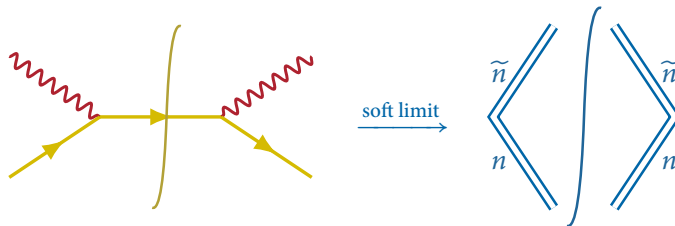


Figure 8.10: In the soft limit, all possible soft contributions between the quark legs are resummed into on-LC Wilson line segments. This gives rise to the soft function as depicted on the right.

On the other hand, the LC divergences can be managed in different ways. The most common way is to regulate the ‘on-LC-ness’ of the LC Wilson line segment by slightly putting it off-LC and introducing a regulator ζ :²

$$\zeta \stackrel{\text{def}}{=} \frac{k \cdot n}{|n|}, \quad (8.44)$$

that measures how much off-LC the segment is. As always, k is the momentum of the struck parton before the interaction, and n is the direction of the Wilson line segment (the same direction as the struck quark after the interaction). The on-LC segment is retrieved in the limit $\zeta \rightarrow \infty$ (which is equivalent to $n^2 \rightarrow 0$). A similar regulator is introduced for the LC-divergences in the FF:

$$\zeta_h \stackrel{\text{def}}{=} \frac{p \cdot \tilde{n}}{|\tilde{n}|}, \quad (8.45)$$

These two regulators will act as rapidity cut-offs, softening the overlapping divergences. The TMD and FF then gain an extra dependence on ζ resp. ζ_h :

$$f(x, \mathbf{k}_\perp, \zeta, \mu^2), \quad D(z, \mathbf{p}_\perp, \zeta_h, \mu^2). \quad (8.46)$$

Now we can give a rigorous definition for the factorisation of the SIDIS cross-section:

Factorisation in SIDIS

$$\begin{aligned} \frac{\partial^2 \sigma_{\gamma^* p}}{\partial z \partial q_\perp^2} &\sim |H(\mu_F^2)|^2 \int d^2 \mathbf{k}_\perp d^2 \mathbf{p}_\perp d^2 \mathbf{l}_\perp \delta^{(2)}(\mathbf{k}_\perp - \mathbf{p}_\perp + \mathbf{l}_\perp + \mathbf{q}_\perp) \\ &\quad \times \sum_q e_q^2 f^q(x, \mathbf{k}_\perp, \zeta, \mu_F^2) D^q(z, \mathbf{p}_\perp, \zeta_h, \mu_F^2) S(\mathbf{l}_\perp, \mu_F^2). \end{aligned} \quad (8.47)$$

This is illustrated in Figure 8.11. The hard part is perturbatively calculable and

² Not to be confused with the ζ momentum fraction in $P_h^- = \zeta p^-$, that is integrated over in the FF.

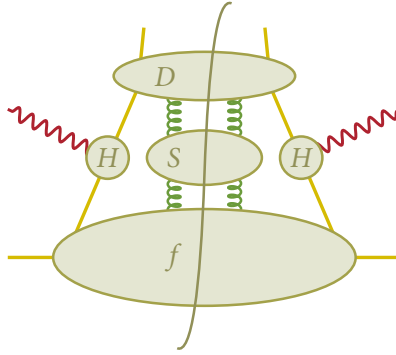


Figure 8.11: Factorisation in SIDIS: the bull diagram. All IR divergences are absorbed in the soft factor S , that hence only interacts with the TMD and FF. Note that there is no real radiation coming from the hard part.

normalised:

$$|H(\mu_F^2)|^2 = 1 + \mathcal{O}(\alpha_s), \quad (8.48)$$

and does not contain real radiation. This factorisation formula is only valid at small transverse momenta (of the order of the proton mass or smaller), and has been proven at one loop and leading twist.³

The factorisation formula can be simplified by Fourier transforming into impact parameter space, as the δ -function makes that all densities depend on the same impact parameter b_\perp . Furthermore, it is convenient to redefine the TMD and FF in order to absorb the soft function:

$$f^q(x, \mathbf{b}_\perp, \zeta, \mu_F^2) \stackrel{\text{def}}{=} \sqrt{S(\mathbf{b}_\perp, \mu_F^2)} f^q(x, \mathbf{b}_\perp, \zeta, \mu_F^2), \quad (8.49a)$$

$$D^q(z, \mathbf{b}_\perp, \zeta_h, \mu_F^2) \stackrel{\text{def}}{=} \sqrt{S(\mathbf{b}_\perp, \mu_F^2)} D^q(z, \mathbf{b}_\perp, \zeta_h, \mu_F^2). \quad (8.49b)$$

There are some subtleties in doing this—as one also has to divide out all self-energy contributions—but we don't delve into these technicalities. The factorisation formula is then:

$$\frac{\partial^2 \sigma_{\gamma^* p}}{\partial z \partial q_\perp^2} \sim |H(\mu_F^2)|^2 \int d^2 \mathbf{b}_\perp e^{-i \mathbf{b}_\perp \cdot \mathbf{q}_\perp} \sum_q e_q^2 f^q(x, \mathbf{b}_\perp, \zeta, \mu_F^2) D^q(z, \mathbf{b}_\perp, \zeta_h, \mu_F^2). \quad (8.50)$$

We can now derive evolution equations in a similar way as in the DGLAP case, viz. by demanding that the cross section is independent on the factorisation scale μ_F and the rapidity cut-offs ζ and ζ_h . It can then be shown that:

³ In the regime with large transversal momenta, regular collinear factorisation can be applied.

CS Evolution Equations for TMDs and FFs

$$\frac{\partial}{\partial \ln \zeta} \ln f(x, b, \zeta, \mu) = K(b, \mu), \quad (8.51a)$$

$$\frac{\partial}{\partial \ln \mu} \ln f(x, b, \zeta, \mu) = \gamma_F(\zeta, \mu), \quad (8.51b)$$

which are known as the Collins-Soper (CS) evolution equations. The same equations apply for D as well (with ζ replaced by ζ_h), as for any TMD or FF. $K(b, \mu)$ is the CS kernel, and γ_F is the anomalous dimension of the TMD. The kernel is perturbatively calculable but only for small \mathbf{q}_\perp (but this is something we don't mind, as at large \mathbf{q}_\perp TMD-factorisation is broken anyway). The kernel and the anomalous dimension satisfy the following RGE:

CS Renormalisation Group Equation

$$\frac{\partial K(b, \mu)}{\partial \ln \mu} = \frac{\partial \gamma_F(\zeta, \mu)}{\partial \ln \zeta} = \gamma_K(\alpha_s), \quad (8.52)$$

where γ_K is the anomalous dimension of the kernel. It is easily calculated at one-loop to equal:

$$\gamma_K = -2 \frac{\alpha_s C_F}{\pi} + \mathcal{O}(\alpha_s^2). \quad (8.53)$$

We will show in Section 11.4 that there is an easy relation between the anomalous dimension of the kernel and the cusp anomalous dimension (where the latter is introduced in Section 10.2):

$$\gamma_K \equiv -2\Gamma_{\text{cusp}}, \quad (8.54)$$

where the factor 2 arises from the fact that there are 2 cusps in the squared amplitude (between the incoming quark and the outgoing Wilson line).

We can solve the CS evolution equations for f :

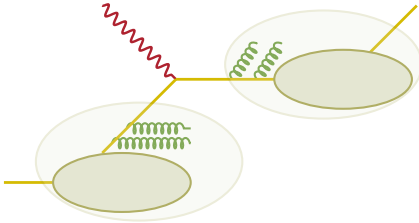
$$f(\zeta, b, \mu) = f(\zeta_0, b, \mu_0) e^{K(b, \mu_0) \ln \frac{\zeta}{\zeta_0} + \int_{\mu_0}^{\mu} d \ln \mu' (\gamma_F(\zeta, \mu') - \gamma_K(\mu') \ln \frac{\zeta}{\mu'})}, \quad (8.55)$$

where the exponential factor evolves the TMD from (ζ_0, μ_0) to (ζ, μ) .

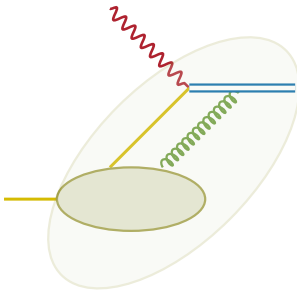
About the Rapidity Cut-Offs

Before we end this chapter, we make a few remarks on the rapidity cut-offs. First we note that they have a significant physical meaning, namely they disentangle

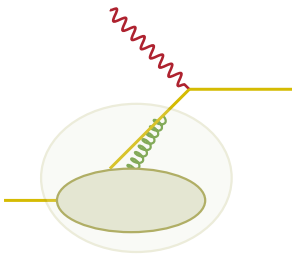
different gluon contributions and sort them in the right density, the **TMD** or the **FF**. Let us illustrate this a bit more elaborately. Suppose the incoming quark is in the **LC** plus direction, then the outgoing quark is in the **LC** minus direction. Naively, we would assume that all radiation from the incoming quark goes into the **TMD**, and all radiation from the outgoing quark goes into the **FF**:



But this is of course not true, as the Wilson line in the **TMD** is in the **LC minus** direction, and resums gluons that are collinear to the incoming quark:



But a gluon that is radiated from the incoming quark and collinear to the incoming quark, is absorbed by the **TMD's** evolution (following the same idea as in [Figure 5.10](#)) and hence also enters the **TMD**:



So we conclude that it doesn't matter from which line the gluon is radiated, but that it is its direction that matters, i.e. collinear to the incoming quark. In other words, all gluons radiated in the **LC** plus direction go into the **TMD**. A similar reasoning can be applied to the **FF**, such that all gluons radiated in the **LC** minus direction go into the **FF**. To know what to do with gluons that are not collinearly

radiated, we look at their rapidity Y . The **LC** plus direction is associated with $Y = +\infty$ and the **LC** minus direction with $Y = -\infty$, so it is tempting to absorb all gluons with positive Y into the **TMD** and all gluons with negative Y into the **FF**. But then we are absorbing too much, because gluons with small rapidity (positive or negative) are *hard*, and have to remain in the hard part. This is exactly what ζ and ζ_h do, as they separate these different regions:

$$Y < \zeta_h \rightarrow \text{FF}, \quad (8.56a)$$

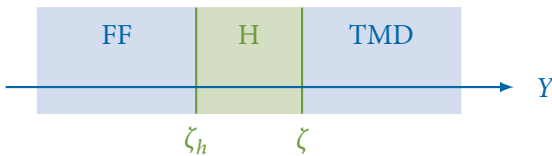
$$\zeta_h < Y < \zeta \rightarrow \text{H}, \quad (8.56b)$$

$$\zeta < Y \rightarrow \text{TMD}, \quad (8.56c)$$

from which also naturally follows

$$\zeta \zeta_h \equiv Q^2, \quad (8.57)$$

because hard gluons are parameterised by $Y \leq Q$. We can show this pictorially:



Another remark about the rapidity cut-offs is that—as we mentioned when introducing them—there are different ways to treat the **LC** divergences. The main reason why one would like to use a different method is that calculations with off-**LC** segments are much more involving than with on-**LC** segments (as we experienced ourselves when calculating the results in [Equation 7.71](#) and [Equation 7.81](#)).

One method is to adapt the renormalisation procedure to subtract the double pole as well, as is commonly done with Wilson loops (see [Section 10.2](#)). However, as this has to be done consistently on all contributions of the **TMD**, it quickly becomes quite cumbersome.

Another method—which is quite recent—is to extract besides the soft factor a collinear factor from the squared amplitude as well. It will have a similar singularity structure, and all rapidity divergences cancel out when combining diagrams.

Last, we discovered that by applying geometrical evolution on the **TMD**, the area derivation (which lies at the basis of the geometric evolution) removes a pole as well. This is investigated in deep detail in [Chapter 11](#).

QCD TOWARDS SMALL- x

In this chapter we will briefly review the small- x framework, which describes the behaviour of QCD in the asymptotic limit $x_B \rightarrow 0$. We will see how in this limit the gluon density dominates, and satisfies evolution equations in x , the so-called BFKL equations. The gluon density grows exponentially without bound until it would start violating causality. At this moment, gluon recombination effects start to dominate and act as a damping effect on the exponential growth. They manifest themselves as extra non-linear terms in the evolution equations, which are then known as the BK equations, while the full framework that includes these non-linear terms is known as *saturation*.

For further reading, see e.g. [76–78] for a general reading, [79–81] on the BFKL equation, [82–85] on the BK equation, [86–93] on saturation and [94–104] for a more present-day approach to saturation.

9.1 EVOLUTION IN LONGITUDINAL MOMENTUM FRACTION

Let us now go back to the case of DIS, and instead of adding transversal momentum dependence, we investigate what happens in the small- x limit. As we know, the DGLAP evolution equations are fully governed by the splitting functions (see Equations 5.71):

$$\begin{aligned}
 P_{qq}(x) &= C_F \frac{1+x^2}{1-x}, \\
 P_{qg}(x) &= \frac{1}{2} (x^2 + (1-x)^2), \\
 P_{gq}(x) &= C_F \frac{1+(1-x)^2}{x}, \\
 P_{gg}(x) &= 2N_c \left(\frac{x}{1-x} + \frac{1-x}{x} + x(1-x) \right).
 \end{aligned}$$

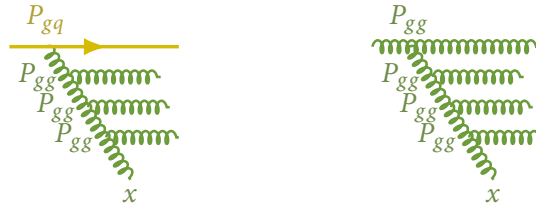


Figure 9.1: Two typical ladder diagrams: at small- x only gluons survive, both in the case of an initial quark or gluon.

It is clear that in the limit $x \rightarrow 0$, only the singular terms in P_{gq} and P_{gg} remain:

$$P_{gq}(x) \xrightarrow{x \rightarrow 0} C_F \frac{1}{x}, \tag{9.1a}$$

$$P_{gg}(x) \xrightarrow{x \rightarrow 0} 2 N_c \frac{1}{x}. \tag{9.1b}$$

It doesn't matter whether we start with a quark or a gluon, at small- x only the splitting functions that result in a gluon remain. This is illustrated in Figure 9.1, which are known as *ladder diagrams*. The small- x DGLAP evolution equations are (see Equation 5.70):

$$\frac{\partial}{\partial \ln \mu^2} q_i(x, \mu^2) = 0, \tag{9.2a}$$

$$\frac{\partial}{\partial \ln \mu^2} g(x, \mu^2) = \frac{\alpha_s}{2\pi} \int_x^1 \frac{d\xi}{\xi} \left[C_F \frac{\xi}{x} \sum_j q_j\left(\frac{x}{\xi}, \mu^2\right) + 2N_c \frac{\xi}{x} g\left(\frac{x}{\xi}, \mu^2\right) \right]. \tag{9.2b}$$

We can then solve these for the gluon distribution:

$$xg(x, \mu^2) = \tilde{Q}(x, \mu^2) + \frac{\alpha_s N_c}{\pi} \int_{\mu_0^2}^{\mu^2} d \ln \mu'^2 \int_x^1 \frac{d\xi}{\xi} \xi g\left(\frac{x}{\xi}, \mu'^2\right), \tag{9.3a}$$

$$\tilde{Q}(x, \mu^2) = \frac{\alpha_s C_F}{2\pi} \ln \frac{\mu^2}{\mu_0^2} \int_x^1 d\xi \sum_j q_j\left(\frac{x}{\xi}\right). \tag{9.3b}$$

Note that because of its vanishing energy evolution, the quark density has no energy dependence at small- x . This also implies that \tilde{Q} is negligible, as it remains constant while g grows exponentially. So we can safely assume that in the small- x limit the evolution of the gluon density is given by:

$$xg(x, \mu^2) = \frac{\alpha_s N_c}{\pi} \int_{\mu_0^2}^{\mu^2} d\ln \mu'^2 \int_x^1 \frac{d\xi}{\xi} \xi g\left(\frac{x}{\xi}, \mu'^2\right). \quad (9.4)$$

This integral equation is of the so-called *Fredholm* type:

$$\phi(x) = f(x) + \lambda \int_a^b dy K(x, y)\phi(y),$$

where $\lambda < 1$ is an expansion parameter. It is even of double-Fredholm type, as this form holds in x and μ^2 at the same time. Fredholm type integrals can be solved by iteration (giving a Liouville-Neumann series). If we define:

$$u_0(x) = f(x),$$

$$u_1(x) = \int dy K(x, y)f(y),$$

$$u_2(x) = \int dy_1 dy_2 K(x, y_1)K(y_1, y_2)f(y_2),$$

...

the solution of a Fredholm type integral is given by

$$\phi(x) \equiv \sum_{i=0}^{\infty} \lambda^i u_i(x). \quad (9.5)$$

As the starting distribution for the gluon density we just take a constant:

$$f(x) = xg_0(x, \mu^2) = C.$$

The Neumann series is hence given by (using $\lambda \equiv \frac{\alpha_s N_c}{\pi}$):

$$u_0(x, \mu^2) \equiv C,$$

$$u_1(x, \mu^2) \equiv C \int_{\mu_0^2}^{\mu^2} d\ln \mu'^2 \int_x^1 d\ln \xi = C \ln \frac{\mu^2}{\mu_0^2} \ln \frac{1}{x},$$

$$u_2(x, \mu^2) \equiv C \int_{\mu_0^2}^{\mu^2} \int_{\mu_0^2}^{\mu'^2} d\ln \mu'^2 d\ln \mu''^2 \int_x^1 \int_{\xi_1}^1 d\ln \xi_1 d\ln \xi_2 = C \left(\frac{1}{2} \ln^2 \frac{\mu^2}{\mu_0^2} \right) \left(\frac{1}{2} \ln^2 \frac{1}{x} \right),$$

$$u_n(x, \mu^2) \equiv C \left(\frac{1}{n!} \ln^n \frac{\mu^2}{\mu_0^2} \right) \left(\frac{1}{n!} \ln^n \frac{1}{x} \right).$$

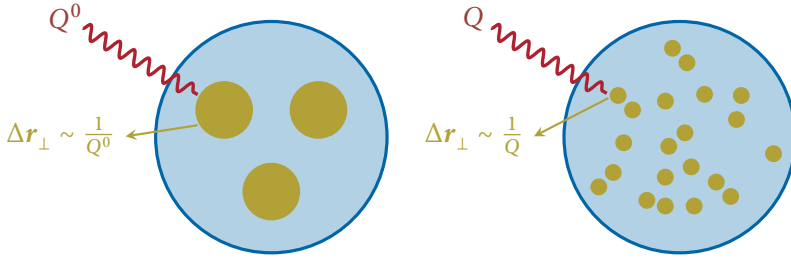


Figure 9.2: An illustration of the effect of the **DGLAP** evolution on the contents of a proton. Shown here is the transversal plane, as the proton has little or no longitudinal extent because it is highly boosted. On the left, a probe at low energy Q^0 does not have much resolution, hence it can only interact with the valence quarks. On the right, a probe at much higher energy $Q \gg Q^0$ has much more resolving power and can observe the sea quarks and gluons as well. Because of the increased energy scale, the spatial extent of the partons decreases (as observed by the probe). Hence the higher Q , the more the proton gets filled with smaller partons.

The full result for the gluon distribution is then given by **Equation 9.5**:

Gluon Distribution at Small- x	
$xg(x, \mu^2) = C \left(e^{\sqrt{\frac{\alpha_s N_c}{\pi} \ln \frac{\mu^2}{\mu_0^2} \ln \frac{1}{x}}} \right)^2 . \tag{9.6}$	(9.6)

This is called the double leading-logarithm approximation (**DLLA**). The interpretation of this result is of paramount importance. First of all, it is literally a resummation of gluon radiations—where each gluon in the ladder contributes a factor $\frac{\alpha_s N_c}{\pi} \ln \frac{\mu^2}{\mu_0^2} \ln \frac{1}{x}$ —with an additional factor $1/(n!)1/(n!)$ for a ladder with n gluons (this is due to the ordering of the gluons). Furthermore, this equation tells us that the gluon density increases as Q^2 increases and/or x decreases. The first is just a re-expression of the **DGLAP** evolution (more correct its small- x approximation as in **Equation 9.2a**). It orders successive gluon radiation in function of energy:¹

$$\mu_0^2 \ll \mu_1^2 \ll \dots \ll Q^2 . \tag{9.7}$$

The effect of the **DGLAP** evolution on the contents of a proton is illustrated in **Figure 9.2**. A proton that is highly boosted in the longitudinal direction will have little or no longitudinal extent. The transversal plane remains unaffected,

¹ Note that for the upper energy scale μ^2 one normally chooses the hard scale Q^2 .

so the proton resembles a pancake: flat and round. At a low scale Q^0 , the hard probe (a virtual photon) does not have enough resolving power to deeply probe the proton, hence it only observes the valence quarks. At much higher energies $Q \gg Q^0$, the probe is able to resolve much shorter distances Δr_\perp , and can interact with sea quarks and gluons as well (the latter via boson-gluon fusion). From the point of view of the probe, when increasing Q , the proton gets more constituents that are of a smaller spatial extent.

The fact that $xg(x)$ increases when x decreases also implies a strong ordering in x :

$$1 \gg x_1 \gg x_2 \gg \dots \gg x. \quad (9.8)$$

So pure **DGLAP** implies a strong ordering in μ^2 , while the **DLLA** (which is **DGLAP** at small- x) implies a strong ordering both in μ^2 and x . The third option—relaxing the ordering condition on μ^2 and only keeping ordering in x —is possible as well, and is very useful as it defines an evolution in x —*only* in x , independent of μ^2 . However, as in **DGLAP** k_\perp -dependence was resummed due to its strong ordering in μ^2 , relaxing this condition means that we can only define evolution equations in x if we add k_\perp -dependence to the gluon density, and define it by the requirement that after k_\perp -integration we should retrieve the original integrated gluon density:

$$xg(x, Q^2) \stackrel{\text{def}}{=} \frac{1}{\pi} \int^{Q^2} d^2\mathbf{k}_\perp f(x, \mathbf{k}_\perp, Q^2), \quad (9.9)$$

where the factor $1/\pi$ will cancel after integrating the angular part. Note that the integration has an upper cut-off Q^2 , and that we defined f with a scale factor of x inside. The unintegrated gluon density satisfies the so-called Balitsky-Fadin-Kuraev-Lipatov (**BFKL**) evolution equation:

BFKL Equation

$$\frac{\partial}{\partial \ln \frac{1}{x}} f(x, k_\perp^2) = \frac{\alpha_s N_c}{\pi^2} \int \frac{d^2\mathbf{q}_\perp}{(\mathbf{k}_\perp - \mathbf{q}_\perp)^2} \left[f(x, q_\perp^2) - \frac{1}{2} \frac{k_\perp^2}{q_\perp^2} f(x, k_\perp^2) \right], \quad (9.10)$$

where all instances of the gluon density are evaluated at the same scale μ^2 . As there is now no ordering in transverse momenta, the partons generated by the **BFKL** equations will retain their transverse size after evolution. This is the most important difference as compared to **DGLAP**, and is illustrated in **Figure 9.3**. It directly implies that for a given Q defining the spatial extent of all partons there exists an x_S which is the unitary limit, i.e. for all $x < x_S$ at the given Q , the probability to find a parton in the proton becomes bigger than one. A different

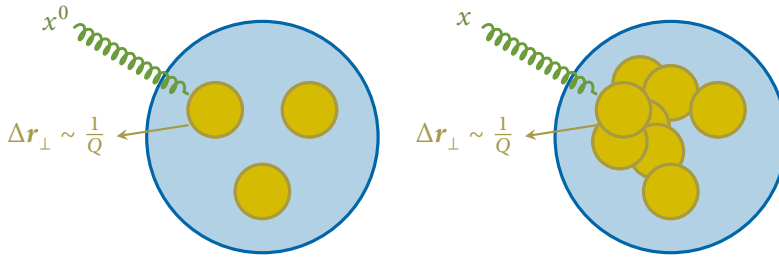


Figure 9.3: An illustration of the effect of the **BFKL** evolution on the contents of a proton. On the left, a probe with large momentum fraction x^0 probes the gluon density at large- x so it will only see a few partons. On the right, a probe with a much smaller fraction $x \ll x^0$ hits the proton and hence directly probes the gluon density at much smaller x . At small- x , the gluon density is exponentially larger and hence the probe sees a lot more partons. However, there spatial extent remains of the same order as before, as the energy scale remains unchanged. It seems as if the partons overlap each other. This is not a problem as long as unitarity is not violated, i.e. as long as there are not more partons than reasonably ‘fit’ inside the proton. As a rule of thumb, we estimate the unitarity condition to be violated when the total surface of the partons is bigger than the surface of the proton. In this case, an approach including saturation is needed.

approach is needed to avoid this scenario, namely the framework of *saturation* which we will treat in the next section.

When using the unintegrated gluon density to describe the proton, collinear factorisation is replaced by \mathbf{k}_\perp -factorisation. As we are mainly working with the gluon distribution, the elementary process is that of boson-gluon fusion (see [Figure 5.11](#)), for which the factorised cross section is given by:

$$\sigma(ep \rightarrow e q \bar{q}) = \int \frac{dy}{y} \frac{dx}{x} dQ^2 d^2 \mathbf{k}_\perp \hat{\sigma}(\hat{s}, \mathbf{k}_\perp, Q^2) f(x, \mathbf{k}_\perp, Q^2). \quad (9.11)$$

It has however only been proven at small- x . This is one of the main differences with the **TMD** framework, where factorisation has been proven independently of x , but only up to certain orders of $1/Q$.

We can express the differences between **DGLAP**, **DLA** and **BFKL** by the resummation of logarithms they induce. There are two types of logarithms that can possibly contribute to the resummation factor, namely the transverse logarithms $\ln \frac{\mu^2}{\mu_0^2}$ and the longitudinal logarithms $\ln \frac{1}{x}$. How these are resummed depends on which are dominant in combination with α_s . In the **DGLAP** case x is fixed and $\alpha_s \ll 1$, hence

$$\alpha_s \ln \frac{1}{x} \ll 1. \quad (9.12)$$

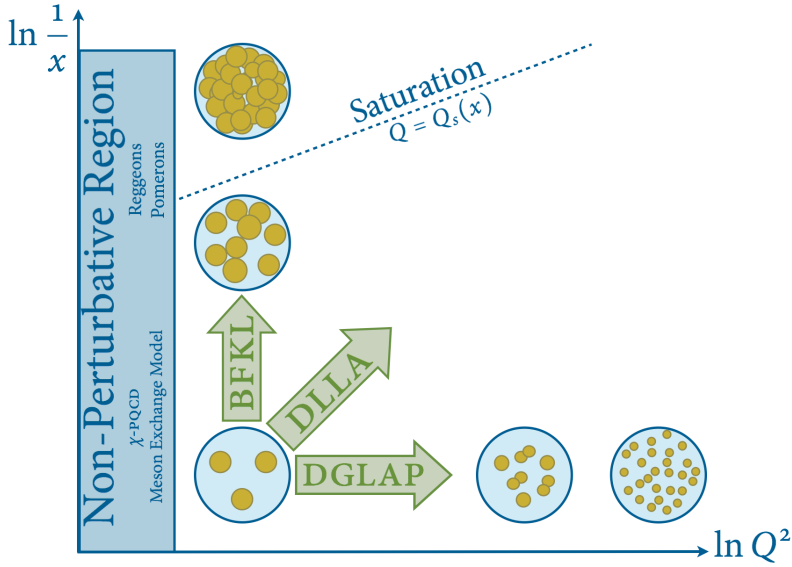


Figure 9.4: A QCD evolution roadmap. Evolving the parton density at constant x towards increasing Q^2 leads to an increase in the number of partons and a decrease of their spatial extent, saturation is never reached. This evolution is governed by the DGLAP equations. Evolving the parton density at constant Q^2 towards decreasing x also leads to an increase in the number of partons but keeps their spatial extent fixed, hence for small enough x the parton density becomes saturated. This evolution is governed by the BFKL equations. The DLLA is a combined evolution in x and Q^2 . When Q^2 is too low, a perturbative approach is no longer possible and different approaches are needed.

Because α_s runs in function of Q^2 , we have that

$$\alpha_s \ln \frac{\mu^2}{\mu_0^2} \sim 1, \tag{9.13}$$

which implies we have to resum these contributions. In the BFKL case it is the other way round, and we have to resum the contributions

$$\alpha_s \ln \frac{1}{x}. \tag{9.14}$$

In the DLLA both contributions separately are subleading:

$$\alpha_s \ln \frac{1}{x} \ll 1, \qquad \alpha_s \ln \frac{\mu^2}{\mu_0^2} \ll 1.$$

but their combination has to be resummed:

$$\alpha_s \ln \frac{1}{x} \ln \frac{\mu^2}{\mu_0^2} \sim 1. \quad (9.15)$$

We have collected these insights in [Figure 9.4](#), where the different evolutions are depicted graphically.

9.2 THE BK EQUATION AND SATURATION

We have seen that in the small- x limit the gluon density grows exponentially, ultimately violating the unitarity bound. We need to somehow adapt the [BFKL](#) equation to tame the exponential growth. But let us first have a look at the origin of this problematic behaviour. Both [DGLAP](#) and [BFKL](#) (and [DLLA](#)) are constructed from the splitting functions (see [Equations 5.71](#)) as a starting point. However, these don't give a full description of the possible processes inside the proton, as they only describe splittings, hence augmentations of the number of partons. However, these splitting functions could also be read in the inverse way, as *recombinations* of partons. It are these effects that are missing in [DGLAP](#) and [BFKL](#), and one can show that they become dominant once the proton is getting saturated.

If we write the [BFKL Equation 9.10](#) schematically as a convolution over a kernel, i.e. :

$$\frac{\partial}{\partial \ln \frac{1}{x}} f = \frac{\alpha_s N_c}{\pi^2} \mathcal{K}_{\text{BFKL}} \otimes f, \quad (9.16)$$

the recombination effects will manifest themselves as a quadratic term:

$$\frac{\partial}{\partial \ln \frac{1}{x}} f = \frac{\alpha_s N_c}{\pi^2} \mathcal{K}_{\text{BFKL}} \otimes [f - f^2]. \quad (9.17)$$

This equation is known as the Balitsky-Kovchegov ([BK](#)) equation. It is quite complicated to fully express it in function of the unintegrated density. Instead, calculations in the saturation framework are mostly done in the so-called *dipole picture*. In this picture, we boost to a frame where the struck parton before and after the interaction can be represented as a created pair (a dipole). This is illustrated in [Figure 9.5](#) for a quark dipole (the dipole can be a gluon dipole as well). Working with dipoles has a lot of advantages, one of these is e.g. that gluon radiation is *colour coherent*, which means that successive radiations are angular

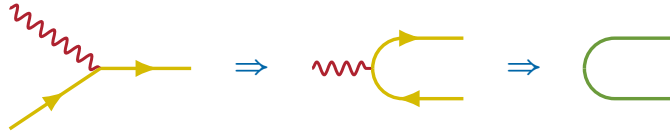


Figure 9.5: Illustration of the dipole picture. We boost to a frame where the incoming parton becomes outgoing, such that we can interpret the diagram as a photon fluctuating into a dipole. The third diagram shows the dipole as an index diagram (where only the colour structure is drawn). Index diagrams are introduced in Section 10.1.

ordered towards smaller angles when radiated from the dipole and towards larger angles when radiated before the dipole:

$$\theta < \psi, \tag{9.18a}$$

$$\theta > \psi. \tag{9.18b}$$

It is possible to define evolution equations based on colour coherence, the so-called Catani-Ciafaloni-Fiorani-Marchesini (CCFM) evolution equations. These are much more difficult to solve, but they are the best way to implement evolution in Monte Carlo generators (the relevant generator is called CASCADE).

The basic dynamical object in the dipole picture is the dipole scattering amplitude $\mathcal{N}(x, \mathbf{r}_\perp)$. This amplitude is supposed to have a unitary bound, i.e. $\mathcal{N} \leq 1$. The dipole cross section is then given by

$$\sigma(x, \mathbf{r}_\perp) \equiv \sigma_0 \mathcal{N}(x, \mathbf{r}_\perp), \tag{9.19}$$

which can be related to the unintegrated gluon density by:

$$\sigma(x, \mathbf{r}_\perp) = \frac{4\pi\alpha_s}{3} \int \frac{d^2\mathbf{k}_\perp}{k_\perp^4} f(x, k_\perp^2) (1 - e^{i\mathbf{k}_\perp \cdot \mathbf{r}_\perp}), \tag{9.20a}$$

$$f(x, k_\perp^2) = \frac{3}{16\pi^3 \alpha_s} k_\perp^2 \mathcal{F}_{k_\perp} [\Delta\sigma(x, \mathbf{r}_\perp)], \tag{9.20b}$$

where Δ is the Laplacian operator in cylinder coordinates. The scattering amplitude can also depend on an impact parameter \mathbf{b}_\perp , which represents the trans-

versal distance between the centre of the dipole and the target. The regular densities are then retrieved by integration over \mathbf{b}_\perp with an extra factor 2:

$$f(x, \mathbf{r}_\perp) = 2\pi \int_0^\infty db^2 f(x, \mathbf{r}_\perp, b^2) \quad (9.21)$$

$$\sigma(x, \mathbf{r}_\perp) = 2\pi \int_0^\infty db^2 \sigma(x, \mathbf{r}_\perp, b^2) \quad (9.22)$$

We can express the BFKL equation in function of the dipole amplitude:

Dipole BFKL Equation

$$\frac{\partial}{\partial \ln \frac{1}{x}} \mathcal{N}(\mathbf{r}_\perp, \mathbf{b}_\perp, x) = \frac{\alpha_s N_c}{2\pi^2} \int d^2 \mathbf{z}_\perp \frac{r_\perp^2}{r_{1\perp}^2 r_{2\perp}^2} [\mathcal{N}_1 + \mathcal{N}_2 - \mathcal{N}], \quad (9.23)$$

where

$$\mathbf{r}_\perp \stackrel{N}{=} \mathbf{x}_{1\perp} - \mathbf{x}_{0\perp}, \quad \mathbf{r}_{1\perp} \stackrel{N}{=} \mathbf{x}_{1\perp} - \mathbf{z}_\perp, \quad \mathbf{r}_{2\perp} \stackrel{N}{=} \mathbf{z}_\perp - \mathbf{x}_{0\perp}, \quad (9.24a)$$

$$\mathbf{b}_\perp \stackrel{N}{=} \frac{1}{2}(\mathbf{x}_{1\perp} + \mathbf{x}_{0\perp}), \quad \mathbf{b}_{1\perp} \stackrel{N}{=} \frac{1}{2}(\mathbf{x}_{1\perp} + \mathbf{z}_\perp), \quad \mathbf{b}_{2\perp} \stackrel{N}{=} \frac{1}{2}(\mathbf{z}_\perp + \mathbf{x}_{0\perp}), \quad (9.24b)$$

$$\mathcal{N} \stackrel{N}{=} \mathcal{N}(\mathbf{r}_\perp, \mathbf{b}_\perp, x), \quad \mathcal{N}_1 \stackrel{N}{=} \mathcal{N}(\mathbf{r}_{1\perp}, \mathbf{b}_{1\perp}, x), \quad \mathcal{N}_2 \stackrel{N}{=} \mathcal{N}(\mathbf{r}_{2\perp}, \mathbf{b}_{2\perp}, x). \quad (9.24c)$$

We can interpret the dipole BFKL equation as a dipole splitting into two dipoles, as illustrated in [Figure 9.6](#). It is now not difficult to add the quadratic term that ensures saturation, leading to the BK equation in the dipole picture:

Dipole BK Equation

$$\frac{\partial}{\partial \ln \frac{1}{x}} \mathcal{N} = \frac{\alpha_s N_c}{2\pi^2} \int d^2 \mathbf{z}_\perp \frac{r_\perp^2}{r_{1\perp}^2 r_{2\perp}^2} [\mathcal{N}_1 + \mathcal{N}_2 - \mathcal{N} - \mathcal{N}_1 \mathcal{N}_2], \quad (9.25)$$

The BK equation naturally introduces the *saturation scale* $Q_s(x)$ at which saturation effects become important. It is a curve in the (Q, x) kinematical plane (see [Figure 9.4](#)), and its definition is model-dependent. It acts as an IR cut-off, screening the non-perturbative part, hence making saturation physics consistently perturbative.

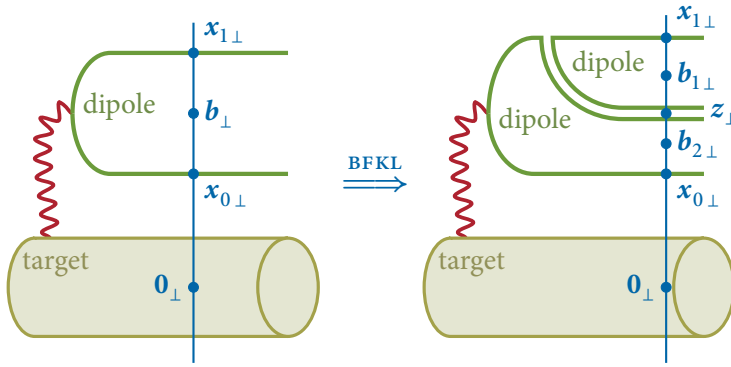


Figure 9.6: In the dipole picture, the **BFKL** evolution is an evolution in dipoles, i.e. new dipoles are created during the evolution. A gluon that is radiated from the dipole can be represented as two fundamental lines (see Equation 10.13). This essentially splits the dipole in two at the point z_{\perp} , as is illustrated in the second diagram.

Comparison to Population Statistics

In order to understand a bit more how the quadratic term induces saturation, we make a comparison to mathematical biology, where a similar procedure is used.² The most basic model for population growth links the growth to the population density (the more animals are present, the more animals reproduce and the more offsprings will arise):

$$\dot{N}(t) = \kappa N(t) \quad \Rightarrow \quad N(t) = N_0 e^{\kappa t} . \tag{9.26}$$

This cannot be a realistic model, as it is possible for the population to overpopulate: if there are too many animals, the lack of food and limited space will decrease the growth. The simplest way to implement this is to let the growth parameter decrease for increasing N :

$$\kappa \rightarrow \kappa (1 - N) .$$

This introduces the quadratic term to the growth equation, which is commonly known as the logistic equation:

$$\dot{N}(t) = \kappa [N(t) - N^2(t)] \quad \Rightarrow \quad N(t) = \frac{e^{\kappa t}}{e^{\kappa t} + \frac{1-N_0}{N_0}} . \tag{9.27}$$

² It is not the case that the addition of the quadratic term to the **BFKL** equation is motivated from biology. The quadratic term follows directly from the recombination effects of the partons. We just make the comparison here to simplify understanding the effect at hand.

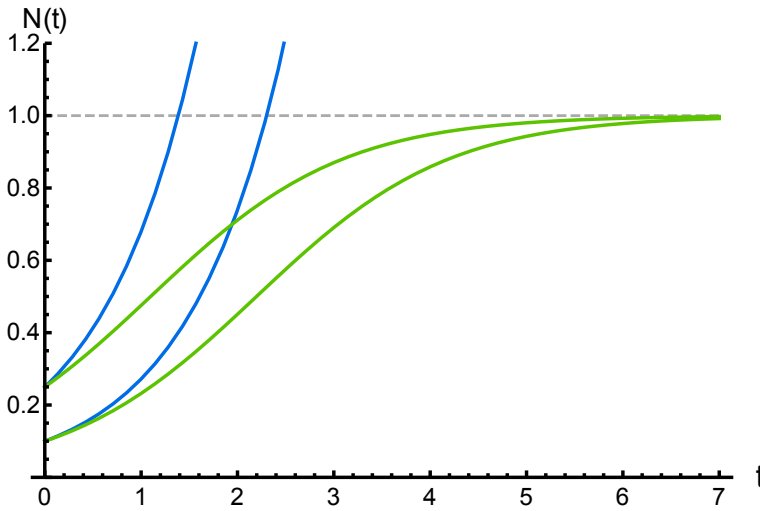


Figure 9.7: Comparison between regular exponential growth (in blue) and the logistic equation (in green) for two initial values ($N_0 = 0.1$ and $N_0 = 0.25$). Note that the logistic growth saturates towards the same value (here equal to 1), independently of the initial condition.

The comparison between the two formulae is made in [Figure 9.7](#). The important thing to remark is that the logistic equation always saturates towards the same value, independently of N_0 . The same is of course true with the [BK](#) equation.

The GBW model

The [BK](#) equation is an exact analytical equation, but difficult to deal with. It is however possible to create models that are inspired on the mechanism in the [BK](#) equations to describe similar saturated behaviour. The most easy (and most well-known) saturation model is the Golec-Biernat Wüsthoff ([GBW](#)) model [105]. It parameterises the dipole amplitude as:

GBW Model

$$\mathcal{N}(x, r_{\perp}) = 1 - e^{-\frac{1}{4} \frac{r_{\perp}^2}{R_0^2(x)}}, \quad (9.28)$$

where the *saturation radius* is modelled as

$$R_0^2(x) \stackrel{\text{def}}{=} \frac{1}{Q_0^2} \left(\frac{x}{x_0} \right)^{\lambda}. \quad (9.29)$$

The factor in front is just a constant to set the scale:

$$Q_0 \stackrel{\text{def}}{=} 1 \text{ GeV}. \quad (9.30)$$

The saturation radius is intimately related to the saturation scale:

$$Q_s^2 \equiv \frac{1}{R_0^2}. \quad (9.31)$$

When comparing to data, the dipole cross section is used:

$$\sigma(x, r_{\perp}) = \sigma_0 \left(1 - e^{-\frac{1}{4} r_{\perp}^2 Q_s^2} \right) \quad (9.32)$$

Note that the dipole amplitude has as requested a unitary bound $\mathcal{N} \leq 1$. The model has been compared to HERA data, and the parameters σ_0 , x_0 and λ have been fit [85, 106]:

$$\sigma_0 = 23.03 \text{ mb}, \quad \lambda = 0.288, \quad x_0 = 3.04 \cdot 10^{-4}, \quad (9.33)$$

with $\chi^2 = 1.18$, deeming it a good fit. The dipole cross section is plot in [Figure 9.8](#) for a few values of x . The cross section value at the saturation radius is independent of x :

$$\sigma_s = \sigma_0 \left(1 - e^{-\frac{1}{4}} \right) \approx 5.09. \quad (9.34)$$

Using [Equations 9.20](#), we can calculate the unintegrated gluon density in the GBW model:

$$f(x, k_{\perp}^2) = \frac{3\sigma_0}{4\pi^2\alpha_s} R_0^2(x) k_{\perp}^4 e^{-R_0^2(x) k_{\perp}^2}. \quad (9.35)$$

It is however common in literature to define the gluon density with an extra factor $(1-x)^7$, motivated by power counting:

$$f(x, k_{\perp}^2) = \frac{3\sigma_0}{4\pi^2\alpha_s} (1-x)^7 R_0^2(x) k_{\perp}^4 e^{-R_0^2(x) k_{\perp}^2}, \quad (9.36)$$

which is the definition we will use in the next section.

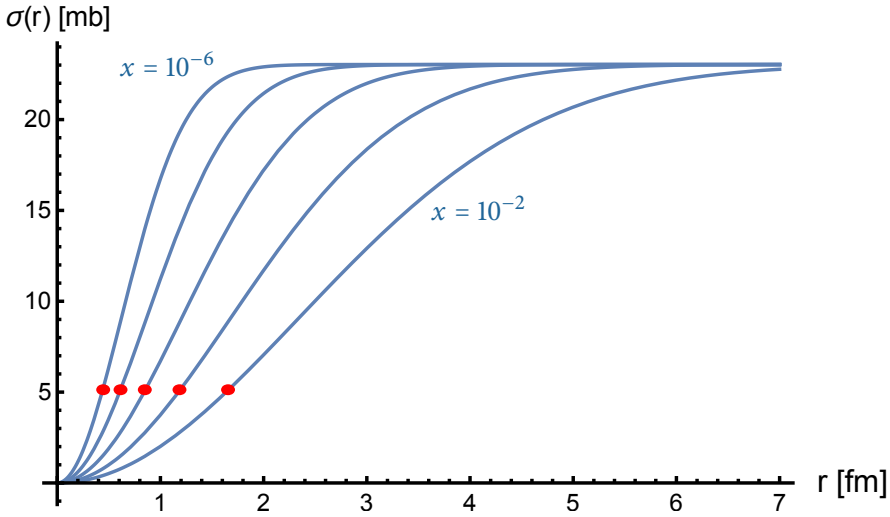


Figure 9.8: Plot of the **GBW** dipole cross section for $x = 10^{-2}, \dots, 10^{-6}$. The red dots are the saturation radii for the given x .

9.3 TRANSVERSAL ENERGY FLOW

It is not so obvious to look for **BFKL** and **BK** signatures in data. Measurements of the F_2 structure function at **HERA** show a rise for decreasing x which is in perfect agreement with **BFKL** predictions. However, F_2 is not suited—due to its inclusive nature—to discriminate between conventional dynamics and **BFKL**, as the observed rise can as well be explained using regular **DGLAP** evolution. An adequate approach is to include final-state properties in the measurement. A good example is the transversal energy flow coming from a small- x gluon ladder, which has already successfully been used to look for **BFKL** signatures in **HERA** data [106–109]. We will apply this formalism to include saturation effects.

Because in **BFKL** and **BK** there is no longer an ordering in μ^2 , we expect to find more transversal energy in the central region, between the main jet and the proton remnants, as illustrated in **Figure 9.9**. The definition of the E_T flow is given by [108]:

$$\xi_j \frac{\partial E_T}{\partial \xi_j} = \frac{1}{\sigma} \int dk_{\perp j}^2 \xi_j \frac{\partial^2 \sigma}{\partial \xi_j \partial k_{\perp j}^2} |\mathbf{k}_{\perp j}|, \quad (9.37)$$

where σ is the total cross section in the range (x, Q^2) , and a sum over j is implied. In order to clarify the notation a bit, we drop the \perp -notation on the

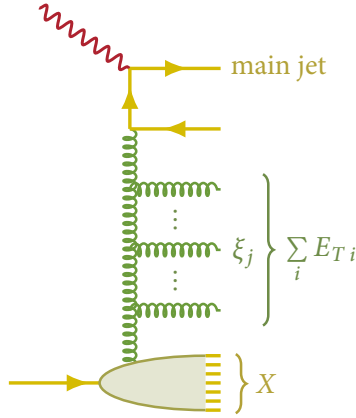


Figure 9.9: Definition of the transversal energy flow. In a boson-gluon fusion process, the energies of the gluons radiated in the ladder are summed to give the full E_T flow. We expect to find more transversal gluons in a [BFKL](#) framework.

momenta. Just remember that every momentum represents only its transversal component. We can express the differential cross section as a function of the differential structure functions:

$$\frac{\partial^2 \sigma}{\partial \xi_j \partial k_j^2} = \frac{4\pi\alpha^2}{xQ^4} \left[(1-y) \frac{\partial^2 F_2}{\partial \xi_j \partial k_j^2} + \frac{1}{2} y^2 \frac{\partial^2 (2xF_1)}{\partial \xi_j \partial k_j^2} \right], \quad (9.38a)$$

$$y = \frac{Q^2}{xs}. \quad (9.38b)$$

We need the total cross section to use it as a normalisation in the denominator of (9.37). It is given by:

$$\begin{aligned} \sigma &= \frac{4\pi\alpha^2}{xQ^4} \int_{(x,0)}^{(1,Q^2)} d\xi_j dk_j^2 \left[(1-y) \frac{\partial^2 F_2}{\partial \xi_j \partial k_j^2} + \frac{1}{2} y^2 \frac{\partial^2 (2xF_1)}{\partial \xi_j \partial k_j^2} \right], \\ &= \frac{4\pi\alpha^2}{xQ^4} \left[(1-y) (F_T(x, Q^2) + F_L(x, Q^2)) + \frac{y^2}{2} F_T(x, Q^2) \right]. \end{aligned}$$

We can express the differential structure functions as:

$$\begin{aligned} \xi_j \frac{\partial^2 F_{1,2}}{\partial \xi_j \partial k_j^2} &= 3 \frac{\alpha_s}{\pi^2} \frac{1}{k_j^2} \int \frac{d^2 \mathbf{k}_p}{k_p^2} \frac{d^2 \mathbf{k}_\gamma}{k_\gamma^2} \mathcal{F}_{1,2} \left(\frac{x}{\xi_j}, k_\gamma^2, Q^2 \right) \\ &\quad \times f(\xi_j, k_p^2) \delta^{(2)}(\mathbf{k}_j - \mathbf{k}_\gamma - \mathbf{k}_p). \end{aligned}$$

\mathcal{F}_i and f are the soft gluon resummations above resp. below the j -th gluon. This gives:

$$\begin{aligned}\xi_j \frac{\partial E_T}{\partial \xi_j} &= 3 \frac{\alpha_s}{\pi^2} \frac{1}{F(x, Q^2)} \int dk_j^2 \frac{d^2 \mathbf{k}_p}{k_p^2} \frac{d^2 \mathbf{k}_\gamma}{k_\gamma^2} \frac{1}{\sqrt{k_j^2}} \\ &\quad \times \mathcal{F} \left(\frac{x}{\xi_j}, k_\gamma^2, Q^2 \right) f(\xi_j, k_p^2) \delta^{(2)}(\mathbf{k}_j - \mathbf{k}_\gamma - \mathbf{k}_p), \\ F &= \left(1 - y + \frac{y^2}{2} \right) F_T + (1 - y) F_L, \\ \mathcal{F} &= \left(1 - y + \frac{y^2}{2} \right) \mathcal{F}_T + (1 - y) \mathcal{F}_L.\end{aligned}$$

To integrate the δ -function over \mathbf{k}_j , we shift the k_j -integration back to its component form:

$$\begin{aligned}dk_j^2 &= \frac{1}{2\pi} dk_j^2 d\phi = \frac{1}{\pi} k_j dk_j d\phi = \frac{1}{\pi} d^2 \mathbf{k}_j, \\ \xi_j \frac{\partial E_T}{\partial \xi_j} &= 3 \frac{\alpha_s}{\pi^3} \frac{1}{F} \int \frac{d^2 \mathbf{k}_p}{k_p^2} \frac{d^2 \mathbf{k}_\gamma}{k_\gamma^2} \frac{1}{\sqrt{(\mathbf{k}_p + \mathbf{k}_\gamma)^2}} \mathcal{F} \left(\frac{x}{\xi_j}, k_\gamma^2, Q^2 \right) f(\xi_j, k_p^2), \\ &= \frac{3\alpha_s}{2\pi^2} \frac{1}{F} \int \frac{dk_p^2}{k_p^2} \frac{d^2 \mathbf{k}_\gamma}{k_\gamma^2} d\varphi \mathcal{F} \left(\frac{x}{\xi_j}, k_\gamma^2, Q^2 \right) f(\xi_j, k_p^2) \\ &\quad \times \frac{1}{\sqrt{k_p^2 + k_\gamma^2 + 2k_p k_\gamma \cos \varphi}}.\end{aligned}$$

The integration over φ can still be done exactly, using:

$$\begin{aligned}\int_0^{2\pi} \frac{d\varphi}{\sqrt{A + B \cos \varphi}} &= \frac{4}{\sqrt{A + B}} K \left(\frac{2B}{A + B} \right), \\ \xi_j \frac{\partial E_T}{\partial \xi_j} &= \frac{\alpha_s}{\pi^2} \frac{6}{F} \int \frac{dk_p^2}{k_p^2} \frac{dk_\gamma^2}{k_\gamma^2} \mathcal{F} \left(\frac{x}{\xi_j}, k_\gamma^2, Q^2 \right) f(\xi_j, k_p^2) \\ &\quad \times \frac{1}{k_p + k_\gamma} K \left(\frac{4k_p k_\gamma}{(k_p + k_\gamma)^2} \right),\end{aligned}$$

where $K(m)$ is the complete elliptic integral of the first kind, which is divergent for $m \geq 1$ (see [Equations B.9](#)). Next we use the transformation $k_p = aL$ and $k_\gamma = (1 - a)L$ as defined in [Equations B.11](#):

$$\xi_j \frac{\partial E_T}{\partial \xi_j} = \frac{\alpha_s}{\pi^2} \frac{24}{F} \int_0^1 \int_0^\infty \frac{da dL}{a(1-a)L^2} \mathcal{F} \left(\frac{x}{\xi_j}, (1-a)L, Q^2 \right) f(\xi_j, aL) K(4a(1-a)).$$

This integral is divergent at $a = \frac{1}{2}$, and at the borders $a = 0$, $a = 1$ and $L = 0$. We expect however that the divergences at the borders will cancel out, because generally we can factorise out at least k_p from f and k_y from \mathcal{F} without introducing (additional) divergences in f or \mathcal{F} .

Calculation of the Structure Functions

We can calculate F_T and F_L in coordinate space or in momentum space. In coordinate space we use the dipole cross section and the photon wave functions (of $q\bar{q}$ fluctuations) to get:

$$F_{T,L}(x, Q^2) = \frac{Q^2}{2\pi \alpha_{\text{em}}} \sum_q \int \rho d\rho |\Psi_{T,L}^q(z, \rho)|^2 \sigma(\tilde{x}_q, \rho) \quad (9.39a)$$

$$|\Psi_L^q(z, \rho)|^2 = 6 \frac{\alpha_{\text{em}}}{4\pi^2} e_q^2 \int_0^1 dz 4z^2 (1-z)^2 Q^2 K_0^2(\epsilon\rho) \quad (9.39b)$$

$$|\Psi_T^q(z, \rho)|^2 = 6 \frac{\alpha_{\text{em}}}{4\pi^2} e_q^2 \int_0^1 dz [(z^2 + (1-z)^2) \epsilon^2 K_1^2(\epsilon\rho) + m_q^2 K_0^2(\epsilon\rho)] \quad (9.39c)$$

$$\epsilon^2 = z(1-z) Q^2 + m_q^2 \quad (9.39d)$$

where we added a mass correction to x :

$$\tilde{x}_q = \frac{Q^2 + 4m_q^2}{Q^2} x \quad (9.40)$$

In momentum space we use the unintegrated PDF and the photon impact factors to get (see [110]):

$$F_{T,L}(x, Q^2) = \frac{Q^2}{8\pi^2 \alpha_{\text{em}}} \sum_q \int \frac{dk^2}{k^4} \Phi_{T,L}^q(k^2, Q^2) f(\tilde{x}_q, k^2), \quad (9.41a)$$

$$\Phi_L^q(k^2, Q^2) = 16\pi \alpha_{\text{em}} \alpha_s e_q^2 \int_0^1 dz d\zeta Z^{-1} [z(1-z)\zeta^2(1-\zeta)^2 k^2 Q^2], \quad (9.41b)$$

$$\Phi_T^q(k^2, Q^2) = 2\pi \alpha_{\text{em}} \alpha_s e_q^2 \int_0^1 dz d\zeta Z^{-1} [(z^2 + (1-z)^2)(\zeta^2 + (1-\zeta)^2)\zeta(1-\zeta) k^2 Q^2]$$

$$+ \left(\zeta^2 + (1 - \zeta)^2 \right) m_q^2 k^2 + 4z(1 - z) \zeta(1 - \zeta) m_q^2 \Big], \quad (9.41c)$$

$$Z = \left(z(1 - z) k^2 + \zeta(1 - \zeta) Q^2 + m_q^2 \right) \left(\zeta(1 - \zeta) Q^2 + m_q^2 \right). \quad (9.41d)$$

Numerical Evaluation of the E_T -Flow

To evaluate the E_T -Flow integral, we cut out a small region around $a = \frac{1}{2}$

$$\begin{aligned} \xi_j \frac{\partial E_T}{\partial \xi_j} &= \Delta_\epsilon I + \frac{\alpha_s}{\pi^2} \frac{24}{F(x, Q^2)} \left(\int_0^{\frac{1}{2}-\epsilon} + \int_{\frac{1}{2}+\epsilon}^1 \right) \int_0^\infty \frac{da dL}{a(1-a)L^2} \\ &\quad \times \mathcal{F} \left(\frac{x}{\xi_j}, (1-a)L, Q^2 \right) f(\xi_j, aL) K(4a(1-a)), \end{aligned}$$

for some ϵ which is small enough to make $\Delta_\epsilon I$ reliable, but not too small to make sure that the main integration part will still converge fast enough. We expand the elliptic function around 1 to approximate $\Delta_\epsilon I$:

$$\begin{aligned} \Delta_\epsilon I &= \frac{\alpha_s}{\pi^2} \frac{24}{F(x, Q^2)} \int_{\frac{1}{2}-\epsilon}^{\frac{1}{2}+\epsilon} \int_0^\infty da dL \frac{\mathcal{F}((1-a)L) f(aL) K(4a(1-a))}{a(1-a)L^2}, \\ &= \frac{\alpha_s}{\pi^2} \frac{96}{F(x, Q^2)} \int_{-\epsilon}^\epsilon \int_0^\infty da dL \frac{\mathcal{F}(\left(\frac{1}{2}-a\right)L) f\left(\left(\frac{1}{2}+a\right)L\right) K(1-4a^2)}{(1-4a^2)L^2}, \end{aligned}$$

$$K(1-4a^2) \approx \ln 2 - \ln |a| + (\ln 2 - 1 - \ln |a|) a^2 + \frac{9}{4} \left(\ln 2 - \frac{7}{6} - \ln |a| \right) a^4.$$

Furthermore we use the following approximation formula (for given N , where $a > 0$):

$$\int_{-a}^a dx f(x) \ln |x| \approx \frac{a}{N} f(0) \ln \frac{a}{2\pi N} + \frac{a}{N} \sum_{i=-N, i \neq 0}^N w_i f\left(i \frac{a}{N}\right) \ln \left| i \frac{a}{N} \right| \quad (9.42)$$

$$w_{|N|} = \frac{5}{12} \quad w_{|N-1|} = \frac{13}{12} \quad w_{|i|} = 1 \quad \forall i \neq N, i \neq N-1 \quad (9.43)$$

We use simplified quark masses and fixed coupling constants:

$$m_q = \{0.15, 0.15, 1.5, 0.15\}, \quad \alpha_{em} = \frac{1}{137}, \quad \alpha_s = 0.2.$$

For the gluon density, we use the GBW model (see Equation 9.36), and for \mathcal{F} we use a model that is inspired on the GBW model [111]:

$$\mathcal{F}_{GBW}(z, k, Q) = N_d(Q^2) \frac{\sigma_0}{2\pi^2\alpha_s} (1-z)^5 Q^2 k^4 R_0^2(z) e^{-k^2 R_0^2(z)}, \quad (9.44)$$

with the same parameters as the GBW gluon density and

$$N_d(Q^2) \approx 1.46. \quad (9.45)$$

Our results are shown in Figure 9.10. In the large- x_B regime more transversal gluons are radiated at higher Q^2 compared to low Q^2 , while the small- x_B regime is insensitive to Q^2 .

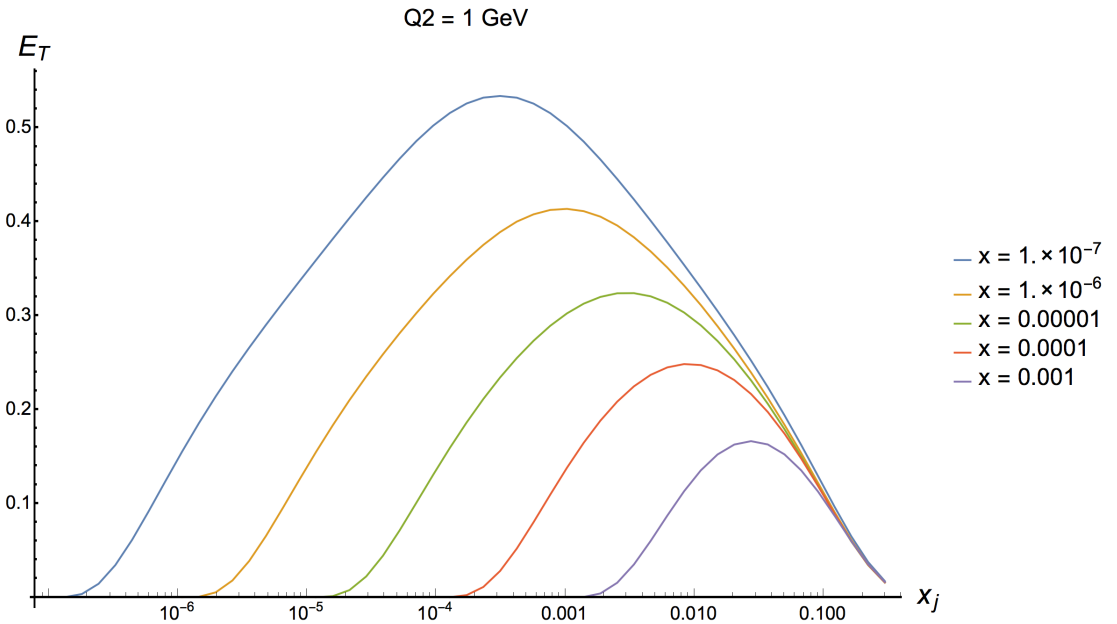
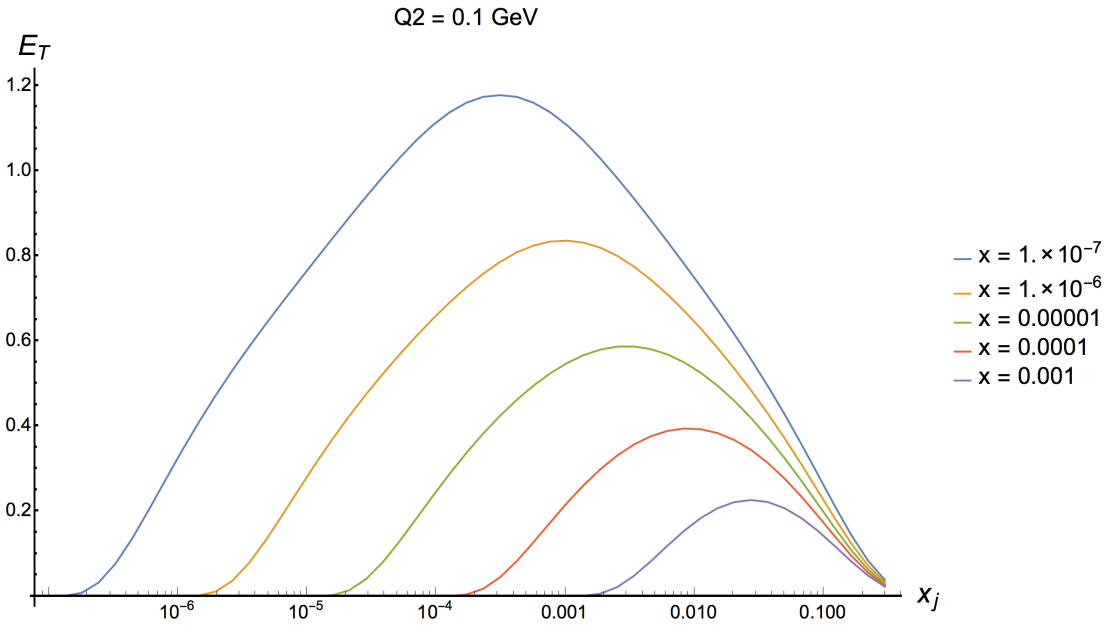
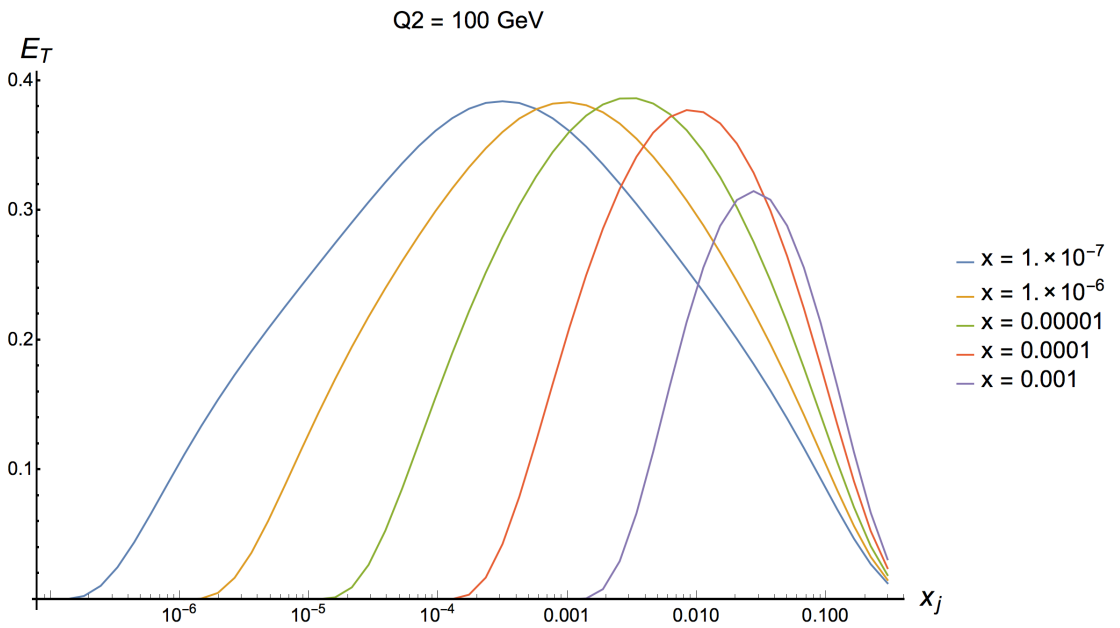
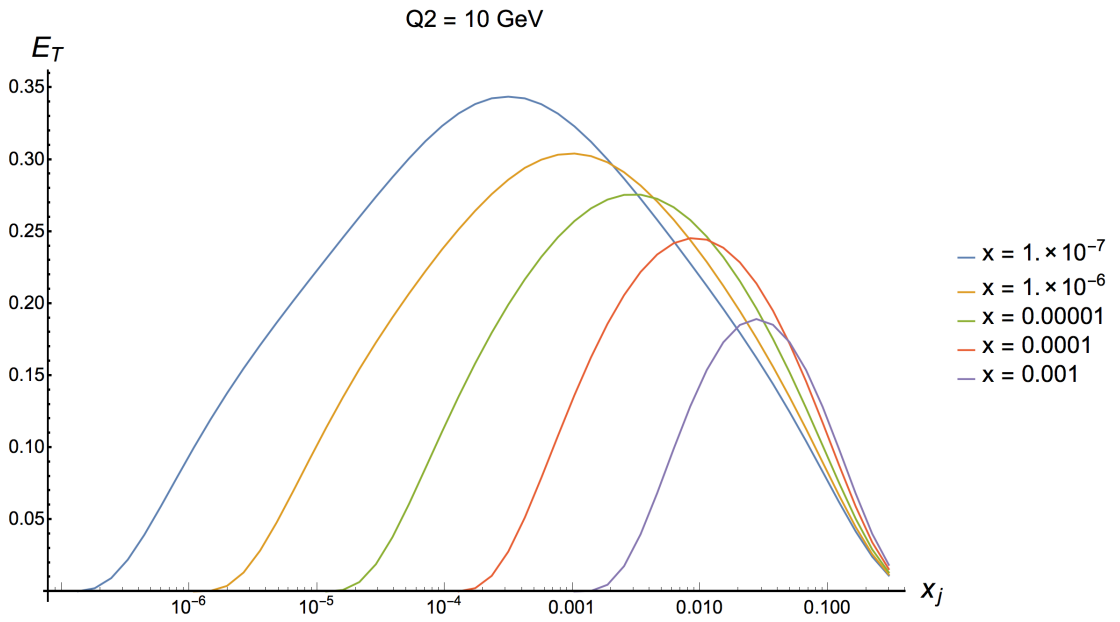


Figure 9.10: Plot of the transversal energy flow in the GBW model for 4 values of Q^2 . We see that in the large- x_B regime more transversal gluons are radiated at higher Q^2 , while the small- x_B regime is insensitive to Q^2 .



(continuation of [Figure 9.10](#))

Part III

WILSON LOOPS AND EVOLUTION

WILSON LOOPS AND LOOP SPACE

In this chapter we will introduce Wilson loops as elementary bricks that allow us to fully recast **QCD** in loop space using the multicolour limit, essentially trading coordinate dependence for path dependence. We start by introducing the large- N_c framework, which—although unrealistic—can give more insight to the non-perturbative behaviour of **QCD**. We will mostly follow the excellent lecture notes by Makeenko [112] in this section. Next we will treat the renormalisation of Wilson loops, and investigate how the energy evolution is governed by Γ_{cusp} , the cusp anomalous dimension.

It will provide us with a solid base to our investigation of the geometric evolution of Wilson loops in [Chapter 11](#). As always we try to avoid going too deep into details. See e.g. [113–124] for a more profound treatment of the topics covered in this and the next chapter.

10.1 LARGE N_c -LIMIT

We saw in Subsection [Running Coupling in QCD: Asymptotic Freedom](#) on page 116 and onwards that **QCD** is asymptotically free due to the particular behaviour of the strong coupling α_s , which invalidates any perturbative approach at energies smaller than Λ_{QCD} . There is however another possibility, that avoids this invalidation by promoting the number of colours N_c to a variable. If we then expand the interaction exponential e^{iS_I} in function of N_c , we can keep the expansion convergent—even when α_s is larger than one—by making N_c large enough to compensate for α_s . To see this, we note that the former enters in the denominator of the evolution of the latter (see [Equation 4.84](#)):

$$\alpha_s(\mu) = \frac{\alpha_s 0}{1 - \frac{\alpha_s 0}{4\pi} b_0 \ln \frac{\mu^2}{\mu_0^2}},$$

where

$$b_0^{\text{su}(n)} = -\frac{11}{3}N_c + \frac{2}{3}N_f.$$

In other words, if α_s tends towards values bigger than one, we have to increase N_c just enough to compensate for the growth in α_s , hence keeping the expansion convergent. It is then logical that in the limit $N_c \rightarrow \infty$ the expansion is convergent *to all orders in α_s* [125], i.e. the large- N_c limit gives a non-perturbative description of QCD.

Of course this is not a realistic treatment, as we know that the number of colours is fixed to 3, and it becomes even less realistic at energies where $\alpha_s \gtrsim 1$. However, it can tell us a lot about the dominant regions in certain processes.

Colour Representation

To use the large- N_c framework in practice, we first investigate the method of *colour representations*, where the colour part of a diagram is depicted and calculated separately from the rest of a Feynman diagram. For this purpose, we define a so-called *matrix-field* by absorbing a Lie generator in the gauge field, such that the latter has manifest fundamental indices but no adjoint indices:

$$A_{ij}^\mu \stackrel{\text{def}}{=} A_a^\mu (t^a)_{ij}. \quad (10.1)$$

To calculate the matrix-field propagator, we use the Fierz identity (see Equation A.77):

$$\left\langle A_\mu^{ij}(x) A_\nu^{kl}(y) \right\rangle = \left(\frac{1}{2} \delta^{il} \delta^{kj} - \frac{1}{2N_c} \delta^{ij} \delta^{kl} \right) D_{\mu\nu}(x, y). \quad (10.2)$$

If we now focus on the colour structure—that is we forget the momentum part and express the propagator in *index space*, using only the fundamental indices—we can write the matrix-gluon propagator as

Matrix-Field Propagator

$$\begin{array}{c} i \\ \bullet \\ \text{-----} \\ \bullet \\ j \end{array} \begin{array}{c} l \\ \bullet \\ \text{-----} \\ \bullet \\ k \end{array} = \frac{1}{2} \begin{array}{c} i \rightarrow l \\ \leftarrow k \end{array} - \frac{1}{2N_c} \begin{array}{c} i \rightarrow \\ \leftarrow j \end{array} \begin{array}{c} l \\ \leftarrow k \end{array}, \quad (10.3)$$

where the green lines are ‘quark-like’ lines, i.e. they have the same colour structure as quarks (being in the fundamental representation), but of course not the same momentum nor Dirac structure. Although the Kronecker δ ’s

seem to indicate that there is some freedom in the direction of the arrow, we have to impose that the matrix-gluon can be written as two quark-like lines in *opposite* directions. This is motivated by the hermiticity of A_μ^{ij} , that amounts an interchange of i and j to a complex conjugation. Another way to see this is to realise that the fundamental index literally represents colour flow, and a gluon always carries a colour and an anticolour.

We can use this pictorial representation to investigate the colour structure of e.g. quark-antiquark scattering (with an additional factor ig per vertex):

$$\begin{array}{c} \text{diagram} \end{array} = -\frac{g^2}{2} \left(\begin{array}{c} \text{diagram 1} \\ \text{diagram 2} \end{array} - \frac{1}{N_c} \begin{array}{c} \text{diagram 3} \\ \text{diagram 4} \end{array} \right) \quad (10.4)$$

The square then becomes:

$$\left| \begin{array}{c} \text{diagram} \end{array} \right|^2 = \frac{g^4}{4} \left(\begin{array}{c} \text{diagram 1} \\ \text{diagram 2} \end{array} - \frac{2}{N_c} \begin{array}{c} \text{diagram 3} \end{array} + \frac{1}{N_c^2} \begin{array}{c} \text{diagram 4} \end{array} \right) \quad (10.5)$$

Note that there is no difference between the yellow and the green lines—both are fundamental index lines—but we keep the difference as a reminder of the original line. The major simplification of this technique now lies in the fact that every loop (which is just defined as a closed index line) contributes the same factor N_c , independent of its underlying physical origin. This is because both internal loops and external particles are summed over colour, giving a factor $\delta^{ii} = N_c$. Furthermore, we can move index lines at will if we don't tear them,¹ such that the topological equivalence lies only in the counting of loops, and not in the form of these loops. From the moment an index line is closed, it is considered a loop, no matter how this loop looks.

In the case of Equation 10.5, the first and the last term have two loops and hence each contribute a factor N_c^2 , while the second term has only one loop and contributes a factor N_c . The result is then

$$\left| \begin{array}{c} \text{diagram} \end{array} \right|^2 = \frac{g^4}{4} (N_c^2 - 2 + 1) = \frac{g^4}{2} N_c C_F, \quad (10.6)$$

which is indeed the correct result. Often we will average over incoming colour, implying that we divide by an additional N_c , giving the common result $\frac{g^4}{2} C_F$.

¹ Because there is no coordinate dependence, only fundamental index dependence.

We don't need squared amplitudes to make use of colour representations, e.g. the colour structure for the quark self-energy can be calculated in an easy manner as well:

$$\begin{aligned}
 \text{quark self-energy} &= -\frac{g^2}{2} \left(\text{quark with gluon loop} - \frac{1}{N_c} \text{quark} \right), \\
 &= -\frac{g^2}{2} \left(N_c \text{quark} - \frac{1}{N_c} \text{quark} \right), \\
 &= -g^2 C_F \text{quark}.
 \end{aligned} \tag{10.7}$$

This is a logical result, because the two vertices give a total colour factor $t^a t^a = C_F$. The colour representation method works, and is a very useful tool to investigate the colour structure of a diagram (and it is especially beneficial for complex diagrams). Let us verify a few more relations. A tadpole is indeed zero:

$$\begin{aligned}
 \text{tadpole} &= \frac{ig}{2} \left(\text{quark loop} - \frac{1}{N_c} \text{quark} \right) \\
 &= \frac{ig}{2} \left(1 - \frac{N_c}{N_c} \right) \text{quark} = 0.
 \end{aligned}$$

The gluon propagator with a quark loop is just a factor times the gluon propagator:

$$\begin{aligned}
 \text{gluon with quark loop} &= -\frac{g^2}{4} \left(\text{quark loop} - \frac{2}{N_c} \text{quark} + \frac{1}{N_c^2} \text{quark} \right), \\
 &= -\frac{g^2}{2} \left(\frac{1}{2} \text{quark} - \frac{1}{2N_c} \text{quark} \right), \\
 &= -\frac{g^2}{2} \text{gluon}.
 \end{aligned}$$

This is just a demonstration of $\text{tr } t^a t^b = \frac{1}{2} \delta^{ab}$. The 3-gluon vertex gets a particularly easy matrix depiction. To calculate it, we note that in the matrix-field representation it is given by

$$\begin{aligned}
 \text{3-gluon vertex} &= g f^{abc} t_{ij}^a t_{kl}^b t_{mn}^c.
 \end{aligned} \tag{10.8}$$

Using Equation A.84a, we can simplify this into

$$\begin{aligned}
 g f^{abc} t_{ij}^a t_{kl}^b t_{mn}^c &= -i g t_{ij}^a t_{kl}^b (t_{mx}^a t_{xn}^b - t_{mx}^b t_{xn}^a), \\
 &= -\frac{i}{4} g \left[\delta_{il} \delta_{jm} \delta_{nk} - \frac{1}{N_c} (\delta_{ij} \delta_{ml} \delta_{nk} + \delta_{in} \delta_{jm} \delta_{kl}) + \frac{1}{N_c^2} \delta_{ij} \delta_{kl} \delta_{mn} \right] \\
 &\quad + \frac{i}{4} g \left[\delta_{in} \delta_{jk} \delta_{lm} - \frac{1}{N_c} (\delta_{ij} \delta_{ml} \delta_{nk} + \delta_{in} \delta_{jm} \delta_{kl}) + \frac{1}{N_c^2} \delta_{ij} \delta_{kl} \delta_{mn} \right], \\
 &= -\frac{i}{4} g (\delta_{il} \delta_{jm} \delta_{nk} - \delta_{in} \delta_{jk} \delta_{lm}).
 \end{aligned}$$

In other words, pictorially we have

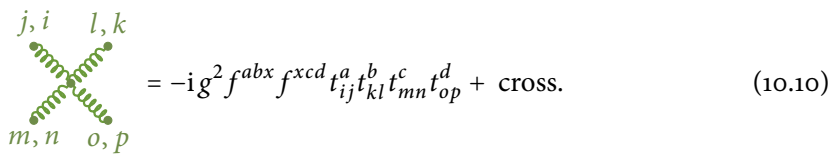
3-Matrix Vertex



The gluon propagator with a gluon loop is then easily calculated:

$$\begin{aligned}
 \text{Gluon with loop} &= -\frac{g^2}{16} \left(2 \text{Diagram 1} - 2 \text{Diagram 2} \right), \\
 &= -\frac{g^2}{4} N_c \left(\frac{1}{2} \begin{matrix} i \rightarrow l \\ j \leftarrow k \end{matrix} - \frac{1}{2N_c} \text{Diagram 3} \right), \\
 &= -\frac{g^2}{4} N_c \text{Diagram 4}.
 \end{aligned}$$

The calculation of the 4-gluon vertex goes similar to the 3-gluon vertex, but is a bit more involved. In matrix-field representation, the former is given by

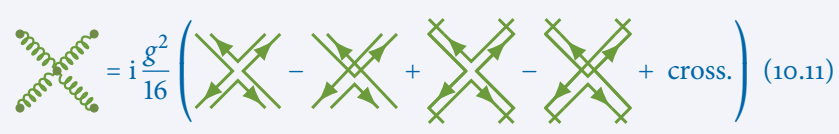


Because we have

$$\begin{aligned}
 -i g^2 f^{abx} f^{xcd} t_{ij}^a t_{kl}^b t_{mn}^c t_{op}^d &= i \frac{g^2}{16} \left[\delta_{il} \delta_{jo} \delta_{kn} \delta_{mp} - \delta_{in} \delta_{jk} \delta_{lo} \delta_{mp} \right. \\
 &\quad \left. - \delta_{il} \delta_{jm} \delta_{kp} \delta_{on} + \delta_{ip} \delta_{jk} \delta_{lm} \delta_{on} \right],
 \end{aligned}$$

we can write

4-Matrix Vertex



$$= i \frac{g^2}{16} \left(\text{diagram 1} - \text{diagram 2} + \text{diagram 3} - \text{diagram 4} + \text{cross.} \right) \quad (10.11)$$

Colour Representation in the Large- N_c Limit

Let us now investigate how the colour representation simplifies in the large- N_c limit. The most important simplification is in the matrix propagator, which is now

$$\langle A_\mu^{ij}(x) A_\nu^{kl}(y) \rangle \rightarrow \frac{1}{2} \delta^{il} \delta^{kj} D_{\mu\nu}(x, y), \quad (10.12)$$

or symbolically:

$$\text{diagram} = \frac{1}{2} \text{diagram} \quad (10.13)$$

Furthermore, we focus on the gauge sector of **QCD**, i.e. $N_f = 0$. This will allow us to make a straightforward power counting of index diagrams. First we note that from [Equation 4.84](#) automatically follows that in the large- N_c limit

$$\alpha_s \sim \frac{1}{N_c}. \quad (10.14)$$

In gauge-only **QCD**, there are three vertex functions: the 3-gluon vertex and the ghost vertex, which both give a factor $N_c^{-1/2}$, and the 4-gluon vertex, which gives a factor N_c^{-1} . Every closed loop gives an additional factor N_c , as it is a trace of the fundamental identity matrix. With this information, we can power count any index diagram. Take for instance the gluon loop correction to the gluon propagator, where now the second diagram vanishes in the large- N_c limit:



The two 3-gluon vertices add a factor N_c^{-1} , and the inner loop adds a factor N_c . In other words, while in standard **pQCD** this is an **NLO** diagram, in the large- N_c approach it contributes already at **LO**. This might sound a bit strange at first, but is something typical for multicolour frameworks. More generally, we state that

in the large- N_c limit only planar diagrams contribute to the LO result. Indeed, if we consider e.g. the planar diagram



we immediately see that it is an LO diagram (we have N_c^{-1} from the 4-gluon vertex, N_c^{-3} from the six 3-gluon vertices, and N_c^4 from the four closed loops). On the other hand, a possible non-planar counterpart of this diagram is



and this is an NNLO result because it scales as $\mathcal{O}(N_c^{-2})$, as there is only one inner loop (by following the inner index line, we see that it is indeed the contour of a single loop). This is easily generalised. For any planar diagram it is true that adding a loop corresponds to adding two 3-gluon vertices or one 4-gluon vertex. Hence the order of any n -loop planar diagram (with two external gluons) is

$$n\text{-loop planar diagram} \sim (g^2 N_c)^n \sim \mathcal{O}(1). \quad (10.15)$$

For non-planar diagrams we use a mathematical tool. In general, it is possible to draw any non-planar diagram without self-crossings on a general Riemann surface with a certain genus h , where the latter corresponds to the number of *holes* in the surface. E.g. a sphere has genus $h = 0$, and a torus (a doughnut) has genus $h = 1$. The non-planar diagram sketched above can be drawn on a torus without self-crossings, hence it has genus $h = 1$. It can be shown [112] that for any diagram (with two external gluons) its large- N_c scaling behaviour is given by

$$\text{genus-}h \text{ diagram} \sim (N_c^{-2})^h. \quad (10.16)$$

Already now we can draw two important conclusions:

- A. The expansion in $1/N_c$ rearranges perturbation theory diagrams in function of their *topology*.

- b. Only planar diagrams survive the large- N_c limit, and more specific *all* planar diagrams survive this limit. This can be translated directly to regular pQCD: *a planar diagram is always dominant with respect to a non-planar diagram.*

This is an important result, as there are far less planar diagrams than non-planar ones. The number of all planar diagrams with n loops grows as e^n , while the number of all general diagrams with n loops grows as $n!$. Take e.g. the ladder diagrams in quark-antiquark scattering consisting of n gluons. There is only one planar ladder diagram for every n , but there are $n! - 1$ non-planar ladder diagrams.

Equation 10.16 can be easily extended to any number of external gluons. We have [112]:

$$\text{genus-}h \text{ diagram for an } n\text{-point Greens' function} \sim (N_c)^{1-\frac{n}{2}-h}. \quad (10.17)$$

Furthermore, re-introducing quarks is trivial: We allow every single line to be a quark as well. Quark loops are always vanishing in the large- N_c limit, as they add vertices but no index loops. Consider e.g. the quark loop correction to the gluon propagator:

$$\text{quark loop correction to gluon propagator} = -\frac{g^2}{4} \text{gluon loop} \sim \mathcal{O}(N_c^{-1}), \quad (10.18)$$

So we don't have to take them into account at LO. In practice, a Greens' function will always be 'closed' by external quark or gluon lines. E.g. a possible closed 3-point function can be drawn as



In order to avoid introducing self-crossings (which would make the diagram non-planar, and hence vanishing in the large- N_c limit), we contract the indices of the external lines in a cyclic order. Every closed Greens' function gains a factor $(ig)^n$ per external leg, coming from the n vertices needed to close the function. The inner part of the diagram can be associated with a colour trace of the gauge fields, i.e.

$$\mathcal{G}_{\mu_1 \dots \mu_n}^n(x_1, \dots, x_n) \equiv \frac{1}{N_c} (ig)^n \text{tr} \langle A_1 \dots A_n \rangle, \quad (10.19)$$

where the factor $1/N_c$ follows from the normalisation condition

$$\mathcal{G}^0 \stackrel{\text{def}}{=} 1. \quad (10.20)$$

With this definition, all Green's functions contribute at LO so that they are finite (except \mathcal{G}^1 , which is a tadpole and hence vanishes). Now to get a general result, we integrate over all possible external path insertion points x_i . Note that these points are bound to the path \mathcal{C} formed by the external lines, hence the integration is a contour integral along \mathcal{C} . As the cyclic ordering of the fundamental indices is automatically implied by an ordering along the path \mathcal{C} , making the integrations path-ordered is sufficient to avoid self-crossings. The n -th order Green's function is then given by:

$$\mathcal{P} \oint_{\mathcal{C}} dx_1^{\mu_1} \cdots \oint_{\mathcal{C}} dx_n^{\mu_n} \mathcal{G}_{\mu_1 \cdots \mu_n}^n(x_1, \dots, x_n). \quad (10.21)$$

Note that all coordinates are integrated out, and all indices are traced. The only variable that remains is the path \mathcal{C} , the topological outline of the external lines. The full QCD result for a set of external lines on a path \mathcal{C} is then an all-order resummation of all closed Greens' functions that are connected to this path:

$$\sum_n \mathcal{P} \oint_{\mathcal{C}} dx_1^{\mu_1} \cdots \oint_{\mathcal{C}} dx_n^{\mu_n} \mathcal{G}_{\mu_1 \cdots \mu_n}^n(x_1, \dots, x_n). \quad (10.22)$$

But this is exactly the definition of the gauge-invariant Wilson loop:

Gauge-Invariant Wilson loop

$$\mathcal{U}^{\mathcal{C}} = \sum_n \mathcal{P} \oint_{\mathcal{C}} dx_1^{\mu_1} \cdots \oint_{\mathcal{C}} dx_n^{\mu_n} \mathcal{G}_{\mu_1 \cdots \mu_n}^n(x_1, \dots, x_n), \quad (10.23a)$$

$$\equiv \frac{1}{N_c} \text{tr} \langle 0 | \mathcal{P} e^{ig \oint_{\mathcal{C}} dx^\mu A_\mu} | 0 \rangle, \quad (10.23b)$$

$$\sim \text{[diagrams]} + \dots + \text{[diagrams]} + \dots + \text{[diagrams]} + \dots \quad (10.23c)$$

where the path \mathcal{C} is depicted naively as a circle.

Another useful property is the factorisation of correlators. If we consider a general correlator that is a product of colourless operators:

$$\langle O_1 \cdots O_n \rangle, \quad (10.24)$$

it can be shown [112] that all possible LO diagrams built from this operators consist of exactly n separable sub-diagrams, i.e. that all (partially) connected

diagrams are of $\mathcal{O}(N_c^{-1})$ or smaller. This immediately implies that the correlator factorises:

$$\langle O_1 \cdots O_n \rangle = \langle O_1 \rangle \cdots \langle O_n \rangle + \mathcal{O}\left(\frac{1}{N_c^2}\right). \quad (10.25)$$

This will be particularly interesting when considering Wilson loops that are defined over separated loops, i.e.

$$\begin{aligned} \langle 0 | \frac{1}{N_c} \text{tr} e^{\frac{ig\oint dx^\mu A_\mu}{c}} \cdots \frac{1}{N_c} \text{tr} e^{\frac{ig\oint dx^\mu A_\mu}{c}} | 0 \rangle = \\ \frac{1}{N_c} \text{tr} \langle 0 | e^{\frac{ig\oint dx^\mu A_\mu}{c}} | 0 \rangle \cdots \frac{1}{N_c} \text{tr} \langle 0 | e^{\frac{ig\oint dx^\mu A_\mu}{c}} | 0 \rangle + \mathcal{O}\left(\frac{1}{N_c^2}\right) \end{aligned} \quad (10.26)$$

We have shown that in the large- N_c limit all information on the gauge sector of QCD is fully encoded in Wilson loops, trading coordinate dependence for path dependence. In other words we have shown that it is possible to fully recast QCD in loop space in the multicolour limit. Unfortunately, it seems to be impossible to make the same connection between QCD and loop space for finite N_c . It is however possible to get partial results for QCD objects from calculations in loops space, by treating the loop space approach as an effective theory within some (quite stringent) conditions. E.g. Tsou succeeded in calculating the CKM and MNS matrices to good agreement with experimental data using loop space variables [126]. Motivated by this, we now take Wilson loops as basic building bricks in QCD, and investigate their properties.

10.2 RENORMALISATION OF WILSON LOOPS AND Γ_{CUSP}

A first difficulty that we encounter when working with Wilson loops is that—due to their non-locality—they are not necessarily renormalisable using regular methods due to the emergence of extra *rapidity divergences* (which are linked to the Wilson line regulators η in e.g. Equation 6.27a). This isn't a problem in regular pQCD (where Wilson loops are used as soft factors for TMDs) because they will cancel with extra divergences from the collinear TMD factor. However, if we want to recast QCD with Wilson loop as its basic elements, the latter have to be well-defined themselves, before cancellation. It has been shown [117–121, 124, 127, 128] that a Wilson loop is *multiplicatively* renormalisable to all orders of perturbation theory if the path has a finite number of self-intersections and cusps. Furthermore, the Wilson loop can be made finite if the path is smooth

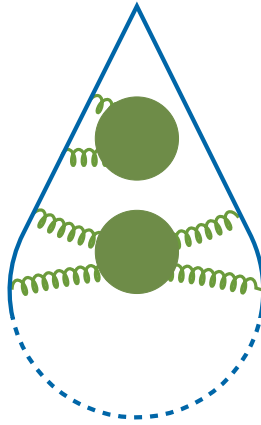


Figure 10.1: A Wilson loop with a cusp in its path. The two legs are semi-infinite lines, that are connected at infinity (illustrated by the dashed line). The blobs are just a representation of the two possible inner diagrams: we can have blobs connected to one of the legs, and blobs connecting both legs.

(without cusps and self-interactions). In the latter case, the renormalisation of the Wilson loop reduces to the regular renormalisation procedure.

So for a smooth path \mathcal{C} , the renormalised Wilson loop will depend on the renormalised coupling and the renormalisation scale:

$$\mathcal{U}_R^{\mathcal{C}}(g_R, \mu), \quad (10.27)$$

but not on the regulator ϵ as it is finite in the limit $\epsilon \rightarrow 0$. However, when the path is not smooth but contains a finite number of cusps², parameterised by Minkowskian angles χ_i , it will contain extra singularities that cannot be removed with the regular renormalisation procedure. Consider e.g. the diagram in Figure 10.1, which is a smooth path except for the upper cusp point. After regular renormalisation, the loop isn't finite yet but still depends on the regulator:

$$\mathcal{U}_R^{\mathcal{C}\chi}(g_R, \mu, \epsilon). \quad (10.28)$$

This is due to an extra singularity that originates from the cusp. We have to modify our renormalisation scheme to also absorb this singularity into a multiplicative factor Z_{cusp} :

$$\mathcal{U}_R^{\mathcal{C}}(g_R, \mu) = Z_{\text{cusp}}(\chi, g_R, \mu, \epsilon) \mathcal{U}_R^{\mathcal{C}\chi}(g_R, \mu, \epsilon). \quad (10.29)$$

² A cusp is characterised by a non-continuous derivative.

The multiplicatively renormalised Wilson loop with one cusp satisfies an adjusted Callan-Symanzik equation (see [Equation 4.81](#)):

$$\left(\frac{\partial}{\partial \ln \mu} + \beta(g_R) \frac{\partial}{\partial g_R} + \Gamma_{\text{cusp}}(\chi, g_R) \right) \ln \mathcal{U}_R \equiv 0, \quad (10.30)$$

where we could interpret the origin of Γ_{cusp} as an order-by-order combination of the anomalous dimensions of the different fields inside the exponential. From a loop space point of view, it can only depend on the cusp angle χ , as there are no other path parameters that define the cusp. The precise form of the path cannot have an influence on Γ_{cusp} , as the latter vanishes for all smooth paths, independent of their specific structure. The only difference now is the addition of a cusp, which is path-local. We can zoom in on the cusp, until its only defining parameter is its angle, hence its influence on the Wilson loop renormalisation as well can only depend on the angle.

Note that the Callan-Symanzik equation gets a Γ_{cusp} contribution for every cusp inside the path. For a contour with several cusps, it has to be adapted to

$$\left(\frac{\partial}{\partial \ln \mu} + \beta(g_R) \frac{\partial}{\partial g_R} + \sum_{\text{cusps}} \Gamma_{\text{cusp}}(\chi, g_R) \right) \ln \mathcal{U}_R \equiv 0,$$

The cusp anomalous dimension is defined as the logarithmic energy derivative of the regularly renormalised Wilson loop (see also Subsection [Mass Dimension Analysis](#) on page 96 and onwards for an introduction to mass dimensions):

Cusp Anomalous Dimension

$$\Gamma_{\text{cusp}} \stackrel{\text{def}}{=} - \lim_{\epsilon \rightarrow 0} \frac{d}{d \ln \mu} \ln \mathcal{U}_{\tilde{R}}(g_R, \mu, \epsilon), \quad (10.31)$$

where \mathcal{U} is defined on a path with exactly one cusp. When expanding the loop in orders of α_s , we find (extracting α_s from the contributions for clarity):

$$\ln \left[1 + \alpha_s \mathcal{U}_1 + \frac{1}{2} \alpha_s^2 \mathcal{U}_2 + \mathcal{O}(\alpha_s^3) \right] = \alpha_s \mathcal{U}_1 + \frac{1}{2} \alpha_s^2 (\mathcal{U}_2 - \mathcal{U}_1^2) + \mathcal{O}(\alpha_s^3), \quad (10.32)$$

which is a helpful tool to simplify the Callan-Symanzik equation and the definition of the cusp anomalous dimension.

We can now easily calculate Γ_{cusp} at one loop using the path structure as in [Figure 10.1](#) for $\mathcal{U}_{\tilde{R}}$. It has been shown in [\[124\]](#) that—at least at LO—the self-energy blobs reduce to the opposite of the vertex correction blob evaluated at zero angle, i.e. :

$$\mathcal{U}_{\tilde{R}} = \mathcal{U}_{\tilde{R}}|_{\text{self}} + \mathcal{U}_{\tilde{R}}|_{\text{vertex}} = \mathcal{U}_{\tilde{R}}(\chi) - \mathcal{U}_{\tilde{R}}(0). \quad (10.33)$$

We already calculated $\mathcal{U}_{\tilde{R}}(\chi)$ in [Chapter 7](#), it is exactly the LO 2-gluon blob connecting two adjoining off-LC segments as given in [Equation 7.81](#):

$$\mathcal{W}_{11}^{JK}|_{\epsilon} = \frac{\alpha_s}{2\pi} \chi \coth \chi \left[\frac{1}{\epsilon} + \ln \frac{n_K^2 n_J^2 - (n_K \cdot n_J)^2}{4} + \ln \frac{\mu^2}{\eta^2} + \Upsilon \right]. \quad (10.34)$$

The only thing missing is the path function, which we get from [Equation 7.24b](#):

$$\mathcal{U}_{\tilde{R}}(\chi) = \Phi_{11}(J, K) \mathcal{W}_{11}^{JK}, \quad (10.35a)$$

$$\Phi_{11}(J, K) = (-)^{\phi_J + \phi_K} C_F. \quad (10.35b)$$

The path goes from $-\infty$ to the cusp along a direction n^μ , and from the cusp back to $-\infty$ along a different direction \tilde{n}^μ . The path segments are hence:

$$\begin{aligned} \rightrightarrows & \bullet \quad n, r, \\ \leftarrow\leftarrow & \bullet \quad \tilde{n}, r. \end{aligned}$$

We know we can rewrite the first segment as (see [Equation 6.66a](#)):

$$\rightrightarrows \bullet = \leftarrow\leftarrow \bullet \Big|_{n \rightarrow -n}.$$

Because we have two similar segments, the path function remains positive, i.e. $\Phi_{11}(J, K) = C_F$. The sign difference in n results in a sign difference in χ because

$$n \rightarrow -n \quad \Rightarrow \quad n \cdot \tilde{n} \rightarrow -n \cdot \tilde{n} \quad \Rightarrow \quad \chi \rightarrow -\chi.$$

In other words (note that $\cosh(-\chi) = \cosh \chi$):

$$\mathcal{U}_{\tilde{R}}(\chi) = -\frac{\alpha_s}{2\pi} C_F \chi \coth \chi \left[\frac{1}{\epsilon} + \ln \frac{n_K^2 n_J^2 - (n_K \cdot n_J)^2}{4} + \ln \frac{\mu^2}{\eta^2} + \Upsilon \right]. \quad (10.36)$$

Now we apply [Equation 10.33](#) and use the limit

$$\lim_{\chi \rightarrow 0} \chi \coth \chi = 1, \quad (10.37)$$

to get

$$\mathcal{U}_{\tilde{R}} = -\frac{\alpha_s}{2\pi} C_F (\chi \coth \chi - 1) \left[\frac{1}{\epsilon} + \ln \frac{n_K^2 n_J^2 - (n_K \cdot n_J)^2}{4} + \ln \frac{\mu^2}{\eta^2} + \Upsilon \right]. \quad (10.38)$$

To get the cusp anomalous dimension is now only a matter of changing the sign and taking the derivative to $\ln \mu$ (also using [Equation 10.32](#)). This gives:

Cusp Anomalous Dimension at One Loop

$$\Gamma_{\text{cusp}} = \frac{\alpha_s}{\pi} C_F (\chi \coth \chi - 1). \quad (10.39)$$

Note that it is divergent in the limit $\chi \rightarrow \infty$ (the on-**LC** limit), so we need to recalculate it in this limit. This is not surprisingly, as also the contributions themselves are totally different in the off-**LC** limit (single pole) and the on-**LC** limit (double pole).

Renormalisation of Wilson Loops on the Light-Cone

Having segments that are light-like further complicates matters, because besides extra cusp divergences we now also have additional light-cone divergences that emerge from the divergent limit $\chi \rightarrow \infty$. This time we cannot simply adapt the regular renormalisation procedure, as Equation 10.30 is no longer valid due to the emergence of a double pole—already at one loop (see Equation 7.71). Hence we need to redefine the renormalisation procedure in order to subtract the double pole [129].

The cusp angle is defined as (see Equation 7.73):

$$\cosh \chi \stackrel{\text{def}}{=} \frac{n \cdot \tilde{n}}{|n| |\tilde{n}|}.$$

It diverges in case of light-like segments because then $|n|, |\tilde{n}| \rightarrow 0$, hence the non-divergent part of the on-**LC** cusp angle is given by $n \cdot \tilde{n}$. To subtract the extra **LC** divergences, the Callan-Symanzik equation is redefined with an additional derivative to the non-divergent cusp angle part:

$$\left[\frac{\partial}{\partial \ln n \cdot \tilde{n}} \left(\frac{\partial}{\partial \ln \mu} + \beta(g_R) \frac{\partial}{\partial g_R} \right) + \sum_{\text{cusps}} \Gamma_{\text{cusp}}(\chi, g_R) \right] \ln \mathcal{U}_R^{\text{LC}} \equiv 0, \quad (10.40)$$

where $[n \cdot \tilde{n}]$ stands for one of the pole prescriptions as defined in Equations 3.142 (most commonly, the principal value prescription is chosen in this case). In practice, it implies that the cusp anomalous dimension is now defined with an additional derivative:

On-**LC** Cusp Anomalous Dimension

$$\Gamma_{\text{cusp}}^{\text{LC}} \stackrel{\text{def}}{=} - \lim_{\epsilon \rightarrow 0} \frac{d}{d \ln \mu} \frac{d}{d \ln n \cdot \tilde{n}} \ln \mathcal{U}_R(g_R, \mu, \epsilon), \quad (10.41)$$

where again \mathcal{U} is defined over a path with exactly one cusps, as for example

Figure 10.1. In the next chapter $n \cdot \tilde{n}$ will take the role of the Mandelstam energy s . The result for light-like segments is given by [Equation 7.71](#) (we already dropped the terms that won't contribute):

$$\mathcal{W}_{11}|_{\text{LC}} = \frac{\alpha_s}{2\pi} \left[\frac{1}{\epsilon} \ln \frac{\mu^2}{\eta^2} + \frac{1}{2} \left(\ln \frac{n \cdot \tilde{n}}{2} + \ln \frac{\mu^2}{\eta^2} \right)^2 \right].$$

The path structure remains the same as in the off-LC case, so we have:

$$\mathcal{U}_{\tilde{R}} = -\frac{\alpha_s}{2\pi} C_F \left[\frac{1}{\epsilon} \ln \frac{\mu^2}{\eta^2} + \frac{1}{2} \left(\ln \frac{n \cdot \tilde{n}}{2} + \ln \frac{\mu^2}{\eta^2} \right)^2 \right]. \quad (10.42)$$

Taking the double derivative is just straightforward (again using [Equation 10.32](#)):

On-LC Cusp Anomalous Dimension at One Loop

$$\Gamma_{\text{cusp}} = \frac{\alpha_s}{\pi} C_F. \quad (10.43)$$

For easy reference later, we also list the on-LC Γ_{cusp} at two loop [[124](#), [130](#)]:

On-LC Cusp Anomalous Dimension at Two Loop

$$\Gamma_{\text{cusp}} = \frac{\alpha_s^2}{4\pi^2} C_F \left[\left(\frac{67}{9} - \frac{\pi^2}{3} \right) N_c - \frac{10}{9} N_f \right]. \quad (10.44)$$

This is of course scheme-dependent. The given result has been calculated in the regular $\overline{\text{MS}}$ -scheme.

GEOMETRIC EVOLUTION

As we saw before in the previous chapter, a Wilson Loop is a fully gauge-invariant object, and can as such be used as a basic building block to fully recast [QCD](#) in loop space. Objects in loop space can then exhibit dualities to objects in coordinate space. In this chapter we address a connection between the energy evolution of polygonal light-like Wilson exponentials and the geometry of loop space. As the former have a singularity structure similar to [TMDs](#), this connection might induce a duality between energy evolution and geometric evolution.

We will start this chapter with a short motivation for our interest in the geometric behaviour of Wilson loops. Next we investigate the dynamical behaviour of Wilson loops in loop space, which will lead to the so-called [MM](#) equation that describe loop evolution in function of the area of the path. However, the [MM](#) equation has its limitations, and are expected to be invalid for the most common interesting paths, namely paths containing cusps. We follow a slightly different approach by investigating the geometrical evolution of a Wilson quadrilateral on the null plane, which will lead to a conjectured evolution equation, that we can apply on [TMDs](#) as well.

11.1 MOTIVATION: WILSON LOOPS IN SUPER YANG-MILLS

Recently, a lot of research is aimed at the investigation of a duality between planar Wilson loops and gluon scattering amplitudes in $\mathcal{N} = 4$ Super Yang-Mills theory [[131–141](#)]. The duality connects N -gluon planar scattering amplitudes to Wilson loops consisting of N light-like segments, see [Figure 11.1](#). We will investigate this topic as a motivation for our interest in Wilson loops.

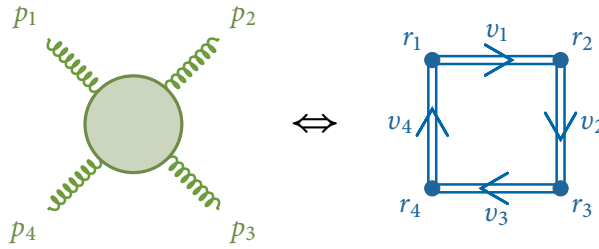


Figure 11.1: The N -gluon planar scattering amplitude in SYM is dual to a Wilson loop with N light-like segments. This is illustrated here for $N = 4$. The gluon momenta p_i are dual to the segment separation vectors $v_i = r_{i+1} - r_i$ of the Wilson loop.

Super Yang-Mills Theory

Super Yang-Mills is the supersymmetric extension to Yang-Mills theory, with a strong conformal symmetry. It cannot be a realistic theory—as it describes *unbroken* supersymmetry—but can be used as a toy theory to investigate problems that are difficult to approach in realistic theories. In any conformal theory, all physics are scale-invariant. The latter naturally implies that it is independent on distance coordinates, and that all information is encoded in the *angles* describing the system. Furthermore, as an unbroken supersymmetric theory, all particles it describes have the same mass (and are hence massless).

SYM is interesting in its own right, as it is associated with a lot of other theories. It is the theory living on the boundary of a 5-dimensional anti-de Sitter space (a common compactification of the 10-dimensional type IIB string theory), and, using the holographic principle, it fully describes the latter. It is also deeply connected to $\mathcal{N} = 8$ supergravity, one of the easiest field theories that include gravity. Finally, it can also (partially) be related to QCD , which is where our interest lies. As it appears, the *leading transcendentality* component [142] is exactly the same in QCD as in SYM . The important fact is that calculations in SYM are much easier than in the other theories,¹ such that we can gain new insights in calculational techniques and possibly find dualities between objects in SYM and realistic theories like QCD .

¹ As an illustration: calculations in SYM have been done up to *six loops*. The techniques developed to achieve this, can be partially adapted to use them in more realistic theories.

Planar Scattering Amplitudes

We will investigate planar gluon scattering by looking at on-shell scattering. An on-shell gluon is fully determined by its momentum p_i (with $p_i^2 = 0$), its helicity $h_i = \pm$ and its colour index a_i . Due to the underlying symmetries in **SYM**, the amplitude is constrained by its helicity structure: amplitudes where all gluons, or all but one, have the same helicity vanish, i.e. :

$$\mathcal{M}^{++++} = \mathcal{M}^{-++++} = \mathcal{M}^{-----} = \mathcal{M}^{+-----} = 0, \quad (11.1)$$

where the amplitudes are understood as the sum over all crossings. This immediately implies that e.g. up to 5 gluons, the only non-vanishing amplitudes are the 4-gluon amplitude \mathcal{M}^{--++} and the 5 gluon amplitudes \mathcal{M}^{--+++} and \mathcal{M}^{++--- . These are so-called *maximally helicity violating*—as is any diagram where 2 particles have helicity opposite to the remaining $n-2$ particles—because they maximally violate helicity conservation at tree level. Such amplitudes can be calculated with the Parke-Taylor formula [143]:

$$|\mathcal{M}^{--+\dots+}|^2 = \frac{4}{n} (N_c^2 - 1) \left(\frac{g^2 N_c}{2} \right)^{n-2} \sum_{\text{permutations}} \frac{1}{p_1 \cdot p_2 p_2 \cdot p_3 \cdots p_n \cdot p_1} + \mathcal{O}(N_c^{-2}, g^2).$$

As **SYM** is fully massless, it will suffer from **IR** divergences. It can be shown that e.g. for the 4-gluon amplitude the divergences can be separated out, and the amplitude takes the surprisingly simple form

$$\ln \mathcal{M}_4 = \text{IR div.} + \frac{1}{2} \Gamma_{\text{cusp}} \ln^2 \frac{s}{t} + \text{const}, \quad (11.2)$$

where s and t are the Mandelstam energy variables:

$$s = (p_1 + p_2)^2, \quad (11.3a)$$

$$t = (p_1 + p_3)^2. \quad (11.3b)$$

Watch the sign in the definition of t , this is opposite to the regular definition. This separation of **IR** divergences has been proven up to 3 loops in [144], and only two years later up to 4 loops in [145]. Similar relations have been proven for higher n . It is exactly this expression that will be related to a rectangular light-like Wilson loop [133]:

$$\ln \mathcal{M}_4 = \ln \mathcal{U}_{\square} + \mathcal{O}(N_c^{-2}), \quad (11.4)$$

where the rectangular Wilson loop is defined as a loop over the rectangular contour as depicted in [Figure 11.1](#), traced over colour indices and evaluated in the ground state:

$$\mathcal{U}_{\square} \stackrel{\text{def}}{=} \frac{1}{N_c} \text{tr} \langle 0 | \mathcal{P} e^{\int_{\square} \text{ig} \phi dz^{\mu} A_{\mu}} | 0 \rangle. \quad (11.5)$$

The contour is built from 4 segments with separation vectors

$$v_i \stackrel{\text{def}}{=} r_{i+1} - r_i. \quad (11.6)$$

The segments are assumed to be light-like, and hence $v_i^2 \stackrel{\text{def}}{=} 0$. Using dimensional regularisation to regulate the IR-divergences one can show that at 1-loop the SYM scattering amplitude equals (see [133, 134], and compare with Equation 11.2):

$$\ln \mathcal{M}_4 = \Gamma_{\text{cusp}} \left[-\frac{1}{\epsilon_{\text{IR}}^2} \left(\frac{-s}{\mu_{\text{IR}}^2} \right)^{\epsilon_{\text{IR}}} - \frac{1}{\epsilon_{\text{IR}}^2} \left(\frac{-t}{\mu_{\text{IR}}^2} \right)^{\epsilon_{\text{IR}}} + \frac{1}{2} \ln^2 \frac{s}{t} + \text{const} \right]. \quad (11.7)$$

On the other hand, we will show in Section 11.3 that the first order contribution of the rectangular Wilson loop is equal to (now using dimensional regularisation in the regular way, viz. to treat the UV divergences):

$$\ln \mathcal{U}_{\square} = \frac{\alpha_s N_c}{\pi} \frac{1}{2} \left[-\frac{1}{\epsilon_{\text{UV}}^2} \left[-(v_1+v_2)^2 \mu_{\text{UV}}^2 \right]^{\epsilon_{\text{UV}}} - \frac{1}{\epsilon_{\text{UV}}^2} \left[-(v_2+v_3)^2 \mu_{\text{UV}}^2 \right]^{\epsilon_{\text{UV}}} + \frac{1}{2} \ln^2 \frac{(v_1+v_2)^2}{(v_2+v_3)^2} + \text{const} \right]. \quad (11.8)$$

Furthermore, because in the large N_c -limit

$$C_F = \frac{N_c}{2} + \mathcal{O}(N_c^{-2}),$$

we can write the factor in front as

$$\frac{\alpha_s N_c}{\pi} \frac{1}{2} = \Gamma_{\text{cusp}} + \mathcal{O}(N_c^{-2}).$$

So we see that Equation 11.4 indeed holds—at most up to a constant term—if we identify the separation vectors with the on-shell momenta:

$$v_i \equiv p_i, \quad (v_1+v_2)^2 \equiv s, \quad (v_2+v_3)^2 \equiv t. \quad (11.9)$$

More specifically, we can state that there exists a duality between a rectangular light-like Wilson loop and the 4-gluon planar scattering amplitude in super Yang-Mills theory, that relates the gluon momenta p_i to the segment lengths v_i , and the IR singularities of the amplitude to the UV singularities of the loop in the following way:

$$\epsilon_{\text{IR}} \equiv \epsilon_{\text{UV}}, \quad \mu_{\text{IR}} \equiv \mu_{\text{UV}}^{-1}. \quad (11.10)$$

This relation has been proven at higher orders as well, both at weak and strong coupling. Unfortunately, this relation only holds in a supersymmetric theory.

Korchemskaia and Korchemsky showed that when considering QCD the relation only holds in the Regge limit [146]. However, the investigation of Wilson loops in QCD is interesting anyway, as they share e.g. the same singularity structure as TMDs, and can be used to calculate soft factors.

11.2 WILSON LOOPS IN LOOP SPACE

In the previous chapter we have made the first steps to show how Wilson loops can be used as elementary building bricks to completely recast QCD in loop space (see also [113–123]). In this section we will investigate this a bit deeper, and look at their geometric behaviour. To achieve this, the definition of a Wilson loop needs to be extended to make it (possibly) dependent on multiple contours. We define a n -th order Wilson loop (consisting of n sub-loops) as:²

$${}_n\mathcal{U}^{C_1, \dots, C_n} = \langle 0 | \Phi^{C_1} \dots \Phi^{C_n} | 0 \rangle, \quad (11.11)$$

where each sub-loop is defined as

$$\Phi^C = \frac{1}{N_c} \text{tr} \mathcal{P} \text{Exp} \left\{ i g \oint_C dz^\mu A_\mu(z) \right\}. \quad (11.12)$$

Thus each sub-loop is Lorentz and Dirac invariant, but only together they are evaluated in the ground state to form a n -th order Wilson loop. Note that a ${}_1\mathcal{U}$ loop coincides with our original definition in Equation 10.23b (when evident from context, we will just write it as \mathcal{U}). Treating these n -th order Wilson loops as elementary objects in loop space, we note that all gauge kinematics are encoded in a ${}_1\mathcal{U}$ loop (which we have shown in Chapter 2, where we even used Wilson loops to introduce the gauge field to begin with). On the other hand, all gauge dynamics are governed by a set of geometrical evolution equations, the Makeenko-Migdal (MM) equations [147–151]:

Makeenko-Migdal Equation

$$\partial^\nu \frac{\delta}{\delta \sigma_{\mu\nu}(z)} {}_1\mathcal{U}^C = g^2 N_c \oint_C du^\mu \delta^{(4)}(z-u) {}_2\mathcal{U}^{C_{zu} C_{uz}}. \quad (11.13)$$

Here a path \mathcal{C} gets deformed by taking two opposite points z and u , and bringing them infinitesimally close, such that we separate a newly-formed closed contour

² We write the loop order index on the left of \mathcal{U} to avoid confusion with the expansion order index as in Equation 6.12.

from the original one. In other words, we deform the contour \mathcal{C} into two closed contours \mathcal{C}_{zu} and \mathcal{C}_{uz} that are still connected in one point.

Of special importance are the two geometrical operations we introduced in the MM equations, namely the path derivative ∂_μ and the area derivative $\frac{\delta}{\delta\sigma_{\mu\nu}(z)}$ [147–151]:

$$\partial_\mu \Phi^{\mathcal{C}} = \lim_{|\delta z_\mu| \rightarrow 0} \frac{\Phi^{\delta z_\mu^{-1} \mathcal{C} \delta z_\mu} - \Phi^{\mathcal{C}}}{|\delta z_\mu|}, \tag{11.14}$$

$$\frac{\delta}{\delta\sigma_{\mu\nu}(z)} \Phi^{\mathcal{C}} = \lim_{|\delta\sigma_{\mu\nu}(z)| \rightarrow 0} \frac{\Phi^{\mathcal{C} \delta \mathcal{C}} - \Phi^{\mathcal{C}}}{|\delta\sigma_{\mu\nu}(z)|}. \tag{11.15}$$

The path derivative resembles most our standard notion of a derivative: it measures the variation of the contour while keeping the area constant:

$$\partial_\mu \Phi^{\mathcal{C}} = \lim_{\not{\rightarrow} \rightarrow 0} \frac{\text{Diagram 1} - \text{Diagram 2}}{\not{\rightarrow}}.$$

On the other hand, the area derivative is the most intuitive interpretation of a geometric derivative: it quantifies the variation of a contour by comparing the original contour \mathcal{C} with a new contour containing small (non area-conserving) deformations $\delta\mathcal{C}$:

$$\frac{\delta}{\delta\sigma_{\mu\nu}(z)} \Phi^{\mathcal{C}} = \lim_{\delta \rightarrow 0} \frac{\text{Diagram 1} - \text{Diagram 2}}{\delta}.$$

When parameterising the path as $z^\mu(\lambda)$, the area derivative can also be expressed in the so-called *Polyakov* form, which can be helpful for certain calculations:

$$\frac{\delta}{\delta\sigma_{\mu\nu}(z(\lambda))} = \int_{\lambda+i\epsilon}^{\lambda-i\epsilon} d\kappa \delta(\kappa - \lambda) \frac{\delta}{\delta x_\mu(\kappa)} \frac{\delta}{\delta x_\nu(\lambda)}. \tag{11.16}$$

Although the MM equations provide an elegant method to describe the evolution of a generalised Wilson loop solely in function of its path, they have their limitations. For starters, they are not closed since the evolution of \mathcal{U} depends on ${}_2\mathcal{U}$. Formally, this limitation is superfluous in the large N_c limit since then we can make use of the factorisation property ${}_2\mathcal{U}^{C_1, C_2} \approx \mathcal{U}^{C_1} \mathcal{U}^{C_2}$ (see Equation 10.26), making the MM equations closed. The remaining limitations on the MM equa-

tions are more severe. For one, the evolution equations are derived by applying the Schwinger-Dyson equations

$$\langle 0 | \nabla_\mu F^{\mu\nu} | 0 \rangle = i \langle 0 | \frac{\delta}{\delta A_\nu} | 0 \rangle \quad (11.17)$$

on the Mandelstam formula

$$\frac{\delta}{\delta \sigma_{\mu\nu}(z)} \Phi^C = ig \operatorname{tr}(F^{\mu\nu} \Phi^{Cz}), \quad (11.18)$$

and using Stokes' theorem (see e.g. [112] for a nice derivation). The Mandelstam formula relates the geometric behaviour of a loop to its gauge content. However, it is not known whether it remains well-defined for all types of paths, while similar issues arise with the area derivative. In particular, all contours containing one or more cusps induce some problematic behaviour, as it is (at least) not straightforward to define *continuous* area differentiation inside a cusp, nor it is to continuously deform a contour in a general topology [C][16, 17, 152–154]. This is somewhat bothersome, as most interesting dynamics lie in contours with cusps. There are similar problems with Stokes' theorem. It is however possible to generalise the latter to be valid for any continuous path containing a finite number of cusps. A last concern is that there are no known general solutions to the MM equations in 4D Minkowskian spacetime. Recently a few developments in the field of twistor theory have shown the MM equations to be valid, but when implemented in a completely different space, viz. twistor space.

11.3 EVOLUTION OF LIGHT-LIKE RECTANGULAR LOOPS

In order to maximally simplify the MM equations, we restrict ourselves to the investigation of rectangular loops with light-like segments. This restriction lowers the dimensionality to a 2-dimensional case, and it fixes the cusp angles to constant values that are conserved under any valid path or area variation, hence removing any angle-dependent contributions that would make the area derivation operator ill-defined.

The loop structure for rectangular on-LC Wilson loops is shown in Figure 11.2a. Because of the light-like segments, the Wilson loop is automatically planar, and for simplicity we choose it to lie on the null-plane, i.e. $r_{\perp i} = 0$. The loop is fully defined by its four cusp points r_1, \dots, r_4 but it will be convenient to express the result in function of the variables v_1, \dots, v_4 that are defined as segment separation vectors:

$$v_i \stackrel{\text{def}}{=} r_{i+1} - r_i. \quad (11.19)$$

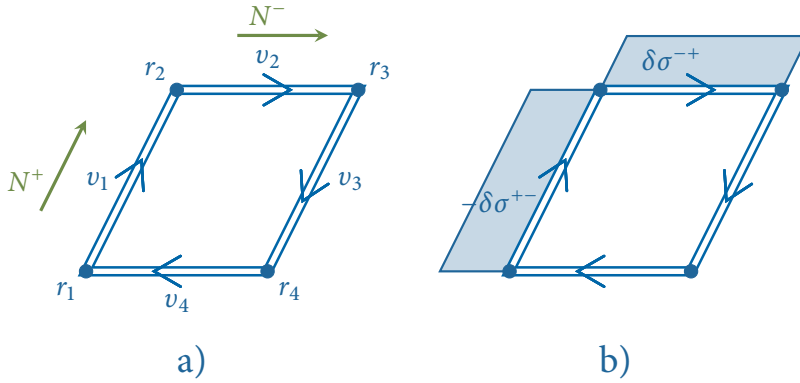


Figure 11.2: a) Rectangular Wilson loop with light-like segments, on the null plane ($\mathbf{r}_{\perp i} = 0$). The segment separation vectors are defined in Equation 11.19. From a geometrical point of view, the loop is fully characterised by the two independent LC directions N^\pm . b) Geometric evolution of the loop.

Comparing this definition with the path parameterisations as we are used to from Chapter 6, we see that the separation vectors are just a rescaling of the path direction vectors:

$$v_i = |r_{i+1} - r_i| n_i. \quad (11.20)$$

Because the segments are light-like, this directly implies that the squares of the separation vectors vanish:

$$v_i^2 \sim n_i^2 \equiv 0. \quad (11.21)$$

We prefer these variables over the direction vectors, so that we can express the result in function of the Mandelstam energy variables (see Equations 11.3):

$$s = (v_1 + v_2)^2 = 2v_1 \cdot v_2, \quad t = (v_2 + v_3)^2 = 2v_2 \cdot v_3. \quad (11.22)$$

From a geometrical point of view, the loop is fully characterised by the two independent LC directions N^+ and N^- . These directions are related to the separation vectors, and more specifically we normalise them to equal the latter:

$$N^+ = v_1 = -v_3, \quad N^- = v_2 = -v_4. \quad (11.23)$$

The area differentiations are now well-defined at the cusp points. In every cusp there are two area derivatives, different on the left side or the right side of the cusp. Only two area derivatives are linearly independent:

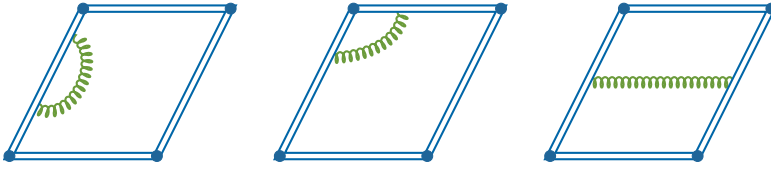


Figure 11.3: At LO, the rectangular Wilson loop has three types of diagrams: a self-energy diagram that vanishes in the on-LC case, a cusp correction, and a correction containing two cusps.

$$\delta\sigma^{-+} = N^- \delta N^+, \quad (11.24a)$$

$$\delta\sigma^{+-} = N^+ \delta N^-. \quad (11.24b)$$

The area derivatives are illustrated in Figure 11.2b. To see how each side of a cusp has a different area derivative, we investigate the area derivatives in the point r_2 :

$$\delta\sigma(r_2)^R = \delta\sigma^{-+}, \quad \delta\sigma(r_2)^L = -\delta\sigma^{+-}, \quad (11.25)$$

The minus sign in $\delta\sigma(r_2)^L$ comes from our choice of N^+ and N^- in Figure 11.2a.

Rectangular Light-Like Loop Calculation at One-Loop

We now calculate the one-loop contribution of this loop in Feynman gauge. We will do this calculation in coordinate space, as at one-loop calculations with Wilson loops (and finite Wilson lines in general) tend to be easier in coordinate representation (however at higher orders, momentum representation is preferable). In coordinate representation, the gluon propagator in Feynman gauge equals:

$$D_{\mu\nu}^{ab}(x-y) = -g_{\mu\nu} \delta^{ab} \frac{(\pi\mu^2)^\epsilon}{4\pi^2} \Gamma(1-\epsilon) \frac{1}{[-(x-y)^2 + i\epsilon]^{1-\epsilon}}. \quad (11.26)$$

The NLO contribution is then given by (remember that colour indices are traced over and divided by N_c):

$$\frac{1}{2} (ig)^2 C_F \mathcal{P} \oint dx^\mu dy^\nu D_{\mu\nu}(x-y), \quad (11.27)$$

We have three types of diagrams, as illustrated in Figure 11.3. The first type—the

self-energy diagrams—vanish because the segments are light-like $v_i \cdot v_i = v_i^2 = 0$. The contribution of the second diagram is

$$\mathcal{U}_{\text{cusp}} = -g^2 C_F \frac{(\pi\mu^2)^\epsilon}{4\pi^2} \int_0^1 d\lambda \, d\kappa \frac{v_i \cdot v_{i+1} \Gamma(1-\epsilon)}{[-(r_i + v_i \lambda - r_{i+1} - v_{i+1} \kappa)^2 + i\epsilon]^{1-\epsilon}}. \quad (11.28)$$

We can rewrite the denominator as

$$\begin{aligned} -(r_i + v_i \lambda - r_{i+1} - v_{i+1} \kappa)^2 &= -(v_i(\lambda - 1) - v_{i+1} \kappa)^2, \\ &= 2v_i \cdot v_{i+1}(\lambda - 1)\kappa, \end{aligned}$$

where the last step is valid because the separation vectors are light-like. The contribution is now

$$\begin{aligned} \mathcal{U}_{\text{cusp}} &= -\frac{1}{2} g^2 C_F \frac{(\pi\mu^2)^\epsilon}{4\pi^2} \Gamma(1-\epsilon) (-2v_i \cdot v_{i+1})^\epsilon \int_0^1 d\lambda \frac{1}{(\lambda - 1)^{1-\epsilon}} \int_0^1 d\kappa \frac{1}{\kappa^{1-\epsilon}}, \\ &= -\frac{1}{2} g^2 C_F \frac{(\pi\mu^2)^\epsilon}{4\pi^2} \Gamma(1-\epsilon) (-2v_i \cdot v_{i+1})^\epsilon \frac{1}{\epsilon^2}. \end{aligned} \quad (11.29)$$

To sum over the four cusps, we relate $2v_i \cdot v_{i+1}$ to the Mandelstam variables (see [Equation 11.22](#)):

$$s = 2v_1 \cdot v_2 = 2v_3 \cdot v_4, \quad t = 2v_2 \cdot v_3 = 2v_4 \cdot v_1,$$

so that we have

$$\sum \mathcal{U}_{\text{cusp}} = -\frac{\alpha_s}{\pi} C_F (\pi\mu^2)^\epsilon \Gamma(1-\epsilon) \frac{1}{\epsilon^2} ((-s + i\epsilon)^\epsilon + (-t + i\epsilon)^\epsilon). \quad (11.30)$$

In principle the last diagram in [Figure 11.3](#) vanishes as well because of the light-like segments, but it is however interesting to calculate it, as at higher orders it might give a non-zero contribution. It is given by:

$$\begin{aligned} \mathcal{U}_{2\text{cusp}} &= g^2 C_F \frac{(-\pi\mu^2)^\epsilon}{4\pi^2} \int_0^1 d\lambda \, d\kappa \frac{v_i \cdot v_{i+2} \Gamma(1-\epsilon)}{(r_i + v_i \lambda - r_{i+2} - v_{i+2} \kappa)^{2(1-\epsilon)}}, \\ \sum \mathcal{U}_{2\text{cusp}} &= \frac{\alpha_s}{2\pi} C_F (\pi\mu^2)^\epsilon \left(\ln^2 \frac{s}{t} + \pi^2 \right). \end{aligned} \quad (11.31)$$

Note that this contribution indeed vanishes, as $s = -t$ and hence

$$\ln^2 \frac{s}{t} + \pi^2 = \ln^2(-1) + \pi^2 = 0,$$

because we are evaluating logarithms in the region $[0, 2\pi]$ (and hence $\ln(-1) = i\pi$). So the full contribution up to first order is simply:

$$\mathcal{U}_{\square} = 1 - \frac{\alpha_s C_F}{\pi} (2\pi\mu^2)^\epsilon \Gamma(1-\epsilon) \left[\frac{1}{\epsilon^2} \left(-\frac{s}{2}\right)^\epsilon + \frac{1}{\epsilon^2} \left(-\frac{t}{2}\right)^\epsilon \right].$$

Expressing this result in function of the LC directions N^+ and N^- , we get:

$$\mathcal{U}_{\square} = 1 - \frac{\alpha_s C_F}{\pi} (2\pi\mu^2)^\epsilon \Gamma(1-\epsilon) \left[\frac{1}{\epsilon^2} (-N^+ N^- + i\epsilon)^\epsilon + \frac{1}{\epsilon^2} (N^+ N^- + i\epsilon)^\epsilon \right].$$

We saw in the previous chapter that an on-LC Wilson loop cannot be renormalised in the regular way, but needs an additional derivative $\partial/\partial n \cdot \tilde{n}$ (see Equation 10.40). But $n \cdot \tilde{n}$ is in this case exactly $N^+ N^-$. Inspired by the area derivatives in Equations 11.24, we define a logarithmic area derivative as

Logarithmic Area Derivative

$$\frac{\delta}{\delta \ln \sigma} \stackrel{\text{def}}{=} \sigma^{+-} \frac{\delta}{\delta \sigma^{+-}} + \sigma^{-+} \frac{\delta}{\delta \sigma^{-+}} = N^- \frac{\delta}{\delta N^-} + N^+ \frac{\delta}{\delta N^+}. \quad (11.32)$$

It lowers the divergence with one order:

$$\frac{\delta}{\delta \ln \sigma} \ln \mathcal{U}_{\square} = -2 \frac{\alpha_s C_F}{\pi} (2\pi\mu^2)^\epsilon \Gamma(1-\epsilon) \frac{1}{\epsilon} \left[(-N^+ N^- + i\epsilon)^\epsilon + (N^+ N^- + i\epsilon)^\epsilon \right],$$

such that we can now apply regular renormalisation by making a logarithmic energy derivation and taking the limit $\epsilon \rightarrow 0$:

$$\frac{d}{d \ln \mu} \frac{\delta}{\delta \ln \sigma} \ln \mathcal{U}_{\square} = -4 \frac{\alpha_s C_F}{\pi} = -4\Gamma_{\text{cusp}}. \quad (11.33)$$

Not only is this in perfect agreement with the on-LC Callan-Symanzik Equation 10.40, the important fact is that we derived this result from a geometrical point of view, using the area infinitesimals Equations 11.24 which we calculated from Equation 11.15. In other words, we established a connection between the geometry of loop space and the dynamical properties of its fundamental objects, viz. light-like Wilson loops, by constructing its geometric evolution.

It is logical to interpret Equation 11.33 as a resummation of all cusps in the path. In other words, for any closed polygonal path that is planar and consists of light-like segments, we have

Geometric Evolution of On-LC Planar Loop

$$\frac{d}{d \ln \mu} \frac{\delta}{\delta \ln \sigma} \ln \mathcal{U} = - \sum_{\text{cusps}} \Gamma_{\text{cusp}}. \quad (11.34)$$

This is a really strong result. Not only does it provide a description of the

geometrical behaviour of light-like objects in loop space, it also holds at all orders. To motivate this, we express the on-LC cusp anomalous dimension as the asymptotic limit of the angle-dependent cusp anomalous dimension for large angles [129]:

$$\Gamma_{\text{cusp}}(\chi, \alpha_s) \xrightarrow{\chi \rightarrow \infty} \chi \Gamma_{\text{cusp}}(\alpha_s), \quad (11.35)$$

where $\Gamma_{\text{cusp}}(\alpha_s)$ is the on-LC cusp anomalous dimension. We know that in the LC limit, the angle is not well defined because it develops additional divergences due to $|n|, |\tilde{n}| \rightarrow 0$, which we can parameterise as (see Equation 7.73 for the definition of the cusp angle):

$$\chi = \cosh^{-1} \frac{n \cdot \tilde{n}}{|n| |\tilde{n}|} \xrightarrow{|n|, |\tilde{n}| \rightarrow 0} \frac{(n \cdot \tilde{n})^\epsilon}{\epsilon} = \frac{\sigma^\epsilon}{\epsilon}, \quad (11.36)$$

where $\sigma = n \cdot \tilde{n}$ is the area of the loop. Then we can rewrite Equation 11.35 as

$$\Gamma_{\text{cusp}}(\chi, \alpha_s) \xrightarrow{\chi \rightarrow \infty} \frac{\sigma^\epsilon}{\epsilon} \Gamma_{\text{cusp}}(\alpha_s), \quad (11.37)$$

The area derivation removes the pole:

$$\frac{\delta}{\delta \ln \sigma} \Gamma_{\text{cusp}}(\chi, \alpha_s) = \sigma^\epsilon \Gamma_{\text{cusp}}(\alpha_s) \xrightarrow{\epsilon \rightarrow 0} \Gamma_{\text{cusp}}(\alpha_s). \quad (11.38)$$

Finally, we fill in the original definition of the angle-dependent cusp anomalous dimension (see Equation 10.31):

$$\sum_{\text{cusps}} \Gamma_{\text{cusp}}(\chi, \alpha_s) = - \lim_{\epsilon \rightarrow 0} \frac{d}{d \ln \mu} \ln \mathcal{U}, \quad (11.39a)$$

$$\frac{\delta}{\delta \ln \sigma} \frac{d}{d \ln \mu} \ln \mathcal{U} = - \sum_{\text{cusps}} \frac{\delta}{\delta \ln \sigma} \Gamma_{\text{cusp}}(\chi, \alpha_s) = - \sum_{\text{cusps}} \Gamma_{\text{cusp}}(\alpha_s), \quad (11.39b)$$

which is indeed our result in Equation 11.34.

11.4 GEOMETRIC EVOLUTION OF TMDS

The most important point about this whole derivation is that this and the former chapter are equally valid when applied to regular Wilson lines, as intuitively we can ‘close’ any Wilson line structure by connecting its endpoints at infinity (which doesn’t add any gauge content, see Equation 6.27c). This is especially interesting

for TMDs and their associated soft factors, whose singularity structures are fully determined by their Wilson line structures.

The singularity structure of a TMD is quite intricate. Typically, there are 3 classes of divergences at one loop:

- A. Regular UV poles, which can be subtracted by a normal renormalisation procedure.
- B. Pure rapidity divergences which depend on an additional rapidity cut-off but don't necessarily violate regular renormalisation. These are the divergences associated with the ζ and ζ_h regulators, and they are manageable as they are resummed using the CS evolution equation.
- C. Overlapping divergences which are a combination of the former two, that stem from (partially) light-like Wilson line segments. These are comparable to the typical LC double poles, and similarly break regular renormalisation. In the standard TMD formalism, these are avoided by putting the segments slightly off-shell using the ζ and ζ_h regulators.

We will now motivate that instead of avoiding overlapping divergences, we can allow the Wilson segments inside a TMD to be on-LC, if we treat its evolution geometrically. The TMD rapidity cut-off is given by (see Equation 8.44)

$$\zeta = \lim_{|n| \rightarrow 0} \frac{k \cdot n}{|n|} = \lim_{|n| \rightarrow 0} \frac{N^+ N^-}{|n|}, \quad (11.40)$$

so that differentiating w.r.t. $\ln \zeta$ can be written as

$$\begin{aligned} \frac{\delta}{\delta \ln \zeta} &= \zeta \frac{\delta N^+}{\delta \zeta} \frac{\delta}{\delta N^+} + \zeta \frac{\delta N^-}{\delta \zeta} \frac{\delta}{\delta N^-}, \\ &= N^+ \frac{\delta}{\delta N^+} + N^- \frac{\delta}{\delta N^-}. \end{aligned}$$

Comparing this to Equation 11.32, we immediately see that

$$\frac{\delta}{\delta \zeta} \equiv \frac{\delta}{\delta \ln \sigma}. \quad (11.41)$$

Our conjecture in Equation 11.34 then tells us that the TMD has to satisfy

$$\frac{d}{d \ln \mu} \frac{\delta}{\delta \ln \sigma} \ln f = - \sum_{\text{cusps}} \Gamma_{\text{cusp}}. \quad (11.42)$$

But how many cusps does the TMD have? Let us have a look at the possibilities in

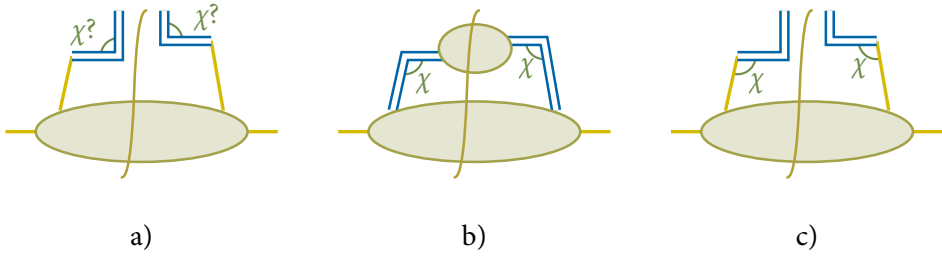


Figure 11.4: a) The only two cusps in a **TMD** are spurious cusps. b) When including the **FF**, two cusps appear. c) We conclude that the **TMD** (and the **FF** as well) contains two ‘hidden’ cusps, which are parameterised by the angle between the **LC** Wilson line and the incoming (resp. outgoing) quark.

Figure 11.4. The first thing we need to realise, is that there exist different types of cusps. What we will call an *externally driven* cusp, is a cusp that is somehow the emergence of a physical interaction. Consider e.g. **Figure 11.1**, where we could interpret the rectangular loop as the soft part of the 4-gluon scattering diagram with a quark box. The cusps in the soft part (the rectangular loop) are just the remnants of the quark-gluon interactions of the box. If we would e.g. remove the gluon on the top left, the Wilson line path on the left would have continued in a straight line (but probably in a different direction) up to the next cusp. If we re-add the fourth gluon in the hard part, the fourth cusp reappears in the soft part as well. That is why we call it externally driven.

Another type of cusp that might appear is what we will call a *spurious* cusp. For starters, it is not externally driven, but merely a result from a mathematical trick. One such example is a cusp that is formed at infinity. The Feynman rule in **Equation 6.27c** tells us that the part of a Wilson line that is connected to infinity does not transfer momentum, and equals just a factor 1. This directly implies that we can connect different Wilson line segments at infinity at will, and this is a perfect example of a spurious cusp. The important consideration is that a spurious cusp cannot contribute to the geometric evolution of Wilson line structures.³ This is why it is important to make the distinction between different type of cusps.

The most common Wilson line structure of a **TMD**, as represented in **Figure 11.4a**, has two cusps, but both of these cusps are positioned at ∞^- , and are hence spurious cusps. Where then are the cusps that drive the geometric evolution of the **TMD**? In fact, our focus is too narrow, and we should look at the full picture. In **SIDIS** we have both a **TMD** and an **FF** at the same time, so we should

³ The motivation for this statement is that we can create as many spurious cusps at will without changing the kinematics nor dynamics of the system.

look at them together. If we ignore the transversal parts of the Wilson line,⁴ the **TMD** contains a Wilson line in the n^- direction, and the **FF** contains a line in the n^+ direction. These two lines meet in a cusp, exactly a cusp is externally driven, as it is the remnant of the interaction with the virtual photon. This is illustrated in **Figure 11.4b** (where again the transversal parts are omitted as they don't contribute to the cusp-discussion). So the geometric evolution is clearly visible if we combine both the **TMD** and the **FF**.

We now conjecture a third type of cusp, what we will call a *hidden* cusp. It is the imprint from the externally driven cusp in **Figure 11.4b** acting on the **TMD** and the **FF** separately. It is externally driven, as it directly influenced by the virtual photon, but it is not a cusp between Wilson lines only—instead it is a cusp between a Wilson line and a quark line. This is illustrated in **Figure 11.4c** (where we reinserted the transversal parts for generality). When considering the Wilson line structure of a **TMD**, this cusp is easily overlooked, as it is merely an imprint of the cusp in **Figure 11.4b**. This is why we call it hidden. But it is not unimportant—in fact it is indispensable—as the geometric evolution of a **TMD** is fully governed by its two hidden cusps.

The geometric evolution for the **TMD** is hence given by

Geometric Evolution for TMD

$$\frac{d}{d \ln \mu} \frac{\delta}{\delta \ln \sigma} \ln f = -2\Gamma_{\text{cusp}}. \quad (11.43)$$

At 1-loop we have $\Gamma_{\text{cusp}} = \frac{\alpha_s C_F}{\pi}$ and hence our conjecture is in perfect agreement with the **CS Equation 8.52**, because trivially (see **Equation 8.53**):

$$\gamma_K \equiv -2\Gamma_{\text{cusp}}. \quad (11.44)$$

This result has been confirmed at 2-loop by Dr. Igor Cherednikov and Tom Mertens [153]. So to summarise:

- A. Our conjecture holds, and is as expected applicable on arbitrary Wilson line structures with **LC** segments, like **TMDs**.
- B. We can treat the nasty overlapping divergences coming from **LC** segments by using a geometric description, hence avoiding the need to calculate difficult off-**LC** segments.
- C. There is a one-to-one correspondence between the rapidity derivative and our logarithmic area derivative. This also implies we can apply geometric evolution on the **TMD** to calculate the **CS** kernel (**Equation 8.51a**).

⁴ Which we can safely do in the discussion on the cusps, as they only contribute spurious cusps.

CONCLUSION AND OUTLOOK

In this thesis we deeply investigated some technicalities of QCD. In particular, the main mathematical object of interest in this thesis was a Wilson line—prominently present in many QCD calculations—and to some extent its more exotic nephew, the Wilson loop. After giving a very broad introduction to the mechanics behind QFT in general and QCD in particular in Chapters 1 to 5, we went on to construct a new framework to work with aforementioned Wilson lines in Chapters 6 and 7. This framework is only applicable on piecewise linear Wilson lines, but luckily this is the only type of line that appears in real-life physics in the absence of an external field, as the path of a Wilson line is generally dictated by external driving forces. In the absence of a continuous external field, the Wilson path will lie in a straight line, until it is spontaneously driven in another direction (e.g. due to the interaction with a photon), leading to a piecewise linear path.

We have spent quite some time in Chapter 6 to introduce Wilson lines in a detailed and rigorous way, as general as possible within the piecewise linear assumption. While standard references generally introduce Wilson lines for a specific path direction, e.g. in the LC minus direction, the Feynman rules in Equations 6.27 and all other formulae in Chapters 6 and 7 are valid for any linear path, be it light-like, transversal, or a mixture of both. We have put some emphasis on the finite and fully infinite linear lines, to introduce them with strong mathematical rigour. What remains of Chapter 6 was devoted to the introduction of our new framework, relating different path topologies and combining segments into a piecewise line. In Chapter 7 we first introduced a new technique to calculate products and traces of fundamental Lie generators, with Equation 7.2a and Equations 7.7 as the main result. In the remaining part of Chapter 7 we have put our framework into practice, and have almost a full result at NLO in Equations 7.71, 7.81 and 7.88—where full implies applicable to any piecewise linear Wilson line that exists.

In Chapters 8 and 9 we reviewed two common frameworks in QCD. Chapter 8 was an investigation of the TMD framework, where Wilson lines are heavily used in the gauge invariant definitions of the density functions. In the end of this

chapter, we elaborated a bit on the singularity structure and evolution of **TMDs**, as it is fully governed by the underlying Wilson line structure. **Chapter 9** was an investigation of the small- x approach, where the behaviour of (integrated and unintegrated) **PDFs** is described at small- x . In the end of this chapter, we elaborated on a way to observe saturation in experiment by measuring the transversal energy flow and using the **GBW** model. Although seemingly unrelated to the rest of this thesis, the small- x framework has a strong use of Wilson lines as well—and hence also has potential use in our new framework—be it at a lesser extent than the **TMD** framework.

Finally, in **Chapters 10** and **11** we investigated a special class of Wilson lines—defined on a closed path—called Wilson loops. They are ideal tools to investigate the renormalisation properties of objects built on a Wilson line structure, like **TMDs** and the loops themselves. Renormalisation is governed by the cusp anomalous dimension, if using an adapted renormalisation procedure where additional divergences are subtracted as well. The loop is then said to be multiplicatively renormalisable. In the case of **TMDs** this additional renormalisation is avoided by use of the **CS RGE** and either an off-**LC** shift or an intercancellation between different sub-factors. In **Chapter 11** we moved to loop space in order to describe the evolution of Wilson loops in a geometrical way. We focussed on rectangular planar light-like loops, and derived geometrical evolution equations in a way similar to the regular **MM** equations, but avoiding mathematical tools that would be ill-defined for a cusped contour. In the end, we define the logarithmic area derivative in **Equation 11.32** and conjecture in **Equation 11.34** a geometrical evolution driven by the cusp anomalous dimension and the number of cusps. We show that it holds for the quadrilateral loop, but also for the **TMD** as it is in perfect agreement with the **CS** evolution equations. In this way we have directly shown that there is another way to treat the additional divergences of **TMDs**: instead of an off-**LC** shift or an intercancellation of sub-factors, we can subtract these divergences using our geometrical approach.

OUTLOOK

The two main results in this thesis—the piecewise linear Wilson framework and the geometric evolution—are still in a stage of active research, as both can be further explored and applied, as well as strengthened by going to higher orders. While my supervisor Dr. Igor Cherednikov and fellow Ph.D. student Tom Mertens have chosen to continue the research on loop space and the geometrical behaviour of Wilson lines/loops—further adapting the conjecture in [Equation 11.34](#) to make it mathematically more stable—I prefer to continue with the piecewise linear Wilson line framework. I am currently finishing the **NLO** calculations in Feynman gauge, and will afterwards continue with the first calculations at **NNLO**, as well as start calculating some other blobs, different from the self-interaction blobs, as e.g. blobs connecting an external quark [15]. But my main aim at the moment is to lift this framework out from the pure theoretical regime, into more applied physics. To achieve this, I recently engaged myself into two new collaborations. The first is together with Dr. Ahmad Idilbi, Dr. Miguel García-Echevarría, Prof. Dr. Ignazio Scimemi and Dr. Alexey Vladimirov, on the calculation of the **TMD** collinear and soft factors at **NNLO** [14]. It is a direct application of the framework developed in [Chapters 6](#) and [7](#). The second is together with Prof. Dr. Leonard Gamberg and Dr. Marc Schlegel, on an investigation of the duality between the **GPD E** and the Boer-Mulders and Sivers **TMDs** [13]. For this calculation a lensing function is used which is originally approximated, but can be calculated in a more direct way using [Equations 7.7](#).

Part IV

APPENDICES

CONVENTIONS AND REFERENCE FORMULAE

A.1 NOTATIONAL CONVENTIONS

We will use a few different equal sign, to clarify some of our statements. In particular:

- A. $=$ “...is equal to ...” ,
- B. \equiv “...is required to be equal to ...” ,
- C. $\stackrel{\text{def}}{=}$ “...is defined as ... or ...is defined to equal ...” ,
- D. $\stackrel{\text{sup}}{=}$ “assume ... to be equal to ...”
- E. $\stackrel{\text{N}}{=}$ “...is written as ...” ,
- F. $\stackrel{?}{=}$ “...is maybe equal to ...” (statement has still to be verified) .

In general, we use the same conventions as in [18]. We will e.g. never use the comma notation to denote derivatives (as it is too easily confused with misplaced commas). We will work in natural units:

$$\hbar = c = \varepsilon_0 = k_B = 1. \quad (\text{A.1})$$

This means in particular that the electromagnetic fine structure constant is given by

$$\alpha = \frac{g^2}{4\pi} \approx \frac{1}{137.04}. \quad (\text{A.2})$$

Although α originally only associated to the electromagnetic force, it is common to define a similar constant for the strong force:

$$\alpha_s \stackrel{\text{N}}{=} \frac{g^2}{4\pi}. \quad (\text{A.3})$$

Concerning indices and general variable namings, we try to be as consistent as possible (which is sometimes difficult due to the limited amount of characters available in the alphabet). In particular, we will use:

- A. $r, s, t, u, v, w, x, y, z$ for coordinates ,
- B. k, l, p, q for momenta ,
- C. μ, ν, ρ, σ for Minkowskian indices ,
- D. i, j, k, l for Euclidian indices ,
and for the spatial part of 4-vectors ,
and for fundamental indices (Lie algebra) ,
and for enumerations in sums and products ,
- E. a, b, c, d, e, f, g for adjoint indices (Lie algebra) ,
- F. x, y, z, w for summations of adjoint indices (Lie algebra) ,
- G. $\alpha, \beta, \gamma, \delta$ for Dirac indices .
- H. n for any integer greater than zero ,
and for any directional 4-vector ,
- I. J, K, L, O for Wilson line segments .

We will mainly work in the path integral formalism (see [Chapter 3](#)). This implies that fields aren't operators, but merely *coordinate or momentum functions*. It also implies that we can treat them as plain numbers, commuting with everything. There are two exceptions: spinor fields anticommute by definition, and non-Abelian gauge fields are contracted with Lie generators. However, there is a strong conceptual difference between these fields, and operator fields. E.g. the generator can be extracted from gauge fields:

$$A_\mu \equiv A_\mu^a t^a , \tag{A.4}$$

where now A_μ^a is again just a number (while in canonical quantisation also this part would remain an operator). This might be a bit confusing, as the gauge fields are sometimes used as 'operators', i.e. with the generators absorbed in the field, as it can reveal certain relations a bit easier (see e.g. [Equations 1.56](#)). Just remember that in our treatment they are never operators in a literal way. The same is true for spinor fields, as their anticommuting behaviour can simply be attributed to the Grassmanian coefficients (just numbers) that define it (see e.g. [Equation 3.83](#)).

A.2 VECTORS AND TENSORS

For the Minkowski metric, we take the common convention

$$g^{\mu\nu} = \begin{pmatrix} 1 & 0 & 0 & 0 \\ 0 & -1 & 0 & 0 \\ 0 & 0 & -1 & 0 \\ 0 & 0 & 0 & -1 \end{pmatrix}, \quad (\text{A.5})$$

where Greek indices run over 0, 1, 2, 3 (for t, x, y, z). To denote only the spatial components, we use Roman indices, like i, j , etc. We use the *Einstein notation* convention throughout the whole thesis, meaning that repeated indices are to be summed over. A 4-vector is denoted in italic, a 3-vector in bold and a 2-vector (the transversal components) in bold and with a subscript \perp :

$$p^\mu = (p^0, p^1, p^2, p^3) = (p^0, \mathbf{p}) = (p^0, \mathbf{p}_\perp, p^3), \quad (\text{A.6})$$

while a length is mostly denoted in italic, be it a length of a 4-, 3- or 2-vector. The difference should be clear from context, but when needed for clarity, we use $|\mathbf{p}|$ and $|\mathbf{p}_\perp|$. The scalar product is fully defined by the metric:

$$x \cdot p = x^0 p^0 - \mathbf{x} \cdot \mathbf{p}. \quad (\text{A.7})$$

This implies that we can define a vector with a lower index as

$$p_\mu = g_{\mu\nu} p^\nu = (p^0, -p^1, -p^2, -p^3) = (p^0, -\mathbf{p}) = (p^0, -\mathbf{p}_\perp, -p^3), \quad (\text{A.8})$$

such that

$$x \cdot p = x^\mu p_\mu. \quad (\text{A.9})$$

Note that the index switches places when moving the coordinate to the denominator, as is e.g. the case for the derivative:

$$\frac{\partial}{\partial x^\mu} \stackrel{\text{N}}{=} \partial_\mu. \quad (\text{A.10})$$

The position 4-vector combines time and 3-position, while the 4-momentum combines energy and 3-momentum:

$$x^\mu = (t, \mathbf{x}) \quad p^\mu = (E, \mathbf{p}). \quad (\text{A.11})$$

A particle that sits on its mass-shell (on-shell for short) has

$$p^2 = E^2 - |\mathbf{p}|^2 = m^2. \quad (\text{A.12})$$

All real particles (having timescales and distances larger than the quantum level) are on-shell.

Last we define the symmetrisation (...) and antisymmetrisation [...] of a tensor as

$$A^{(\mu\nu)} = \frac{1}{2} (A^{\mu\nu} + A^{\nu\mu}) , \quad (\text{A.13a})$$

$$A^{[\mu\nu]} = \frac{1}{2} (A^{\mu\nu} - A^{\nu\mu}) . \quad (\text{A.13b})$$

A rank-2 tensor has the peculiar property that it can be split exactly in its symmetric and antisymmetric parts

$$A^{\mu\nu} = A^{(\mu\nu)} + A^{[\mu\nu]} . \quad (\text{A.14})$$

This is in general not true for tensors of higher rank. Symmetrising an antisymmetric tensor returns zero, this implies:

$$A^{(\mu\nu)} B_{[\mu\nu]} = 0 . \quad (\text{A.15})$$

It is straightforward to generalise the definition of symmetrisation to tensors of higher rank:

$$A^{(\mu_1 \cdots \mu_n)} = \frac{1}{n!} (A^{\mu_1 \cdots \mu_n} + \text{all permutations}) , \quad (\text{A.16a})$$

$$A^{[\mu_1 \cdots \mu_n]} = \frac{1}{n!} (A^{\mu_1 \cdots \mu_n} - \text{all odd perm.} + \text{all even perm.}) . \quad (\text{A.16b})$$

A.3 SPINORS AND GAMMA MATRICES

Any field with half-integer spin, i.e. a Dirac field, anticommutes:

$$\psi(x)\psi(y) = -\psi(y)\psi(x) \quad x \neq y . \quad (\text{A.17})$$

We define gamma matrices by their anticommutation relations

$$\{\gamma^\mu, \gamma^\nu\} \equiv 2 g^{\mu\nu} \mathbb{1} , \quad (\text{A.18})$$

with the following additional property:

$$(\gamma^\mu)^\dagger = \gamma^0 \gamma^\mu \gamma^0 . \quad (\text{A.19})$$

Then we can define the Dirac equation for a particle field ψ :

$$(i\rlap{/}\partial - m)\psi = 0. \quad (\text{A.20})$$

where the slash is a shortcut notation for

$$\rlap{/}\partial = \gamma^\mu \partial_\mu. \quad (\text{A.21})$$

We can identify an antiparticle field with $\bar{\psi}$ if we define:

$$\bar{\psi} = \psi^\dagger \gamma^0, \quad (\text{A.22})$$

which satisfies a slightly adapted Dirac equation:

$$i\partial_\mu \bar{\psi} \gamma^\mu + m\bar{\psi} = 0. \quad (\text{A.23})$$

We can expand Dirac fields in function of a set of plane waves:

$$\psi(x) = u^s(p) e^{-ip \cdot x} \quad (p^2 = m^2, p^0 > 0), \quad (\text{A.24a})$$

$$\psi(x) = v^s(p) e^{ip \cdot x} \quad (p^2 = m^2, p^0 < 0), \quad (\text{A.24b})$$

where s is a spin-index. If we define

$$\bar{u} = u^\dagger \gamma^0, \quad \bar{v} = \gamma^0 v^\dagger, \quad (\text{A.25})$$

we can find the *completeness relations* by summing over spin:

$$\sum_s u^s(p) \bar{u}^s(p) = \rlap{/}\not{p} + m, \quad (\text{A.26a})$$

$$\sum_s \bar{v}^s(p) v^s(p) = \rlap{/}\not{p} - m. \quad (\text{A.26b})$$

We will identify

- A. u with an incoming fermion,
- B. \bar{u} with an outgoing fermion,
- C. \bar{v} with an incoming antifermion,
- D. v with an outgoing antifermion.

If we define

$$\gamma^5 \stackrel{\text{N}}{=} i\gamma^0 \gamma^1 \gamma^2 \gamma^3 = -\frac{i}{4!} \varepsilon^{\mu\nu\rho\sigma} \gamma_\mu \gamma_\nu \gamma_\rho \gamma_\sigma, \quad (\text{A.27a})$$

$$\gamma^{\mu\nu} \stackrel{\text{N}}{=} \gamma^{[\mu} \gamma^{\nu]} = \frac{1}{2} (\gamma^\mu \gamma^\nu - \gamma^\nu \gamma^\mu), \quad (\text{A.27b})$$

we can construct a complete Dirac basis:

$$\mathbb{1}, \gamma^\mu, \gamma^{\mu\nu}, \gamma^\mu \gamma^5, \gamma^5. \quad (\text{A.28})$$

We will identify

- A. $\mathbb{1}$ with a scalar,
- B. γ^μ with a vector,
- C. $\gamma^{\mu\nu}$ with a tensor,
- D. $\gamma^\mu\gamma^5$ with a pseudo-vector,
- E. γ^5 with a pseudo-scalar.

Furthermore, γ^5 has the following properties:

$$(\gamma^5)^\dagger = \gamma^5, \quad (\gamma^5)^2 = \mathbb{1}, \quad \{\gamma^5, \gamma^\mu\} = 0. \quad (\text{A.29})$$

Let's list some contraction identities for gamma matrices in ω dimensions:

$$\gamma^\mu \gamma_\mu = \omega, \quad (\text{A.30a})$$

$$\gamma^\mu \gamma^\nu \gamma_\mu = (2 - \omega) \gamma^\nu, \quad (\text{A.30b})$$

$$\gamma^\mu \gamma^\nu \gamma^\rho \gamma_\mu = 4 g^{\nu\rho} + (\omega - 4) \gamma^\nu \gamma^\rho, \quad (\text{A.30c})$$

$$\gamma^\mu \gamma^\nu \gamma^\rho \gamma^\sigma \gamma_\mu = -2 \gamma^\sigma \gamma^\rho \gamma^\nu + (4 - \omega) \gamma^\nu \gamma^\rho \gamma^\sigma. \quad (\text{A.30d})$$

And some trace identities:

$$\text{tr}(\mathbb{1}_{\text{Dirac}}) = 4, \quad (\text{A.31a})$$

$$\text{tr}(\text{odd number of } \gamma\text{'s}) = 0, \quad (\text{A.31b})$$

$$\text{tr}(\gamma^\mu \gamma^\nu) = 4 g^{\mu\nu}, \quad (\text{A.31c})$$

$$\text{tr}(\gamma^\mu \gamma^\nu \gamma^\rho \gamma^\sigma) = 4 (g^{\mu\nu} g^{\rho\sigma} - g^{\mu\rho} g^{\nu\sigma} + g^{\mu\sigma} g^{\nu\rho}), \quad (\text{A.31d})$$

$$\text{tr}(\gamma^{\mu_1} \gamma^{\mu_2} \dots \gamma^{\mu_{n-1}} \gamma^{\mu_n}) = \text{tr}(\gamma^{\mu_n} \gamma^{\mu_{n-1}} \dots \gamma^{\mu_2} \gamma^{\mu_1}). \quad (\text{A.31e})$$

Let us finish this section by listing some useful relations:

$$\not{k} \not{k} = k^2, \quad \not{k} \not{p} + \not{p} \not{k} = 2p \cdot k, \quad \gamma^\mu \not{k} = 2k^\mu - \not{k} \gamma^\mu, \quad (\text{A.32a})$$

$$\not{p} \not{k} \not{p} = 2p \cdot k \not{p} - p^2 \not{k}, \quad \not{p} \not{k} \not{q} \not{p} = 2p \cdot q \not{p} \not{k} - 2p \cdot k \not{p} \not{q} + p^2 \not{k} \not{q}, \quad (\text{A.32b})$$

$$\not{k} \not{p} \not{q} + \not{q} \not{p} \not{k} = 2p \cdot q \not{k} - 2q \cdot k \not{p} + 2k \cdot p \not{q}. \quad (\text{A.32c})$$

A.4 LIGHT-CONE COORDINATES

Light-cone coordinates form a useful basis to represent 4-vectors. For a random vector k^μ , they are defined by

$$k^+ = \frac{1}{\sqrt{2}} (k^0 + k^3), \quad (\text{A.33a})$$

$$k^- = \frac{1}{\sqrt{2}} (k^0 - k^3), \quad (\text{A.33b})$$

$$\mathbf{k}_\perp = (k^1, k^2). \quad (\text{A.33c})$$

We will represent the plus-component first, i.e.

$$k^\mu = (k^+, k^-, \mathbf{k}_\perp). \quad (\text{A.34})$$

One often encounters in literature the notation $(k^-, k^+, \mathbf{k}_\perp)$, but this is merely a matter of convention. The factor $\frac{1}{\sqrt{2}}$ normalises the transformation to unit Jacobian, such that

$$d^\omega k = dk^+ dk^- d^{\omega-2} \mathbf{k}_\perp. \quad (\text{A.35})$$

It is straightforward to show that the scalar product has the form

$$k \cdot p = k^+ p^- + k^- p^+ - \mathbf{k}_\perp \cdot \mathbf{p}_\perp, \quad (\text{A.36a})$$

$$k^2 = 2k^+ k^- - \mathbf{k}_\perp^2. \quad (\text{A.36b})$$

This implies that the metric becomes off-diagonal:

$$g_{\text{LC}}^{\mu\nu} = \begin{pmatrix} 0 & 1 & 0 & 0 \\ 1 & 0 & 0 & 0 \\ 0 & 0 & -1 & 0 \\ 0 & 0 & 0 & -1 \end{pmatrix}. \quad (\text{A.37})$$

We will drop the index LC when clear from context. Note that this basis is not orthonormal. Note also that

$$g^{\mu\nu} g_{\nu\rho} = \delta_\rho^\mu, \quad g^{\mu\nu} g_{\mu\nu} = 4, \quad (\text{A.38})$$

just like the Cartesian metric. We can also define two light-like basis-vectors:

$$n_+^\mu = (1^+, 0^-, \mathbf{0}_\perp), \quad (\text{A.39a})$$

$$n_-^\mu = (0^+, 1^-, \mathbf{0}_\perp). \quad (\text{A.39b})$$

These are light-like vectors, and maximally non-orthogonal:

$$n_+^2 = 0, \quad n_-^2 = 0, \quad n_+ \cdot n_- = 1. \quad (\text{A.40})$$

Watch out, as lowering the index switches the light-like components because of the form of the metric:

$$n_{+\mu} = (0^+, 1^-, \mathbf{0}_\perp), \quad (\text{A.41a})$$

$$n_{-\mu} = (1^+, 0^-, \mathbf{0}_\perp), \quad (\text{A.41b})$$

such that they project out the other light-like component of a vector:

$$k \cdot n_+ = k^-, \quad k \cdot n_- = k^+. \quad (\text{A.42})$$

In other words, we can write

$$k = (k \cdot n_-) n_+ + (k \cdot n_+) n_- - \mathbf{k}_\perp^2. \quad (\text{A.43})$$

For Dirac matrices in LC-coordinates, we have

$$\{\gamma^+, \not{k}\} = 2 g^{+\mu} k_\mu = 2k^+ \quad \Rightarrow \quad \gamma^+ \not{k} = 2k^+ - \not{k} \gamma^+. \quad (\text{A.44})$$

Note that

$$(\gamma^+)^2 = (\gamma^-)^2 = 0, \quad \frac{1}{2} \{\gamma^+, \gamma^-\} = 1,$$

such that [Equation A.18](#) remains valid in light-cone coordinates.

We can use the light-like basis vectors to construct a metric for nothing but the transversal part:

$$g_\perp^{\mu\nu} = g^{\mu\nu} - 2 n_+^{(\mu} n_-^{\nu)} \quad (\text{A.45a})$$

$$= \begin{pmatrix} 0 & 0 & 0 & 0 \\ 0 & 0 & 0 & 0 \\ 0 & 0 & -1 & 0 \\ 0 & 0 & 0 & -1 \end{pmatrix}. \quad (\text{A.45b})$$

Note that

$$g_\perp^{\mu\nu} g_{\perp\nu\rho} = \delta_\rho^\mu - n_+^\mu n_{-\rho} - n_-^\mu n_{+\rho}, \quad g_\perp^{\mu\nu} g_{\perp\mu\nu} = 2. \quad (\text{A.46})$$

Last we can define an antisymmetric metric:

$$\varepsilon_\perp^{\mu\nu} = \varepsilon^{+\mu\nu} \quad (\text{A.47a})$$

$$= \begin{pmatrix} 0 & 0 & 0 & 0 \\ 0 & 0 & 0 & 0 \\ 0 & 0 & 0 & 1 \\ 0 & 0 & -1 & 0 \end{pmatrix}, \quad (\text{A.47b})$$

where we adopt the convention $\epsilon^{0123} = \epsilon^{+-12} = +1$.

A.5 FOURIER TRANSFORMS AND DISTRIBUTIONS

The Heaviside step function is defined as

$$\theta(x) = \begin{cases} 0 & x < 0 \\ 1 & x > 0 \end{cases}, \quad (\text{A.48})$$

and is undefined for $x = 0$ (sometimes it is hard-coded to equal 0, 1 or $1/2$, but we leave it undefined). It can be used to limit integration borders:

$$\int_{-\infty}^{+\infty} dx \theta(x-a) f(x) = \int_a^{+\infty} dx f(x), \quad (\text{A.49a})$$

$$\int_{-\infty}^{+\infty} dx \theta(a-x) f(x) = \int_{-\infty}^a dx f(x). \quad (\text{A.49b})$$

The Dirac δ -function is defined as the derivative of the θ -function:

$$\delta(x) = \frac{d}{dx} \theta(x), \quad \Rightarrow \int dx \delta(x) = 1, \quad (\text{A.50})$$

and is zero everywhere, except at $x = 0$. A generalisation to n dimensions is straightforward:

$$\int d^n x \delta^n(x) = 1. \quad (\text{A.51})$$

The most important use of the Dirac δ -function is the *sifting property*, which follows straight from [Equation A.51](#):

$$\int d^n x f(x) \delta^n(x-t) = f(t). \quad (\text{A.52})$$

However, for non-infinite borders, the sifting property gains additional θ -functions:

$$\int_a^b dx \delta(x-c) f(x) = \theta(b-c) \theta(c-a) f(c). \quad (\text{A.53a})$$

Similar properties can be derived for the θ -function:

$$\int_a^b dx \theta(x-c) f(x) = \theta(a-c) \int_a^b dx f(x) + \theta(b-c) \theta(c-a) \int_c^b dx f(x), \quad (\text{A.53b})$$

$$\int_a^b dx \theta(c-x) f(x) = \theta(c-b) \int_a^b dx f(x) + \theta(b-c) \theta(c-a) \int_a^c dx f(x). \quad (\text{A.53c})$$

When dealing with on-shell conditions, we often encounter the combination of a Heaviside θ and a Dirac δ function. To save space, we define the short-hand notation

$$\delta^+(p^2 - m^2) \stackrel{\text{N}}{=} \delta(p^2 - m^2) \theta(p^0). \quad (\text{A.54})$$

When working in LC-coordinates, the integration over p^0 is replaced by an integration over p^+ , hence in this case we define the short-cut as

$$\delta^+(p^2 - m^2) \stackrel{\text{N}}{=} \delta(p^2 - m^2) \theta(p^+). \quad (\text{A.55})$$

Another short-hand notation we will often use to save space is

$$\delta^{(n)}(x) \stackrel{\text{N}}{=} (2\pi)^n \delta^{(n)}(x), \quad (\text{A.56})$$

because a δ -function is often accompanied with powers of 2π . The combination of the two is trivial:

$$\delta^+(x) \stackrel{\text{N}}{=} 2\pi \delta(p^2 - m^2) \theta(p^+). \quad (\text{A.57})$$

When dealing with Fourier transforms, we will use the following conventions:

$$\tilde{f}(k) = \int d^4x f(x) e^{ik \cdot x}, \quad (\text{A.58a})$$

$$f(x) = \int \frac{d^4k}{(2\pi)^4} \tilde{f}(k) e^{-ik \cdot x}. \quad (\text{A.58b})$$

The tilde will always be omitted, as the function argument specifies clearly enough whether we are dealing with the coordinate or momentum representation. Note that due to the Minkowski metric, Fourier transforms over spatial components have the signs in their exponents flipped:

$$f(x) = \int \frac{d^3\mathbf{k}}{(2\pi)^3} \tilde{f}(\mathbf{k}) e^{i\mathbf{k} \cdot \mathbf{x}}, \quad (\text{A.59a})$$

$$\tilde{f}(\mathbf{k}) = \int d^3\mathbf{x} f(x) e^{-i\mathbf{k} \cdot \mathbf{x}}, \quad (\text{A.59b})$$

and the same for two-dimensional Fourier transforms. When necessary to emphasise the Fourier transform itself, we will use the notation

$$\mathcal{F}_k [f(x)] \stackrel{\text{N}}{=} \int d^4x f(x) e^{ik \cdot x}, \quad (\text{A.60})$$

$$\mathcal{F}_x^{-1} [f(k)] \stackrel{\text{N}}{=} \int \frac{d^4k}{(2\pi)^4} f(k) e^{-ik \cdot x}. \quad (\text{A.61})$$

An ‘empty’ Fourier transform gives a δ -function:

$$\mathcal{F}_k [1] = \int d^n x e^{ik \cdot x} \equiv (2\pi)^n \delta^{(n)}(k), \quad (\text{A.62a})$$

$$\mathcal{F}_x^{-1} [1] = \int \frac{d^n k}{(2\pi)^n} e^{-ik \cdot x} \equiv \delta^{(n)}(x), \quad (\text{A.62b})$$

and the Fourier transform of $1/k$ leads to a Heaviside θ -function:

$$\mathcal{F}_x \left[\frac{1}{k} \right] \equiv \theta(x) = -\lim_{\varepsilon \rightarrow 0} \frac{1}{2\pi i} \int_{-\infty}^{+\infty} dk \frac{1}{k + i\varepsilon} e^{-ikx}, \quad (\text{A.63a})$$

$$= -\lim_{\varepsilon \rightarrow 0} \frac{1}{2\pi i} \int_{-\infty}^{+\infty} dk \frac{1}{k - i\varepsilon} e^{ikx}, \quad (\text{A.63b})$$

where the integration should be made by choosing the appropriate complex contour. A Dirac δ -function having a complex argument is in general not well-defined, as its exponential representation is divergent:¹

$$\delta^n(x + iy) \stackrel{?}{=} \int \frac{d^n k}{(2\pi)^n} e^{-ik(x+iy)} = \mathcal{F}_x^{-1} [e^{ky}]. \quad \not\equiv \quad (\text{A.64})$$

But we will allow this notation anyway, because sometimes a function acts as a *nascent δ_ε -function*, which implies that—in combination with the sifting property—it behaves exactly the same as a regular δ -function (mostly under certain conditions). It is possible that such nascent δ_ε -functions allow for complex arguments, and still retain their sifting property (see e.g. the discussion of the infinite Wilson line on page 174). It is for these situations that we allow the notation of a complex δ -function, but we keep in mind that it can only be used together with the sifting property, and has no exponential representation.

¹ The only non-divergent Fourier transform of a linear real exponential is that of $e^{-a|x|}$ with $a > 0$.

To conclude this section, we list two other common transformations. First we have the Laplace transform:

$$f(x) = \frac{1}{2\pi i} \int_{c-i\infty}^{c+i\infty} d^n s f(s) e^{s \cdot x}, \tag{A.65a}$$

$$f(s) = \int_0^\infty d^n x f(x) e^{-s \cdot x}, \tag{A.65b}$$

and second the Mellin transform:

$$f(x) = \frac{1}{2\pi i} \int_{c-i\infty}^{c+i\infty} d^n s f(s) x^{-s}, \tag{A.66a}$$

$$f(s) = \int_0^\infty d^n x f(x) x^{s-1}, \tag{A.66b}$$

which is quite common in QCD (it is e.g. the driving transform behind the convolution in the DGLAP equations, see Equations 5.45). Both for the inverse Laplace integral as the inverse Mellin integral, c is chosen such that it is bigger than all singularities in $f(s)$.

A.6 LIE ALGEBRA

Representations

Let's revise some basic colour algebra. As is well known, the group which governs QCD is $SU(3)$, but for the sake of generality we list some basic rules and derive some properties for $SU(N)$ (more specifically, for $\mathfrak{su}(n)$, the corresponding Lie algebra of $SU(N)$). The latter is fully defined by $d_A = N^2 - 1$ linearly independent Hermitian generators t^a and their commutation relations

$$[t^a, t^b] = i f^{abc} t^c, \tag{A.67}$$

where the f^{abc} are real and fully antisymmetric constants (the so-called structure constants). The structure constants themselves satisfy the *Jacobi identity*:

$$f^{abx} f^{xcd} - f^{acx} f^{xbd} + f^{adx} f^{xbc} = 0. \tag{A.68}$$

From a mathematician's point of view, any set of generators (not necessarily Hermitian) that satisfy the commutation relations and the Jacobi identity define a Lie algebra.

In practice we will work with representations of the algebra, where the generators are represented by $d_R \times d_R$ Hermitian matrices, with d_R the dimension of the representation. Two representations of particular interest are first the fundamental representation which has dimension $d_F = N$.² It has the additional unique property that its matrices, if complemented with the identity matrix, form a set

$$(\mathbb{1}, t^a) .$$

that acts as a basis for the generator products under matrix multiplication.

The second important representation is the adjoint representation, which is constructed from the structure constants:

$$(T^a)_{bc} = -if^a_{bc} ,$$

and has dimension $d_A = N^2 - 1$. We will make the distinction in notation by writing the fundamental with lowercase t and the adjoint with uppercase T . Note that in literature several different notations exist (e.g. t_F and t_A).

Properties

All matrices are traceless in every representation:

$$\text{tr}(t^a) = 0 . \tag{A.69}$$

The trace of two matrices is zero if they are different:

$$\text{tr}(t^a t^b) = D_R \delta^{ab} . \tag{A.70}$$

D_R is a constant depending on the representation. In the fundamental representation this is by convention almost always $D_F = \frac{1}{2}$. Summing all squared matrices gives an operator that commutes with all other generators (and combinations of generators), the so-called Casimir operator

$$t^a t^a = C_R \mathbb{1} , \tag{A.71}$$

² A small remark: when working in QCD, It is common to denote the dimension of the fundamental representation by N_c , as it represents the number of colours used in the theory. In this section of the appendix we will use the notation N to keep it general, but in the body of this thesis we will use the notation N_c to enhance interpretation.

Again, C_R is a constant depending on the representation. Both constants can be easily related

$$t^a t^a = C_R \mathbb{1} \Rightarrow \text{tr}(t^a t^a) = C_R \text{tr}(\mathbb{1}) = C_R d_R, \quad (\text{A.72a})$$

$$\text{tr}(t^a t^b) = D_R \delta^{ab} \Rightarrow \text{tr}(t^a t^a) = D_R \delta^{aa} = D_R d_A, \quad (\text{A.72b})$$

$$\Rightarrow \frac{C_R}{d_A} = \frac{D_R}{d_R}.$$

These properties are valid for any representation, not only the adjoint. Let us now list the constants for the fundamental and the adjoint representation:

$$\begin{aligned} D_F &= \frac{1}{2}, & D_A &= 2D_F d_F = N, \\ C_F &= D_F \frac{d_A}{d_F} = \frac{N^2 - 1}{2N}, & C_A &= D_A = N, \\ d_F &= N, & d_A &= d_F^2 - 1 = N^2 - 1. \end{aligned}$$

Because in the fundamental representation we have a basis that spans its full product space, we can derive additional properties that are not valid in other representations. First of all, the anticommutator has to be an element of the algebra, and thus a linear combination of the identity and the generators:

$$\{t^a, t^b\} = \frac{1}{N} \delta^{ab} \mathbb{1} + d^{abc} t^c. \quad (\text{A.73})$$

The constant in front of the identity was calculated by taking the trace and comparing to [Equation A.70](#), while d^{abc} can be retrieved, as well as f^{abc} , from

$$f^{abc} = -\frac{i}{D_R} \text{tr}([t_R^a, t_R^b] t_R^c), \quad (\text{A.74a})$$

$$d^{abc} = 2 \text{tr}(\{t^a, t^b\} t^c). \quad (\text{A.74b})$$

[Equation A.74a](#) is valid in any representation, while [Equation A.74b](#) only makes sense in the fundamental representation.

Because almost every calculation ends with a full colour trace, having the identity matrix written implicitly is dangerous, as one might forget to add the factor N coming from its trace. For this reason we will often write $\frac{\mathbb{1}}{N}$ together, as it is a factor that is trace-normalised to one.

It is easy to check that the d^{abc} are fully symmetric and that they vanish when contracting any two indices:

$$d^{aab} = d^{baa} = d^{aba} = 0.$$

It is interesting to note that in $SU(2)$ all d^{abc} vanish. By combining the commutation rules with the anticommutation rules we can find another useful property:

$$\begin{aligned} t^a t^b &= \frac{\{t^a, t^b\} + [t^a, t^b]}{2} \\ &= \frac{1}{2} \delta^{ab} \frac{\mathbb{1}}{N} + \frac{1}{2} h^{abc} t^c, \end{aligned} \quad (\text{A.75})$$

where we defined

$$h^{abc} = d^{abc} + i f^{abc}. \quad (\text{A.76})$$

h^{abc} is Hermitian and cyclic in its indices:

$$\begin{aligned} h^{abc} &= \bar{h}^{bac} = \bar{h}^{cba} = \bar{h}^{acb}, \\ h^{abc} &= h^{bca} = h^{cab}, \\ h^{aab} &= h^{baa} = h^{aba} = 0. \end{aligned}$$

A last useful property is the Fierz identity

$$(t^a)_{ij} (t^a)_{kl} = \frac{1}{2} \delta_{il} \delta_{jk} - \frac{1}{2N} \delta_{ij} \delta_{kl}. \quad (\text{A.77})$$

It is straightforward to prove this identity; first we write a general element of the fundamental representation as

$$X = c^0 \mathbb{1} + i c^a t^a, \quad (\text{A.78})$$

which is true only in the fundamental representation.³ The c^0 and c^a are easily calculated:

$$\begin{aligned} c^0 &= \frac{1}{N} \text{tr}(X), \\ c^a &= -2i \text{tr}(X t^a). \end{aligned}$$

We then get the requested by calculating $\frac{\partial(X)^{ij}}{\partial(X)^{kl}} = \delta^{ik} \delta^{jl}$. The Fierz identity is especially handy to rearrange traces containing contractions:

$$\text{tr}(A t^a B t^a C) = \frac{1}{2} \text{tr}(AC) \text{tr}(B) - \frac{1}{2N} \text{tr}(ABC), \quad (\text{A.79a})$$

$$\text{tr}(t^a B t^a) = C_F \text{tr}(B), \quad (\text{A.79b})$$

$$\text{tr}(A t^a B) \text{tr}(C t^a D) = \frac{1}{2} \text{tr}(ADCB) - \frac{1}{2N} \text{tr}(AB) \text{tr}(CD), \quad (\text{A.79c})$$

where A, B, C, D are expressions built from t^a 's. But it can be used for standard products as well, e.g.

$$t^a A t^a = \frac{N}{2} \text{tr}(A) \frac{\mathbb{1}}{N} - \frac{1}{2N} A. \quad (\text{A.80})$$

³ This is because in other representations the set $\{\mathbb{1}, t_F^a\}$ doesn't span the full product space.

Useful Formulae

To conclude, we list—without proof—some useful properties of the constants f^{abc} , d^{abc} and h^{abc} . Most of these are easy to prove by straightforward calculation, but see [155] for a nice approach using tensor products for the more difficult ones.

The Jacobi identity can be extended to include d^{abc} , now with all positive signs:

$$f^{abx} d^{xcd} + f^{acx} d^{xbd} + f^{adx} d^{xbc} = 0. \quad (\text{A.81})$$

If we want to find a Jacobi identity with h^{abc} , we have to add the hermitian conjugate due to the sign change:

$$f^{abx} h^{xcd} + f^{acx} \bar{h}^{xbd} + f^{adx} h^{xbc} = 0. \quad (\text{A.82})$$

A Jacobi identity with only d^{abc} also exists, but only in $SU(3)$:

$$d^{abx} d^{xcd} + d^{acx} d^{xbd} + d^{adx} d^{xbc} = \frac{1}{3} (\delta^{ab} \delta^{cd} + \delta^{ac} \delta^{bd} + \delta^{ad} \delta^{bc}). \quad (\text{A.83})$$

Contracting any of the structure constants with a generator gives:

$$f^{abx} t^x = -i (t^a t^b - t^b t^a), \quad (\text{A.84a})$$

$$d^{abx} t^x = t^a t^b + t^b t^a - \delta^{ab} \frac{\mathbb{1}}{N}, \quad (\text{A.84b})$$

$$h^{abx} t^x = 2t^a t^b - \delta^{ab} \frac{\mathbb{1}}{N}, \quad (\text{A.84c})$$

$$\bar{h}^{abx} t^x = 2t^b t^a - \delta^{ab} \frac{\mathbb{1}}{N}. \quad (\text{A.84d})$$

Contracting any of the structure constants with two generators gives:

$$f^{axy} t^x t^y = i \frac{N}{2} t^a, \quad (\text{A.85a})$$

$$d^{axy} t^x t^y = \frac{N^2 - 4}{2N} t^a, \quad (\text{A.85b})$$

$$h^{axy} t^x t^y = -\frac{2}{N} t^a, \quad (\text{A.85c})$$

$$\bar{h}^{axy} t^x t^y = \frac{N^2 - 2}{N} t^a. \quad (\text{A.85d})$$

Contracting any of the structure constants with three generators gives:

$$f^{xyz}t^xt^yt^z = i\frac{N^2}{2}C_F\frac{\mathbb{1}}{N}, \quad (\text{A.86a})$$

$$d^{xyz}t^xt^yt^z = \frac{N^2-4}{2}C_F\frac{\mathbb{1}}{N}, \quad (\text{A.86b})$$

$$h^{xyz}t^xt^yt^z = -2C_F\frac{\mathbb{1}}{N}, \quad (\text{A.86c})$$

$$\bar{h}^{xyz}t^xt^yt^z = (N^2-2)C_F\frac{\mathbb{1}}{N}, \quad (\text{A.86d})$$

Tracing any two structure constants gives:

$$f^{xay}fy^{bx} = -N\delta^{ab}, \quad (\text{A.87a})$$

$$d^{xay}fy^{bx} = 0, \quad (\text{A.87b})$$

$$d^{xay}d^{ybx} = \frac{N^2-4}{N}\delta^{ab}, \quad (\text{A.87c})$$

$$h^{xay}h^{ybx} = 2\frac{N^2-2}{N}\delta^{ab}, \quad (\text{A.87d})$$

$$h^{xay}\bar{h}^{ybx} = -\frac{4}{N}\delta^{ab}, \quad (\text{A.87e})$$

$$\bar{h}^{xay}\bar{h}^{ybx} = 2\frac{N^2-2}{N}\delta^{ab}. \quad (\text{A.87f})$$

And tracing any three structure constants gives:

$$f^{xay}fy^{bz}f^{zcx} = -\frac{N}{2}f^{abc}, \quad (\text{A.88a})$$

$$d^{xay}fy^{bz}f^{zcx} = -\frac{N}{2}d^{abc}, \quad (\text{A.88b})$$

$$d^{xay}d^{ybz}f^{zcx} = \frac{N^2-4}{2N}f^{abc}, \quad (\text{A.88c})$$

$$d^{xay}d^{ybz}d^{zcx} = \frac{N^2-12}{2N}d^{abc}, \quad (\text{A.88d})$$

$$h^{xay}h^{ybz}h^{zcx} = 2\frac{N^2-3}{N}h^{abc}, \quad (\text{A.88e})$$

$$h^{xay}h^{ybz}\bar{h}^{zcx} = -\frac{2}{N}(2h^{abc} + \bar{h}^{abc}), \quad (\text{A.88f})$$

$$h^{xay}\bar{h}^{ybz}\bar{h}^{zcx} = -\frac{2}{N}(h^{abc} + 2\bar{h}^{abc}), \quad (\text{A.88g})$$

$$\bar{h}^{xay}\bar{h}^{ybz}\bar{h}^{zcx} = 2\frac{N^2-3}{N}\bar{h}^{abc}. \quad (\text{A.88h})$$

Tracing four structure constants quickly becomes messy, so we only list a few f and d combinations:

$$f^{x a y} f^{y b z} f^{z c w} f^{w d x} = \delta^{a d} \delta^{b c} + \frac{1}{2} (\delta^{a b} \delta^{c d} + \delta^{a c} \delta^{b d}) + \frac{N}{4} (f^{a d x} f^{x b c} + d^{a d x} d^{x b c}), \quad (\text{A.89a})$$

$$f^{x a y} f^{y b z} f^{z c w} d^{w d x} = \frac{N}{4} (f^{a d x} d^{x b c} - d^{a d x} f^{x b c}), \quad (\text{A.89b})$$

$$f^{x a y} f^{y b z} d^{z c w} d^{w d x} = \frac{1}{2} (\delta^{a c} \delta^{b d} - \delta^{a b} \delta^{c d}) - \frac{N^2 - 8}{4N} f^{a d x} f^{x b c} - \frac{N}{4} d^{a d x} d^{x b c}, \quad (\text{A.89c})$$

$$f^{x a y} d^{y b z} f^{z c w} d^{w d x} = \frac{1}{2} (\delta^{a b} \delta^{c d} - \delta^{a c} \delta^{b d}) - \frac{N}{4} (f^{a d x} f^{x b c} + d^{a d x} d^{x b c}), \quad (\text{A.89d})$$

$$(\text{A.89e})$$

A.7 SUMMARY OF THE NOETHER THEOREMS

We make a short summary of the Noether theorems we defined in [Chapter 1](#). Given the following transformation:

$$x^\mu \rightarrow x^\mu + \epsilon^a X^{\mu a}, \quad (\text{A.90a})$$

$$\phi_i \rightarrow \phi_i + \epsilon^a \Phi_i^a + (\partial_\mu \epsilon^a) \Omega_i^{\mu a}, \quad (\text{A.90b})$$

the Noether theorems on page [14](#) and [27](#) state that if the Lagrangian remains invariant up to a divergence, i.e.

$$\delta \mathcal{L} \equiv \partial_\mu (\epsilon^a K^\mu), \quad (\text{A.91})$$

we can construct the following quantities (the Noether tensor resp. Noether current resp. Noether charge):

$$F^{\mu\nu a} \stackrel{\text{def}}{=} \frac{\partial \mathcal{L}}{\partial \partial_\nu \phi_i} \Omega_i^{\mu a}, \quad (\text{A.92a})$$

$$\mathcal{J}^{\mu a} \stackrel{\text{def}}{=} \frac{\partial \mathcal{L}}{\partial \partial_\mu \phi_i} \Phi_i^a + \frac{\delta \mathcal{L}}{\delta \phi_i} \Omega_i^{\mu a} - \left(\frac{\partial \mathcal{L}}{\partial \partial_\mu \phi_i} \partial_\nu \phi_i - \mathcal{L} \delta_\nu^\mu \right) X^{\nu a} - K^{\mu a}, \quad (\text{A.92b})$$

$$Q^a \stackrel{\text{def}}{=} \int d^3 \mathbf{x} \mathcal{J}^{0 a}, \quad (\text{A.92c})$$

that are conserved

$$\partial_\mu \partial_\nu F^{\mu\nu a} \equiv 0, \quad (\text{A.93a})$$

$$\partial_\mu \mathcal{J}^{\mu a} \equiv 0, \quad (\text{A.93b})$$

$$\dot{Q}^a \equiv 0, \quad (\text{A.93c})$$

and satisfy the additional relation

$$\partial_\nu F^{\nu\mu a} \equiv \mathcal{J}^{\mu a}. \quad (\text{A.94})$$

Furthermore, the equations of motion are given by

$$\frac{\delta \mathcal{L}}{\delta \phi_i} \Phi_i^a \equiv \partial_\mu \left(\frac{\delta \mathcal{L}}{\delta \phi_i} \Omega_i^{\mu a} \right), \quad (\text{A.95})$$

where the variational derivative is given by:

$$\frac{\delta \mathcal{L}}{\delta \phi_i} \stackrel{\text{def}}{=} \frac{\partial \mathcal{L}}{\partial \phi_i} - \partial_\mu \frac{\partial \mathcal{L}}{\partial \partial_\mu \phi_i}. \quad (\text{A.96})$$

In case of a local internal symmetry, the defined charges don't have a physical interpretation and can be ignored. In case of a global symmetry, we have $\Omega_i^{\mu a} = 0$, implying there is no Noether tensor (and the relation in [Equation A.94](#) is invalidated). The [ELEM](#)s then simplify into

$$\frac{\delta \mathcal{L}}{\delta \phi_i} \equiv 0.$$

A.8 FEYNMAN RULES FOR QCD

The full Lagrangian for QCD is given by:

$$\begin{aligned} \mathcal{L} = & \bar{\psi} (i \not{\partial} - m) \psi - \frac{1}{4} (\partial_\mu A_\nu^a - \partial_\nu A_\mu^a)^2 + g \bar{\psi} \not{A} \psi \\ & - g f^{abc} (\partial_\mu A_\nu^a) A^{\mu b} A^{\nu c} - \frac{1}{2} g^2 f^{abx} f^{xcd} A_\mu^a A_\nu^b A^{\mu c} A^{\nu d}, \quad (\text{A.97}) \end{aligned}$$

where $\not{A} \stackrel{\text{N}}{=} A_\mu^a \gamma^\mu t^a$. The sum over gluon polarisation states depends on the gauge, and equals (where in both equations we have made the additional gauge choice $\xi = 0$):

$$\sum_{\text{pol}} \varepsilon_\mu(k) \bar{\varepsilon}_\nu(k) = -g^{\mu\nu} \quad (\text{Lorentz}) \quad (\text{A.98a})$$

$$\sum_{\text{pol}} \varepsilon_\mu(k) \bar{\varepsilon}_\nu(k) = -g^{\mu\nu} + \frac{2k^{(\mu} n^{\nu)}}{n \cdot k} \quad (\text{LC}) \quad (\text{A.98b})$$

where the light-cone gauge is defined by the vector n^- as $n^- \cdot A = A^+ = 0$. The Lagrangian gives rise to the following (extensive) list of Feynman rules (see the next doublepage):

Feynman Rules

$$i, s \xrightarrow{p} \text{fermion vertex} = u_i^s(p) \quad (\text{initial}) \quad (\text{A.99a})$$

$$\text{fermion vertex} \xrightarrow{p} i, s = \bar{u}_i^s(p) \quad (\text{final}) \quad (\text{A.99b})$$

$$i, s \xleftarrow{p} \text{fermion vertex} = \bar{v}_i^s(p) \quad (\text{initial}) \quad (\text{A.99c})$$

$$\text{fermion vertex} \xleftarrow{p} i, s = v_i^s(p) \quad (\text{final}) \quad (\text{A.99d})$$

$$\mu, a \xrightarrow{k} \text{gluon vertex} = \varepsilon_\mu^a(k) \quad (\text{initial}) \quad (\text{A.99e})$$

$$\text{gluon vertex} \xrightarrow{k} \mu, a = \bar{\varepsilon}_\mu^a(k) \quad (\text{final}) \quad (\text{A.99f})$$

$$i \xrightarrow{p} j = i \delta^{ij} \frac{\not{p} + m}{p^2 - m^2 + i\epsilon} \quad (\text{A.99g})$$

$$i \xrightarrow{p} \text{crossed} j = \delta^{ij} \delta^+(p^2 - m^2) (\not{p} + m) \quad (\text{A.99h})$$

$$a, \mu \xrightarrow{k} \text{gluon vertex} b, \nu \stackrel{\text{Lorentz}}{=} \frac{-i \delta^{ab}}{k^2 + i\epsilon} \left[g^{\mu\nu} - (1 - \xi) \frac{k^\mu k^\nu}{k^2} \right] \quad (\text{A.99i})$$

$$a, \mu \xrightarrow{k} \text{gluon vertex} b, \nu \stackrel{\text{LC}}{=} \frac{-i \delta^{ab}}{k^2 + i\epsilon} \left[g^{\mu\nu} - 2 \frac{k_{(\mu} n_{\nu)}}{k \cdot n} + \xi \frac{k^2 k_\mu k_\nu}{(k \cdot n)^2} \right] \quad (\text{A.99j})$$

$$a, \mu \xrightarrow{k} \text{gluon vertex} b, \nu \stackrel{\text{Lorentz}}{=} -\delta^{ab} \delta^+(k^2) g^{\mu\nu} \quad (\text{A.99k})$$

$$a, \mu \xrightarrow{k} \text{gluon vertex} b, \nu \stackrel{\text{LC}}{=} -\delta^{ab} \delta^+(k^2) \left(g^{\mu\nu} - 2 \frac{k_{(\mu} n_{\nu)}}{k \cdot n} \right) \quad (\text{A.99l})$$

$$a \text{---} k \text{---} b = \frac{i \delta^{ab}}{k^2 + i\epsilon} \quad (\text{only Lorentz gauges}) \quad (\text{A.99m})$$

$$\text{double line vertex} \xrightarrow{k, n} = \frac{i}{n \cdot k + i\eta} \quad (\text{A.99n})$$

$$\text{double line vertex} \text{---} k, n \text{---} = \delta(n \cdot k + i\eta) \quad (\text{A.99o})$$

$$i \xrightarrow{p} \text{photon vertex} j = i g_{EM} \mu_{EM}^\epsilon \gamma^\mu \delta_{ij} \quad (\text{A.99p})$$

Feynman Rules

$$\begin{aligned}
 & \begin{array}{c} i \longrightarrow \text{---} \longrightarrow j \\ \text{---} \\ \mu, a \end{array} = ig\mu^\epsilon \gamma^\mu (t^a)_{ji} & \text{(A.99q)} \\
 & \begin{array}{c} a \cdots \text{---} \cdots k \cdots c \\ \text{---} \\ \mu, b \end{array} = g\mu^\epsilon f^{abc} k^\mu \quad (\text{only Lorentz gauges}) & \text{(A.99r)} \\
 & \begin{array}{c} k, n \\ \text{---} \text{---} \\ i \text{---} \text{---} j \\ \text{---} \\ \mu, a \end{array} = ig\mu^\epsilon n^\mu (t^a)_{ji} & \text{(A.99s)} \\
 & r \text{---} \text{---} \xrightarrow{k} = e^{ir \cdot k} & \text{(A.99t)} \\
 & \text{=====} + \infty = 1 \quad (\text{no momentum flow}) & \text{(A.99u)} \\
 & \begin{array}{c} \nu, b \quad \rho, c \\ \text{---} \quad \text{---} \\ p \quad q \\ \text{---} \\ \mu, a \end{array} = g\mu^\epsilon f^{abc} [g^{\mu\nu}(k-p)^\rho + g^{\nu\rho}(p-q)^\mu + g^{\rho\mu}(q-k)^\nu] & \text{(A.99v)} \\
 & \begin{array}{c} \nu, b \quad \rho, c \\ \text{---} \quad \text{---} \\ \mu, a \quad \sigma, d \end{array} = -ig^2 \mu^{2\epsilon} [f^{abx} f^{xcd} (g^{\mu\rho} g^{\nu\sigma} - g^{\mu\sigma} g^{\nu\rho}) - f^{acx} f^{xbd} (g^{\mu\sigma} g^{\nu\rho} - g^{\mu\nu} g^{\rho\sigma}) + f^{adx} f^{xbc} (g^{\mu\nu} g^{\rho\sigma} - g^{\mu\rho} g^{\nu\sigma})] & \text{(A.99w)}
 \end{aligned}$$

Furthermore:

- A. Momentum conservation is imposed at every vertex.
- B. Loop momenta have to be integrated with an additional factor $1/(2\pi)^4$.
- C. Fermion loops (hence ghost loops as well) add an additional factor -1.
- D. All Feynman rules are complex conjugated when on the right side of a final-state cut. Additionally, the 3-gluon vertex and the ghost vertex change sign if on the right side of a final-state cut.
- E. The final result has to be divided by the symmetry factor of the diagram. For a cut diagram: multiply with a symmetry factor for each side.
- F. For each set of k indistinguishable particles in the final state, divide by $k!$.
- G. Impose momentum conservation between initial and final states.
- H. Divide by the flux factor. It is $4\sqrt{(p_1 \cdot p_2)^2 - m_1^2 m_2^2}$ when there are exactly two incoming particles.

INTEGRATIONS

In this appendix we list some common techniques to solve integrals, and give some reference formulae as well.

B.1 REFERENCE INTEGRALS

We start with regular integrals, sorted by type. Note that we omitted the constant term $+c$ that appears in indefinite integrals because of space constraints.

Algebraic Integrals

The easiest type of algebraic integrals are binomial integrals:

$$\int dx (x^n + \alpha)^m = \sum_0^m \binom{m}{k} \frac{1}{nk+1} x^{nk+1} a^{m-k}, \quad (\text{B.1a})$$

$$\int dx (x^n + \alpha)^m x^n = \sum_0^{m+1} \binom{m+1}{k} \frac{k}{m+1} \frac{1}{nk+1} x^{nk+1} a^{m+1-k}, \quad (\text{B.1b})$$

$$\int dx (x^n + \alpha)^m (x^p + b)^r = \sum_{k=0}^m \sum_{l=0}^r \binom{m}{k} \binom{r}{l} \frac{1}{nk+pl+1} x^{nk+pl+1} a^{m-k} b^{r-l}. \quad (\text{B.1c})$$

Next we have rational integrals. First some properties of complex logarithms:

$$\arctan x = \frac{i}{2} \ln \frac{1-ix}{1+ix} \quad (\text{B.1d})$$

$$\operatorname{artanh} x = \frac{1}{2} \ln \frac{1+x}{1-x} \quad (\text{B.1e})$$

$$\ln(-1) = i\pi + 2ik\pi \quad \ln(1) = 2ik\pi \quad (\text{B.1f})$$

$$\ln(i) = \frac{i\pi}{2} + 2ik\pi \quad \ln(-i) = 3\frac{i\pi}{2} + 2ik\pi \quad (\text{B.1g})$$

For the correct derivation of complex logarithms, use polar representation: $i = e^{i(\frac{\pi}{2} + 2k\pi)} \Rightarrow \ln(i) = \frac{i\pi}{2} + 2ik\pi$. We evaluate logarithms in the region $[0, 2\pi]$. Rational integrals will almost always result in a combination of polynomials and/or logarithms:

$$\int dx \frac{1}{1+x^2} = \frac{i}{2} \ln \frac{1-ix}{1+ix}, \quad (\text{B.1h})$$

$$\int dx \frac{1}{1-x^2} = \frac{1}{2} \ln \frac{1+x}{1-x}, \quad (\text{B.1i})$$

$$\int dx \frac{1}{ax^2+bx+c} = \begin{cases} \frac{1}{\sqrt{\Delta}} \ln \frac{\sqrt{\Delta}-(2ax+b)}{\sqrt{\Delta}+(2ax+b)} & \Delta > 0, \\ \frac{-2}{2ax+b} & \Delta = 0, \\ \frac{i}{\sqrt{\Delta}} \ln \frac{\sqrt{\Delta}-i(2ax+b)}{\sqrt{\Delta}+i(2ax+b)} & \Delta < 0, \end{cases} \quad (\Delta = b^2 - 4ac) \quad (\text{B.1j})$$

$$\int dx \frac{x}{ax^2+bx+c} = \begin{cases} \frac{1}{2a} \ln(ax^2+bx+c) + \frac{b}{2a\sqrt{\Delta}} \ln \frac{\sqrt{\Delta}+(2ax+b)}{\sqrt{\Delta}-(2ax+b)} & \Delta > 0, \\ \frac{1}{a} \ln(2ax+b) + \frac{b}{a} \frac{1}{2ax+b} & \Delta = 0, \\ \frac{1}{2a} \ln(ax^2+bx+c) - \frac{ib}{2a\sqrt{-\Delta}} \ln \frac{\sqrt{-\Delta}-i(2ax+b)}{\sqrt{-\Delta}+i(2ax+b)} & \Delta < 0, \end{cases} \quad (\text{B.1k})$$

$$\int dx \frac{x^n}{x-a} = a^n \ln(x-a) + \sum_{k=0}^{n-1} a^k \frac{x^{n-k}}{n-k}, \quad (\text{B.1l})$$

$$\int dx \frac{x^n}{(x-a)^2} = n a^{n-1} \ln(x-a) + \frac{a^n}{a-x} + \sum_{k=1}^{n-1} \frac{k}{n-k} a^{k-1} x^{n-k}, \quad (\text{B.1m})$$

$$\int dx \frac{x^n}{\prod_m (x-a_i)} = \sum_{i=1}^m \frac{a_i^n}{\prod_{j \neq i} (a_i - a_j)} \ln(x-a_i) + \sum_{k=1}^{n-1} \sum_{i=1}^m \frac{a_i^k}{\prod_{j \neq i} (a_i - a_j)} \frac{x^{n-k}}{n-k}. \quad (\text{B.1n})$$

Algebraic integrals with real exponents lead to a Beta function (see [Equation B.7a](#)) or an incomplete Beta function (see [Equation B.7c](#)):

$$\int_0^\infty dx \frac{x^\alpha}{(x+a)^\beta} = a^{1+\alpha-\beta} B(\beta-\alpha-1, \alpha+1), \quad (\text{B.1o})$$

$$\int_c^\infty dx \frac{(x+a)^\alpha}{(x+b)^\beta} = (b-a)^{1+\alpha-\beta} B\left(\frac{b-a}{b+c}; \beta-\alpha-1, \alpha+1\right). \quad (\text{B.1p})$$

Logarithmic Integrals

The most common logarithmic integrals contain a logarithm and a polynomial:

$$\int dx x^n \ln|x+\alpha| = \frac{1}{n+1} \left((x^{n+1} - (-\alpha)^{n+1}) \ln|x+a| - \sum_1^{n+1} \frac{x^k (-\alpha)^{n+1-k}}{k} \right), \quad (\text{B.2a})$$

$$\int dx x^n \ln \left| \frac{x+\alpha}{x-\alpha} \right| \stackrel{n \text{ odd}}{=} \frac{1}{n+1} \left((x^{n+1} - \alpha^{n+1}) \ln \left| \frac{x+a}{x-a} \right| + 2 \sum_0^{n/2} \frac{x^{2k+1} \alpha^{n-2k}}{2k+1} \right), \quad (\text{B.2b})$$

$$\int dx x^n \ln \left| \frac{x+\alpha}{x-\alpha} \right| \stackrel{n \text{ even}}{=} \frac{1}{n+1} \left(x^{n+1} \ln \left| \frac{x+a}{x-a} \right| + \alpha^{n+1} \ln|x^2-a^2| + \sum_1^{n/2} \frac{x^{2k} \alpha^{n+1-2k}}{k} \right). \quad (\text{B.2c})$$

We also list a few integrals of a logarithm divided by x :

$$\int dx \frac{\ln(x-a)}{x-a} = \frac{1}{2} \ln^2(x-a), \quad (\text{B.2d})$$

$$\int dx \frac{\ln(x-a)}{x-b} \stackrel{a \neq b}{=} \ln(x-b) \ln(b-a) - \text{Li}_2 \left(\frac{x-b}{a-b} \right), \quad (\text{B.2e})$$

$$\int dx \frac{\ln(x-a)}{(x-a)^2} = -\frac{1}{x-a} (\ln(x-a) + 1), \quad (\text{B.2f})$$

$$\int dx \frac{\ln(x-a)}{(x-b)^2} \stackrel{a \neq b}{=} \frac{1}{b-a} \left[\ln(x-b) - \frac{x-a}{x-b} \ln(x-a) \right], \quad (\text{B.2g})$$

$$\int dx \frac{\ln(x-a)}{(x-a)(x-b)} \stackrel{a \neq b}{=} \frac{1}{b-a} \left[\ln(x-b) \ln(b-a) - \frac{1}{2} \ln^2(x-a) \right. \\ \left. \text{Li}_2 \left(\frac{x-b}{a-b} \right) \right], \quad (\text{B.2h})$$

$$\int dx \frac{\ln(x+a)}{(x-b)(x-c)} \stackrel{a \neq b \neq c}{=} \frac{1}{b-c} \left[\ln(x-b) \ln(b-a) - \ln(x-c) \ln(c-a) \right. \\ \left. - \text{Li}_2 \left(\frac{x-b}{a-b} \right) + \text{Li}_2 \left(\frac{x-c}{a-c} \right) \right], \quad (\text{B.2i})$$

where Li_2 is the dilogarithm, a specific form of the polylogarithm Li_s (see Subsection [Polylogarithms](#) on page 341 and onwards). Note that the distinction between $a = b$ and $a \neq b$ is mathematically not needed, but we prefer to explicitly state the different integral as the limit $b \rightarrow a$ is not so obvious.

Cyclometric Integrals

We list two important cyclometric integrals:

$$\int dx \arctan x = x \arctan x - \frac{1}{2} \ln(1+x^2), \quad (\text{B.3a})$$

$$\int dx \operatorname{artanh} x = x \operatorname{artanh} x + \frac{1}{2} \ln(1-x^2). \quad (\text{B.3b})$$

Gaussian Integrals

Gaussian integrals are by far the most common integrals in physics in general. We list the most common one-dimensional integrals:

$$\int_{-\infty}^{+\infty} dx e^{-ax^2} = \sqrt{\frac{\pi}{a}}, \quad (\text{B.4a})$$

$$\int_{-\infty}^{+\infty} dx e^{-ax^2+bx+c} = \sqrt{\frac{\pi}{a}} e^{\frac{b^2}{4a}+c}, \quad (\text{B.4b})$$

$$\int_0^{\infty} dx x^{2n} e^{-ax^2} = \frac{1}{2} \frac{(2n-1)!!}{2^n a^n} \sqrt{\frac{\pi}{a}} = \frac{1}{2} \frac{\Gamma(n+\frac{1}{2})}{a^{n+\frac{1}{2}}}, \quad (\text{B.4c})$$

$$\int_0^{\infty} dx x^{2n+1} e^{-ax^2} = \frac{1}{2} \frac{n!}{a^{n+1}} = \frac{1}{2} \frac{\Gamma(n+1)}{a^{n+1}}, \quad (\text{B.4d})$$

$$\int_0^{\infty} dx x^n e^{-ax^2+bx+c} = \frac{1}{2} e^{\frac{b^2}{4a}+c} \sum_0^n \binom{n}{k} \left(\frac{b}{2a}\right)^{n-k} \frac{\Gamma(\frac{k+1}{2})}{a^{\frac{k+1}{2}}}, \quad (\text{B.4e})$$

and the most common multidimensional integrals:

$$\int d^n x e^{-x_i A^{ij} x_j} = \sqrt{\frac{\pi^n}{\det A}}, \quad (\text{B.4f})$$

$$\int d^n x e^{-x_i A^{ij} x_j + b^i x_i + c} = \sqrt{\frac{\pi^n}{\det A}} e^{\frac{1}{4} b^i (A^{-1})_{ij} b^j + c}, \quad (\text{B.4g})$$

$$\int d^n x x_{\mu_1} \cdots x_{\mu_n} e^{-x_i A^{ij} x_j} \stackrel{n \text{ even}}{=} \sqrt{\frac{\pi^n}{\det A}} A_{(\mu_1 \mu_2}^{-1} A_{\mu_3 \mu_4}^{-1} \cdots A_{\mu_{n-1} \mu_n)}^{-1}, \quad (\text{B.4h})$$

where always only the symmetric part of A contributes to the determinant. One special integral is one that is encountered often when variables are chained:

$$\int dx_1 \cdots dx_n e^{i\lambda[(x_1-a)^2+(x_2-x_1)^2+\cdots+(b-x_n)^2]} = \sqrt{\frac{1}{n+1} \left(\frac{i\pi}{\lambda}\right)^n} e^{i\frac{\lambda}{n+1}(b-a)^2}. \quad (\text{B.4i})$$

Gaussian integrals can also be expressed as integrations over complex variables. Then the square root is gone, and an i^n is added:

$$\int d^n z d^n \bar{z} e^{-\bar{z}_i A^{ij} z_j} = \frac{(2\pi i)^n}{\det A}, \tag{B.4j}$$

$$\int d^n z d^n \bar{z} e^{-\bar{z}_i A^{ij} z_j + \bar{w}^i z_i + \bar{z}^i u_i} = \frac{(2\pi i)^n}{\det A} e^{\bar{w}^i (A^{-1})_{ij} u^j}. \tag{B.4k}$$

Discrete Integrals

For completeness and because we need it in [Chapter 2](#), we give the discrete approximation to the integral over an infinitesimal line segment $[a, a + \epsilon]$:

$$\int_a^{a+\epsilon} dx f(x) \approx \epsilon f\left(a + \frac{\epsilon}{2}\right). \tag{B.5a}$$

A macroscopic integral can then be approximated as a sum of such infinitesimal segments:

$$\int_a^b dx f(x) \approx \sum_i^n (x_i - x_{i-1}) f\left(\frac{x_i + x_{i-1}}{2}\right), \tag{B.5b}$$

where $x_0 = a$ and $x_n = b$. We can use the same method to discretise line integrals:

$$\int_a^{a+\epsilon} dx^\mu f_\mu(x) \approx \epsilon^\mu f_\mu\left(a + \frac{\epsilon}{2}\right), \tag{B.5c}$$

$$\int_a^b dx^\mu f_\mu(x) \approx \sum_i^n (x_i - x_{i-1})^\mu f_\mu\left(\frac{x_i + x_{i-1}}{2}\right). \tag{B.5d}$$

B.2 SPECIAL FUNCTIONS AND INTEGRAL TRANSFORMS

In this section we list some common integral relations and transforms, and special functions.

Gamma Function

The Gamma Function is probably the most well-known special function. It is defined as

$$\Gamma(z) \stackrel{\text{def}}{=} \int_0^{\infty} dt \, t^{z-1} e^{-t} \quad \Re(z) > 0. \quad (\text{B.6a})$$

For $n \in \mathbb{N}_0$ it is related to the factorial:

$$\Gamma(n) = (n-1)! \quad (\text{B.6b})$$

and has a similar ‘factorial’ property, but for all z :

$$\Gamma(z+1) = z\Gamma(z). \quad (\text{B.6c})$$

We can also relate it to the double factorial (now for $n \in \mathbb{N}$, i.e. n can be zero):

$$\Gamma\left(n + \frac{1}{2}\right) = \sqrt{\pi} \frac{(2n-1)!!}{2^n}, \quad (\text{B.6d})$$

where the double factorial multiplies every second number:

$$a!! \stackrel{\text{def}}{=} a(a-2)(a-4)\dots \quad (\text{B.6e})$$

which gives the logical relation

$$a! \equiv a!!(a-1)!! \quad (\text{B.6f})$$

An important value of the Gamma function is

$$\Gamma\left(\frac{1}{2}\right) = \sqrt{\pi}, \quad (\text{B.6g})$$

which is just a re-expression of a Gaussian integral. There are four inter-related *reflection formulae*:

$$\Gamma(z)\Gamma(1-z) = \frac{\pi}{\sin(\pi z)}, \quad (\text{B.6h})$$

$$\Gamma(z)\Gamma(-z) = -\frac{\pi}{z \sin(\pi z)}, \quad (\text{B.6i})$$

$$\Gamma\left(z + \frac{1}{2}\right)\Gamma\left(\frac{1}{2} - z\right) = \frac{\pi}{\cos(\pi z)}, \quad (\text{B.6j})$$

$$\Gamma(2z) = \frac{1}{\sqrt{\pi}} 2^{2z-1} \Gamma(z)\Gamma\left(z + \frac{1}{2}\right). \quad (\text{B.6k})$$

The Gamma function has poles in 0 and all negative integers. It can however be expanded around these poles:

$$\Gamma(\epsilon - n) = \frac{(-)^n}{n!} \left(\frac{1}{\epsilon} + \psi^{(0)}(n+1) + \mathcal{O}(\epsilon) \right) \quad n \in \mathbb{N}_0, \quad (\text{B.6l})$$

where $\psi^{(0)}$ is the digamma function, defined as the logarithmic derivative of the Gamma function:

$$\psi^{(0)}(z) \stackrel{\text{def}}{=} \frac{\Gamma'(z)}{\Gamma(z)}. \quad (\text{B.6m})$$

For integer values $n > 0$ it equals

$$\psi^{(0)}(n) = -\gamma_E + \sum_{j=1}^{n-1} \frac{1}{j}. \quad (\text{B.6n})$$

The Gamma function is especially useful when solving integrals, as we can often express the integral at hand in the form [Equation B.6a](#). For easy reference, we list a representation with a quadratic exponential:

$$\int_0^\infty dt \, t^{\alpha-1} e^{-t^2} = \frac{1}{2} \Gamma\left(\frac{\alpha}{2}\right) \quad \Re(\alpha) > 0. \quad (\text{B.6o})$$

We can extend [Equation B.6a](#) to allow for a complex contour. This gives the following complex Gamma representations, that are bound to strict convergence criteria:

$$\int_0^\infty dt \, t^{\alpha-1} e^{i(A+iB)t} = \Gamma(\alpha) i^\alpha (A+iB)^{-\alpha} \quad \forall A, B > 0, \Re(\alpha) > 0, \quad (\text{B.6p})$$

$$\int_0^\infty dt \, t^{\alpha-1} e^{-i(A-iB)t} = \Gamma(\alpha) (-i)^\alpha (A+iB)^{-\alpha} \quad \forall A, B > 0, \Re(\alpha) > 0, \quad (\text{B.6q})$$

$$\int_0^\infty dt \, t^{\alpha-1} e^{\pm iAt} = \Gamma(\alpha) (\pm i)^\alpha A^{-\alpha} \quad \forall A, 0 < \Re(\alpha) < 1. \quad (\text{B.6r})$$

Note that integrals with an exponent $e^{i(A-iB)t}$ or $e^{-i(A+iB)t}$ are divergent for $B > 0$. For easy reference, we also list some complex quadratic representations:

$$\int_0^{\infty} dt \, t^{\alpha-1} e^{i(A+iB)t^2} = \frac{1}{2} \Gamma\left(\frac{\alpha}{2}\right) i^{\frac{\alpha}{2}} (A+iB)^{-\frac{\alpha}{2}} \quad \forall A, B > 0, \Re(\alpha) > 0, \quad (\text{B.6s})$$

$$\int_0^{\infty} dt \, t^{\alpha-1} e^{-i(A-iB)t^2} = \frac{1}{2} \Gamma\left(\frac{\alpha}{2}\right) (-i)^{\frac{\alpha}{2}} (A-iB)^{-\frac{\alpha}{2}} \quad \forall A, B > 0, \Re(\alpha) > 0, \quad (\text{B.6t})$$

$$\int_0^{\infty} dt \, t^{\alpha-1} e^{\pm iAt^2} = \frac{1}{2} \Gamma\left(\frac{\alpha}{2}\right) (\pm i)^{\frac{\alpha}{2}} A^{-\frac{\alpha}{2}} \quad \forall A, 0 < \Re(\alpha) < 2. \quad (\text{B.6u})$$

Beta Function

The Beta function is defined as

$$B(\alpha, \beta) \stackrel{\text{def}}{=} \int_0^1 dt \, t^{\alpha-1} (1-t)^{\beta-1} \quad \Re(\alpha), \Re(\beta) > 0, \quad (\text{B.7a})$$

It can be expressed in terms of Γ -functions:

$$B(\alpha, \beta) \equiv \frac{\Gamma(\alpha)\Gamma(\beta)}{\Gamma(\alpha + \beta)}. \quad (\text{B.7b})$$

When solving complex integrals, it is sometimes convenient to use the incomplete Beta function, which is defined as

$$B(z; \alpha, \beta) \stackrel{\text{def}}{=} \int_0^z dt \, t^{\alpha-1} (1-t)^{\beta-1}, \quad (\text{B.7c})$$

such that

$$B(1; \alpha, \beta) \equiv B(\alpha, \beta). \quad (\text{B.7d})$$

A useful property is its mirror symmetry:

$$B(x; \alpha, \beta) = B(1-x; \beta, \alpha), \quad (\text{B.7e})$$

which follows directly from the definition. Especially helpful is its series expansion (see [156]):

$$B(x; \alpha, \beta) = \frac{1}{\alpha} x^{\alpha} (1-x)^{\beta} \left(1 + \sum_{n=0}^{\infty} \frac{B(\alpha+1, n+1)}{B(\alpha+\beta, n+1)} x^{n+1} \right). \quad (\text{B.7f})$$

Polylogarithms

When integrating logarithms, the result will often depend on the so-called polylogarithm, which is defined by its series expansion:

$$\text{Li}_s(z) \stackrel{\text{def}}{=} \sum_{k=1}^{\infty} \frac{z^k}{k^s}. \quad (\text{B.8a})$$

It can also be defined as a recursive integral:

$$\text{Li}_{s+1}(z) = \int_0^z dt \frac{\text{Li}_s(t)}{t}. \quad (\text{B.8b})$$

For $s \leq 1$ and s integer, the polylogarithm can be expressed as a regular function:

$$\text{Li}_1(z) = -\ln(1-z), \quad (\text{B.8c})$$

$$\text{Li}_0(z) = \frac{z}{1-z}, \quad (\text{B.8d})$$

$$\text{Li}_{-n}(z) = \left(z \frac{\partial}{\partial z} \right)^n \frac{z}{1-z}. \quad (\text{B.8e})$$

The polylogarithm of 0 is always 0 itself, and the polylogarithm of 1 equals the Riemann ζ -function:

$$\text{Li}_s(0) = 0, \quad (\text{B.8f})$$

$$\text{Li}_s(1) = \zeta(s). \quad (\text{B.8g})$$

Of particular interest is the following asymptotic behaviour:

$$\text{Li}_s(e^\epsilon) = \Gamma(1-s)(-\epsilon)^{s-1}, \quad (\text{B.8h})$$

which is valid for $|\epsilon| \rightarrow 0$ and $\Re(s) < 1$. The polylogarithm emerges naturally in the solution to Bose-Einstein and Fermi-Dirac integrals:

$$\int_0^{\infty} dk \frac{k^s}{e^{k-\mu} - 1} = \Gamma(s+1) \text{Li}_{s+1}(e^\mu), \quad (\text{B.8i})$$

$$\int_0^{\infty} dk \frac{k^s}{e^{k-\mu} + 1} = -\Gamma(s+1) \text{Li}_{s+1}(-e^\mu), \quad (\text{B.8j})$$

where Γ is just the Gamma function.

The most common polylogarithm is the dilogarithm Li_2 . Three particular values are:

$$\text{Li}_2(1) = \zeta(2) = \frac{\pi^2}{6}, \quad \text{Li}_2(0) = 0, \quad \text{Li}_2(-1) = -\frac{\pi^2}{12}. \quad (\text{B.8k})$$

It satisfies some additional useful properties:

$$\text{Li}_2(z) + \text{Li}_2(-z) = \frac{1}{2} \text{Li}_2(z^2), \quad (\text{B.8l})$$

$$\text{Li}_2(z) + \text{Li}_2(1-z) = \frac{\pi^2}{6} - \ln z \ln(1-z), \quad (\text{B.8m})$$

$$\text{Li}_2(z) + \text{Li}_2\left(\frac{1}{z}\right) = -\frac{\pi^2}{6} - \frac{1}{2} \ln^2(-z), \quad (\text{B.8n})$$

$$\text{Li}_2(1-z) + \text{Li}_2\left(1 - \frac{1}{z}\right) = -\frac{1}{2} \ln^2 z, \quad (\text{B.8o})$$

$$\text{Li}_2(-z) - \text{Li}_2(1-z) + \frac{1}{2} \text{Li}_2(1-z^2) = -\frac{\pi^2}{12} - \ln z \ln(1+z). \quad (\text{B.8p})$$

However only the first two relations are valid for the full complex plane.

Elliptic K-Function

The elliptic K -function is defined as:

$$K(k) \stackrel{\text{def}}{=} \int_0^{2\pi} d\varphi \frac{1}{\sqrt{1 - k \sin^2 \varphi}}. \quad (\text{B.9a})$$

It is divergent for $k = 1$ and becomes complex for $k > 1$. A related integral is

$$\int_0^{2\pi} d\varphi \frac{1}{\sqrt{a + b \cos \varphi}} = \frac{4}{\sqrt{a+b}} K\left(\frac{2b}{a+b}\right), \quad (\text{B.9b})$$

which is divergent for $a = \pm b$.

Integral Transforms

An integral transform that we will use a lot, is the so-called *Schwinger parameterisation*, which is a complex exponential integral representation for a denominator (where $k \in \mathbb{R}$ and $\varepsilon > 0$):

$$\frac{1}{k+i\varepsilon} = -i \int_0^{\infty} d\alpha e^{i(k+i\varepsilon)\alpha}, \quad (\text{B.10a})$$

$$\frac{1}{k-i\varepsilon} = i \int_0^{\infty} d\alpha e^{-i(k-i\varepsilon)\alpha}. \quad (\text{B.10b})$$

We can summarise this if we define $\sigma = \pm 1$ to be the sign in front of $i\varepsilon$:

$$\frac{1}{k+i\sigma\varepsilon} = -i\sigma \int_0^{\infty} d\alpha e^{i\sigma(k+i\sigma\varepsilon)\alpha}. \quad (\text{B.10c})$$

Note that we can use lower half integrals as well:

$$\frac{1}{k+i\varepsilon} = -i \int_{-\infty}^0 d\alpha e^{-i(k+i\varepsilon)\alpha}, \quad (\text{B.10d})$$

$$\frac{1}{k-i\varepsilon} = i \int_{-\infty}^0 d\alpha e^{i(k-i\varepsilon)\alpha}. \quad (\text{B.10e})$$

It is possible to define a similar parameterisation with a real exponential, but then the sign of k matters:

$$\frac{1}{k} = \int_0^{\infty} d\alpha e^{-k\alpha} \quad k > 0, \quad (\text{B.10f})$$

$$\frac{1}{k} = - \int_0^{\infty} d\alpha e^{k\alpha} \quad k < 0. \quad (\text{B.10g})$$

Having to split up an expression in two terms in function of the sign of k is a bit cumbersome, which is why we won't use the latter parameterisation.

Another parameterisation we will often use is the so-called xL parameterisation, that is used to simplify integrals of the form

$$\int_0^{\infty} \int_0^{\infty} d\alpha d\beta f(\alpha, \beta). \quad (\text{B.11a})$$

The trick is to use the parameterisation:

$$\alpha = xL, \quad \beta = (1-x)L, \quad d\alpha d\beta = L dL dx. \quad (\text{B.11b})$$

The integral then simplifies into

$$\int_0^1 dx \int_0^L dL L f(xL, (1-x)L), \quad (\text{B.11c})$$

which is often easier to solve when starting with the L integration. It can be easily generalised to any number of integrations:

$$(n-1)! \int_0^1 dx_1 \cdots dx_n \int_0^L dL \delta\left(1 - \sum^n x_i\right) L^{n-1} f(x_1L, \dots, x_nL). \quad (\text{B.11d})$$

The normalisation comes from the fact that

$$\int_0^1 dx_1 \cdots dx_n \delta\left(1 - \sum^n x_i\right) = \frac{1}{(n-1)!}. \quad (\text{B.11e})$$

One word of caution however, as the δ -function will chain its influence in all the x_i integrations. This is due to the fact that for non-infinite borders, the sifting property gains additional θ -functions (see [Equations A.53](#)). This implies in general:

$$\begin{aligned} & \int_0^1 dx_1 \cdots \int_0^1 dx_n \delta\left(1 - \sum^n x_i\right) f(x_1, \dots, x_n) \\ &= \int_0^1 dx_1 \int_0^{1-x_1} dx_2 \int_0^{1-x_1-x_2} dx_3 \cdots \int_0^{1-\sum^{n-2} x_i} dx_{n-1} f(x_1, \dots, x_{n-1}, 1-\sum^{n-1} x_i), \quad (\text{B.11f}) \\ &= \int_0^1 dt_1 dt_2 \cdots dt_{n-1} t_1^{n-2} t_2^{n-3} \cdots t_{n-2} \\ & \quad \times f(1-t_1, t_1(1-t_2), t_1 t_2(1-t_3), \dots, t_1 t_2 \cdots t_{n-1}). \quad (\text{B.11g}) \end{aligned}$$

To get to the last step, we used the transformation

$$x_i = \left(\prod_j^{i-1} t_j \right) (1-t_i).$$

Each of these three expressions can be more easy to use or not, depending on the structure of f .

If we combine the Schwinger and the xL -parameterisation, we get the well-known *Feynman parameterisation*:

$$\frac{1}{A} \frac{1}{B} = \int_0^1 dx \frac{1}{(xA + (1-x)B)^2}. \quad (\text{B.12a})$$

We can easily generalise this for n fractions, each with a power m_i :

$$\frac{1}{A_1^{m_1} \dots A_n^{m_n}} = \frac{\Gamma\left(\sum m_i\right)}{\Gamma(m_1) \dots \Gamma(m_n)} \int_0^1 dx_1 \dots dx_n \delta\left(1 - \sum x_i\right) \frac{x_1^{m_1-1} \dots x_n^{m_n-1}}{\left(\sum x_i A_i\right)^{\sum m_i}}. \quad (\text{B.12b})$$

Whether we use the Schwinger parameterisation, the xL -parameterisation or the Feynman parameterisation is situation-dependent, but remains above all a matter of personal taste. Closely related to these parameterisations is the fact that we can use the Gamma function to our advantage:

$$\frac{1}{A^\alpha} = \frac{1}{\Gamma(\alpha)} \int_0^\infty dt t^{\alpha-1} e^{-At}, \quad (\text{B.13})$$

which can be a huge simplification when A is not too complicated.

Totally unrelated to the integral transformations but still worth mentioning, an important property of line integrals is the *gradient theorem*:

$$\int_a^b dx^\mu \partial_\mu f(x) \equiv f(b) - f(a). \quad (\text{B.14})$$

B.3 DIMENSIONAL REGULARISATION

Dimensional regularisation is introduced in Subsection [Regularisation](#) on page 91 and onwards. Here we will list some common loop integrals as a quick reference. Most common loop integrands can be transformed into the form $(k^2 - \Delta)^{-n}$, for which we will give a set of solutions. Furthermore, integrands with momenta in the numerator can be simplified as well. First of all, terms with an odd power

of k vanish by symmetric integration. Also by symmetry arguments, we can replace:

$$k^\mu k^\nu \rightarrow \frac{k^2}{\omega} g^{\mu\nu}, \quad (\text{B.15a})$$

$$k^\mu k^\nu k^\rho k^\sigma \rightarrow \frac{k^4}{\omega(\omega+2)} (g^{\mu\nu} g^{\rho\sigma} + g^{\mu\rho} g^{\nu\sigma} + g^{\mu\sigma} g^{\nu\rho}). \quad (\text{B.15b})$$

The most straightforward way to use dimensional regularisation, is when the integrand only depends on k^2 . Because then we can make a Wick rotation, move to spherical coordinates and calculate the angular part separately:

$$\int \frac{d^{\omega-1}\Omega}{(2\pi)^\omega} = \frac{2}{(4\pi)^{\frac{\omega}{2}} \Gamma\left(\frac{\omega}{2}\right)}. \quad (\text{B.16})$$

Dimensional regularisation is often accompanied by a subtraction scheme. We will only use the $\overline{\text{MS}}$ scheme, and mostly with Collins' convention of dividing the result by a factor

$$S_\epsilon = \frac{(4\pi)^\epsilon}{\Gamma(1-\epsilon)}. \quad (\text{B.17})$$

The more common regular subtraction is done by dividing by

$$S_\epsilon = (4\pi e^{-\gamma_E})^\epsilon, \quad (\text{B.18})$$

but we prefer Collins' convention as it works better with the double poles that originate from LC segments.

Euclidian Integrals

Let us now list some common Euclidian integrals in dimensional regularisation. On the second line of each integral we give the condition for it to be divergent and the expansion in the poles for the latter case.

$$\int \frac{d^\omega k_E}{(2\pi)^\omega} \frac{1}{(k_E^2 + \Delta)^n} = \frac{1}{(4\pi)^{\frac{\omega}{2}}} \frac{\Gamma\left(n - \frac{\omega}{2}\right)}{\Gamma(n)} \Delta^{\frac{\omega}{2}-n}, \quad (\text{B.19a})$$

$$\left(\begin{array}{l} d \geq 2n \\ d \text{ even} \end{array} \right) = \frac{\Delta^{\frac{d}{2}-n}}{(4\pi)^{\frac{d}{2}}} \frac{(-)^{\frac{d}{2}-n}}{(n-1)! \left(\frac{d}{2}-n\right)!} \left(\frac{1}{\epsilon} - \gamma_E + \sum_j^{\frac{d}{2}-n} \frac{1}{j} + \ln 4\pi - \ln \Delta \right),$$

$$\int \frac{d^\omega k_E}{(2\pi)^\omega} \frac{k_E^2}{(k_E^2 + \Delta)^n} = \frac{1}{(4\pi)^{\frac{\omega}{2}}} \frac{\omega}{2} \frac{\Gamma\left(n - \frac{\omega}{2} - 1\right)}{\Gamma(n)} \Delta^{\frac{\omega}{2}+1-n}, \quad (\text{B.19b})$$

$$\left(\begin{array}{l} d \geq 2n-2 \\ d \text{ even} \end{array} \right) = \frac{\Delta^{\frac{d}{2}+1-n}}{(4\pi)^{\frac{d}{2}}} \frac{\omega}{2} \frac{(-)^{\frac{d}{2}+1-n}}{(n-1)! (\frac{d}{2}+1-n)!} \left(\frac{1}{\epsilon} - \gamma_E + \sum_j \frac{1}{j} + \ln 4\pi - \ln \Delta \right),$$

$$\int \frac{d^\omega k_E}{(2\pi)^\omega} \frac{k_E^4}{(k_E^2 + \Delta)^n} = \frac{1}{(4\pi)^{\frac{\omega}{2}}} \frac{\omega(\omega+2)}{4} \frac{\Gamma(n - \frac{\omega}{2} - 2)}{\Gamma(n)} \Delta^{\frac{\omega}{2}+2-n}, \quad (\text{B.19c})$$

$$\left(\begin{array}{l} d \geq 2n-4 \\ d \text{ even} \end{array} \right) = \frac{\Delta^{\frac{d}{2}+2-n}}{(4\pi)^{\frac{d}{2}}} \frac{\omega(\omega+2)}{4} \frac{(-)^{\frac{d}{2}-n}}{(n-1)! (\frac{d}{2}+2-n)!} \left(\frac{1}{\epsilon} - \gamma_E + \sum_j \frac{1}{j} + \ln 4\pi - \ln \Delta \right).$$

We can generalise an Euclidian dimensionally regulated integral to real positive values of the exponents, as

$$\int \frac{d^\omega k_E}{(2\pi)^\omega} \frac{(k_E^2)^\alpha}{(k_E^2 + \Delta)^\beta} = \frac{1}{(4\pi)^{\frac{\omega}{2}}} \Delta^{\frac{\omega}{2}+\alpha-\beta} \frac{\Gamma(\alpha + \frac{\omega}{2}) \Gamma(\beta - \alpha - \frac{\omega}{2})}{\Gamma(\frac{\omega}{2}) \Gamma(\beta)}. \quad (\text{B.20})$$

From this we can deduce that

$$\int d^\omega k_E (k_E^2)^\alpha = 0, \quad (\text{B.21})$$

because in the denominator we have $\Gamma(\beta) \xrightarrow{\beta \rightarrow 0} 1/\beta$, hence the fraction goes to zero in this limit. This is valid $\forall \alpha \geq 0$. For any function that only depends on the square of the momenta, we can write:

$$\int \frac{d^\omega k_E}{(2\pi)^\omega} k_E^{\mu_1} \dots k_E^{\mu_n} f(k_E^2) = \delta^{(\mu_1 \mu_2 \dots \mu_{n-1} \mu_n)} \frac{1}{(4\pi)^{\frac{\omega}{2}}} \frac{\Gamma(\frac{n}{2} + \frac{1}{2})}{\Gamma(\frac{\omega}{2} + \frac{n}{2})} \frac{2}{\sqrt{\pi}} \int_0^\infty df k_E^{\omega-1+n} f(k_E^2), \quad (\text{B.22})$$

for n even (for odd n the integral is zero). Note that in the case of a Minkowskian integral, the δ -functions are replaced with $g^{\mu\nu}$'s.

Wick Rotation and Minkowskian Integrals

Calculating Minkowskian loop integrals can be straightforwardly done by Wick rotating the momenta to Euclidian space, by making the substitution

$$k^0 \stackrel{\text{def}}{=} i k_E^0 \quad k^2 = -k_E^2. \quad (\text{B.23})$$

There are some intricacies with Wick rotations, as one has to make sure not to cross the poles. See [Section 7.3](#) for a digression on this topic. Furthermore, one has to be consistent in the whole formulation. E.g. δ -functions change as well under a Wick rotation:

$$\delta^{(n)}(k) = i \delta_E^{(n)}(k_E). \quad (\text{B.24})$$

To see this, we move to the exponential representation of the δ -function:

$$\delta^{(n)}(k) = \int \frac{d^n x}{(2\pi)^n} e^{i k \cdot x} = i \int \frac{d^n x_E}{(2\pi)^n} e^{-i k_E \cdot x_E} = i \delta_E^{(n)}(k_E).$$

The Mikowskian loop integrals are then the same as the Euclidian ones, up to a possible sign difference:

$$\int \frac{d^\omega k}{(2\pi)^\omega} \frac{1}{(k^2 - \Delta)^n} = i \frac{(-)^n}{(4\pi)^{\frac{\omega}{2}}} \frac{\Gamma(n - \frac{\omega}{2})}{\Gamma(n)} \Delta^{\frac{\omega}{2} - n}, \quad (\text{B.25a})$$

$$\left(\begin{array}{l} d \geq 2n \\ d \text{ even} \end{array} \right) = i \frac{\Delta^{\frac{d}{2} - n}}{(4\pi)^{\frac{d}{2}}} \frac{(-)^{\frac{d}{2}}}{(n-1)! (\frac{d}{2} - n)!} \left(\frac{1}{\epsilon} - \gamma_E + \sum_j^{\frac{d}{2} - n} \frac{1}{j} + \ln 4\pi - \ln \Delta \right),$$

$$\int \frac{d^\omega k}{(2\pi)^\omega} \frac{k^2}{(k^2 - \Delta)^n} = i \frac{(-)^{n+1}}{(4\pi)^{\frac{\omega}{2}}} \frac{\omega}{2} \frac{\Gamma(n - \frac{\omega}{2} - 1)}{\Gamma(n)} \Delta^{\frac{\omega}{2} + 1 - n}, \quad (\text{B.25b})$$

$$\left(\begin{array}{l} d \geq 2n - 2 \\ d \text{ even} \end{array} \right) = i \frac{\Delta^{\frac{d}{2} + 1 - n}}{(4\pi)^{\frac{d}{2}}} \frac{\omega}{2} \frac{(-)^{\frac{d}{2}}}{(n-1)! (\frac{d}{2} + 1 - n)!} \left(\frac{1}{\epsilon} - \gamma_E + \sum_j^{\frac{d}{2} + 1 - n} \frac{1}{j} + \ln 4\pi - \ln \Delta \right),$$

$$\int \frac{d^\omega k}{(2\pi)^\omega} \frac{k^4}{(k^2 - \Delta)^n} = i \frac{(-)^n}{(4\pi)^{\frac{\omega}{2}}} \frac{\omega(\omega+2)}{4} \frac{\Gamma(n - \frac{\omega}{2} - 2)}{\Gamma(n)} \Delta^{\frac{\omega}{2} + 2 - n}, \quad (\text{B.25c})$$

$$\left(\begin{array}{l} d \geq 2n - 4 \\ d \text{ even} \end{array} \right) = i \frac{\Delta^{\frac{d}{2} + 2 - n}}{(4\pi)^{\frac{d}{2}}} \frac{\omega(\omega+2)}{4} \frac{(-)^{\frac{d}{2}}}{(n-1)! (\frac{d}{2} + 2 - n)!} \left(\frac{1}{\epsilon} - \gamma_E + \sum_j^{\frac{d}{2} + 2 - n} \frac{1}{j} + \ln 4\pi - \ln \Delta \right).$$

We list some other common Minkowskian integrals:

$$\int \frac{d^\omega k}{(2\pi)^\omega} \ln(k^2 - a) = -\frac{i}{(4\pi)^{\frac{\omega}{2}}} \Gamma\left(-\frac{\omega}{2}\right) a^{\frac{\omega}{2}}, \quad (\text{B.26a})$$

$$\int \frac{d^\omega k}{(2\pi)^\omega} e^{ak^2 - ib \cdot k} = \frac{i}{(4\pi)^{\frac{\omega}{2}}} a^{-\frac{\omega}{2}} e^{\frac{b^2}{4a}}, \quad (\text{B.26b})$$

$$\int \frac{d^\omega k}{(2\pi)^\omega} \frac{1}{(-k^2)^\alpha} e^{-ib \cdot k} = \frac{i}{4^\alpha \pi^{\frac{\omega}{2}}} \frac{\Gamma(\frac{\omega}{2} - \alpha)}{\Gamma(\alpha)} \frac{1}{(-b^2)^{\frac{\omega}{2} - \alpha}}. \quad (\text{B.26c})$$

Two transversal integrations:

$$\int \frac{d^{\omega-2} \mathbf{k}_\perp}{(2\pi)^{\omega-2}} e^{-i\alpha k_\perp^2} = \frac{1}{(4\pi)^{\frac{\omega}{2}-1}} \frac{1}{(i\alpha)^{\frac{\omega}{2}-1}}, \quad (\text{B.27a})$$

$$\int \frac{d^{\omega-2} \mathbf{k}_\perp}{(2\pi)^{\omega-2}} \frac{1}{(k_\perp^2)^\alpha} e^{i\mathbf{k}_\perp \cdot \mathbf{b}_\perp} = \frac{1}{4^\alpha \pi^{\frac{\omega}{2}-1}} \frac{\Gamma\left(\frac{\omega}{2} - \alpha - 1\right)}{\Gamma(\alpha)} \frac{1}{(b_\perp^2)^{\frac{\omega}{2}-\alpha-1}}. \quad (\text{B.27b})$$

One integral that frequently appears after making a (dimensionally regulated) transverse momentum integration is:

$$\int \frac{d\mathbf{k}^+ d\mathbf{k}^-}{(2\pi)^2} e^{i(a\mathbf{k}^+ \mathbf{k}^- + p^+ \mathbf{k}^- + p^- \mathbf{k}^+ + i\epsilon)} = \frac{1}{2\pi} \frac{1}{a} e^{-\frac{i}{a} p^+ p^-}. \quad (\text{B.28})$$

B.4 PATH INTEGRALS

Here we list some results with path integrals from [Section 3.1](#).

Properties

Every path integral is required to be linear and translation invariant. A rotation of the fields gives an extra determinant in front. These properties can be written together as:

$$\int \mathcal{D}\phi (aF[\phi] + bG[\phi]) = a \int \mathcal{D}\phi F[\phi] + b \int \mathcal{D}\phi G[\phi], \quad (\text{B.29a})$$

$$\int \mathcal{D}\phi F[L\phi + \chi] = \det L \int \mathcal{D}\phi F[\phi], \quad (\text{B.29b})$$

where we used the short-hand notation

$$L\phi \stackrel{\text{N}}{=} \int d^4x L(y, x)\phi(x), \quad (\text{B.30})$$

inside the functional F . We will keep using this short-hand, just remember that the fields are integrated over their coordinates. The real scalar Gaussian path integral is given by:

$$\int \mathcal{D}\phi e^{\phi K \phi} = N_G \frac{1}{\sqrt{\det K}}, \quad (\text{B.31a})$$

$$\phi K \phi \stackrel{N}{=} - \int d^4x d^4y \phi(x) K(x, y) \phi(y), \quad (\text{B.31b})$$

$$N_G = \lim_{n \rightarrow \infty} \sqrt{\pi^n}. \quad (\text{B.31c})$$

If there is an extra linear term in the Gaussian exponent, we can complete the square:

$$\int \mathcal{D}\phi e^{-\phi K \phi + J \phi} = e^{\frac{1}{4} J K^{-1} J} \int \mathcal{D}\phi e^{-\phi K \phi}. \quad (\text{B.32})$$

We can use this property to calculate Gaussian integrals with extra field factors in front of the exponential:

$$\int \mathcal{D}\phi \phi_1 \cdots \phi_n e^{-\phi K \phi} = \frac{\delta}{\delta J_1} \cdots \frac{\delta}{\delta J_n} e^{\frac{1}{4} J K^{-1} J} \Big|_{J=0} \int \mathcal{D}\phi e^{-\phi K \phi}, \quad (\text{B.33})$$

$$= \frac{(n-1)!!}{2^{\frac{n}{2}}} K_{(i_1 i_2}^{-1} \cdots K_{i_{n-1} i_n}^{-1}) \int \mathcal{D}\phi e^{-\phi K \phi}. \quad (\text{B.34})$$

Complex scalar Gaussian path integrals are calculated in a similar way:

$$\int \mathcal{D}\phi \mathcal{D}\bar{\phi} e^{-\bar{\phi} K \phi} = \frac{N_{\bar{G}}}{\det A}, \quad (\text{B.35a})$$

$$N_{\bar{G}} = \lim_{n \rightarrow \infty} (2\pi i)^n, \quad (\text{B.35b})$$

$$\int \mathcal{D}\phi \mathcal{D}\bar{\phi} e^{-\bar{\phi} K \phi + \bar{J} \phi + J \bar{\phi}} = e^{\bar{J} K^{-1} J} \int \mathcal{D}\phi \mathcal{D}\bar{\phi} e^{-\bar{\phi} K \phi}, \quad (\text{B.35c})$$

$$\begin{aligned} \int \mathcal{D}\phi \mathcal{D}\bar{\phi} \phi_{i_1} \bar{\phi}_{j_1} \cdots \phi_{i_n} \bar{\phi}_{j_n} e^{-\bar{\phi} K \phi} &= \frac{\delta}{\delta J_{i_1}} \frac{\delta}{\delta \bar{J}_{j_2}} \cdots \frac{\delta}{\delta J_{i_n}} \frac{\delta}{\delta \bar{J}_{j_n}} e^{\bar{J} K^{-1} J} \Big|_{J, \bar{J}=0} \\ &\times \int \mathcal{D}\phi \mathcal{D}\bar{\phi} e^{-\bar{\phi} K \phi}. \end{aligned} \quad (\text{B.35d})$$

In analogy with the discrete integration, we can give a path integral definition for the functional δ -function:

$$\delta(\phi) = \int \mathcal{D}\omega e^{i \int d^4x \phi(x) \omega(x)}. \quad (\text{B.36})$$

BIBLIOGRAPHY

- [1] I. O. CHEREDNIKOV, T. MERTENS, and F. F. VAN DER VEKEN (2014). *Wilson Lines in Quantum Field Theory*. De Gruyter Studies in Mathematical Physics. De Gruyter, Berlin. (Cited on page [v](#).)
- [2] I. O. CHEREDNIKOV, T. MERTENS, and F. F. VAN DER VEKEN (2013). “Cusped light-like Wilson loops in gauge theories.” *Phys. Part. Nucl.* **44**, 250–259. [arXiv:1210.1767 \[hep-ph\]](#) (Cited on pages [v](#) and [xii](#).)
- [3] I. O. CHEREDNIKOV, T. MERTENS, and F. F. VAN DER VEKEN (2012). “Evolution of cusped light-like Wilson loops and geometry of the loop space.” *Phys. Rev.* **D86**, 085035. [arXiv:1208.1631 \[hep-th\]](#) (Cited on pages [v](#) and [xii](#).)
- [4] F. F. VAN DER VEKEN (2014). “Piecewise linear Wilson lines.” EPJ Web Conf. In print. [arXiv:1409.3190 \[hep-ph\]](#) (Cited on pages [v](#) and [xi](#).)
- [5] F. F. VAN DER VEKEN (2014). “Calculation of colour traces and generators.” In preparation to submit to *Phys. Lett. B*. (Cited on pages [v](#) and [xi](#).)
- [6] F. F. VAN DER VEKEN (2014). “Working with piecewise linear Wilson lines.” In preparation to submit to *Phys. Rev. D*. (Cited on pages [v](#) and [xi](#).)
- [7] I. O. CHEREDNIKOV, T. MERTENS, P. TAELS, and F. F. VAN DER VEKEN (2014). “Evolution of transverse-distance dependent parton densities at large- x_B and geometry of the loop space.” *Int. J. Mod. Phys. Conf. Ser.* **25**, 1460006. [arXiv:1308.3116 \[hep-ph\]](#) (Cited on pages [vi](#) and [xii](#).)
- [8] F. F. VAN DER VEKEN (2013). “Evolution and dynamics of cusped light-like Wilson loops.” *PoS Hadron2013*, 134. [arXiv:1405.4017 \[hep-ph\]](#) (Cited on pages [vi](#) and [xii](#).)
- [9] F. F. VAN DER VEKEN (2013). “Evolution and dynamics of cusped light-like Wilson loops.” *Nuovo Cim.* **C36**, 89–94. [arXiv:1302.6765 \[hep-th\]](#) (Cited on pages [vi](#) and [xii](#).)

- [10] F. F. VAN DER VEKEN, I. O. CHEREDNIKOV, and T. MERTENS (2012). “Evolution and dynamics of cusped light-like Wilson loops in loop space.” AIP Conf. Proc. **1523**, 272–275. [arXiv:1212.4345 \[hep-th\]](#) (Cited on pages [vi](#) and [xii](#).)
- [11] I. O. CHEREDNIKOV, T. MERTENS, and F. F. VAN DER VEKEN (2012). “Loop space and evolution of the light-like Wilson polygons.” Int. J. Mod. Phys. Conf. Ser. **20**, 109–117. [arXiv:1208.5410 \[hep-th\]](#) (Cited on pages [vi](#) and [xii](#).)
- [12] F. F. VAN DER VEKEN (2014). “A new approach to piecewise linear Wilson lines.” Submitted to Int. J. Mod. Phys. Conf. Ser. [arXiv:1411.3372 \[hep-ph\]](#) (Cited on pages [vi](#) and [xi](#).)
- [13] L. P. GAMBERG, M. SCHLEGEL, and F. F. VAN DER VEKEN (2014). “Final state interactions and the Boer-Mulders function.” Work in Progress. (Cited on pages [vi](#) and [308](#).)
- [14] M. GARCÍA ECHEVARRÍA, A. S. IDILBI, I. SCIMEMI, and F. F. VAN DER VEKEN (2014). “Universality of the soft function in QCD.” Work in Progress. (Cited on pages [vi](#) and [308](#).)
- [15] F. F. VAN DER VEKEN (2014). “Computational techniques for Wilson lines.” Work in Progress. (Cited on pages [vi](#) and [308](#).)
- [16] I. O. CHEREDNIKOV and T. MERTENS (2014). “Fréchet derivative for light-like Wilson loops.” Submitted. [arXiv:1401.2721 \[hep-th\]](#) (Cited on pages [xii](#) and [297](#).)
- [17] T. MERTENS (2014). “Generalized loop space and TMDs.” EPJ Web Conf. **73**, 02011. (Cited on pages [xii](#) and [297](#).)
- [18] M. E. PESKIN and D. V. SCHROEDER (1995). *An Introduction to quantum field theory*. Advanced Book Program. Westview Press, Boulder, CO. (Cited on pages [2](#), [12](#), [46](#), [62](#), [114](#), [121](#), and [310](#).)
- [19] R. J. RIVERS (1987). *Path Integral Methods in Quantum Field Theory*. Cambridge monographs on mathematical physics. Cambridge University Press, Cambridge. (Cited on pages [2](#), [46](#), and [62](#).)
- [20] U. MOSEL (2004). *Path integrals in field theory: An introduction*. Springer, Berlin. (Cited on pages [2](#), [46](#), [62](#), [75](#), and [82](#).)
- [21] F. MANDL and G. SHAW (2010). *Quantum Field Theory*. John Wiley & Sons, Chichester, 2nd edition. (Cited on pages [2](#), [46](#), and [75](#).)

- [22] M. SREDNICKI (2007). *Quantum field theory*. Cambridge University Press, Cambridge. (Cited on pages 2 and 121.)
- [23] H. GOLDSTEIN, C. P. J. POOLE, and J. L. SAFKO (2000). *Classical Mechanics*. Addison Wesley, San Francisco, CA, 3th edition. (Cited on pages 4 and 5.)
- [24] I. M. GELFAND and S. V. FOMIN (1963). *Calculus of Variations*. Dover Publications, Mineola, NY. (Cited on pages 5 and 24.)
- [25] E. NEUENSCHWANDER, DWIGHT (2011). *Emmy Noether's Wonderful Theorem*. The Johns Hopkins University Press, Baltimore. (Cited on page 5.)
- [26] F. SCHWABL (2005). *Advanced Quantum Mechanics*. Springer, Berlin. (Cited on page 16.)
- [27] M. CASELLE (2000). "Lattice gauge theories and the ads / cft correspondence." *Int. J. Mod. Phys. A*15, 3901–3966. [arXiv:hep-th/0003119](https://arxiv.org/abs/hep-th/0003119) [hep-th] (Cited on page 42.)
- [28] L. FADDEEV and V. POPOV (1967). "Feynman diagrams for the Yang-Mills field." *Phys. Lett.* B25, 29–30. (Cited on page 80.)
- [29] G. LEIBBRANDT (1987). "Introduction to noncovariant gauges." *Rev. Mod. Phys.* 59, 1067. (Cited on page 88.)
- [30] M. POLJSAK (1994). "A note on the extended mandelstam-leibbrandt prescription for gauge theories in temporal gauge." *Phys. Lett.* B320, 74–82. (Cited on page 88.)
- [31] J. C. COLLINS (1984). *Renormalization*. Cambridge Monographs on Mathematical Physics. Cambridge University Press, Cambridge. (Cited on pages 93, 113, 114, and 220.)
- [32] G. LEIBBRANDT (1975). "Introduction to the technique of dimensional regularization." *Rev. Mod. Phys.* 47, 849. (Cited on page 93.)
- [33] J. COLLINS (2011). *Foundations of perturbative QCD, Cambridge monographs on particle physics, nuclear physics and cosmology*, vol. 32. Cambridge University Press, Cambridge. (Cited on pages 111, 121, 154, 188, and 229.)
- [34] R. D. FIELD (1989). *Applications of Perturbative QCD, Frontiers in Physics*, vol. 77. Addison-Wesley, Reading, MA. (Cited on page 121.)

- [35] R. K. ELLIS, W. J. STIRLING, and B. R. WEBBER (1996). *QCD and collider physics, Cambridge monographs on particle physics, nuclear physics and cosmology*, vol. 8. Cambridge University Press, Cambridge. (Cited on page 121.)
- [36] J. R. FORSHAW and D. A. ROSS (1997). *Quantum chromodynamics and the pomeron, Cambridge Lecture Notes in Physics*, vol. 9. Cambridge University Press, Cambridge. (Cited on page 121.)
- [37] T. MUTA (1998). *Foundations of Quantum Chromodynamics: An Introduction to Perturbative Methods in Gauge Theories, World Scientific Lecture Notes in Physics*, vol. 78. World Scientific, Singapore. (Cited on page 121.)
- [38] V. BARONE and E. PREDAZZI (2002). *High-energy particle diffraction. Theoretical and Mathematical Physics*. Springer, Berlin. (Cited on page 121.)
- [39] A. D. MARTIN (2008). “Proton structure, partons, QCD, DGLAP and beyond.” *Acta Phys.Polon.* **B39**, 2025–2062. [arXiv:0802.0161 \[hep-ph\]](#) (Cited on page 134.)
- [40] P. KOTKO (2014). “Wilson lines and gauge invariant off-shell amplitudes.” *JHEP* **1407**, 128. [arXiv:1403.4824 \[hep-ph\]](#) (Cited on page 172.)
- [41] J. S. BALL and T.-W. CHIU (1980). “Analytic properties of the vertex function in gauge theories. 2.” *Phys. Rev.* **D22**, 2550. (Cited on page 210.)
- [42] A. I. DAVDYCHEV, P. OSLAND, and O. TARASOV (1996). “Three gluon vertex in arbitrary gauge and dimension.” *Phys. Rev.* **D54**, 4087–4113. [arXiv:hep-ph/9605348 \[hep-ph\]](#) (Cited on page 210.)
- [43] J. C. COLLINS and D. E. SOPER (1981). “Back-To-Back Jets in QCD.” *Nucl. Phys.* **B193**, 381. (Cited on page 229.)
- [44] J. C. COLLINS and D. E. SOPER (1982). “Parton Distribution and Decay Functions.” *Nucl. Phys.* **B194**, 445. (Cited on page 229.)
- [45] J. C. COLLINS, D. E. SOPER, and G. F. STERMAN (1983). “Factorization for One Loop Corrections in the Drell-Yan Process.” *Nucl. Phys.* **B223**, 381. (Cited on page 229.)
- [46] J. C. COLLINS, D. E. SOPER, and G. F. STERMAN (1982). “Does the Drell-Yan Cross-section Factorize?” *Phys. Lett.* **B109**, 388. (Cited on page 229.)
- [47] J. C. COLLINS, D. E. SOPER, and G. F. STERMAN (1985). “Transverse Momentum Distribution in Drell-Yan Pair and W and Z Boson Production.” *Nucl. Phys.* **B250**, 199. (Cited on page 229.)

- [48] X.-D. JI, J.-P. MA, and F. YUAN (2005). “QCD factorization for semi-inclusive deep-inelastic scattering at low transverse momentum.” *Phys. Rev. D* **71**, 034005. [arXiv:hep-ph/0404183 \[hep-ph\]](#) (Cited on page 229.)
- [49] X.-D. JI, J.-P. MA, and F. YUAN (2004). “QCD factorization for spin-dependent cross sections in DIS and Drell-Yan processes at low transverse momentum.” *Phys. Lett.* **B597**, 299–308. [arXiv:hep-ph/0405085 \[hep-ph\]](#) (Cited on page 229.)
- [50] X.-D. JI and F. YUAN (2002). “Parton distributions in light cone gauge: Where are the final state interactions?” *Phys. Lett.* **B543**, 66–72. [arXiv:hep-ph/0206057 \[hep-ph\]](#) (Cited on page 229.)
- [51] D. BOER, P. MULDER, and F. PIJLMAN (2003). “Universality of T odd effects in single spin and azimuthal asymmetries.” *Nucl. Phys.* **B667**, 201–241. [arXiv:hep-ph/0303034 \[hep-ph\]](#) (Cited on page 229.)
- [52] J. C. COLLINS and F. HAUTMANN (2000). “Infrared divergences and nonlightlike eikonal lines in Sudakov processes.” *Phys. Lett.* **B472**, 129–134. [arXiv:hep-ph/9908467 \[hep-ph\]](#) (Cited on page 229.)
- [53] F. HAUTMANN (2007). “Endpoint singularities in unintegrated parton distributions.” *Phys. Lett.* **B655**, 26–31. [arXiv:hep-ph/0702196 \[HEP-PH\]](#) (Cited on page 229.)
- [54] A. BELITSKY and A. RADYUSHKIN (2005). “Unraveling hadron structure with generalized parton distributions.” *Phys. Rept.* **418**, 1–387. [arXiv:hep-ph/0504030 \[hep-ph\]](#) (Cited on page 229.)
- [55] A. V. BELITSKY, X. JI, and F. YUAN (2003). “Final state interactions and gauge invariant parton distributions.” *Nucl. Phys.* **B656**, 165–198. [arXiv:hep-ph/0208038 \[hep-ph\]](#) (Cited on pages 229 and 247.)
- [56] A. BACCHETTA, U. D’ALESIO, M. DIEHL, and C. A. MILLER (2004). “Single-spin asymmetries: The Trento conventions.” *Phys. Rev. D* **70**, 117504. [arXiv:hep-ph/0410050 \[hep-ph\]](#) (Cited on pages 229 and 238.)
- [57] A. BACCHETTA (2011). “Transverse-momentum-dependent parton distributions (TMDs).” *AIP Conf. Proc.* **1374**, 29–34. [arXiv:1012.2315 \[hep-ph\]](#) (Cited on page 229.)
- [58] A. BACCHETTA. “Transverse momentum distributions.” URL http://www2.pv.infn.it/~bacchett/teaching/Bacchetta_

- [Trento2012.pdf](#). Lecture notes at the ECT* doctoral training programme. (Cited on pages [229](#) and [244](#).)
- [59] D. BOER, M. DIEHL, R. MILNER, R. VENUGOPALAN, et al. (2011). “Gluons and the quark sea at high energies: Distributions, polarization, tomography.” A report on the joint BNL/INT/JLab program. [arXiv:1108.1713 \[nucl-th\]](#) (Cited on pages [229](#) and [238](#).)
- [60] S. MERT AYBAT and T. C. ROGERS (2011). “TMD factorization and evolution for TMD correlation functions.” *Int. J. Mod. Phys. Conf. Ser.* **04**, 97–105. (Cited on page [229](#).)
- [61] S. M. AYBAT, A. PROKUDIN, and T. C. ROGERS (2012). “Calculation of TMD Evolution for Transverse Single Spin Asymmetry Measurements.” *Phys. Rev. Lett.* **108**, 242003. [arXiv:1112.4423 \[hep-ph\]](#) (Cited on page [229](#).)
- [62] S. M. AYBAT, J. C. COLLINS, J.-W. QIU, and T. C. ROGERS (2012). “The QCD Evolution of the Sivers Function.” *Phys. Rev.* **D85**, 034043. [arXiv:1110.6428 \[hep-ph\]](#) (Cited on page [229](#).)
- [63] E. AVSAR (2012). “TMD factorization and the gluon distribution in high energy QCD.” Unpublished. [arXiv:1203.1916 \[hep-ph\]](#) (Cited on page [229](#).)
- [64] J. COLLINS (2013). “TMD theory, factorization and evolution.” Unpublished. [arXiv:1307.2920 \[hep-ph\]](#) (Cited on page [229](#).)
- [65] I. CHEREDNIKOV and N. STEFANIS (2008). “Renormalization, Wilson lines, and transverse-momentum dependent parton distribution functions.” *Phys. Rev.* **D77**, 094001. [arXiv:0710.1955 \[hep-ph\]](#) (Cited on page [229](#).)
- [66] I. CHEREDNIKOV and N. STEFANIS (2008). “Wilson lines and transverse-momentum dependent parton distribution functions: A Renormalization-group analysis.” *Nucl. Phys.* **B802**, 146–179. [arXiv:0802.2821 \[hep-ph\]](#) (Cited on page [229](#).)
- [67] I. CHEREDNIKOV and N. STEFANIS (2009). “Renormalization-group properties of transverse-momentum dependent parton distribution functions in the light-cone gauge with the Mandelstam-Leibbrandt prescription.” *Phys. Rev.* **D80**, 054008. [arXiv:0904.2727 \[hep-ph\]](#) (Cited on page [229](#).)

- [68] N. STEFANIS and I. CHEREDNIKOV (2009). “Renormalization-group anatomy of transverse-momentum dependent parton distribution functions in QCD.” *Mod. Phys. Lett. A* **24**, 2913–2923. [arXiv:0910.3108 \[hep-ph\]](#) (Cited on page 229.)
- [69] I. CHEREDNIKOV, A. KARANIKAS, and N. STEFANIS (2010). “Wilson lines in transverse-momentum dependent parton distribution functions with spin degrees of freedom.” *Nucl. Phys.* **B840**, 379–404. [arXiv:1004.3697 \[hep-ph\]](#) (Cited on page 229.)
- [70] I. CHEREDNIKOV and N. STEFANIS (2011). “Transverse-momentum-dependent parton distributions at the edge of the lightcone.” *Int. J. Mod. Phys. Conf. Ser.* **4**, 135–145. [arXiv:1108.0811 \[hep-ph\]](#) (Cited on page 229.)
- [71] X.-D. JI, J.-P. MA, and F. YUAN (2005). “Transverse-momentum-dependent gluon distributions and semi-inclusive processes at hadron colliders.” *JHEP* **0507**, 020. [arXiv:hep-ph/0503015 \[hep-ph\]](#) (Cited on page 236.)
- [72] F. DOMINGUEZ, C. MARQUET, B.-W. XIAO, and F. YUAN (2011). “Universality of unintegrated gluon distributions at small x .” *Phys. Rev.* **D83**, 105005. [arXiv:1101.0715 \[hep-ph\]](#) (Cited on page 237.)
- [73] A. BACCHETTA, C. BOMHOF, P. MULDER, and F. PIJLMAN (2005). “Single spin asymmetries in hadron-hadron collisions.” *Phys. Rev.* **D72**, 034030. [arXiv:hep-ph/0505268 \[hep-ph\]](#) (Cited on page 245.)
- [74] M. BUFFING and P. MULDER (2014). “Color entanglement for azimuthal asymmetries in the Drell-Yan process.” *Phys. Rev. Lett.* **1129**, 092002. [arXiv:1309.4681 \[hep-ph\]](#) (Cited on page 245.)
- [75] M. BUFFING and P. MULDER (2014). “Color effects for transverse momentum dependent parton distribution functions in hadronic processes.” [arXiv:1410.6345 \[hep-ph\]](#) (Cited on page 245.)
- [76] Y. V. KOVCHegov (2011). “Introduction to the Physics of Saturation.” *Nucl. Phys.* **A854**, 3–9. [arXiv:1007.5021 \[hep-ph\]](#) (Cited on page 254.)
- [77] Y. V. KOVCHegov (2013). “Introduction to the physics of saturation.” *AIP Conf. Proc.* **1520**, 3–26. (Cited on page 254.)
- [78] Y. V. KOVCHegov and E. LEVIN (2012). *Quantum chromodynamics at high energy, Cambridge monographs on particle physics, nuclear physics and*

- cosmology*, vol. 33. Cambridge University Press, Cambridge. (Cited on page 254.)
- [79] E. A. KURAEV, L. N. LIPATOV, and V. S. FADIN (1976). “Multi - Reggeon Processes in the Yang-Mills Theory.” *Sov. Phys. JETP* **44**, 443–450. (Cited on page 254.)
- [80] E. KURAEV, L. LIPATOV, and V. S. FADIN (1977). “The Pomeranchuk Singularity in Nonabelian Gauge Theories.” *Sov. Phys. JETP* **45**, 199–204. (Cited on page 254.)
- [81] I. BALITSKY and L. LIPATOV (1978). “The Pomeranchuk Singularity in Quantum Chromodynamics.” *Sov. J. Nucl. Phys.* **28**, 822–829. (Cited on page 254.)
- [82] I. BALITSKY (1996). “Operator expansion for high-energy scattering.” *Nucl. Phys.* **B463**, 99–160. [arXiv:hep-ph/9509348 \[hep-ph\]](#) (Cited on page 254.)
- [83] Y. V. KOVCHEGOV (1999). “Small x $F(2)$ structure function of a nucleus including multiple pomeron exchanges.” *Phys. Rev.* **D60**, 034008. [arXiv:hep-ph/9901281 \[hep-ph\]](#) (Cited on page 254.)
- [84] Y. V. KOVCHEGOV (2000). “Unitarization of the BFKL pomeron on a nucleus.” *Phys. Rev.* **D61**, 074018. [arXiv:hep-ph/9905214 \[hep-ph\]](#) (Cited on page 254.)
- [85] E. IANCU, K. ITAKURA, and S. MUNIER (2004). “Saturation and BFKL dynamics in the HERA data at small x .” *Phys. Lett.* **B590**, 199–208. [arXiv:hep-ph/0310338 \[hep-ph\]](#) (Cited on pages 254 and 266.)
- [86] L. GRIBOV, E. LEVIN, and M. RYSKIN (1983). “Semihard Processes in QCD.” *Phys. Rept.* **100**, 1–150. (Cited on page 254.)
- [87] K. J. GOLEC-BIERNAT and M. WUSTHOFF (1998). “Saturation effects in deep inelastic scattering at low Q^2 and its implications on diffraction.” *Phys. Rev.* **D59**, 014017. [arXiv:hep-ph/9807513 \[hep-ph\]](#) (Cited on page 254.)
- [88] A. STASTO, K. J. GOLEC-BIERNAT, and J. KWIECINSKI (2001). “Geometric scaling for the total $\gamma^* p$ cross-section in the low x region.” *Phys. Rev. Lett.* **86**, 596–599. [arXiv:hep-ph/0007192 \[hep-ph\]](#) (Cited on page 254.)

- [89] K. KUTAK and J. KWIECINSKI (2003). “Screening effects in the ultrahigh-energy neutrino interactions.” *Eur. Phys. J.* **C29**, 521. [arXiv:hep-ph/0303209 \[hep-ph\]](#) (Cited on page 254.)
- [90] J. BARTELS and K. KUTAK (2008). “A Momentum Space Analysis of the Triple Pomeron Vertex in pQCD.” *Eur. Phys. J.* **C53**, 533–548. [arXiv:0710.3060 \[hep-ph\]](#) (Cited on page 254.)
- [91] J. L. ALBACETE and C. MARQUET (2010). “Azimuthal correlations of forward di-hadrons in d+Au collisions at RHIC in the Color Glass Condensate.” *Phys. Rev. Lett.* **105**, 162301. [arXiv:1005.4065 \[hep-ph\]](#) (Cited on page 254.)
- [92] A. DUMITRU, K. DUSLING, F. GELIS, J. JALILIAN-MARIAN, et al. (2011). “The Ridge in proton-proton collisions at the LHC.” *Phys. Lett.* **B697**, 21–25. [arXiv:1009.5295 \[hep-ph\]](#) (Cited on page 254.)
- [93] J. ALBACETE, J. MILHANO, P. QUIROGA-ARIAS, and J. ROJO (2012). “Linear vs Non-Linear QCD Evolution: From HERA Data to LHC Phenomenology.” *Eur. Phys. J.* **C72**, 2131. [arXiv:1203.1043 \[hep-ph\]](#) (Cited on page 254.)
- [94] E. IANCU, A. LEONIDOV, and L. MCLERRAN (2002). “The Color glass condensate: An Introduction.” Lecture notes. [arXiv:hep-ph/0202270 \[hep-ph\]](#) (Cited on page 254.)
- [95] E. IANCU and R. VENUGOPALAN (2003). “The Color glass condensate and high-energy scattering in QCD.” Unpublished. [arXiv:hep-ph/0303204 \[hep-ph\]](#) (Cited on page 254.)
- [96] E. IANCU (2009). “Color Glass Condensate and its relation to HERA physics.” *Nucl. Phys. Proc. Suppl.* **191**, 281–294. [arXiv:0901.0986 \[hep-ph\]](#) (Cited on page 254.)
- [97] F. GELIS, E. IANCU, J. JALILIAN-MARIAN, and R. VENUGOPALAN (2010). “The Color Glass Condensate.” *Ann. Rev. Nucl. Part. Sci.* **60**, 463–489. [arXiv:1002.0333 \[hep-ph\]](#) (Cited on page 254.)
- [98] K. KUTAK, K. GOLEC-BIERNAT, S. JADACH, and M. SKRZYPEK (2012). “Nonlinear equation for coherent gluon emission.” *JHEP* **1202**, 117. [arXiv:1111.6928 \[hep-ph\]](#) (Cited on page 254.)
- [99] K. KUTAK (2012). “Nonlinear extension of the CCFM equation.” Unpublished. [arXiv:1206.1223 \[hep-ph\]](#) (Cited on page 254.)

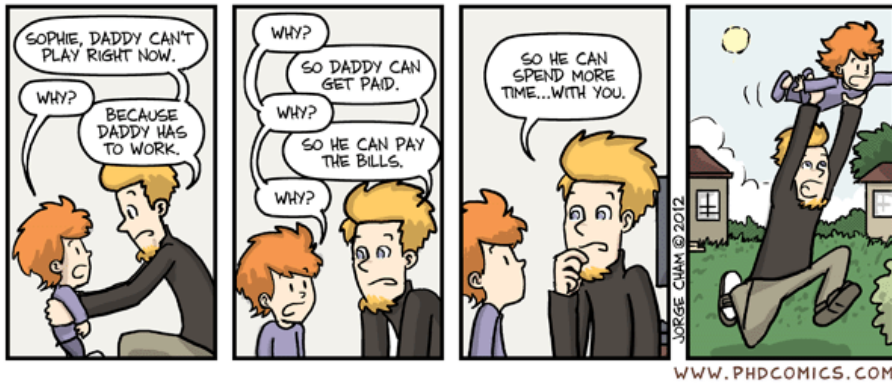
- [100] K. KUTAK and S. SAPETA (2012). “Gluon saturation in dijet production in p-Pb collisions at Large Hadron Collider.” *Phys. Rev.* **D86**, 094043. [arXiv:1205.5035 \[hep-ph\]](#) (Cited on page 254.)
- [101] K. KUTAK (2012). “Resummation in nonlinear equation for high energy factorisable gluon density and its extension to include coherence.” *JHEP* **1212**, 033. [arXiv:1206.5757 \[hep-ph\]](#) (Cited on page 254.)
- [102] M. DEAK (2013). “Estimation of saturation and coherence effects in the KGBJS equation - a non-linear CCFM equation.” *JHEP* **1307**, 087. [arXiv:1209.6092 \[hep-ph\]](#) (Cited on page 254.)
- [103] K. KUTAK and D. TOTON (2013). “Gluon saturation scale from the KGBJS equation.” *JHEP* **1311**, 082. [arXiv:1306.3369 \[hep-ph\]](#) (Cited on page 254.)
- [104] K. KUTAK (2014). “Hard scale dependent gluon density, saturation and forward-forward dijet production at the LHC.” Unpublished. [arXiv:1409.3822 \[hep-ph\]](#) (Cited on page 254.)
- [105] K. J. GOLEC-BIERNAT and M. WUSTHOFF (1999). “Saturation in diffractive deep inelastic scattering.” *Phys. Rev.* **D60**, 114023. [arXiv:hep-ph/9903358 \[hep-ph\]](#) (Cited on page 265.)
- [106] K. J. GOLEC-BIERNAT, J. KWIECINSKI, A. D. MARTIN, and P. SUTTON (1994). “Transverse energy flow at HERA.” *Phys. Lett.* **B335**, 220–225. [arXiv:hep-ph/9405400 \[hep-ph\]](#) (Cited on pages 266 and 267.)
- [107] J. KWIECINSKI, A. D. MARTIN, and P. SUTTON (1992). “Deep inelastic events containing a measured jet as a probe of QCD behavior at small x.” *Phys. Rev.* **D46**, 921–930. (Cited on page 267.)
- [108] J. KWIECINSKI, A. D. MARTIN, P. SUTTON, and K. J. GOLEC-BIERNAT (1994). “QCD predictions for the transverse energy flow in deep inelastic scattering in the HERA small x regime.” *Phys. Rev.* **D50**, 217–225. [arXiv:hep-ph/9403292 \[hep-ph\]](#) (Cited on page 267.)
- [109] C. ADLOFF et al. (2000). “Measurements of transverse energy flow in deep inelastic scattering at HERA.” *Eur. Phys. J.* **C12**, 595–607. [arXiv:hep-ex/9907027 \[hep-ex\]](#) (Cited on page 267.)
- [110] S. BONDARENKO (2011). “Gluon density and $F(2)$ functions from BK equation with local impact parameter dependence in DIS on nuclei.” *Nucl. Phys.* **A853**, 71–96. (Cited on page 270.)

- [111] L. MOTYKA and N. TIMNEANU (2003). “Unintegrated gluon in the photon and heavy quark production.” *Eur.Phys.J.* **C27**, 73–85. [arXiv:hep-ph/0209029 \[hep-ph\]](#) (Cited on page 272.)
- [112] Y. M. MAKEENKO (1995). “Non-perturbative methods in gauge theory.” Lecture notes. (Cited on pages 276, 282, 283, 284, and 297.)
- [113] S. MANDELSTAM (1968). “Feynman rules for electromagnetic and Yang-Mills fields from the gauge independent field theoretic formalism.” *Phys. Rev.* **175**, 1580–1623. (Cited on pages 276 and 295.)
- [114] K. G. WILSON (1974). “Confinement of quarks.” *Phys. Rev.* **D10**, 2445–2459. (Cited on pages 276 and 295.)
- [115] Y. NAMBU (1979). “QCD and the string model.” *Phys. Lett.* **B80**, 372. (Cited on pages 276 and 295.)
- [116] A. M. POLYAKOV (1979). “String representations and hidden symmetries for gauge fields.” *Phys. Lett.* **B82**, 247–250. (Cited on pages 276 and 295.)
- [117] V. DOTSENKO and S. VERGELES (1980). “Renormalizability of Phase Factors in the Nonabelian Gauge Theory.” *Nucl. Phys.* **B169**, 527. (Cited on pages 276, 285, and 295.)
- [118] A. M. POLYAKOV (1980). “Gauge fields as rings of glue.” *Nucl. Phys.* **B164**, 171–188. (Cited on pages 276, 285, and 295.)
- [119] I. Y. AREFEVA (1980). “Quantum contour field equations.” *Phys. Lett.* **B93**, 347–353. (Cited on pages 276, 285, and 295.)
- [120] N. CRAIGIE and H. DORN (1981). “On the renormalization and short distance properties of hadronic operators in QCD.” *Nucl. Phys.* **B185**, 204. (Cited on pages 276, 285, and 295.)
- [121] S. AOYAMA (1982). “The Renormalization of the String Operator in QCD.” *Nucl. Phys.* **B194**, 513. (Cited on pages 276, 285, and 295.)
- [122] N. STEFANIS (1984). “Gauge invariant quark two point green’s function through connector insertion to $\mathcal{O}(\alpha_s)$.” *Nuovo Cim.* **A83**, 205. (Cited on pages 276 and 295.)
- [123] I. BALITSKY and V. M. BRAUN (1989). “Evolution equations for QCD string operators.” *Nucl. Phys.* **B311**, 541–584. (Cited on pages 276 and 295.)

- [124] G. KORCHEMSKY and A. RADYUSHKIN (1987). “Renormalization of the Wilson Loops Beyond the Leading Order.” Nucl. Phys. **B283**, 342–364. (Cited on pages [276](#), [285](#), [287](#), and [290](#).)
- [125] G. ’T HOOFT (1974). “A Planar Diagram Theory for Strong Interactions.” Nucl. Phys. **B72**, 461. (Cited on page [277](#).)
- [126] S. T. TSOU (2003). “Electric magnetic duality and the dualized standard model.” Int. J. Mod. Phys. **A18S2**, 1–40. [arXiv:hep-th/0110256 \[hep-th\]](#) (Cited on page [285](#).)
- [127] J.-L. GERVAIS and A. NEVEU (1980). “The Slope of the Leading Regge Trajectory in Quantum Chromodynamics.” Nucl. Phys. **B163**, 189. (Cited on page [285](#).)
- [128] R. A. BRANDT, F. NERI, and M.-A. SATO (1981). “Renormalization of Loop Functions for All Loops.” Phys. Rev. **D24**, 879. (Cited on page [285](#).)
- [129] I. KORCHEMSKAYA and G. KORCHEMSKY (1992). “On lightlike Wilson loops.” Phys. Lett. **B287**, 169–175. (Cited on pages [289](#) and [302](#).)
- [130] M. GARCÍA ECHEVARRÍA, A. IDILBI, A. SCHÄFER, and I. SCIMEMI (2013). “Model independent evolution of transverse momentum dependent distribution functions (TMDs) at NNLL.” Eur. Phys. J. **C73**, 2636. URL <http://arxiv.org/abs/1208.1281>. [arXiv:1208.1281 \[hep-ph\]](#) (Cited on page [290](#).)
- [131] L. F. ALDAY and J. M. MALDACENA (2007). “Gluon scattering amplitudes at strong coupling.” JHEP **0706**, 064. [arXiv:0705.0303 \[hep-th\]](#) (Cited on page [291](#).)
- [132] L. F. ALDAY and J. MALDACENA (2007). “Comments on gluon scattering amplitudes via ads/cft.” JHEP **0711**, 068. [arXiv:0710.1060 \[hep-th\]](#) (Cited on page [291](#).)
- [133] J. DRUMMOND, J. HENN, G. KORCHEMSKY, and E. SOKATCHEV (2008). “On planar gluon amplitudes/wilson loops duality.” Nucl. Phys. **B795**, 52–68. [arXiv:0709.2368 \[hep-th\]](#) (Cited on pages [291](#), [293](#), and [294](#).)
- [134] J. DRUMMOND, G. KORCHEMSKY, and E. SOKATCHEV (2008). “Conformal properties of four-gluon planar amplitudes and Wilson loops.” Nucl. Phys. **B795**, 385–408. [arXiv:0707.0243 \[hep-th\]](#) (Cited on pages [291](#) and [294](#).)

- [135] Y. MAKEENKO (2003). “Light cone Wilson loops and the string / gauge correspondence.” JHEP 0301, 007. [arXiv:hep-th/0210256 \[hep-th\]](#) (Cited on page 291.)
- [136] L. F. ALDAY, B. EDEN, G. P. KORCHEMSKY, J. MALDACENA, et al. (2011). “From correlation functions to wilson loops.” JHEP 1109, 123. [arXiv:1007.3243 \[hep-th\]](#) (Cited on page 291.)
- [137] N. BEISERT and C. VERGU (2012). “On the geometry of null polygons in full $n=4$ superspace.” Phys. Rev. D86, 026006. [arXiv:1203.0525 \[hep-th\]](#) (Cited on page 291.)
- [138] N. BEISERT, S. HE, B. U. SCHWAB, and C. VERGU (2012). “Null polygonal Wilson loops in full $n=4$ superspace.” J. Phys. A45, 265402. [arXiv:1203.1443 \[hep-th\]](#) (Cited on page 291.)
- [139] A. BELITSKY, G. KORCHEMSKY, and E. SOKATCHEV (2012). “Are scattering amplitudes dual to super Wilson loops?” Nucl. Phys. B855, 333–360. [arXiv:1103.3008 \[hep-th\]](#) (Cited on page 291.)
- [140] A. BELITSKY (2012). “OPE for null Wilson loops and open spin chains.” Phys. Lett. B709, 280–284. [arXiv:1110.1063 \[hep-th\]](#) (Cited on page 291.)
- [141] A. BELITSKY (2012). “A note on two-loop superloop.” Phys. Lett. B718, 205–213. [arXiv:1207.1924 \[hep-th\]](#) (Cited on page 291.)
- [142] S. MOCH, V. J., and A. VOGT (2005). “The quark form-factor at higher orders.” JHEP 0508, 049. [arXiv:hep-ph/0507039 \[hep-ph\]](#) (Cited on page 292.)
- [143] S. J. PARKE and T. TAYLOR (1986). “An amplitude for n gluon scattering.” Phys. Rev. Lett. , 2459. (Cited on page 293.)
- [144] Z. BERN, L. J. DIXON, and V. A. SMIRNOV (2005). “Iteration of planar amplitudes in maximally supersymmetric Yang-Mills theory at three loops and beyond.” Phys. Rev. D72, 085001. [arXiv:hep-th/0505205 \[hep-th\]](#) (Cited on page 293.)
- [145] Z. BERN, M. CZAKON, L. J. DIXON, D. A. KOSOWER, et al. (2007). “The four-loop planar amplitude and cusp anomalous dimension in maximally supersymmetric yang-mills theory.” Phys. Rev. D75, 085010. [arXiv:hep-th/0610248 \[hep-th\]](#) (Cited on page 293.)

- [146] I. KORCHEMSKAYA and G. KORCHEMSKY (1996). “Evolution equation for gluon Regge trajectory.” *Phys. Lett.* **B387**, 346–354. [arXiv:hep-ph/9607229 \[hep-ph\]](#) (Cited on page 295.)
- [147] A. A. MIGDAL (1977). “Multicolor QCD as dual resonance theory.” *Annals Phys.* **109**, 365. (Cited on pages 295 and 296.)
- [148] Y. MAKEENKO and A. A. MIGDAL (1979). “Exact equation for the loop average in multicolor QCD.” *Phys. Lett.* **B88**, 135. (Cited on pages 295 and 296.)
- [149] A. A. MIGDAL (1980). “Properties of the loop average in QCD.” *Annals Phys.* **126**, 279–290. (Cited on pages 295 and 296.)
- [150] Y. MAKEENKO and A. A. MIGDAL (1981). “Quantum chromodynamics as dynamics of loops.” *Nucl. Phys.* **B188**, 269. (Cited on pages 295 and 296.)
- [151] A. A. MIGDAL (1983). “Loop equations and $1/N$ expansion.” *Phys. Rept.* **102**, 199–290. (Cited on pages 295 and 296.)
- [152] T. MERTENS (2013). “Generalized loop space and TMDs.” *PoS Hadron2013*, 135. (Cited on page 297.)
- [153] I. O. CHEREDNIKOV and T. MERTENS (2014). “On geometric scaling of light-like Wilson polygons: Higher orders in α_s .” *Phys. Lett.* **B734**, 198–202. [arXiv:1404.6713 \[hep-th\]](#) (Cited on pages 297 and 305.)
- [154] T. MERTENS and P. TAELS (2013). “Evolution of light-like Wilson loops with a self-intersection in loop space.” *Phys. Lett.* **B727**, 563–567. [arXiv:1308.5296 \[hep-ph\]](#) (Cited on page 297.)
- [155] P. DITTNER (1971). “Invariant tensors in $SU(3)$.” *Commun. Math. Phys.* **22**, 238–252. (Cited on page 325.)
- [156] M. ABRAMOWITZ and I. STEGUN (1965). *Handbook of Mathematical Functions*. Dover Publications, NY. (Cited on page 340.)



PILED HIGHER AND DEEPER by Jorge Cham

www.phdcomics.com

COLOPHON

This document was typeset using the typographical look-and-feel classicthesis developed by André Miede. The style was inspired by Robert Bringhurst's seminal book on typography "*The Elements of Typographic Style*". classicthesis is available for both LaTeX and LyX:

<http://code.google.com/p/classicthesis/>

Happy users of classicthesis usually send a real postcard to the author, a collection of postcards received so far is featured here:

<http://postcards.miede.de/>

Final Version as of 1st December 2014 (classicstyle).

Antwerpen, December 2014

Frederik Van der Veken

TAQ – Theoretical Aspects of QCD